



Universidad de Oviedo

Departamento de Química Orgánica e Inorgánica

Programa de Doctorado: Síntesis y Reactividad Química

***Synthesis of Hetero- and Carbocycles by Stoichiometric and
Catalytic Strategies in Organometallic Chemistry***

Sergio Sánchez Alonso

Tesis Doctoral

2023



Universidad de Oviedo

Departamento de Química Orgánica e Inorgánica

Programa de Doctorado: Síntesis y Reactividad Química

***Synthesis of Hetero- and Carbocycles by Stoichiometric and
Catalytic Strategies in Organometallic Chemistry***

Sergio Sánchez Alonso

Memoria presentada para optar al grado de Doctor en Química orgánica con
Mención de Doctor Internacional

Dissertation submitted to apply for the degree of Doctor of Philosophy in
Organic Chemistry with International Doctor Mention



RESUMEN DEL CONTENIDO DE TESIS DOCTORAL

1.- Título de la Tesis	
Español/Otro Idioma: <i>Síntesis de hetero- y carbociclos mediante estrategias catalíticas y estequiométricas en química organometálica</i>	Inglés: <i>Synthesis of hetero- and carbocycles by stoichiometric and catalytic strategies in organometallic chemistry</i>
2.- Autor	
Nombre: Sergio Sánchez Alonso	DNI/Pasaporte/NIE:
Programa de Doctorado: Síntesis y Reactividad Química	
Órgano responsable: Universidad de Oviedo	

RESUMEN (en español)

La Tesis doctoral aquí recogida puede encuadrarse en el ámbito de la Catálisis Organometálica, específicamente dentro del área de la catálisis homogénea empleando catalizadores carbofílicos de oro (I). Dentro de la misma se recogen y exponen los resultados derivados del estudio realizado para la obtención de diferentes compuestos hetero- y carbocíclicos, tanto mediante aproximaciones estequiométricas como a través de procesos catalizados por complejos de oro. Esta memoria se ha dividido en tres capítulos bien diferenciados atendiendo al tipo de transformación descrita, tal como se expone a continuación.

El primer capítulo recoge el estudio de cicloadición formal [3+3] entre alcoxi alquilcarbenos de Fischer y 4,5-dihidro-1,2,4-oxadiazoles para la síntesis de pirimidin-4(3*H*)-onas. Dicha transformación ha permitido sintetizar diferentes derivados de estos importantes N-heterociclos de forma totalmente regio- y quimioselectiva, con rendimientos de buenos a moderados y una gran tolerancia a grupos funcionales. Diferentes estudios de Resonancia Magnética Nuclear han permitido sugerir posibles rutas mecanísticas y descartar otras, si bien han resultado ser no concluyentes. Cabe también destacar que este proceso representa el primer ejemplo de una reacción de cicloadición [3+3] en la que participan 4,5-dihidro-1,2,4-oxadiazoles.

En el segundo capítulo se describe una reacción de cicloaromatización de ésteres "push-pull" 2,4-dien-6-inocarboxílicos con topología atípica [0,5], catalizada por complejos de oro (I). En este estudio se encontraron condiciones para la obtención de 2-alcoxibenzoatos 6-sustituídos de forma altamente eficiente y regioselectiva en su mayoría, representando así una mejora y extensión del mismo proceso ya descrito para los correspondientes ácidos carboxílicos. Asimismo, se realizaron cálculos computacionales DFT para racionalizar aquellos ejemplos en los que se obtuvieron mezclas de productos de cicloaromatización-[0,5] como [1,6]. Desafortunadamente, las pequeñas diferencias energéticas observadas no permitieron llegar a una explicación satisfactoria.

En el tercer capítulo se encuentran los resultados logrados en el desarrollo de una reacción de cicloadición [4+2] intermolecular entre ésteres 2,4-dien-6-inocarboxílicos "push-pull" e inamidas, constituyendo una reacción de tipo tetrahidro-Diels-Alder (TDDA). Esta metodología permitió acceder a derivados de anilinas tetrasustituídos con rendimientos excelentes y completa regioselectiva. Además, se llevaron a cabo cálculos computacionales DFT para apoyar el mecanismo propuesto por el que transcurre esta transformación.



RESUMEN (en Inglés)

The doctoral thesis collected here can be framed within the field of Organometallic Catalysis, specifically within the area of homogeneous catalysis using gold (I) carbophilic catalysts. Herein are presented and discussed the results derived from the study carried out to obtain different hetero- and carbocyclic compounds, both through stoichiometric approaches and catalytic processes using gold complexes. This thesis is divided into three distinct chapters according to the type of transformation described, as outlined below.

The first chapter presents the study of a formal [3+3]-cycloaddition between alkoxy alkynyl Fischer carbenes and 4,5-dihydro-1,2,4-oxadiazoles for the synthesis of pyrimidin-4(3*H*)-ones. This transformation has allowed the synthesis of various derivatives of these important N-heterocycles in a completely regio- and chemoselective manner, with yields ranging from good to moderate and a high tolerance to functional groups. Different Nuclear Magnetic Resonance studies have suggested possible mechanistic pathways while ruling out others, although they have not been conclusive. It is also worth noting that this process represents the first example of a [3+3]-cycloaddition reaction involving 4,5-dihydro-1,2,4-oxadiazoles.

The second chapter describes an atypical [0,5]-cycloaromatization reaction of "push-pull" 2,4-dien-6-ynoic acid esters, catalysed by gold (I) complexes. In this study, conditions were found for the efficient and regioselective synthesis of 6-substituted 2-alkoxybenzoates, representing an improvement and extension of the previously described process for the corresponding carboxylic acids. Additionally, computational DFT calculations were performed to rationalize cases where mixtures of [0,5]- and [1,6]-cyclization products were obtained. Unfortunately, the small energy differences observed did not allow for a satisfactory explanation.

The third chapter presents the results achieved in the development of an intermolecular [4+2]-cycloaddition reaction between "push-pull" 2,4-dien-6-ynoic acid esters and ynamides, constituting a tetrahydro-Diels-Alder (TDDA) type reaction. This methodology allowed access to tetrasubstituted aniline derivatives with excellent yields and complete regioselectivity. Computational DFT calculations were also carried out to support the proposed mechanism for this transformation.

**SR. PRESIDENTE DE LA COMISIÓN ACADÉMICA DEL PROGRAMA DE DOCTORADO
EN SÍNTESIS Y REACTIVIDAD QUÍMICA**

Agradecimientos

Aunque siempre dije que no iba a hacer agradecimientos, llegado este momento me doy cuenta de que una tesis doctoral es muy larga, te pasan muchas cosas durante tanto tiempo y siempre hay mucha gente a la que agradecerle algo.

Aunque lo normal es empezar agradeciendo a la familia, el jefe... siento que las primeras palabras de agradecimiento deben ser para Sergio, ya que esta tesis no habría sido posible sin él. Bien podría decirse que mereces título y medio de doctor en química. Cada vez que mencionaba la necesidad de buscar información sobre un tema, tú ya lo habías hecho en poco tiempo. Por no hablar del verano en el que te quedaste trabajando por mí mientras yo estaba de estancia. Además, esta memoria bien podría considerarse en gran parte tuya. Hay muchas otras cosas que tú y yo sabemos y que te agradezco profundamente. De verdad, gracias por todo. Eres la persona más especial que he conocido nunca y te querré siempre.

También me gustaría expresar mi agradecimiento a mi director de tesis, Enrique. Gracias por ayudarme siempre en todo lo que necesité, tanto en aspectos relacionados con la química como en trámites burocráticos o asuntos personales. A veces eran cosas triviales y otras veces eran temas más interesantes, pero siempre intentaste ayudarme en todo. Realmente, te estoy muy agradecido.

Además, quisiera agradecer a Isabel Merino su ayuda en los diferentes experimentos que necesité realizar (ya nunca olvidaré hacer el "atma" en el NAV400) y por ese congreso tan especial para mí en Jaca. También quiero agradecer a Isabel Menéndez por los cálculos computacionales realizados en esta tesis (y por ende a Lucía Quintana), pero sobre todo por estar siempre disponible para resolver mis dudas, a pesar de mi absoluta ignorancia en el tema.

Por otro lado, deseo expresar mi profundo agradecimiento a mi familia. A pesar de la distancia y de que en muchas ocasiones no entendían los temas de los que hablaba, siempre me han brindado su apoyo incondicional. Sin vosotros, no habría sido posible llegar hasta aquí. Gracias a su constante apoyo, un chaval de un pequeño pueblo de 300 habitantes en Extremadura, hijo de agricultores, puede hoy decir que es Doctor en Química.

Y, por supuesto, quiero expresar mi más sincero agradecimiento a todas las personas de esta maravillosa tierra, Asturias (y también a aquellos que no son de aquí, pero que han estado conmigo disfrutándola tanto como yo). Quiero agradecer

a los veteranos que estuvieron presentes desde mi llegada y me brindaron su apoyo desde el principio: Berto, Enol, LuciFlow, Lucía, Manu, Miguel, Patri, Raquelina, Raquel Barroso, Silvia, Tati... (puede que se me escape algún nombre, ya que éramos muchos al principio, aún recuerdo mi primer año lleno de espichas...). A medida que el tiempo avanzaba, llegó el relevo generacional pisando fuerte, al que también deseo agradecer de corazón: Álvaro, Ana, Helena, Lali, Laura, Paula, Puri, Sara... Gracias por los viajes, vermús, congresos, espichas, orquestas... También quiero agradecer a todos esos compañeros y compañeras que vinieron de fuera y a los que siempre recordaré: Hikaru, Lucciana, y especialmente a Davide y Kota. Y finalmente, gracias inmensas a mis mejores amigos que he encontrado aquí: Darío, Diego, Iratxe, Martino, Patari, Ross y Sergio. Compartimos mil y una anécdotas de estos años juntos: viajes a Italia, Palomero, Vitoria, Múnich, ...; rutas senderistas, quedadas y mucho más. Aunque a veces no sea la persona más expresiva del mundo y parezca que todo me da igual, quiero que sepáis que siempre estaré aquí para vosotros si me necesitáis.

Abbreviations

$^{\circ}\text{C}$	Celsius degrees
$\%V_{bur}$	Percent buried volume
α	Fine-structure constant
a_{rel}	Relativistic Bohr atomic radius
δ	Chemical shift
Δ	Heat
\hbar	Reduced Planck's constant
ϕ	<i>Tolman angle</i>
v_e	Speed of the electron
Ac	Acetate
Alk	Alkyl
Aq	Acqueus
Ar	Aryl
c	Speed of light constant
c-	Cyclo
COSY	COrelated SpectroscopY
Cy	Cyclohexyl
<i>dig</i>	Digonal
DCM	DiChloroMethane
DCE	DiChloroEthane
DDA	Dehydro-Diels-Alder

DDDA	Di-Dehydro-Diels Alder
DEPT	Distrosionless Enhacement by Polarization Transfer
DFT	Density Funtional Theory
DMF	DiMethylFormamide
DMSO	DiMethylSulfOxide
<i>dr</i>	Diastereomeric ratio
E ⁺	Electrophile
EDG	Electron-Donating Group
<i>ee</i>	Enantiomeric excess
EI	Electron Ionization
ESI	ElectroSpray Ionization
Equiv.	Equivalents
Et	Ethyl
EWG	Electron-Withdrowing Group
FG	Functional Group
GAI	Gold Affinity Index
hν	Electromagnetic radiation
HBX	Hydrogen Bond Basicity Index
HDDA	Hexa-Dehidro-Diels Alder
H-DDDA	Hetero-Di-Dehydro-Diels Alder
H-TDDA	Hetero-Tetra-Dehydro-Diels Alder
Hex	Hexane
HMBC	Hetero Multiple Bond Correlation
HOMO	Highest Occupied Molecular Orbital

HPLC	High-Pressure Liquid Chromatography
HRMS	High-Resolution Mass Spectrometry
HSQC	Hetero Single Quantum Correlation
<i>i</i> Pr	<i>iso</i> -Propyl
IPr	2,6-diisopropylphenyl-imidazol-2-ylidene
<i>J</i>	Coupling constant
JohnPhos	(2-Biphenyl)di- <i>tert</i> -butylphosphine
L	Ligand
LA	Lewis Acid
LG	Leaving Group
LUMO	Lowest Unoccupied Molecular Orbital
<i>m</i> -	<i>Metha</i> -
M	Metal
m_{rel}	Relativistic mass
m/z	Charge/mass relation
Me	Methyl
Ms	Mesityl
MS	Molecular sieves
n.c.	Non-quantified
<i>n</i> Bu	<i>n</i> -Butyl
NHC	<i>N</i> -Heterocyclic Carbene
NMR	Nuclear Magnetic Resonance
NOE	Nuclear Overhauser Effect

NOESY	Nuclear Overhauser Enhancement Spectroscopy
<i>n</i> Pe	<i>n</i> -Pentyl
Ns	Nosyl
Nu ⁻	Nucleophile
<i>o</i> -	<i>Ortho</i> -
on	Overnight
<i>p</i> -	<i>Para</i> -
p.	page
P	Product
PDDA	Penta-Dehydro-Diels Alder
Ph	Phenyl
Ph. D.	Doctor of Philosophy
pp.	pages
ppm	Parts per million
Pr	Propyl
R _f	Retention factor
rt	Room temperature
S	Substrate
Solv	Solvent
SPhos	2-Dicyclohexylphosphino-2',6'-dimethoxybiphenyl
t	Time
T	Temperature
<i>t</i> Bu	<i>tert</i> -Butyl

TBS	<i>tert</i> -Butylsilyl
TDDA	Tetra-Dehydro-Diels Alder
<i>Tet</i>	Tetragonal
Tf	Triflic
THF	TetraHydroFurane
TLC	Thin Layer Chromatography
TMS	TriMethylSilyl
Tol	Tolyl
<i>Tri</i>	Trigonal
Ts	Tosyl
TS	Transition State
vs	versus
XPhos	2-Dicyclohexylphosphino-2',4',6'- triisopropylbiphenyl

Resumen

La Tesis doctoral aquí recogida puede encuadrarse en el ámbito de la Catálisis Organometálica, específicamente dentro del área de la catálisis homogénea empleando catalizadores carbofílicos de oro (I), si bien en el *Capítulo I* se llevan a cabo reacciones estequiométricas. Dentro de la misma se recogen y exponen los resultados derivados del estudio realizado para la obtención de diferentes compuestos hetero- y carbocíclicos, tanto mediante aproximaciones estequiométricas como a través de procesos catalizados por complejos de oro. Esta memoria se ha dividido en tres capítulos bien diferenciados atendiendo al tipo de transformación descrita, tal como se expone a continuación.

El primer capítulo recoge el estudio de cicloadición formal [3+3] entre alcoxi alquilcarbenos de Fischer y 4,5-dihidro-1,2,4-oxadiazoles para la síntesis de pirimidin-4(3*H*)-onas. Dicha transformación ha permitido sintetizar diferentes derivados de estos importantes *N*-heterociclos de forma totalmente regio- y quimioselectiva, con rendimientos de buenos a moderados y una gran tolerancia a grupos funcionales. Cabe también destacar que este proceso representa el primer ejemplo de una reacción de cicloadición [3+3] en la que participan 4,5-dihidro-1,2,4-oxadiazoles.

En el segundo capítulo se describe una reacción de cicloaromatización de ésteres “*push-pull*” 2,4-dien-6-inocarboxílicos con topología inusual [0,5], catalizada por complejos de oro (I). En este estudio se encontraron condiciones para la obtención de 2-alcoxibenzoatos sustituidos en la posición 6 de forma altamente eficiente y

regioselectiva en su mayoría, representando así una mejora y extensión de este proceso ya descrito para los correspondientes ácidos carboxílicos. Asimismo, se realizaron cálculos computacionales DFT para racionalizar aquellos ejemplos en los que se obtuvieron mezclas de productos de cicloaromatización [0,5] y [1,6].

En el tercer capítulo se encuentran los resultados logrados en el desarrollo de una reacción de cicloadición [4+2] intermolecular entre ésteres 2,4-dien-6-inocarboxílicos “*push-pull*” e inamidas, constituyendo una reacción de tipo tetrahidro-Diels-Alder (TDDA). Esta metodología permitió acceder a derivados de anilinas tetrasustituídos con rendimientos excelentes y completa regioselectividad. Además, se llevaron a cabo cálculos computacionales DFT para apoyar el mecanismo propuesto para esta transformación.

Summary

The doctoral thesis collected here can be framed within the field of Organometallic Catalysis, specifically within the area of homogeneous catalysis using gold (I) carbophilic catalysts, although in *Chapter 1* stoichiometric reactions are reported. Herein are presented and discussed the results derived from the study carried out to obtain different hetero- and carbocyclic compounds, both through stoichiometric approaches and catalytic processes using gold complexes. This thesis is divided into three distinct chapters according to the type of transformation described, as outlined below.

The first chapter presents the study of a formal [3+3]-cycloaddition between alkoxy alkynyl Fischer carbenes and 4,5-dihydro-1,2,4-oxadiazoles for the synthesis of pyrimidin-4(3*H*)-ones. This transformation has allowed the synthesis of various derivatives of these important *N*-heterocycles in a completely regio- and chemoselective manner, with yields ranging from good to moderate and a high tolerance to functional groups. It is also worth noting that this process represents the first example of a [3+3]-cycloaddition reaction involving 4,5-dihydro-1,2,4-oxadiazoles.

The second chapter describes an atypical [0,5]-cycloaromatization reaction of “*push-pull*” 2,4-dien-6-ynoic acid esters, catalysed by gold (I) complexes. In this study, conditions were found for the efficient and regioselective synthesis of 6-substituted 2-alkoxybenzoates, representing an improvement and extension of the previously described process for the corresponding carboxylic acids. Additionally,

computational DFT calculations were performed to rationalize cases where mixtures of [0,5]- and [1,6]-cyclization products were obtained.

The third chapter presents the results achieved in the development of an intermolecular [4+2]-cycloaddition reaction between "*push-pull*" 2,4-dien-6-ynoic esters and ynamides, constituting a tetrahydro-Diels-Alder (TDDA) type reaction. This methodology allowed access to tetrasubstituted aniline derivatives with excellent yields and complete regioselectivity. Computational DFT calculations were also carried out to support the proposed mechanism for this transformation.

Index

Introduction.....	1
General background.....	5
1 Gold catalysis. Carbophilic activation.....	7
1.1 Properties of Gold.....	8
1.2 Gold-catalysed transformations involving carbon-carbon multiple bonds.....	22
Chapter I: Chemo- and regioselective synthesis of pyrimidin-4(3H)-ones by formal [3+3]-cycloaddition between 4,5-dihydro-1,2,4-oxadiazoles and chromium alkoxy alkynyl Fischer carbene complexes.....	35
1 Introduction.....	37
2 Bibliographic background.....	39
2.1 General reactivity of group 6 metal alkynyl carbene complexes.....	41
2.2 4,5-Dihydro-1,2,4-oxadiazoles in organic synthesis.....	48
3 Results and discussion.....	53
3.1 Synthesis of starting materials.....	54
3.2 Initial experiment and structural elucidation.....	56
3.3 Optimization of the reaction conditions.....	58
3.4 Scope of the reaction.....	60
3.5 Reaction mechanism.....	66
4 Conclusions.....	73
Chapter II: Gold-catalysed cycloaromatization of “push-pull” alkyl (and silyl) 2,4-dien-6-yne carboxylates. Synthesis of alkyl 6-substituted 2-alkoxybenzoate derivatives.....	75
1 Introduction.....	77
2 Bibliographic background.....	79
2.1 Reactivity of 1, <i>n</i> -enynes.....	80

2.2	Cycloisomerization reactions of 1,3-dien-5-yne.	86
2.3	"Push-pull" 2,4-dien-6-yne.	98
3	Results and discussion.....	101
3.1	Synthesis of starting materials.	102
3.2	Optimization of the reaction conditions.	105
3.3	Scope of the reaction.....	107
3.4	Reaction mechanism.	110
4	Conclusions.	121
Chapter III: Gold-catalysed reaction between "push-pull" alkyl (and silyl) 2,4-dien-6-yne carboxylates and ynamides. Synthesis of tetrasubstituted anilines		123
1	Introduction.	125
2	Bibliographic background.....	127
2.1	Cycloaddition reactions catalysed by gold.	128
2.2	Ynamides as building blocks in gold catalysis.....	131
2.3	Dehydro-Diels-Alder reactions.	138
2.4	"Push-pull" 2,4-dien-6-yne in intermolecular reactions.	144
3	Results and discussion.....	149
3.1	Synthesis of starting materials.	149
3.2	Initial experiment and structural elucidation.....	151
3.3	Optimization of the reaction conditions.	153
3.4	Scope of the reaction.....	154
3.5	Reaction mechanism.	157
4	Conclusions.	163
General conclusions.....		165
Conclusiones Generales.....		169
Experimental section		173
1	General aspects.....	175

1.1	General considerations.....	175
1.2	Instrumental techniques.....	176
2	Experimental procedures.....	177
2.1	Experimental procedures described in Chapter I.....	177
2.2	Experimental procedures described in Chapter II.....	199
2.3	Experimental procedures described in Chapter III.....	218
<i>Annex I: Nuclear Magnetic Resonance (NMR) spectra.....</i>		231
1	Chapter I.....	233
2	Chapter II.....	270
3	Chapter III.....	307
<i>Annex II: Complete computational data.....</i>		329
1	Chapter II.....	332
<i>Annex III: Crystallographic data.....</i>		337

Introduction

This Ph. D. dissertation is located within the fields of Organometallic Chemistry and Organic Synthesis, specifically framed in the area of homogenous gold catalysis.

In recent decades, catalysis has emerged as a crucial tool for synthetic chemists, enabling the development of increasingly selective and sustainable methodologies. Among these catalysts, those based on noble metals have assumed a pivotal role in large-scale industrial processes, owing to their ability to facilitate a wide range of reactions.

In this context, gold catalysis has undergone a phenomenon often referred to as the "golden rush" in recent years, witnessing an exponential growth in applications and transformations facilitated by gold species. Several years ago, our research group became intrigued by these processes and embarked on a journey to expand our knowledge in this field, making significant contributions along the way.

The results described herein are focused on the development of novel stoichiometric and catalytic strategies for the construction of six-membered hetero- and carbocycles starting from unsaturated systems. Moreover, DFT calculations, as well as experimental mechanism studies, were conducted aiming to shed light to and rationalize the different proposed mechanisms.

This Dissertation has been divided into three Chapters, preceded by a General Background section.

The General Background has been divided into two parts: the first part explores the fundamental properties that influence gold catalytic cycles, while the second part provides an overview of representative examples in the field of homogeneous gold catalysis.

The achieved results have been compiled in the following manner:

- Chapter I: Chemo- and regioselective synthesis of pyrimidin-4(3*H*)-ones by formal [3+3]-cycloaddition between 4,5-dihydro-1,2,4-oxadiazoles and chromium alkoxy alkynyl Fischer carbene complexes.
- Chapter II: Gold-catalysed cycloaromatization of “*push-pull*” alkyl (and silyl) 2,4-dien-6-yne carboxylates. Synthesis of alkyl 6-substituted 2-alkoxybenzoate derivatives.
- Chapter III: Gold-catalysed reaction between “*push-pull*” alkyl (and silyl) 2,4-dien-6-yne carboxylates and ynamides. Synthesis of tetrasubstituted anilines.

Later, the General Conclusions that can be extracted from this thesis have been discussed.

Lastly, an Experimental section details the synthetic procedures employed in this study and provides characterization data for the synthesized compounds. Furthermore, three separate Appendices at the end compile the recorded NMR spectra, the details of the performed DFT computational calculations and the obtained X-Ray Diffraction data.

General background

1 Gold catalysis. Carbophilic activation.

Gold is a metal with a long and rich history that spans thousands of years. It was first used by civilizations such as the Egyptians, who utilized it in the creation of jewelry, currency, and for religious purposes. Due to its scarcity, stunning appearance, and longevity, gold was highly regarded and has played a significant role in human history ever since.

From a chemical perspective, gold was among the earliest elements to be discovered and isolated by humans. However, within the field of chemical catalysis, it was long considered a "dead metal" until its first application in heterogeneous catalysis using gold nanoparticles. Gold catalysts have been found to be highly effective in facilitating a range of heterogeneous reactions, including the hydrogenation of alkenes¹ and the oxidation of alcohols.² However, its first application in homogeneous catalysis is more recent.³ Given that this thesis is focused on homogeneous gold catalysis and that this area has seen significant advancements in recent decades, going forward, when discussing catalysis with gold, the focus will be exclusively on homogeneous gold catalysis.

Among the benefits of using gold as a catalyst its high level of activity and its stability are the two more valuable ones. Unlike other metal catalysts, such as palladium and platinum, gold is less prone to poisoning and leaching. These features

¹ Sermon, P. A.; Bond, G. C.; Wells, P. B. *J. Chem. Soc., Faraday Trans. 1* **1979**, *75*, 385-394.

² Guan, B.; Xing, D.; Cai, G.; Wan, X.; Yu, N.; Fang, Z.; Yang, L.; Zhangjie. *S. J. Am. Chem. Soc.* **2005**, *127*, 18004-18005.

³ Ito, Y.; Sawamura, M.; Hayashi, T. *J. Am. Chem. Soc.* **1986**, *108*, 6406-6407.

make gold catalysts a more reliable option for industrial applications, where efficiency and consistency are important.

However, there are also limitations to the use of gold as a catalyst. One of the main ones is the high cost of gold, which makes it an expensive option for industrial applications. Moreover, it has the highest normal reduction potential of all metals (1.48 V). This property, a priori, implies lower reactivity but also allows it to be recovered to its active form. In addition, the mechanisms of gold-catalysed reactions are still not well understood, making it difficult to optimize the conditions for these reactions.⁴

Despite these disadvantages, the use of gold as a catalyst has steadily increased, reflecting the growing interest and importance of this area of study. This has led to a better understanding of the mechanism by which gold catalyses reactions, as well as the optimization of its use in various industrial processes.

This introduction will be structured in two sections. First, the most relevant theoretical aspects of gold catalysis will be explained, followed by the discussion of the existing background and published work on the topic in recent years.

1.1 Properties of Gold.

1.1.1 Relativistic effects.

Gold, a chemical element with atomic number $Z = 79$, is situated in group 11 of the periodic table and has an electronic configuration of $[\text{Xe}] 4f^{14} 5d^{10} 6s^1$, making it part of the transition metals. However, simply based on its location in the periodic table, it is not possible to understand its significant properties and unique chemical behaviour. This exceptional reactivity is a result of the well-known relativistic effects that are present in the gold element.⁵

To understand these effects, it is important to mention the Albert Einstein's Theory of Relativity.⁶ Although the concept of "relativity" in relation to the quantum

⁴ Lu, Z.; Li, T.; Mudshinge, S. R.; Xu, B.; Hammond, G. B. *Chem. Rev.* **2021**, *121*, 8452-8477.

⁵ a) Autschbach, J. J. *Chem. Phys.* **2012**, *136*, 150902-150917; b) Pyykkö, P. *Annu. Rev. Phys. Chem.* **2012**, *63*, 45-64.

⁶ Einstein, A. *Annalen der Physik* **1905**, *17*, 891-921.

theory of electrons was first introduced in 1928 by Paul Dirac,⁷ he initially undervalued its effect on the determination of atomic and molecular structure in relation to Coulomb forces. It was not until Bertha Swirles presented a relativistic model in 1935,⁸ and subsequent studies in the 1970s and 80s,⁹ that it was recognized as a vital factor in the study of heavy elements in the periodic table.

The term "relativistic effects" refers to the deviations observed between theoretical predictions and actual observations. Within the group of metals, gold stands out due to its unique relativistic effects, which provide insight into both its chemical reactivity and physical properties.

In order to find the appropriate treatment, it is important to examine one of the most well-known outcomes in this theory and its connection to the relativistic Bohr atomic radius (a_{rel}), which are both outlined in Equation GB.1.

$$m_{rel} = \frac{m_0}{\sqrt{1-(v_e/c)^2}} \qquad a_{rel} = \frac{\hbar}{m_{rel}c\alpha}$$

Equation GB.1: Equations for relativistic mass (m_{rel}) and relativistic Bohr radius (a_{rel}).

The first equation relates the relativistic mass (m_{rel}) to the uncorrected mass (m_0), considering the speed of the electron (v_e). The second equation demonstrates the relationship between the relativistic Bohr atomic radius (a_{rel}) and the relativistic mass, where c is the speed of light constant, \hbar is the reduced Planck's constant, and α is the fine-structure constant.

From a qualitative perspective, a higher charge or atomic number of the nucleus leads to an increase in the speed of electrons, causing an increase in relativistic mass and a reduction in the relativistic Bohr atomic radius. This suggests that electrons in the s and p orbitals are located near the nucleus, providing a shield for electrons in the d and f orbitals. In simpler terms, the s and p orbitals will contract while the d and f orbitals will expand.

⁷ Dirac, P. A. M. *Proc. R. Soc. A.* **1929**, *123*, 714-733.

⁸ Swirles, B. *Proc. R. Soc. A.* **1935**, *152*, 625-649.

⁹ a) Pitzer, K. S. *Acc. Chem. Res.* **1979**, *12*, 271-276; b) Pyykkö, P. *Chem. Rev.* **1988**, *88*, 563-594.

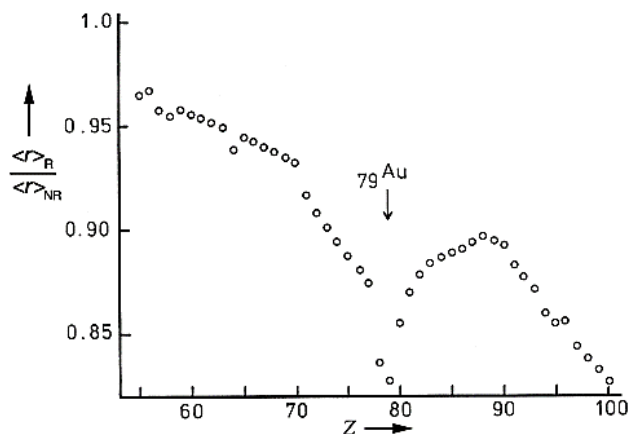


Figure GB.1: 6s orbital contraction.

It is believed that this significant relativistic effect, that affects more to heavier elements and particularly to Pt and Au (Figure GB.1),¹⁰ may be a result of the overlap between the 6s valence shell orbital, which undergoes a contraction, and the 5d orbital, which experiences an expansion. This leads to a strong σ -interaction between the gold atom and its ligands compared to other metals.¹¹ As a result, gold (I) complexes are d^{10} type, which generally display a bicoordinated linear geometry with 14 electrons, while Cu (I) and Ag (I) complexes exhibit a tri- or tetraordinated geometry. In contrast, Au (III) complexes are d^8 , which are known to have a square-planar geometry with 16 electrons. These two oxidation states are prevalent in gold catalysis, although a range of other oxidation states have been documented in gold species.¹²

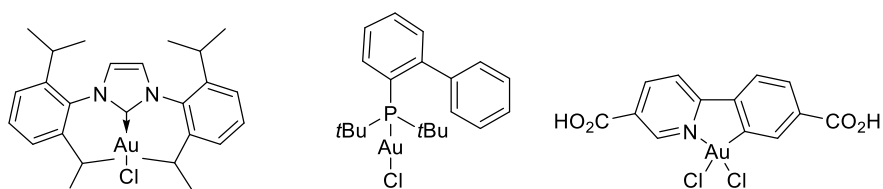


Figure GB.2: Examples of commonly found Au (I) and Au (III) complexes.

¹⁰ Leyva-Pérez, A.; Corma, A. *Angew. Chem. Int. Ed.* **2012**, *51*, 614-635.

¹¹ a) Autsschbach, L.; Sekeierski, S.; Seth, M.; Schwerdtfeger, P.; Schwarz, W. H. E. *J. Comput. Chem.* **2002**, *23*, 804-813; b) Gorin, D. J.; Toste, F. D. *Nature* **2007**, *446*, 395-403.

¹² Lin, J.; Zhang, S.; Guan, W.; Yang, G.; Ma, Y. *J. Am. Chem. Soc.* **2018**, *140*, 9545-9550.

Furthermore, this contraction gives rise to the well-known "aurophilic" behaviour of this metal,¹³ leading to a tendency for gold to form Au-Au interactions with bond lengths ranging from 2.50 to 3.50 Å and stabilization effects similar to hydrogen bonding.

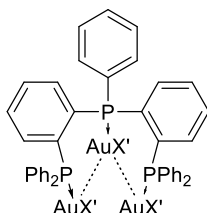


Figure GB.3: Example of aurophilic interaction between gold atoms.

As a result of the contraction of the 6s orbital, the electrons are brought closer to the nucleus, leading to an increase in the electronegativity and ionization potential of the metal (9.22 eV) when compared to other metals in the group like silver (7.57 eV) or copper (7.72 eV).¹⁴

The marked relativistic effects in this metal result in a lower electron-electron interaction in the diffuse 5d orbitals. This means that more energy is needed to remove an electron. This could be the reason why gold is less likely to undergo redox processes, such as the oxidative addition or the reductive elimination that is typical of other transition metals.¹⁵ Nevertheless, despite being a challenging area, several examples of this reactivity have been successfully demonstrated.¹⁶

Concerning their nucleophilicity, gold complexes are less nucleophilic compared to other similar systems, such as copper complexes, because the electrons in the 6s orbital are more stabilized, as previously explained. This decrease in nucleophilicity is not only due to the 6s orbital contraction, but also to the 5d orbital expansion,

¹³ a) Schmidbaur, H.; Schier, A. *Chem. Soc. Rev.* **2012**, *41*, 370-412; b) Blasco, D.; Reboiro, F.; Sundholm, D.; Olmos, M. A.; Monge, M.; López-de-Luzuriaga, J. M. *Dalton Trans.* **2023**, *52*, 2219-2222.

¹⁴ Cronje, S.; Djordjevic, B.; Schmidbaur, H. *Chem. Phys.* **2005**, *311*, 151-161.

¹⁵ Huang, B; Hu, M.; Toste, F. D. *Trends Chem.* **2020**, *2*, 707-720.

¹⁶ a) Chintawar, C. C.; Yadav, A. K.; Patil, N. T. *Angew. Chem. Int. Ed.* **2020**, *59*, 11808-11813; b) Ye, L.-W.; Zhu, X.-Q.; Sahani, R. L.; Xu, Y.; Qian, P.-C.; Liu, R.-S. *Chem. Rev.* **2021**, *121*, 9039-9112.

which results in higher electron retention due to reduced electron-electron repulsions.

Besides, the contraction of the $6s$ and $6p$ valence orbitals due to relativistic effects results in a decrease in the energy of the Lowest Unoccupied Molecular Orbital (LUMO), which is primarily composed of $6s$ and $6p$ orbitals with a roughly equal contribution of s and p character (Figure GB.4). This decrease in energy leads to increased electronegativity and heightened Lewis acidity.

Additionally, since the Au (I) cation is large and diffuse, distributing its positive charge among its ligands, orbital interactions are favoured over charge interactions, making it simpler to add a second ligand. As a result, the LAu^+ cation is considered a "soft" Lewis acid that selectively activates "soft" electrophiles, such as π systems. This behaviour is particularly noteworthy as it provides exceptional potential for producing and stabilizing intermediate carbocationic reactions from alkynes, alkenes, or allenes in the presence of other functional groups.

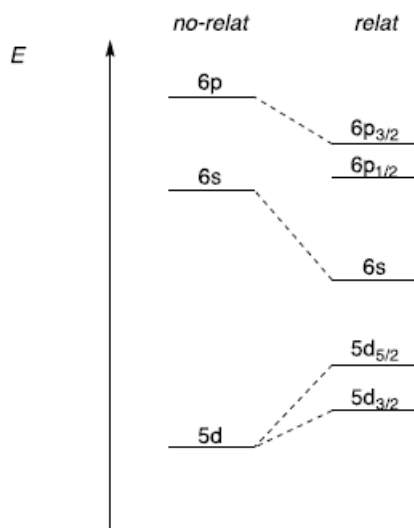


Figure GB.4: Diagram of Energy Levels for Gold's Atomic Orbitals.

Activation of alkynes with gold complexes is more common than activation of alkenes due to the differences in their electronic properties. It is known that alkynes have lower HOMOs and LUMOs than their alkenes analogues, making them less

nucleophilic and more electrophilic.¹⁷ Besides, computational studies suggest that the [ethene-Au]⁺ complex is more stabilized than the [ethyne-Au]⁺ complex.¹⁸ Because of these reasons, it is thought that gold complexes show a preference for alkynes over alkenes.

1.1.2 Ligand-dependent effects.

The research in chemical catalysis using gold has demonstrated that the type of ligand complexed to the metal plays a crucial role, similar to what is seen in catalysis with other metals. Two key factors that determine its effectiveness in catalysis are the electronic and steric properties of the ligand.

These properties often work together in a complementary manner. However, in some cases, one effect may be more dominant. The two main families of ligands used in this type of catalysis are *N*-heterocyclic carbene (NHC) type ligands and phosphine type ligands (Figure GB.5). The electronic and steric differences between these two types of ligands will be the focus of comparison.

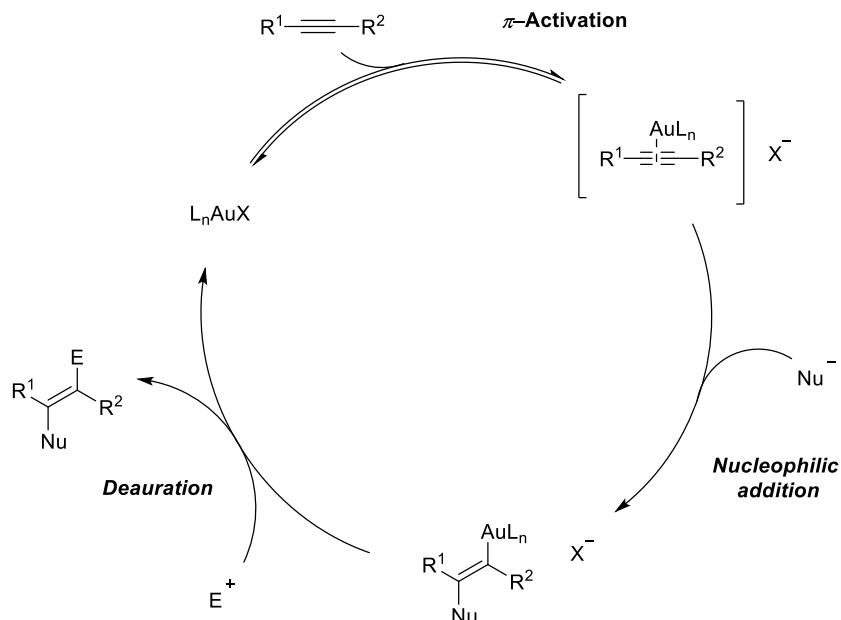


Figure GB.5: Gold complexes with *N*-heterocyclic carbenes (NHC) and phosphine type ligands.

To ensure clarity, a brief overview of the key steps in gold catalysis (as illustrated in Scheme GB.1) will be provided. The process begins with the electrophilic activation of the C-C unsaturated bond by gold, followed by a nucleophilic attack to the activated unsaturated system (generating an alkenyl-gold intermediate in the case of alkynes or an alkyl-gold intermediate for alkenes) following Markovnikov's rules, and finally, a deauration stage takes place when the reaction with an electrophile (normally a proton) occurs and the catalyst is recovered.

¹⁷ Fleming, I. *Frontier Orbitals and Organic Chemical Reactions*. **1976**, 23-32.

¹⁸ Nechaev, M. S.; Rayon, V. M.; Frenking, G. *J. Phys. Chem. A*. **2004**, *108*, 3134-3142.



Scheme GB.1: General mechanism of a gold-catalysed reaction.

- **Electronic properties**

Electron-donor ligands, such as *N*-heterocyclic carbenes (NHC) or phosphine derivatives with electron-donating groups in the aromatic ring, are considered electronically rich. These ligands present higher in energy HOMOs and can stabilize cationic complexes by donating electron density to the metal. On the other hand, electron-withdrawing ligands, such as phosphoramidites, phosphites or phosphines with acceptor substituents in the aromatic ring, remove electron density from the metal, lowering the energy of its LUMO, and facilitating its coordination to unsaturated systems.¹⁹

Taking this into account, as demonstrated by some authors like Xu and co-workers in their kinetic studies about the different stages of the mechanism in model substrates,²⁰ electron-donating ligands stabilize and facilitate the deauration process. On the other hand, electron-withdrawing ligands increase the Lewis acidity of the complex, favouring the π -activation of the unsaturated C-C bond and the subsequent nucleophilic attack.

¹⁹ Huynh, H. V. *Chem. Rev.* **2018**, *118*, 9457-9492.

²⁰ Wang, W.; Hammond, G. B.; Xu, B. *J. Am. Chem. Soc.* **2012**, *134*, 5697-5705.

- **Steric effects**

The volume of the ligand plays a significant role in gold catalysis through the non-bonding interactions between the reactant and the catalyst. These interactions can greatly impact the conformation and reactivity, ultimately determining the success of the process.

Tolman was the first one to attempt to measure the steric influence of the ligand volume using a parameter (*Tolman angle*, ϕ).²¹ This parameter is defined as the conical angle formed by taking the origin of the vertex, which would be where the metal atom is located, 2.28 \AA from the phosphorus atom (regardless of the metal centre) and is tangent to the Van der Waals radius of the atoms furthest from the substituent (Figure GB.6). When ligands are bulkier, the Tolman angle also increases. The applicability of this parameter is often limited as it can mostly be reliably measured in symmetrical phosphines, which restricts its utility.

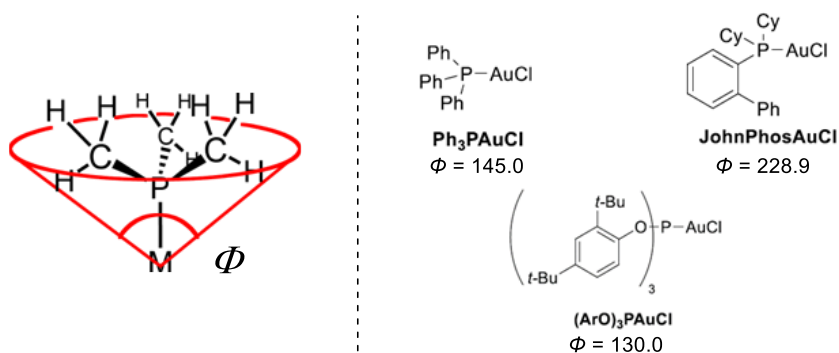


Figure GB.6: Tolman angle (ϕ) representation and values for some phosphine- and phosphite-type gold (I) chloride complexes.

Given that the Tolman angle is mostly applicable to phosphines and that NHC-type ligands have gained popularity in gold catalysis in recent years, other authors have attempted to quantify these steric effects. Nolan described the concept of *Percent buried volume* ($\%V_{bur}$), which is defined as the percentage of the total volume of a sphere occupied by the ligand bound to the metal, at an average distance of typically 2.00 \AA (Figure GB.7).²²

²¹ Tolman, C. A. *Chem. Rev.* **1977**, *77*, 313-348.

²² a) Hillier, A. C.; Sommer, W. J.; Yong, B. S.; Petersen, J. L.; Cavallo, L.; Nolan, S. P. *Organometallics* **2003**, *22*, 4322-4326; b) Clavier, H.; Nolan, S. P. *Chem. Commun.* **2010**, *46*,

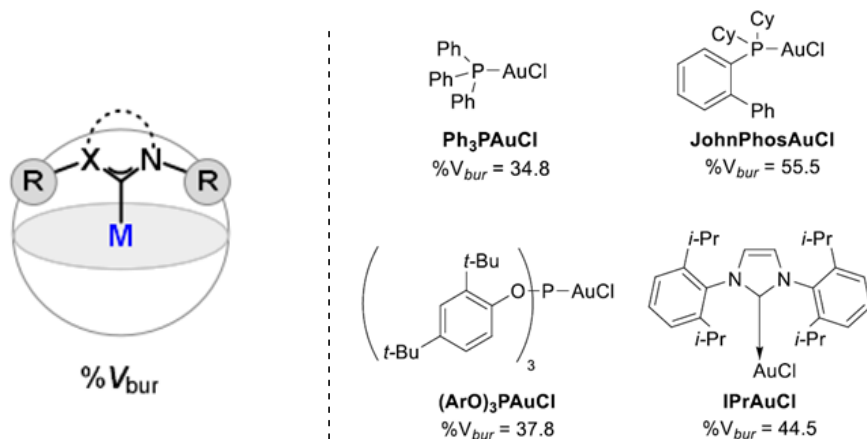


Figure GB.7: Percent buried volume ($\%V_{bur}$), representation and its values for four common gold (I) chloride complexes.

1.1.3 Counterion-depending properties.

Regarding the influence that counterions have on gold catalysis, in recent years, studies such as those by Hammond⁴ or Hashmi²³ have shed light on this area. This topic had not been extensively studied in the past, and the most common practice was to use halides as counterions due to the great stability of the complexes formed.

Initially perceived as advantageous, these highly stable complexes later presented a challenge due to the significant energy barrier required for their use in catalysis. The activation of unsaturated C-C bonds in gold (I) complexes demands a free coordination site, which complicates their application. Hence, a new generation of counterions with lower coordination abilities, such as OTs^- , Ntf_2^- , BF_4^- , or SbF_6^- , have been widely adopted.

Classifying counterions and predicting their behaviour based on their properties is challenging due to the influence of various factors, such as: stability of the complex formed, distribution of the ionic pair, and the counterion's affinity for gold or proton.

841-861; c) Gómez-Suárez, A.; Nelson, D. J.; Nolan, S. P. *Chem. Commun.* **2017**, 53, 2650-2660.

⁴ Lu, Z.; Li, T.; Mudshinge, S. R.; Xu, B.; Hammond, G. B. *Chem. Rev.* **2021**, 121, 8452-8477.

²³ Schießl, J.; Schulmeister, J.; Doppiu, A.; Wörner, E.; Rudolph, M.; Karch, R.; Hashmi S. K. *Adv. Synt. Catal.* **2018**, 360, 3949-3959.

Talking about stability of gold complex, Hammond, Xu, and co-workers have conducted fascinating studies demonstrating how using different counterions with the same ligand against a model substrate can significantly affect the reaction outcome.²⁴ Although these studies have highlighted the counterion's important role, its precise mechanism has yet to be established. Experimental observations indicate that cationic gold complexes with weakly coordinating counterions are typically unstable and may not be isolable without a stabilizing molecule, such as a nitrile.²⁵

Previous research has shown that the Au (I) catalysis mechanism involves various steps of coordination and decoordination of the gold atom, ligand, counterion, and C-C unsaturated bond. To further investigate and take advantage of these processes, recent studies have employed DFT and NMR techniques.²⁶ The coordination of an unsaturated system can result in three possible cation/anion orientations, as can be seen in the Figure GB.8. If the anion remains close to the alkene/alkyne, the reaction can occur (left). However, if the anion stays near the ligand, the reaction may slow down or even cease (right). The reason for this observation has not been extensively rationalized by the authors.

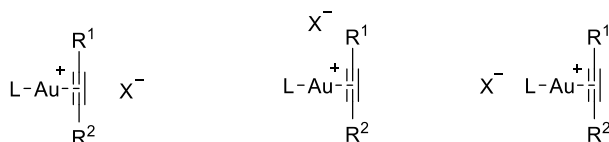


Figure GB.8: Possible orientations in gold (I)-alkyne π -complexes in solution.

The counterion's affinity for gold can hinder the reaction, as seen previously. Several studies have attempted to quantify the influence of this affinity, such as Hammond and co-workers' work, which defines a new parameter - the *Gold Affinity Index (GAI)* - utilizing dissociation energies of well-known counterions in gold catalysis.²⁷ This leads to a consistency between the theoretical values of this index and the experimental results.

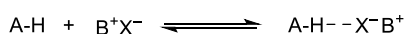
²⁴ Kumar, M.; Jasisnski, J.; Hammond, G. B.; Xu, B.; *Chem. Eur. J.* **2014**, *20*, 3113-3119.

²⁵ a) Raabe, I.; Krossing, I. *Angew. Chem. Int. Ed.* **2004**, *43*, 2066-2090; b) Mézailles, N.; Ricard, L.; Gagosz, F. *Org. Lett.* **2005**, *7*, 4133-4136.

²⁶ a) Zuccaccia, D.; Belpassi, L.; Tarantelli, F.; Macchioni, A. *J. Am. Chem. Soc.* **2009**, *131*, 3170-3171; b) Ciancaleoni, G.; Belpassi, L.; Tarantelli, F.; Zuccaccia, D.; Macchioni, A. *Dalton Trans.* **2013**, *42*, 4122-4131.

²⁷ Lu, Z.; Han, J.; Okoromoba, E. O.; Shimizu, N.; Amii, H.; Tormena, C. F.; Hammond, G. B.; Xu, B. *Org. Lett.* **2017**, *19*, 5848-5851.

Similar to how the affinity of a counterion for gold can be measured, attempts have been made to quantify its ability to capture protons in certain mechanisms. To do this, various authors have developed the *Hydrogen Bond Basicity Index*, based on the energy of hydrogen bonds.^{4,28} A comprehensive database of hydrogen-bond basicity, measured by pK_{HBX} (Scheme GB.2), has been reported after quantification. Most compounds have a pK_{HBX} in the range of 1-6, with a higher number indicating higher hydrogen-bond basicity. Generally, smaller hydrogen bonding basicity is shown by larger and more charge-delocalized anions ($I^- < Br^- < Cl^- < OAc^-$). This index has been shown to have better correlation with experimental data than pK_a .



$$K_c = [A-H \cdots X^-B^+] / [A-H][B^+X^-]$$

$$pK_{HBX} = \log K_c$$

Scheme GB.2: Definition of pK_{HBX} of a reaction.

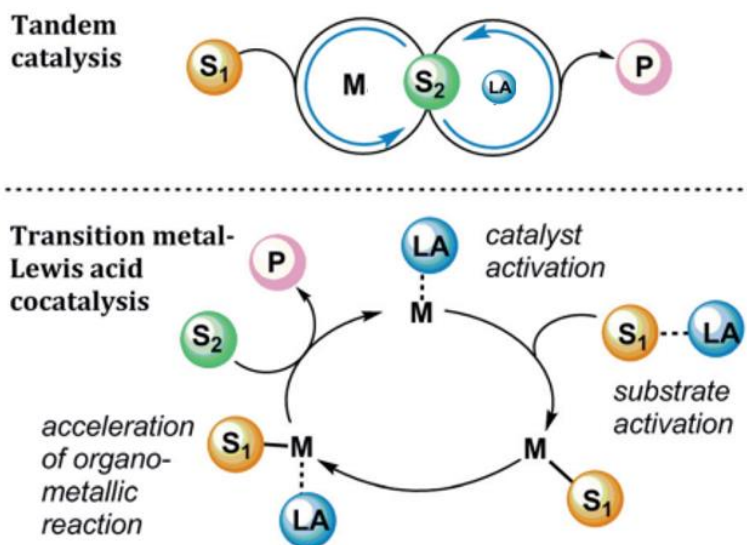
1.1.4 Additive-depending effects.

The use of various additives in transition metal catalysis has been thoroughly investigated to enhance performance and selectivity.²⁹ Typically, two primary roles have been assigned to these additives, leading to either tandem catalysis or co-catalysis. Scheme GB.3 shows that tandem catalysis occurs when the additive enters a catalytic cycle that is completely distinct from the cycle of the metallic catalyst, while in co-catalysis, both catalysts operate within the same cycle. In the first case, it is easier to accurately assign the role of the additive in the reaction, while in the second case, the additive can participate in multiple steps, making it more challenging to fully comprehend its function.

⁴ Lu, Z.; Li, T.; Mudshinge, S. R.; Xu, B.; Hammond, G. B. *Chem. Rev.* **2021**, *121*, 8452-8477.

²⁸ Laurence, C.; Brameld, K. A.; Graton, J. R. M.; Le Questel, J.-Y.; Renault, E. *J. Med. Chem.* **2009**, *52*, 4073–4086.

²⁹ a) Wang, C.; Xi, Z. *Chem. Soc. Rev.* **2007**, *36*, 1395-1406; b) Beca, J.; Döbereiner, G. E. *Org. Biomol. Chem.* **2019**, *17*, 2055-2069.



Scheme GB.3: Tandem catalysis vs cocatalysis. S1, S2 = Substrates; M =Metal complex; LA= Lewis acid; P= Products.

In the same manner, in the field of Au (I) catalysis, researchers have also explored the use of additives for similar purposes. The work conducted by Hammond and co-workers over the past few years is of utmost importance.⁴ It provides a classification of additives used in this field, which are grouped into four categories based on their function in the catalytic cycle. These categories are hydrogen bond acceptors, activators/reactivators, acid cocatalysts, and promoters.

- **Hydrogen bond acceptors**

As previously mentioned, an additive can donate a proton in the protodeauration stage of the Au (I) catalytic cycle (Scheme GB.1, p. 14). However, it could also trap the gold complex and compete with the unsaturated system during the initial π -activation step, ultimately hindering the catalytic cycle. To address these complications, studies have been conducted on model substrates in the presence or absence of various additives,³⁰ and also correlating the result with their Hydrogen

⁴ Lu, Z.; Li, T.; Mudshinge, S. R.; Xu, B.; Hammond, G. B. *Chem. Rev.* **2021**, *121*, 8452-8477.

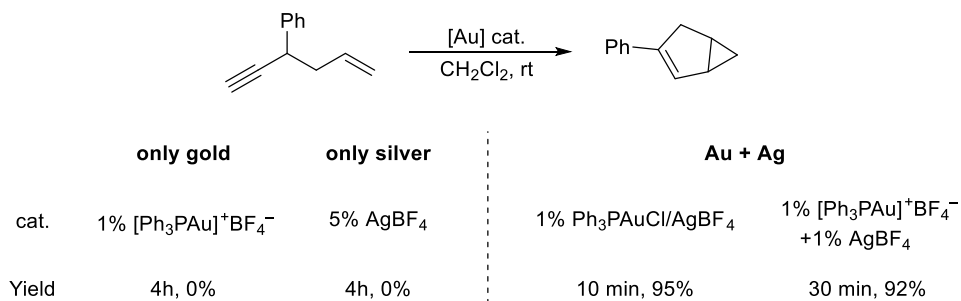
³⁰ Kumar, M.; Hammond, G. B.; Xu, B. *Org. Lett.* **2014**, *16*, 3452-3455.

²⁷ Laurence, C.; Brameld, K. A.; Graton, J. R. M.; Le Questel, J.-Y.; Renault, E. *J. Med. Chem.* **2009**, *52*, 4073-4086.

Bonding Index (pK_{HBX}).^{27,31} The conclusion reached is that additives with a high pK_{HBX} facilitate the protodeauration step, as they may act as transporters for the acidic proton in the intermediate. On the other hand, additives with low pK_{HBX} deactivate the reaction since they have a high tendency to bind to gold, thereby preventing π -activation from occurring.

- **Activators/reactivators as catalysts**

Although gold halides have been widely used in this field, they may not always be active enough as catalysts due to their high stability. Therefore, a common practice is to perform a counterion exchange using silver salts as additives. Nonetheless, recent studies have revealed that the effect of adding silver salts to the reaction may not be as straightforward as once assumed.³² Apart from counterion exchange, silver may also play different roles in the reaction, such as bimetallic catalysis, where the reaction does not occur when using just gold or silver alone (Scheme GB.4, *left*), but it does occur when both are used together (Scheme GB.4, *right*).

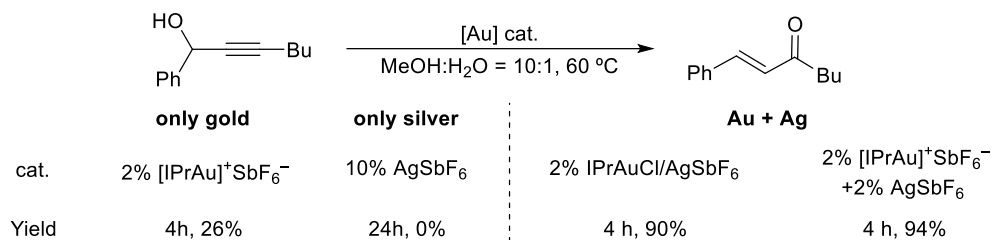


Scheme GB.4: Example of Au / Ag bimetallic catalysis.

It also may play the role of silver-assisted catalysis where the reaction takes place in the absence of silver (Scheme GB.5, *left*), producing one product with low yield, but when silver is added the yield of the reaction improves (Scheme GB.5, *right*).

³¹ a) Okoromba O. E.; Han, J.; Hammond, G. B.; Xu, B. *J. Am. Chem. Soc.* **2014**, *136*, 14381-14384; b) Han, J.; Lu, Z.; Flach, A. L.; Paton, R. S.; Hammond, G. B.; Xu, B. *Chem. Eur. J.* **2015**, *21*, 11687-11691.

³² a) Wang, D.; Cai, R.; Sharma, S.; Jirak, J.; Thummanapelli, S. K.; Akhmedov, N. G.; Zhang, H.; Liu, X.; Petersen, J. L.; Shi, X. *J. Am. Chem. Soc.* **2012**, *134*, 9012-9019; b) Homs, A.; Escofet, I.; Echavarren, A. M. *Org. Lett.* **2013**, *15*, 5782-5785; c) Zhdanko, A.; Maier, M. E. *ACS Catal.* **2015**, *5*, 5994-6004.

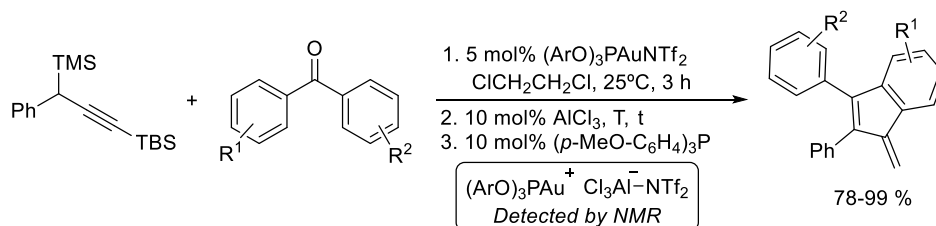


Scheme GB.5: Example of silver-assisted gold catalysis.

• Acidic cocatalysts

The catalytic activity of gold complexes can be enhanced by combining them with different Brønsted and Lewis acids, thereby improving their performance. To gain insight into these transformations, Hammond and his team conducted several studies with model reactions.³³ While a detailed mechanism for how these additives work was not provided, and their effectiveness was not consistently demonstrated, three potential roles for acidic cocatalysts were proposed. These roles include acting as a Lewis/Brønsted-acid-assisted Lewis acid catalyst, where the acidic additive can coordinate one of the gold ligands or counterions, thus increasing its electrophilicity.

Santamaría, Ballesteros and co-workers have demonstrated an exceptional example of using a Lewis acid to enhance the catalytic activity of gold. Their work showed that by utilizing AlCl₃ as a Lewis acid, the counterion's capacity to capture the LAu⁺ cation was reduced, resulting in an increased electrophilicity and improved reaction yield (Scheme GB.6).³⁴ They could also detect the real intermediate involved in the catalytic cycle, [LAu]⁺[AlCl₃]⁻, by ³¹P and ¹⁹F NMR experiments.



Scheme GB.6: Example of enhancement using a Lewis acid in gold catalysis.

³³ Barrio, P.; Kumar, M.; Lu, Z.; Han, J.; Xu, B.; Hammond, G. B. *Chem. Eur. J.* **2016**, *22*, 16410-16414.

³⁴ Fernández, S.; Santamaría, J.; Ballesteros, A. *Adv. Synth. Catal.* **2022**, *364*, 1286-1294.

The cocatalyst could also aid in the regeneration of catalytically active species, preventing the formation of non-reactive gold acetylides from terminal alkynes. Additionally, the cocatalyst may slow down decay processes by influencing the decomposition of the gold catalyst.

- **Promoters**

Hammond and co-workers recognized that certain gold complexes can be highly unstable yet reactive due to their electrophilic nature.³⁵ In an effort to improve several reactions, they explored the use of CTf_3^- as a counterion in gold catalysts, which is prepared by combining the gold catalyst with KCTf_3 (they called it promoter, because does not interact with other acidic or basic species in the reaction). This novel approach has the potential to enhance the performance of gold catalysts and improve their efficiency in certain reactions.

In summary, considering the complexity of transformations catalysed by gold complexes, the rational design of ligands remains a challenging task. Currently, the process of selecting the most suitable ligand to carry out a catalytic process is still a trial-and-error methodology of the ligand to be used rather than a rational design based on theoretical foundations, although all these studies have also contributed to bringing us closer to achieving it.

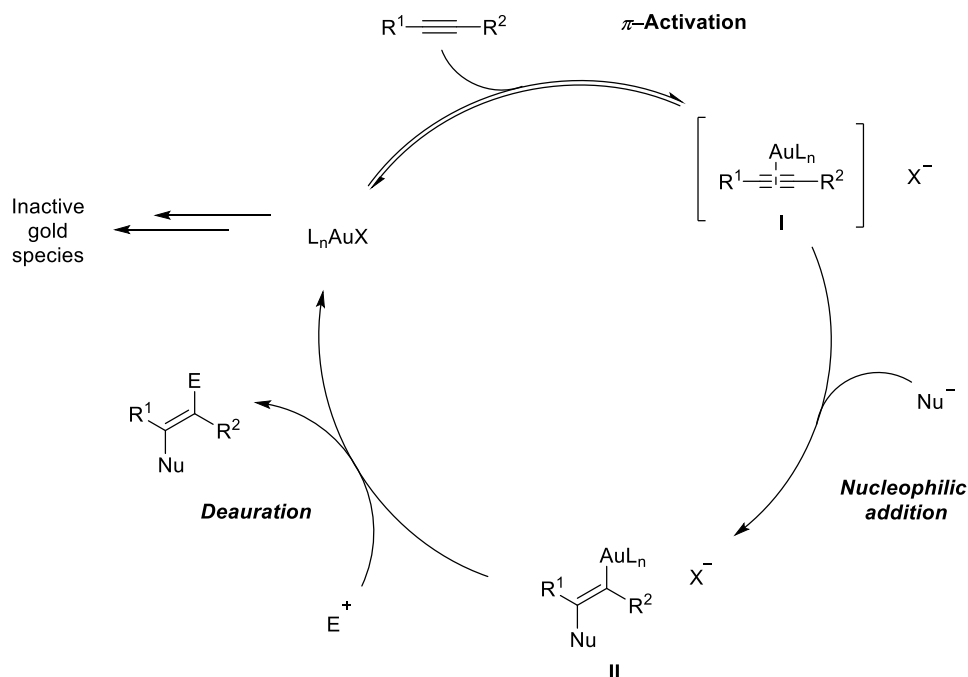
1.2 Gold-catalysed transformations involving carbon-carbon multiple bonds.

Carbophilic activation, which involves the activation of multiple carbon-carbon bonds, is an area where gold complexes have been shown to play a significant role. As the present dissertation focuses on this type of activation, an overview of some of the general aspects of these transformations will be provided.

In this carbophilic activation, the general mechanism for an alkyne (Scheme GB.7) starts with the π -coordination of the catalyst to the unsaturated C-C bond. This reduces the electron density of the π -cloud, giving it an electrophilic character

³⁵ Han, J.; Lu, Z.; Wang, W.; Hammond, G. B.; Xu, B. *Chem. Commun.* **2015**, *51*, 13740-13743.

(Intermediate I). Next, a nucleophile can attack this intermediate following Markovnikov's rules (Intermediate II). Finally, the reaction takes place with an electrophile, mainly a proton in a protodeauration process, and the catalyst is recovered. However, the gold catalyst may be susceptible to poisoning processes that can produce inactive gold species.



Scheme GB.7: Mechanism of a model gold-catalysed reaction initiated by alkyne activation.

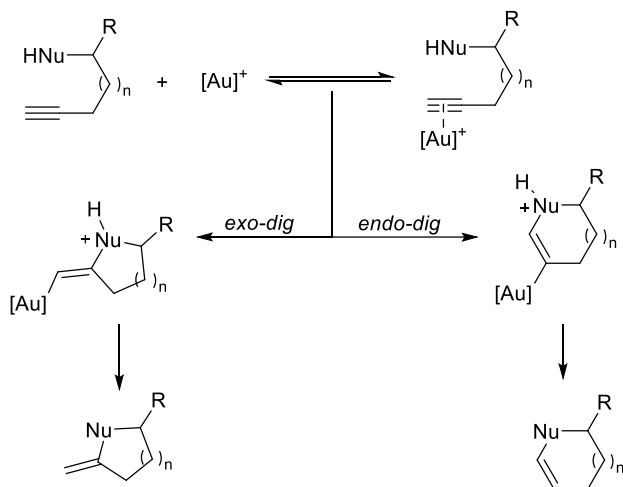
When this process occurs intramolecularly, it provides a highly versatile route for forming carbocycles and heterocycles - compounds of significant interest to both organic and medicinal chemistry.

Typically, the regiochemistry of intramolecular reactions on metal-unsaturated system complexes follows the Baldwin rules,³⁶ which categorize cyclizations based on three criteria:

- The size of the newly formed cycle, determined by the number of bonds it contains.

³⁶ Baldwin, J.E. *J. Chem. Soc., Chem. Commun.* **1976**, 734-736.

- Whether the bond broken during the process is found outside the new cycle in the final product (*exo*) or within the cycle (*endo*).
- The electrophilic center's geometry, which can be tetragonal (*tet*), trigonal (*tri*), or digonal (*dig*).



Scheme GB.8: Different ways in which nucleophiles can intramolecularly react with C-C triple bonds.

While it may appear that this provides a lot of possibilities for cyclizing, it is important to note that some are more advantageous than others.

	3		4		5		6		7	
Type	<i>exo</i>	<i>endo</i>	<i>exo</i>	<i>endo</i>	<i>exo</i>	<i>endo</i>	<i>exo</i>	<i>endo</i>	<i>exo</i>	<i>endo</i>
<i>tet</i>	✓		✓		✓	✗	✓	✗	✓	
<i>trig</i>	✓	✗	✓	✗	✓	✗	✓	✓	✓	✓
<i>dig</i>	✗	✓	✗	✓	✓	✓	✓	✓	✓	✓

Table GB.1: Un-/favoured ring closures following Baldwin's rules.

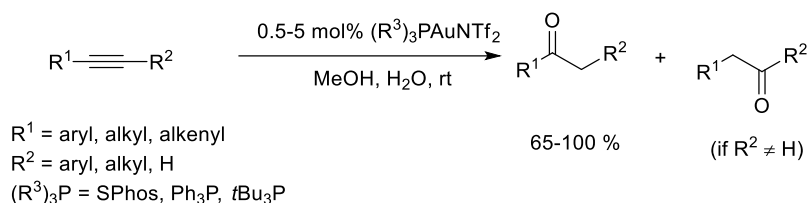
The diversity of reported gold-catalysed transformations presents a challenge for compiling and classifying them. In light of this and given its relevance to the theme of this memory, I have chosen to narrow my focus to transformations that involve alkyne activation followed by nucleophilic attack. Although there are other relevant

transformations such as gold redox catalysis, activation of diazo-compounds or photochemistry with gold, these topics will not be discussed in this dissertation.³⁷

This section of the thesis will showcase a number of significant examples of intramolecular and intermolecular nucleophilic additions to alkynes, which have been discovered in recent years. These examples will demonstrate the versatility and applicability of this synthetic approach in modern organic chemistry.

1.2.1 Addition of O-nucleophiles to alkynes.

In the context of industrial applications, the hydration of alkynes is a highly significant reaction. While processes using Hg (II) salts have been developed in the past, recent years have witnessed the emergence of less toxic alternatives that utilize Au (I) salts and very low catalyst loadings. Scheme GB.9 illustrates an example of this reaction, which can be achieved with minimal amounts of catalyst. These novel processes hold immense promise for sustainable and environmentally conscious industrial chemistry.³⁸

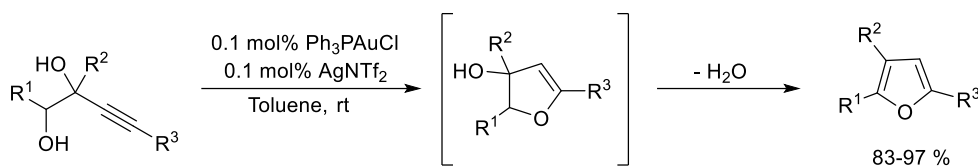


Scheme GB.9: Hydration of alkyne catalysed by gold (I) salts.

³⁷ For recent reviews see: a) Miege, F.; Meyer, C.; Cossy, J. *Beilstein J. Org. Chem.* **2011**, *7*, 717-734; b) Rudolph, M.; Hashmi, S. K. *Chem. Soc. Rev.* **2012**, *41*, 2448-2462; c) Wei, F.; Song, C.; Ma, Y.; Zhou, L.; Tung, C.-H.; Xu, Z. *Sci. Bull.* **2015**, *60*, 1479-1492; d) Ma, B.; Liu, L.; Zhang, J. *Asian J. Org. Chem.* **2018**, *7*, 2015-2025; e) Vicente, R. *Chem. Rev.* **2021**, *121*, 162-226; f) Witzel, S.; Hashmi, S. K.; Xie, J. *Chem. Rev.* **2021**, *121*, 8868-8925; g) Zheng, Z.; Ma, X.; Cheng, X.; Zhao, K.; Gutman, K.; Li, T.; Zhang, L. *Chem. Rev.* **2021**, *121*, 8979-9038; h) Hendrich, C. M.; Sekine, K.; Koshikawa, T.; Tanaka, K.; Hashmi, S. K. *Chem. Rev.* **2021**, *121*, 9113-9163.

³⁸ Teles, J. H.; Brode, S.; Chabanas, M. *Angew. Chem. Int. Ed.* **1998**, *37*, 1415-1418; b) Mizushima, E.; Sato, K.; Hayashi, T.; Tanaka, M. *Angew. Chem. Int. Ed.* **2002**, *41*, 4563-4565; c) Marion, N.; Ramón, R. S.; Nolan, S. P. *J. Am. Chem. Soc.* **2009**, *131*, 448-449; d) Leyva, A.; Corma, A. *J. Org. Chem.* **2009**, *74*, 2067-2074; e) Rzhnevskiy, S. A.; Philippova, A. N.; Chesnokov, G. A.; Agheshina, A. A.; Minaeva, L. I.; Topchiy, M. A.; Nechaev, M. S.; Asachenko, A. F. *Chem. Commun.* **2021**, *57*, 5686-5689; f) Hobsteter, A. W.; Badajoz, M. A.; Lo Fiego, M. J.; Silbestri, F. *ACS Omega* **2022**, *7*, 21788-21799.

Another noteworthy example of the employment of *O*-nucleophiles involves the intramolecular gold-catalysed formation of furans, outlined in Scheme GB.10.³⁹



Scheme GB.10: Intramolecular reaction catalysed by gold to obtain furanes.

In addition, carboxylic acids, carbonates, carbamates, and other carbonyl compounds can function as nucleophiles, reacting with gold-activated triple bonds to form diverse heterocyclic compounds with one or more heteroatoms.⁴⁰

1.2.2 Addition of *N*-nucleophiles to alkynes.

Gold-catalysed hydroamination processes have also shown promising developments, similar to those observed in other catalytic reactions. Utimoto first described this type of reaction,⁴¹ and since then, several studies have highlighted the efficiency of this method.⁴² For instance, the example shown in Scheme GB.11 involves a sequential hydroamination catalysed by gold (I) and enantioselective

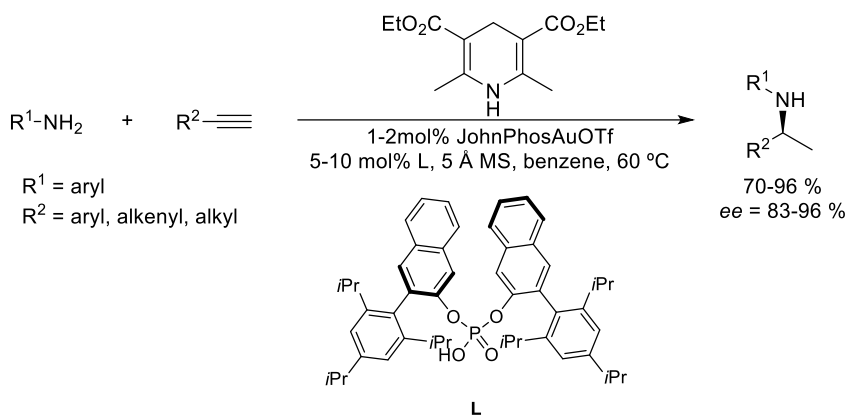
³⁹ a) Aponick, A.; Li, C. -Y.; Malinge, J.; Marques, E. F. *Org. Lett.* **2009**, *11*, 4624-4627; b) Egi, M.; Yamaguchi, Y.; Fujiwara, N.; Akai, S. *Org. Lett.* **2009**, *11*, 5002-5005; c) Iqbal, A.; Sahraoui, E.-H.; Leeper, F. J. *Beilstein J. Org. Chem.* **2014**, *10*, 2580-2585; d) Cheng, X.; Wang, Z.; Quintanilla, C. D.; Zhang, L. *J. Am. Chem. Soc.* **2019**, *141*, 3787-3791.

⁴⁰ a) Hashmi, S. K.; Sinha, P. *Adv. Synth. Catal.* **2004**, *346*, 432-438; b) Yao, T.; Zhang, X.; Larock, R. C. *J. Am. Chem. Soc.* **2004**, *126*, 11164-11165; c) Genin, E.; Toullec, P. Y.; Antoniotti, S.; Brancour, C.; Genêt, J.-P.; Michelet, V. *J. Am. Chem. Soc.* **2006**, *128*, 3112-3113; d) Enomoto, T.; Girard, A. -L.; Yasui, Y.; Takemoto, Y. *J. Org. Chem.* **2009**, *74*, 9158-9164; e) Buzas, A.; Istrate, F.; Le Goff, X. F.; Odabachian, Y.; Gagosz, F. *J. Organomet. Chem.* **2009**, *694*, 515-519; f) Luo, T.; Dai, M.; Zheng, S.-L.; Schreiber, S. L. *Org. Lett.* **2011**, *13*, 2834-2836; g) Chen, Y.; Chen, M.; Liu, Y. *Angew. Chem. Int. Ed.* **2012**, *51*, 6493-6497; h) Han, X.; Retailleau, P.; Gandon, V.; Voituriez, A. *Chem. Commun.* **2020**, *56*, 9457-9460; i) Suárez-Rodríguez, T.; Suárez-Sobrino, Á. L.; Ballesteros, A. *Chem. Eur. J.* **2021**, *27*, 13079-13084; j) Rawat, V. K.; Higashida, K.; Sawamura, M. *ACS Catalysis* **2022**, *12*, 8325-8330.

⁴¹ a) Fukuda Y.; Utimoto K.; Nozaki, H. *Heterocycles* **1987**, *25*, 297-300; b) Fukuda, Y.; Utimoto, K. *Synthesis* **1991**, *11*, 975-978.

⁴² a) Liu, X.-Y.; Che, C.-M. *Org. Lett.* **2009**, *11*, 4204-4207; b) Fustero, S.; Ibáñez, I.; Barrio, P.; Maestro, M. A.; Catalán, S. *Org. Lett.* **2013**, *15*, 832-835; c) Soklou, K. E.; Marzag, H.; Bouillon, J.-P.; Marchivie, M.; Routier, S.; Plé, K. *Org. Lett.* **2020**, *22*, 5973-5977.

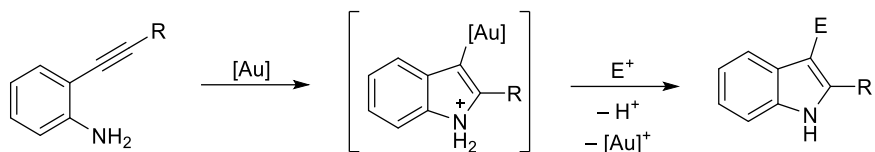
transfer hydrogenation using a chiral phosphoric acid, demonstrating the versatility and usefulness of this approach.



Scheme GB.11: Hydroamination and transfer hydrogenation of alkynes catalysed by gold (I).

Given the special importance of indoles in the field of heterocycles, numerous hydroamination reactions have been investigated in recent years for the synthesis of these *N*-heterocycles. Specifically, gold has been used as catalyst in some of these transformations. Within hydroamination reactions of alkynes, cascade processes have also been developed in which 2-alkynylanilines react intramolecularly to form the intermediate with the indole skeleton (Scheme GB.12). Subsequent reaction with electrophiles present in the medium leads to the formation of 2,3-disubstituted indoles. It is noteworthy that in these cascade reactions, the gold catalyst promotes two processes of different nature: carbophilic activation and electrophile activation.⁴³

⁴³ a) Arcadi, A.; Bianchi, G.; Marinelli, F. *Synthesis* **2004**, 610-618. b) Alfonsi, M.; Arcadi, A.; Aschi, M.; Bianchi, G.; Marinelli, F. *J. Org. Chem.* **2005**, *70*, 2265-2273. c) Zhang, Y.; Donahue, J. P.; Li, C.-J. *Org. Lett.* **2007**, *9*, 627-630. d) Brand, J. P.; Chevalley, C.; Waser, J. *Beilstein J. Org. Chem.* **2011**, *7*, 565-569; e) Simm, P. E.; Sekar, P.; Richardson, J.; Davies, P. W. *ACS Catalysis* **2021**, *11*, 6357-6362.



Scheme GB.12: Cascade reaction for the obtention of indoles using gold catalyst.

Besides amines, a range of nitrogen-containing compounds, including imines, azides, carbamates, and amides, have also been used as nucleophiles in gold-catalysed C–N bond formation reactions. These alternative nucleophiles have facilitated the development of new synthetic routes for the obtention of nitrogen-containing heterocycles, demonstrating the versatility and potential of gold catalysis in organic synthesis.⁴⁴

1.2.3 Addition of C-nucleophiles.

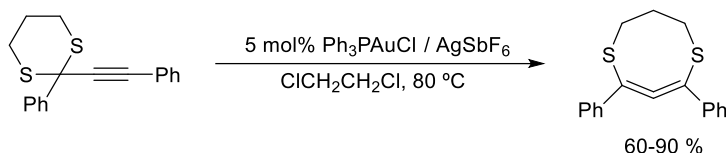
The formation of C–C bonds is arguably the most powerful tool in organic synthesis. Gold has demonstrated remarkable catalytic abilities in promoting diverse processes for constructing these bonds when the nucleophile involved is a carbon atom.

In regard to intramolecular reactions, the field of 1-5 or 1,6-enyne cycloisomerization has received extensive attention, with Echavarren and his group contributing significantly to its study. Furthermore, intermolecular cyclizations have also been the subject of extensive research. Given the close relationship of these reactions with *Chapters 2* and *3* of the thesis, a comprehensive exploration of these topics will be provided in those respective chapters.

⁴⁴ a) Gorin, D. J.; Davis, N. R.; Toste, F. D. *J. Am. Chem. Soc.* **2005**, *127*, 11260-11261; b) Kusama, H.; Miyashita, Y.; Takaya, J.; Iwasawa, N. *Org. Lett.* **2006**, *8*, 289-292; c) Ritter, S.; Horino, Y.; Lex, J.; Schmalz, H.-G. *Synlett* **2006**, *19*, 3309-3313; d) Istrate, F. M.; Gagosz, F. *Org. Lett.* **2007**, *9*, 3181-3184; e) Nakamura, I.; Okamoto, M.; Terada, M. *Org. Lett.* **2010**, *12*, 2453-2455; f) Benedetti, E.; Lemièrre, G.; Chapellet, L.-L.; Penoni, A.; Palmisano, G.; Malacria, M.; Goddard, J.-P.; Fensterbank, L. *Org. Lett.* **2010**, *12*, 4396-4399; g) Ye, S. Y.; Yu, Z.-X. *Org. Lett.* **2010**, *12*, 804-807; h) Davies, P. W.; Martin, N. J. *J. Organomet. Chem.* **2011**, *696*, 159-164; i) Basceken, S.; Kaya, S.; Balci, M. *J. Org. Chem.* **2015**, *80*, 12552-12561; j) Han, X.; Gaignard-Gaillard, Q.; Retailleau, P.; Gandon, V.; Vouturiez, A. *Chem. Commun.* **2022**, *58*, 3043-3046; k) Liu, C.; Bolognani, A.; Song, L.; Van Meervelt, L.; Peshkov, V. A.; Van der Eycken, E. V. *Org. Lett.* **2022**, *24*, 8536-8541.

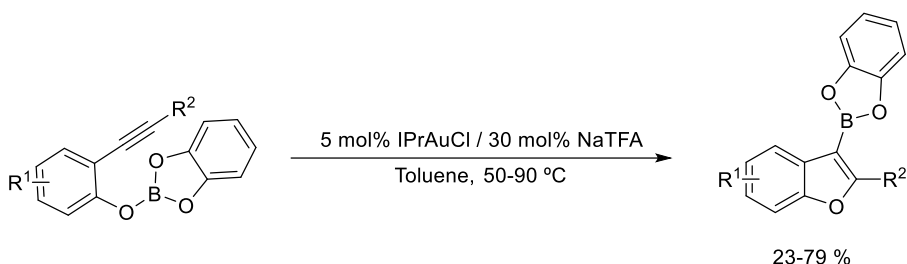
1.2.4 Addition of other nucleophiles to alkynes.

In recent years, in addition to oxygen-, nitrogen-, and carbon-derived nucleophiles, researchers have developed new reactions using a variety of nucleophiles to create highly complex and interesting compounds. One such example is the use of sulphur as a nucleophile to synthesize 8-membered cyclic dithioallenes, shown in Scheme GB.13.⁴⁵



Scheme GB.13: Example of intramolecular reaction with sulphur as nucleophile.

The gold (I) catalysed alkoxyboration of alkynes offers a similar transformation that can be utilized to produce *O*-heterocyclic boronic acid derivatives, as outlined in Scheme GB.14 for 3-benzofurane boronic esters.⁴⁶



Scheme GB.14: Intramolecular reaction to obtain *O*-heterocyclic boronic acid derivatives.

Such advancements not only provide valuable insights into the fundamental principles of organic chemistry, but also accelerate the way for the development of novel synthetic methodologies with broad applications in various fields of science and technology.

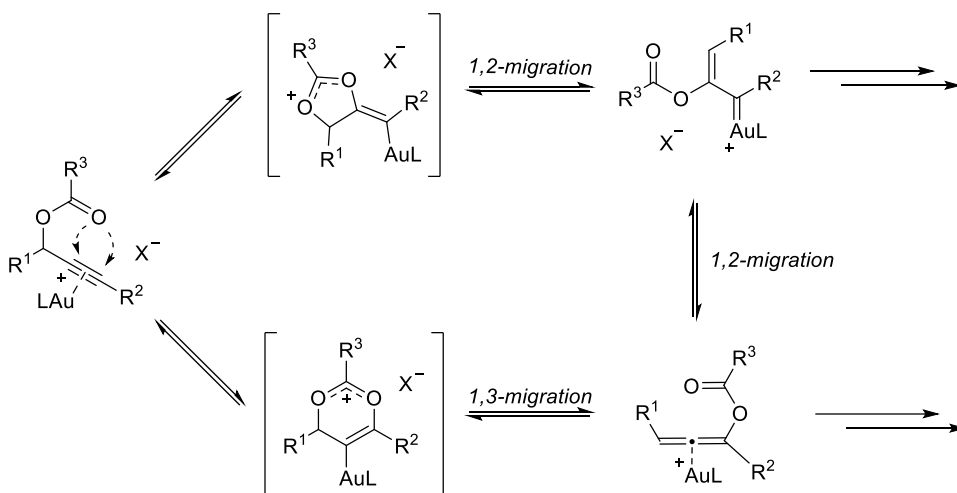
⁴⁵ Zhao, X.; Zhong, Z.; Peng, L.; Zhang, W.; Wang, J. *Chem. Commun.* **2009**, 2535-2537.

⁴⁶ Himer, J. J.; Faizi, D. J.; Blum, S. A. *J. Am. Chem. Soc.* **2014**, *136*, 4740-4745.

1.2.5 Propargyl carboxylate migrations.

While propargyl carboxylate migration may not be the central theme of this dissertation, its significance in the realm of gold catalysis cannot be underestimated, as it provides a flexible pathway to a myriad of captivating subsequent reactions, resulting in diverse functional structures. Therefore, a brief summary will be shown to highlight its significance in this area of study.

Carboxylates derived from propargylic alcohols or propargylamines are considered privileged structures due to their accessibility and high synthetic potential.⁴⁷ Upon activation by gold carbophilic species, these substrates can undergo two distinct pathways: [1,2] or [1,3]-carboxy migration (Scheme GB.15). The first pathway involves a *5-exo-dig* reaction, yielding a gold carbene intermediate. The second pathway proceeds through a *6-endo-dig* cyclization to form a carboxyallene π -complex, which can subsequently undergo a new [1,2]-migration leading also to the same carbene intermediate.



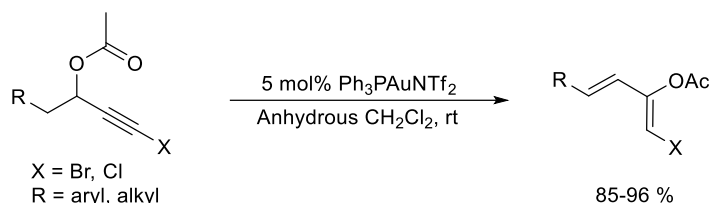
Scheme GB.15: General pathways in the isomerization of propargylic carboxylates.

The steric and electronic factors of the alkyne's carbon atom dictate which intermediate is more favourable. Large substituents and electronically-rich aryl rings

⁴⁷ For selected examples see: a) Marion, N.; Nolan, S. P. *Angew. Chem. Int. Ed.* **2007**, *46*, 2750-2752; b) Shu, X.-Z.; Shu, D.; Scienebeck, C. M.; Tang, W. *Chem. Soc. Rev.* **2012**, *41*, 7698-7711; c) Tejedor, D.; Méndez-Abt, G.; Cotos, L.; Garcia-Tellado, F. *Chem. Soc. Rev.* **2013**, *42*, 458-471; d) Kumar, R. K.; Bi, X. *Chem. Commun.* **2016**, *52*, 853-868.

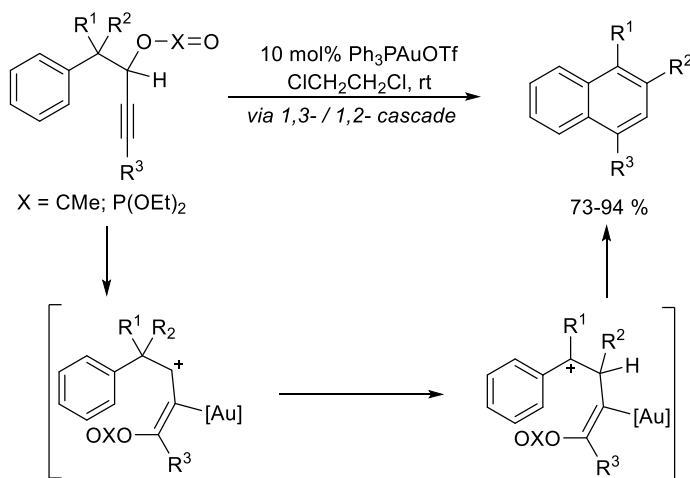
tend to stabilize the positive charge on the C_β , thus favouring [1,3]-migration. Conversely, hydrogen or electron-withdrawing groups tend to promote [1,2]-migration.⁴⁸

An example of [1,2]-migration can be demonstrated through the synthesis of 1-halo-2-carboxy-1,3-dienes using propargylic carboxylates (Scheme GB.16). This process involves a gold (I) catalysed 1,2-ester migration in CH_2Cl_2 .⁴⁹



Scheme GB.16: 1,2-Migration of halo-substituted propargyl carboxylates.

In the synthesis of substituted naphthalenes from propargylic esters catalysed by gold (I), a [1,3]-migration of the acyloxy group is followed by a [1,2]-migration of the alkyl or aryl group and concludes with hydroarylation (Scheme GB.17). This example proves the occurrence of a [1,3]-migration reaction, resulting in the desired product.⁵⁰



Scheme GB.17: Example of [1,3]-migration to obtain naphthalene derivatives.

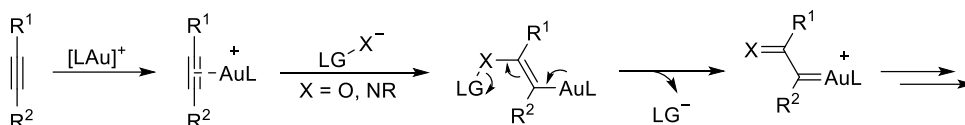
⁴⁸ Soriano, E.; Marco-Contelles, J. *Chem. Eur. J.* **2008**, *14*, 6771-6779.

⁴⁹ Marco-Contelles, J.; Soriano, E. *Chem. Eur. J.* **2008**, *13*, 1350-1357.

⁵⁰ Dudnik, A. S.; Schwier, T.; Gevorgyan, V. *Org. Lett.* **2008**, *10*, 1465-1468.

1.2.6 Formation of α -oxo and α -imino gold carbene complexes.

In recent years, there has been a significant research effort devoted to the search for gold-catalysed carbene intermediates. To address the safety concerns associated with the classic diazo-intermediate method, researchers have been exploring alternative approaches that involve using a heteronucleophile with a leaving group to attack the gold-activated alkyne. This results in the formation of a carbene intermediate through retrodonation, leading to a C-heteroatom bond at the alpha position (Scheme GB.18). Depending on the choice of nucleophile, either an α -oxo carbene or an α -imino carbene can be generated, when an *O*-nucleophile or *N*-nucleophile is used, respectively.⁵¹

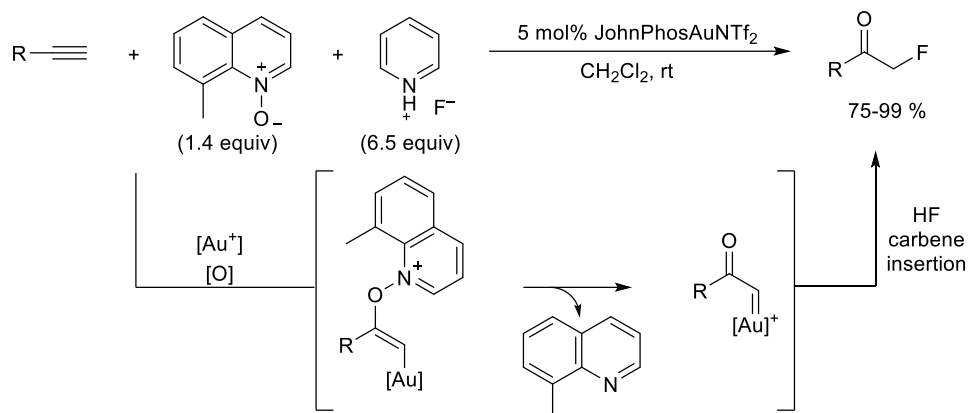


Scheme GB.18: Generation of α -oxo and α -imino gold (I) carbenes.

There are multiple methods for producing α -oxo carbenes, but one of the most frequently used approaches is through the use of *N*-oxide derivatives to generate this intermediate, which can then be trapped. For instance, Xu and co-workers have developed an effective oxofluorination reaction of terminal alkynes, which involves the insertion of the gold carbene intermediate into the H-F bond (Scheme GB.19).⁵²

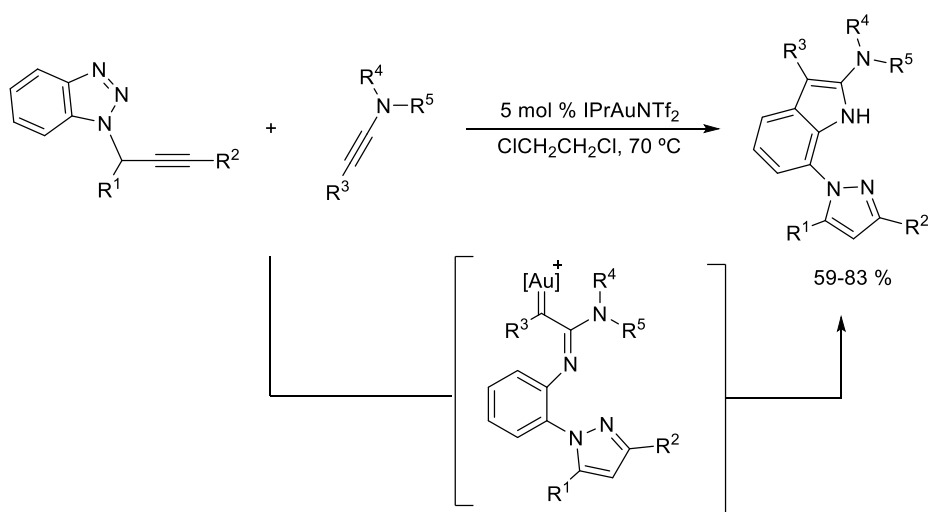
⁵¹ For selected reviews see: a) Zhang, L. *Acc. Chem. Res.* **2014**, *47*, 877-888; b) Aguilar, E.; Santamaría, J. *Org. Chem. Front.* **2019**, *6*, 1513-1540; c) Bhunia, S.; Ghosh, P.; Patra, S. R. *Adv. Synth. Catal.* **2020**, *362*, 3664-3708; d) Zhao, X.; Rudolph, M.; Asiri, A. M.; Hashmi, A. S. *Front. Chem. Sci. Eng.* **2020**, *14*, 317-349.

⁵² Zeng, X.; Liu, S.; Shi, Z.; Liu, G.; Xu, B. *Angew. Chem. Int. Ed.* **2016**, *55*, 10032-10036.



Scheme GB.19: Synthesis of α -fluoroketone through an α -oxo carbene as intermediate.

On the other hand, Santamaría, Ballesteros and co-workers have conducted impressive research on α -imino carbenes, exemplified by their use of benzotriazole precursors and ynamides as reagents for synthesizing indoles (Scheme GB.20). Their approach involves an α -imino gold carbene intermediate, followed by intramolecular C-H insertion, to obtain a great variety of indole derivatives in good to very good yields.⁵³



Scheme GB.20: Synthesis of indoles through an α -imino gold carbene.

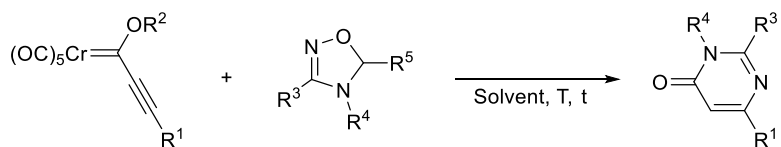
⁵³ Allegue, D.; González, J.; Fernández, S.; Santamaría, J.; Ballesteros, A. *Adv. Synth. Catal.* **2019**, *361*, 758-768.

Chapter I:

Chemo- and regioselective synthesis of pyrimidin-4(3H)-ones by formal [3+3]-cycloaddition between 4,5-dihydro-1,2,4-oxadiazoles and chromium alkoxy alkynyl Fischer carbene complexes.

1 Introduction.

In this chapter a synthesis of pyrimidin-4(3*H*)-ones, via a formal [3+3]-cycloaddition between chromium alkynyl carbene complexes with 4,5-dihydro-1,2,4-oxadiazoles, is presented (Scheme 1.1). The reaction's optimal conditions and its scope have been explored, as well.

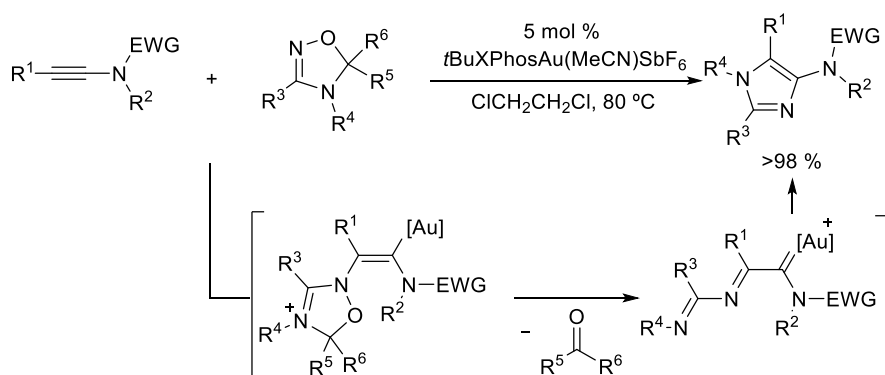


Scheme 1.1: Formal [3+3]-cycloaddition to obtain pyrimidin-4(3*H*)-ones.

In addition, several NMR studies have been conducted to enhance the understanding of the mechanism underlying this transformation.

2 Bibliographic background.

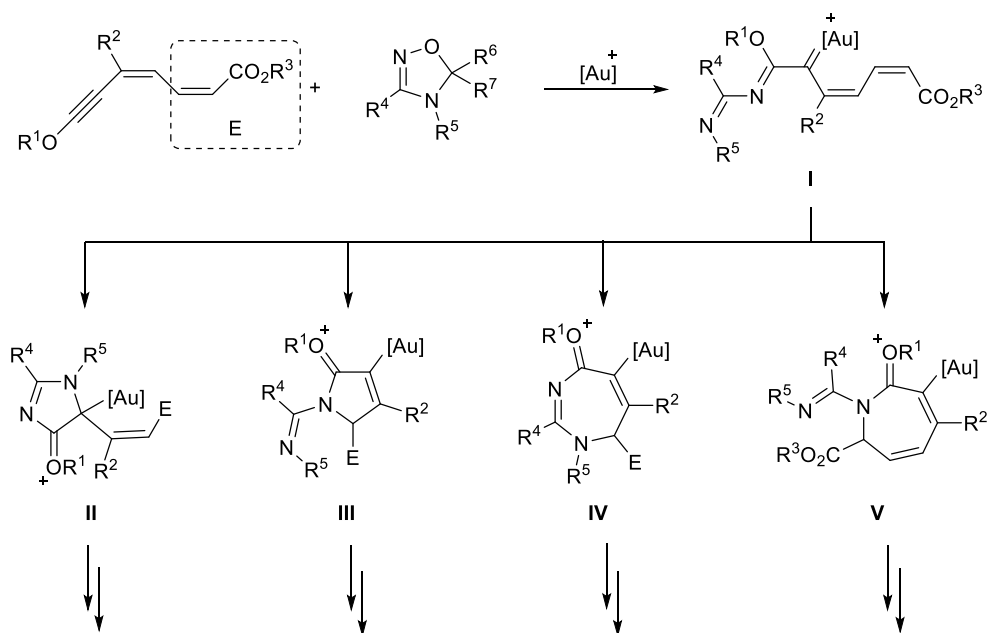
In 2017, Liu and co-workers reported a novel gold-catalysed reaction between ynamides and 4,5-dihydro-1,2,4-oxadiazoles,¹ which resulted in the formation of 4-aminoimidazoles via a [3+2]-cycloaddition. In this transformation the authors proposed that, after an initial nucleophilic attack of the oxadiazole derivative to the activated ynamide, a fragmentation of this 5-membered ring would generate an α -imino gold carbene while releasing a carbonyl compound (Scheme 1.2). Further cyclization of the gold carbene complex would generate the final product in a regioselective fashion.



Scheme 1.2: Gold-catalysed synthesis of 4-aminoimidazoles.

¹ Xu, W.; Wang, G.; Sun, N.; Liu, Y. *Org. Lett.* **2017**, *19*, 3307-3310.

Based on this innovative work, it was aimed to investigate the potential of 2,4-dien-6-ynecarboxylic esters as activated alkyne analogues of the ynamides in a similar reaction with 4,5-dihydro-1,2,4-oxadiazoles. The group's previous experience working with 2,4-dien-6-ynecarboxylic esters has provided valuable insights into their unique "push-pull" behaviour,² which arises from the presence of an activated alkyne attached to two double bonds and an electron-withdrawing group on the terminal bond. This, combined with the potential of 4,5-dihydro-1,2,4-oxadiazoles as promising three-atom synthons, makes the current reaction particularly intriguing from a synthetic chemistry perspective. The formation of an α -imino gold carbene presents several opportunities for vinylogous attack, as illustrated in Scheme 1.3, leading to multiple possible products.

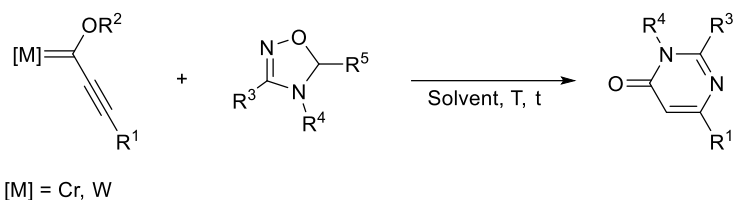


Scheme 1.3: Envisioned mechanistic pathways for this transformation.

Unfortunately, the attempts to obtain a defined major product from this reaction were unsuccessful, probably due to the existence of many different reactive positions, resulting in complex mixtures instead.

² a) Barluenga, J.; Fernandez-Rodriguez, M. A.; García-García, P.; Aguilar, E. *J. Am. Chem. Soc.* **2008**, *130*, 2764-2765; b) García-García, P.; Fernandez-Rodriguez, M. A.; Aguilar, E. *Angew. Chem. Int. Ed.* **2009**, *48*, 5534-5537; c) Fernández-García, J. M.; Fernandez-Rodriguez, M. A.; Aguilar, E. *Org. Lett.* **2011**, *13*, 5172-5175.

However, given our group's past experience with group 6 metal alkynyl carbene complexes,³ which seemed also potential reagents for a reaction with 4,5-dihydro-1,2,4-oxadiazoles, it was decided to investigate this alternative transformation, which led to pyrimidin-4(3*H*)-one derivatives (Scheme 1.4).



Scheme 1.4: Obtention of pyrimidin-4(3*H*)-ones via [3+3]-cycloaddition of Fischer-alkynyl carbene complexes and 4,5-dihydro-1,2,4-oxadiazoles.

After successfully synthesizing a pyrimidin-4(3*H*)-one via a [3+3] formal cyclization with good yield, it was aimed to extend the scope of this reaction and investigate its mechanism.

Because the reaction to be studied in this chapter involves Fischer alkynyl carbene complexes and 4,5-dihydro-1,2,4-oxadiazoles as starting materials, a brief overview of the properties, synthesis, and general reactivity of both compound families will be presented.

2.1 General reactivity of group 6 metal alkynyl carbene complexes.

A carbene is a highly reactive intermediate in organic chemistry. It contains a neutral carbon atom with two valences and two unshared valence electrons (Figure 1.1). Its general formula is $R-(C:)-R'$ or $R=C:$, where R represents substituents or hydrogen atoms.



Figure 1.1: Formal representation of a carbene.

³ Barluenga, J.; Aguilar, E. *Adv. Organomet. Chem.* **2017**, *67*, 1-150.

Despite their significant instability, some of them are stable at room temperature and have been synthesized, isolated, and used as reagents or catalysts in many chemical reactions.⁴ A stable carbene, also referred to as a persistent carbene, is the one that exhibits exceptional stability. The most well-known and predominant subgroup of stable carbenes are *N*-heterocyclic carbenes (NHC), also known as Arduengo carbenes.⁵ One of the most common ways known to stabilize carbenes is their complexation with a metal, playing an important role the oxidation state of the metal, the ligands attached to it and the substituents on the carbene carbon.

In this manner, metal-carbene complexes are formed and can be mainly divided into two types:

- Schrock-type carbenes

They feature a group 4 or 5 metal with a high oxidation state, π -donor ligands, and carbonated substituents. This combination makes the carbene carbon highly nucleophilic.

- Fischer-type carbenes

Fischer's carbenes feature a group 6, 7, or 8 metal in a low oxidation state, with metal ligands that are π -acceptors, typically carbonyls, and π -donor substituents, such as alkoxy- or dialkylamine groups, to stabilize the carbene complex. This combination makes the carbene carbon highly electrophilic.

$\begin{array}{c} \text{Cp} \quad \text{H} \\ \quad / \\ \text{Cl}-\text{Ta}=\text{C} \\ \quad \backslash \\ \text{Cl} \quad \text{tBu} \end{array}$	$\begin{array}{c} \text{R} \\ \\ (\text{OC})_5\text{W}=\text{C} \\ \\ \text{R}' \end{array}$	$\begin{array}{c} \text{OMe} \\ \\ (\text{OC})_5\text{Cr}=\text{C} \\ \\ \text{R} \end{array}$
Schrock-type carbene	Non-stabilized Fischer-type carbene	Stabilized Fischer-type carbene
Group 4 or 5 metal with high oxidation state	Group 6, 7 or 8 metal with low oxidation state	Group 6, 7 or 8 metal with low oxidation state
π -Donor ligands	π -Acceptor ligands	π -Acceptor ligands
Carbonated substituents	Carbonated substituents	Carbonated and π -donor substituents
Carbene carbon nucleophilic	Carbene carbon electrophilic	Carbene carbon electrophilic

Scheme 1.5: Comparison between Schrock-type carbene and non-/stabilized Fischer-type carbenes.

⁴ a) Bourissou, D.; Guerret, O.; Gabbai, F. P.; Bertrand, G. *Chem. Rev.* **2000**, *100*, 39-92; b) Frémont, P.; Marion, N.; Nolan, S. P. *Coord. Chem. Rev.* **2009**, *253*, 862-892.

⁵ a) Hopkinson, M. N.; Richter, C.; Schedler, M.; Glorius, F. *Nature* **2014**, *510*, 485-496; b) Bellotti, P.; Koy, M.; Hopkinson, M. N.; Glorius, F. *Nat. Rev. Chem.* **2021**, *5*, 711-725.

Carbene chemistry has been an intense field of research for years, resulting in a plethora of described transformations. Among them, cyclopropanation, C-H insertion, metathesis and carbene dimerization remain as the most characteristic ones.

Metal carbene complexes have drawn even greater attention during the last decades due to their fascinating versatility. Although Schrock and NHC complexes are interesting reagents, the focus will be narrowed on the reactivity of Fischer-type group 6 metal carbene complexes, since they are closely related to the transformation described in this chapter.

Indeed, the specific focus will be on the reactivity of stabilized Fischer-type metal-carbene complexes bearing an alkyne substituent, although other with different substituents on the carbene carbon and non-stabilized Fischer-type metal-carbene complexes have also been widely researched.^{3,6}

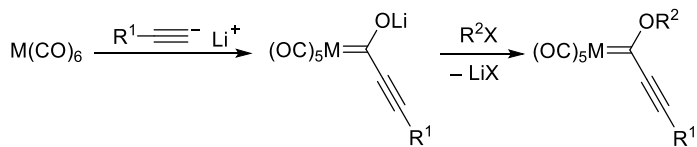
The most commonly used method for synthesizing alkynyl Fischer alkoxycarbene complexes (alkynyl-FCCs) involves adding a lithium acetylide reagent to a hexacarbonyl metal, which forms an acyl metalate (Scheme 1.6). This metalate then undergoes in-situ *O*-alkylation using hard alkylating reagents, such as $R^2OSO_2CF_3$ (R^2OTf) or Meerwein's salt (R^3OBF_4).⁷ There are alternative methods available for synthesizing alkynyl-FCCs with alkoxy groups derived from triflates that are more challenging to prepare, as well as aminocarbene complexes.⁸

³ Barluenga, J.; Aguilar, E. *Adv. Organomet. Chem.* **2017**, *67*, 1-150.

⁶ For selected reviews in the field, see: a) de Meijere, A.; Schirmer, H.; Duetsch, M. *Angew. Chem. Int. Ed.* **2000**, *39*, 3964-4002; b) Barluenga, J.; Santamaría, J.; Tomás, M. *Chem. Rev.* **2004**, *104*, 2259-2284; c) Wu, Y. T.; de Meijere, A. *Top. Organomet. Chem.* **2004**, *13*, 21-57; d) Barluenga, J.; Martínez, S. *ARKIVOK*, **2006**, *7*, 129-147; e) Kagoshima, H.; Fuchibe, K.; Akiyama, T. *Chem. Record.* **2007**, *7*, 104-114; f) Dötz K. H.; Stendel, J. *Chem Rev.* **2009**, *109*, 3227-3274; g) Aguilar, E.; López, L. A.; *Science of Synthesis, Knowledge Updates 2014/2*. Stuttgart, Germany: Georg Thieme Verlag KG; **2014**, *2*, 1; h) Santamaría, J.; Aguilar, E. *Org. Chem. Front.* **2016**, *3*, 1561-1588; i) Wang, K.; Wang, J. *Synlett* **2019**, *30*, 542-551; j) Hoskocová, I.; Ludvík, J. *Curr. Opin. Electrochem.* **2019**, *15*, 65-174. k) Bera, T.; Pandey, K.; Ali, R. *ChemistrySelect* **2020**, *5*, 5239-5267; l) Feliciano, A.; Vázquez, J. L.; Benítez-Puebla, L. J.; Velazco-Cabral, I.; Cruz, D. C.; Delgado, F.; Vázquez, M. A. *Chem. Eur. J.* **2021**, *32*, 8233-8251.

⁷ Fischer, E. O.; Maasböl, A. *Angew. Chem. Int. Ed.* **1964**, *3*, 580-581.

⁸ a) Connor, J. A.; Jones, E. M.; *J. Chem. Soc. A*, **1971**, 3368-3372; b) Kreissel, F. *Chem. Inform.* **1985**, *16*, 1; c) Yamashita, A.; Toy, A.; Ghazal, N. B.; Muchmore, C. R. *J. Org. Chem.* **1989**, *54*, 4481-4483; d) Hegedus, L. S.; Schwindt, M. A.; De Lombaert, S.; Imwinkelried, R. *J. Am. Chem. Soc.* **1990**, *112*, 2264-2273; e) Sodeberg, B. C.; Hegedus, L. S.; Sierra, M. A. *J. Am.*



M = Cr, Mo, W

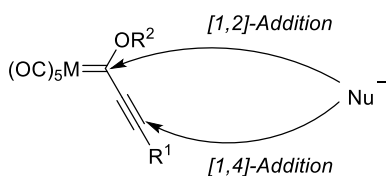
R¹ = Alkyl, alkenyl, alkynyl, (Hetero)aryl, TMS

R²X = (R²)₃OBF₄, R²OSO₂CF₃, R²OSO₂F, R²I

Scheme 1.6: Common synthesis of alkynyl-FCCs.

Regarding their usefulness in organic synthesis, chromium complexes are the most widely used group 6 FCCs due to their optimal combination of reactivity, stability, and accessibility. Tungsten carbene complexes exhibit greater stability, whereas molybdenum complexes tend to be more reactive than their chromium counterparts. Additionally, chromium carbene complexes have a better tendency towards CO ligand insertion compared to tungsten or molybdenum analogues, primarily due to differences in metal-CO strength resulting from backbonding.⁹

The reactions reported in the literature in which alkynyl-FCCs participate as reagents involve a nucleophile attacking the carbene. The alkynyl carbene complex has two electrophilic positions, the carbene carbon and the β -carbon of the triple bond. In this sense, [1,2]-addition or [1,4]-addition can occur, being subjected to the nucleophile, the reaction conditions, and the nature of the carbene complex (Scheme 1.7). As a result, acyclic, carbocyclic, or heterocyclic products may be formed, depending also on the aforementioned variables.

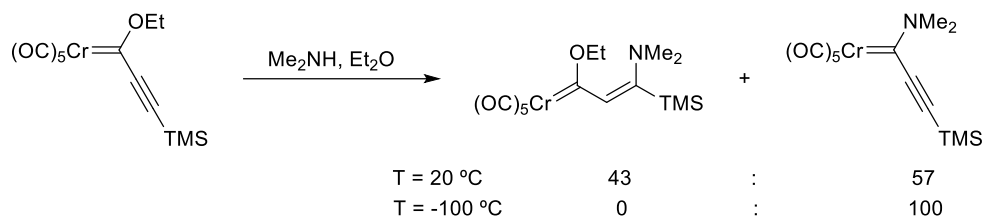


Scheme 1.7: [1,2]-Addition vs [1,4]-addition in alkynyl alkoxy Fischer-carbene complexes.

Chem. Soc. **1990**, *112*, 4364-4374; f) Vernier, J. M.; Hegedus, L. S.; Miller, D. B. *J. Org. Chem.* **1992**, *57*, 6914-6920.

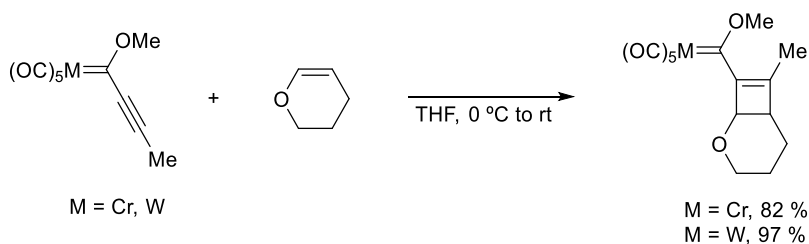
⁹ Fernández, I.; Sierra, M. A.; Gómez-Gallego, M.; Mancheño, M. J.; Cossío, F. P. *Chem. Eur. J.* **2005**, *11*, 5988-5996.

Scheme 1.8 depicts the formation of acyclic products via reaction of a chromium carbene complex with dimethylamine. The reaction results in a mixture of products from [1,2]-addition and [1,4]-addition at room temperature, but at low temperature only the [1,2]-addition adduct is formed. This observation leads to the conclusion that [1,2]-addition is the preferred pathway for secondary amines at low temperatures.¹⁰



Scheme 1.8: Nucleophilic addition of secondary amines to alkoxy alkynyl FCCs.

However, most of the examples reported in the bibliography employing alkynyl-FCCs as starting material lead to cyclic compounds. For instance, in the Scheme 1.9 the reaction between an alkynyl-FCC and an electron-rich alkene, such as an enol ether, yields cyclobutene carbene complexes with complete regioselectivity at room temperature.¹¹ In this example, the FCC reacts exclusively through the triple bond while the carbene carbon remains unaltered. This reaction takes place for both chromium and tungsten alkynyl carbene complexes.



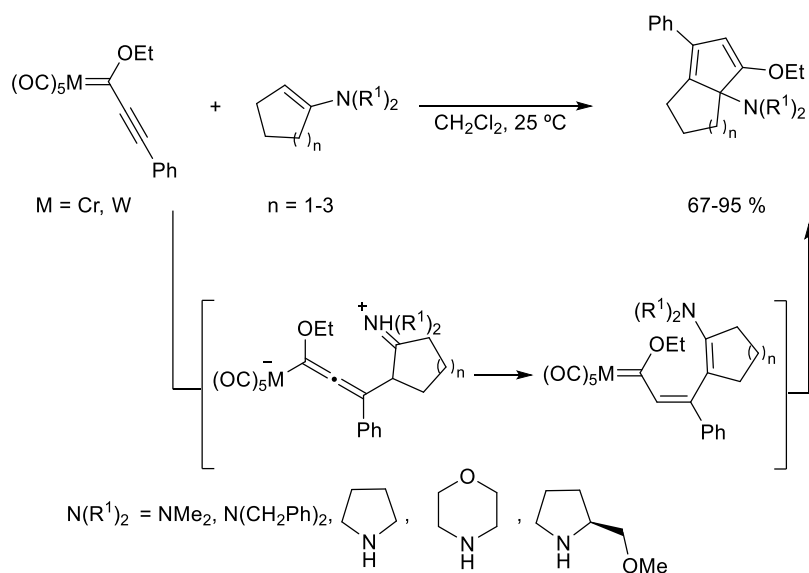
Scheme 1.9: Synthesis of cyclobutenes via [2+2]-reaction sequence.

¹⁰ Duetsch, M.; Stein, F.; Lackmann, R.; Pohl, E.; Herbst-Irmer, R.; de Meijere, A. *Chem. Ber.* **1992**, *125*, 2051-2065.

¹¹ Wulff, W. D.; Faron, K. L.; Su, J.; Springer, J. P.; Rheingold, A. L. *J. Chem. Soc. Perkin. Trans.* **1997**, *1*, 197-199.

The reaction with enamines, also electron-rich alkenes, such as tertiary 1-aminocycloalkenes, yields a different type of carbocycles. Thus, cyclopentadiene rings are obtained in good yields at room temperature (Scheme 1.10).¹² The reaction is believed to begin with a nucleophilic [1,4]-addition of the enamine to form zwitterionic allene-type species. Because of steric reasons related to the size of the nucleophile, the alternative addition to the carbene carbon should be disfavoured. These allene-type intermediates then evolve into 1-metalla-1,3,5-hexatrienes by intramolecular [1,3]-hydrogen transfer, and the reaction products are ultimately formed via an overall formal [3+2]-carbocyclization.

Remarkably, in this case, both triple bond carbons and the carbene carbon are involved in the reaction. Therefore, FCCs may behave as C2- or C3-synthons depending on the nucleophile employed and the reaction conditions.

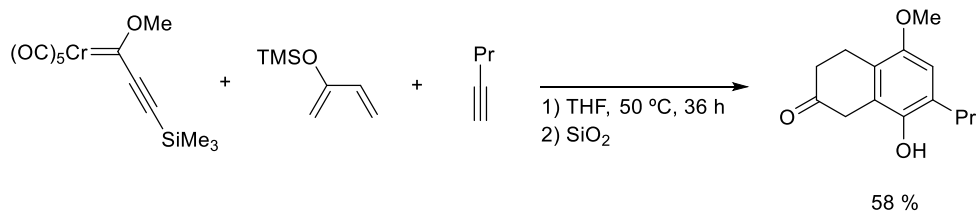


Scheme 1.10: Synthesis of cyclopentadienes from alkynyl-FCCs.

In addition, a facile route to obtain tetrahydronaphthalene derivatives is the tandem [4+2]-cycloaddition/Dötz benzannulation sequence, employing alkynyl-FCCs, a diene, and an alkyne (Scheme 1.11).¹³ This method serves as an illustrative example for the synthesis of six-membered carbocyclic rings.

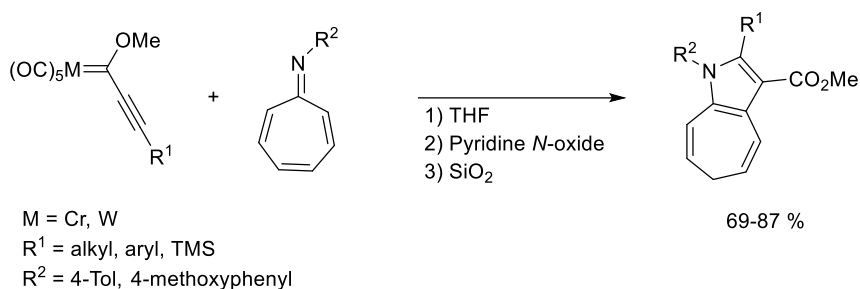
¹² Meyer, A. G.; Aumann, R. *Synlett*, **1995**, 1011-1013.

¹³ Wulff, W. D.; Yang, D. C. *J. Am. Chem. Soc.* **1984**, *106*, 7565-7567.



Scheme 1.11: Preparation of substituted dihydronaphthalene derivative accomplished through [4+2]-cycloaddition/Dötz benzannulation reaction.

Regarding the use of FCCs in heterocyclic synthesis, a noteworthy example of 5-membered heterocycle synthesis involves the reaction of alkynyl-FCCs with heptafulvene derivatives, which leads to the formation of cycloheptatriene-fused pyrrole derivatives via a [8+2]-cycloaddition reaction (Scheme 1.12).¹⁴ Again, in this example the FCC reacts exclusively through the triple bond.



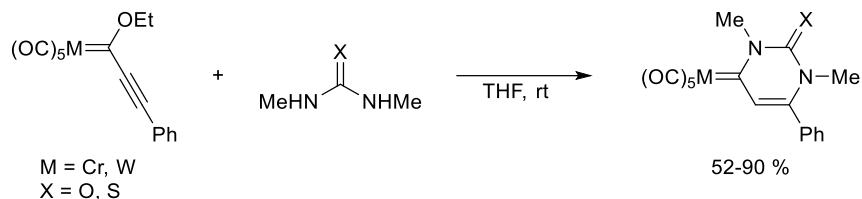
Scheme 1.12: Obtention of 1,6-dihydrocyclohepta[*b*]pyrrole derivatives.

Various reactions have been reported for obtaining 6-membered heterocycles using alkyne-FCCs.¹⁵ Particularly noteworthy, due to its relative similarity with the reaction under study in this chapter, is the reaction between alkynyl-FCCs and 1,3-dinitrogen nucleophiles such as symmetric *N*-alkylureas (X = O) or -thioureas (X = S),

¹⁴ Barluenga, J.; García-Rodríguez, J.; Suárez-Sobrino, A. L.; Tomás, M. *Chem. Eur. J.* **2009**, *15*, 8800-8806.

¹⁵ a) Aumann, R.; Heinen, H.; Dartmann, M.; Krebs, B. *Chem. Ber.* **1991**, *124*, 2343-2347; b) Aumann, R.; Kobmeier, M.; Roths, K.; Fröhlich, R. *Synlett* **1994**, *12*, 1041-1044; c) Barluenga, J.; Tomás, M.; López-Peigrín, J. A.; Rubio, E. *Tet. Lett.* **1997**, *38*, 3981-3984; d) Barluenga, J.; Tomás, M.; Ballesteros, A.; Santamaría, J.; Suárez-Sobrino, A. *J. Org. Chem.* **1997**, *62*, 9229-9235; e) Polo, R.; Moretó, J. M.; Schick, U.; Ricart, S. *Organometallics* **1998**, *17*, 2135-2137; f) Barluenga, J.; López, L. A.; Martínez, S.; Tomás, M. *Synlett* **1999**, *2*, 219-221.

which leads to cyclic FCCs that can be converted into uracil fragments through oxidation (Scheme 1.13).¹⁶ This example illustrates a case where FCCs behave as C3-synthons by reacting through the carbene carbon and both atoms of the triple bond.



Scheme 1.13: Uracil derivatives synthesized through reactions of alkynyl-FCCs with ureas and thioureas.

As mentioned in the previous examples, FCCs have been found to participate in reactions leading to the formation of acyclic, carbocyclic, and heterocyclic compounds. Mostly, they can act as either C2- or C3-synthons, depending on the nucleophile used and the reaction conditions.

2.2 4,5-Dihydro-1,2,4-oxadiazoles in organic synthesis.

Obtaining heterocyclic compounds has always been an objective for synthetic chemists, given their importance as part of numerous natural structures, such as nitrogenous bases in DNA and vitamins.¹⁷ In this sense, the use of 4,5-dihydro-1,2,4-oxadiazoles as precursors for the synthesis of various heterocycles, behaving as [N-C-N] synthons, could provide significant benefits in this field.

In the last years, the core structure of 4,5-dihydro-1,2,4-oxadiazoles has been found in products of significant biological importance, including pesticides,¹⁸ insecticides¹⁹ and kinase inhibitors²⁰ (Figure 1.2).

¹⁶ D'Acunto, M.; Tommasone, S.; Talotta, C.; Brancatelli, G.; Geremia, S.; Valletta, E.; Merlo, F. M.; Macchi, B.; Gaeta, C.; Neri, P.; Spinella, A. *RSC Adv.* **2016**, *6*, 75002-75005.

¹⁷ A) Gilchrist, T. L.; *Heterocyclic Chemistry, 3rd ed. Addison Wesley: Essex, England, 1997*, 414 pp; b) Alvarez-Builla, J.; Vaquero, J. J.; Barluenga, J. *Modern Heterocyclic Chemistry, Wiley-VCH Verlag GmbH & Co. KGaA* **2011**, 2533 pp.

¹⁸ Lv, M.; Ma, Q.; Zhang, S.; Xu, H.; *Bioorg. Med. Chem. Lett.* **2021**, *51*, 128356-128361.

¹⁹ Zhang, Y.; Shang, J.; Li, H.; Liu, H.; Song, H.; Wang, B.; Li, Z. *Chin. Chem. Lett.* **2020**, *31*, 1276-1280.

²⁰ Yamamoto, K.; Yoshikawa, Y.; Ohue, M.; Inuki, S.; Ohno, H.; Oishi, S. *Org. Lett.* **2019**, *21*, 373-377.

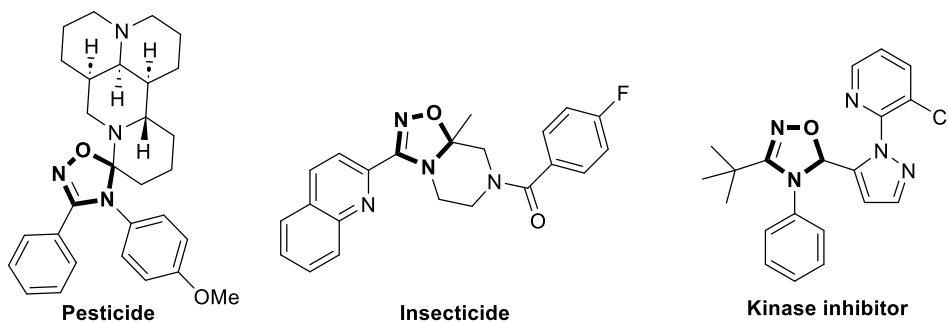
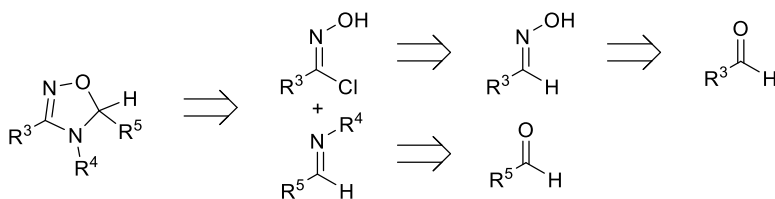


Figure 1.2: 4,5-dihydro-1,2,4-oxadiazoles presents in the nature.

Among the different approaches for the synthesis of 4,5-dihydro-1,2,4-oxadiazoles, the most common one involves a condensation between an oxime chloride and an imine, as illustrated in Scheme 1.14. In turn, the oxime chloride is obtained by chlorinating the oxime formed by reacting the corresponding aldehyde with hydroxylamine.²¹ Similarly, the imine required for the formation of 4,5-dihydro-1,2,4-oxadiazoles is obtained by reacting the aldehyde with the required amine.²²



Scheme 1.14: Retrosynthesis of 4,5-dihydro-1,2,4-oxadiazoles.

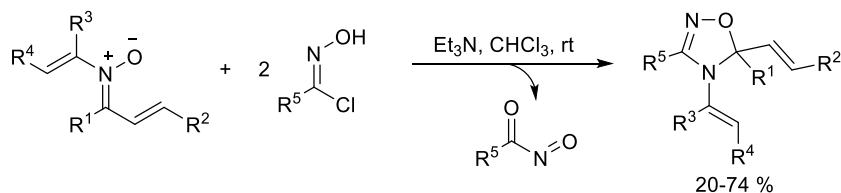
The previous method may present challenges when attempting to obtain 4,5-dihydro-1,2,4-oxadiazole derivatives with specific substituents.²³ Therefore, alternative syntheses have been developed which offer a more feasible approach for those cases. One such example is presented in Scheme 1.15, where an imine oxide is used for the synthesis of 4,5-dialkenyl-4,5-dihydro-1,2,4-oxadiazoles.²⁴

²¹ Zheng, H.; McDonald, R.; Hall, D. G. *Chem. Eur. J.* **2010**, *16*, 5454-5460.

²² Schaufelberger, F.; Hu, L.; Ramström, O. *Chem. - A Eur. J.* **2015**, *21*, 9776-9783.

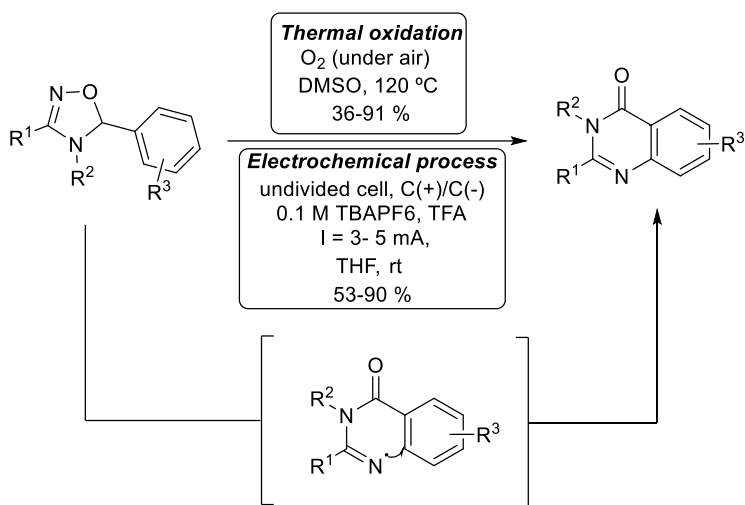
²³a) Coutouli-Argyropoulou, E.; Malamidou-Xenikaki, E.; Mentzafos, D.; Terzis, A. *J. Heterocyclic Chem.* **1990**, *27*, 1185-1189; b) Azizian, J.; Jadidi, K.; Mehrdad, M.; Sarrafi, Y. *Synth. Comm.* **2000**, *30*, 2309-2315; c) Shi, G.; He, X.; Shang, Y.; Xiang, L.; Yang, C.; Han, G.; Du, B. *Chin. J. Chem.* **2016**, *34*, 901-909.

²⁴ Nong, C.-M.; Lv, S.-N.; Shi, W.-M.; Liang, C.; Su, G.-F.; Mo, D.-L. *Org. Lett.* **2023**, *25*, 267-271.



Scheme 1.15: Alternative method to obtain 4,5-dihydro-1,2,4-oxadiazoles.

On the other hand, the use of 4,5-dihydro-1,2,4-oxadiazoles in organic synthesis is very limited, and they have been mainly employed as starting materials in intramolecular reactions. For instance, they can be used as precursors to *N*-centered radicals in intramolecular reactions to obtain quinazolines. This transformation may be achieved either through thermal oxidation²⁵ or by electrochemical means, proceeding via transient iminyl radical species (Scheme 1.16).²⁶



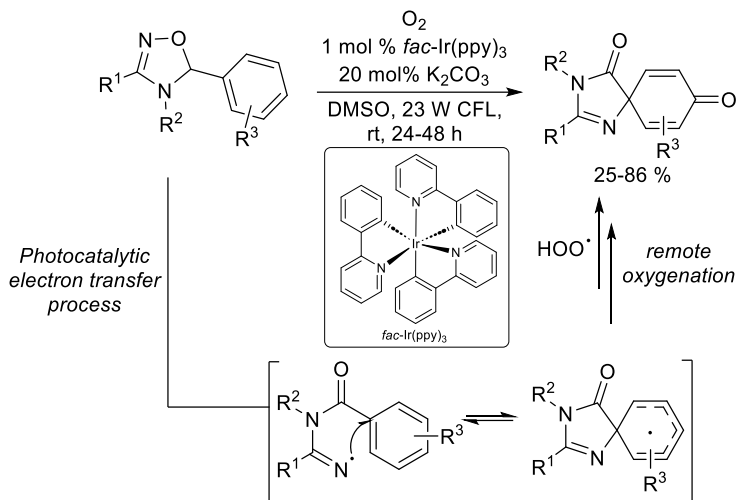
Scheme 1.16: Obtention of quinazolines from 4,5-dihydro-1,2,4-oxadiazoles.

A different outcome happens when 4,5-dihydro-1,2,4-oxadiazoles are treated in the presence of an iridium catalyst under photocatalytic conditions, whereby a selective *ipso*-attack occurs after the formation of the iminyl radical species, ultimately leading to spiro-azalactams through remote oxygenation (Scheme 1.17).²⁷

²⁵ Wang, Y.-F.; Zhang, F.-L.; Chiba, S. *Org. Lett.* **2013**, *15*, 2842-2845.

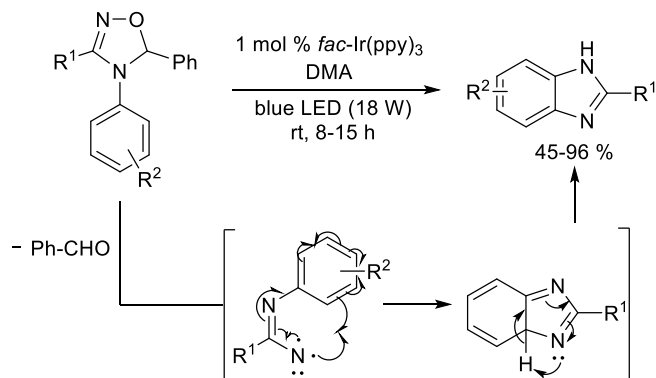
²⁶ Hwang, H. S.; E. J. Cho. *Org. Lett.* **2021**, *23*, 5148-5152.

²⁷ Soni, V. K.; Hwang, H. S.; Moon, Y. K.; Park, S.-W.; You, Y.; Cho, E. J. *J. Am. Chem. Soc.* **2019**, *141*, 10538-10545.



Scheme 1.17: Obtention of spiro-azalactams via photocatalytic electron transfer.

In addition, energy transfer catalysis under LED conditions can drive the rearrangement of these compounds to form benzimidazoles via a nitrene intermediate and extrusion of benzaldehyde, as long as the *sp*³ nitrogen atom is linked to an aromatic group (Scheme 1.18).²⁸

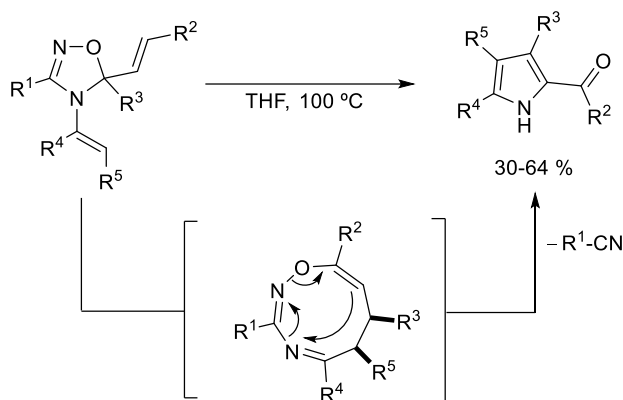


Scheme 1.18: Synthesis of benzimidazoles under LED conditions.

When the 4,5-dihydro-1,2,4-oxadiazoles bear alkenyl substituents at positions 4 and 5 they can undergo a thermal [3,3]-rearrangement leading to a 6,7-dihydro-

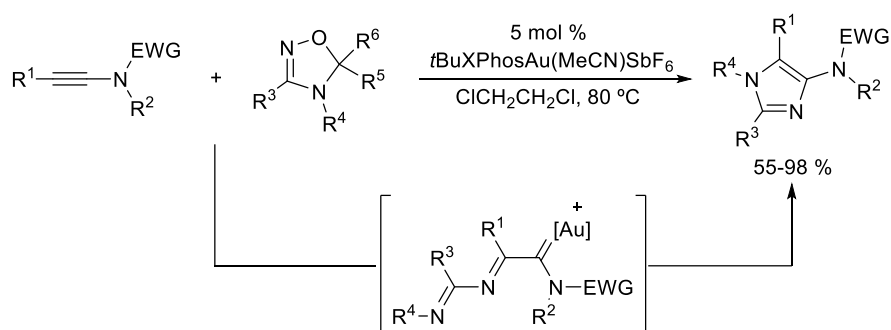
²⁸ Park, D. D.; Min, K. H.; Kang, J.; Hwang, H. S.; Soni, V. K.; Cho, C.-G.; Cho, E. J. *Org. Lett.* **2020**, *22*, 1130-1134.

1,2,4-oxadiazonine intermediate, ultimately producing 2-acyl pyrroles via the extrusion of nitrile (Scheme 1.19).²³



Scheme 1.19: Obtention of pyrroles through a thermal [3,3]-rearrangement.

All the transformations reported so far belong to intramolecular reactions; however, the role of 4,5-dihydro-1,2,4-oxadiazoles as [N-C-N] synthons has been scarcely studied and, in fact, the only example of an intermolecular transformation reported so far is the one shown in Scheme 1.20 and mentioned at the beginning of the chapter. In that example, the synthesis of 4-aminoimidazoles takes place in moderate to excellent yields through a [3+2]-cycloaddition reaction between ynamides and 4,5-dihydro-1,2,4-oxadiazoles, via a gold α -imino carbene complex intermediate.¹



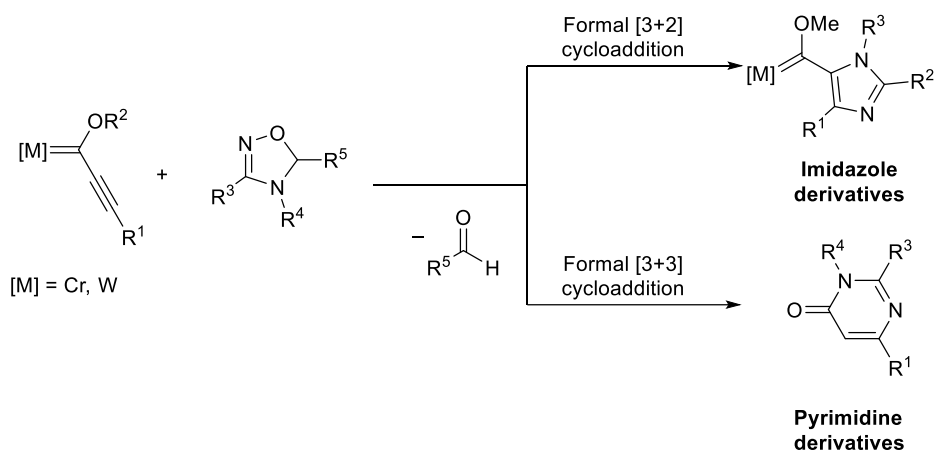
Scheme 1.20: Synthesis of 4-aminoimidazoles catalysed by gold (I).

²³ Nong, C.-M.; Lv, S.-N.; Shi, W.-M.; Liang, C.; Su, G.-F.; Mo, D.-L. *Org. Lett.* **2023**, *25*, 267-271.

¹ Xu, W.; Wang, G.; Sun, N.; Liu, Y. *Org. Lett.* **2017**, *19*, 3307-3310.

3 Results and discussion.

This chapter aims to investigate the reaction between alkynyl alkoxy Fischer carbene complexes and 4,5-dihydro-1,2,4-oxadiazoles. Considering the previously described reactivity for these substrates, two reaction pathways were expected to occur (Scheme 1.21). The first one would involve a formal [3+2]-cycloaddition that should lead to the formation of imidazole derivatives. In the second one, a formal [3+3]-cycloaddition would take place yielding the corresponding pyrimidine derivatives.

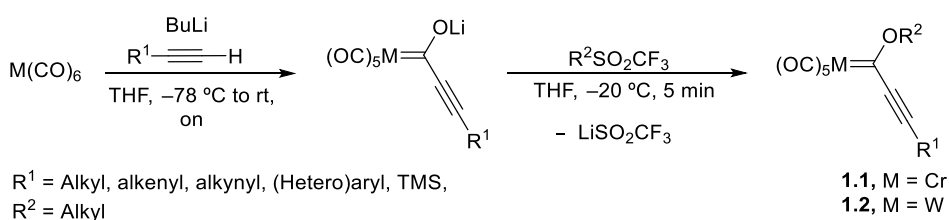


Scheme 1.21: [3+2] vs [3+3]-cycloaddition.

3.1 Synthesis of starting materials.

The synthesis of alkynyl FCCs, which serve as starting materials in our reaction, was achieved via the classical Fischer synthesis (Scheme 1.22).⁷ This procedure involves the deprotonation of the corresponding acetylene with a strong base, typically BuLi (butyl lithium), followed by nucleophilic attack on one of the CO groups in $M(CO)_6$, leading to the formation of the corresponding lithium salt. The reaction is set up in a dry Schlenk flask under N_2 atmosphere, using THF (tetrahydrofurane) as solvent, at $-78^\circ C$ and left to react at room temperature overnight.

In the second step, a one-pot *O*-alkylation reaction is carried out adding a strong alkylating agent such as MeOTf ($R^2SO_2CF_3$) to the reaction mixture and let them react at $-20^\circ C$ for 5 minutes to yield the desired final product. This synthetic route has been widely used in the preparation of alkynyl FCCs due to its high efficiency and excellent yields.



Scheme 1.22: Synthesis followed to obtain alkynyl-FCCs.

On the other hand, the synthesis of 4,5-dihydro-1,2,4-oxadiazoles **1.3** was carried out using the methodology described in Scheme 1.23.²¹ To obtain these compounds, this synthetic pathway has been commonly employed due to its simplicity and high yields. The scheme outlines the reaction conditions and the key intermediates involved.

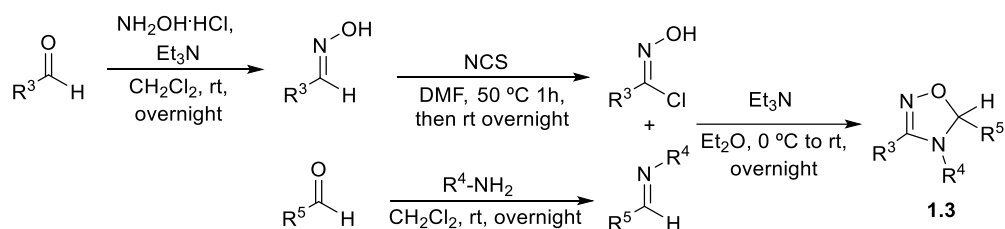
To obtain the corresponding oxime, the appropriate aldehyde is reacted with hydroxylamine in dichloromethane (DCM) in a dry Schlenk under a N_2 atmosphere at room temperature, using triethylamine (Et_3N) as a base. Once the oxime is obtained, it is chlorinated with *N*-chlorosuccinimide (NCS) in *N,N*-dimethylformamide (DMF) at $50^\circ C$ for 1 hour, followed by allowing it to react overnight at room temperature to prepare the oxime chloride. In a similar way, to obtain the required imine for the

⁷ Fischer, E. O.; Maasböl, A. *Angew. Chem. Int. Ed.* **1964**, *3*, 580-581.

²¹ Schaufelberger, F.; Hu, L.; Ramström, O. *Chem. - A Eur. J.* **2015**, *21*, 9776-9783.

formation of 4,5-dihydro-1,2,4-oxadiazoles **1.3**, the aldehyde is reacted overnight with the corresponding amine in DCM in a dry Schlenk under N₂ atmosphere.

With the corresponding oxime chloride and imine in hands, they are mixed in a dry Schlenk flask under N₂ atmosphere, using Et₃N as a base and diethylether (Et₂O) as the solvent, at 0 °C and left to react at room temperature overnight, to obtain 4,5-dihydro-1,2,4-oxadiazoles **1.3**.



Scheme 1.23: Synthesis followed to obtain 4,5-dihydro-1,2,4-oxadiazoles **1.3**.

The procedure outlined above was employed to synthesize a diverse set of 4,5-dihydro-1,2,4-oxadiazoles **1.3**, which are listed in Table 1.1 along with their respective yields for the cycloaddition step. The moieties were varied by incorporating different aliphatic or aromatic groups, resulting in a range of synthesized compounds.

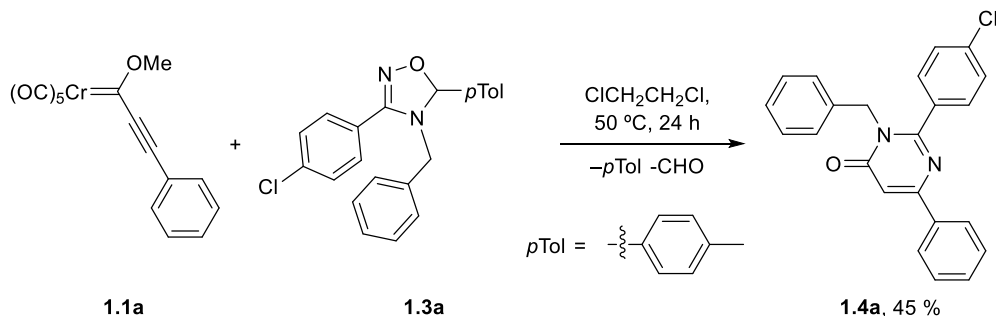
Entry	4,5-dihydro-1,2,4-oxadiazole	R ³	R ⁴	R ⁵	%Yield, 1.3 ^[a]
1	1.3a	<i>p</i> Cl-C ₆ H ₄	Bn	<i>p</i> Tol	88
2	1.3b	<i>p</i> MeO-C ₆ H ₄	Bn	<i>p</i> Tol	83
3	1.3c	Ph	Bn	<i>p</i> Tol	32
4	1.3d	<i>o</i> Tol	Bn	<i>p</i> Tol	34
5	1.3e	<i>o</i> Br-C ₆ H ₄	Bn	<i>p</i> Tol	47
6	1.3f	<i>m</i> Cl-C ₆ H ₄	Bn	<i>p</i> Tol	10
7	1.3g	<i>s</i> Bu	Bn	<i>p</i> Tol	15
8	1.3h	<i>p</i> Cl-C ₆ H ₄	<i>p</i> MeO-C ₆ H ₄	Ph	63
9	1.3i	<i>p</i> Cl-C ₆ H ₄	Ph	<i>p</i> Tol	32
10	1.3j	<i>p</i> Cl-C ₆ H ₄	<i>n</i> Bu	<i>p</i> Tol	32
11	1.3k	<i>p</i> MeO-C ₆ H ₄	<i>n</i> Bu	<i>p</i> Tol	49
12	1.3l	<i>p</i> Cl-C ₆ H ₄	<i>p</i> MeO-C ₆ H ₄	<i>p</i> Tol	61
13	1.3m	<i>p</i> Cl-C ₆ H ₄	<i>p</i> MeO-C ₆ H ₄ -CH ₂ -	<i>p</i> Tol	54
14	1.3n	<i>p</i> MeO-C ₆ H ₄	H	<i>p</i> Tol	11
15	1.3o	2-Furyl	Bn	<i>p</i> Tol	57

^[a] Isolated yield for the [3+2]-cycloaddition step.

Table 1.1: Scope of 4,5-dihydro-1,2,4-oxadiazoles **1.3**.

3.2 Initial experiment and structural elucidation.

Based on the aforementioned hypothesis, alkynyl-FCC **1.1a** and 4,5-dihydro-1,2,4-oxadiazole **1.3a** were chosen as model substrates for an initial attempt. Thus, when a mixture of **1.1a** and 1.2 equivalents of **1.3a** in DCE was heated at 50 °C for 24h, pyrimidin-4(3*H*)-one **1.4a** was obtained and could be isolated in 45% yield (Scheme 1.24).



Scheme 1.24: Obtention of pyrimidin-4(3*H*)-one **1.4a** in the first attempt.

It was easy to determine by NMR techniques that the reaction product corresponded to a [3+3]-cycloadduct (Scheme 1.21, p. 53), and no product of [3+2]-cycloaddition was obtained. However, it was not as clear whether the obtained compound was **1.4a** or its regioisomer **1.4a'** (Figure 1.3, *top*). To treat to identify the product obtained, a NOESY (Nuclear Overhauser Enhancement Spectroscopy) was performed (Figure 1.3, *bottom*).³²

To determine whether the obtained regioisomer is **1.4a** or **1.4a'**, the proton signals at carbon 7 are the most informative. If the obtained regioisomer is **1.4a**, the protons in this position will exhibit NOE effects with those at carbons 9 and 13. On the other hand, if the obtained isomer is **1.4a'**, these protons should also exhibit NOE effects with those at positions 17 (Figure 1.3). As shown, there is no signal in the spectrum in the overlap between the proton signals at carbon 7 and those at carbons 17, which suggests that the regioisomer obtained is **1.4a**. Nevertheless, the absence of NOE does not necessarily confirm the non-existence of the compound, being therefore not possible to draw a definitive conclusion. It is plausible that the

³² Anet, F. A. L.; Bourn, A. J. R. *J. Am. Chem. Soc.* **1965**, *87*, 5250-5251.

regioisomer obtained was **1.4a'** and that other factors contributed to the lack of NOE.

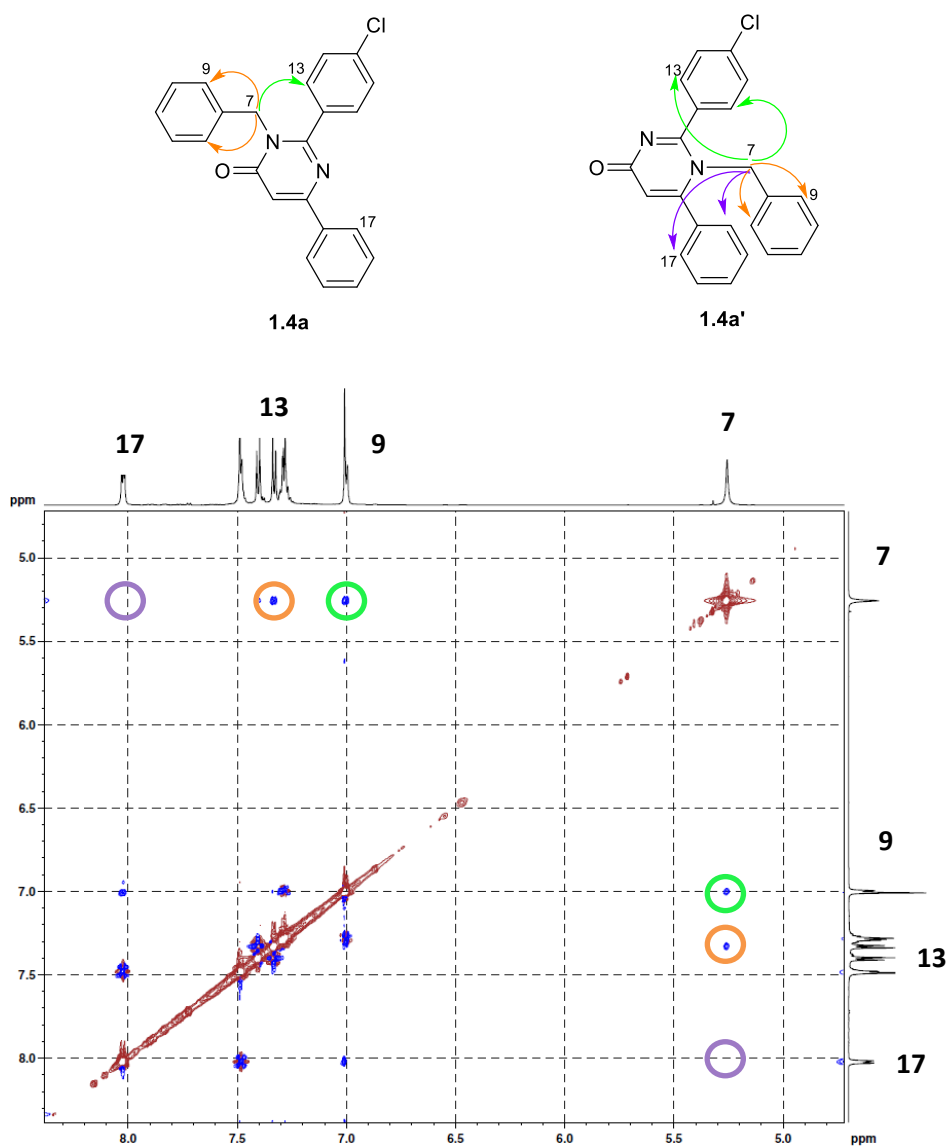


Figure 1.3: NOESY spectrum of derivative **1.4a**.

Therefore, it was decided to fully access to the structure of the reaction product by obtaining the X-ray diffraction structure of one product **1.4**. In this sense, during the expansion of the scope of the reaction (as it will be seen later) a single

monocrystal of compound **1.4c** could be obtained in a mixture of hexane and dichloromethane (Figure 1.4). From here, it can be seen that N1 (unsubstituted nitrogen) is bonded to C6, which comes from the beta position of the FCC, and that N3 is bonded to the former carbenic carbon. Therefore, it was confirmed that the structure obtained for pyrimidin-4(3*H*)-ones **1.4** corresponds to the derivatives of regioisomer **1.4a**, and not **1.4a'**, and that the assumptions made by NMR elucidations were correct (Figure 1.3). The bond distances of C-C, C-H, C-N, and C-O are consistent with those expected for both single and double bonds (see Annex III).

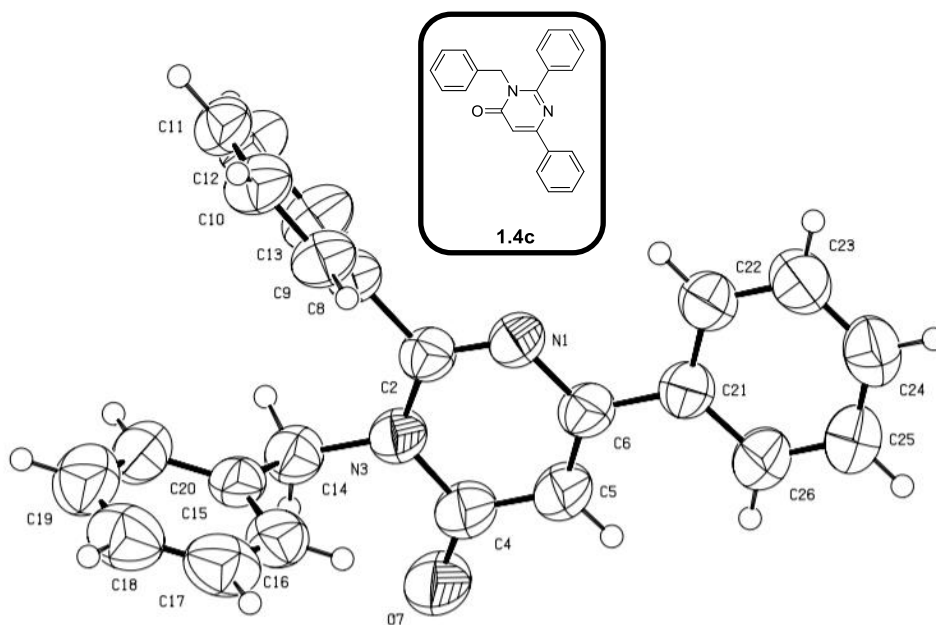


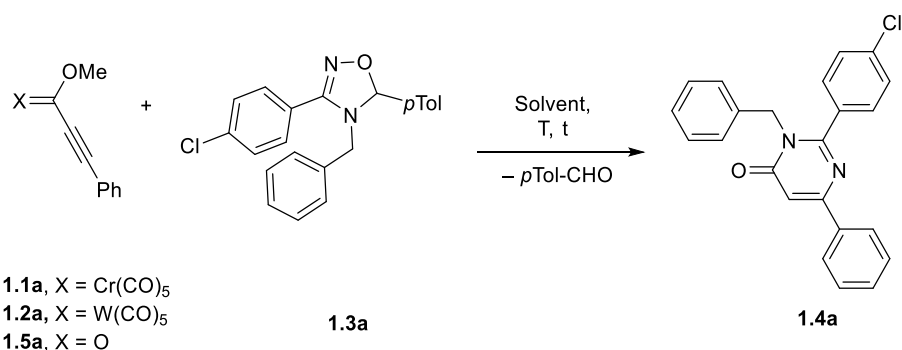
Figure 1.4: X-Ray diffraction structure of pyrimidin-4(3*H*)-one **1.4c**.

3.3 Optimization of the reaction conditions.

As previously mentioned, a formal [3+3]-cycloaddition has taken place between the starting materials. In this regard, the 4,5-dihydro-1,2,4-oxadiazole **1.3a** acts as a regioselective [N-C-N] synthon after *p*-tolualdehyde extrusion. Moreover, the NMR experiments allowed us to determine the structure of the final product as a pyrimidin-4(3*H*)-one. Given that there is only one previous example of 4,5-dihydro-1,2,4-oxadiazoles acting as [N-C-N] synthon, we decided to explore this reaction in further detail.

In order to maximize the yield of pyrimidin-4(3*H*)-one **1.4a**, different reaction conditions were explored, investigating the effect of variables such as temperature,

solvent, stoichiometry, and reaction time. The experimental results of these analyses are summarized in Table 1.2.



Entry	FCC 1.1	1.1a:1.3a	T	t	Solvent	%Yield, 1.4a ^[a]
1	1.1a	1:1.2	60	24	DCE	59
2	1.1a	1:1.2	70	24	DCE	17
3	1.1a	1:1.2	60	24	THF	(23)
4	1.1a	1:1.2	60	24	Hexane	(14)
5	1.1a	1:1.2	60	24	1,4-Dioxane	(36)
6	1.1a	1:1.2	60	24	Toluene	(44)
7	1.1a	1:1.2	60	24	DCM	(52) ^[b]
8	1.1a	1:2	60	24	DCE	40
9	1.1a	1:1.2	60	24	DCE	54 ^[c]
10	1.1a	1:1.2	rt	96	DCE	66 ^[d]
11	1.1a	1:1.5	60	36	DCE	80(81)
12	1.2a	1:1.5	60	48	DCE	37
13	1.5a	1:1.5	60	48	DCE	--

^[a] Isolated yield; in brackets, NMR estimated yield using 1,3,5-trimethoxybenzene as internal standard. ^[b] Reaction performed in a sealed tube. ^[c] **1.1a** was added dropwise for 2h over **1.3a** at 60 °C. ^[d] Reaction carried out at rt.

Table 1.2: Optimization of the reaction conditions.

The results gathered in Table 1.2 demonstrate that a slight increase in temperature from 50 (in our initial attempt) to 60 °C improved the reaction yield to 59 % (*Entry 1*). However, a further increase in temperature resulted in a dramatic

drop in yield (*Entry 2*). Various solvents were also tested, including THF, hexane, 1,4-dioxane, toluene, and DCM, but none of them lead to better results (*Entries 3-7*).

Other optimization parameters such as increasing the amount of 4,5-dihydro-1,2,4-oxadiazole **1.3a** (*Entry 8*) or adding the dissolved carbene **1.1a** dropwise onto the 4,5-dihydro-1,2,4-oxadiazole **1.3a** (*Entry 9*) did not result in an improvement in the reaction yield. Subsequently, leaving the reaction at room temperature for a longer period of time was attempted, and it was found that the yield rose to 66 % (*Entry 10*). As a result, the reaction conditions were reverted to the optimum temperature of 60 °C but left for a longer time than in the first attempts, resulting in a yield of 80 % (*Entry 11*).

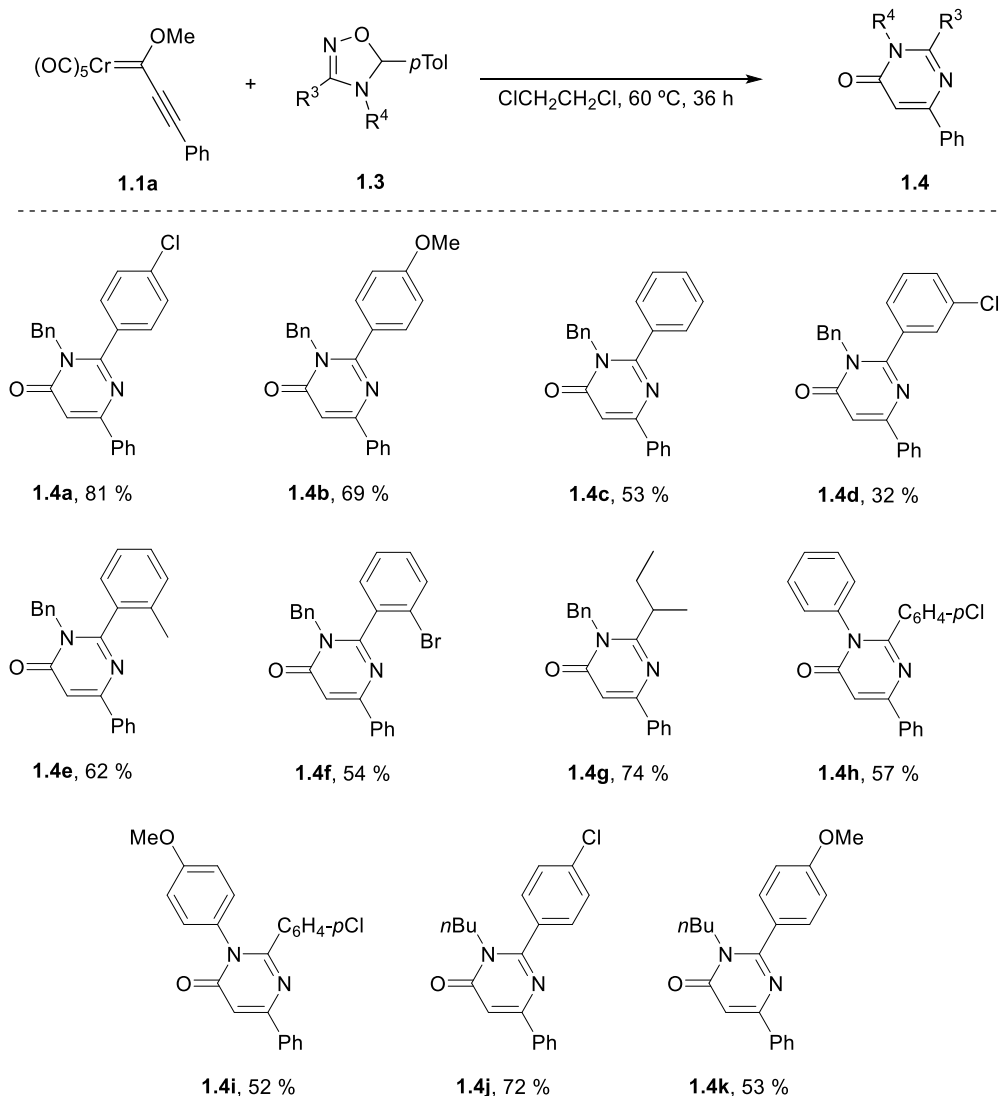
Finally, two additional experiments were also conducted. The first one was performed using W-alkynyl-FCC **1.2a**, which yielded a poorer outcome (*Entry 12*), proving that Cr-FCCs behave better than W-FCCs for this transformation. The second one was carried out with the corresponding alkynoic ester **1.5a**, but no reaction product was obtained (*Entry 13*). This result highlights the role of the metal moiety, showcasing an additional example of a superior performance of the FCCs over their ester analogues. This fact has already been established in the literature,³³ where the performance of FCCs has been compared to that of the corresponding ester (even when is activated by a Lewis acid) and better results have been obtained with FCCs. This is why these compounds have been referred to as "super esters".

As a conclusion of the optimization process, the best conditions found were a 1:1.5 ratio of Cr-alkynyl-FCC **1.1a** and 4,5-dihydro-1,2,4-oxadiazole **1.3a**, in DCE at 60 °C for 36 hours.

3.4 Scope of the reaction.

Once the optimum conditions for this transformation were established, the generalization process was started by modifying the R³ and R⁴ substituents of **3** (Scheme 1.25).

³³ a) Anderson, B. A.; Wulff, W. D.; Powers, T. S.; Tribbitt, S.; Rheingold, A. L. *J. Am. Chem. Soc.* **1992**, *114*, 10784-10798; b) Barluenga, J.; Aznar, F.; Barluenga, S. *J. Chem. Soc., Chem. Commun.* **1995**, 1973-1974; c) Barluenga, J.; Fernández-Rodríguez, M. A.; Aguilar, E. *Org. Lett.* **2002**, *4*, 3659-3662.

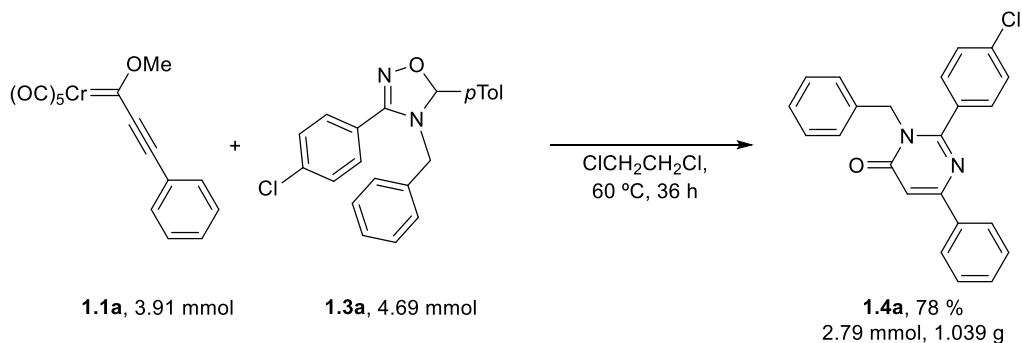


Scheme 1.25: Scope of positions R^3 y R^4 of 4,5-dihydro-1,2,4-oxadiazole **1.3**.

Thus, position R^3 of the 4,5-dihydro-1,2,4-oxadiazole **1.3** tolerates various aromatic substituents, including those with electron-withdrawing (**1.4a, d, f, h-j**) and electron-donating (**1.4b, e, k**) groups, as well as Ph (**1.4c**). Substituents such as *meta*- (**1.4d**) and *ortho*-substituted aromatic (**1.4e, f**), as well as a secondary aliphatic group (**1.4g**), are also feasible at that position. Furthermore, at position R^4 , satisfactory yields of the corresponding pyrimidin-4(3*H*)-ones can be achieved using both alkyl [benzyl (**1.4a-g**) and *n*-butyl (**1.4j, k**)] and aryl [phenyl (**1.4h**), and *p*-methoxyphenyl

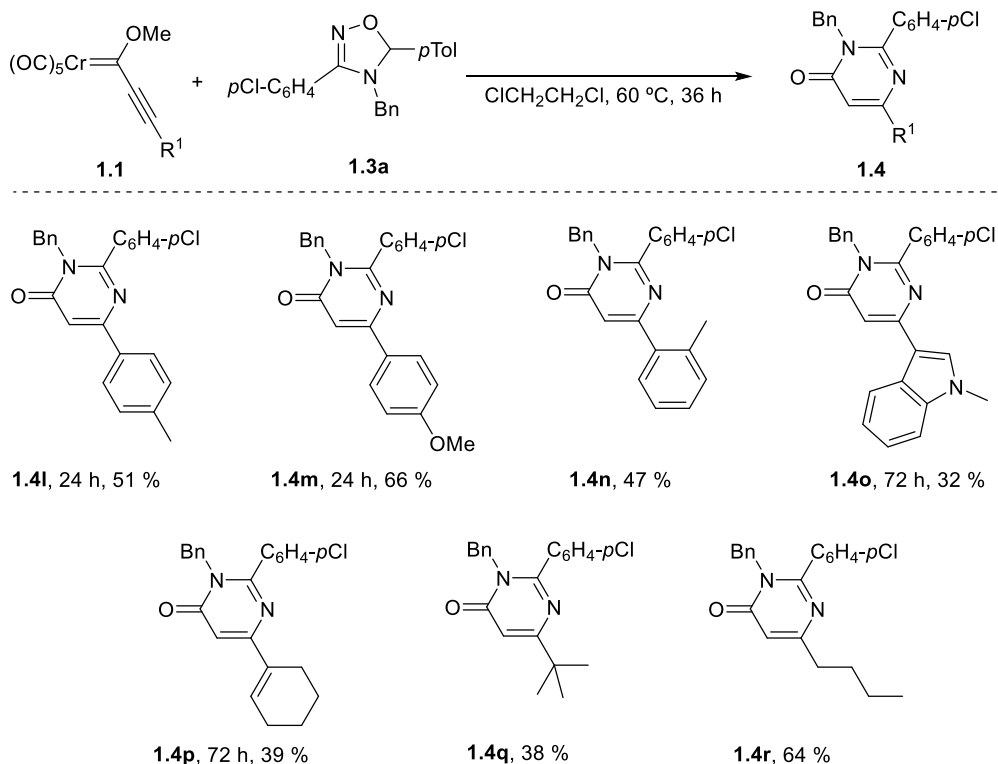
(**1.4i**)] groups as substituents. Moderate to good yields were observed in all the cases.

Under optimized reaction conditions, a gram-scale reaction was carried out between **1.1a** and **1.3a**, resulting in the synthesis of 1.039 g of **1.4a** in a 71% yield. The method's synthetic potential is demonstrated by this transformation, highlighting its applicability in industrial scales. (Scheme 1.26).



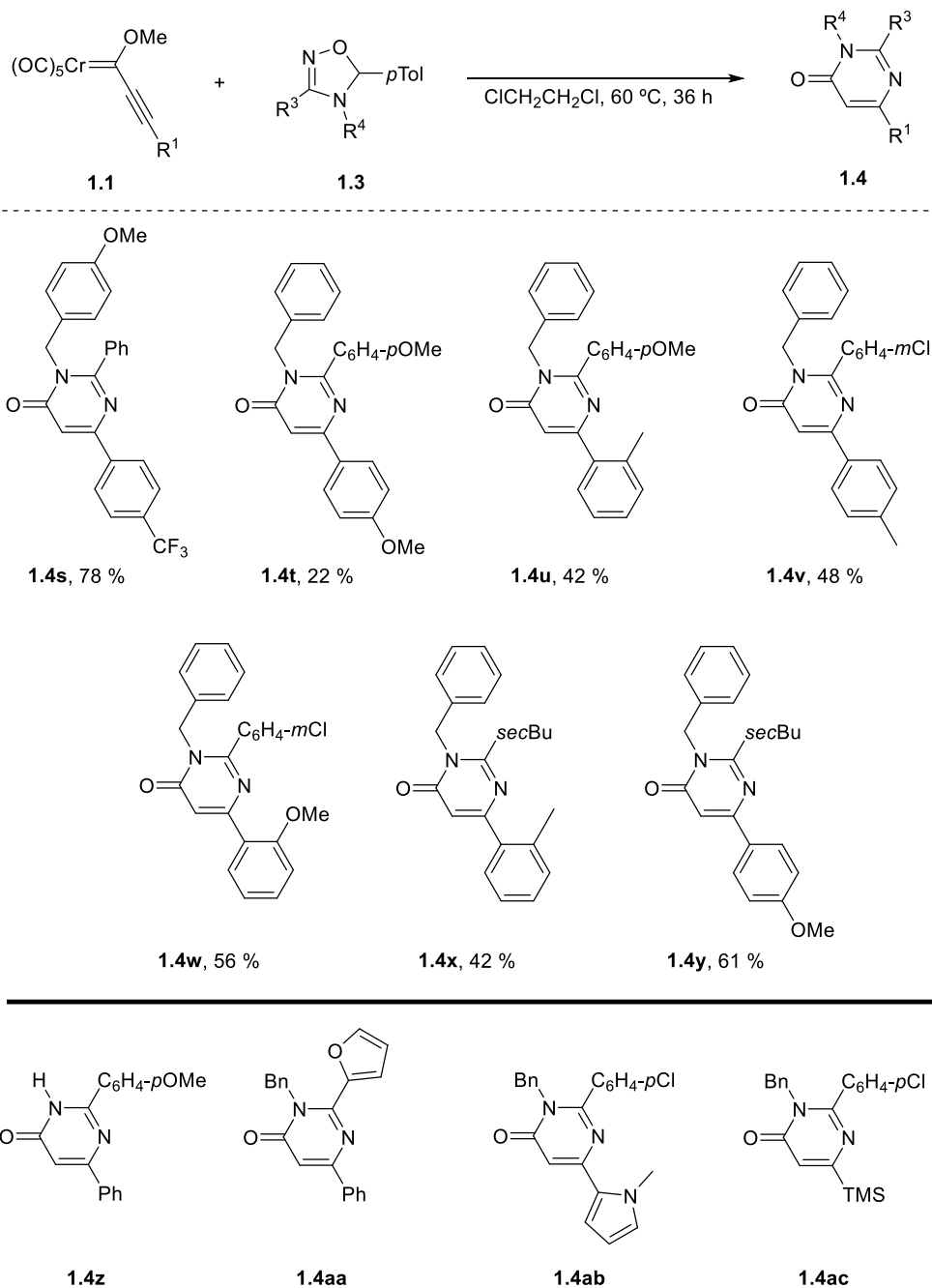
Scheme 1.26: Gram-scale reaction.

Regarding the substitution pattern of the Fischer carbene complex **1.1** (Scheme 1.27), the reaction can tolerate electron-donating (**1.4l**, **m**, **n**) aromatic substituents at that position. Substituents such as *ortho*-substituted phenyl groups (**1.4n**) and heteroaromatics (**1.4o**) can also be used satisfactorily, along with alkenyl (**1.4p**), primary (**1.4r**), and tertiary (**1.4q**) alkyl groups. In all cases, moderate to good yields were observed. In some cases (**1.4o**, **1.4p**), the reaction had to be left for longer period of time until complete consumption of the starting alkynyl-FCC **1.1** was achieved, while in other cases, particularly for aromatic substituents bearing electron-donating groups at *para*-position (**1.4l**, **1.4m**), the reaction proceeded faster than for obtaining **1.4a**.

Scheme 1.27: Scope of position R^1 of alkyne-FCCs.

Scheme 1.28, *top* shows other pyrimidin-4(3H)-ones **1.4** that were also obtained during the expansion of the scope of the reaction in order to create a sufficiently broad family of compounds to understand the interesting aspects of this reaction. In all cases, yields similar to those shown previously were obtained, except for **1.4t** which was synthesized in a 22 % yield.

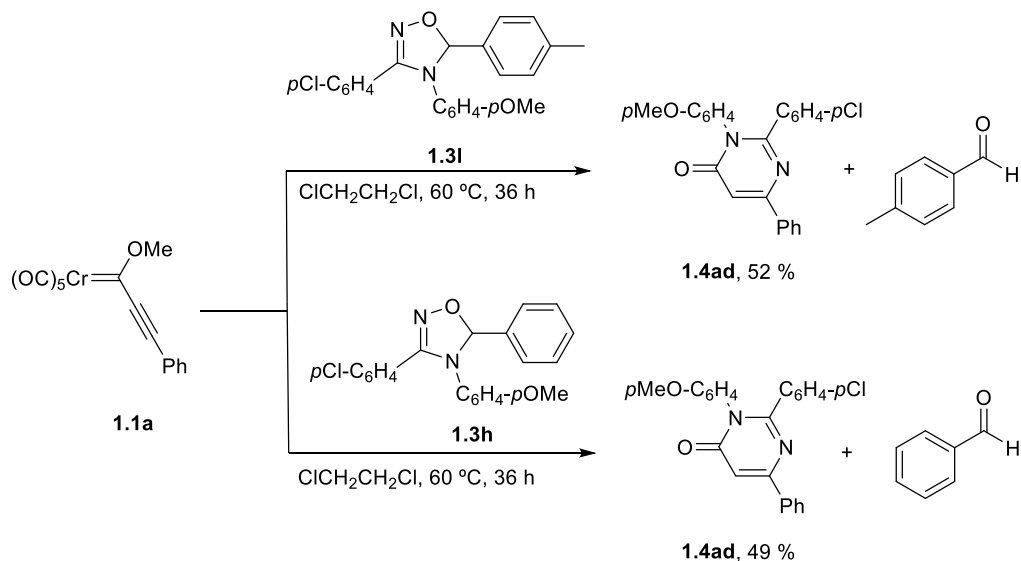
Nevertheless, the [3+3]-cycloaddition could not be achieved in specific cases (Scheme 1.28, *bottom*). The aim was to obtain the derivatives of pyrimidin-4(3H)-one (**1.4z**) unsubstituted at the R^4 position, as well as bearing a furan (**1.4aa**) at the R^3 position, but these options were unsuccessful. Additionally, attempts to introduce another heterocycle, *N*-methylpyrrole (**1.4ab**), at the R^1 position failed, as well as the test made to place the TMS group at the R^1 position (**1.4ac**).



Scheme 1.28: Other combinations tolerated (*top*) and unsuccessful attempts of obtain pyrimidin-4(3*H*)-ones (*bottom*).

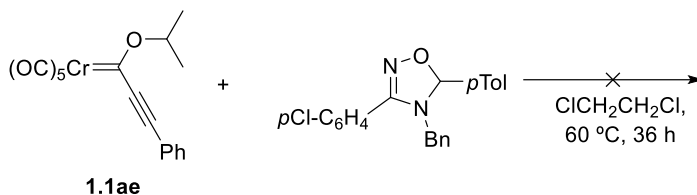
The influence of the group that is released from the 4,5-dihydro-1,2,4-oxadiazole was examined to determine whether it would have any effect on the reaction yield.

For this purpose, two analogous 4,5-dihydro-1,2,4-oxadiazoles **1.3** were synthesized, with two slightly different aromatic groups (Ph, **1.3h** and *p*Tol **1.3i**) at the position of interest (Scheme 1.29). The reactions were carried out under the same optimal conditions, and the yield of the obtained pyrimidin-4(3*H*)-one **1.4ad** was very similar. Therefore, it can be concluded that the nature of the released aromatic aldehyde has little or no influence on the reaction yield, for the cases considered.



Scheme 1.29: Experiment to test the influence of the leaving group.

Other parameter to be analysed, which also may give some hints about the reaction mechanism, is the influence of the alkoxy group of the alkynyl-FCC **1.1**. For this purpose, carbene **1.1ae** with a bulkier group, such as *i*Pr, was subjected to the reaction conditions (Scheme 1.30). No defined product was obtained in this case even at a longer period of time, observing eventually decomposition of the carbene. Therefore, it can be concluded that the presence of a bulkier group at that position inhibits the reaction under study. It is important to note that a bulky alkoxy substituent hinders the attack at the carbene carbon.



Scheme 1.30: Study of influence of alkoxy group on reaction development.

3.5 Reaction mechanism.

After considering all the aforementioned information, a reaction mechanism was proposed (Scheme 1.31). It must begin with the more nucleophilic sp^2 N atom of the 4,5-dihydro-1,2,4-oxadiazole **1.3** moiety undergoing an initial 1,4-addition to the β -carbon atom of the triple bond of alkynyl-FCC **1.1**, which would result in the formation of zwitterionic species **1.I**.^{11,34}

Subsequently, the allenyl metalate **1.I** would undergo evolution via a cyclization step that would involve a [1,2]-pentacarbonylmetal migration to form a (2*H*)-1,3,5-oxadiazocinium intermediate **1.II** (Route A). While ring closure to medium-sized rings involving a [1,2]-Cr shift is a well-documented reaction,³⁵ the formation of an eight-membered ring intermediate as proposed here is unprecedented. It should be noted that the use of a carbene complex with a bulky alkoxy group (as shown in Scheme 1.30) would prevent this step from proceeding.

Next, a 6π -electrocyclization reaction would lead to the formation of metalated 6-methoxy-7-oxa-1,3-diazabicyclo[4.2.0]octa-2,4-dien-1-ium **1.III**,³⁶ which would undergo the elimination of the corresponding aldehyde to produce a new

¹¹ Wulff, W. D.; Faron, K. L.; Su, J.; Springer, J. P.; Rheingold, A. L. *J. Chem. Soc. Perkin. Trans.* **1997**, *1*, 197-199.

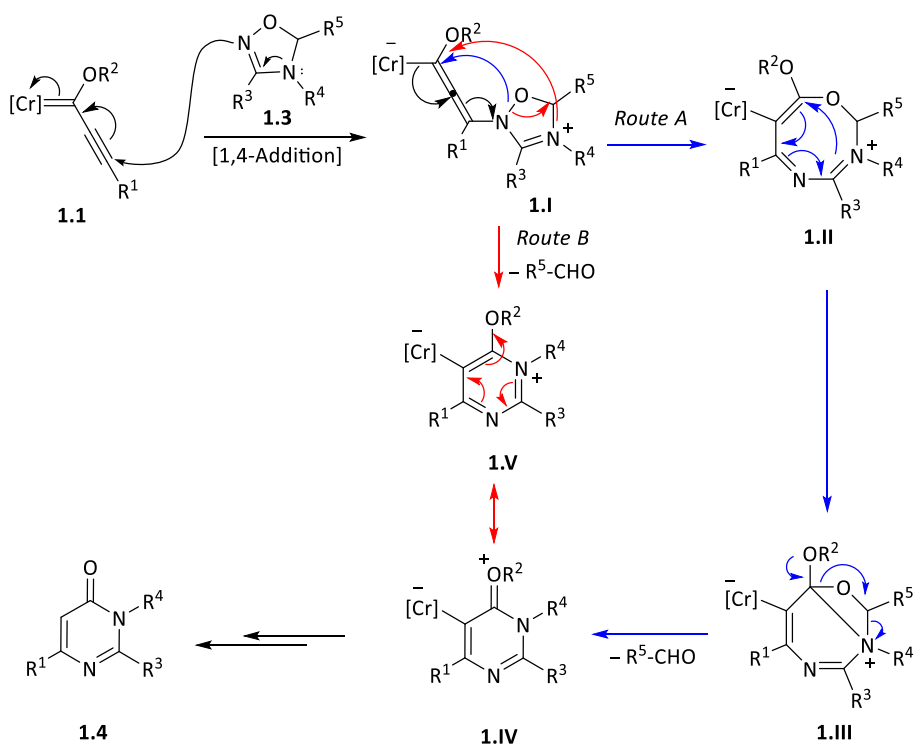
³⁴ a) Santiago, A.; Gómez-Gallego, M.; Ramírez de Arellano, C.; Sierra, M. A. *Chem. Commun.* **2013**, *49*, 1112-1114; b) Giner, E. A.; Santiago, A.; Gómez-Gallego, M.; Ramírez de Arellano, C.; Poulten, R. C.; Whittlesey, M. K.; Sierra, M. A. *Inorg. Chem.* **2015**, *54*, 5450-5461.

³⁵ a) Barluenga, J.; Tomás, M.; Ballesteros, A.; Santamaría, J.; Carbajo, R. J.; López-Ortiz, F.; García-Granda, S.; Pertierra, P. *Chem. Eur. J.*, **1996**, *2*, 88-97; b) Barluenga, J.; Martínez, S.; Suárez-Sobrino, Á. L.; Tomás, M. *J. Am. Chem. Soc.* **2002**, *124*, 5948-5949; c) Barluenga, J.; Martínez, S.; Suárez-Sobrino, Á. L.; Tomás, M. *Organometallics* **2006**, *25*, 2337-2343; d) Gómez, A.; Funes-Ardoiz, I.; Sampedro, D.; Santamaría, J. *Org. Lett.* **2018**, *20*, 4099-4102.

³⁶ García-García, P.; Fernández-Rodríguez, M. A.; Aguilar, E. *Angew. Chem. Int. Ed.* **2009**, *48*, 5534-5537.

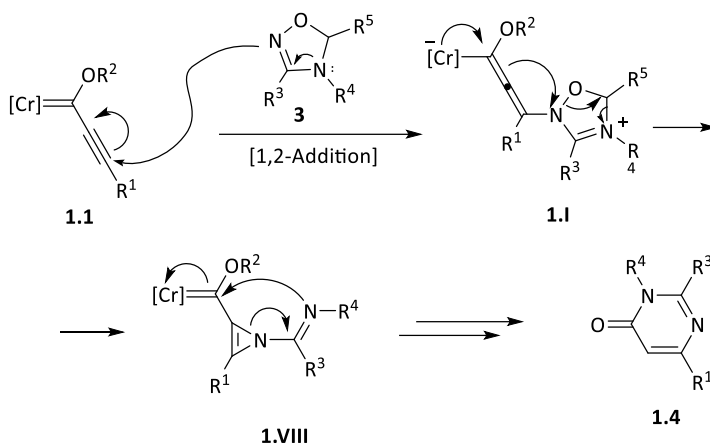
zwitterionic pyrimidine derivative **1.IV**. Finally, protodemetalation of intermediate **1.IV** would lead to the isolation of pyrimidin-4(3*H*)-one **1.4**.

Although this may be the most plausible mechanism, based on experimental evidence in the literature for similar reactions as discussed earlier, an alternative pathway (*Route B*) cannot be ruled out. The different approach involves the formation of intermediate **1.IV** directly through the advancement of intermediate **1.I** to **1.V** in a concerted process, which is a resonant form of intermediate **1.IV**, ultimately leading to the formation of the final product **1.4**.



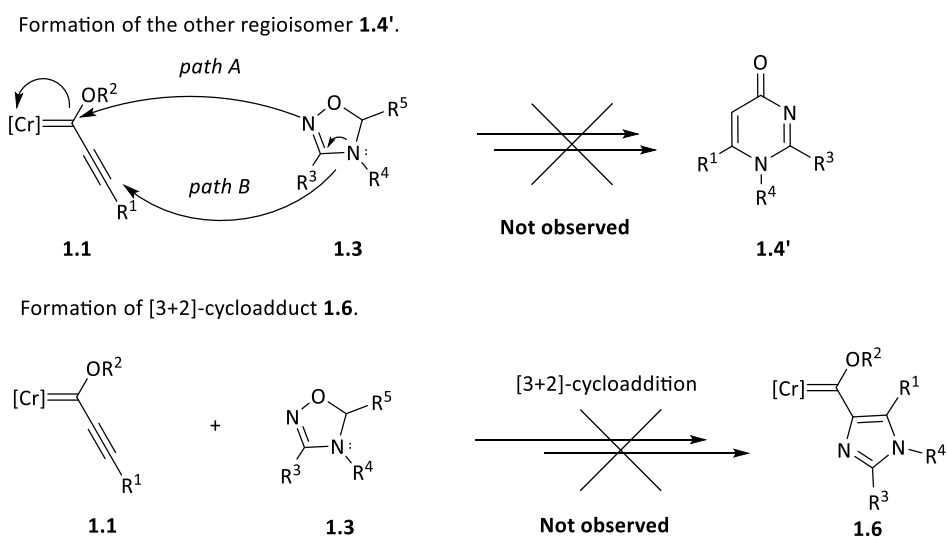
Scheme 1.31: Proposed mechanism of the reaction.

Another alternative mechanism also initially considered would involve the formation of the final product **1.4** via an intermediate containing an azirine ring **1.VIII**. This intermediate would be formed through the evolution of intermediate **I** with releasing of the aldehyde moiety (Scheme 1.32). Nevertheless, this mechanism is less probable based on the known reactivity of FCCs.



Scheme 1.32: Alternative mechanisms initially considered for the reaction through azirine intermediate **1.VIII**.

In addition, based on the experimental results, where there is no evidence of the formation of regioisomers **1.4'** (Scheme 1.33, *top*) or the cycloadduct **1.6** (Scheme 1.33, *bottom*), the following mechanistic options were discarded. In the first case, the regioisomers **1.4'** could be formed either by nucleophilic attack of the sp N to the carbene carbon (*path A*) or, less probable, through attack of the sp^2 N to the β position of the alkyne as well (*path B*). On the other hand, no [3+2]-cycloaddition occurs as cycloadduct **1.6** (or its regioisomer) is not detected.



Scheme 1.33: Alternative discarded mechanisms for this transformation.

In order to gather evidence supporting any of the possible mechanism intermediates, a reaction was conducted in a Schlenk flask using the same model substrates **1.1a** and **1.2a** and monitored by NMR. The reaction was carried out at room temperature in 1,2-dichloroethane, following the standard procedure described before. After one day, a sample was transferred to an NMR tube and a capillary tube of D₂O was introduced to record a ¹H-NMR spectrum with solvent suppression.

Two approaches were taken to monitor the reaction. Firstly, the initial NMR sample was left under the reaction conditions and monitored daily. Secondly, a fresh sample was taken from the reaction flask every day and a new ¹H-NMR spectrum was recorded using a new NMR tube and a capillary tube of D₂O. The second approach provided cleaner and more significant spectra than the first one. Therefore, these spectra will be used for further analysis discussion (Figure 1.5).

The piled spectra were obtained over a 3-day period for monitoring the formation of the final product. The red marks indicate the signals that correspond to 4,5-dihydro-1,2,4-oxadiazole **1.3a**. The green marks represent the extruded *p*-tolualdehyde, while the purple mark indicates the final product **1.4a**. The blue marks represent the signals of the possible intermediate detected represented by **1.I**. There are two regions of the spectra that provide significant information in this study. The first region corresponds to the aromatic methyl groups between 2.0-2.4 ppm (*p*Tol region), and the second region (benzyl region) corresponds to benzyl protons around 4.0-4.5 ppm.

On the first day, three signals on the *p*Tol region of the spectrum that correspond to the 4,5-dihydro-1,2,4-oxadiazole **1.3a**, to the possible intermediate **I** and to the extruded *p*-tolualdehyde are observed. Moreover, one signal around 4 ppm that corresponds to the benzylic protons and one signal around 6 ppm that is assigned to the CH proton, both belonging to the 4,5-dihydro-1,2,4-oxadiazole **1.3a**, are also observed. In addition, different signals that correspond to the pyrimidin-4(3*H*)-one **1.4** also appear. Finally, a singlet around 10 ppm that correspond to the proton of the extruded *p*-tolualdehyde is detected.

On the second day, the signals for *p*-tolualdehyde, the intermediate, and the final product increase, while the signals for the starting material decrease, indicating the expected progression of the reaction.

By day 3, the signal for the intermediate do not increase at the same rate as before. In fact, the intensity of the intermediate signal is much smaller than that of

p-tolualdehyde, unlike on day 2, where they are similar. This suggests that the intermediate is evolving into the final product.

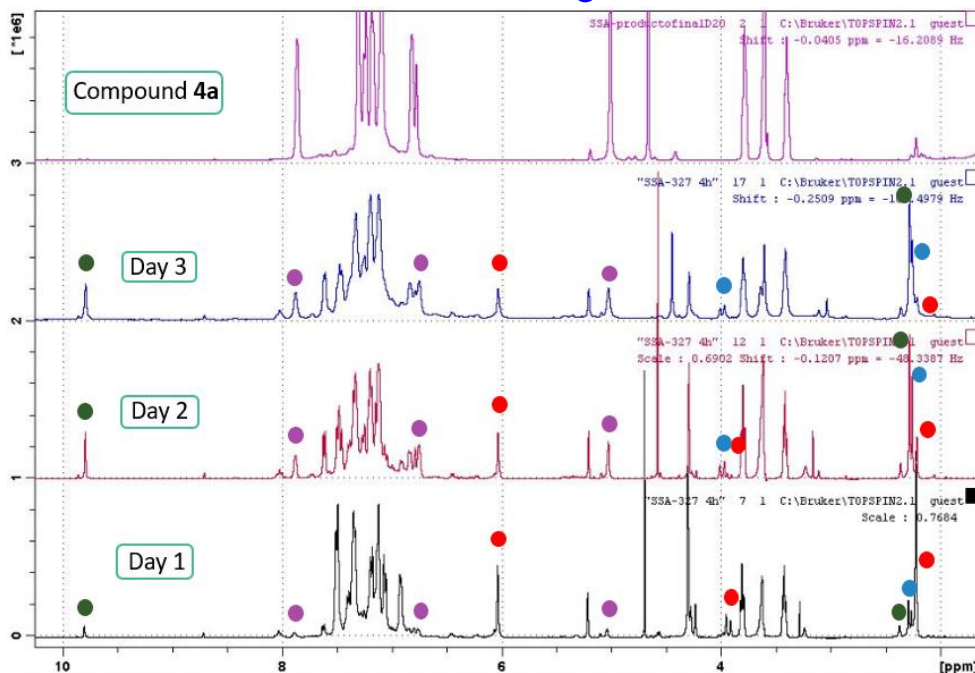
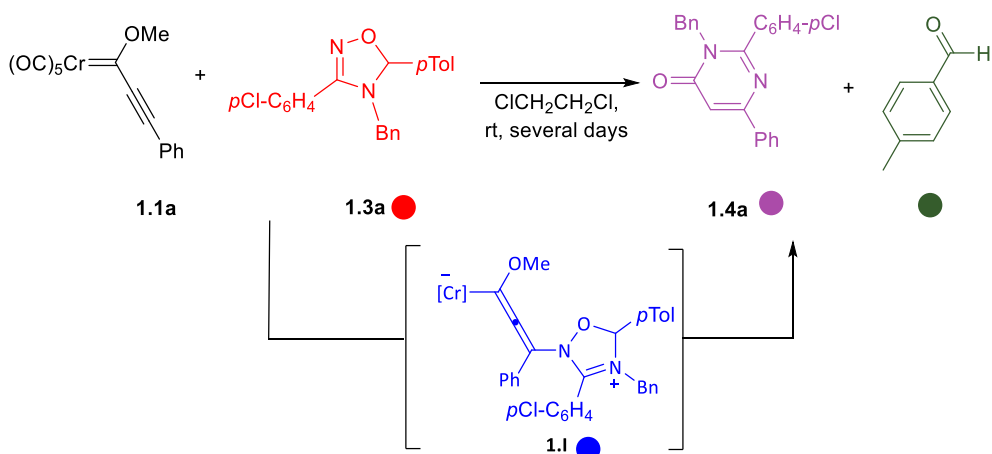


Figure 1.5: $^1\text{H-NMR}$ spectra with solvent suppression piled at 1 to 3 days and the final product.

Going in detail to the regions mentioned before, in the 4,5-dihydro-1,2,4-oxadiazole and the released *p*-tolualdehyde, there is an aromatic methyl group, which is absent in the final product. Hence, in the *p*Tol region (Figure 1.6, right) in addition to the signals corresponding to these two species (red and green marks, Figure 1.5), a new signal (blue mark) that appears initially (day 1), grows (days 1-3)

and then decreases gradually (day 3-7) is observed. This signal can be assigned to the reaction intermediate.

Regarding the benzyl region (Figure 1.6, *left*), the protons appear as an AB quartet in the starting material due to their diastereotopicity because of the presence of a stereocenter. However, in the final product, they appear as a singlet because there is no stereocenter. It is important to note that a new signal (blue mark), which also appears as an AB quartet, is observed in that region. This signal can be also assigned to the reaction intermediate, as it follows the same trend as the previously described methyl group.

Based on these findings, we conclude that the observed reaction intermediate should contain diastereotopic benzyl protons and an aromatic methyl group. Therefore, allenyl metallate **1.1** marked in blue in Figure 1.5 is the most possible representation of such reaction intermediate. However, it could not be confirmed as no signal for the allenyl carbon could be observed in the ^{13}C NMR spectra. No other intermediate was detected in the NMR experiments.

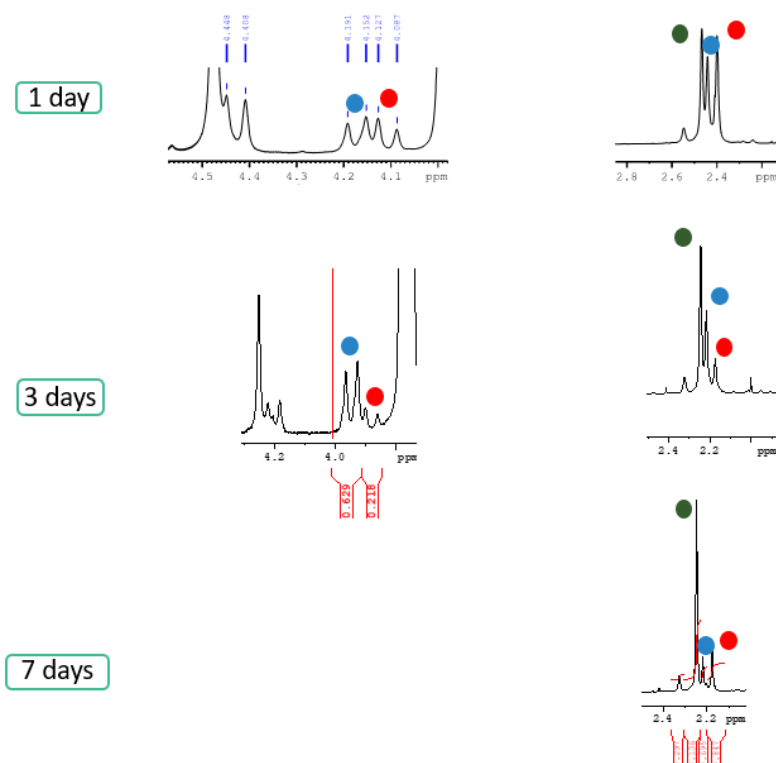


Figure 1.6: Expansions of selected signals (Days 1, 3, 7) in the ^1H -NMR spectra.

Therefore, although attempts were made to elucidate the structure of the intermediate detected, the collected NMR evidences were inconclusive, and the identity of the true intermediate remains unclear.

4 Conclusions.

A [3+3]-cycloaddition reaction has been described, using chromium alkoxy alkynyl carbene complexes and 4,5-dihydro-1,2,4-oxadiazoles to synthesize pyrimidin-4(3*H*)-ones. These findings represent the first reported example of 4,5-dihydro-1,2,4-oxadiazole participating in a [3+3]-cycloaddition reaction.

The study presents a reliable method for synthesizing pyrimidin-4(3*H*)-ones with moderate to good yields. The transformation demonstrated tolerance towards a broad range of substitution patterns in both aromatic and aliphatic moieties in various positions of the scaffold.

The [3+2]-cycloaddition product **1.6**, as well as the other possible regioisomer **1.4'**, have never been detected, indicating that the reaction proceeds with complete regio- and chemoselectivity.

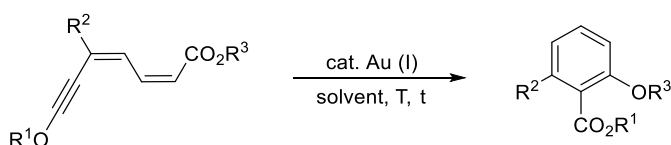
The proposed mechanism for this transformation would involve the formation of an allenyl metalate intermediate that would further evolve either in a concerted manner or through an eight-membered ring intermediate to produce the final pyrimidin-4(3*H*)-ones.

Chapter II:

Gold-catalysed cycloaromatization of “*push-pull*” alkyl (and silyl) 2,4-dien-6-yne carboxylates. Synthesis of alkyl 6-substituted 2-alkoxybenzoate derivatives.

1 Introduction.

In this section, a cycloaromatization with unusual topology of “push-pull” 2,4-dien-6-ynecarboxylic esters, catalysed by gold, is explained. The process results in alkyl 6-substituted 2-alkoxybenzoates with complete regioselectivity and excellent yields, utilizing only small quantities of gold (I) catalyst. (Scheme 2.1). The reaction's optimal conditions and generality have been explored, as well.

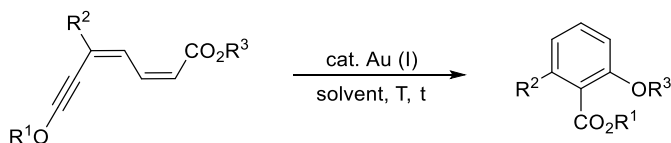


Scheme 2.1: Synthesis of methyl 6-substituted 2-alkoxybenzoates catalysed by gold.

Several theoretical computational studies have been conducted to gain a better understanding of the mechanism involved in this transformation.

2 Bibliographic background.

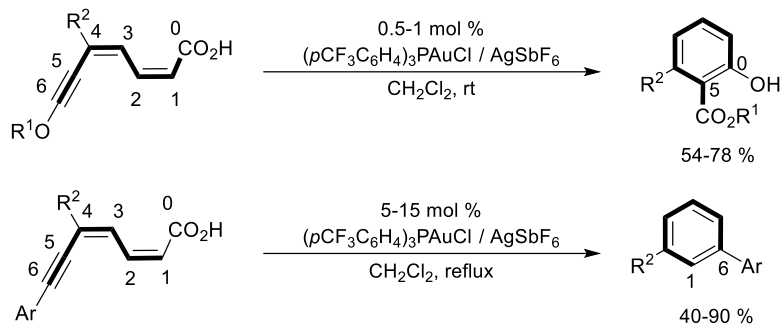
As part of the investigation into the cyclization reaction of "push-pull" 2,4-dien-6-ynecarboxylic esters with ynamides (see *Chapter 3*), it was found that an additional by-product was formed. This by-product was identified as the result of an intramolecular cyclization reaction of "push-pull" 2,4-dien-6-ynecarboxylic esters (as shown in Scheme 2.2).



Scheme 2.2: Gold-catalysed synthesis of alkyl 6-substituted 2-alkoxybenzoates.

In 2009, Aguilar and co-workers published a research on the gold-catalysed cyclization of "push-pull" 2,4-dien-6-ynecarboxylic acids with total regioselectivity and low catalyst amounts to generate alkyl 6-substituted salicylates (Scheme 2.3, *top*).¹ The study revealed an unconventional cycloaromatization process that occurred between carbons 0 and 5, instead of the expected reaction between carbons 1 and 6 which takes place for common 2,4-dien-6-ynecarboxylic acids (without a donor group in the alkynyl moiety, Scheme 2.3, *bottom*).

¹ García-García, P.; Fernández-Rodríguez, M. A.; Aguilar, E. *Angew. Chem. Int. Ed.* **2009**, *48*, 5534-5537.



Scheme 2.3: Gold-catalysed cycloaromatization of “push-pull” 2,4-dien-6-yne carboxylic acids (*top*) vs non-“push-pull” 2,4-dien-6-yne carboxylic acids (*bottom*).

Since the reaction with the corresponding esters remains unexplored, it was decided to investigate the reaction conditions and its scope, and gain insight into its possible mechanism.

As highlighted in the *General Background* (see pp. 25-28), studies have been conducted on the attack of different nucleophiles, such as *O*-, *N*-, *C*- or other hetero-nucleophiles on gold-activated multiple carbon-carbon bonds. While this cyclization reaction can be categorized as an intramolecular addition of an *O*-nucleophile to an activated triple bond, it yields a carbocycle as the final product.

Specifically, in this section, the intramolecular addition of *C*-nucleophiles will be reviewed, providing a brief summary of the reactivity of 1,*n*-enynes, followed by a more extensive review about cycloisomerizations of 1,3-dien-5-yne, as they are more directly related to the “push-pull” 2,4-dien-6-yne carboxylic esters used as starting materials for the reaction under research in this chapter.

2.1 Reactivity of 1,*n*-enynes.

The most studied reactions in this field are the cycloisomerizations of 1,*n*-enynes, which all together represent a very useful method to form carbon-carbon bonds. These reactions are highly valuable in synthetic organic chemistry, as they allow the creation of intricate molecular structures, through fully intramolecular mechanistically complex processes, but from readily available starting materials.

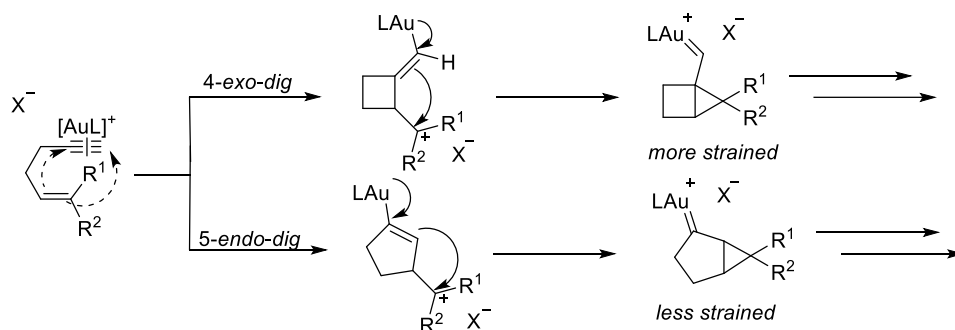
It is important to emphasize that other transition metals have been employed for this kind of transformations. However, they usually activate the alkene and alkyne moieties at the same time via π -coordination, triggering migratory insertion or

metallacycle formation processes.² On the other hand, as gold (I) complexes are linearly bicoordinated, they cannot perform such organometallic steps, forcing these reactions to proceed via carbene intermediates and skeletal rearrangements.

Although 1,*n*-enyne with different chain lengths have been studied, 1,5- and 1,6-enynes continue to be the most widely researched substrates in this field as they provide an entry to 5- and 6-membered carbocycles, with the contributions of Echavarren and his group being particularly noteworthy.³

2.1.1 Cycloisomerization of 1,5-enynes.

Typically, 1,5-enynes undergo endocyclic cycloisomerization reactions. This preference can be explained by the formation of a less strained bicyclo[3.1.0]hexane system in the endocyclic reaction, as opposed to the more strained bicyclo[2.1.0]pentane system that would result from exocyclic reactions (Scheme 2.4). Nevertheless, different strategies have been used to switch the selectivity of the cyclization from *endo-dig* to *exo-dig*.⁴



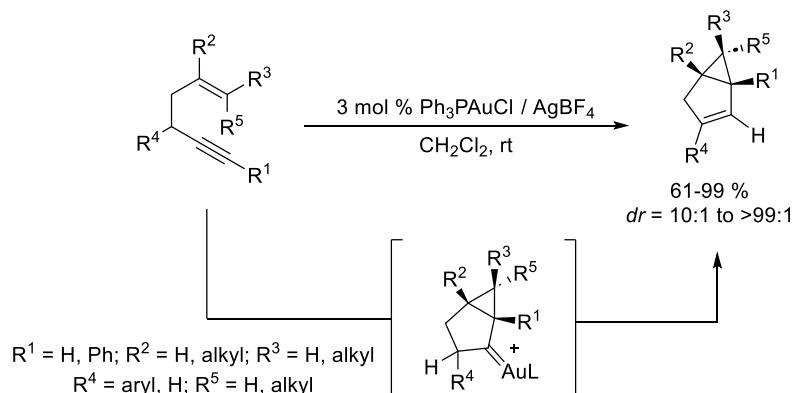
Scheme 2.4: General pathways for the cycloisomerization of 1,5-enynes.

² a) Aubert, C.; Buisine, O.; Malacria, M. *Chem. Rev.* **2002**, *102*, 813-834; b) Marinetti, A.; Jullien, H.; Voituriez, A. *Chem. Soc. Rev.* **2012**, *41*, 4884-4908; c) Muratore, M. E.; Homs, A.; Obradors, C.; Echavarren, A. M. *Chem. Asian. J.* **2014**, *9*, 3066-3082; d) Stathakis, C. I.; Gkizis, P. L.; Zografos, A. L. *Nat. Prod. Rep.* **2016**, *33*, 1093-1117.

³ For selected reviews of 1,*n*-enyne cycloisomerization, see: a) Obradors, C.; Echavarren, A. M. *Acc. Chem. Res.* **2014**, *47*, 902-912; b) Dorel, R.; Echavarren, A. M. *Chem. Rev.* **2015**, *115*, 9028-9072; c) Marín-Luna, M.; Nieto, O.; Silva, C. *Front. Chem.* **2019**, *7*, 1-22.

⁴ a) Shibata, T.; Ueno, Y.; Kanda, K. *Synlett* **2006**, *3*, 411-414; b) Sanjuan, A. M.; Rashid, M. A.; García-García, P.; Martínez-Cuevas, A.; Fernández Rodríguez, M. A.; Rodríguez, F.; Sang, R. *Chem. - Eur. J.* **2015**, *21*, 3042-3052.

One example of alkyl- and aryl-substituted 1,5-enynes which undergo stereospecific cycloisomerization to produce bicyclo[3.1.0]hexene derivatives is depicted in Scheme 2.5.⁵ The outcome can be attributed to the formation of a gold-carbene intermediate via a 5-*endo-dig* reaction, followed by a [1,2]-hydrogen shift. The stereoselectivity and stereospecificity of the transformation can be explained by half-chair transition states, where the large groups occupy pseudoequatorial positions.



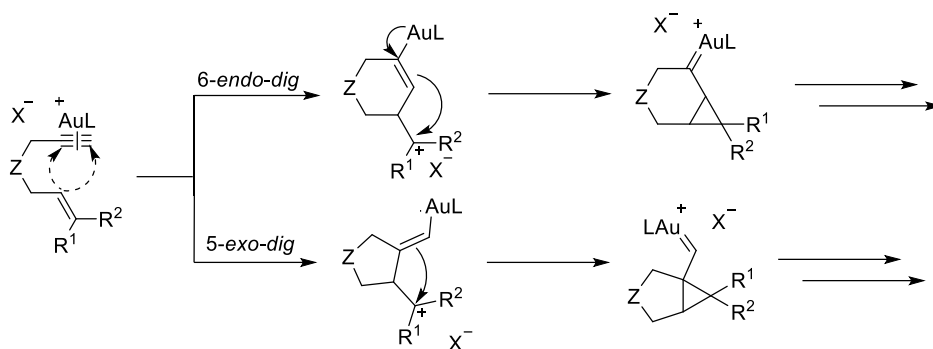
Scheme 2.5: Synthesis of bicyclo[3.1.0]hexenes by *endo-dig* 1,5-enynes cycloisomerization.

2.1.2 Cyloisomerization of 1,6-enynes.

From a mechanistic perspective, the most extensively researched transformations catalysed by gold (I) involve cycloisomerizations of 1,6-enynes. These reactions have frequently served as prototypes for identifying novel processes and catalyst activities. In general terms, in the absence of nucleophiles or directing groups, these reactions follow a 5-*exo-dig* (kinetically favoured for terminal alkynes) or a 6-*endo-dig* (preferred for internal and heteroatom-tethered-alkynes) cyclization mechanism (as shown in Scheme 2.6).⁶ This process involves the generation of a cyclic intermediate through the interaction of the substrate with the gold catalyst, followed by a cascade of bond-breaking and bond-forming events that ultimately lead to the desired product.

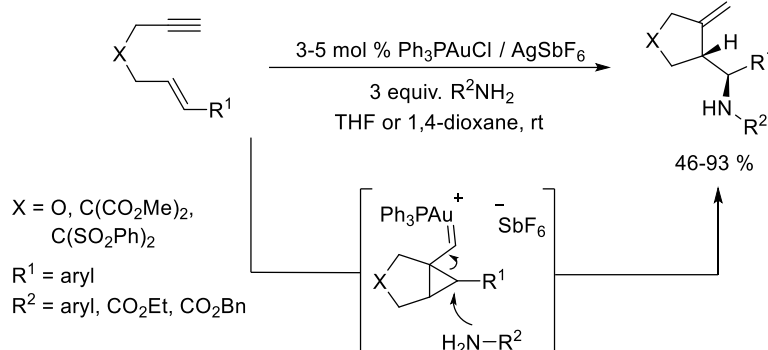
⁵ Luzung, M. R.; Markham, J. P.; Toste, F. D. *J. Am. Chem. Soc.* **2004**, *126*, 10858-10859.

⁶ a) Nieto-Oberhuber, C.; Muñoz, M. P.; Buñuel, E.; Nevado, C.; Cardenas, D. J.; Echavarren, A. M. *Angew. Chem. Int. Ed.* **2004**, *43*, 2402-2406; b) Nieto-Oberhuber, C.; Lopez, S.; Muñoz, M. P.; Cardenas, D. J.; Buñuel, E.; Nevado, C.; Echavarren, A. M. *Angew. Chem. Int. Ed.* **2005**, *44*, 6146-6148; c) Escribano-Cuesta, A.; Perez-Galán, P.; Herrero-Gómez, E.; Sekine, M.; Braga, A. A. C.; Maseras, F.; Echavarren, A. M. *Org. Biomol. Chem.* **2012**, *10*, 6105-6111.



Scheme 2.6: General pathways for the cycloisomerization of 1,6-enynes.

1,*n*-Enynes exhibit a shared reactivity pattern that includes the trapping of cyclopropyl gold carbenes via cyclopropanation, C-H insertion, or nucleophilic addition, besides skeletal rearrangement.⁷ Scheme 2.7 illustrates a 1,6-enyne aminocyclization process.⁸ The formation of a cyclopropyl gold carbene intermediate is followed by a conjugated addition of the amine to generate the final product.



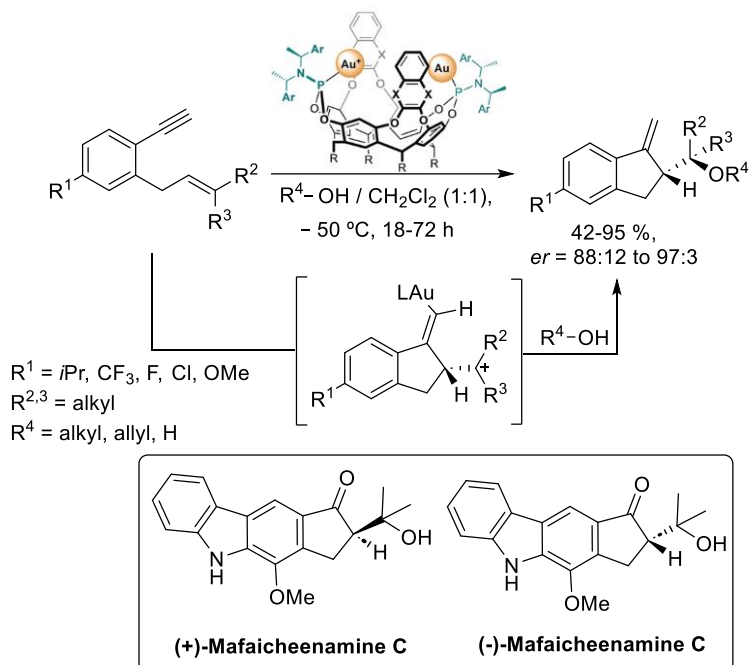
Scheme 2.7: Cycloisomerization of a 1,6-enyne followed by intermolecular trapping.

Echavarren and co-workers have conducted experimental and computational investigations to elucidate the reaction mechanisms, applying them to achieve gold

⁷ a) Pérez-Galán, P.; Waldmann, H.; Kumar, K. *Tetrahedron* **2016**, *72*, 3647-3652; b) Bao, M.; Lu, W.; Cai, Y.; Qiu, L.; Xu, X. *J. Org. Chem.* **2017**, *82*, 13386-13395; c) Davenel, V.; Nisole, C.; Fontaina-Vive, F.; Fourquez, J. -M.; Chollet, A. -M.; Michelet, V. *J. Org. Chem.* **2020**, *85*, 12657-12669.

⁸ Leseurre, L.; Toullec, P. Y.; Genêt, J.-P.; Michelet, V. *Org. Lett.* **2007**, *9*, 4049-4052.

catalysts with enhanced reaction selectivity.⁹ A remarkable consequence of their findings is illustrated in Scheme 2.8, not only due to the use of these new chiral gold catalysts to obtain indene derivatives with high selectivity, but also because this approach allows the synthesis of carbazole alkaloid (+)-mafaicheenamine C and its enantiomer in high *er*.¹⁰



Scheme 2.8: Enantioselective alkoxy cyclization of 1,6-enynes.

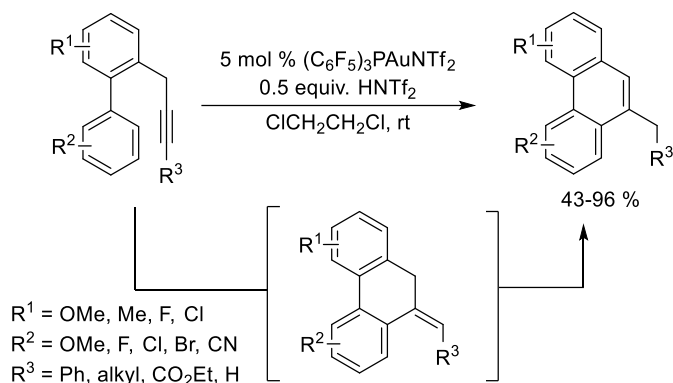
2.1.3 Alkyne hydroarylation.

Hydroarylation reactions catalysed by gold have also been important transformations in the reactivity of enynes. From a mechanistic point of view, it can be described either as a Friedel-Crafts process or, alternatively, through the formation of a gold cyclopropylcarbene intermediate. In this reaction, a C–C bond is

⁹ a) Jiménez-Núñez, E.; Echavarren, A. M. *Chem. Rev.* **2008**, *108*, 3326-3350; b) Pérez-Galán, P.; López-Carrillo, V.; Echavarren, A. M. *Contrib. Sci.* **2010**, *6*, 143-153; c) Zuccarello, G.; Mayans, J. G.; Escofet, I.; Scharnagel, D.; Kirillova, M. S.; Pérez-Jimeno, A. H.; Calleja, P.; Boothe, J. R.; Echavarren, A. M. *J. Am. Chem. Soc.* **2019**, *141*, 11858-11863; d) Zuccarello, G.; Zanini, M.; Echavarren, A. M. *Isr. J. Chem.* **2020**, *60*, 360-372.

¹⁰ Martín-Torres, I.; Ogalla, G.; Yang, J. -M.; Rinaldi, A.; Echavarren, A. M. *Angew. Chem. Int. Ed.* **2021**, *60*, 9339-9344.

formed between an aromatic ring (which, if electron-rich, is more prone to act as a nucleophile) and a gold-activated alkyne.¹¹ In the example presented in Scheme 2.9, phenanthrene derivatives are formed by a 6-*exo-dig* hydroarylation reaction of *o*-propargylbiaryls.¹²



Scheme 2.9: Synthesis of phenanthrenes by 6-*exo-dig* hydroarylation.

2.2 Cycloisomerization reactions of 1,3-dien-5-yne.

1,3-Dien-5-yne are highly versatile conjugated dienyne with a rich reactivity, being involved in a wide variety of cyclization reactions that have been applied to the formation of carbocycles of different sizes, as well as heterocycles.¹³ This review will focus on the synthesis of 6-membered rings, as they are directly related to the reaction that will be developed in this chapter.

According to García-García and co-workers,^{13c} three different groups of cycloaromatization reactions can be established, for 1,3-dien-5-yne. Firstly, the classical [1,6]-cycloaromatizations, where the new bond is created between the terminal carbon of the external alkene and the terminal carbon of the alkyne, and all

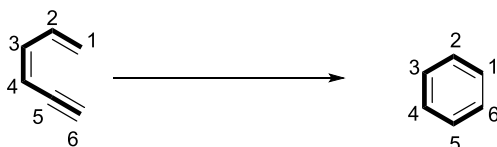
¹¹ a) Liu, X.-Y.; Che, C.-M. *Angew. Chem. Int. Ed.* **2008**, *47*, 3805-3810; b) Morán-Poladura, P.; Suárez-Pantiga, S.; Piedrafita, M.; Rubio, E.; González, J. M. *J. Organomet. Chem.* **2011**, *696*, 12-15; c) Aparece, M. D.; Vadola, P. A. *Org. Lett.* **2014**, *16*, 6008-6011; d) Liu, C.; Van Meervelt, L.; Peshkov, V. A.; Van der Eycken, E. V. *Org. Chem. Front.* **2022**, *9*, 4619-4624.

¹² Shu, C.; Li, L.; Chen, C. B.; Shen, H. C.; Ye, L. W. *Chem. - Asian J.* **2014**, *9*, 1525-1529.

¹³ a) Zimmermann, G. *Eur. J. Org. Chem.* **2001**, *3*, 457-471; b) Hitt, D. M.; O'Connor, J. M. *Chem. Rev.* **2011**, *111*, 7904-7922; c) Aguilar, E.; Sanz, R.; Fernández-Rodríguez, M. A.; García-García, P. *Chem. Rev.* **2016**, *116*, 8256-8311.

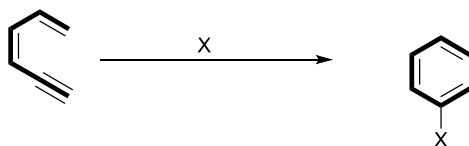
substituents remain bonded to the same carbon as they were in the starting material (Scheme 2.10, *top*). Secondly, cycloaromatizations that also follow a [1,6]-topology, but involve additional transformations, such as incorporation of new moieties or migration of existing groups (Scheme 2.10, *medium*). Finally, cycloaromatizations that do not follow a [1,6]-topology, i.e., those where the six carbon atoms of the new aromatic ring are not the six carbon atoms of the diene-yne skeleton in the starting material (Scheme 2.10, *bottom*). In these cycloisomerizations with unusual topology, products of cycloaromatization can be obtained between carbons 0 and 5 or between carbons 2 and 7, as will be seen later.

Classical [1,6]-cycloaromatization



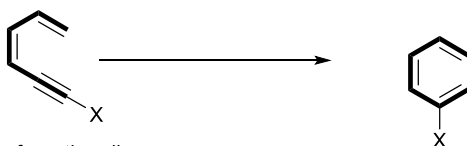
[1,6]-Cycloaromatization involving additional transformations

Cycloaromatization with further transformations

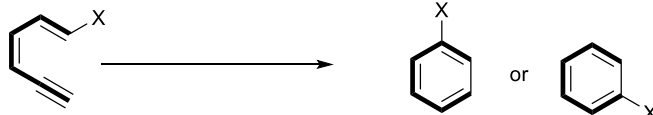


Cycloaromatization with migration

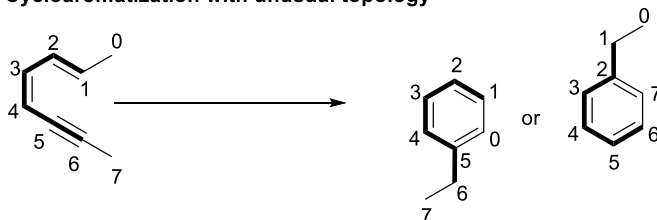
from the alkyne



from the alkene



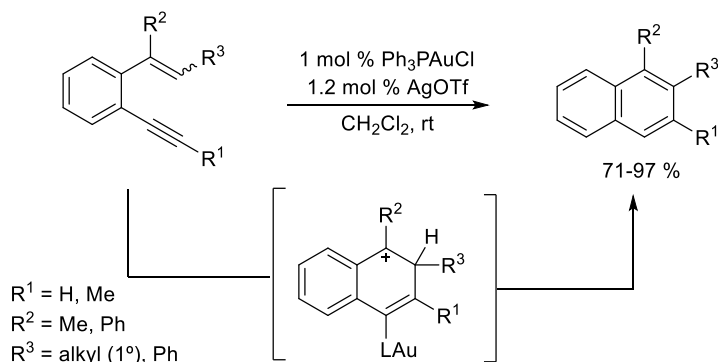
Cycloaromatization with unusual topology



Scheme 2.10: Classification of 1,3-dien-5-yne cycloaromatizations.

2.2.1 Classical [1,6]-cycloisomerizations.

These reactions have been extensively studied, particularly towards the end of the last century. Acid- or base-promoted/catalysed reactions,¹⁴ as well as those catalysed by different metals such as Pt, Pd, or Rh, have been reported.¹⁵ However, as gold is the metal employed in this chapter, an example of gold (I)-catalysed cycloaromatization is provided in Scheme 2.11. A synthesis of 1,2,3-trisubstituted naphthalene derivatives in good to excellent yields through a 6-*endo-dig* cycloaromatization of aromatic 1,3-dien-5-yne that possess a substituent on their alkyne terminus, employing a mixture of Ph₃PAuCl/AgOTf as catalyst, has been reported by Kanda.¹⁶



Scheme 2.11: Gold-catalysed cycloaromatization of *o*-(alkynyl)styrenes.

2.2.2 [1,6]-Cycloaromatizations involving additional transformations.

In these reactions, additional transformations take place alongside the cycloaromatization event, such as the integration of new moieties or the migration or removal of existing groups. As a result, the structure of the final product differs

¹⁴ a) Wang, Y.; Xu, J.; Burton, D. J. *J. Org. Chem.* **2006**, *71*, 7780-7784; b) Mukherjee, A.; Pati, K.; Liu, R.-S. *J. Org. Chem.* **2009**, *74*, 6311-6314; c) Zhao, G.; Zhang, Q.; Zhou, H. *Adv. Synth. Catal.* **2013**, *355*, 3492-3496; d) Mitsudo, K.; Sato, H.; Yamasaki, A.; Kamimoto, N.; Goto, J.; Mandai, H.; Suga, S. *Org. Lett.* **2015**, *17*, 4858-4861.

¹⁵ a) Kang, D.; Kim, J.; Oh, S.; Lee, P. H. *Org. Lett.* **2012**, *14*, 5636-5639; b) Kozma, Á.; Deden, T.; Carreras, J.; Wille, C.; Petuskova, J.; Rust, J.; Alcarazo, M. *Chem. - Eur. J.* **2014**, *20*, 2208-2214; c) Kinoshita, H.; Tohjima, T.; Miura, K. *Org. Lett.* **2014**, *16*, 4762-4765.

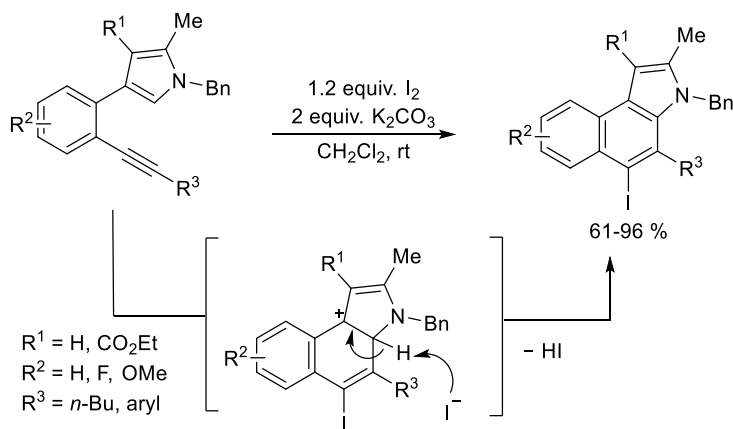
¹⁶ Shibata, T.; Ueno, Y.; Kanda, K. *Synlett* **2006**, *3*, 411-414.

from what would be produced through a "conventional" cycloaromatization, in terms of the number and/or position of substituents.

- **Cycloaromatizations accompanied by further functionalization.**

One of the most significant transformations of this type is the halocycloaromatization reaction, which involves activating the triple bond through coordination with a halogen atom.¹⁷ The process is similar to the previously mentioned metal-catalysed transformations, but in this case, the halogen atom becomes part of the cyclized product. However, there are a few differences with the metal-catalysed reaction, in which the catalyst is used in small amounts and the final product does not contain the metal moiety, because a protodemetalation process takes place and leads to the regeneration of the catalytic species.

In this regard, Scheme 2.12 shows a halocycloaromatization of 4-(2-alkynylaryl)pyrroles using I₂ as promotor of the reaction, activating the C-C triple bond, to produce 3*H*-benzo[*e*]indoles, where the iodine atom is finally incorporated at position 5.¹⁸

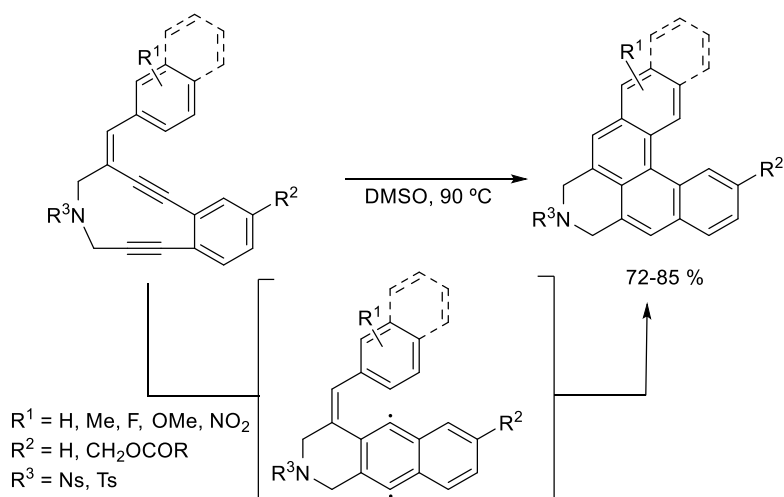


Scheme 2.12: Synthesis of the 5-iodo 3*H*-benzo[*e*]indoles by iodocyclization.

¹⁷ a) Crone, B.; Kirsch, S. F.; Umland, K.-D. *Angew. Chem. Int. Ed.* **2010**, *49*, 4661-4664; b) Yan, Q.; Cai, K.; Zhang, C.; Zhao, D. *Org. Lett.* **2012**, *14*, 4654-4657; c) Martins, G. M.; Zeni, G.; Back, D. F.; Kaufman, T. S.; Silveira *Adv. Synth. Catal.* **2015**, *357*, 3255-3261; d) Zhi, S.; Yao, H.; Zhang, W. *Molecules* **2023**, *28*, 1145-1202.

¹⁸ Martins, G. M.; Zeni, G.; Back, D. F.; Kaufman, T. S.; Silveira, C. C. *Adv. Synth. Catal.* **2015**, *357*, 3255-3261.

Another scenario where this type of reaction occurs is when either the alkyne or alkene group of the dienyne are transformed before the cyclization event happens, being more extended the first one.¹⁹ An example of the aforementioned reaction involving previous modification on the alkyne moiety is depicted in Scheme 2.13. Basak and co-workers have described a polycyclization reaction initiated by a Bergman cyclization of an enediyne moiety that includes the alkyne of the 1,3-dien-5-yne. This leads to the formation of a diradical which undergoes cyclization with the external aromatic ring of the initial 1-aryl-1-en-3-yne, resulting in helicene derivatives with varying substitution patterns on the external aromatic rings.²⁰



Scheme 2.13: Synthesis of helicenes initiated by Bergman cyclization.

- **Cycloaromatizations with migration or loss of alkene/alkyne moiety.**

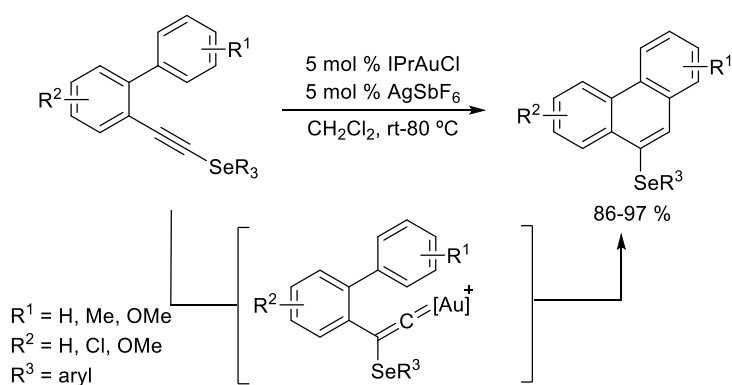
Other changes from the "standard" cycloaromatization category involve a migration phase, being the substituent position in the product of cycloaromatization

¹⁹ a) Saito, K.; Sogou, H.; Suga, T.; Kusama, H.; Iwasawa, N. *J. Am. Chem. Soc.* **2011**, *133*, 689-691; b) Mohamed, R. K.; Mondal, S.; Gold, B.; Evoniuk, C. J.; Banerjee, T.; Hanson, K.; Alabugin, I. V. *J. Am. Chem. Soc.* **2015**, *137*, 6335-6349; c) Pati, K.; Michas, C.; Allenger, D.; Piskun, I.; Coutros, P. S.; dos Passos Gomes, G.; Alabugin, I. V. *J. Org. Chem.* **2015**, *80*, 11706-11717; d) Xu, X.-D.; Cao, T.-T.; Meng, Y.-N.; Zhou, G.; Guo, Z.; Li, Q.; Wei, W.-T. *ACS Sust. Chem. Eng.* **2019**, *7*, 13491-13496; e) Watson, H. A.; Manaviazar, S.; Steeds, H. G.; Hal, K. H. *Tetrahedron* **2020**, *76*, 131061-131082; f) Yuling Lu, Y.; Zhang, J.; Duan, X.; Yang, B.; Zhao, C.; Gu, L.; Chen, C.; Zhu, H.; Ye, Y.; Luo, Z.; Zhang, Y. *J. Org. Chem.* **2023**, *88*, 2393-2403.

²⁰ Roy, S.; Anoop, A.; Biradha, K.; Basak, A. *Angew. Chem. Int. Ed.* **2011**, *50*, 8316-8319.

different from the initially expected one. The group that migrates can be a substituent of either the triple²¹ or the double bond.²² Additionally, in specific instances, the loss of a substituent during the cycloaromatization process has been reported.²³

Scheme 2.14 showcases an example where a selenyl group migration in the alkynyl moiety concurrently takes place during the cycloaromatization process under gold catalysis, likely involving a vinylidene intermediate. As a result, selenylphenanthrenes with diverse substitutions at both arene rings can be produced in very good yields.²⁴



Scheme 2.14: Cycloaromatization accompanied of selenyl group migration of *o*-(selenylalkynyl)biphenyls.

On the other hand, Scheme 2.15 shows a reaction leading to cycloaromatization with [1,2]-migration of one of the double bond substituents.²⁵ The reaction starts

²¹ a) Nakae, T.; Ohnishi, R.; Kitahata, Y.; Soukawa, T.; Sato, H.; Mori, S.; Okujima, T.; Uno, H.; Sakaguchi, H. *Tetrahedron Lett.* **2012**, *53*, 1617-1619; b) Huang, G.; Cheng, B.; Xu, L.; Li, Y.; Xia, Y. *Chem. -Eur. J.* **2012**, *18*, 5401-5415; c) Johansen, T.; Golz, C.; Alcarazo, M. *Angew. Chem. Int. Ed.* **2020**, *59*, 22779-22784.

²² a) Lian, J.-J.; Odedra, A.; Wu, C.-J.; Liu, R.-S. *J. Am. Chem. Soc.* **2005**, *127*, 4186-4187; b) Khosravi, H.; Ghazvini, H. J.; Kamangar, M.; Rominger, F.; Balalaie, S. *Chem. Comm.* **2022**, *58*, 2164-2167.

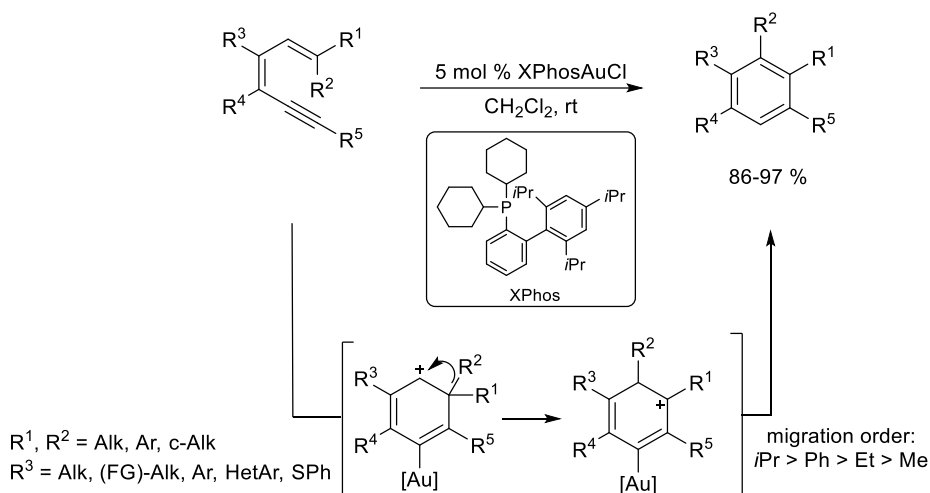
²³ a) Matsumoto, S.; Takase, K.; Ogura, K. *J. Org. Chem.* **2008**, *73*, 1726-1731; b) Saito, K.; Sogou, H.; Suga, T.; Kusama, H.; Iwasawa, N. *J. Am. Chem. Soc.* **2011**, *133*, 689-691; c) Mohamed, R. K.; Mondal, S.; Gold, B.; Evoniuk, C. J.; Banerjee, T.; Hanson, K.; Alabugin, I. V. *J. Am. Chem. Soc.* **2015**, *137*, 6335-6349.

²⁴ Lim, W.; Rhee, Y. H. *Eur. J. Org. Chem.* **2013**, *2013*, 460-464.

²⁵ García-García, P.; Martínez, A.; Sanjuan, A. M.; Fernández-Rodríguez, M. A.; Sanz, R. *Org. Lett.* **2011**, *13*, 4970-4973.

with the nucleophilic attack of the olefin to the gold-coordinated triple bond, generating a carbocation intermediate. Then, the migration of R^2 results in the conversion of a secondary carbocation to a more stable tertiary carbocation. Notably, for these 1,3-dien-5-yne, a conventional cycloaromatization cannot occur as the aromatization by simple proton elimination is prevented due to the disubstitution in one of the carbon atoms of the standard intermediate.

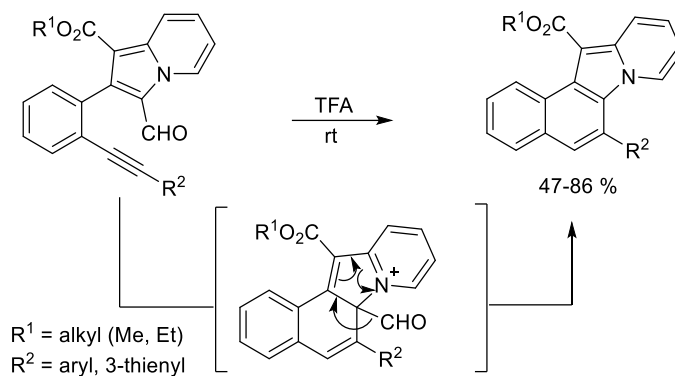
Remarkably, a fully regioselective shift occurs when both substituents at the β position of the double bond are distinct, with groups possessing a greater ability to stabilize positive charge migrating preferentially. This methodology enables the regioselective synthesis of highly substituted benzene rings with various groups located at the five points of diversity, yielding good results.



Scheme 2.15: Gold-catalysed cycloaromatization of 1,3-dien-5-yne accompanied by selective migration from the olefin.

Finally, as an example of substituent loss, Scheme 2.16 depicts a cycloaromatization of 2-[*o*-(alkynyl)phenyl]indolizine-3-carbaldehydes that occurs with concurrent deformylation.²⁶ This process is facilitated by triflic acid at room temperature. The authors propose that the deformylation takes place to restore aromaticity following the initial heteroaryl group attack on the alkyne.

²⁶ Jung, Y.; Kim, I. *Org. Lett.* **2015**, *17*, 4600-4603.



Scheme 2.16: Deformylative cycloaromatization of *o*-(alkynyl)heterobiaryls.

2.2.3 Cycloaromatizations with unusual topology.

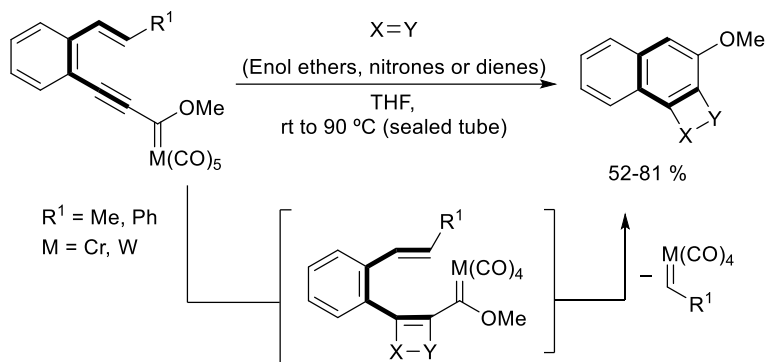
As previously shown, the majority of cycloaromatizations involving 1,3-dien-5-ynes occur with a [1,6]-topology, meaning the resulting aromatic ring incorporates all six carbon atoms of the dienyne system. While rare, other topologies have been observed, being the most common the [0,5]-topology (where a carbon atom linked to the terminal position of the olefin is connected to the internal position of the alkyne),²⁷ but also having a few cases with [2,7]-topology.²⁸

In this sense, in a process that leads to a cycloaromatization product with [2,7]-topology plus additional transformation, Barluenga and co-workers have reported a method for synthesizing naphthalenes fused with various carbo- and heterocycles using *o*-(alkenyl)arylalkynyl Fischer carbene complexes; the resulting aromatic ring incorporates both carbon atoms of the alkyne while excluding the terminal carbon of the olefin. Thus, when exposed to enol ethers, nitrones, or dienes, the aforementioned substrates undergo regioselective [2+2], [3+2], or [4+2]-cycloadditions, respectively, with the alkyne, resulting in intermediate carbene complexes. These intermediates can be converted to naphthalene derivatives through a metathesis process initiated by the dissociation of an irreversible carbonyl ligand upon heating (Scheme 2.17).²⁹

²⁷ a) Bera, K.; Sarkar, S.; Jalal, S.; Jana, U. *J. Org. Chem.* **2012**, *77*, 8780-8786; b) Kondoh, A.; Aoki, T.; Terada, M. *Chem. -Eur. J.* **2015**, *21*, 12577-12580.

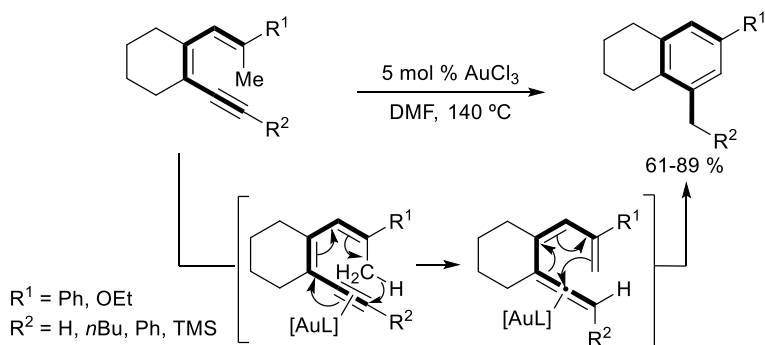
²⁸ Zhang, X.; Feng, C.; Jiang, T.; Li, Y.; Pan, L.; Xu, X. *Org. Lett.* **2015**, *17*, 3576-3579.

²⁹ Barluenga, J.; Andina, F.; Aznar, F.; Valdes, C. *Org. Lett.* **2007**, *9*, 4143-4146.



Scheme 2.17: Synthesis of carbo- and heterocycle-fused naphthalenes from dienyne-tethered Fischer carbene complexes.

Although also scarce, cycloisomerizations with [0,5]-topology are more common. Thus, the metal-catalysed cycloaromatization of 1,3-dien-5-yne that contain internal alkynes and have substituents bearing α -protons on the olefin is described in Scheme 2.18.³⁰ The obtention of the final products involves the formation of a new bond between the α -carbon of one of the substituents on the olefin and the internal carbon atom of the alkyne. Notably, AuCl_3 has been demonstrated to be an effective catalyst for this reaction.

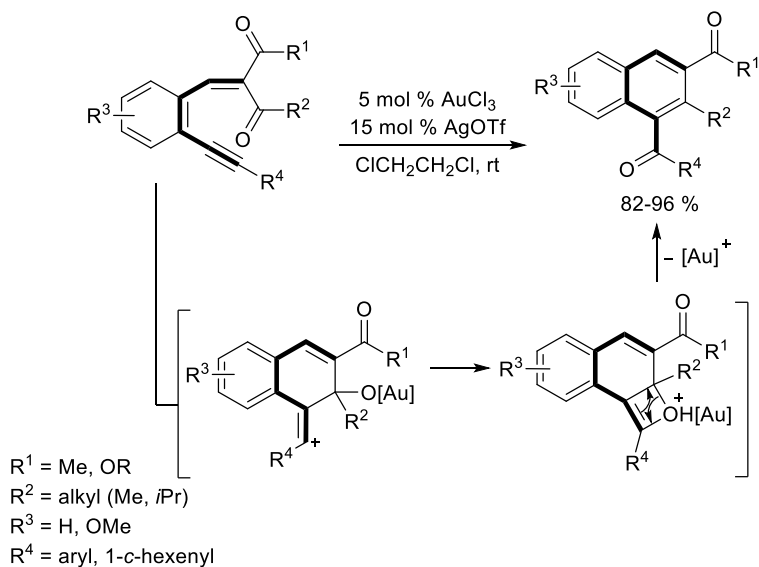


Scheme 2.18: Cycloaromatization of 1,3-dien-5-yne triggered by [1,7]-hydrogen shift.

In Scheme 2.19 *o*-(alkynyl)styrenes with terminal carbonyl substituents in the external olefin are used to obtain naphthalene derivatives. $\text{Au}(\text{OTf})_3$ has been

³⁰ Lian, J.-J.; Lin, C.-C.; Chang, H.-K.; Chen, P.-C.; Liu, R.-S. *J. Am. Chem. Soc.* **2006**, *128*, 9661-9667.

identified as an efficient catalyst for this transformation, in comparison with PtCl_2 or thermal heating.³¹ The authors propose a mechanistic pathway involving a nucleophilic attack of the alkyne on the activated carbonyl group, leading to the generation of an alkenyl cation that is subsequently intramolecularly trapped by the nucleophilic O-[Au] moiety. Finally, a retro-[2+2]-cycloaddition affords the observed naphthalene derivatives.

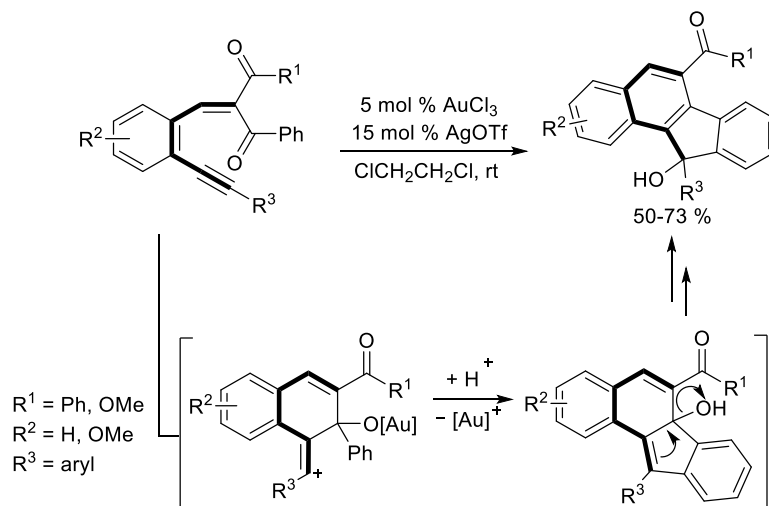


Scheme 2.19: Cycloaromatization of *o*-(alkynyl)styrenes catalysed by gold (III).

When in the previous example R^2 is a phenyl ring, benzo[*a*]fluorene derivatives are obtained from *o*-(alkynyl)styrenes (Scheme 2.20). The reaction, conducted with catalytic amounts of $\text{Au}(\text{OTf})_3$, proceeds efficiently to afford the desired products in moderate to good yields.³² According to the proposed mechanism, the intermediate alkenyl cation undergoes a Friedel-Crafts type cyclization in this case, followed by protodemetalation and double bond isomerization.

³¹ Liu, L.; Zhang, J. *Synthesis* **2014**, *46*, 2133-2142.

³² Liu, L.; Zhang, J. *Angew. Chem. Int. Ed.* **2009**, *48*, 6093-6096.

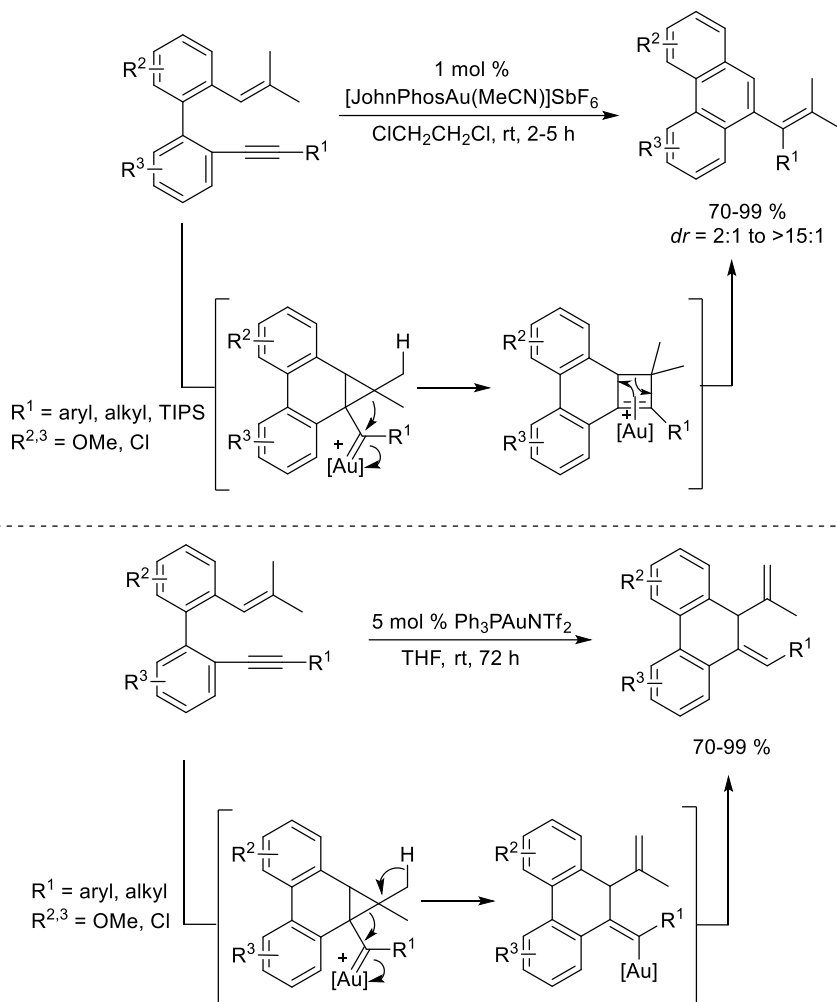


Scheme 2.20: Cycloaromatization of *o*-(alkynyl)styrenes with phenyl ketone substituent in the double bond.

A specific category of 1,7-enynes known as *o*'-alkenyl-*o*-alkynylbiaryls can be subjected to a cycloisomerization reaction with a gold (I) catalyst, resulting in the formation of phenanthrene and dihydrophenanthrene derivatives with high yields. The reaction outcome is significantly influenced by the choice of solvent, which prompts a change in the evolution of the gold intermediate and plays a crucial role in the reaction's success (Scheme 2.21).³³

The authors postulated that the reaction begins by activating the acetylene in the starting enyne upon binding to the gold complex, followed by an intramolecular 6-*exo-dig* nucleophilic addition of the alkene moiety to form a cyclopropylgold (I) carbene intermediate. In the presence of DCE as solvent, the cyclopropyl ring expands to form a cyclobutene-gold (I) complex. Then, this complex undergoes ring opening of the cyclobutene and subsequent demetalation to produce phenanthrene derivatives (Scheme 2.21, *top*). Conversely, when using THF, the cyclopropylgold (I) carbene intermediate experiences proton elimination, generating an alkenylgold species that subsequently undertakes protodemetalation to yield dihydrophenanthrene derivatives bearing an exocyclic double bond (Scheme 2.21, *bottom*).

³³ Milián, A.; García-García, P.; Pérez-Redondo, A.; Sanz, R.; Vaquero, J. J.; Fernández-Rodríguez, M. A. *Org. Lett.* **2020**, *22*, 8464-8469.



Scheme 2.21: Cycloisomerization reaction of *o'*-alkenyl-*o*-alkynylbiaryls using a gold (I) catalyst.

2.3 "Push-pull" 2,4-dien-6-yne.

"Push-pull" 2,4-dien-6-yne derivatives (Figure 2.1) can be regarded as unique 1,3-dien-5-yne because of their electron-donating group that activates the triple bond, and a second conjugated double bond linked to an electron-withdrawing group.³⁴

³⁴ Barluenga, J.; García-García, P.; de Saa, D.; Fernández-Rodríguez, M. A.; Bernardo de la Rúa, R.; Ballesteros, A.; Aguilar, E.; Tomás, M. *Angew. Chem. Int. Ed.* **2007**, *46*, 2610-2612.

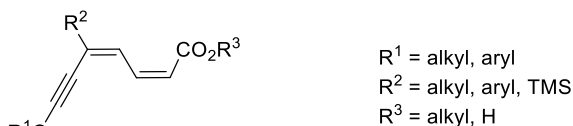
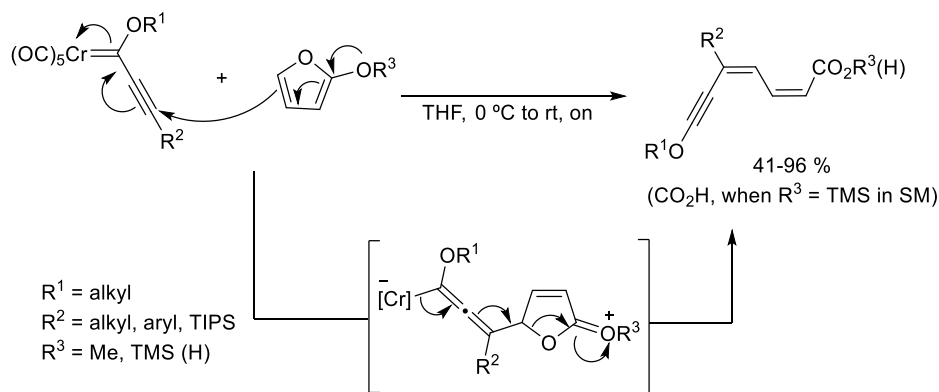


Figure 2.1: "Push-pull" 2,4-dien-6-yne derivatives.

Barluenga, and co-workers have recently studied the synthesis of "push-pull" 2,4-dien-6-yne derivatives and their behaviour as starting materials in cycloaddition and cycloisomerization reactions. They are obtained in good yields just mixing chromium Fischer alkoxyalkynylcarbene complexes and 2-alkoxyfurans (Scheme 2.22).³⁴ According to the proposed mechanism, the reaction is initiated by a Michael-type attack of 2-alkoxyfuran to the triple bond of FCC. This leads to the formation of an allenyl-type metalate intermediate, which subsequently evolves with the opening of the furan ring and loss of metal to obtain the desired "push-pull" 2,4-dien-6-yne derivatives. "Push-pull" 2,4-dien-6-ynecarboxylic acids can be directly synthesized by in-situ desilylation of the corresponding 2,4-dien-6-yne that should be TMS-silylated at the R^3 position when 2-trimethylsilyloxyfuran is employed as starting material; nevertheless, the silylated 2,4-dien-6-yne is never obtained, only observing the carboxylic acid as product.



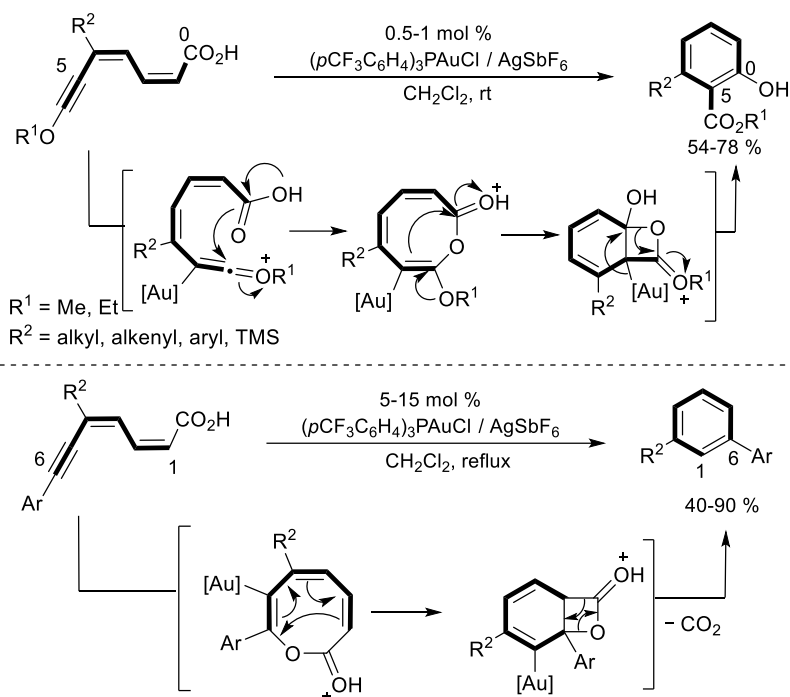
Scheme 2.22: Synthesis of "push-pull" 2,4-dien-6-yne derivatives.

"Push-pull" 2,4-dien-6-ynecarboxylic acids have been shown to undergo cycloaromatization reactions (*see below*), while the carboxylic esters partake mainly in intermolecular cycloaddition reactions, as will be discussed in *Chapter 3*.

In this sense, Aguilar and co-workers have reported on the synthesis of salicylic acid derivatives by a gold-catalysed cycloaromatization of "push-pull" 7-alkoxy-2,4-

dien-6-ynecarboxylic acids (Scheme 2.23, *top*).¹ The reaction employs remarkably low catalyst loadings and is initiated by a nucleophilic attack of the carboxylic acid to the gold-coordinated triple bond, forming an eight-membered-ring intermediate. This is followed by an alkoxy-group-promoted intramolecular attack to the activated carbonyl group, leading to a bicyclic [4.2.0] intermediate. The final product is obtained after ring opening of the four-membered ring with concomitant aromatization.

Interestingly, when an aromatic group is attached to the alkyne moiety, the classic [1,6]-cycloaromatization takes place through an intramolecular cyclization-decarboxylation process (Scheme 2.23, *bottom*). This demonstrates the importance of having an electron-donating group in the alkyne position to achieve a cyclization with [0,5]-topology with these substrates.

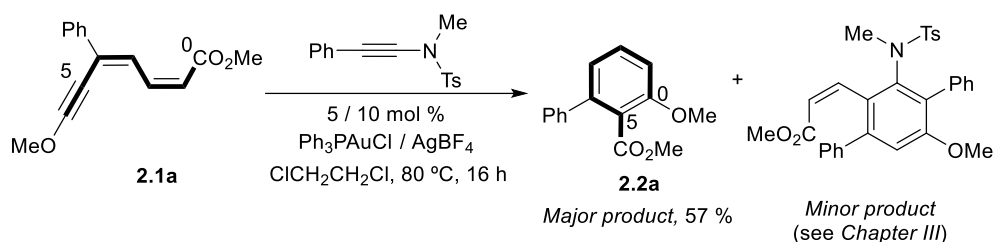


Scheme 2.23: Gold-catalysed cycloaromatization of “push-pull” 2,4-dien-6-yne carboxylic acids vs non-“push-pull” 2,4-dien-6-ynecarboxylic acids.

¹ García-García, P.; Fernández-Rodríguez, M. A.; Aguilar, E. *Angew. Chem. Int. Ed.* **2009**, *48*, 5534-5537.

3 Results and discussion.

During the study on the cyclization reaction of "push-pull" 2,4-dien-6-ynecarboxylic ester **2.1a** with an ynamide (see Chapter 3), unexpected by-product **2.2a** emerged as major outcome. It was identified as methyl 6-phenyl-2-methoxybenzoate, coming from the intramolecular cyclization reaction of "push-pull" 2,4-dien-6-ynecarboxylic ester **2.1a** (Scheme 2.24).

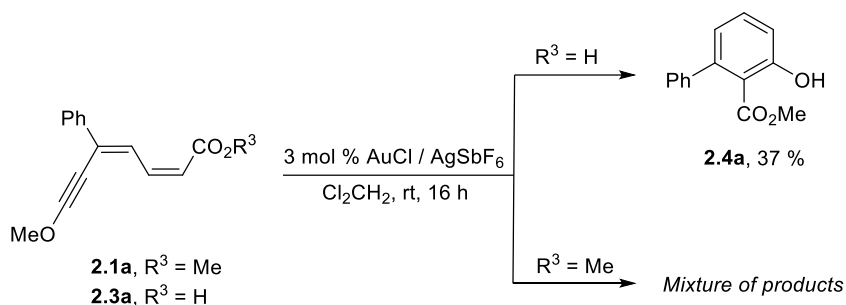


Scheme 2.24: Gold-catalysed synthesis of methyl 6-substituted 2-alkoxybenzoate **2a**.

The unexpected cycloaromatization with unusual [0,5]-topology was a significant advancement in the research conducted by this group. Previously, the group had reported on the gold-catalysed cyclization of "push-pull" 7-methoxy-2,4-dien-6-ynecarboxylic acids, which generated methyl 6-substituted 2-hydroxybenzoates with total regioselectivity and low catalyst amount (Scheme 2.25).¹ However, the

¹ García-García, P.; Fernandez-Rodriguez, M. A.; Aguilar, E. *Angew. Chem. Int. Ed.* **2009**, *48*, 5534-5537.

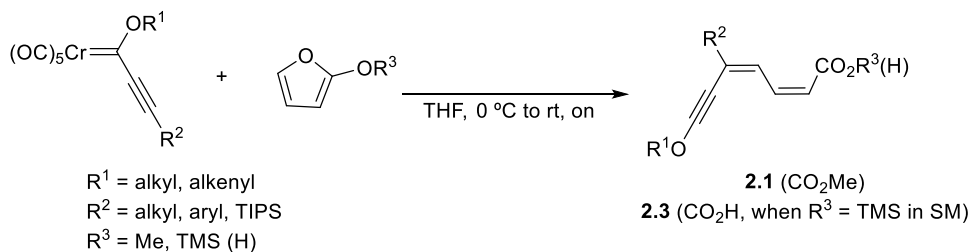
reaction with the corresponding esters led to a mixture of products under the previously explored conditions,³⁷ so this result prompted to investigate the reaction.



Scheme 2.25: Previously explored condition with "push-pull" 2,4-dien-6-yne carboxylic esters.

3.1 Synthesis of starting materials.

The synthesis of "push-pull" 2,4-dien-6-yne carboxylic esters, which serve as starting material in the reaction under research, was achieved as previously reported (Scheme 2.26).³⁴ The reaction is set up under inert atmosphere conditions, using THF as solvent and cooling down to 0 °C, and let reach room temperature overnight.



Scheme 2.26: Synthesis of "push-pull" 2,4-dien-6-yne derivatives.

A diverse set of "push-pull" 2,4-dien-6-yne derivatives **2.1** was synthesized using the procedure outlined above and their yield are listed in Table 2.1. Two different

³⁷ García-García, P. *Ph. D. Thesis dissertation, University of Oviedo, 2007.*

³⁴ Barluenga, J.; García-García, P.; de Saa, D.; Fernández-Rodríguez, M.A.; Bernardo de la Rúa, R.; Ballesteros, A.; Aguilar, E.; Tomás, M. *Angew. Chem. Int. Ed.* **2007**, *46*, 2610-2612.

positions of diversity were successfully analysed, and a wide range of aromatic and aliphatic moieties, as well as a silyl group, were installed.

Entry	"Push-pull" 2,4-dien-6-yne derivatives	R ¹	R ²	R ³	%Yield, 2.1 ^[a]
1	2.1a	Me	Ph	Me	79
2	2.1b	Me	<i>p</i> Tol	Me	59
3	2.1c	Me	<i>p</i> MeO-C ₆ H ₄	Me	89
4	2.1d	Me	<i>p</i> Cl-C ₆ H ₄	Me	75
5	2.1e	Me	<i>p</i> Br-C ₆ H ₄	Me	38
6	2.1f	Me	<i>p</i> CF ₃ -C ₆ H ₄	Me	56
7	2.1g	Me	<i>o</i> MeO-C ₆ H ₄	Me	49
8	2.1h	Me	<i>o</i> Tol	Me	59
9	2.1i	Me	<i>o</i> Cl-C ₆ H ₄	Me	59
10	2.1j	Me	<i>m</i> MeO-C ₆ H ₄	Me	39
11	2.1k	Me	<i>m</i> Cl-C ₆ H ₄	Me	64
12	2.1l	Me	<i>n</i> Pentyl	Me	64
13	2.1m	Me	cyclopropyl	Me	81
14	2.1n	Me	<i>t</i> Bu	Me	48
15	2.1o	Me	TIPS	Me	95 ^[b]
16	2.1p	Me	<i>N</i> -Me-pyrrolyl	Me	41
17	2.1q	Me	2-Furyl	Me	12
18	2.1r	Me	<i>N</i> -Me-indol-2-yl	Me	45
19	2.1s	Me	<i>N</i> -Me-indol-3-yl	Me	47
20	2.1t	Et	Ph	Me	54
21	2.1u	<i>i</i> -Pr	Ph	Me	59

^[a] Isolated yield of "push-pull" 2,4-dien-6-yne derivatives **2.1**. ^[b] Mixture 1:1 of diastereomers.

Table 2.1: Scope of "push-pull" 2,4-dien-6-yne derivatives **2.1**.

In an effort to expand the scope of "push-pull" 2,4-dien-6-yne carboxylic esters **2.1** various attempts were made to introduce other heterocycles in R² position, such as furyl or thiophenyl rings. Regrettably, none of these attempts have been successful to date.

On the other hand, while the formation of Me esters at R³ position is straightforward, because 2-methoxyfuran is a commercial reagent, the synthesis of esters (or amides) bearing alkyl groups different from Me proved to be challenging

(Scheme 2.27). The most obvious route was thought to be the synthesis of the corresponding "push-pull" 2,4-dien-6-ynecarboxylic acid **2.3** followed by its esterification. However, these attempts using different reported procedures did not lead to satisfactory results, such as the in-situ generation of a mixed anhydride³⁹ or an acyl chloride derivative,⁴⁰ the use of carbodiimides as activating agents⁴¹ or the use of H₂SO₄ as a Brønsted acid catalyst.⁴²



Process	Result obtained
In-situ generation of mixed anhydride	--
In-situ generation of an acyl chloride derivative	--
Carbodiimides as activating agents	--
H ₂ SO ₄ as Brønsted acid	--

Scheme 2.27: Unsuccessful synthesis of "push-pull" 2,4-dien-6-yne derivatives with R³ ≠ Me.

However, the approach developed by Brückner to synthesize 2-triisopropylfuran⁴³ could be employed for the preparation of 2-isopropyl- and 2-triisopropylsilylfuran from 2-furanone, and they were in-situ made react with pentacarbonyl(1-methoxy-3-phenylpropynylidene)chromium (0) (Table 2.2, top). In this manner, new "push-pull" 2,4-dien-6-ynecarboxylic esters, with R³ ≠ Me were successfully synthesized although in low to moderate yields (Table 2.1).

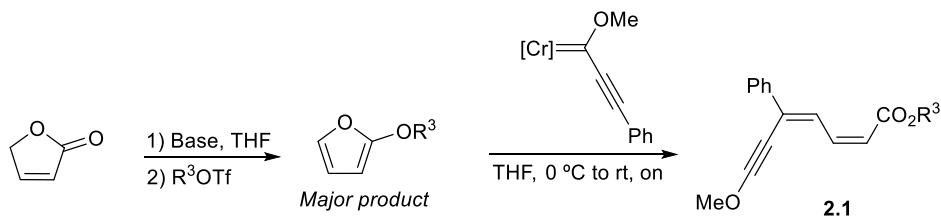
³⁹ Wakasugi, K.; Iida, A.; Misaki, T.; Nishii, Y.; Tanabe, Y. *Adv. Synth. Catal.* **2003**, *345*, 1209-1214.

⁴⁰ a) Hata, T.; Iwata, S.; Seto, S.; Urabe, H. *Adv. Synth. Catal.* **2012**, *354*, 1885-1889; b) Mao, W.; Oestreich, M. *Org. Lett.* **2020**, *22*, 8096-8100.

⁴¹ a) Sorg, A.; Siegel, K.; Brückner, R. *Chem. Eur. J.* **2005**, *11*, 1610-1624; b) Persich, P.; Llaveria, J.; Lhermet, R.; de Haro, T.; Stade, R.; Kondoh, A.; Fürstner, A. *Chem. Eur. J.* **2013**, *19*, 13047-13058; c) Soltani, Y.; Wilkins, L. L.; Melen, R. L. *Angew. Chem. Int. Ed.* **2017**, *56*, 11995-11999.

⁴² Tian, P.-P.; Cai, S.-H.; Liang, Q.-J.; Zhou, X.-Y.; Xu, Y.-H.; Loh, T.-P. *Org. Lett.* **2015**, *17*, 1636-1639.

⁴³ Neumeyer, M.; Brückner, R. *Eur. J. Org. Chem.* **2017**, *17*, 2512-2539.

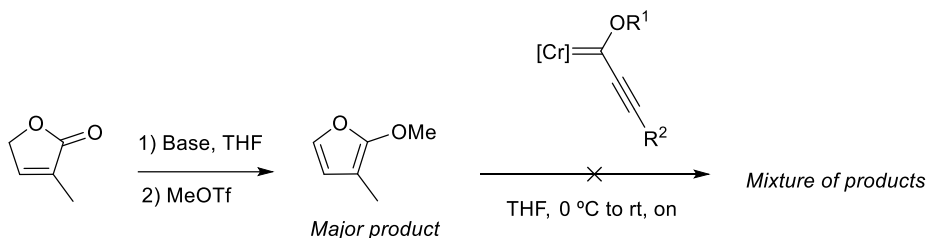


Entry	"Push-pull" 2,4-dien-6-yne derivatives	R ¹	R ²	R ³	%Yield, 2.1 ^[a]
1	2.1v	Me	Ph	<i>i</i> Pr	33
2	2.1w	Me	Ph	TIPS	15

^[a] Isolated yield of "push-pull" 2,4-dien-6-yne derivatives **2.1** from furan-2-one.

Table 2.2: Scope of "push-pull" 2,4-dien-6-yne derivatives **2.1** with R³ ≠ Me.

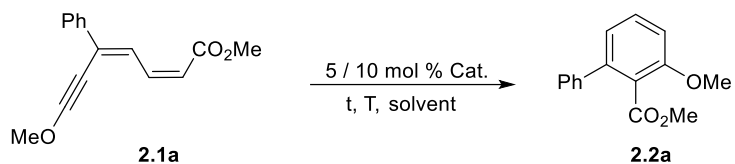
Nevertheless, the attempts to extend this procedure to 3-methylfuran-2-one to obtain "push-pull" 2,4-dien-6-yne carboxylic esters with substitution at position 1 of the dienyne system resulted in a mixture of undefined products (Scheme 2.28).



Scheme 2.28: Unsuccessful attempts of having "push-pull" 2,4-dien-6-yne derivatives substituted at the double bond positions.

3.2 Optimization of the reaction conditions.

After the initial result already mentioned (Scheme 2.24, *p.* 101; and Table 2.3, *Entry 1*), different reaction conditions such as temperature, catalyst system, solvent, stoichiometry, and reaction time were investigated. The experimental results of these analyses are summarized in Table 2.3.



Cat.

A = $\text{Ph}_3\text{PAuCl} / \text{AgBF}_4$

B = $(\text{RO})_3\text{PAuCl} / \text{AgBF}_4$ (R = 2,4-di-*t*-butylphenyl-)

C = $(p\text{CF}_3\text{-C}_6\text{H}_4)\text{PAuCl} / \text{AgBF}_4$

D = $(\text{RO})_3\text{PAuCl} / \text{AgOTf}$

E = $(\text{RO})_3\text{PAuCl} / \text{AgOTs}$

F = $(\text{RO})_3\text{PAuNTf}_2$

Entry	Catalyst	time (h)	T (°C)	Solvent	%Yield, 2.2a ^[a]
1	A	16	80	DCE	57 ^[b]
2	B	16	rt	DCE	40 ^[b,c]
3	C	2	60	DCE	67
4	A	1	rt	DCE	18
5	AuCl_3	2	60	DCE	71
6	C	2	60	Toluene	25
7	C	2	60	Dioxane	nr ^[d]
8	C	2	60	DMF	nr
9	D	2	60	DCE	nr
10	E	2	60	DCE	nr
11	B	2	60	DCE	99 ^[e] (96) ^[f]
12	B	2	60	DCE	36 ^[g]
13	F	2	60	DCE	16
14	B	2	60	DCE	60 ^[h]
15	AgBF_4	2	60	DCE	nr

^[a] Yield estimated by NMR using 1,3,5-trimethoxybenzene as internal standard. ^[b] Reaction performed in the presence of ynamide. ^[c] 10/10 mol% cat Au/Ag. ^[d] nr = no reaction (s.m. was recovered). ^[e] 2.5/5 mol% cat Au/Ag. ^[f] Isolated product yield. ^[g] 2.5/2.5 mol% cat Au/Ag. ^[h] 1/2.5 mol% cat Au/Ag.

Table 2.3: Optimization of the reaction conditions.

Thus, more electrophilic catalysts, such as (2,4-di-*t*-butylphenyloxy)₃PAuCl/AgBF₄ (cat. B) or (*p*CF₃-C₆H₄)₃PAuCl/AgBF₄ (cat. C), resulted in moderate variations in the reaction yield (*Entries 2 and 3*). However, a decrease in the yield was observed when using cat. A at rt for 1 h (*Entry 4*). Notably, AuCl₃ alone in DCE at 60 °C produced a good reaction yield (*Entry 5*). Solvent screening showed that toluene, 1,4-dioxane, or DMF were less efficient or unsuitable (*Entries 6-8*), and other silver salts tested as cocatalyst were also ineffective (*Entries 9-10*). Remarkably, anisole derivative **2.2a** was obtained quantitatively using 2.5/5 mol% of cat. B at 60 °C for 2 hours in DCE (*Entry 11*). Reducing the amount of the silver cocatalyst decreased the reaction yield

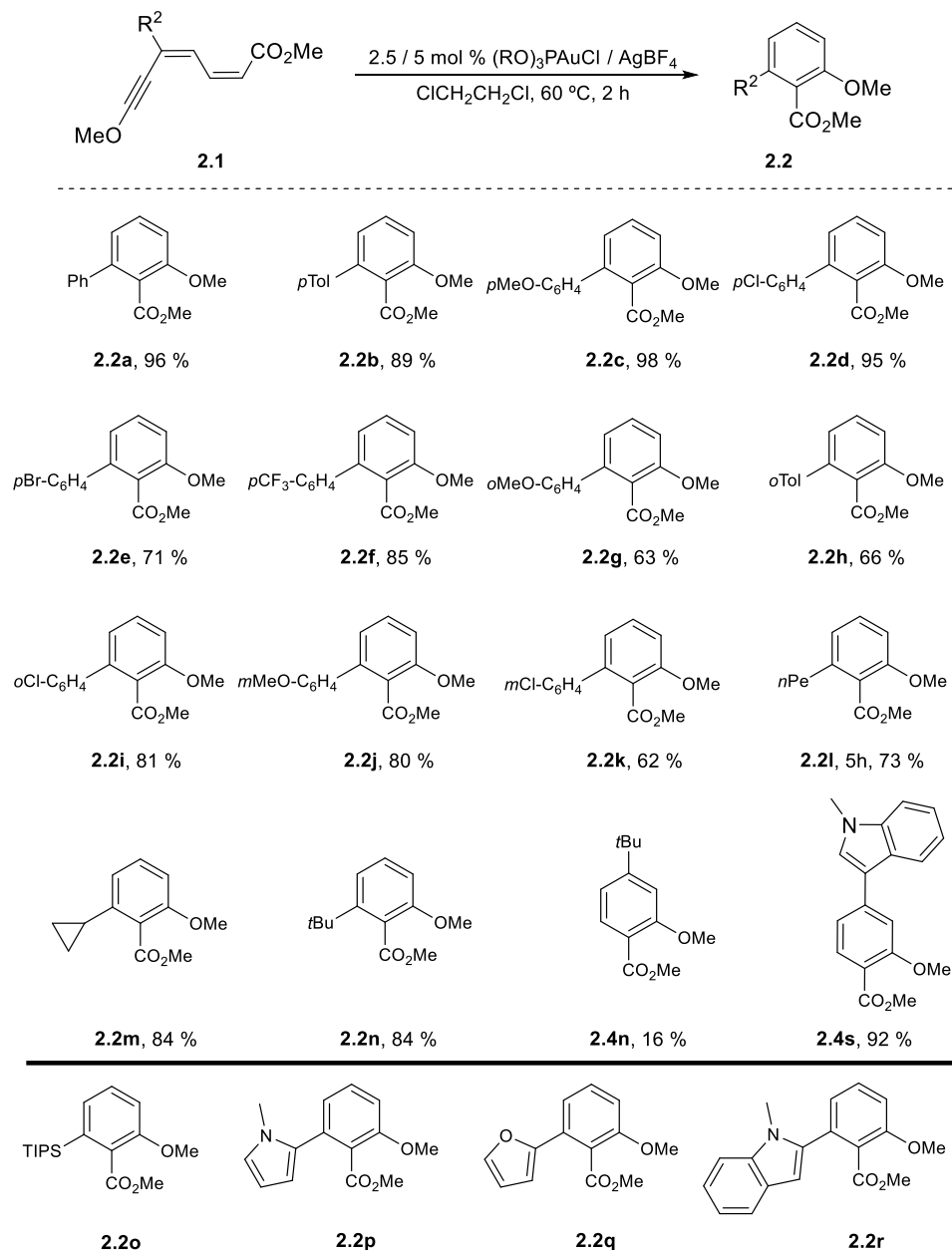
(Entry 12), as well as only using gold as catalyst (Entry 13). Diminishing the amount of both catalysts also reduced the reaction yield (Entry 14). Interestingly, using a double catalytic amount of AgBF_4 vs Au (I) salt led to higher reaction yields, although AgBF_4 alone was not active (Entry 15). Taking into consideration that the reaction also occurs without a silver cocatalyst (Entries 5 and 13), this can be considered as an example of silver-assisted gold catalysis.

As a conclusion of the optimization process, the best conditions found required to use a mixture of 2.5/5 mol% of $(\text{RO})_3\text{PAuCl}/\text{AgBF}_4$ in DCE at 60 °C for 2 hours.

3.3 Scope of the reaction.

Once the best conditions for the formation of methyl 2-methoxy-6-phenylbenzoate **2.2a** from "push-pull" 2,4-dien-6-yne derivative **2.1a** were determined, the scope of the reaction was established by modifying the R^2 group of the starting material (Scheme 2.29, top).

Significant or nearly quantitative yields were obtained when R^2 was an aromatic group that contained electron-donating *para*-substituents (**2.2b, c**). When methyl dienynecarboxylates contained *para*-electron-withdrawing substituted aryl groups, the expected methyl 2-methoxy-6-substitutedbenzoate derivatives **2.2** were also obtained in excellent yields, such as for $\text{R}^2 = \text{Cl}$ (**2.2d**), or good yields for $\text{R}^2 = \text{Br}, \text{CF}_3$ (**2.2e, f**). *Ortho*-substituted aromatic methyl diyne carboxylates also produced the corresponding benzoates with synthetically useful yields, although lower than those of the analogous *para*-isomers (**2.2g-i**). The reaction also tolerated *meta*-substitution with both electron-donating (**2.2j**) and electron-withdrawing (**2.2k**) substrates. Dienyne carboxylates with aliphatic substituents underwent the expected cycloaromatization reaction with satisfactory yields, having examples of primary (**2.2l**), secondary (**2.2m**), or tertiary (**2.2n**) alkyl substituents. In the latter case, a small amount of product **2.4n** was also isolated, formed by a conventional [1,6]-cycloaromatization reaction. In the case of *N*-methylindol-3-yl at R^2 position the [1,6]-cycloaromatization product (**2.4s**) was obtained in 92 % yield.

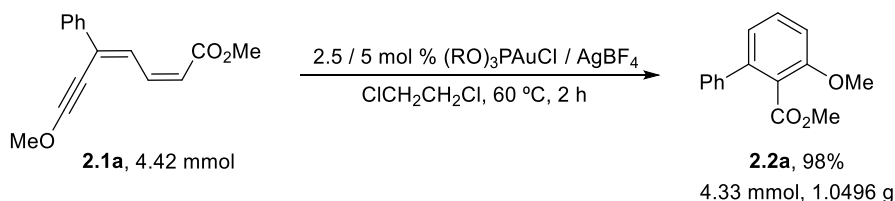


Scheme 2.29: Scope at the position R² of "push-pull" 2,4-dien-6-yne derivatives **2.1**

Additional attempts to introduce other groups in order to create a sufficiently wide range of compounds to better understand the potential of this reaction were unsuccessful (Scheme 2.29, *bottom*). Thus, no defined product could be obtained when attempting to introduce a silylated group, such as the triisopropylsilyl moiety (**2.2o**). Similarly, all tests to introduce heterocycles at the R² position also failed, as

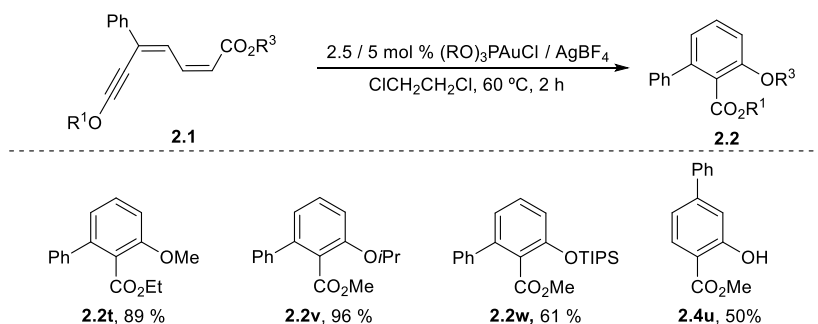
N-methylpyrrolyl (**2.2p**), 2-furanyl (**2.2q**) and *N*-methylindol-2-yl (**2.2r**) only furnished products arising from the polymerization of the starting "push-pull" 2,4-dien-6-yne. It may be worth to emphasize the different behaviour found when having at R² a *N*-methylindol-3-yl (**2.4s**) vs *N*-methylindol-2-yl (**2.2r**); in the first case, the [1,6]-cycloaromatization product was obtained while only polymerization products were detected in the second one.

Under optimized reaction conditions, a gram-scale reaction performed with the "push-pull" 2,4-dien-6-yne **2.1a** resulted in the obtention of 1.0496 g of 2,3-disubstituted anisole derivative **2.2a** in 98% yield. This transformation showcases the method's synthetic potential and its suitability for large-scale industrial applications (Scheme 2.30).



Scheme 2.30: Gram-scale cycloaromatization reaction.

Scheme 2.31 (*top*) shows other alkyl 6-substituted 2-alkoxybenzoate derivatives **2.2** that were also obtained during the expansion of the scope of the reaction, modifying in this case the substituents at positions R¹ and R³ in the "push-pull" 2,4-dien-6-yne **2.1**. For instance, replacing the methoxy group with an ethoxy group at the R¹ position was well-tolerated, resulting in the formation of the 2,3-disubstituted benzoate derivative **2.2t** with good yield. At the R³ position, an isopropyl group (**2.2v**) as well as a silylated moiety, such as the triisopropyl silyl group (**2.2w**), could be also installed in moderate yields.

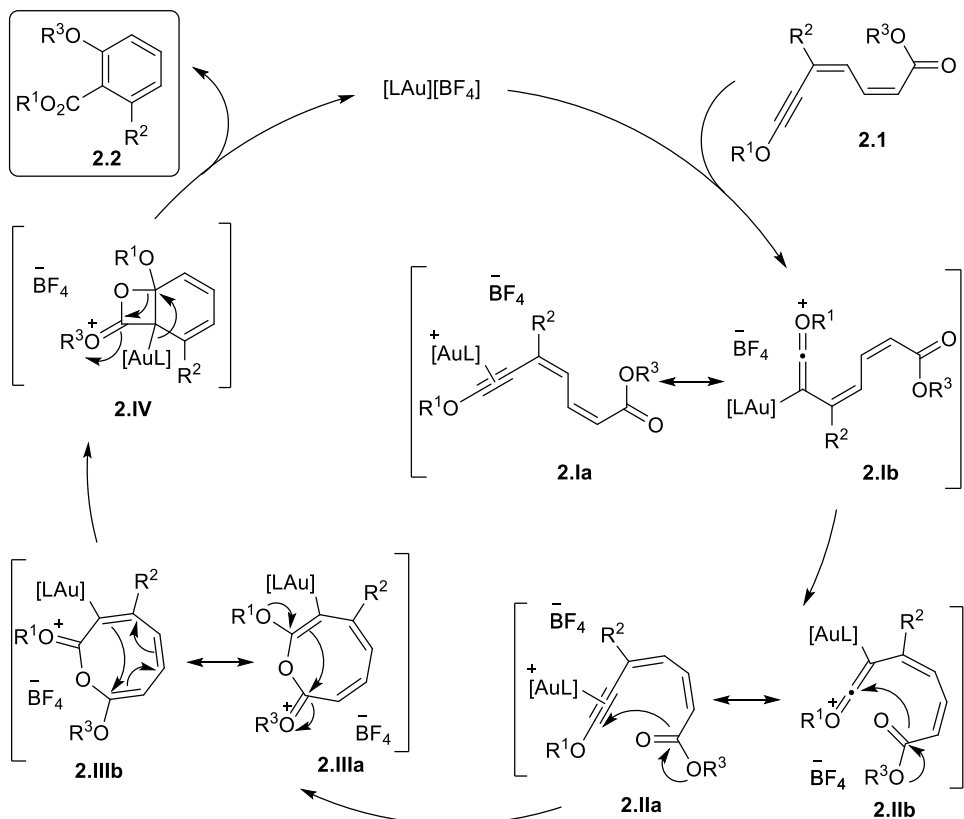


Scheme 2.31: Scope at the positions R¹ and R³ of "push-pull" 2,4-dien-6-yne derivatives **2.1**.

On the other hand, when placing a bulky group at the R¹ position (Scheme 2.31, *bottom*), such as *iso*-propyl (**2.2u**), the product obtained was the one coming from conventional [1,6]-cycloaromatization, with the additional loss of the *iso*-propyl moiety (**2.4u**).

3.4 Reaction mechanism.

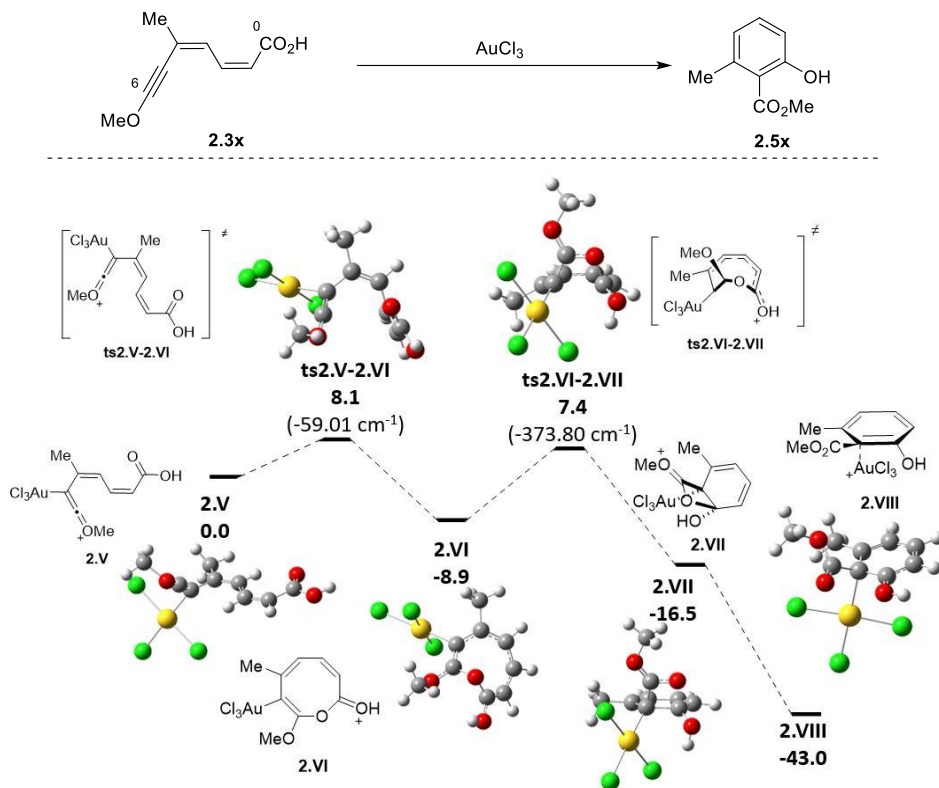
According to the proposed mechanism (Scheme 2.32), the gold catalyst should initially activate the C-C triple bond, which would be then stabilized by the alkoxy group's donation. Subsequently, the *s-trans*-form **2.Ia** would undergo isomerization to the *s-cis*-form **2.IIa**, followed by a nucleophilic attack of the carboxy group to the triple bond, leading to the formation of cyclooctatrienic intermediate **2.IIIa**. A nucleophilic attack promoted by the alkoxy group would lead to the generation of bicyclic intermediate **2.IV**. Finally, the [4.2.0] intermediate **2.IV** would be opened to yield the final product **2.2** while the gold catalyst initiates a new catalytic cycle.



Scheme 2.32: Proposed reaction mechanism.

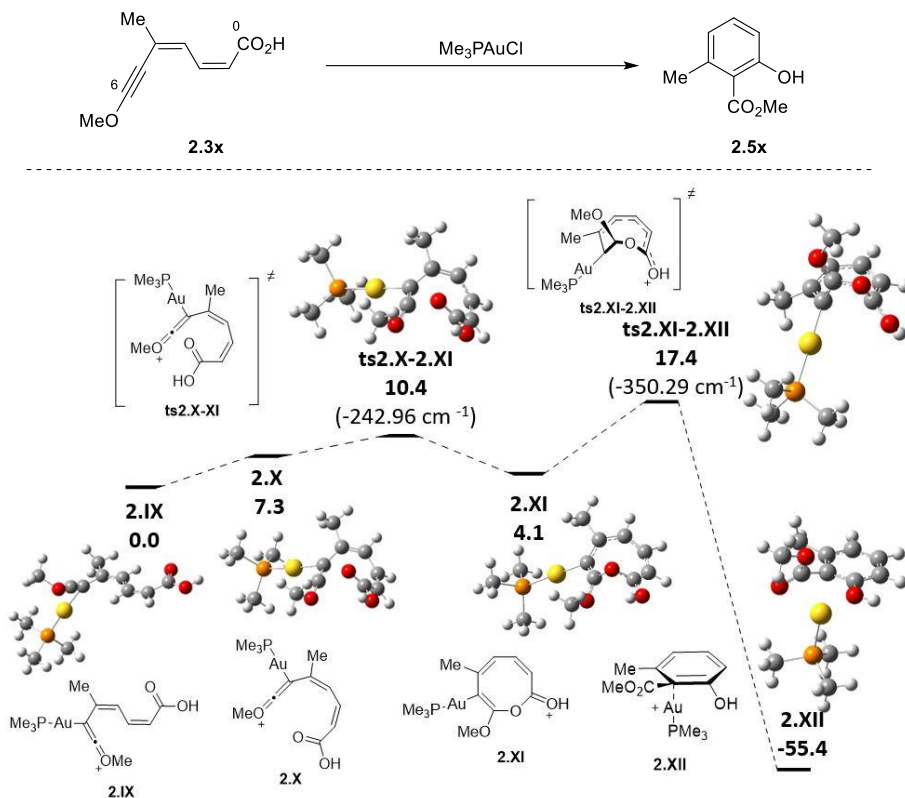
In order to obtain mechanistic insights, quantum chemical calculations were conducted. First of all, as it remained unexplored, the cycloisomerization reaction of "push-pull" 2,4-dien-6-ynecarboxylic acids, using AuCl₃ and Me₃PAuCl as catalysts, were calculated, and the methyl derivative (**2.3x**, R² = Me) was chosen as the reaction model for the calculations.

In the catalytic cycloisomerization with AuCl₃ (Scheme 2.33), the initial step of the mechanism involves the metal catalyst complexing to the substrate's triple bond to form intermediate **2.V**. Following this, an *s-trans-s-cis* isomerization occurs through **ts2.V-2.VI** (8.1 kcal/mol). The *s-trans* isomer of **2.V** and a transition state for the *O*-nucleophilic attack of the carboxylic group on the most electrophilic of the two *sp* C atoms were expected after **ts2.V-2.VI**, but **ts2.V-2.VI** led straightforwardly to the cyclooctatrienic intermediate **2.VI** (−8.9 kcal/mol). Both expected structures are probably very similar in geometry and energy to **ts2.V-2.VI**, so they could not be found at the theoretical level used, although assumed to exist as transient structures between **ts2.V-2.VI** and **2.VI**. Intermediate **2.VI** then undergoes a second intramolecular nucleophilic attack, this time from the electron-rich C5 (the atom bonded to the gold catalyst), to the activated carbonyl group via **ts2.VI-2.VII** (7.4 kcal/mol). The outcome is the stable [4.2.0]-bicyclic intermediate **2.VII** (−16.5 kcal/mol). Subsequently, a final aromatization triggers the ring-opening of the four-membered cycle in **2.VII**, leading to the highly stable intermediate **2.VIII** (−43.0 kcal/mol). This occurs before demetallation and regeneration of the catalyst which, when released, can be incorporated into a new cycle.



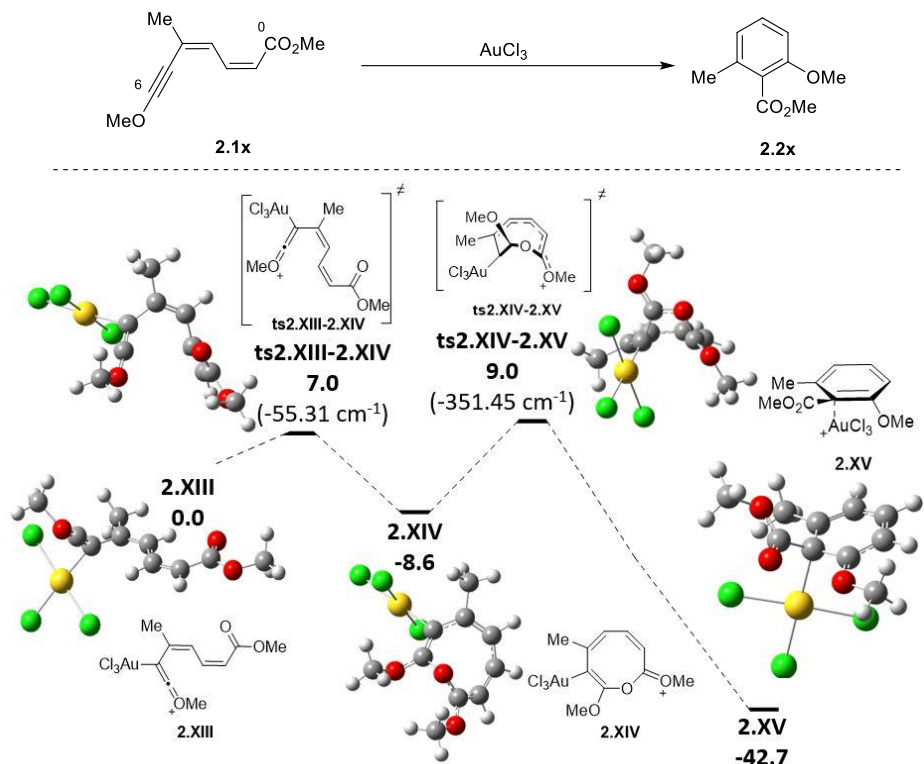
Scheme 2.33: Cycloisomerization of "push-pull" 2,4-dien-6-ynecarboxylic acid **2.3x** catalysed by AuCl₃, intermediates and transition states optimized using the B3LYP/6-31(G) (LANL2DZ for gold) computational level.

The replacement for a bulkier ligand in the gold catalyst, as well as the change in gold oxidation state (Scheme 2.34), has a minor impact on the reaction profile just described. No transition state for the isomerization of the *s-trans* **2.IX** into the *s-cis* isomer **2.X** could be found, probably because it is very similar to **2.X** both in geometry and energy. However, **ts2.X-2.XI** performs the *O*-nucleophilic attack of the carboxylic group on C6. The only noticeable effect is a slight increase in the energy barrier (2.3 kcal/mol) for the formation of **ts2.X-2.XI** compared to the analogue **ts2.V-2.VI** (shown in Scheme 2.33). Similarly, the energy barrier for **ts2.XI-2.XII** is 1.1 kcal/mol higher than its analogous **ts2.VI-2.VII**. On the other hand, the energy released during the formation of the cycloaromatized intermediate **2.XII** is 12.4 kcal/mol bigger than in the formation of **2.VIII**, without detecting the formation of bicyclic [4.2.0] intermediate in this case.



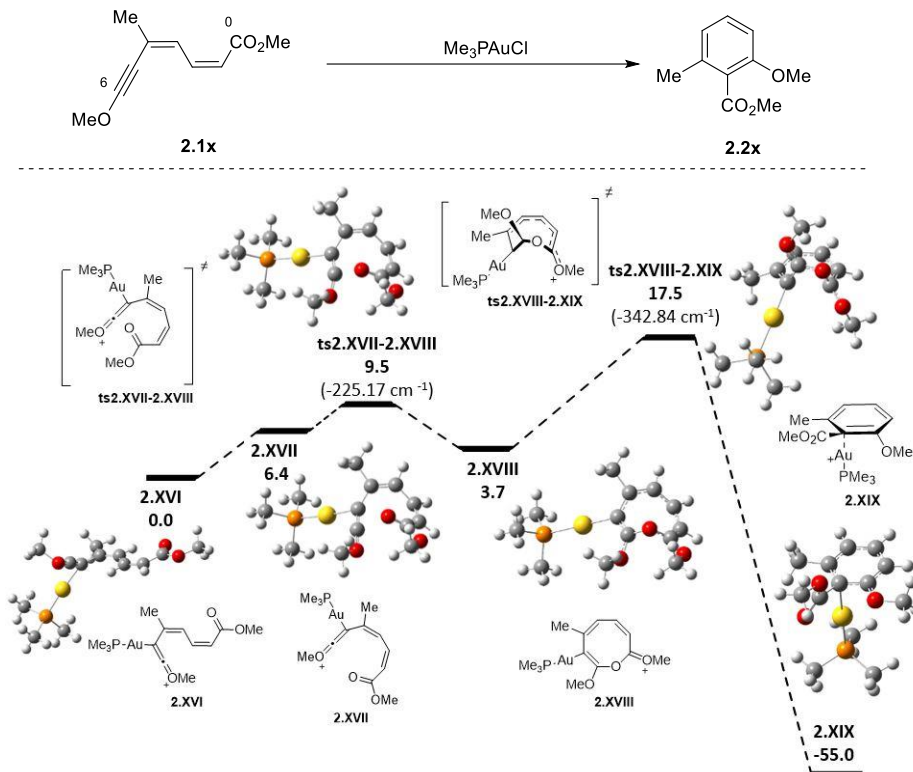
Scheme 2.34: Cycloisomerization of "push-pull" 2,4-dien-6-ynecarboxylic acid **2.3x** catalysed by Me_3PAuCl , intermediates and transition states optimized using the B3LYP/6-31(G) (LANL2DZ for gold) computational level.

The replacement of the carboxylic acid group by a methyl ester group in the "push-pull" 1,3-dien-5-yne molecule has also little impact on the reaction mechanism in terms of the structures involved and their relative energies (Scheme 2.35). Once again, two reaction steps are observed for the reaction catalysed by AuCl_3 , consisting of consecutive intramolecular nucleophilic attacks, firstly from the carbonyl-ester oxygen to C6 and then from C5 to the activated carbonyl-ester carbon atom. The energy barriers of both steps are less than 11 kcal/mol. These small barriers coupled with the high stability of the aromatic 6-membered cyclic intermediate **2.XV** (-42.7 kcal/mol), suggest a fast and direct reaction. The only difference observed in the reaction of the ester compared to that of the acid in the AuCl_3 catalysed reaction is the absence of a stable bicyclic [4.2.0] intermediate, analogous to **2.VII** in Scheme 2.33; it becomes a transient structure and **ts2.XIV-2.XV** directly yields the aromatic intermediate **2.XV** before demetallation.



Scheme 2.35: Cycloisomerization of "push-pull" 2,4-dien-6-ynecarboxylic ester **2.1x** catalysed by AuCl₃, intermediates and transition states optimized using the B3LYP/6-31(G) (LANL2DZ for gold) computational level.

The theoretical studies with Me₃PAuCl as the catalyst in the transformation of "push-pull" 2,4-dien-6-ynecarboxylic ester **2.1x** have also been performed (Scheme 2.36). Again, in this case, upon coordination of the Me₃PAuCl catalyst to the triple bond of the reactant, no transition state (ts) was found between *s-trans* **2.XVI** (0.0 kcal/mol) and *s-cis* isomer **2.XVII** (6.4 kcal/mol). The first nucleophilic attack has a 9.5 kcal/mol barrier and leads to the formation of the eight-membered cycle **2.XVIII**, which is 3.7 kcal/mol higher in energy than the reactant. Subsequently, the second nucleophilic attack occurs with a Gibbs energy barrier of 17.5 kcal/mol, directly yielding the highly stable aromatic intermediate **2.XIX**. Thus, the Gibbs energy barriers for both steps are very similar to those observed when using AuCl₃ for the same ester, both measured from the most stable previous intermediate.



Scheme 2.36: Cycloisomerization of "push-pull" 2,4-dien-6-ynecarboxylic ester **2.1x** catalysed by Me_3PAuCl , intermediates and transition states optimized using the B3LYP/6-31(G) (LANL2DZ for gold) computational level.

Some noteworthy observations related to the effect of the catalyst and the exchange of acid/ester functionalities can be summarised from these calculations, all of them aligned with the previously proposed mechanism for the formation of the [0,5]-cycloaromatization product. Firstly, with AuCl_3 the transition state for the *s-trans-s-cis* isomerization presents a low imaginary frequency (which corresponds to a "wide" transition state in the reaction potential energy surface) and leads straightforwardly to the eight-membered cyclic intermediate, whereas with the Me_3PAuCl catalyst the isomerization is done through a hypothetical transition state very similar to the *s-cis* intermediate that evolves to the eight-membered cycle through a "narrow" transition state (with large absolute value of its imaginary frequency). Secondly, for both acid and ester functionalities, the eight-membered cyclic intermediate is relatively more stable in the AuCl_3 -catalysed cycloisomerization. This is attributed to stabilizing H-bonds formed between the methyl groups at C4 and the methoxy fragment. However, this difference in stability

has little impact on the barrier of the limiting step. Thirdly, only the AuCl₃-catalysed cyclization of "push-pull" 2,4-dien-6-ynecarboxylic acids produced the stable bicyclic [4.2.0] intermediate **2.VII**, whereas it becomes a transient structure in the other cases (i.e. the cyclization of the acid with Me₃PAuCl, the cyclization of carboxylic esters with AuCl₃ and with Me₃PAuCl). Finally, the product still linked to the catalyst is more stable in the presence of Me₃PAuCl than with AuCl₃. In the following calculations Me₃PAuCl catalyst was considered to make them more similar to the experimental conditions.

The [1,6]-cyclization product was observed in small amount when R² = *t*-Bu and as a main product when R² = *N*-methylindol-3-yl (Scheme 2.29, *p.* 106). Besides, it was the product classically expected, so it is worthy to explore the mechanism for its formation and to compare it with that obtained for the [0,5]-cyclization. The initial reaction model employed in the DFT calculations was again the methyl derivative **2.1x** (R² = Me). The energy profile for the formation of [1,6]-product product is displayed in Scheme 2.37, (*left, p.*116) together with that for the formation of the [0,5]-product Scheme 2.37 (*right*) for the sake of comparison. Two potential pathways were discovered in the formation of the [1,6]-cycloaromatization product **2.4x** but only that with the lowest energy barrier will be followed by the system and discussed in this section (see full DFT calculations *Annex II*).

The calculations revealed that reaction paths leading to both products were possible, but the formation of product **2.2x** from the unconventional [0,5]-cycloaromatization pathway was slightly favoured due to its lower Gibbs energy barrier (17.5 vs 18.7 kcal/mol). On the other hand, product **2.4x**, is thermodynamically favoured by 3.6 kcal/mol (−58.6 vs −55.0 kcal/mol), but experimental observations confirm that kinetics control the process.

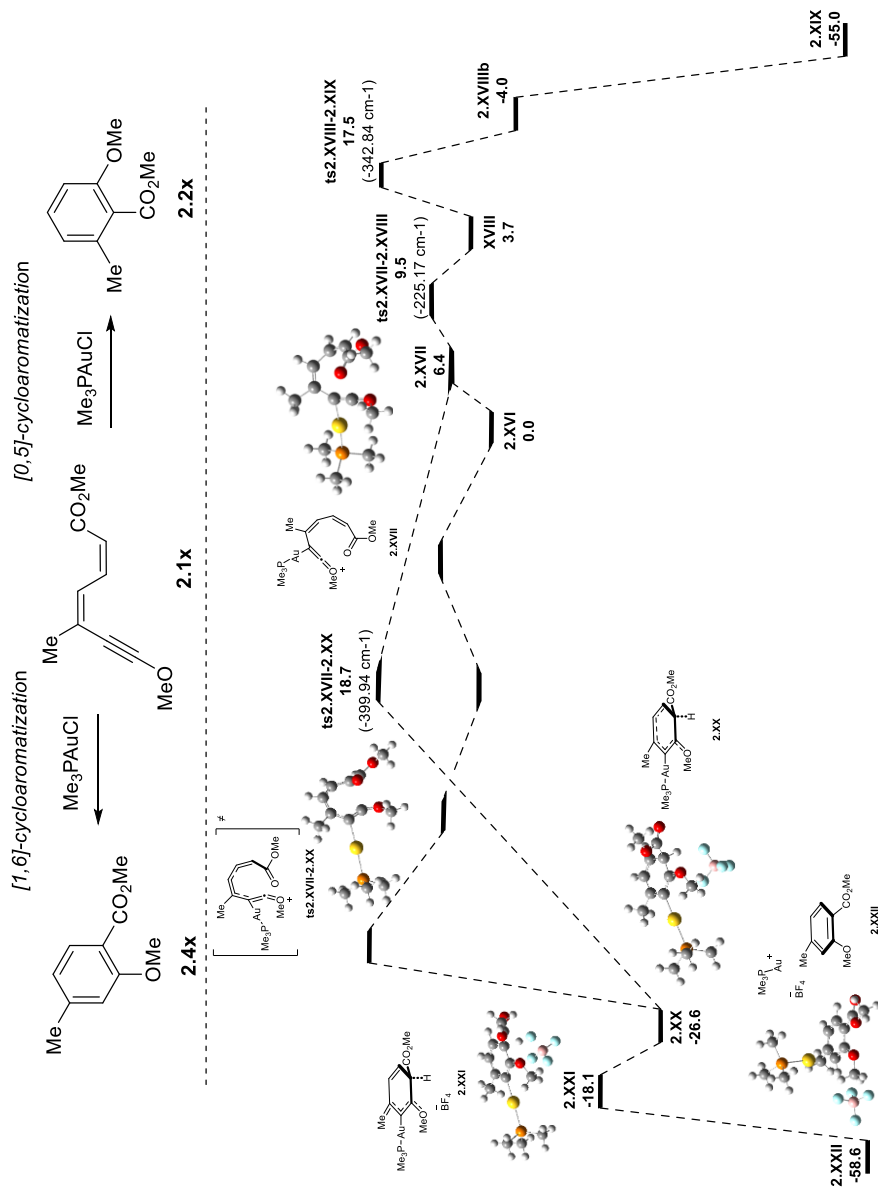
In the case of R² = *t*Bu (**2.1n**), where a mixture of [0,5]-cycloaromatization product (**2.2n**, 84 %) and [1,6]-cycloaromatization product (**2.4n**, 16 %) was experimentally obtained (Scheme 2.29, *p.* 106), it was decided to also conduct theoretical studies on the reaction profiles for both reaction routes (Scheme 2.38, *p.*117). According to the theoretical calculations, both reaction pathways were found to be feasible. Again, computations indicate kinetics preference for the [0,5]-cyclization product over the [1,6]-one (barriers of 15.4 vs 18.3 kcal/mol) with a thermodynamic preference for the [1,6]-cyclization product (−60.4 vs −52.4 kcal/mol). Although there is larger kinetic preference for the [0,5]-product than in the case of R² = Me, thermodynamics strongly favours (by 8.0 kcal/mol) the formation of the [1,6]-

product. This could explain the presence of a small amount of the [1,6]-cyclization product experimentally observed.

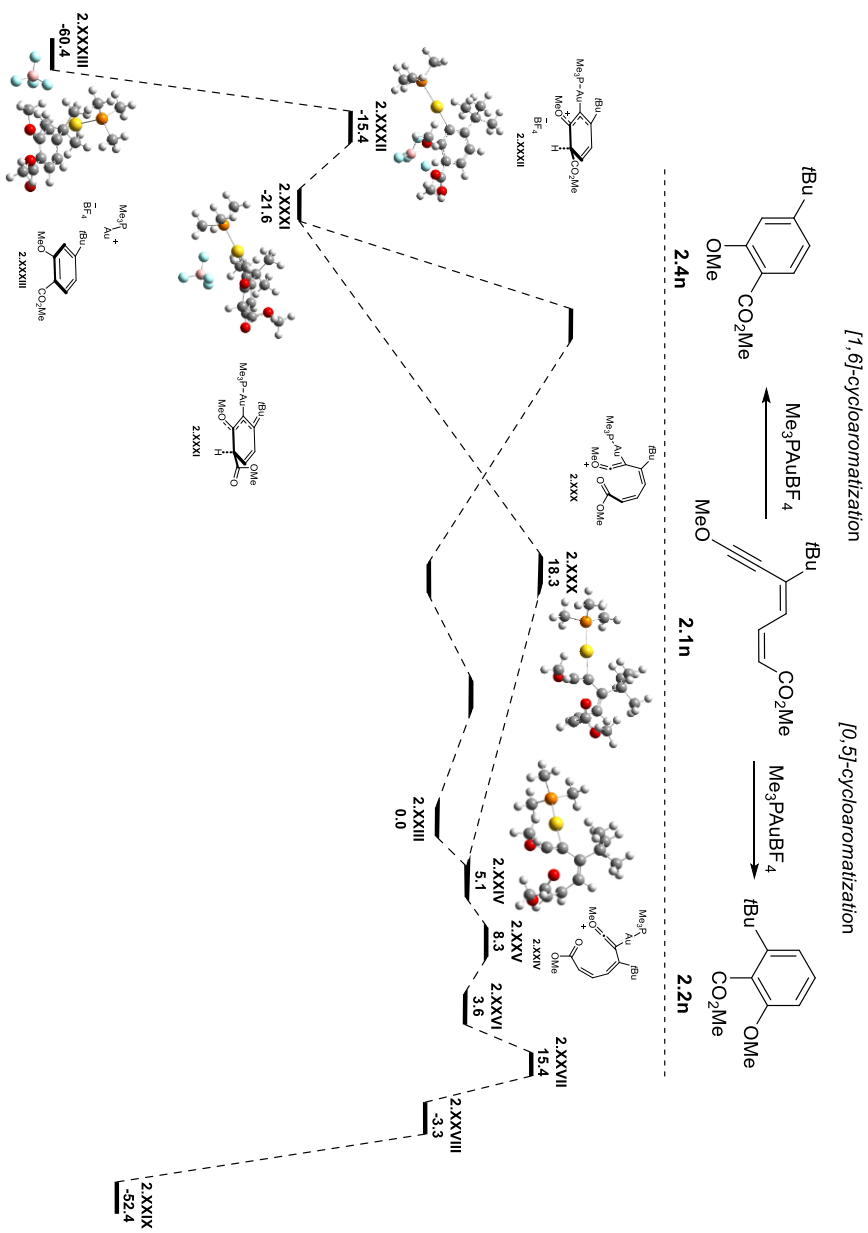
In the case of $R^2 = N$ -methylindol-3-yl (**2.1s**), only the [1,6]-cycloaromatization product (**2.4s**, 92 %) was experimentally obtained (Scheme 2.29, *p.106*). However, the calculations showed once more a kinetics preference for the [0,5]-cyclization product **2.2s** over the [1,6]-one **2.4s** (17.2 vs 18.9 kcal/mol), being the [1,6]-product more stable than the [0,5]-one by 7.1 kcal/mol (Scheme 2.39, *p.118*).

At this point it necessary to highlight that the difference in the barriers for [0,5]- vs [1,6]-additions are in the range of 1.2–2.9 kcal/mol for the three studied systems. These small differences make it difficult to reproduce the experimental findings with a standard computational level as the one used here. More accurate theoretical levels would be needed to reproduce the subtle energy differences determining the experimental selectivity. However, they are highly demanding in terms of computational resources for systems of the size here considered. Computational results inform about the similarity of the rate limiting energies of both routes and clearly confirm the mechanistic proposal for the reactions under study.

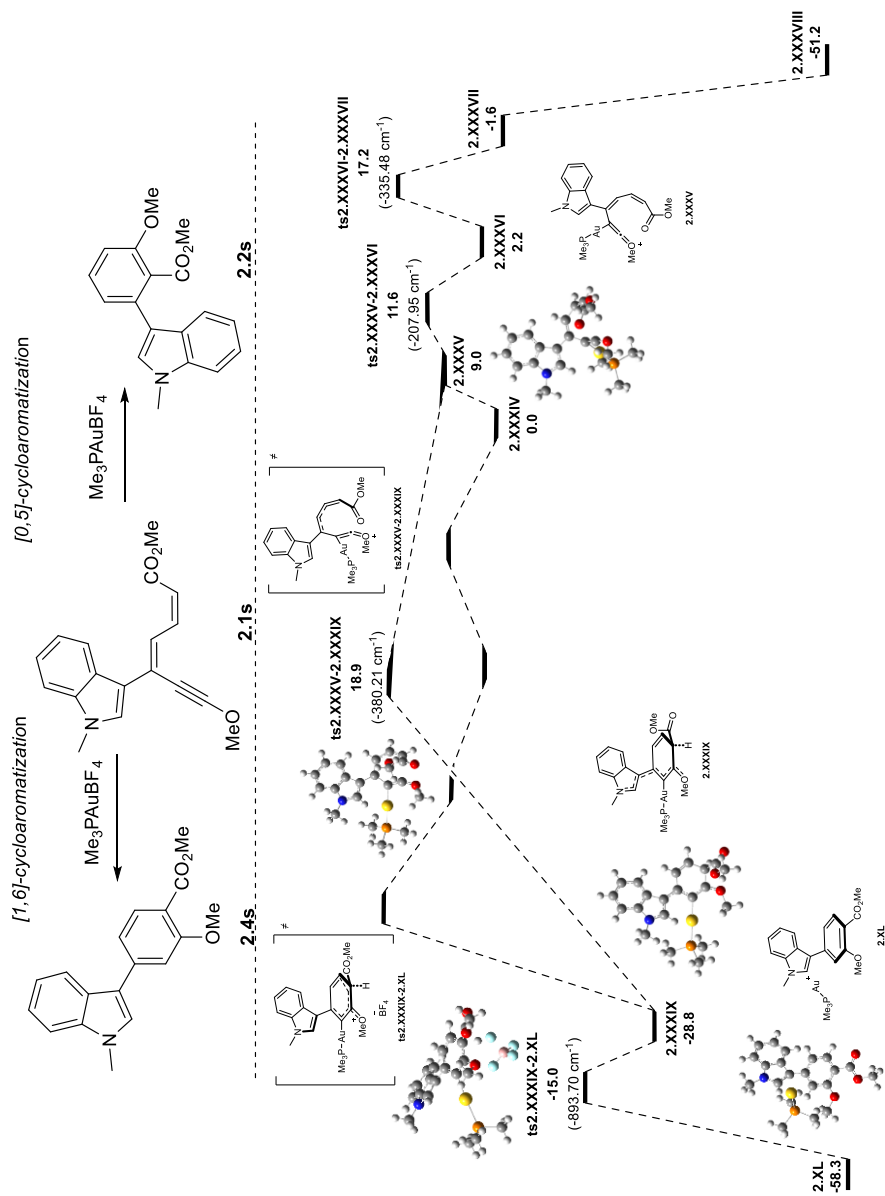
Finally, in the case of $R^1 = iso$ -propyl and $R^2 = phenyl$ (**2.1u**), only the [1,6]-cycloaromatization product (**2.4u**, 50 %) was experimentally obtained (Scheme 2.40, *p.119*), accompanied with the elimination of the *iso*-propyl fragment. The calculations performed keeping the *iso*-propyl fragment linked to the O atom suggest that the formation of the kinetic product **2.2u** (–49.8 kcal/mol) via the [0,5]-cycloaromatization pathway should be favoured due to its lower Gibbs energy barrier (19.8 vs 22.6 kcal/mol) compared to the more stable thermodynamic product **2.4u** (–54.1 kcal/mol) from the [1,6]-cycloaromatization pathway (2.8 $\Delta\Delta G$). New routes need to be theoretically explored to reproduce experimental results.



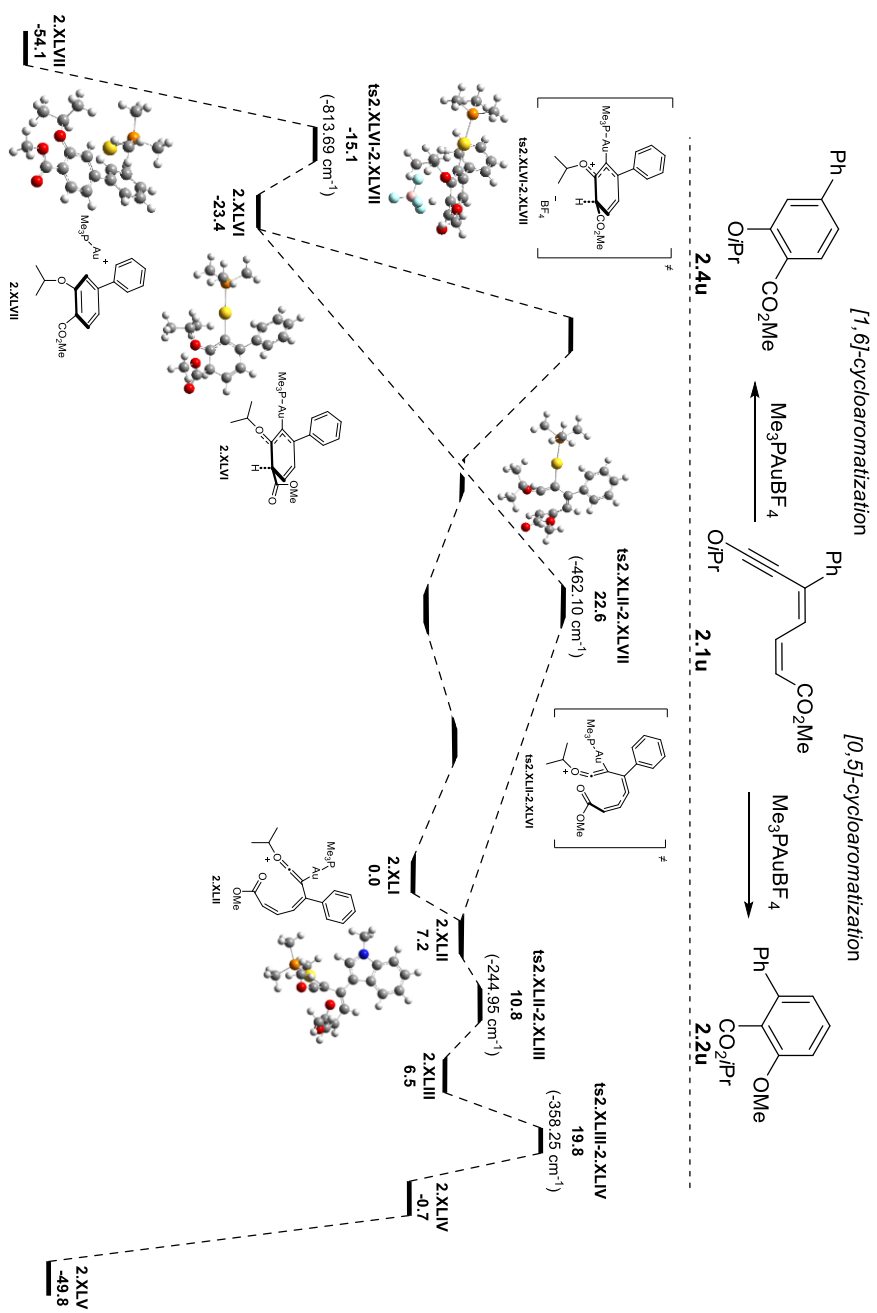
Scheme 2.37: Intermediates and transition states for the two cycloisomerization pathways of "push-pull" 2,4-dien-6-ynecarboxylic ester 2.1x ($R^2 = \text{Me}$), catalysed by Me_3PAuCl , obtained using the B3LYP/6-31(G) (LANL2DZ for gold)



Scheme 2.38: Intermediates and transition states for the two cycloisomerization pathways of "push-pull" 2,4-dien-6-ynecarboxylic ester 2.1n ($R^2 = tBu$), catalysed by Me_3PAuBF_4 , obtained using the B3LYP/6-31(G) (LANL2DZ for gold)



Scheme 2.39: Intermediates and transition states for the two cycloisomerization pathways of "push-pull" 2,4-dien-6-ynecarboxylic ester **2.1s** (R² = *N*-methylindol-3-yl), catalysed by Me₃PAuBF₄, obtained using the B3LYP/6-31(G) (LANL2DZ for gold) computational level.



Scheme 2.40: Intermediates and transition states for the two cycloisomerization pathways of "push-pull" 2,4-dien-6-ynecarboxylic ester **2.1u** ($\text{R}^1 = \text{Pr}$), catalysed by $\text{Me}_3\text{PAuBF}_4$, obtained using the B3LYP/6-31(G) (LANL2DZ for gold) computational level.

In summary, based on these theoretical calculations, it is difficult to establish a general conclusion as to why the product of [0,5]-cycloaromatization is formed in some cases and the product of [1,6]-cycloaromatization is formed in others, or both in some cases, as the energy differences are often minimal. Furthermore, it is important to consider that many factors can influence gold-catalysed reactions (see *General Background*), as the solvent, the effect of silver, ... which are not always accounted for in theoretical studies. It is worth noting that, by running the reaction at 60 °C, both products could potentially be formed with these small energy differences.

4 Conclusions.

This chapter describes a gold-catalysed cycloaromatization reaction of *"push-pull"* 2,4-dien-6-ynecarboxylic esters with unusual topology. The study represents an upgrade and expansion upon a previously reported example of cycloaromatization of *"push-pull"* 2,4-dien-6-ynecarboxylic acids.

The process yields 6-substituted 2-alkoxybenzoates with excellent yields and complete regioselectivity, using only small amounts of gold (I) catalyst. Notably, the transformation is tolerant to a wide range of substitution patterns in different positions of the scaffold.

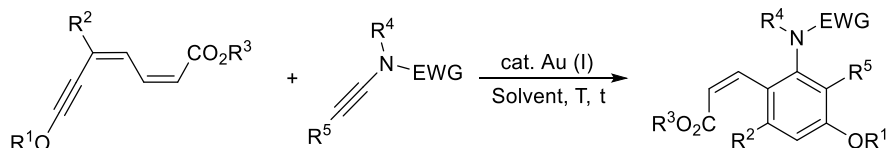
In some cases, a mixture of the [0,5]-cycloaromatization and the [1,6]-cycloaromatization product, or only the [1,6]-cycloaromatization product, has been obtained. Computational DFT theoretical calculations have been performed to try to rationalize these experimental findings. These calculations have shown that both reaction pathways are feasible and that the energetic differences between the rate limiting barriers of both processes are small enough to make difficult the prediction of the reaction outcome.

Chapter III:

Gold-catalysed reaction between “*push-pull*” alkyl (and silyl) 2,4-dien-6-yne carboxylates and ynamides. Synthesis of tetrasubstituted anilines.

1 Introduction.

In this Chapter a gold-catalysed procedure for the synthesis of tetra-substituted anilines by reaction between “push-pull” alkyl (and silyl) 2,4-dien-6-yne carboxylates and ynamides is described. This process occurs with complete regioselectivity and excellent yields, utilizing only small quantities of gold (I) catalyst (Scheme 3.1). The reaction’s optimal conditions and generality have been explored as well.

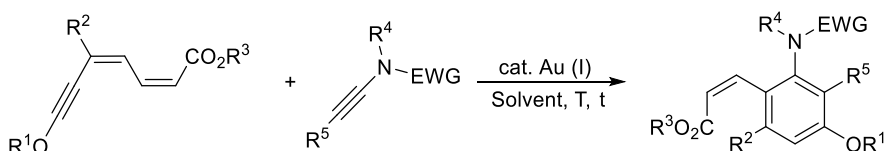


Scheme 3.1: Transformation studied in this Chapter.

In addition, theoretical computational studies have been carried out to improve the understanding of the mechanism underlying this transformation.

2 Bibliographic background.

As previously mentioned, the unique behaviour of “push-pull” 2,4-dien-6-yne compared to other enynes has led our group to focus on studying the reactivity of these compounds with different nucleophiles (see examples later on p. 144-148). In an effort to further expand knowledge in this field, the unexplored reaction between these compounds and ynamides catalysed by gold was investigated, which led to tetrasubstituted anilines through a tetrahydro-Diels-Alder cycloaddition reaction (Scheme 3.2).



Scheme 3.2: Obtention of aniline derivatives through a reaction between “push-pull” 2,4-dien-6-yne and ynamides.

The interesting result obtained, in which a benzene ring substituted in 5 positions with 6 possible diversity points is obtained through a completely regioselective reaction, seemed sufficiently intriguing to continue studying it.

As the reaction being developed in this chapter involves a cycloaddition between “push-pull” 2,4-dien-6-yne and ynamides, a review of the literature on these compounds as starting materials will be conducted. The bibliographic background of the gold-catalysed intermolecular cycloaddition reactions is also considered in this chapter (the intramolecular ones have been covered in *Chapter II*). It is worth noting that this transformation can also be viewed as an example of a tetrahydro-Diels-

Alder reaction. To provide a comprehensive understanding of this transformation type, an overview of dehydro-Diels-Alder reactions will be presented as well.

2.1 Cycloaddition reactions catalysed by gold.

Among the most widely used tools for the creation of carbocyclic and heterocyclic compounds, catalytic intermolecular reactions involving gold have been particularly significant.¹ Several examples of [2+1],² [2+2], [3+2], [4+2], [4+3],³ [6+2],⁴ [8+2]⁵ or [2+2+2]⁶ have been reported in the literature. Among these, the [2+2], [3+2] and [4+2] reactions have been more extensively studied, and they are the ones outlined in this short review.

2.1.1 [2+2]-Cycloaddition.

[2+2]-Cycloaddition is perhaps the most straightforward way to access four-membered rings.⁷ The Echavarren group was the first one to describe a formal [2+2]-

¹ a) Lautens, M.; Klute, W.; Tam, W. *Chem. Rev.* **1996**, *96*, 49-92; b) Fruhauf, H. W. *Chem. Rev.* **1997**, *97*, 523-596; c) López, F.; Mascareñas, J. L. *Beilstein J. Org. Chem.* **2011**, *7*, 1075-1094; d) Vilhelmsen, M. H.; Hashmi, S. K. *PATAI'S Chemistry of Functional Groups*, **2015**; e) Dorel, R.; Echavarren, A. M. *Chem. Rev.* **2015**, *115*, 9028-9072; e) Echavarren, A. M.; Muratore, M. E.; López-Carrillo, V.; Escribano-Cuesta, V.; Huguet, N.; Obradors, C. *Organic Reactions, Chapter 1, Vol. 92*, **2017**; f) Bhakta, S.; Ghosh, T.; *Asian J. Org. Chem.* **2021**, *10*, 496-505; g) Escofet, I.; Zuccarello, G.; Echavarren, A. M. *Adv. Organom. Chem.* **2022**, *77*, 1-42.

² a) Johansson, M. J.; Gorin, D. J.; Staben, S. T.; Toste, F. D. *J. Am. Chem. Soc.* **2005**, *127*, 18002-18003; b) Solorio-Alvarado, C. R.; Wang, Y.; Echavarren, A. M. *J. Am. Chem. Soc.* **2011**, *133*, 11952-11955; c) Briones, J. F.; Davies, H. M. L. *J. Am. Chem. Soc.* **2012**, *134*, 11916-11919; d) Hong, T.; Liu, Y.; Zhao, K.; Cheng, S.; Liu, Q.; Zhang, S.; Zhong, Y.; Li, X.; Zhao, Z. *Org. Biomol. Chem.*, **2023**, *21*, 3684-3690.

³ a) Karad, S. N.; Bhunia, S.; Liu, R.-S. *Angew. Chem. Int. Ed.* **2012**, *51*, 8722-8726; b) Zhang, S.; Tang, A.; Chen, P.; Zhao, Z.; Miao, M.; Ren, H. *Org. Lett.* **2020**, *22*, 848-853; c) Wang, X.; Lv, R.; Li, X. *Org. Chem. Front.* **2022**, *9*, 5292-5298.

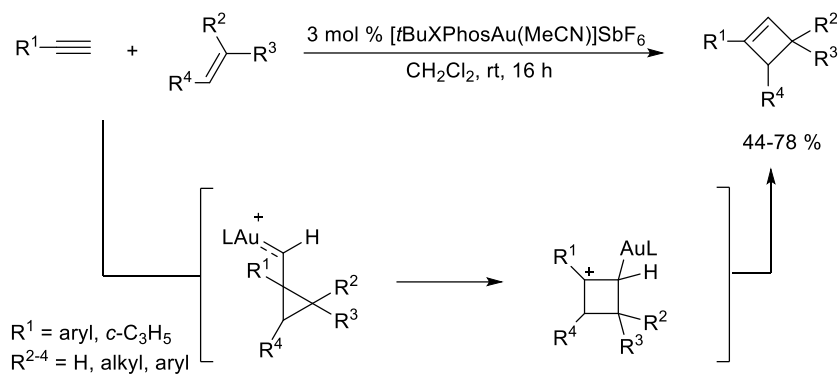
⁴ Tenaglia, A.; Gaillard, S. *Angew. Chem. Int. Ed.* **2008**, *47*, 2454-2457.

⁵ Suárez-Rodríguez, T.; Suárez-Sobrinho, A. L.; Ballesteros, A. *Chem. Eur. J.* **2021**, *27*, 7154-7159.

⁶ a) Kramer, S.; Odabachian, Y.; Overgaard, J.; Rottländer, M.; Gagosz, F.; Skrydstrup, T. *Angew. Chem. Int. Ed.* **2011**, *50*, 5090-5094; b) Faustino, H.; Varela, I.; Mascareñas, J. L.; López, F. *Chem. Sci.* **2015**, *6*, 2903-2908; c) Dubovtsev, A. Y.; Shcherbakov, N. V.; Dar'in, D. V.; Kukushkin, V. Y. *Adv. Synth. Catal.* **2020**, *362*, 2672-2682.

⁷ a) Luzung, M. R.; Mauleón, P.; Toste, F. D. *J. Am. Chem. Soc.* **2007**, *129*, 12402-12403; b) Teller, H.; Flügge, S.; Goddard, R.; Fürstner, A. *Angew. Chem. Int. Ed.* **2010**, *49*, 1949-1953; c) Faustino, H.; Bernal, P.; Castedo, L.; López, F.; Mascareñas, J. L. *Adv. Synth. Catal.* **2012**,

intramolecular cycloaddition of enynes catalysed by Au (I) to give cyclobutenes.⁸ Later, this same research group developed the intermolecular version of this reaction using terminal alkynes and mono-, di-, and trisubstituted alkenes, which leads to the formation of polysubstituted cyclobutenes through a gold carbene complex intermediate (Scheme 3.3).⁹



Scheme 3.3: [2+2]-Cycloaddition reaction catalysed by gold (I).

2.1.2 [3+2]-Cycloaddition.

Accessing five-membered rings is perhaps most easily achieved through [3+2]-cycloaddition.¹⁰ In addition to the common mechanism of activation of the π -bonds, gold can also activate 1,3-dipoles. This was demonstrated by the work of Toste and co-workers,¹¹ who used azlactones and *N*-phenylmaleimide to obtain Δ^1 -pyrroline

354, 1658-1664; d) Teller, H.; Corbet, M.; Mantilli, L.; Gopakumar, G.; Goddard, R.; Thiel, W.; Fürstner, A. *J. Am. Chem. Soc.* **2012**, *134*, 15331-15342; e) Montserrat, S.; Faustino, H.; Lledós, A.; Mascareñas, J. L.; López, F.; Ujaque, G. *Chem. Eur. J.* **2013**, *19*, 15248-15260; f) Ha, S.; Lee, Y.; Kwak, Y.; Mishra, A.; Yu, E.; Ryou, B.; Park, C.-M. *Nat. Commun.* **2020**, *11*, 2509-2521; g) Zanini, M.; Cataffo, A.; Echavarren, A. M. *Org. Lett.* **2021**, *23*, 8989-8993.

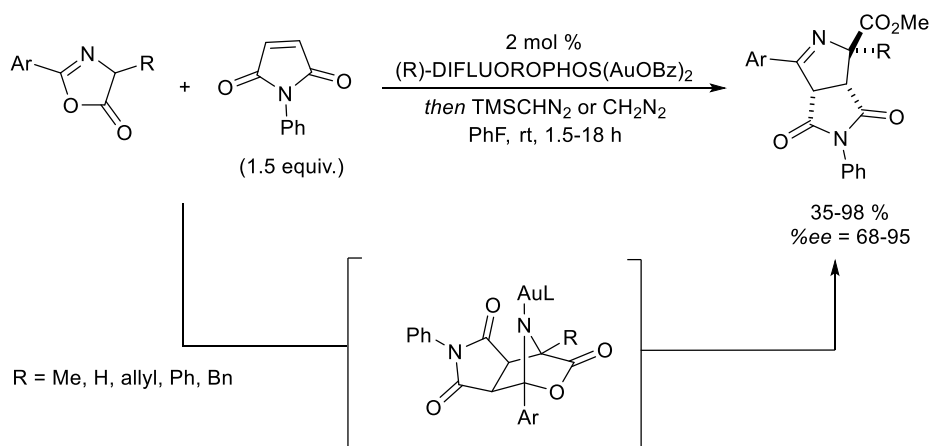
⁸ Nieto-Oberhuber, C.; López, S.; Jiménez-Núñez, E.; Echavarren, A. M. *Chem. Eur. J.* **2006**, *12*, 5916-5923.

⁹ López-Carrillo, V.; Echavarren, M. A. *J. Am. Chem. Soc.* **2010**, *132*, 9292-9294.

¹⁰ a) Lian, J. J.; Chen, P. C.; Lin, Y. P.; Ting, H. C.; Liu, R. S. *J. Am. Chem. Soc.* **2006**, *128*, 11372-11373; b) Yamamoto, K.; López, E.; Barrio, P.; Borge, J.; López, L. A. *Chem. Eur. J.* **2020**, *26*, 6999-7003; c) Koshikawa, T.; Nagashima, Y.; Tanaka, K. *ACS Catal.* **2021**, *11*, 1932-1937; d) Xu, B.; Zhang, Z.-M.; Han, J.; Gu, G.; Zhang, J. *Chin J. Chem.* **2022**, *40*, 1407-1412.

¹¹ Melhado, A. D.; Luparia, M.; Toste, F. D. *J. Am. Chem. Soc.* **2007**, *129*, 12638-12639.

derivatives via a tricyclo[5.2.1.0^{2,6}]decane intermediate (Scheme 3.4) obtaining moderate to excellent enantiomeric excesses.



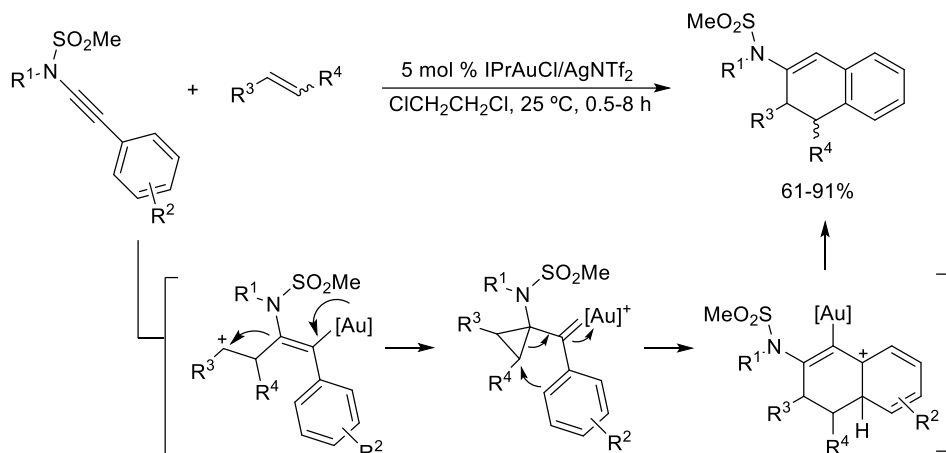
Scheme 3.4: Formal [3+2]-cycloaddition catalysed by gold (I).

2.1.3 [4+2]-Cycloaddition.

The [4+2]-cycloaddition reaction is undoubtedly the most widely used strategy for accessing six-membered rings.¹² In Scheme 3.5, a gold-catalysed [4+2]-cycloaddition reaction is depicted, which occurs between ynamides and aromatic olefins.¹³ This reaction involves a formal [4+2]-cycloaddition with alkenes and, as far as we know, it represents the only intermolecular example of such type of reactivity for ynamides. The key intermediate for this transformation would be an α -cyclopropyl gold carbene complex, generated after a three-step sequence: activation of the ynamide by the catalyst, nucleophilic attack of the alkene and retrodonation-cyclopropanation. The final product would arise from a S_EAr process followed by protodeauration. It is worth noting that, for this example, the ynamide behaves as a 4-atom synthon in the [4+2]-cycloaddition reaction. This reaction is also a case of a dehydro-Diels-Alder reaction, which will be discussed in further detail later on this chapter.

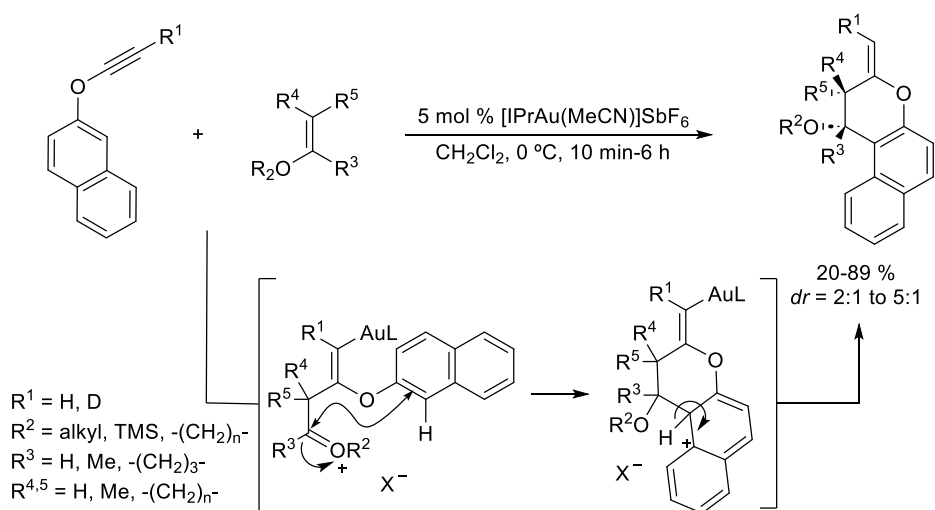
¹² a) Faustino, H.; López, F.; Castedo, L.; Mascareñas, J. L. *Chem. Sci.* **2011**, *2*, 633-637; b) Papar, V. V.; Jadhav, A. M.; Liu, R.-S. *J. Am. Chem. Soc.* **2011**, *133*, 20728-20731; c) Zhang, X.-Q.; Xu, T.; Zhang, C.; Wang, C.; Wang, Y. *Org. Chem. Front.* **2023**, *10*, 680-685.

¹³ Dateer, R. B.; Shaibu, B. S.; Liu, R.-S. *Angew. Chem. Int. Ed.* **2012**, *51*, 113-117.



Scheme 3.5: [4+2]-Cycloaddition reaction between ynamides and aromatic olefins.

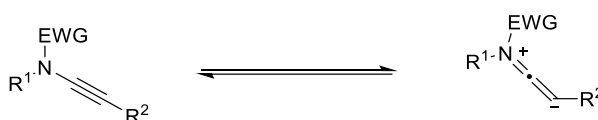
More recently, Ballesteros and co-workers reported that chromene derivatives are produced via intermolecular formal [4+2]-cycloaddition when *O*-aryl ynol ethers and enol ethers are reacted in the presence of a gold (I) catalyst. The proposed mechanism involves the addition of the enol ether to the activated triple bond followed by an intramolecular Friedel-Crafts-type acylation reaction (Scheme 3.6).⁵



Scheme 3.6: Formal [4+2]-cycloaddition reaction to obtain chromene derivatives.

2.2 Ynamides as building blocks in gold catalysis.

Ynamides have emerged as the most extensively studied compounds among heteroatom-activated alkynes. The polarization in their structure, attributed to their equilibrium with the keteneiminium ion (Scheme 3.7),¹⁴ is typically reduced by the presence of an electron-attracting group. This facilitates the delocalization of the lone pair electrons on the nitrogen atom, thereby enhancing the molecule's stability. Such attributes, along with the development of suitable methods for their preparation,¹⁵ have supposed an exponential growth in the field of ynamide chemistry.



Scheme 3.7: Equilibrium between ynamides and keteneiminium ion.

Ynamide species, which inherit polarization of the nitrogen lone pair electron to the triple bond, have been extensively employed for the development of innovative synthetic techniques and the creation of uncommon *N*-containing heterocycles. Recently, the versatility of ynamide reactions in umpolung reactivity,¹⁶ radical reactions,¹⁷ and asymmetric synthesis has been thoroughly examined.¹⁸ In this dissertation a comprehensive overview of gold-catalysed transformations of ynamides is going to be summarized, as it is the most related topic with this thesis.

Because of the almost equal distribution of electrons in sp^2/sp hybridized π -orbitals in non-polar alkenes/alkynes, activation by gold catalysts results in low regioselectivity. However, the inherent delocalization of the nitrogen lone pair

⁵ Suárez-Rodríguez, T.; Suárez-Sobrino, A. L.; Ballesteros, A. *Chem. Eur. J.* **2021**, *27*, 7154-7159.

¹⁴ Ficini, J.; *Tetrahedron* **1976**, *32*, 1449-1486.

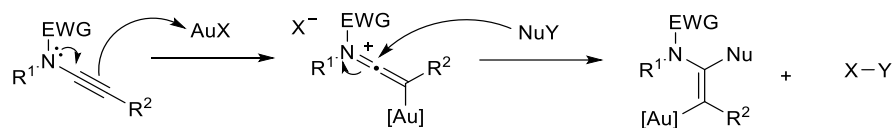
¹⁵ a) Evano, G.; Jouvin, K.; Coste, A. *Synthesis* **2013**, *45*, 17-26; b) Betou, M.; Sallustrau, A.; Toupet, L.; Trolez, Y. *Tetrahedron Lett.* **2015**, *56*, 4627-4630; c) Mansfield, S. J.; Campbell, C. D.; Jones, M. W.; Anderson, E. A. *Chem. Commun.* **2015**, *51*, 3316-3319.

¹⁶ Zhou, B.; Tan, T.-D.; Zhu, X.-Q.; Shang, M.; Ye, L.-W. *ACS Catal.* **2019**, *9*, 6393-6406.

¹⁷ a) Mahe, C.; Cariou, K. *Adv. Synth. Catal.* **2020**, *362*, 4820-4832; b) Tan, T.-T.; Wang, Z.-S.; Qian, P.-C.; Ye, L.-W. *Small Methods* **2021**, *5*, 2000673.

¹⁸ Lynch, C. C.; Sripada, A.; Wolf, C. *Chem. Soc. Rev.* **2020**, *49*, 8543-8583.

causes uneven π -electron distribution, creating an opportunity for a regioselective transformation of ynamides. Thus, when an electron-rich ynamide interacts with a gold complex (or salt), it generates in-situ a polarized keteniminium species, which becomes electrophilic (Scheme 3.8). This electrophilicity leads to easy nucleophilic attack to the α -position of the ynamide.

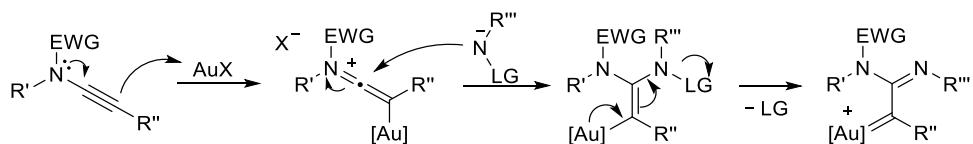


Scheme 3.8: Nucleophilic attack to ynamides activated by a gold catalyst.

The attack of N-, O- and C-nucleophiles among others to gold-activated ynamide species is a valued method for constructing complex hetero- and carbocycles.

2.2.1 N-based nucleophiles.

The use of a gold catalyst in combination with ynamide and a variety of N-based nucleophiles results in the formation of C-N bonds in multiple molecular structures. The reaction between the Au-activated ynamide and N-based nucleophiles which possess a good leaving group such as nitrene-transfer reagents, involves Au-back donation, delocalization, and cleavage of the leaving group, ultimately generating α -imino gold carbene complexes (Scheme 3.9). These α -imino gold carbene intermediates exhibit various types of reactivity and can be utilized in the synthesis of a wide range of heterocycles and structurally complex nitrogen-containing molecules.¹⁹

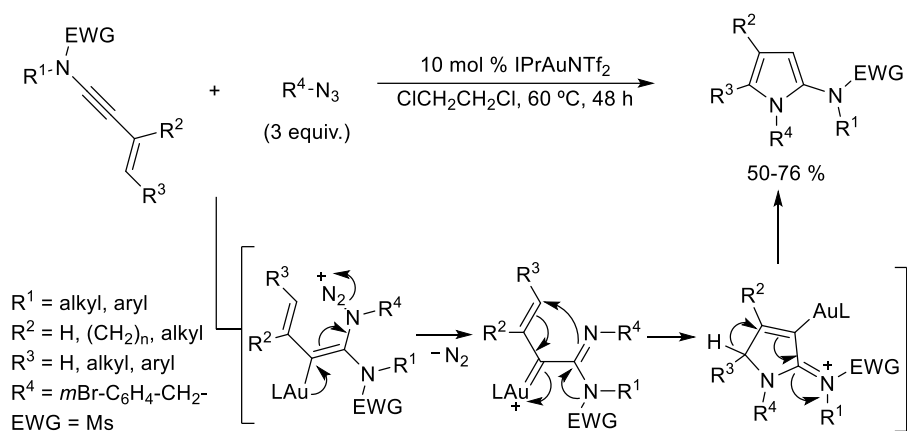


Scheme 3.9: Generic formation of an α -imino gold-carbene intermediate from an ynamide.

¹⁹ a) Davies, P. W.; Cremonesi, A.; Dumitrescu, L. *Angew. Chem. Int. Ed.* **2011**, *50*, 8931-8935; b) Garzo, M.; Davies, P. W. *Org. Lett.* **2014**, *16*, 4850-4853; c) Shu, C.; Wang, Y.-H.; Zhou, B.; Li, X.-L.; Ping, Y.-F.; Lu, X.; Ye, L.-W. *J. Am. Chem. Soc.* **2015**, *137*, 9567-9570; d) Tian, X.; Song, L.; Rudolph, M.; Rominger, F.; Hashmi, A. S. K. *Org. Lett.* **2019**, *21*, 4327-4330.

The reaction already commented in *Chapter I* (Schemes 1.2, p. 39 and 1.20, p.52) is one example that takes advantage of this idea.²⁰

Scheme 3.10 illustrates another reaction of this nature, in which an azide serves as a nitrene transfer reagent and undergoes a [4+1]-cycloaddition with a 3-en-1-ynamide to synthesize 2-aminopyrroles via an aza-Nazarov cyclization mechanism.²¹ Initially, benzyl azide attacks the gold-activated ynamide, resulting in the formation of an alkenyl gold intermediate. Subsequently, an α -imino gold carbene intermediate is generated through the release of N₂ gas. The imine and the terminal alkene then undergo a preferential intramolecular cyclization, leading to the formation of an iminium ion intermediate. Finally, the iminium ion undergoes aromatization and protodeauration, yielding 2-amino-pyrrole derivatives.



Scheme 3.10: Intermolecular ynamide amination and aza-Nazarov cyclization can be catalysed by gold.

2.2.2 O-based nucleophiles.

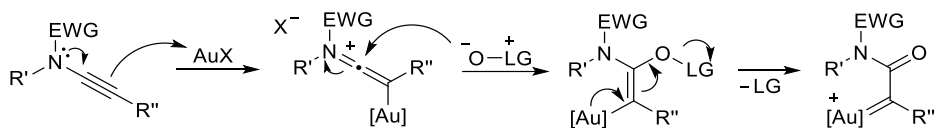
New C-O bonds can be formed by utilizing O-based nucleophiles and gold-activated ynamides.²² Just as α -imino gold carbenes are formed using nitrene-

²⁰ Xu, W.; Wang, G.; Sun, N.; Liu, Y. *Org. Lett.* **2017**, *19*, 3307-3310.

²¹ Shu, C.; Wang, Y.-H.; Shen, C.-H.; Ruan, P.-P.; Lu, X.; Ye, L.-W. *Org. Lett.* **2016**, *18*, 3254-3257.

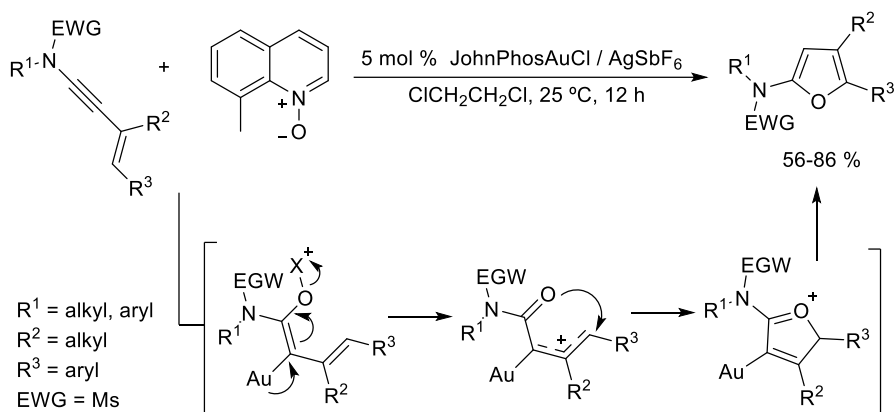
²² a) Karad, S. N.; Bhunia, S.; Liu, R. S. *Angew. Chem. Int. Ed.* **2012**, *51*, 8722-8726; b) Li, D.-Y.; Wei, Y.; Shi, M. *Eur. J. Org. Chem.* **2015**, 4108-4113; c) Prabagar, B.; Mallick, R. K.; Prasad, R.; Gandon, V.; Sahoo, A. K. *Angew. Chem. Int. Ed.* **2019**, *58*, 2365-2370; d) Liu, J.; Zhu, L.; Wan, W.; Huang, X. *Org. Lett.* **2020**, *22*, 3279-3285.

transfer reagents (see Scheme 3.9, p.135), α -oxo gold carbene complexes can also be generated using nucleophilic oxidants (Scheme 3.11).



Scheme 3.11: Generic formation of an α -oxo gold-carbene intermediate from an ynamide.

For instance, the formal [4+1]-cycloaddition reaction catalysed by gold between 3-en-1-ynamides and 8-methyl-quinoline *N*-oxide produces 2-amino furan derivatives (Scheme 3.12).²³ In this process, a proposed oxa-Nazarov cyclization occurs on gold-stabilized allylic cations, which are generated in-situ via the intramolecular attack on the gold-activated ynamide. Subsequently, gold-back-donation results in the formation of the carbene intermediate which undergoes cyclization. Finally, protodeauration and aromatization lead to the desired final products.

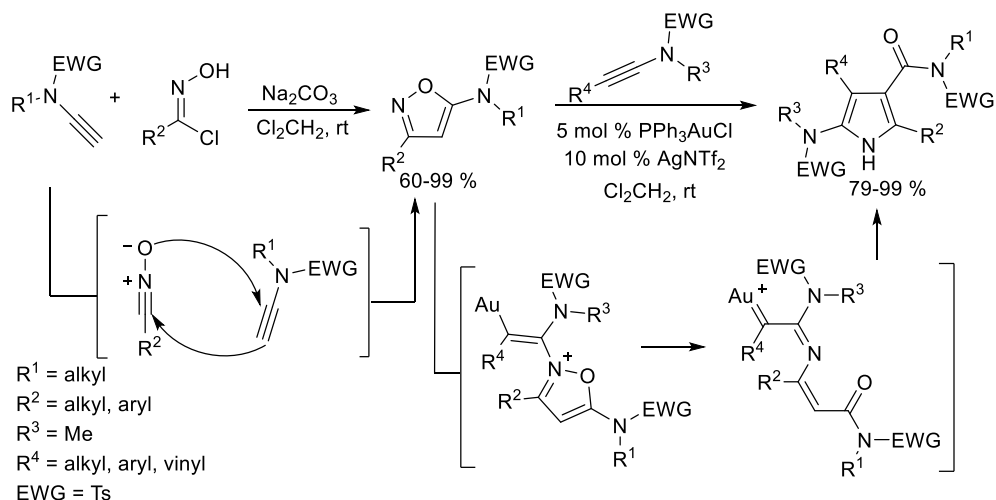


Scheme 3.12: Synthesis of 2-aminofurans achieved the reaction between 3-en-1-ynamides and quinoline oxide using gold catalyst.

In a separate example, Cui and Chen presented an iterative approach for synthesizing isoxazoles and pyrroles through the assembly of nitrile oxides and

²³ Dateer, R. B.; Pati, K.; Liu, R. S. *Chem. Commun.* **2012**, 48, 7200-7202.

ynamides (Scheme 3.13).²⁴ First, the nitrile oxides undergo a metal-free regioselective [3+2]-cycloaddition with terminal ynamides to produce isoxazoles. Then, the attack of the isoxazole on the gold-activated internal ynamides, followed by gold-back donation and intramolecular cyclization of the generated α -imino carbene complex, results in the formation of substituted pyrroles in good to excellent yields.



Scheme 3.13: Iterative assembly of nitrile oxides and ynamides.

2.2.3 C-based nucleophiles.

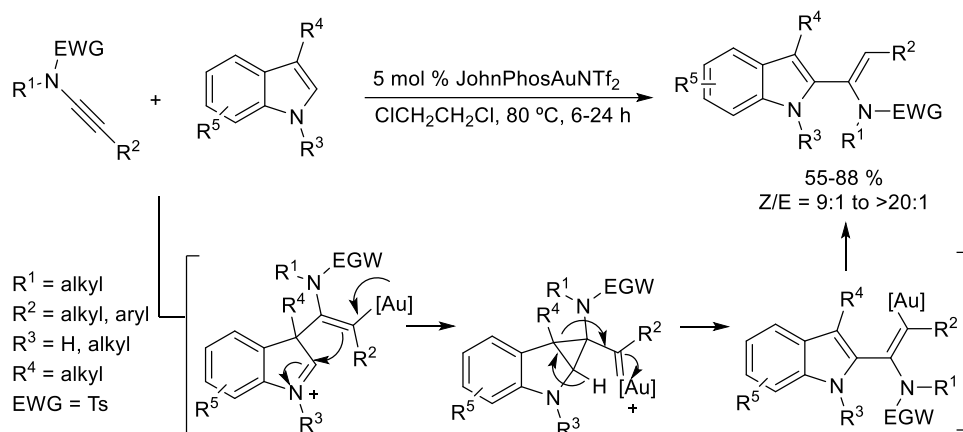
By using C-based nucleophiles and gold-activated ynamides it is possible to create novel carbocyclic compounds.²⁵ Scheme 3.14 illustrates an example of this reaction type, in which a 3-substituted indole undergoes gold-catalysed reaction with ynamides to produce 2-alkenylindole derivatives.²⁶ During this process, the

²⁴ Chen, C.; Cui, S. *J. Org. Chem.* **2019**, *84*, 12157-12164.

²⁵ a) Mak, X. Y.; Crombie, A. L.; Danheiser, R. L. *J. Org. Chem.* **2011**, *76*, 1852-1873; b) Rettenmeier, E.; Schuster, A. M.; Rudolph, M.; Rominger, F.; Gade, C. A.; Hashmi, A. S. K. *Angew. Chem. Int. Ed.* **2013**, *52*, 5880-5884; c) Tokimizu, Y.; Wieteck, M.; Rudolph, M.; Oishi, S.; Fujii, N.; Hashmi, A. S. K.; H. Ohno, H. *Org. Lett.* **2015**, *17*, 604-607; d) Dutta, S.; Yang, S.; Vanjari, R.; Mallick, R. K.; Gandon, V.; Sahoo, A. K. *Angew. Chem. Int. Ed.* **2020**, *59*, 10785-10790; e) Yuan, T.; Tang, Q.; Shan, C.; Ye, X.; Wang, J.; Zhao, P.; Wojtas, L.; Hadler, N.; Chen, H.; Shi, X. *J. Am. Chem. Soc.* **2021**, *143*, 4074-4082.

²⁶ Pirovano, V.; Negrato, M.; Abbiati, G.; Dell'Acqua, M.; Rossi, E. *Org. Lett.* **2016**, *18*, 4798-4801.

indole participates in *anti*-addition to a gold-activated ynamide, forming an alkenyl gold intermediate. This intermediate undergoes subsequent gold-back donation and cyclization to generate a gold-carbene complex conjugated with a cyclopropyl motif. Finally, the ring opening of the cyclopropyl group and a subsequent protodeauration yield the products.



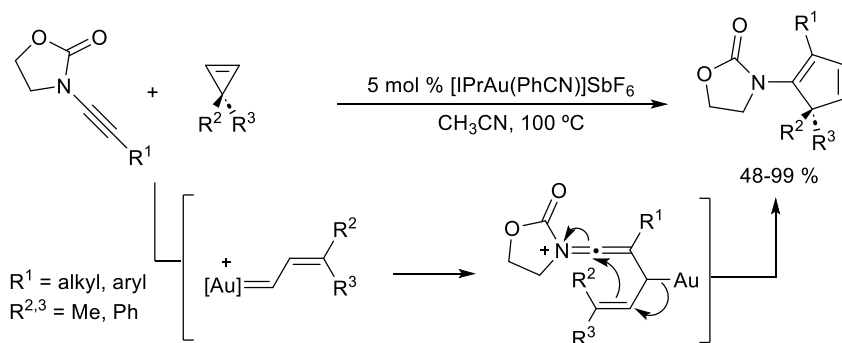
Scheme 3.14: Example of ynamides hydroarylation reaction catalysed by gold.

On the other hand, Huang and co-workers have developed an innovative method for the synthesis of cyclopentadiene derivatives by using a gold-catalysed cycloaddition of ynamides with cyclopropenes. This method involves preferential activation of the alkene over the alkyne (Scheme 3.15).²⁷ The mechanism begins with the activation of the cyclopropene by a cationic gold catalyst, which leads to the formation of an alkenyl carbenoid intermediate. The ynamide then attacks the carbene moiety, resulting in the formation of a keteniminium species. Finally, a deaurative intramolecular cyclization takes place, yielding the cyclopentadiene derivative.

In addition, the reaction already described in Scheme 3.5 (p.131), where ynamides and olefins undergo a [4+2]-cycloaddition process, leading to the formation of six-membered rings belongs also to this type of transformation.¹³

²⁷ Cheng, X.; Zhu, L.; Lin, M.; Chen, J.; Huang, X. *Chem. Commun.* **2017**, 53, 3745-3748.

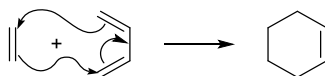
¹³ Dateer, R. B.; Shaibu, B. S.; Liu, R.-S. *Angew. Chem. Int. Ed.* **2012**, 51, 113-117.



Scheme 3.15: Cycloisomerization of ynamides with cyclopropenes catalysed by gold.

2.3 Dehydro-Diels-Alder reactions.

One of the most powerful and well-known C-C bond-forming reactions in organic chemistry is the Diels-Alder (DA) cycloaddition.²⁹ The basic form of the DA reaction is the thermal [4+2]-cycloaddition between 1,3-butadiene (diene) and ethylene (dienophile), resulting in the formation of cyclohexene (Scheme 3.16).



Scheme 3.16: Classical Diels-Alder reaction.

The dehydro-Diels-Alder (DDA) reactions are a type of modified Diels-Alder reactions that involve substrates with increasingly higher oxidation states (Scheme 3.17).³⁰ According to Hoye and co-workers classification,³¹ when an alkyne and a diene react, they undergo a didehydro-Diels-Alder (DDDA) transformation to produce a cyclohexadiene (*type 1 DDDA*);³² in a similar manner, a reaction between an alkene and an enyne would lead to cyclohexadiene through a [1,3]-rearrangement of the proton (*type 2 DDDA*). In the case where an alkyne is present on both the

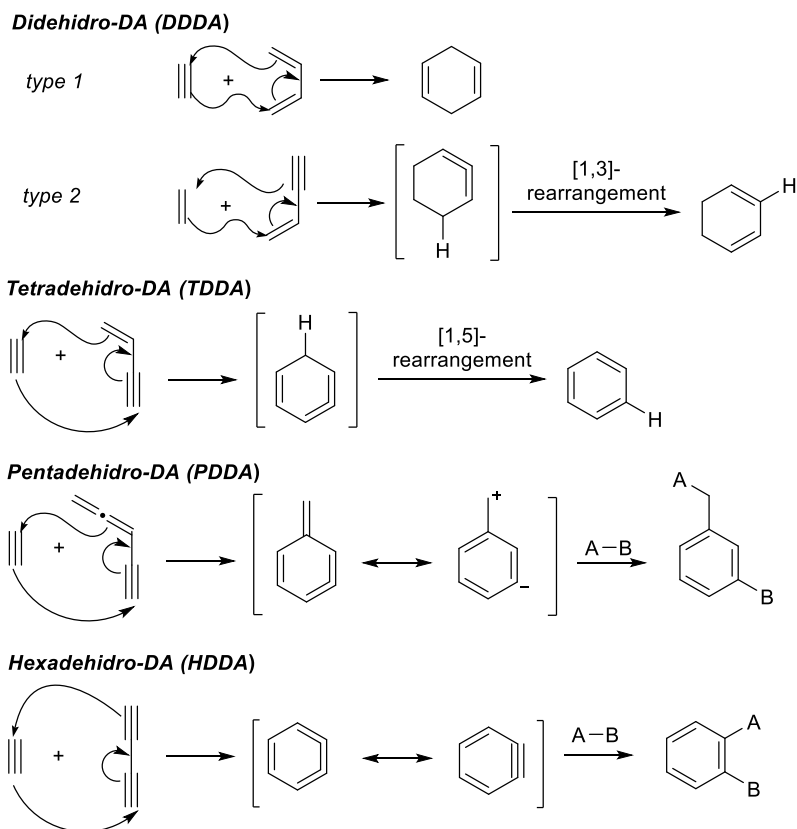
²⁹ Diels, O.; Alder, K. *Justus Liebigs Ann. Chem.* **1928**, *460*, 98-122.

³⁰ a) Wessig, P.; Müller, G. *Chem. Rev.* **2008**, *108*, 2051-2063; b) Johnson, R. P. *J. Phys. Org. Chem.* **2010**, *23*, 283-292; c) Li, W.; Zhou, L.; Zhang, J. *Chem. Eur. J.* **2016**, *22*, 1558-1571.

³¹ Hoye, T. R.; Baire, B.; Niu, D.; Willoughby, P. H.; Woods, B. P. *Nature*, **2012**, *490*, 208-212.

³² a) Brummond, K. M.; Kocsis, L. S. *Acc. Chem. Res.* **2015**, *48*, 2320-2329; b) Bober, A. E.; Proto, J. T.; Brummond, K. M. *Org. Lett.* **2017**, *19*, 1500-1503; c) Chen, X.; Zhong, C.; Lu, Y.; Yao, M.; Guan, Z.; Chen, C.; Zhu, H.; Luo, Z.; Zhang, Y.; *Chem. Commun.* **2021**, *57*, 5155-5158.

enyne and enynophile, it results in the tetrahydro-Diels-Alder (TDDA) variant, which ultimately yields a product in the benzene oxidation state after a [1,5]-rearrangement of the proton. The pentadehydro-Diels-Alder (PDDA) reaction, on the other hand, involves allenyne and alkynes, proceeds via 3-dehydrotoluene species and generates trappable reactive intermediates.³³ Finally, the hexadehydro-Diels-Alder (HDDA) reaction occurs between diynes and alkynes and goes through a benzyne intermediate that can also be trapped.³⁴



Scheme 3.17: Variations of the classical Diels-Alder reaction.

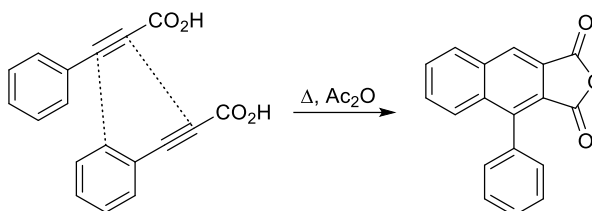
³³ a) Wang, T.; Naredla, R. R.; Thompson, S. K.; Hoyer, T. R. *2*; b) Xu, Q.; Hoyer, T.R. *Angew. Chem. Int. Ed.* **2022**, *61*, e202207510; c) Kraemer, N.; Naredla, R.R.; Hoyer, T.R. *Org. Lett.* **2022**, *24*, 2327-2331

³⁴ a) Lucas L. Fluegel L. L.; Hoyer, T. R. *Chem. Rev.* **2021**, *121*, 2413-2444; b) Lynn, M.; Smela, M.P.; Hoyer, T.R. *Chem. Sci.* **2021**, *12*, 13902-13908; c) Zhu, C.; Hoyer, T.R. *J. Am. Chem. Soc.* **2022**, *144*, 7750-7757; d) Chinta, B.S.; Arora, S.; Hoyer, T.R. *Org. Lett.* **2022**, *24*, 425-429

Given that a wide range of examples of all these types of transformations have been reported in the literature, the focus in this chapter is going to be specifically on TDDA transformations, as the reaction developed here falls within this field. They will be outlined depending on the different ways to initiate these reactions, such as thermal, photochemical, base-promoted, or metal-catalysed methods.

2.3.1 Thermal dehydro-Diels-Alder.

Arylacetylenes have been used as a source of 4 electrons in reactions that require thermal energy to initiate.³⁵ Over 130 years ago, Michael and Bucher reported the dimerization of phenylpropionic acid in the presence of acetic anhydride to produce a tricyclic anhydride (Scheme 3.18, phenyl propionic acid is also the source of 2 electrons in this reaction).³⁶ This was the first reaction known as DDA, although they were not aware of it at the time. Later on, Baddar and colleagues expanded this process to include acid derivatives and substitution on the aromatic ring.³⁷ In addition, the use of heterocyclic derivatives has been described, resulting in the corresponding compounds with fused rings.³⁸



Scheme 3.18: Dimerization reaction of phenylpropionic acid.

³⁵ a) Brown, D.; Stevenson, R. *J. Org. Chem.* **1965**, *30*, 1759-1763; b) Holmes, T. L.; Stevenson, R. *J. Chem. Soc.* **1971**, 2091-2093; c) Rodríguez, D.; Castedo, L.; Domínguez, D. Saá, C. *Synthesis* **2004**, *5*, 761-764; d) Kawano, T.; Suehiro, M.; Ueda, I. *Chem. Lett.* **2006**, *35*, 58-59; e) Shibata, T.; Sekine, A.; Mitake, A.; Kanyiva, K. S. *Angew. Chem. Int. Ed.* **2018**, *57*, 15862-15865.

³⁶ a) Michael, A.; Bucher, J. E. *Chem. Ber.* **1895**, *28*, 2511-2512; b) Michael, A.; Bucher, J. E. *Am. Chem. J.* **1898**, *20*, 89-91; c) Bucher, J. E. *J. Am. Chem. Soc.* **1908**, *30*, 1244-1264.

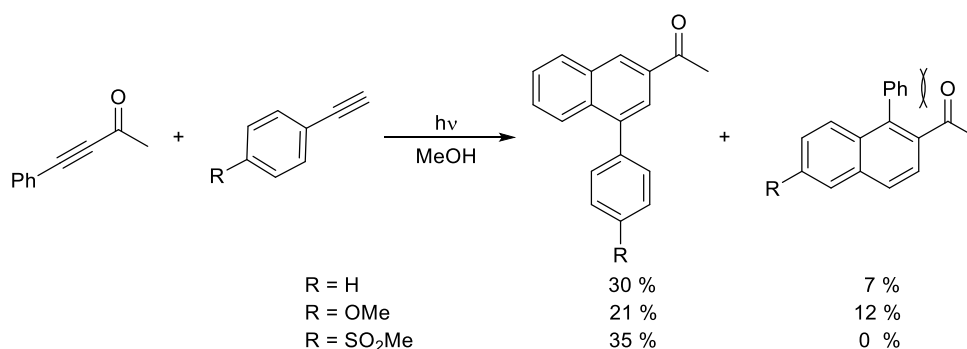
³⁷ a) Baddar, F. G. *J. Chem. Soc.* **1947**, 224-227; b) Baddar, F. G.; El-Assal, L. S. *J. Chem. Soc.* **1948**, 1267-1270; c) Baddar, F. G.; El-Assal, L. S. *J. Chem. Soc.* **1951**, 1844-1847; d) Baddar, F. G.; El-Assal, L. S.; Doss, N. A. *J. Chem. Soc.* **1959**, 1027-1032; e) Baddar, F. G.; Moussa, G. E. M.; Omar, M. T. *J. Chem. Soc.* **1968**, 110-112.

³⁸ Cadby, P. A.; Hearn, M. T. W.; Ward, A. D. *Aust. J. Chem.* **1973**, *26*, 557-570.

Arylacetylenes are the most commonly used “enynophiles” in these reactions, although examples of enynes and diynes have also been reported in the literature.³⁹

2.3.2 Photochemical dehydro-Diels-Alder.

The dehydro-Diels-Alder reaction can also be initiated photochemically. In fact, there are compounds that only evolve through this pathway and not through thermal DDA. In this case, intermolecular reactions take place with very low yields, which can be explained by the short lifetime of their starting materials' excited states, which decompose before encountering the other reactant.⁴⁰ One illustrative example is the regioselective synthesis of 4-substituted 2-acetylnaphthalenes from ynones (Scheme 3.19).⁴¹



Scheme 3.19: Photochemical intermolecular DDA.

This reaction is achieved by irradiating the ynones in the presence of another arylacetylene, resulting in the desired product with only minor amounts of other isomers. The selectivity of this reaction can be attributed to steric hindrance in 1,2,6-

³⁹ a) Fields, E. K.; Meyerson, S. *Tetrahedron Lett.* **1967**, *6*, 571-575; b) Ueda, I.; Sakurai, Y.; Kawano, T.; Wada, Y.; Futai, M. *Tetrahedron Lett.* **1999**, *40*, 319-322; c) Rodríguez, D.; Castedo, L.; Domínguez, D.; Saá, C. *Org. Lett.* **2003**, *5*, 3119-3121; d) Dunetz, J. R.; Danheiser, R. L. *J. Am. Chem. Soc.* **2005**, *127*, 5776-5777; e) Xu, Q.; Hoye, T.R. *J. Am. Chem. Soc.* **2023**, *145*, 9867-9875.

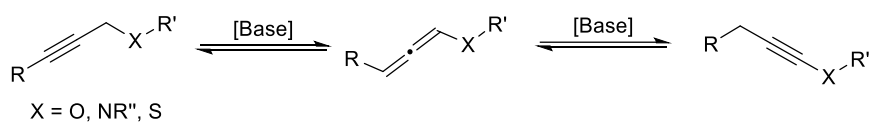
⁴⁰ a) Bryce-Smith, D.; Lodge, J. E. *J. Chem. Soc.* **1963**, 695-701; b) Büchi, G.; Perry, C. W.; Robb, E. W. *J. Org. Chem.* **1962**, *27*, 4106-4107; c) Polman, H.; Mosterd, A.; Bos, H. T. *J. Recl. Trav. Chim. Pays-Bas* **1973**, *92*, 845-854; d) Miyamoto, N.; Nozaki, H. *Bull. Chem. Soc. Jpn.* **1973**, *46*, 1257-1260; e) Xu, F.; Xiao, X.; Hoye, T. R. *J. Am. Chem. Soc.* **2017**, *139*, 8400-8403; f) Wessig, P.; Badetko, D.; Koebe, M. *ChemistrySelect* **2022**, *7*, e202202648.

⁴¹ Wessig, P.; Müller, G.; Pick, C.; Matthes, A. *Synthesis* **2007**, *3*, 464-477.

substituted naphthalene isomers, which are less favoured due to their higher energy states.

2.3.3 Dehydro-Diels-Alder reactions catalysed by bases.

These reactions are catalysed by strong bases and the [4+2]-cycloaddition step is more related to an ordinary Diels-Alder reaction, which is surrounded by isomerization processes. It has been widely acknowledged that propargyl ethers, amines, or thioethers can undergo isomerization to form allenes and heteroatom-substituted acetylenes when treated with strong bases (Scheme 3.20).⁴²



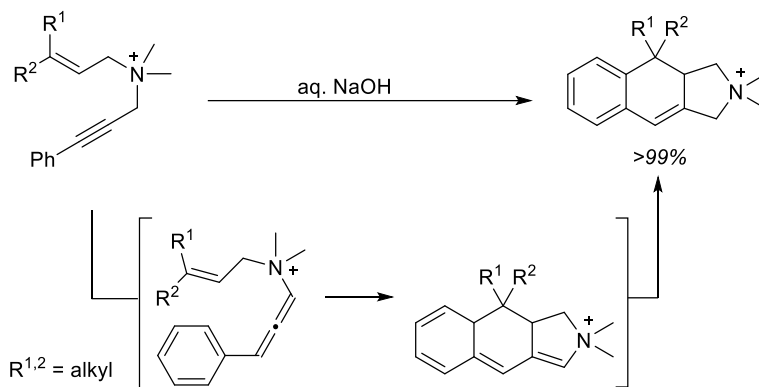
Scheme 3.20: Isomerization of acetylenes catalysed by bases.

Based on this equilibrium, different examples of this type of reaction have been reported.⁴³ One of them is shown in Scheme 3.21, where quaternary allyl propargyl ammonium salts can be used to synthesize dehydronaphthalenes through a concerted [4+2]-cyclization process followed by a [1,5]-hydrogen shift.⁴⁴

⁴² Brandsma, L. *Synthesis of Acetylene, Allenes and Cumulenes: Methods and Techniques*; Elsevier Academic Press: Amsterdam, **2004**.

⁴³ a) Garratt, P. J.; Neoh, S. B. *J. Am. Chem. Soc.* **1975**, *97*, 3255-3257; b) Garratt, P. J.; Neoh, S. B. *J. Org. Chem.* **1979**, *44*, 2667-2674; c) Cheng, Y. S. P.; Garratt, P. J.; Neoh, S. B.; Rumjamebe, V. M. *Isr. J. Chem.* **1985**, *26*, 101-104; d) Chukhadzhyan, E. O.; Chukhadzhyan, E. O.; Shakhatuni, K. G.; Babayan, A. T. *Chem. Heterocycl. Compd.* **1991**, *27*, 594-596; e) Herz, H.-G.; Schatz, J.; Maas, G. *J. Org. Chem.* **2001**, *66*, 3176-3181.

⁴⁴ a) Chukhadzhyan, E. O.; Gevorkyan, A. R.; Chukhadzhyan, E. O.; Kinoyan, F. S. *Russ. J. Org. Chem.* **2005**, *41*, 358-360.



Scheme 3.21: Intramolecular cyclization promoted by a base.

2.3.4 Dehydro-Diels-Alder reactions catalysed by metals.

It has been reported that metals such as platinum and/or rhodium,⁴⁵ or palladium⁴⁶ are able to catalyse this type of reactions. However, for the purpose of this thesis, only the two examples reported catalysed by gold are commented.

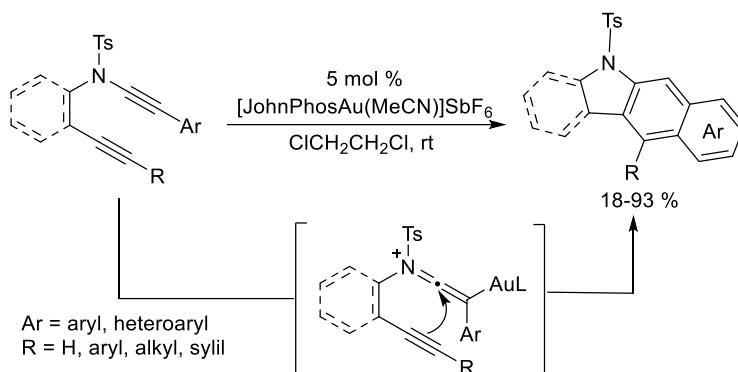
The synthesis of diversely substituted benzo[*b*]carbazoles takes place through a gold-catalysed cycloisomerization of ynamide-ynes via a formal dehydro-Diels–Alder reaction (Scheme 3.22).⁴⁷ The mechanism likely involves the regioselective attack of the pendant alkyne moiety to a keteniminium ion intermediate, followed by benzannulation. Subsequently, a similar reaction was reported where the aromatic

⁴⁵ a) Amer, I.; Blum, J.; Vollhardt, K. P. C. *J. Mol. Catal.* **1990**, *60*, 323-330; b) Badrieh, Y.; Blum, J.; Amer, I.; Vollhard, K. P. C. *J. Mol. Catal.* **1991**, *66*, 295-312; c) Baidossi, W.; H. Schumann, H.; Blum, J. *Tetrahedron* **1996**, *52*, 8349-8364; d) Saito, S.; Salter, M. M.; Gevorgyan, V.; Tsuboya, N.; Tando, K.; Yamamoto, Y. *J. Am. Chem. Soc.* **1996**, *118*, 3970-3971; e) Shibata, T.; Sekine, A.; Mitake, A.; Kanyiva, K. S. *Angew. Chem. Int. Ed.* **2018**, *57*, 15862-15865; f) Thadkapally, S.; Farshadfar, K.; Drew, M. A.; Richardson, C.; Ariaferd, A.; Pyne, S. G.; Hyland, C. J. T. *Chem. Sci.* **2020**, *11*, 10945-10950.

⁴⁶ a) Gevorgyan, V.; Yamamoto, Y. *J. Organomet. Chem.* **1999**, *576*, 232-247; b) Gevorgyan, V.; Takeda, A.; Homma, M.; Sadayori, N.; Radhakrishnan, U.; Yamamoto, Y. *J. Am. Chem. Soc.* **1999**, *121*, 6391-6402; c) Saito, S.; Yamamoto, Y. *Chem. Rev.* **2000**, *100*, 2901-2916; d) Saito, S.; Yamamoto, Y.; Negishi, E. *Handbook of Organopalladium Chemistry for Organic Synthesis Ed. Wiley, New York*, **2002**; e) Rubin, M.; Sromek, A. W.; Gevorgian, V. *Synlett* **2003**, 2265-2291; f) Goh, M. S.; Pfrunder, M. C.; McMurtrie, J. C.; Arnold, D. P. *Asian J. Org. Chem.* **2014**, *3*, 856-869.

⁴⁷ Xu, W.; Wang, G.; Xie, X.; Liu, Y. *Org. Lett.* **2018**, *20*, 3273-3277.

ring was not necessary to increase the rigidity of the structure to have the two alkyne moieties positioned closer in space, leading to indoles.⁴⁸



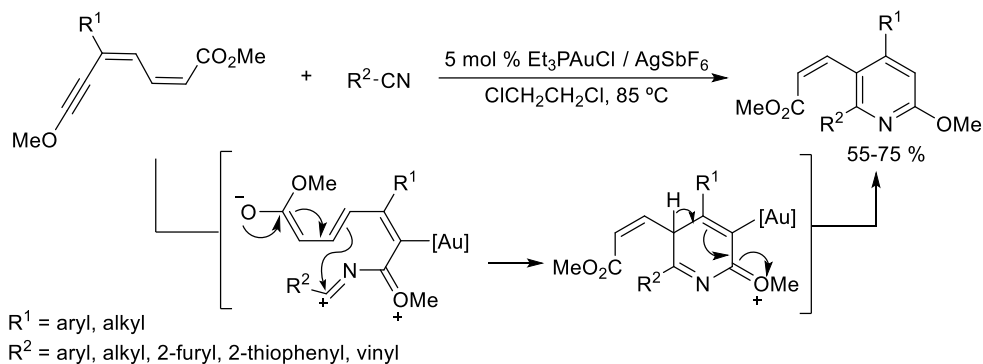
Scheme 3.22: Obtention of benzo[*b*]carbazoles and indoles through a gold (I)-catalysed reaction.

2.4 “Push-pull” 2,4-dien-6-yne in intermolecular reactions.

Our group has been studying the use of “push-pull” 2,4-dien-6-yne systems as starting materials in various intermolecular reactions with different nucleophiles in recent years. The first successful attempt is outlined in Scheme 3.23, in which a regioselective direct access to pyridines was achieved through an intermolecular hetero-tetrahydro-Diels-Alder (H-TDDA) cycloaddition with nitriles catalysed by gold (I).⁴⁹ The reaction occurs via an intramolecular attack and the subsequent addition of the nitrile to the activated C-C bond, furnishing the final pyridine after a protodeauration step.

⁴⁸ Prabagar, B.; Dutta, S.; Gandon, V.; Sahoo, A. K. *Asian J. Org. Chem.* **2019**, *8*, 1128-1132.

⁴⁹ Barluenga, J.; Fernández-Rodríguez, M. A.; García-García, P.; Aguilar E. *J. Am. Chem. Soc.* **2008**, *130*, 2764-2765.



Scheme 3.23: Intermolecular cycloaddition to obtain pyridine derivatives catalysed by gold.

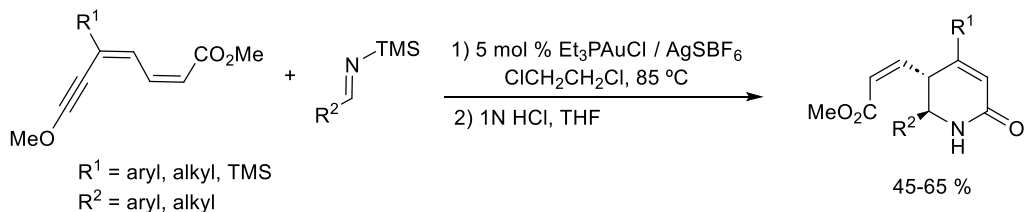
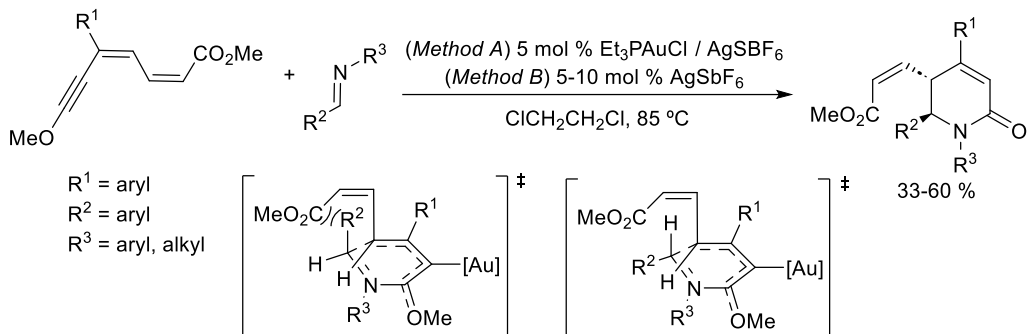
As an extension of this research, an intermolecular hetero-didehydro-Diels-Alder (H-DDDA) reaction catalysed by gold (I) or silver (I) salts between “push-pull” methyl 2,4-dien-6-ynecarboxylates and aldimines (Scheme 3.24, *top*) or silylaldimines (Scheme 3.25, *bottom*) has been achieved, yielding the diastereo- and regioselective formation of 5,6-dihydropyridin-2-ones with good yields.⁵⁰ The selective formation of the *anti* diastereoisomer can be attributed to reduced steric hindrance during the cyclization step, which occurs via a preferred transition state where the R^2 group and the ester moiety are further apart from each other (Scheme 3.24, *top*). This enables the reactants to adopt a conformation that is more favourable for the reaction to occur with greater selectivity towards the *anti* diastereoisomer.

A similar approach was attempted using aldehydes as nucleophiles (Scheme 3.25),^{51,52} although optimal reaction conditions could not be reached. An open-chain product was obtained for most of the conditions tested, being the best ones described by *method A*. On the other hand, under *method B* conditions, the dihydropyranone product could be obtained, but the reaction was not found to be robust, showing lack of reproducibility. The instability of the product under the reaction conditions may be a contributing factor, and further testing is necessary to determine the effectiveness of this transformation.

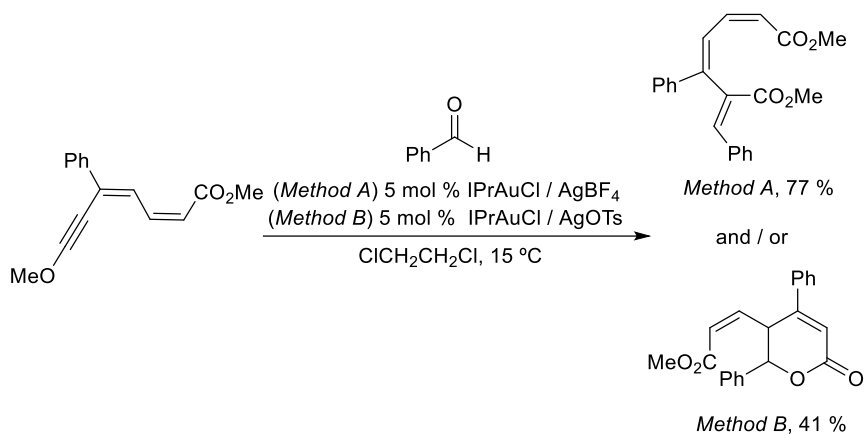
⁵⁰ Fernández-García, J. M.; Fernández-Rodríguez, M. A.; Aguilar E. *Org. Lett.* **2011**, *13*, 5172-5175.

⁵¹ Fernández-García, J. M. *Ph. D. Thesis dissertation, University of Oviedo*, **2013**.

⁵¹ Otero-Diz, E. M. *Master Thesis dissertation, University of Oviedo*, **2014**.



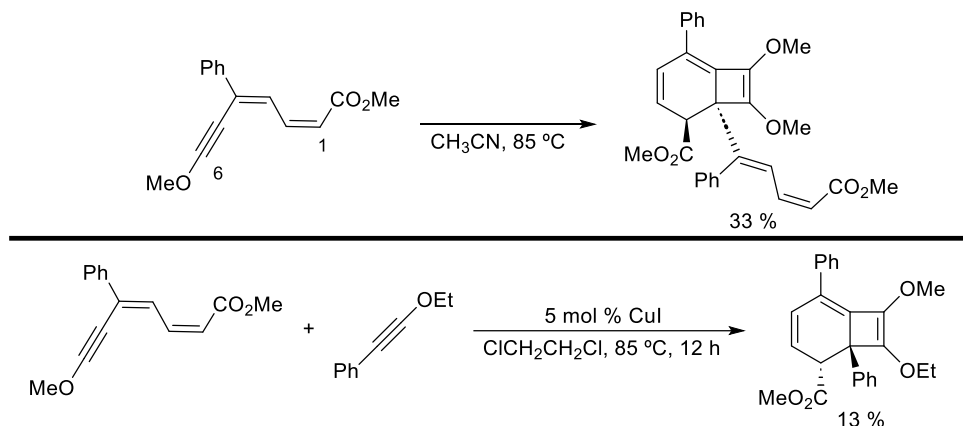
Scheme 3.24: Intermolecular reaction catalysed by gold (I) to obtain 5,6-dihydropyridin-2-ones.



Scheme 3.25: Intermolecular reaction catalysed by gold (I) between a “push-pull” 2,4-dien-6-yne and benzaldehyde.

It was also found that, under certain conditions or upon standing, the “push-pull” 2,4-dien-6-yne carboxylic esters evolve to bicyclo[4.1.0] dimerization products (Scheme 3.26, *top*). These compounds are obtained through an intermolecular cycloaddition reaction where a molecule of 2,4-dien-6-yne reacts through positions 1 and 6, while the other unit reacts through positions 5 and 6 of the

conjugated system. In an attempt to further understand this transformation, the intermolecular reaction between “push-pull” 2,4-dien-6-ynecarboxylic esters and ynol ethers was also studied (Scheme 3.26, *bottom*). Although the product shown in the scheme was better formed under copper catalysis, the reached yields were not satisfactory in any conditions tested so far.⁵¹

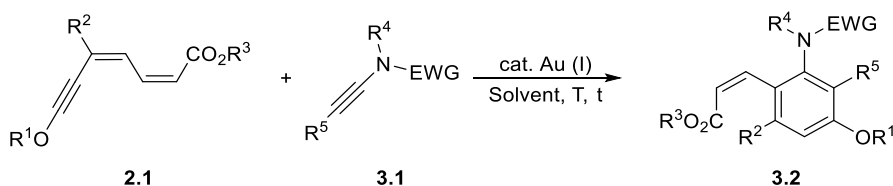


Scheme 3.26: Intramolecular dimerization of “push-pull” 2,4-dien-6-ynes vs intermolecular reaction between “push-pull” 2,4-dien-6-ynes and ynol ethers.

⁵¹ Fernández-García, J. M. *Ph. D. Thesis dissertation, University of Oviedo, 2013.*

3 Results and discussion.

This chapter aims to investigate the reaction between “push-pull” alkyl 2,4-dien-6-yne carboxylates **2.1** and ynamides **3.1** to obtain tetrasubstituted anilines **3.2**. Considering the previously described reactivity for these substrates a [4+2]-cycloaddition reaction, that means a formal TDDA, was expected to occur with complete regioselectivity (Scheme 3.27).



Scheme 3.27: Tetradehydro-Diels-Alder transformation to obtain tetrasubstituted anilines.

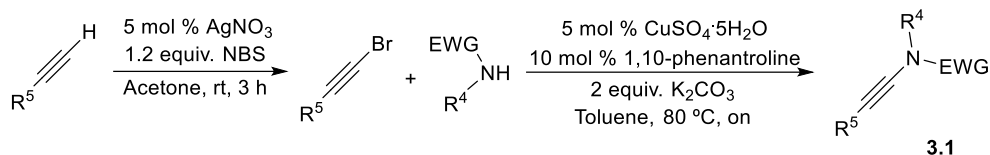
To the best of our knowledge, this is the first reported example where ynamides **3.1** are used as starting materials in gold-catalysed [4+2]-cycloadditions behaving as two-carbon synthons.

3.1 Synthesis of starting materials.

As “push-pull” 2,4-dien-6-yne carboxylates **2.1** were already used as starting materials in the reaction covered in *Chapter 2*, their synthesis and obtained yields have already been described there (*pp. 102-105*).

On the other hand, Hsung’s procedure has been used for the synthesis of the ynamides **3.1** employing 1-bromo-acetylenes (obtained brominating the acetylene)

as substrates to promote an Ullmann coupling (Scheme 3.28).⁵² Alternative methods that use starting materials such as acetylenes or *gem*-dibromovinyls were not required.³⁷



Scheme 3.28: Synthesis of ynamides.

A diverse set of ynamide derivatives **3.1** was prepared using the procedure outlined earlier. Table 3.1 lists the synthesized compounds, which incorporate different alkyl or aryl groups, along with their respective yields.

Entry	Ynamide	R ⁴	EWG	R ⁵	%Yield, 3.1 ^[a]
1	3.1a	Me	Ts	Ph	95
2	3.1b	Me	Ts	<i>p</i> Tol	76
3	3.1c	Me	Ts	<i>p</i> MeO-C ₆ H ₄	75
4	3.1d	Me	Ts	<i>p</i> Cl-C ₆ H ₄	52
5	3.1e	Me	Ts	<i>p</i> Br-C ₆ H ₄	75
6	3.1f	Me	Ts	<i>p</i> CF ₃ -C ₆ H ₄	84
7	3.1g	Me	Ts	<i>o</i> Cl-C ₆ H ₄	36
8	3.1h	Me	Ts	<i>m</i> MeO-C ₆ H ₄	72
9	3.1i	Me	Ts	<i>m</i> Cl-C ₆ H ₄	75
10	3.1j	Me	Ts	cyclohexenyl	42
11	3.1k	Me	Ts	Me	92
12	3.1l	Me	Ts	<i>t</i> Bu	15
13	3.1m	Me	Ts	<i>n</i> Bu	70
14	3.1n	Me	Ts	H	89 ^[b]
15	3.1o	-(CH ₂) ₂ -O-	-(C=O)-	Ph	78

^[a] Isolated yield of the second step (Scheme 3.28) for the obtention of ynamide derivatives **3.1**. ^[b] Obtained through desilylation of the ynamide bearing a TMS group at R⁵ moiety.

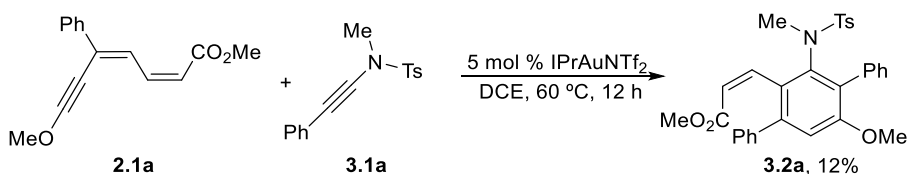
Table 3.1: Scope of ynamide derivatives **3.1** employed.

⁵² Frederick, M. O.; Mulder, J. A.; Tracey, M. R.; Hsung, R. P.; Huang, J.; Kurtz, K. C. M.; Shen, L.; Douglas, C. J. *Am. Chem. Soc.* **2003**, *125*, 2368-2369.

³⁷a) Evano, G.; Jouvin, K.; Coste, A. *Synthesis* **2013**, *45*, 17-26; b) Betou, M.; Sallustrau, A.; Toupet, L.; Trolez, Y. *Tetrahedron Lett.* **2015**, *56*, 4627-4630; c) Mansfield, S. J.; Campbell, C. D.; Jones, M. W.; Anderson, E. A. *Chem. Commun.* **2015**, *51*, 3316-3319.

3.2 Initial experiment and structural elucidation.

To test the viability of the previously mentioned hypothesis, “push-pull” methyl 2,4-dien-6-yne carboxylate **2.1a** and ynamide **3.1a** were chosen as model substrates for the initial attempt. Thus, when a mixture of **2.1a** and 1.5 equivalents of **3.1a** in DCE, in the presence of IPrAuNTf₂ as gold (I) catalyst, was heated at 60 °C for 12h, the tetrasubstituted aniline derivative **3.2a** was obtained and could be isolated in 12% yield (Scheme 3.29). It is worth noting that minor amounts of the cycloisomerization product **2.2a** (described in Chapter II) were observed in the crude reaction mixture.



Scheme 3.29: Obtention of tetrasubstituted aniline **3.2a** in the first attempt.

Several mono- and bidimensional NMR techniques allowed to identify the product as the one arising from a formal tetrahydro-Diels-Alder type [4+2] intermolecular cycloaddition previously proposed (Scheme 3.27, *p.* 149), as a single regioisomer. However, elucidating the relative position of the amido and aryl substituents coming from the ynamide in the ring was not a trivial quest using HSQC and HMBC. To this end, different selective NOE experiments irradiating key positions in the molecule were performed, and the results are collected in Figure 3.1 (*bottom*).

Aiming to simplify the pattern in the aromatic region and distinguish between the aromatic substituents in the ring, tetrasubstituted aniline **3.2p** bearing a *p*-tolyl group, obtained from **2.1a** and **3.1b** (see next section), was chosen as the subject for the NOE experiments. The ¹H-NMR spectra for this compound is provided in Figure 3.1 (*purple*). To determine whether the obtained regioisomer is **3.2p** or **3.2p'**, the proton signals at carbons 8 and 9 in the methyl acrylate unit and the one at position 10 (–NTsMe) are the most informative. If the obtained regioisomer is **3.2p**, the proton at carbon 8 (and less likely at 9) should exhibit NOE effects with those at position 10. On the other hand, if the obtained isomer is **3.2p'**, the opposite combinations would appear: proton at carbon 8 will now have NOE with protons at position 20 (*o*-CH) (Figure 3.1, *top*). To identify the proton at carbon 8 (overlapped with those of the phenyl ring), a selective NOE experiment (*green*) was done irradiating the proton at position 9, showing that the proton at carbon 8 appears at 7.40 ppm. On the other

hand, the signal at 7.38 ppm belongs to the *ortho*-protons in the phenyl ring, as is exposed in the selective NOE irradiating the proton at position 3 (*red*). Turning the attention to the selective NOE of the protons at carbon 10 (*blue*), positive peaks indicating a NOE effect can be observed at 3.42 (–COOMe), at 5.80 (proton at position 9) and slightly at 7.40 ppm (proton at carbon 8). Altogether, it can be concluded that the acrylate moiety is spatially close to the –NTsMe and that the reaction took place in a regioselective manner to generate compound **3.2p** as an exclusive isomer.

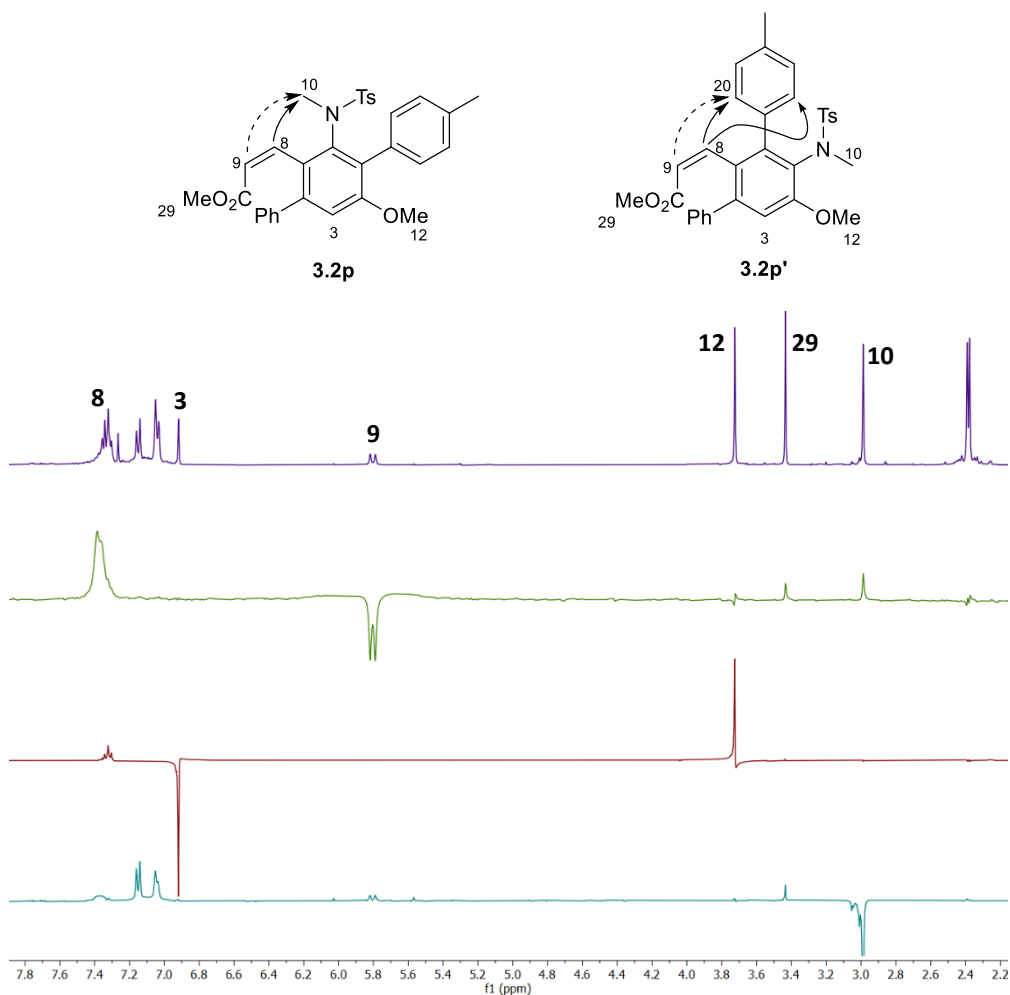
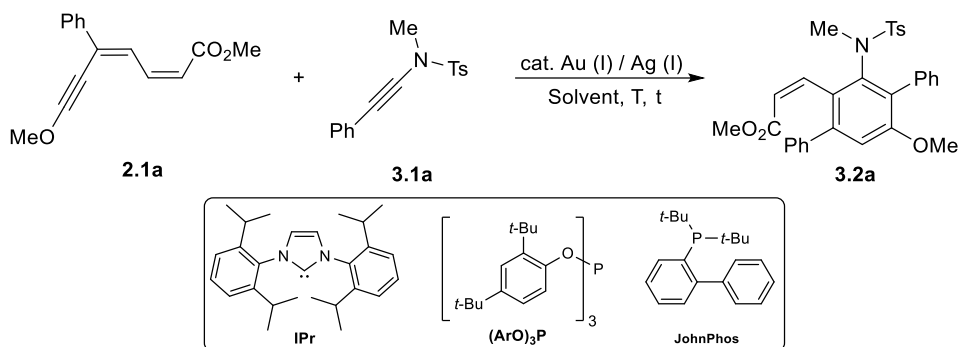


Figure 3.1: Stacked selective NOE spectra obtained for derivative **3.2p**.

3.3 Optimization of the reaction conditions.

Aiming to improve the yield of the [4+2]-cycloaddition reaction between “push-pull” 2,4-dien-6-yne carboxylates **2.1** and ynamides **3.1** to obtain tetrasubstituted anilines **3.2**, different combinations of gold and silver catalysts, starting reagents stoichiometry, reaction times, temperatures, and solvents have been used to study the reaction conditions. “Push-pull” methyl 2,4-dien-6-ynecarboxylate **2.1a** and ynamide **3.1a** were chosen as model substrates. The reaction conditions tested have been summarized in Table 3.2.



Entry	Catalyst A/B (% mol A/% mol B)	2.1a:3.1a	time (h)	T (°C)	Solvent	%Yield, 3.2a ^[a]
1	IPrAuNTf ₂ (5)	1:1.5	12	60	DCE	12 ^[b]
2	IPrAuNTf ₂ (5)	1:2	12	60	DCE	15 ^[b]
3	IPrAuNTf ₂ (5)	1:2	16	60	DCE	19 ^[b]
4	IPrAuNTf ₂ (5)	1:2	16	60	Toluene	15
5	IPrAuNTf ₂ (5)	1:2	16	60	Dioxane	traces
6	IPrAuNTf ₂ (5)	1:2	16	rt	DCE	40
7	IPrAuNTf ₂ (5)	1:2	16	0	DCE	20
8	IPrAuCl/AgSbF ₆ (5/10)	1:2	16	rt	DCE	25
9	IPrAuCl/AgBF ₄ (5/10)	1:2	16	rt	DCE	33
10	Ph ₃ PAuCl/AgBF ₄ (5/10)	1:2	16	rt	DCE	-
11	(ArO) ₃ PAuCl/AgBF ₄ (5/10)	1:2	16	rt	DCE	-
12	JohnPhosAuCl/AgBF ₄ (5/10)	1:2	16	rt	DCE	99
13	[JohnPhosAu(MeCN)]BF ₄ (5)	1:2	16	rt	DCE	40
14	AgBF ₄ (10)	1:2	16	rt	DCE	-

^[a] NMR estimated yield using 1,3,5-trimethoxybenzene as internal standard. ^[b] Minor amounts of the cycloaromatization product **2.2a** (Chapter II) were obtained.

Table 3.2: Optimization of the reaction conditions.

In the initial experiment a 5 mol% of IPrAuNTf₂ catalyst was used with a 1:1.5 ratio of “push-pull” methyl 2,4-dien-6-yne carboxylate **2.1a** / ynamide **3.1a** in dichloroethane. The reaction was heated at 60 °C for 12 hours, resulting in a yield of only 12% for cycloaddition product **3.2a** (Entry 1). By slightly increasing the amount of ynamide **3.1a** added (Entry 2), the yield of **3.2a** improved to 15%. Further experimentation showed that leaving the reaction to proceed for a longer time (Entry 3) increased the yield of product **3.2a** to 19%, as some unreacted “push-pull” methyl 2,4-dien-6-yne carboxylate **2.1a** was found. On the other hand, testing different solvents (Entries 4-5) did not improve the yield. However, varying the temperature (Entries 6-7) provided better results being the best one obtained at room temperature. Finally, different combinations of Au (I) catalysts and silver salts were used (Entries 8-14). Excellent yield of 99% was obtained employing a mixture of 5 mol% of JohnPhosAuCl catalyst and a 10 mol% of AgBF₄ (Entry 12). It is important to note that the use [JohnPhosAu(MeCN)]BF₄ (Entry 13) provided a worse yield, while the reaction did not take place when running only in the presence of the silver salt as catalyst (Entry 14). This suggests that both catalysts are necessary, and the silver salt has a role beyond just providing the counterion, which may explain why a double amount of Ag (I) is required compared to Au (I). Again, as the reaction developed in Chapter 2, this can be considered a case of silver assisted gold-catalysis.

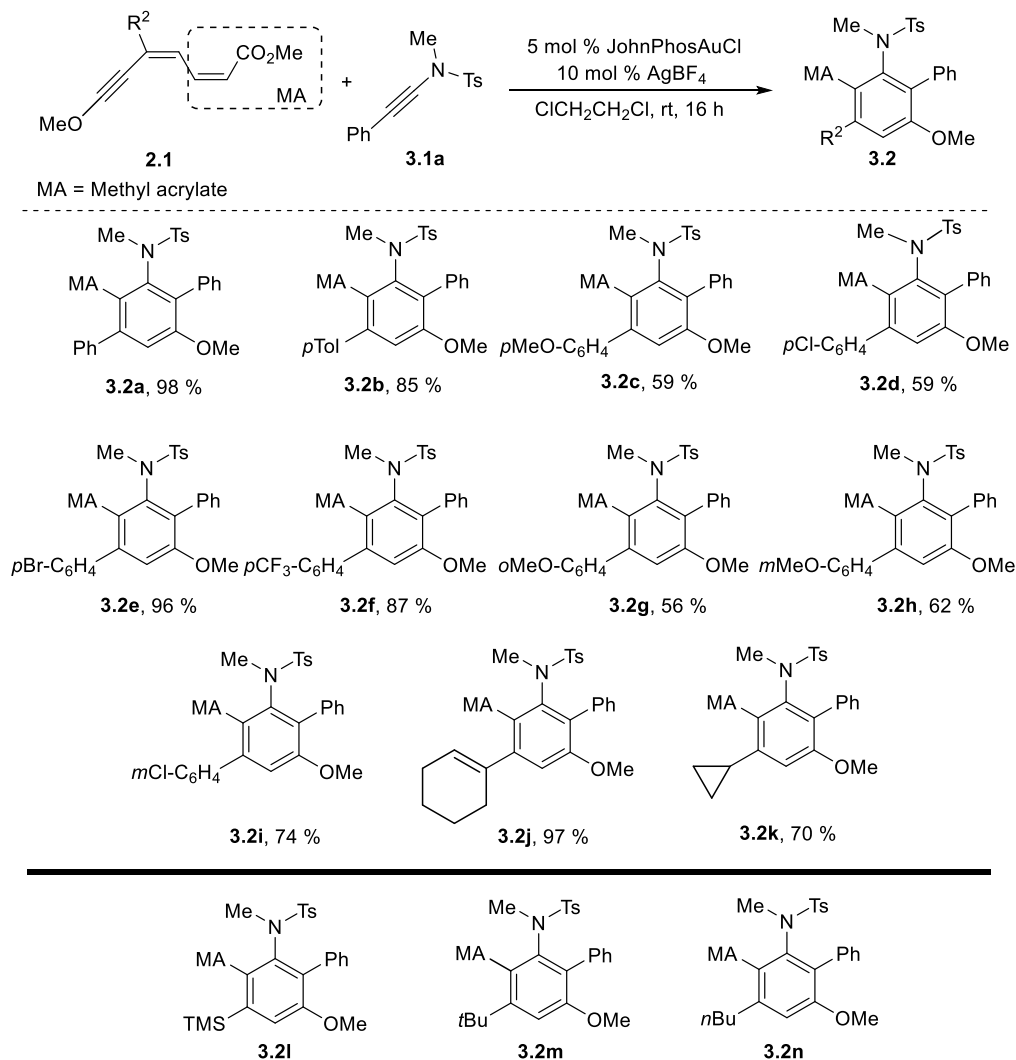
As a conclusion of the optimization process, the best conditions found required to use a mixture of 5/10 mol% of JohnPhosAuCl/AgBF₄ in DCE at room temperature for 16 hours.

3.4 Scope of the reaction.

Once the best conditions for the formation of tetra-substituted aniline **3.2a**, by a tetrahydro-Diels-Alder (TDDA) reaction between “push-pull” methyl 2,4-dien-6-yne carboxylate **2.1a** and ynamide **3.1a**, were determined, the scope of the reaction was established starting by modifying the R² group of the “push-pull” methyl 2,4-dien-6-yne carboxylate **2.1** (Scheme 3.30, top).

Good to excellent yields were achieved with aromatic moieties substituted at the *para*-position with either electron-donating (**3.2b,c**) or electron-withdrawing groups (**3.2d-f**). Additionally, the reaction is tolerant to substitution at the *ortho*- (**3.2g**) and *meta*-positions (**3.2h,i**) of the aromatic ring; in the last case, both for electron-donating and electron-withdrawing groups. Notably, good to excellent yields were also achieved with aliphatic rings, with examples of a cyclohexene (**3.2j**) and a cyclopropyl ring (**3.2k**). It was also attempted to introduce a silylated group at

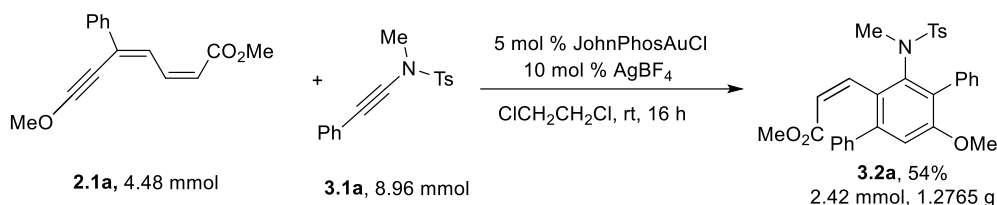
R² substituent in **2.1**, such as the trimethylsilyl moiety (**3.2l**), but a defined product could not be obtained (Scheme 3.30, *bottom*). Similarly, the efforts to introduce acyclic moieties at that position (**3.2m**, **3.2n**) were also unsuccessful.



Scheme 3.30: Scope of the reaction by modifying R² moiety in “push-pull” 2,4-dien-6-yne carboxylate **2.1**.

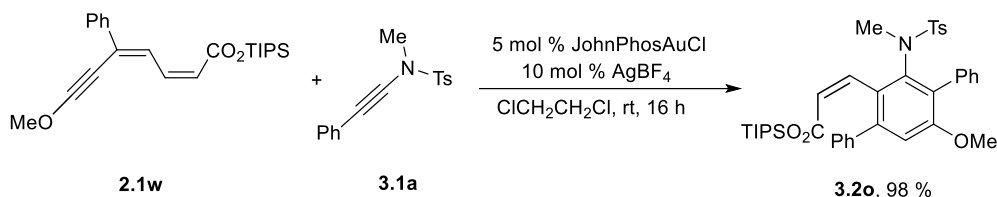
Under optimized reaction conditions, a gram-scale reaction performed with “push-pull” 2,4-dien-6-yne carboxylate **2.1a** and ynamide **3.1a** produced of 1.2765 g of tetra-substituted aniline **3.2a** with a yield of 54%. This transformation showcases

the method's synthetic potential and its suitability for large-scale industrial applications (Scheme 3.31).



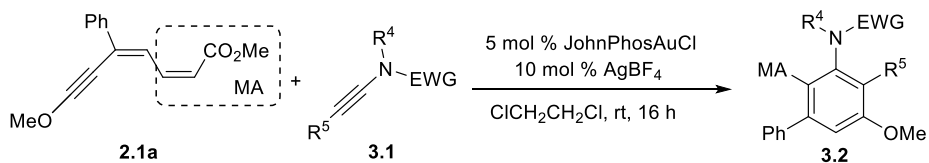
Scheme 3.31: Gram-scale reaction.

At the moment, the modification of the substituent at R³ displays a unique example (Scheme 3.32). Noteworthy, excellent yield of tetrasubstituted aniline **3.2o** was obtained by replacing the methoxy group of the R³ moiety with a triisopropylsilyloxy group.

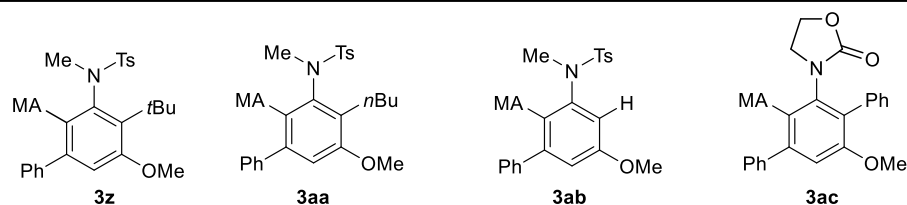
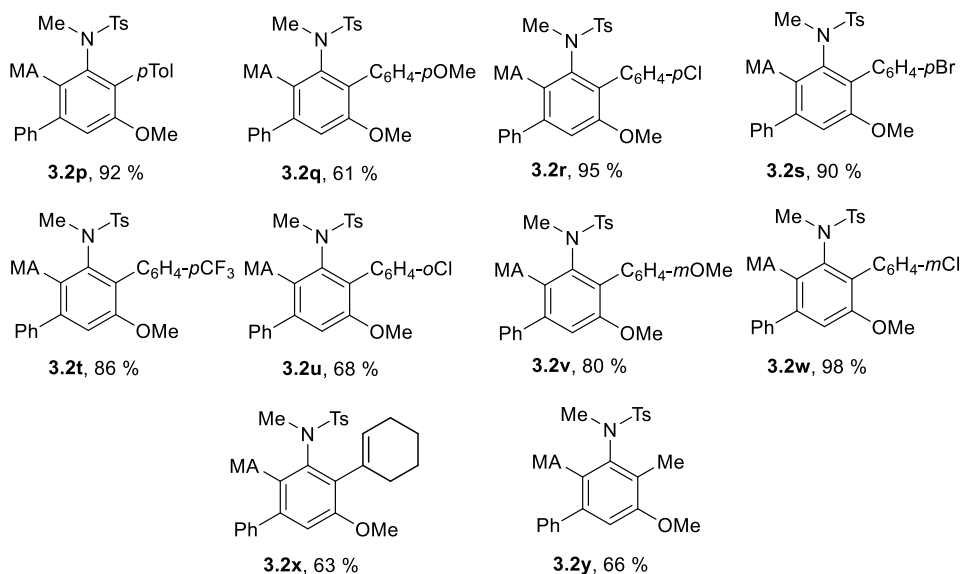


Scheme 3.32: Reaction with "push-pull" 2,4-dien-6-yne carboxylate **2.1w**.

Scheme 3.33 (*top*) shows the scope expanded to include variations at R⁵ moiety of the ynamide **3.1**. Excellent to good yields were obtained when electron-withdrawing (**3.2r-t**) and electron-donating groups (**3.2p, q**) were located at the *para*-position of the aromatic ring. In addition, good yields were attained with substitution at the *ortho*- (**3.2u**) and *meta*-position (**3.2v, w**) of an aromatic ring, where one example has an electron-donating group and the other has an electron-withdrawing group. Notably, the R⁵ position was also tolerant of a cyclohexene ring (**3.2x**) and a methyl group (**3.2y**). In addition, attempts to introduce other aliphatic moieties such as *t*-butyl (**3.2z**), *n*-butyl (**3.2aa**) or a hydrogen atom (**3.2ab**) failed (Scheme 3.33, *bottom*). Finally, one test to substantially modify the substituents of the *N* atom from ynamides **3.2**, installing an oxazolidinone ring (**3.2ac**) instead of the sulfonyl group (modifying both R⁴ and EWG), was completely unsuccessful.

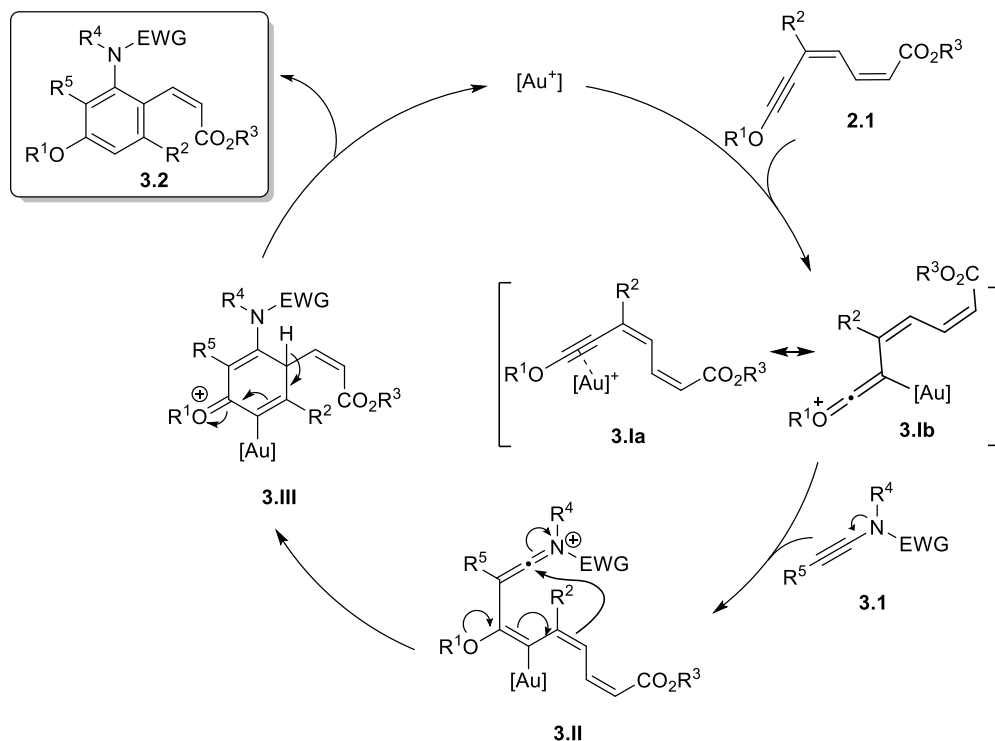


MA = Methyl acrylate

Scheme 3.33: Scope of the reaction by modifying the moieties in ynamide **3.1**.

3.5 Reaction mechanism.

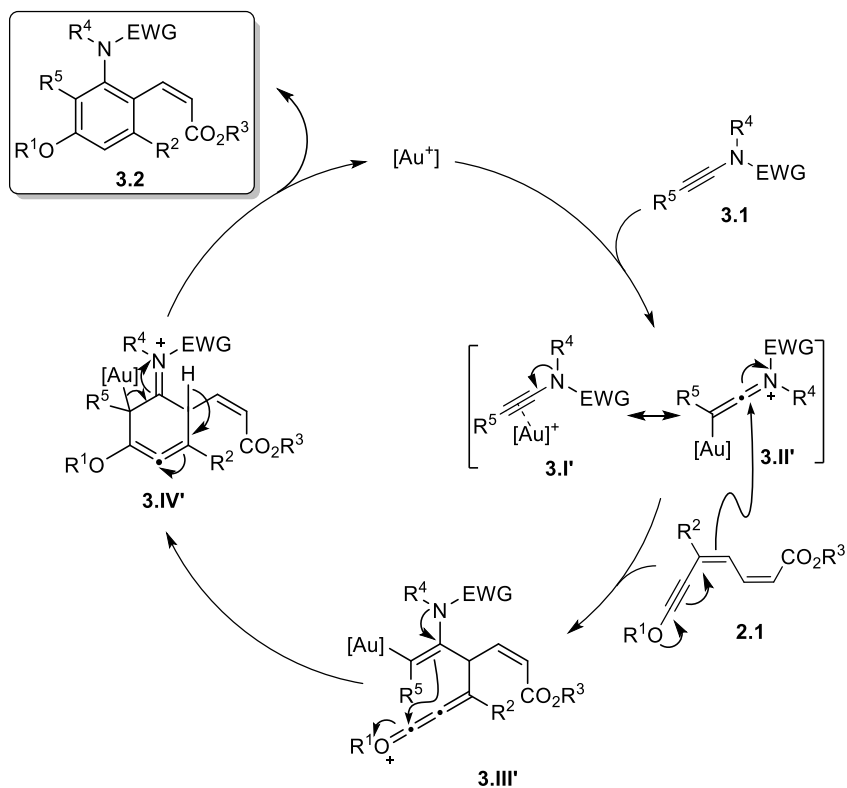
In principle, two mechanistic alternatives can be considered, each one of them involving the initial coordination of the gold catalyst to the triple bond of one or the other of the starting materials. In the first option (Scheme 3.34), the gold catalyst should activate the C-C triple bond of the “*push-pull*” alkyl 2,4-dien-6-ynecarboxylate **2.1** (**3.I**). Later, a nucleophilic attack of the ynamide **3.1** through the beta carbon should take place to form trienyl-keteniminium intermediate **3.II**. After that, an intramolecular cyclization promoted by the alkoxy group would occur to form the 6-membered ring carbocyclic intermediate **3.III**. Finally, a protodeauration process would take place to obtain the final aniline **3.2** and recover the gold catalyst.



Scheme 3.34: Proposed reaction mechanism.

At the alternative mechanism the initial coordination of the gold catalyst with the C-C bond of the ynamide (Scheme 3.35) would lead to the formation of gold keteniminium intermediate **3.II'**. Then, to account for the formation of aniline **3.2**, an intermolecular nucleophilic attack of “push-pull” alkyl 2,4-dien-6-ynecarboxylate **2.1**, through the δ -position of the triple bond should take place to form three-bonded cumulene derived oxonium intermediate **3.III'**, which could further evolve into the cyclic allene intermediate **3.IV'** by intermolecular cyclization. Finally, a [1,3]-hydrogen shift and a deauration process would yield the final product **3.2**.

This cyclic intermediate **3.IV'** could be the possible reason why this mechanism is less prone to occur. Intermediate **3.IV'** is a 6-membered cyclic allene and its formation seems rather difficult because of the inherent strain of having two consecutive double bonds in such small cycles. Therefore, the mechanism depicted in Scheme 3.34 stands as the most plausible option.



Scheme 3.35: Alternative reaction mechanism through ynamide activation.

In order to obtain mechanistic insights, quantum chemical calculations were conducted. The “push-pull” alkyl 2,4-dien-6-ynecarboxylate **2.1x** and ynamide **3.1x** were chosen as model substrates, and Me_3PAuBF_4 as model gold-catalyst (Figure 3.2).

For the first step, it was observed that the coordination of the ynamide by the gold catalyst is energetically more favourable than the coordination of the triple bond in the “push-pull” alkyl 2,4-dien-6-ynecarboxylate (-9.9 vs -2.1 kcal/mol). However, the theoretical exploration of the pathway starting with ynamide coordination did not yield the experimentally obtained product, neither led to any other reaction pathway. In this sense, it can be concluded that the reaction would occur with complete discrimination between two electron-rich alkynes.

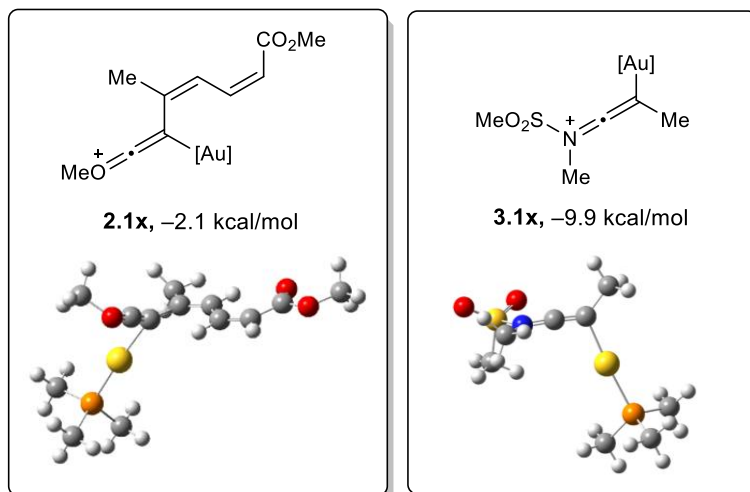
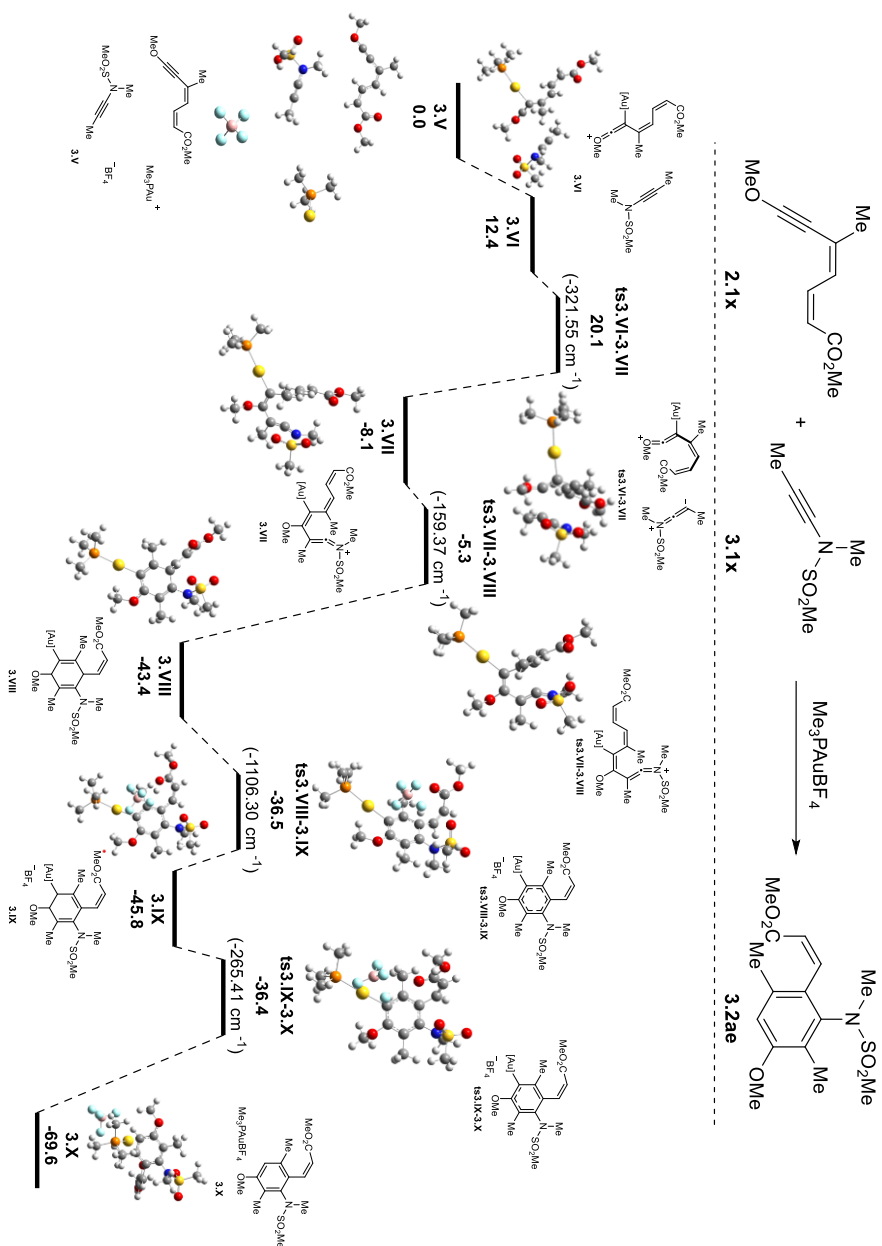


Figure 3.2: Activation of the “push-pull” alkyl 2,4-dien-6-ynecarboxylate **2.1x** vs ynamide **3.1x**.

Therefore, the reaction mechanism would begin with the metal catalyst complexing the triple bond of the “push-pull” alkyl 2,4-dien-6-ynecarboxylate **2.1x** (Scheme 3.36). Then, the ynamide **3.1x** would approach it to form intermediate **3.VI** (12.4 kcal/mol) where both fragments experience a weak interaction. Subsequently, the nucleophilic intermolecular attack of β -carbon of the ynamide **3.1x** to C6 in the “push-pull” alkyl 2,4-dien-6-ynecarboxylate **2.1x** would take place to the trienyl-keteniminium intermediate **3.VII** (–8.1 kcal/mol) where a new C-C bond has been formed. The transition state for this process is the rate limiting one of the whole mechanism and presents a barrier of 20.1 kcal/mol.

Then, intermediate **3.VII** undergoes an intramolecular nucleophilic attack to yield the cyclic intermediate **3.VIII** (–43.4 kcal/mol) through a low energy barrier transition state (–5.3 kcal/mol) where a second C-C bond forms. At intermediate **3.VIII** the final hexacycle is already built and only protodeauration is needed to reach the final product. BF_4^- performs the extraction of the proton from the sp^3 C atom of the diene fragment participating in the lastly formed C-C bond through **ts3.VIII-3.IX** (–36.5 kcal/mol) and its donation to the C atom still linked to the gold catalyst through **ts3.IX-3.X** (–36.4 kcal/mol). Aniline **3.X** is the very stable species (–69.6 kcal/mol) finally formed.



Scheme 3.36: Cycloaddition reaction to obtain **3.2ae** catalysed by Me_3PAuCl , intermediates and transition states optimized using the B3LYP/6-31(G) (LANL2DZ for gold) computational level.

As it can be seen, the theoretical studies supported the proposed mechanism for the reaction, which starts with the activation of the gold catalyst on the triple bond of the “*push-pull*” 2,4-dien-6-ynecarboxylate. Subsequently, an intermolecular nucleophilic attack occurs, followed by an intramolecular cyclization reaction. Finally, a protodeauration process takes place, leading to the formation of tetrasubstituted aniline derivatives **3.2ae**.

4 Conclusions.

This chapter describes a gold-catalysed cyclization reaction of *“push-pull”* alkyl 2,4-dien-6-ynecarboxylate and ynamides through a formal tetrahydro-Diels-Alder (TDDA) process.

The process yields tetrasubstituted anilines with excellent yields and complete regioselectivity. Moreover, the reaction occurs with complete discrimination between two electron-rich alkynes. Notably, the transformation is tolerant to a wide range of substitution patterns in different positions of the scaffold.

Computational DFT (Density Functional Theory) theoretical calculations indicate that the reaction is initiated by a gold complexation of the *“push-pull”* alkyl 2,4-dien-6-ynecarboxylate followed by a nucleophilic attack of the ynamide and intramolecular last nucleophilic attack to close the six-membered cycle.

General conclusions

The utilization of organometallic compounds, specifically alkoxy alkynyl-Fischer carbenes and gold (I) complexes, has facilitated the development of innovative methodologies for synthesizing various six-membered hetero- and carbocycles, both through stoichiometric and catalytic processes.

By investigating the interaction between alkoxy alkynyl-Fischer carbenes and 4,5-dihydro-1,2,4-oxadiazoles, a novel [3+3] formal cycloaddition reaction has been identified, where the 4,5-dihydro-1,2,4-oxadiazoles act as [N-C-N] synthons. This discovery represents the first case of this type of transformation involving these particular *N,O*-heterocycles. The process produces regio- and chemoselectively pyrimidin-4(3*H*)-ones. Furthermore, a novel reaction mechanism was proposed, which involved either a concerted cyclization step or the formation of an eight-membered ring intermediate.

Efforts to explore new intermolecular cycloaddition reactions of "push-pull" 2,4-dien-6-ynecarboxylic esters, utilizing gold catalysis, have led to the observation of their gold-catalysed cycloaromatization with an unusual [0,5]-topology. This finding represented an enhancement of the previously reported [0,5]-cycloaromatization of "push-pull" 2,4-dien-6-ynecarboxylic acids. Due to the occurrence of product mixtures involving [0,5]- and [1,6]-cycloaromatization, computational DFT theoretical calculations have been performed to gain insight into these experimental results. The calculations provided evidence of both reaction pathways although they were inconclusive, as they did not allow to predict the reaction outcome.

Finally, the sought-after intermolecular gold-catalysed reaction between "push-pull" 2,4-dien-6-ynecarboxylic esters and ynamides has been successfully accomplished, leading to the formation of highly substituted aniline derivatives. This transformation exhibits complete discrimination between the two electron-rich alkynes and represents a novel example of a regioselective formal tetrahydro-Diels-Alder reaction. Additionally, a mechanistic proposal has been formulated and validated through DFT theoretical calculations.

Conclusiones Generales

La utilización de compuestos organometálicos, específicamente alcoxi carbenos de Fischer alquinílicos y complejos de oro (I), ha facilitado el desarrollo de metodologías innovadoras para la síntesis de diversos hetero- y carbociclos de seis miembros, tanto mediante procesos estequiométricos como catalíticos.

Al investigar la interacción entre alcoxi alquinil carbenos de Fischer y 4,5-dihidro-1,2,4-oxadiazoles, se ha identificado una novedosa reacción de cicloadición formal [3+3] en la cual los 4,5-dihidro-1,2,4-oxadiazoles actuaron como sintones [N-C-N]. Este descubrimiento representa el primer ejemplo de este tipo de transformación que involucra a estos *N,O*-heterociclos en particular. El proceso produce pirimidin-4(3*H*)-onas de manera regio- y quimioselectiva. Además, se ha propuesto un nuevo mecanismo de reacción, que podría involucrar una ciclación concertada o la formación de un intermedio cíclico de ocho miembros.

Los esfuerzos por explorar nuevas reacciones de cicloadición intermolecular de ésteres 2,4-dien-6-inocarboxílicos "*push-pull*" utilizando catalizadores de oro han conducido a la observación de su cicloaromatización catalizada por oro con una topología inusual [0,5]. Este hallazgo representó una mejora de la cicloaromatización previamente descrita de sus análogos ácidos 2,4-dien-6-inocarboxílicos "*push-pull*". Debido a la aparición de mezclas de productos que involucran ciclaromatizaciones [0,5] y [1,6], se han realizado cálculos teóricos computacionales de DFT para obtener una comprensión de estos resultados experimentales. Dichos cálculos aportaron evidencias de que ambos caminos de reacción ocurren, aunque no fueron concluyentes, ya que no es posible predecir el resultado de la reacción para cada caso.

Finalmente, se ha logrado llevar a cabo la buscada reacción intermolecular catalizada por oro entre ésteres 2,4-dien-6-inocarboxílicos "*push-pull*" e inamidas, lo que ha dado lugar a la formación de derivados de anilina altamente sustituidos. Esta transformación supone una discriminación completa entre los dos alquinos ricos en electrones y representa un nuevo ejemplo de una reacción tetrahydro-Diels-Alder regioselectiva formal. Además, se ha formulado una propuesta mecanística, que ha sido validada a través de cálculos teóricos de DFT.

Experimental section

1 General aspects.

In this section, a detailed account of the experimental aspects relative to the transformations described in the current dissertation is provided. Initially, a summary of the general considerations concerning the working conditions, reagents, and analytical techniques utilized for the isolation and characterization of the various compounds is presented. Subsequently, the experimental procedures for synthesizing the starting materials and the final products, including relevant control experiments are compelled. Additionally, this section encompasses the spectroscopic data associated with these compounds.

1.1 General considerations.

The reactions described in the Results and Discussion sections of this dissertation were conducted in either an inert argon (99.99%) or nitrogen atmosphere (99.99%). The glassware was dried and evacuated before usage. For reactions carried out at temperatures below 0 °C, acetone baths cooled with liquid nitrogen were employed. In instances where maintaining low temperatures for extended periods was necessary, a Cryocool apparatus (Neslab C-100II) was utilized. When heating was required, the reactions were performed in mineral oil baths with temperature control achieved through heating plates equipped with contact thermometers.

Chromatographic purifications were carried out using silica gel 60 (230-400 mesh) as stationary phase. Thin-layer chromatography (TLC) was performed on aluminium plates coated with silica gel 60 and F254 indicator. Visualization of the TLC plates was achieved by exposing them to ultraviolet light or by using phosphomolybdic acid, potassium permanganate, or vanillin dye solutions followed by subsequent heating.

The solvents employed for column chromatography and extractions were commercially purchased with analytical purity grade and used without additional purification. All solvents used in the reactions were dried through distillation over calcium hydride, sodium hydride, or metallic sodium. Other reagents were purified using standard procedures before their utilization.

1.2 Instrumental techniques.

Nuclear Magnetic Resonance (NMR) experiments (^1H , ^{13}C , ^{19}F , DEPT, COSY, HSQC, HMBC and NOESY) were conducted using Bruker AV-300, Bruker DPX-300, Bruker AV-400 or on Bruker AV-600 spectrometers. The chemical shifts (δ) are reported in parts per million (ppm) and referenced to the residual signal of the solvent employed in ^1H -, ^{13}C - and ^{19}F -NMR spectra. Coupling constants (J) are expressed in Hertz (Hz). ^1H NMR: splitting pattern abbreviations are: s (singlet), d (doublet), t (triplet), q (quartet), p (pentet), sext (sextet), at (apparent triplet), dd (double doublet), ddd (double doublet of doublet), adt (apparent double triplet), m (multiplet). ^{13}C NMR: multiplicities were determined by DEPT, abbreviations are: q (CH_3), t (CH_2), d (CH) and s (quaternary carbons), except for compounds bearing fluorine atoms. For these compounds, the abbreviation (q) regarding the carbon multiplicity refers to the F-C coupling and there will be no abbreviation if there is no F-C coupling; the number of hydrogen atoms linked to a determined carbon atom is indicated as C, CH, CH_2 or CH_3 . Standard pulse sequences were employed for the DEPT experiments.

The mass spectra were obtained at the scientific-technical services of the University of Oviedo using either a Finnigan-Matt 95 micro TOF focus (Bruker Daltonics, Bremen, Germany) or Vg AutoSpec M spectrometers to acquire high-resolution mass spectra (HRMS).

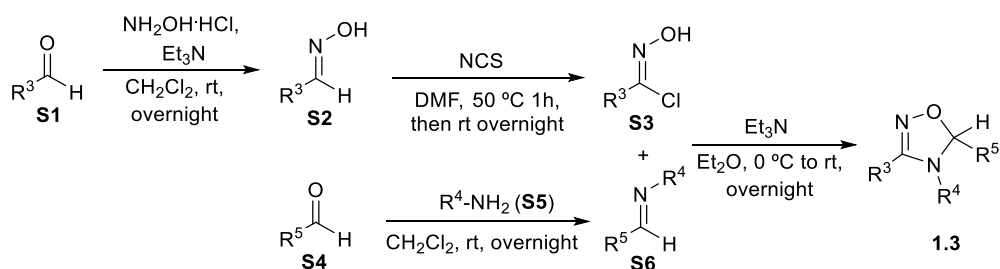
Melting points were determined after purification by column chromatography using a Büchi-Tottoli apparatus. The reported values have not been corrected.

2 Experimental procedures.

2.1 Experimental procedures described in Chapter I.

2.1.1 Synthesis of 4,5-dihydro-1,2,4-oxadiazoles 1.3.

4,5-Dihydro-1,2,4-oxadiazoles **1.3**, were prepared by 1,3-dipolar cycloaddition of nitrile oxides (in situ generated treating *C*-chlorooximes with Et₃N) with aldimines, by a variation of a previously reported procedure.¹ Aldimines were prepared by condensation of *p*-tolualdehyde (benzaldehyde for **1.3h**) with amines.² Hydroxymoyl chlorides (*C*-chlorooximes) were formed by NCS-chlorination of oximes, which were readily prepared by standard condensation between the corresponding aldehyde and hydroxylamine hydrochloride.³ All experimental procedures are detailed below.



Scheme 1. Synthesis followed to obtain 4,5-dihydro-1,2,4-oxadiazoles **1.3**

¹ (a) Alcaide, B.; Mardomingo, C. L.; Plumet, J.; Cativiela, C.; Mayoral, J. A. *Can. J. Chem.* **1987**, *65*, 2050-2056. (b) Xu, W.; Wang, G.; Sun, N.; Liu, Y. *Org. Lett.* **2017**, *19*, 3307-3310.

² Schaufelberger, F.; Hu, L.; Ramström, O. *Chem. Eur. J.* **2015**, *21*, 9776-9783.

³ Zheng, H.; McDonald, R.; Hall, D. G. *Chem. Eur. J.* **2010**, *16*, 5454-5460.

Hydroxylamine hydrochloride (1.39 g, 20 mmol, 2.0 equiv.) and triethylamine (5.58 mL, 40 mmol, 4.0 equiv.) were added to a solution of aldehyde **S1** (10.0 mmol, 1.0 equiv.) in anhydrous DCM (15 mL) in a dry Schlenk flask under N₂ atmosphere. The resulting mixture was stirred at room temperature until consumption of starting materials (usually overnight). Then, saturated NaHCO₃ was added to the reaction mixture at 0 °C and the resulting mixture was extracted with DCM (3 x 20 mL), dried over Na₂SO₄, filtered, and concentrated under reduced pressure. The residue was purified by flash column chromatography to give the oxime **S2** in pure form.

A solution of *N*-chlorosuccinimide (1.34 g, 10.0 mmol, 1.0 equiv.) in DMF (80 mL) was added dropwise to a solution of oxime **S2** (10.0 mmol, 1.0 equiv.) in DMF (80 mL) in a round-bottomed flask over 30 minutes, at 50 °C. The resulting mixture was stirred for 1 hour, and then allowed to stir at room temperature overnight. A mixture of ice-water was added to the reaction mixture and extracted with Et₂O (3 x 20 mL). The combined organic extracts were washed with ice-water and brine, dried over Na₂SO₄, filtered and concentrated under reduced pressure to give hydroxymoyl chlorides **S3** in pure form.

Amine **S5** (10.0 mmol, 1.0 equiv.) was added dropwise via syringe to a solution of aldehyde **S4** (10.0 mmol, 1.0 equiv) in anhydrous DCM (100 mL) in a dry Schlenk flask under N₂ atmosphere in the presence of activated 4 Å MS. The reaction mixture was stirred at room temperature and, upon consumption of starting materials (usually overnight), filtered through a pad of Celite and concentrated under reduced pressure to give imine **S6** in pure form.

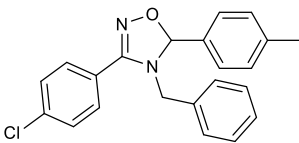
A solution of triethylamine (0.50 – 3.35 mL, 3.60 – 24.0 mmol, 1.2 equiv) in anhydrous Et₂O (22.5 – 150 mL) was added dropwise during 15 min at 0 °C to a solution of hydroxymoyl chloride **S3** (3.30 – 22.0 mmol, 1.1 equiv) and imine **S6** (3.00 – 20.0 mmol, 1.0 equiv) in anhydrous Et₂O (75 mL) in a dry Schlenk under N₂ atmosphere. The reaction was then allowed to stir at room temperature overnight. Then the reaction mixture was filtered through Celite and concentrated under reduced pressure. The residue was purified by silica gel chromatography (HxH/AcOEt 20:1) to give 4,5-dihydro-1,2,4-oxadiazole **1.3** in pure form.

4,5-dihydro-1,2,4-oxadiazole **1.3**⁴ had already been reported in the bibliography.

⁴ Miralinaghi, P.; Salimi, M.; Amirhamzeh, A.; Norouzi, M.; Kandelousi, H. M.; Shafiee, A.; Amini, M. *Med Chem Res* **2013**, *22*, 4253-4262.

On the other hand, 4,5-dihydro-1,2,4-oxadiazoles **1.3n**, **1.3o** have not been characterised because they did not lead to the corresponding pyrimidone-4-(3*H*)-one **1.4** (examples **1.4z-aa**, see *Chapter I*, p. 64).

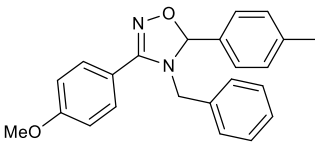
4-Benzyl-3-(4-chlorophenyl)-5-(*p*-tolyl)-4,5-dihydro-1,2,4-oxadiazole (1.3a)

	<p>Yield = 88%, 5329.6 mg (14.69 mmol). Brown-yellow oil. R_f (SiO₂) = 0.2 (Hexane : Ethyl acetate, 8:2). HRMS (ESI): (m/z) calculated for C₂₂H₂₀ClN₂O [M+H]⁺: 363.1259; found: 363.1259.</p>
---	---

¹H-NMR (300 MHz, CDCl₃, 25 °C, TMS): δ (ppm) = 7.74 – 7.61 (m, 2H), 7.55 – 7.43 (m, 2H), 7.42 – 7.35 (m, 2H), 7.35 – 7.27 (m, 3H), 7.27 – 7.19 (m, 2H), 7.14 – 7.02 (m, 2H), 6.27 (s, 1H), 4.47 (d, *J* = 15.9 Hz, 1H), 4.08 (d, *J* = 15.9 Hz, 1H), 2.41 (s, 3H).

¹³C-NMR (75 MHz, CDCl₃, 25 °C): δ (ppm) = 157.3 (s), 139.7 (s), 136.8 (s), 135.5 (s), 134.9 (s), 129.6 (d), 129.4 (d), 128.8 (d), 127.9 (d), 127.8 (d), 127.3 (d), 123.9 (s), 96.9 (d), 49.8 (t), 21.4 (q).

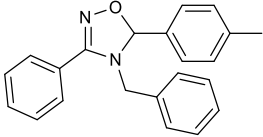
4-Benzyl-3-(4-methoxyphenyl)-5-(*p*-tolyl)-4,5-dihydro-1,2,4-oxadiazole (1.3b)

	<p>Yield = 83%, 897.3 mg (2.5 mmol). Brown-yellow oil. R_f (SiO₂) = 0.3 (Hexane : Ethyl acetate, 8:2). HRMS (ESI): (m/z) calculated for C₂₃H₂₃N₂O₂ [M+H]⁺: 359.1754; found: 359.1750.</p>
---	--

¹H-NMR (300 MHz, CDCl₃, 25 °C, TMS): δ (ppm) = 7.76 – 7.61 (m, 2H), 7.41 – 7.34 (m, 2H), 7.34 – 7.26 (m, 3H), 7.25 – 7.17 (m, 2H), 7.14 – 7.06 (m, 2H), 7.05 – 6.97 (m, 2H), 6.22 (s, 1H), 4.51 (d, *J* = 15.9 Hz, 1H), 4.07 (d, *J* = 15.9 Hz, 1H), 3.86 (s, 3H), 2.39 (s, 3H).

¹³C-NMR (75 MHz, CDCl₃, 25 °C): δ (ppm) = 161.5 (s), 157.9 (s), 139.6 (s), 135.9 (s), 135.4 (s), 129.9 (d, 2CH), 129.4 (d, 2CH), 128.8 (d, 2CH), 127.9 (d, 2CH), 127.8 (d), 127.4 (d, 2CH), 117.4 (s), 114.5 (d, 2CH), 96.5 (d), 55.5 (q), 49.9 (t), 21.4 (q).

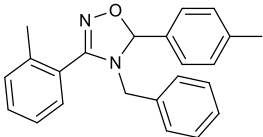
4-Benzyl-3-phenyl-5-(*p*-tolyl)-4,5-dihydro-1,2,4-oxadiazole (1.3c)

	<p>Yield = 32%, 844.9 mg (2.6 mmol).</p> <p>Brown oil.</p> <p>R_f (SiO₂) = 0.4 (Hexane : Ethyl acetate, 8:2).</p> <p>HRMS (ESI): (m/z) calculated for C₂₂H₂₁N₂O [M+H]⁺: 329.1648; found: 329.1649.</p>
---	--

¹H-NMR (300 MHz, CDCl₃, 25 °C, TMS): δ (ppm) = 7.80 – 7.65 (m, 2H), 7.57 – 7.44 (m, 3H), 7.43 – 7.34 (m, 2H), 7.33 – 7.25 (m, 3H), 7.22 (d, *J* = 7.8 Hz, 2H), 7.14 – 7.02 (m, 2H), 6.25 (s, 1H), 4.50 (d, *J* = 15.9 Hz, 1H), 4.06 (d, *J* = 15.8 Hz, 1H), 2.39 (s, 3H).

¹³C-NMR (75 MHz, CDCl₃, 25 °C): δ (ppm) = 158.1 (s), 139.6 (s), 135.7 (s), 135.1 (s), 130.8 (d), 129.3 (d), 129.1 (d), 128.7 (d), 128.4 (d), 127.9 (d), 127.8 (d), 127.4 (d), 125.4 (s), 96.6 (d), 49.7 (t), 21.4 (q).

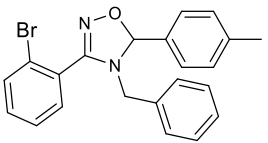
4-Benzyl-3-(*o*-tolyl)-5-(*p*-tolyl)-4,5-dihydro-1,2,4-oxadiazole (1.3d)

	<p>Yield = 34%, 756.2 mg (2.2 mmol).</p> <p>Brown oil.</p> <p>R_f (SiO₂) = 0.4 (Hexane : Ethyl acetate, 8:2).</p> <p>HRMS (ESI): (m/z) calculated for C₂₃H₂₃N₂O [M+H]⁺: 343.1805; found: 343.1804.</p>
---	--

¹H-NMR (300 MHz, CDCl₃, 25 °C, TMS): δ (ppm) = 7.53 (dd, *J* = 7.9, 1.6 Hz, 1H), 7.47 – 7.37 (m, 3H), 7.36 – 7.31 (m, 2H), 7.31 – 7.23 (m, 5H), 7.07 – 6.94 (m, 2H), 6.26 (s, 1H), 4.19 (d, *J* = 15.5 Hz, 1H), 3.85 (d, *J* = 15.5 Hz, 1H), 2.52 (s, 3H), 2.42 (s, 3H).

¹³C-NMR (75 MHz, CDCl₃, 25 °C): δ (ppm) = 156.9 (s), 139.8 (s), 138.0 (s), 135.2 (s), 134.7 (s), 130.9 (d), 130.5 (d), 130.1 (d), 129.5 (d, 2 CH), 128.7 (d, 2CH), 128.1 (d, 2CH), 127.8 (d), 127.6 (d, 2CH), 126.2 (d), 124.6 (s), 95.6 (d), 48.0 (t), 21.4 (q), 19.9 (q).

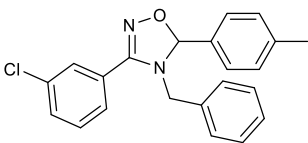
4-Benzyl-3-(2-bromophenyl)-5-(*p*-tolyl)-4,5-dihydro-1,2,4-oxadiazole (1.3e)

	<p>Yield = 47%, 3835.7 mg (9.4 mmol).</p> <p>Yellow solid. mp = 107.5-110.5 °C.</p> <p>R_f (SiO₂) = 0.3 (Hexane : Ethyl acetate, 8:2).</p> <p>HRMS (ESI): (m/z) calculated for C₂₂H₂₀BrN₂O [M+H]⁺: 407.0754; found: 407.0752.</p>
---	--

¹H-NMR (300 MHz, CDCl₃, 25 °C, TMS): δ (ppm) = 7.70 (dd, *J* = 7.8, 1.5 Hz, 1H), 7.58 (dd, *J* = 7.5, 1.9 Hz, 1H), 7.49 – 7.21 (m, 9H), 7.07 – 6.94 (m, 2H), 6.30 (s, 1H), 4.19 (d, *J* = 15.6 Hz, 1H), 3.89 (d, *J* = 15.6 Hz, 1H), 2.41 (s, 3H).

¹³C-NMR (75 MHz, CDCl₃, 25 °C): δ (ppm) = 156.4 (s), 140.0 (s), 135.2 (s), 134.3 (s), 133.6 (d), 132.4 (d), 132.1 (d), 129.5 (d, 2CH), 128.7 (d, 2CH), 128.12 (d, 2CH), 128.08 (d, 2CH), 127.9 (d), 127.8 (d), 126.9 (s), 123.6 (s), 96.4 (d), 47.9 (t), 21.5 (q).

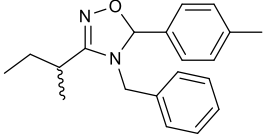
4-Benzyl-3-(3-chlorophenyl)-5-(*p*-tolyl)-4,5-dihydro-1,2,4-oxadiazole (1.3f)

	<p>Yield = 10%, 414.0 mg (1.1 mmol).</p> <p>Brown oil.</p> <p>R_f (SiO₂) = 0.5 (Hexane : Ethyl acetate, 8:2).</p> <p>HRMS (ESI): (m/z) calculated for C₂₂H₂₀ClN₂O [M+H]⁺: 363.1259; found: 363.1259.</p>
---	--

¹H-NMR (300 MHz, CDCl₃, 25 °C, TMS): δ (ppm) = 7.74 (t, *J* = 1.8 Hz, 1H), 7.62 (dt, *J* = 7.4, 1.5 Hz, 1H), 7.50 (dt, *J* = 8.1, 1.6 Hz, 1H), 7.44 (d, *J* = 7.6 Hz, 1H), 7.41 – 7.35 (m, 2H), 7.34 – 7.28 (m, 3H), 7.24 (d, *J* = 7.8 Hz, 2H), 7.15 – 7.05 (m, 2H), 6.27 (s, 1H), 4.49 (d, *J* = 15.8 Hz, 1H), 4.09 (d, *J* = 15.8 Hz, 1H), 2.41 (s, 3H).

¹³C-NMR (75 MHz, CDCl₃, 25 °C): δ (ppm) = 157.0 (s), 139.8 (s), 135.4 (s), 135.0 (s), 134.9 (s), 130.9 (d), 130.4 (d), 129.4 (d), 128.8 (d), 128.3 (d), 128.0 (d), 127.9 (d), 127.3 (d), 127.3 (d), 126.4 (d), 97.0 (d), 49.9 (t), 21.4 (q).

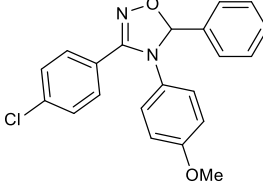
4-Benzyl-3-(sec-butyl)-5-(p-tolyl)-4,5-dihydro-1,2,4-oxadiazole (1.3g)

	<p>Yield = 15%, 320.2 mg (1.0 mmol), as a 4:1 mixture of diastereomers</p> <p>Brown oil.</p> <p>R_f (SiO₂) = 0.4 (Hexane : Ethyl acetate, 8:2).</p> <p>HRMS (ESI): (m/z) calculated for C₂₀H₂₅N₂O [M+H]⁺: 309.1961; found: 309.1956.</p>
---	--

¹H-NMR (300 MHz, CDCl₃, 25 °C, TMS): δ (ppm) = 7.38 – 7.25 (m, 5H, maj + 5H, min), 7.20 – 7.11 (m, 4H, maj + 4H, min), 6.07 (s, 1H, min), 6.04 (s, 1H, maj), 4.41 (d, *J* = 16.4 Hz, 1H, maj + 1H, min), 3.93 (d, *J* = 16.4, 1H, maj + 1H, min), 2.59 – 2.44 (m, 2H, maj + 2 H, min), 2.38 (s, 3H, maj + 3H, min), 1.97 – 1.88 (m, 1H, min), 1.87 – 1.74 (m, 1H, maj), 1.71 – 1.52 (m, 2H, maj + 2H, min), 1.34 (d, *J* = 6.9 Hz, 3H, maj), 1.31 (d, *J* = 6.9 Hz, 3H, min), 1.11 – 0.99 (m, 3H, maj + 3H, min).

¹³C-NMR (75 MHz, CDCl₃, 25 °C): δ (ppm) = 160.3 (s), 139.7 (s), 135.9 (s), 135.0 (s), 129.4 (d, 2CH), 128.90 (d, 2CH, maj), 128.88 (d, 2CH, min), 127.82 (d), 127.79 (d, 2CH, min), 127.7 (d, 2CH, maj), 127.4 (d, 2CH, maj), 127.3 (d, 2CH, min), 95.7 (d, maj), 95.5 (d, min), 47.0 (t, maj), 46.7 (t, min), 31.6 (d, min), 30.9 (d, maj), 28.1 (t, maj), 26.7 (t, min), 21.4 (t), 18.9 (t, min), 16.9 (t, maj), 12.2 (q, min), 11.3 (q, maj).

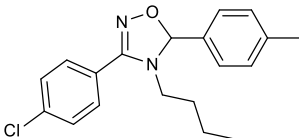
3-(4-Chlorophenyl)-4-(4-methoxyphenyl)-5-(p-phenyl)-4,5-dihydro-1,2,4-oxadiazole (1.3h)

	<p>Yield = 63%, 3007.3 mg (8.2 mmol).</p> <p>Brown oil.</p> <p>R_f (SiO₂) = 0.3 (Hexane : Ethyl acetate, 8:2).</p> <p>HRMS (ESI): (m/z) calculated for C₂₁H₁₈ClN₂O₂ [M+H]⁺: 365.1051; found: 365.1053.</p>
---	---

¹H-NMR (300 MHz, CDCl₃, 25 °C, TMS): δ (ppm) = 7.61 – 7.56 (m, 2H), 7.55 – 7.49 (m, 2H), 7.49 – 7.42 (m, 2H), 7.34 – 7.26 (m, 2H), 6.83 – 6.76 (m, 2H), 6.76 – 6.69 (m, 2H), 6.42 (s, 1H), 3.74 (s, 3H).

¹³C-NMR (75 MHz, CDCl₃, 25 °C): δ (ppm) = 158.2 (s), 155.2 (s), 138.7 (s), 136.5 (s), 133.6 (s), 130.0 (d), 129.4 (d, 2CH), 129.0 (d, 2CH), 128.9 (d, 2CH), 127.6 (d, 2CH), 127.2 (d, 2CH), 124.0 (s), 114.8 (d, 2CH), 101.4 (d), 55.5 (q).

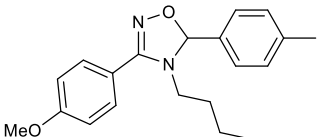
4-Butyl-3-(4-chlorophenyl)-5-(*p*-tolyl)-4,5-dihydro-1,2,4-oxadiazole (1.3j)

	<p>Yield = 32%, 317.7 mg (1.0 mmol). Brown oil.</p> <p>R_f (SiO₂) = 0.5 (Hexane : Ethyl acetate, 8:2).</p> <p>HRMS (ESI): (m/z) calculated for C₁₉H₂₂ClN₂O [M+H]⁺: 329.1415; found: 329.1408.</p>
---	---

¹H-NMR (300 MHz, CDCl₃, 25 °C, TMS): δ (ppm) = 7.65 – 7.54 (m, 2H), 7.50 – 7.41 (m, 4H), 7.29 – 7.19 (m, 2H), 6.28 (s, 1H), 3.20 – 2.88 (m, 2H), 2.40 (s, 3H), 1.58 – 1.31 (m, 1H), 1.34 – 1.06 (m, 3H), 0.76 (t, *J* = 7.3 Hz, 3H).

¹³C-NMR (75 MHz, CDCl₃, 25 °C): δ (ppm) = 157.9 (s), 139.8 (s), 136.7 (s), 136.0 (s), 129.6 (d, 2CH), 129.5 (d, 2CH), 129.3 (d, 2CH), 127.3 (d, 2CH), 124.3 (s), 98.5 (d), 47.3 (t), 30.3 (t), 21.5 (q), 19.9 (t), 13.7 (q).

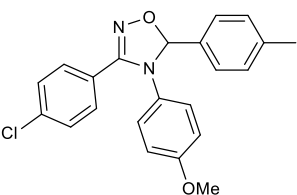
4-Butyl-3-(4-methoxyphenyl)-5-(*p*-tolyl)-4,5-dihydro-1,2,4-oxadiazole (1.3k)

	<p>Yield = 49%, 476.9 mg (1.5 mmol). Brown oil.</p> <p>R_f (SiO₂) = 0.2 (Hexane : Ethyl acetate, 8:2).</p> <p>HRMS (ESI): (m/z) calculated for C₂₀H₂₅N₂O₂ [M+H]⁺: 325.1911; found: 325.1906.</p>
---	---

¹H-NMR (300 MHz, CDCl₃, 25 °C, TMS): δ (ppm) = 7.57 (d, *J* = 8.8 Hz, 2H), 7.46 (d, *J* = 8.1 Hz, 2H), 7.23 (d, *J* = 7.6 Hz, 2H), 6.97 (d, *J* = 8.7 Hz, 2H), 6.25 (s, 1H), 3.83 (s, 3H), 3.10 – 3.01 (m, 2H), 2.38 (s, 3H), 1.48 – 1.37 (m, 1H), 1.32 – 1.04 (m, 3H), 0.82 – 0.66 (m, 3H).

¹³C-NMR (75 MHz, CDCl₃, 25 °C): δ (ppm) = 161.4 (s), 158.6 (s), 139.6 (s), 136.4 (s), 129.7 (d, 2CH), 129.4 (d, 2CH), 127.3 (d, 2CH), 117.8 (s), 114.4 (d, 2CH), 98.1 (d), 55.5 (q), 47.3 (t), 30.4 (t), 21.4 (q), 19.9 (t), 13.7 (q).

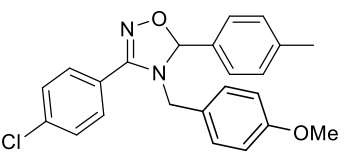
3-(4-Chlorophenyl)-4-(4-methoxyphenyl)-5-(*p*-tolyl)-4,5-dihydro-1,2,4-oxadiazole (1.3l)

	<p>Yield = 61%, 2262.1 mg (6.0 mmol). Brown solid. mp = 116.3-118.9 °C. R_f (SiO₂) = 0.5 (Hexane : Ethyl acetate, 8:2). HRMS (ESI): (m/z) calculated for C₂₁H₁₈ClN₂O₂ [M+H]⁺: 379.1208; found: 379.1216.</p>
---	---

¹H-NMR (300 MHz, CDCl₃, 25 °C, TMS): δ (ppm) = 7.55 – 7.41 (m, 4H), 7.34 – 7.20 (m, 4H), 6.78 (d, *J* = 9.1 Hz, 2H), 6.72 (d, *J* = 9.0 Hz, 2H), 6.39 (s, 1H), 3.74 (s, 3H), 2.41 (s, 3H).

¹³C-NMR (75 MHz, CDCl₃, 25 °C): δ (ppm) = 158.0 (s), 155.2 (s), 140.0 (s), 136.4 (s), 135.7 (s), 133.5 (s), 129.6 (d, 2CH), 129.4 (d, 2CH), 129.0 (d, 2CH), 127.6 (d, 2CH), 127.1 (d, 2CH), 124.0 (s), 114.7 (d, 2CH), 101.4 (d), 55.5 (q), 21.5 (q).

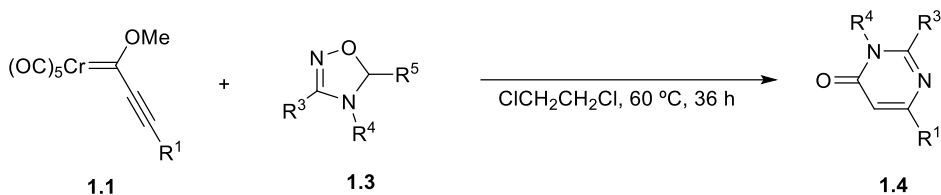
3-(4-chlorophenyl)-4-(4-methoxybenzyl)-5-(*p*-tolyl)-4,5-dihydro-1,2,4-oxadiazole (1.3m)

	<p>Yield = 54%, 1968.2 mg (5.0 mmol). Brown oil. R_f (SiO₂) = 0.4 (Hexane : Ethyl acetate, 8:2). HRMS (ESI): (m/z) calculated for C₂₁H₁₈ClN₂O₂ [M+H]⁺: 393.1364; found: 393.1375.</p>
---	--

¹H-NMR (300 MHz, CDCl₃, 25 °C, TMS): δ (ppm) = 7.65 (d, *J* = 8.4 Hz, 2H), 7.45 (d, *J* = 8.4 Hz, 2H), 7.36 (d, *J* = 8.0 Hz, 2H), 7.21 (d, *J* = 7.8 Hz, 2H), 6.95 (d, *J* = 8.6 Hz, 2H), 6.81 (d, *J* = 8.6 Hz, 2H), 6.21 (s, 1H), 4.40 (d, *J* = 15.6 Hz, 1H), 3.96 (d, *J* = 15.6 Hz, 1H), 3.77 (s, 3H), 2.37 (s, 3H).

¹³C-NMR (75 MHz, CDCl₃, 25 °C): δ (ppm) = 159.1 (s), 157.2 (s), 139.6 (s), 136.7 (s), 134.9 (s), 129.6 (d), 129.3 (d), 129.2 (d), 127. (d)3, 127.1 (s), 123.9 (s), 114.0 (d), 96.6 (d), 55.2 (q), 49.1 (t), 21.3 (q).

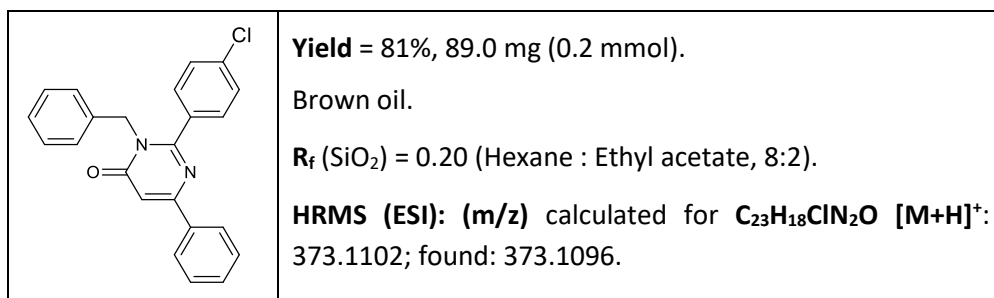
2.1.2 General procedure for the synthesis of pyrimidin-4(3H)-ones **1.4**.



Scheme 2: Synthesis of pyrimidin-4(3H)-ones **1.4**.

The corresponding 4,5-dihydro-1,2,4-oxadiazole **1.3** (0.3-1.5 mmol, 1.5 equiv.) was added to a solution of the corresponding chromium alkoxy alkynyl Fischer carbene complex **1.1** (0.2-1 mmol, 1 equiv.) in DCE (3-15 mL) in a Schlenk flask, at room temperature under argon atmosphere. The mixture was stirred at 60 °C until complete disappearance of the Fischer carbene complex was monitored by TLC (24-72 h). Then, silica gel was added, solvent was evaporated under reduced pressure and the crude residue was purified by column chromatography on silica gel (Hexane/EtOAc: 20:1 to 4:1) to afford pyrimidin-4(3H)-ones **1.4**.

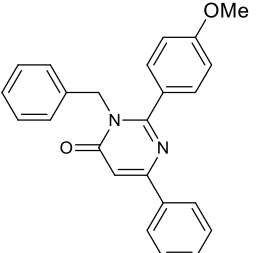
3-Benzyl-2-(4-chlorophenyl)-6-phenylpyrimidin-4(3H)-one (**1.4a**)



¹H-NMR (600 MHz, CDCl₃, 25 °C, TMS): δ (ppm) = 8.12 – 7.88 (m, 2H), 7.49 (d, J = 1.8 Hz, 3H), 7.40 (d, J = 8.4 Hz, 2H), 7.33 (d, J = 8.4 Hz, 2H), 7.30 – 7.22 (m, 3H), 7.00 (s+d, J = 6.9 Hz, 3H), 5.25 (s, 2H).

¹³C-NMR (75 MHz, CDCl₃, 25 °C): δ (ppm) = 163.1 (s), 159.9 (s), 159.6 (s), 136.5 (s), 136.1 (s), 135.9 (s), 133.4 (s), 130.8 (d), 129.6 (d), 128.8 (d), 127.7 (d), 127.1 (d), 126.8 (d), 108.1 (d), 48.8 (t).

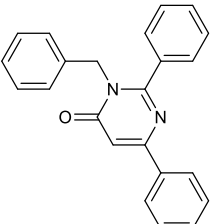
3-Benzyl-2-(4-methoxyphenyl)-6-phenylpyrimidin-4(3H)-one (1.4b)

	<p>Yield = 69%, 76.0 mg (0.2 mmol). Brown solid. mp = 128.7-131.0 °C. R_f (SiO₂) = 0.1 (Hexane : Ethyl acetate, 8:2). HRMS (ESI): (m/z) calculated for C₂₄H₂₀N₂O₂ [M+H]⁺: 369.1598; found: 369.1591.</p>
---	---

¹H-NMR (300 MHz, CDCl₃, 25 °C, TMS): δ (ppm) = 8.08 – 7.99 (m, 2H), 7.51 – 7.44 (m, 3H), 7.38 (d, *J* = 8.4 Hz, 2H), 7.33 – 7.20 (m, 3H), 7.04 (d, *J* = 6.1 Hz, 2H), 6.97 (s, 1H), 6.93 (d, *J* = 8.3 Hz, 2H), 5.31 (s, 2H), 3.87 (s, 3H).

¹³C-NMR (75 MHz, CDCl₃, 25 °C): δ (ppm) = 163.5 (s), 161.1 (s), 160.5 (s), 159.9 (s), 136.5 (s), 136.2 (s), 130.6 (d), 129.9 (d), 128.7 (d), 128.6 (d), 127.5 (d), 127.4 (d), 127.1 (d), 126.8 (d), 113.9 (d), 107.6 (d), 55.6 (q), 49.0 (t).

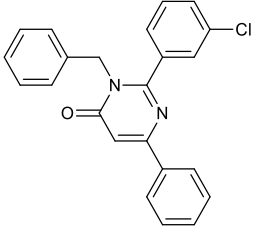
3-Benzyl-2,6-diphenylpyrimidin-4(3H)-one (1.4c)

	<p>Yield = 53%, 53.2 mg (0.2 mmol). Yellow solid. mp = 135.7-138.6 °C. R_f (SiO₂) = 0.1 (Hexane : Ethyl acetate, 8:2). HRMS (ESI): (m/z) calculated for C₂₃H₁₉N₂O [M+H]⁺: 339.1492; found: 339.1483.</p>
---	--

¹H-NMR (300 MHz, CDCl₃, 25 °C, TMS): δ (ppm) = 8.08-7.99 (m, 2H), 7.60 – 7.43 (m, 8H), 7.31 – 7.15 (m, 3H), 7.03-6.94 (s+m, 3H), 5.28 (s, 2H).

¹³C-NMR (75 MHz, CDCl₃, 25 °C): δ (ppm) = 163.2 (s), 160.6 (s), 159.9 (s), 136.3 (s), 136.1 (s), 135.0 (s), 130.6 (d), 130.1 (d), 128.7 (d), 128.6 (d), 128.5 (d), 128.1 (d), 127.5 (d), 127.1 (d), 127.0 (d), 108.0 (d), 48.7 (t).

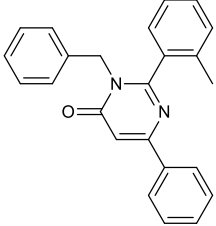
3-Benzyl-2-(3-chlorophenyl)-6-phenylpyrimidin-4(3H)-one (1.4d)

	<p>Yield = 32%, 103.5 mg (0.3 mmol). Yellow oil. R_f (SiO₂) = 0.2 (Hexane : Ethyl acetate, 8:2). HRMS (ESI): (m/z) calculated for C₂₃H₁₈ClN₂O [M+H]⁺: 373.1102; found: 373.1101.</p>
---	---

¹H-NMR (300 MHz, CDCl₃, 25 °C, TMS): δ (ppm) = 8.06 – 7.97 (m, 2H), 7.54 – 7.44 (m, 4H), 7.41 – 7.31 (m, 2H), 7.31 – 7.26 (m, 3H), 7.26 – 7.22 (m, 2H), 7.04 – 6.94 (s+m, 3H), 5.24 (s, 2H).

¹³C-NMR (75 MHz, CDCl₃, 25 °C): δ (ppm) = 163.0 (s), 159.9 (s), 159.2 (s), 136.5 (s), 136.1 (s), 135.9 (s), 134.6 (s), 130.8 (d), 130.3 (d), 129.8 (d), 128.8 (d), 128.7 (d), 128.5 (d), 127.7 (d), 127.1 (d), 126.9 (d), 126.1 (d), 108.3 (d), 48.7 (t).

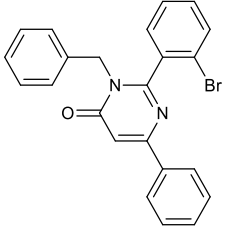
3-Benzyl-6-phenyl-2-(*o*-tolyl)pyrimidin-4(3H)-one (1.4e)

	<p>Yield = 62%, 64.5 mg (0.2 mmol). Brown oil. R_f (SiO₂) = 0.3 (Hexane : Ethyl acetate, 8:2). HRMS (ESI): (m/z) calculated for C₂₄H₂₁N₂O [M+H]⁺: 353.1648; found: 353.1636.</p>
---	---

¹H-NMR (300 MHz, CDCl₃, 25 °C, TMS): δ (ppm) = 8.01 (dd, *J* = 6.7, 3.0 Hz, 2H), 7.51–7.42 (m, 3H), 7.29 – 7.08 (m, 7H), 7.02 (s, 1H), 6.95–6.80 (m, 2H), 5.17 (s, 2H), 1.98 (s, 3H).

¹³C-NMR (75 MHz, CDCl₃, 25 °C): δ (ppm) = 163.3 (s), 160.2 (s), 160.0 (s), 136.2 (s), 136.1 (s), 135.9 (s), 134.5 (s), 130.6 (d), 129.9 (d), 128.7 (d), 128.4 (d), 127.8 (d), 127.7 (d), 127.2 (d), 125.8 (d), 108.2 (d), 47.9 (t), 19.0 (q).

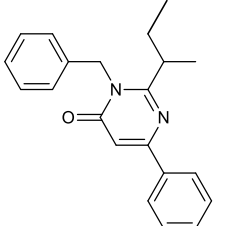
3-Benzyl-2-(2-bromophenyl)-6-phenylpyrimidin-4(3H)-one (1.4f)

	<p>Yield = 54%, 67.2 mg (0.2 mmol).</p> <p>Brown oil.</p> <p>R_f (SiO₂) = 0.2 (Hexane : Ethyl acetate, 8:2).</p> <p>HRMS (ESI): (m/z) calculated for C₂₃H₁₈⁷⁹BrN₂O [M+H]⁺: 417.0597; found: 417.0592.</p>
---	--

¹H-NMR (300 MHz, CDCl₃, 25 °C, TMS): δ (ppm) = 8.06 – 7.94 (m, 2H), 7.69 (dd, *J* = 8.0, 1.2 Hz, 1H), 7.52 – 7.42 (m, 3H), 7.35 (dd, *J* = 7.9, 1.8 Hz, 1H), 7.27 (td, *J* = 7.6, 1.2 Hz 1H), 7.21 (dd, *J* = 5.5, 1.8 Hz, 3H), 7.08 – 7.01 (s+m, 2H), 6.95 – 6.86 (m, 2H) 5.72 (d, *J* = 15.0 Hz, 1H), 4.61 (d, *J* = 15.0 Hz, 1H).

¹³C-NMR (75 MHz, CDCl₃, 25 °C): δ (ppm) = 163.0 (s), 159.9 (s), 159.2 (s), 136.5 (s), 136.1 (s), 135.9 (s), 134.6 (s), 130.8 (d), 130.3 (d), 129.8 (d), 128.8 (d), 128.7 (d), 128.5 (d), 127.7 (d), 127.1 (d), 126.9 (d), 126.1 (d), 108.3 (d), 48.7 (t).

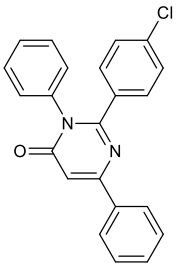
3-Benzyl-2-(sec-butyl)-6-phenylpyrimidin-4(3H)-one (1.4g)

	<p>Yield = 74%, 70,0 mg (0.2 mmol).</p> <p>Brown solid. mp = 77.6-81.6 °C.</p> <p>R_f (SiO₂) = 0.3 (Hexane : Ethyl acetate, 8:2).</p> <p>HRMS (ESI): (m/z) calculated for C₂₁H₂₃N₂O [M+H]⁺: 319.1805; found: 319.1796.</p>
---	---

¹H-NMR (300 MHz, CDCl₃, 25 °C, TMS): δ (ppm) = 8.30 – 7.90 (m, 2H), 7.56 – 7.41 (m, 3H), 7.41 – 7.23 (m, 3H), 7.20 (dd, *J* = 8.0, 1.5 Hz, 2H), 6.90 (s, 1H), 5.52 (d, *J* = 15.9 Hz, 1H), 5.36 (d, *J* = 15.9 Hz, 1H), 3.02 – 2.75 (m, 1H), 2.10 – 1.80 (m, 1H), 1.71 – 1.45 (m, 1H), 1.23 (d, *J* = 6.6 Hz, 3H), 0.76 (t, *J* = 7.4 Hz, 3H).

¹³C-NMR (75 MHz, CDCl₃, 25 °C): δ (ppm) = 166.1 (s), 163.6 (s), 159.6 (s), 136.5 (s), 136.3 (s), 130.5 (d), 128.9 (d), 128.7 (d), 127.6 (d), 127.0 (d), 126.5 (d), 106.3 (d), 45.6 (t), 39.4 (t), 28.8 (t), 19.5 (q), 11.9 (q).

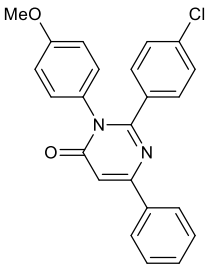
2-(4-Chlorophenyl)-3,6-diphenylpyrimidin-4(3H)-one (1.4h)

	<p>Yield = 57%, 61.2 mg (0.2 mmol). Red solid. mp = 127.0-129.8 °C. R_f (SiO₂) = 0.1 (Hexane : Ethyl acetate, 8:2). HRMS (ESI): (m/z) calculated for C₂₃H₁₈ClN₂O [M+H]⁺: 359.0946; found: 359.0939.</p>
---	--

¹H-NMR (600 MHz, CDCl₃, 25 °C, TMS): δ (ppm) = 8.12 – 7.88 (m, 2H), 7.49 (d, *J* = 1.8 Hz, 3H), 7.40 (d, *J* = 8.4 Hz, 2H), 7.33 (d, *J* = 8.4 Hz, 2H), 7.30 – 7.22 (m, 3H), 7.00 (s+d, *J* = 6.9 Hz, 3H), 5.25 (s, 2H).

¹³C-NMR (150 MHz, CDCl₃, 25 °C): δ (ppm) = 162.9 (s), 160.0 (s), 158.0 (s), 137.0 (s), 136.0 (s), 136.0 (s), 133.5 (s), 130.8 (d), 130.7 (d), 129.3 (d), 128.9 (d), 128.8 (d), 128.7 (d), 128.2 (d), 127.1 (d), 108.1 (d).

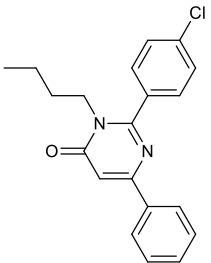
2-(4-Chlorophenyl)-3-(4-methoxyphenyl)-6-phenylpyrimidin-4(3H)-one (1.4i)

	<p>Yield = 52%, 54.6 mg (0.1 mmol). Brown oil. R_f (SiO₂) = 0.4 (Hexane : Ethyl acetate, 8:2). HRMS (ESI): (m/z) calculated for C₁₄H₂₁O₃ [M+H]⁺: 389.1051; found: 389.1050.</p>
---	---

¹H-NMR (300 MHz, CDCl₃, 25 °C, TMS): δ (ppm) = 7.58 (dd, *J* = 6.6, 3.2 Hz, 2H), 7.52 (d, *J* = 8.9 Hz, 2H), 7.48 – 7.41 (m, 3H), 7.30 (d, *J* = 9.5 Hz, 2H), 6.79 (d, *J* = 9.2 Hz, 2H), 6.73 (d, *J* = 9.3 Hz, 2H), 6.42 (s, 1H), 3.75 (s, 3H)

¹³C-NMR (75 MHz, CDCl₃, 25 °C): δ (ppm) = 158.1 (s), 155.1 (s), 138.6 (s), 136.4 (s), 133.5 (s), 129.8 (d), 129.3 (d), 129.0 (d), 128.9 (d), 128.8 (d), 128.3 (s), 127.4 (d), 127.1 (d), 123.9 (s), 114.7 (d), 101.3 (d), 55.4 (q).

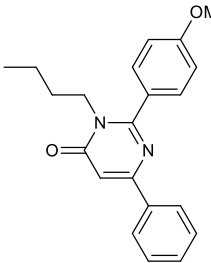
3-Butyl-2-(4-chlorophenyl)-6-phenylpyrimidin-4(3H)-one (1.4j)

	<p>Yield = 72%, 12.2 mg (0.04 mmol).</p> <p>Yellowish solid. mp = 132.0-135.1 °C.</p> <p>R_f (SiO₂) = 0.2 (Hexane : Ethyl acetate, 8:2).</p> <p>HRMS (ESI): (m/z) calculated for C₂₀H₂₀ClN₂O [M+H]⁺: 339.1259; found: 339.1257.</p>
---	--

¹H-NMR (300 MHz, CDCl₃, 25 °C, TMS): δ (ppm) = 7.98 (dd, J = 6.6, 2.9 Hz, 2H), 7.53 (s, 4H), 7.49 – 7.42 (m, 3H), 6.90 (s, 1H), 4.03 – 3.91 (m, 2H), 1.63 (td, J = 7.6, 6.4, 3.4 Hz, 2H), 1.22 (q, J = 7.5 Hz, 2H), 0.82 (t, J = 7.3 Hz, 3H).

¹³C-NMR (75 MHz, CDCl₃, 25 °C): δ (ppm) = 162.9 (s), 159.6 (s), 159.2 (s), 136.3 (s), 136.1 (s), 133.7 (s), 130.6 (d), 129.4 (d), 129.0 (d), 128.7 (d), 127.0 (d), 108.2 (d), 45.7 (t), 30.7 (t), 19.9 (t), 13.5 (q).

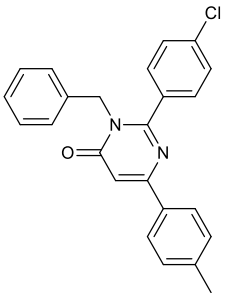
3-Butyl-2-(4-methoxyphenyl)-6-phenylpyrimidin-4(3H)-one (1.4k)

	<p>Yield = 53%, 140.0 mg (0.42 mmol).</p> <p>Brown oil.</p> <p>R_f (SiO₂) = 0.1 (Hexane : Ethyl acetate, 8:2).</p> <p>HRMS (ESI): (m/z) calculated for C₂₁H₂₃N₂O [M+H]⁺: 335.1754; found: 335.1747.</p>
---	---

¹H-NMR (300 MHz, CDCl₃, 25 °C, TMS): δ (ppm) = 8.06 – 7.94 (m, 2H), 7.58 – 7.49 (m, 2H), 7.47 – 7.37 (m, 3H), 7.15 – 6.98 (m, 2H), 6.88 (s, 1H), 4.08 – 3.97 (m, 2H), 3.91 (s, 3H), 1.72 – 1.54 (m, 2H), 1.31 – 1.12 (m, 2H), 0.82 (t, J = 7.3 Hz, 3H).

¹³C-NMR (75 MHz, CDCl₃, 25 °C): δ (ppm) = 163.3 (s), 160.8 (s), 160.2 (s), 159.5 (s), 136.4 (s), 130.4 (d), 129.7 (d), 129.2 (d), 128.7 (d), 127.8 (d), 127.7 (s), 127.0 (d), 126.8 (d), 114.0 (d), 107.7 (d), 55.5 (q), 45.8 (t), 30.7 (t), 19.9 (t), 13.5 (q).

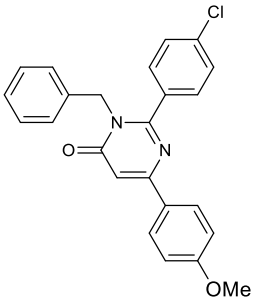
3-Benzyl-2-(4-chlorophenyl)-6-(*p*-tolyl)pyrimidin-4(3*H*)-one (1.4l)

	<p>Yield = 51%, 101.2 mg (0.3 mmol). Brown oil. R_f (SiO₂) = 0.1 (Hexane : Ethyl acetate, 8:2). HRMS (ESI): (m/z) calculated for C₂₄H₂₀ClN₂O [M+H]⁺: 387.1259; found: 387.1251.</p>
---	--

¹H-NMR (300 MHz, CDCl₃, 25 °C, TMS): δ (ppm) = .53 – 7.46 (m, 2H), 7.40 – 7.35 (m, 2H), 7.33-7.25 (m, 7H), 7.07-6.96 (s+m, 3H), 5.26 (s, 2H), 2.49 (s, 3H).

¹³C-NMR (75 MHz, CDCl₃, 25 °C): δ (ppm) = 163.2 (s), 159.9 (s), 159.4 (s), 141.2 (s), 136.4 (s), 136.2 (s), 133.4 (s), 133.1 (s), 129.6 (d), 129.5 (d), 128.8 (d), 128.7 (d), 127.6 (d), 127.0 (d), 126.8 (d), 107.4 (d), 48.7 (t), 21.5 (q).

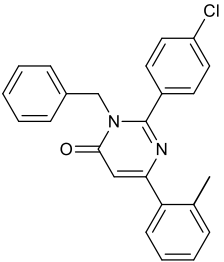
3-Benzyl-2-(4-chlorophenyl)-6-(4-methoxyphenyl)pyrimidin-4(3*H*)-one (1.4m)

	<p>Yield = 66%, 148.1 mg (0.4 mmol). Yellow solid. mp = 118.2-119.6 °C. R_f (SiO₂) = 0.1 (Hexane : Ethyl acetate, 8:2). HRMS (ESI): (m/z) calculated for C₂₄H₂₀ClN₂O₂ [M+H]⁺: 403.1208; found: 403.1202.</p>
---	---

¹H-NMR (300 MHz, CDCl₃, 25 °C, TMS): δ (ppm) = 7.99 (d, *J* = 8.9 Hz, 2H), 7.39 (d, *J* = 8.6 Hz, 2H), 7.31 (d, *J* = 8.5 Hz, 2H), 7.26 (d, *J* = 1.9 Hz, 3H), 6.98 (dt, *J* = 6.9, 2.5 Hz, 4H), 6.92 (s, 1H), 5.23 (s, 2H), 3.88 (s, 3H).

¹³C-NMR (75 MHz, CDCl₃, 25 °C): δ (ppm) = 163.2 (s), 161.8 (s), 159.4 (s), 159.3 (s), 136.4 (s), 136.2 (s), 133.5 (s), 129.6 (d), 128.7 (d), 128.3 (s), 127.6 (d), 126.7 (d), 114.1 (d), 106.4 (d), 55.4 (q), 48.6 (t).

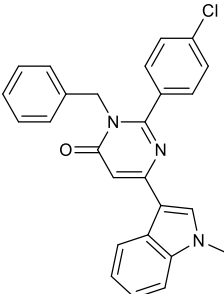
3-Benzyl-2-(4-chlorophenyl)-6-(*o*-tolyl)pyrimidin-4(3*H*)-one (1.4n)

	<p>Yield = 47%, 58.8 mg (0.2 mmol). Yellowish oil.</p> <p>R_f (SiO₂) = 0.1 (Hexane : Ethyl acetate, 8:2).</p> <p>HRMS (ESI): (m/z) calculated for C₂₄H₂₀ClN₂O [M+H]⁺: 387.1259; found: 387.1254.</p>
---	---

¹H-NMR (300 MHz, CDCl₃, 25 °C, TMS): δ (ppm) = 7.50 (dd, *J* = 7.8, 1.8 Hz, 1H), 7.40 – 7.35 (m, 2H), 7.29 (qd, *J* = 4.3, 2.1 Hz, 8H), 7.08 – 6.94 (m, 2H), 6.68 (s, 1H), 5.26 (s, 2H), 2.49 (s, 3H).

¹³C-NMR (75 MHz, CDCl₃, 25 °C): δ (ppm) = 163.2 (s), 162.7 (s), 159.3 (s), 137.2 (s), 136.5 (s), 136.1 (s), 136.0 (s), 133.2 (s), 131.1 (d), 129.5 (d), 129.1 (d), 128.8 (d), 127.7 (d), 126.8 (d), 126.1 (d), 112.8 (d), 48.9 (t), 20.7 (q).

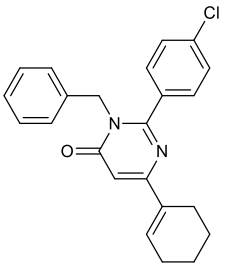
3-Benzyl-2-(4-chlorophenyl)-6-(1-methyl-1*H*-indol-3-yl)pyrimidin-4(3*H*)-one (1.4o)

	<p>Yield = 32%, 82.0 mg (0.2 mmol). Brown solid. mp = 145.3-148.7 °C.</p> <p>R_f (SiO₂) = 0.2 (Hexane : Ethyl acetate, 8:2).</p> <p>HRMS (ESI): (m/z) calculated for C₂₆H₂₁ClN₃O [M+H]⁺: 426.1368; found: 426.1373.</p>
---	---

¹H-NMR (300 MHz, CDCl₃, 25 °C, TMS): δ (ppm) = 8.20 – 8.12 (m, 1H), 7.88 (s, 1H), 7.44 – 7.36 (m, 3H), 7.35 – 7.30 (m, 2H), 7.30-7.25 (m, 5H), 7.05 – 6.98 (m, 2H), 6.95 (s, 1H), 5.23 (s, 2H), 3.85 (s, 3H).

¹³C-NMR (75 MHz, CDCl₃, 25 °C): δ (ppm) = 163.2 (s), 159.0 (s), 157.2 (s), 138.1 (s), 136.6 (s), 136.2 (s), 133.8 (s), 132.5 (d), 129.5 (d), 128.7 (d), 127.5 (d), 126.8 (d), 125.6 (s), 122.6 (d), 121.5 (d), 121.0 (d), 112.9 (s), 110.0 (d), 104.9 (d), 48.4 (t), 33.3 (q).

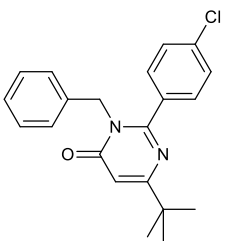
3-Benzyl-2-(4-chlorophenyl)-6-(cyclohex-1-en-1-yl)pyrimidin-4(3H)-one (1.4p)

	<p>Yield = 39%, 43.2 mg (0.1 mmol). Yellow oil. R_f (SiO₂) = 0.3 (Hexane : Ethyl acetate, 8:2). HRMS (ESI): (m/z) calculated for C₂₁H₂₂ClN₂O [M+H]⁺: 377.1415; found: 377.1413.</p>
---	--

¹H-NMR (300 MHz, CDCl₃, 25 °C, TMS): δ (ppm) = 7.36 (d, J = 8.8 Hz, 2H), 7.28 – 7.21 (m, 5H), 7.20 – 7.14 (m, 1H), 6.97 – 6.89 (m, 2H), 6.46 (s, 1H), 5.18 (s, 2H), 2.35 (td, J = 6.1, 5.3, 3.0 Hz, 2H), 2.27 (dt, J = 4.8, 2.1 Hz, 2H), 1.79 (dd, J = 5.9, 2.3 Hz, 2H), 1.67 (dd, J = 5.9, 2.2 Hz, 2H).

¹³C-NMR (75 MHz, CDCl₃, 25 °C): δ (ppm) = 163.6 (s), 160.1 (s), 158.0 (s), 136.3 (s), 136.2 (s), 134.3 (d), 133.6 (s), 133.3 (s), 129.5 (d), 128.7 (d), 127.5 (d), 126.7 (d), 106.1 (d), 48.4 (t), 26.1 (t), 24.9 (t), 22.5 (t), 21.8 (t).

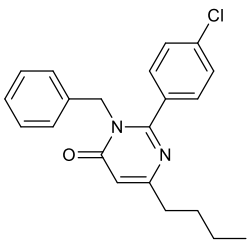
3-Benzyl-6-(tert-butyl)-2-(4-chlorophenyl)pyrimidin-4(3H)-one (1.4q)

	<p>Yield = 38%, 80.7 mg (0.2 mmol). Brown oil. R_f (SiO₂) = 0.3 (Hexane : Ethyl acetate, 8:2). HRMS (ESI): (m/z) calculated for C₂₁H₂₂ClN₂O [M+H]⁺: 353.1415; found: 353.1426.</p>
---	---

¹H-NMR (300 MHz, CDCl₃, 25 °C, TMS): δ (ppm) = 7.35 (d, J = 8.4 Hz, 2H), 7.31 – 7.13 (m, 5H), 6.97 (dd, J = 7.3, 2.2 Hz, 2H), 6.52 (s, 1H), 5.17 (s, 2H), 1.29 (s, 9H).

¹³C-NMR (75 MHz, CDCl₃, 25 °C): δ (ppm) = 173.7 (s), 163.4 (s), 158.4 (s), 136.3 (s), 136.2 (s), 133.5 (s), 129.7 (d), 128.8 (d), 128.7 (d), 127.5 (d), 126.7 (d), 107.8 (d), 48.7 (t), 37.1 (s), 28.6 (q).

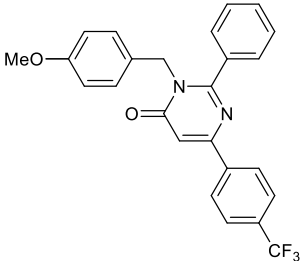
3-Benzyl-6-butyl-2-(4-chlorophenyl)pyrimidin-4(3H)-one (1.4r)

	<p>Yield = 64%, 72.6 mg (0.2 mmol). Yellow oil.</p> <p>R_f (SiO₂) = 0.3 (Hexane : Ethyl acetate, 8:2).</p> <p>HRMS (ESI): (m/z) calculated for C₂₁H₂₂ClN₂O [M+H]⁺: 353.1415; found: 353.1409.</p>
---	---

¹H-NMR (300 MHz, CDCl₃, 25 °C, TMS): δ (ppm) = 7.40 – 7.32 (m, 2H), 7.29 – 7.18 (m, 5H), 6.93 (dd, J = 6.5, 3.1 Hz, 2H), 6.40 (s, 1H), 5.16 (s, 2H), 2.67 – 2.50 (m, 2H), 1.75 – 1.60 (m, 2H), 1.42 (h, J = 7.3 Hz, 2H), 0.96 (t, J = 7.3 Hz, 3H).

¹³C-NMR (75 MHz, CDCl₃, 25 °C): δ (ppm) = 166.8 (s), 162.6 (s), 159.3 (s), 136.4 (s), 136.1 (s), 133.2 (s), 129.4 (d), 128.8 (d), 128.7 (d), 127.6 (d), 126.8 (d), 110.8 (d), 48.6 (t), 37.0 (t), 30.0 (t), 22.3 (t), 13.9 (q).

3-(4-Methoxybenzyl)-2-phenyl-6-(4-(trifluoromethyl)phenyl)pyrimidin-4(3H)-one (1.4s)

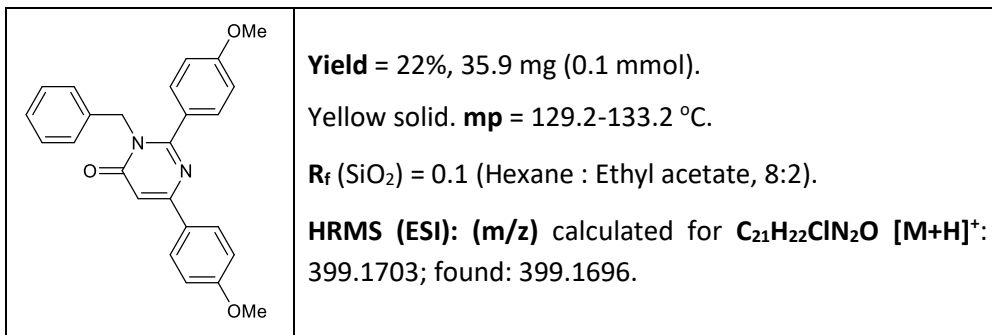
	<p>Yield = 78%, 156.0 mg (0.2 mmol). Yellowish oil.</p> <p>R_f (SiO₂) = 0.5 (Hexane : Ethyl acetate, 8:2).</p> <p>HRMS (ESI): (m/z) calculated for C₂₄H₂₀ClN₂O₂ [M+H]⁺: 437.1471; found: 437.1473.</p>
---	---

¹H-NMR (300 MHz, CDCl₃, 25 °C, TMS): δ (ppm) = 8.15 (d, J = 8.1 Hz, 2H), 7.73 (d, J = 8.1 Hz, 2H), 7.39 (d, J = 8.5 Hz, 2H), 7.35 – 7.18 (m, 4H), 7.09 – 6.84 (m, 6H), 5.32 (s, 2H), 3.88 (s, 3H).

¹³C-NMR (75 MHz, CDCl₃, 25 °C): δ (ppm) = 163.3 (C), 161.3 (C), 161.1 (C), 158.4 (C), 139.8 (C), 136.4 (CH), 132.2 (q, J_{C-F} = 32.4 Hz, C), 130.0 (CH), 129.4 (C), 128.8 (CH), 128.6 (C), 127.7 (CH), 127.6 (CH), 127.3 (CH), 126.9 (CH), 125.7 (q, J_{C-F} = 3.6 Hz, CH), 124.1 (q, $^1J_{C-F}$ = 272.0 Hz, CF₃), 114.0, 108.8, 55.5 (CH₃), 49.2 (CH₂).

¹⁹F-NMR (282 MHz, CDCl₃, 25 °C): δ (ppm) = -62.8.

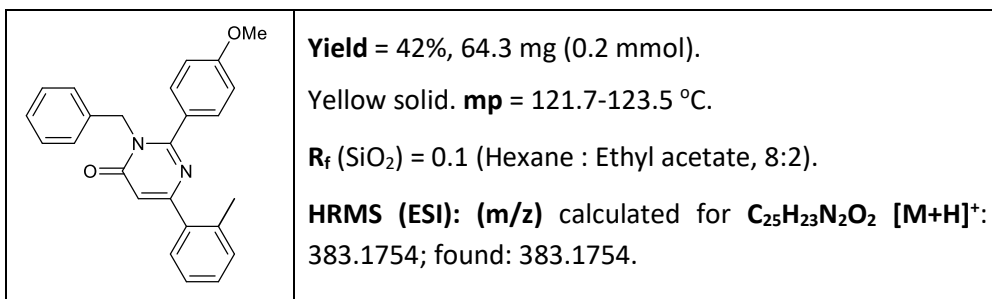
3-Benzyl-2,6-bis(4-methoxyphenyl)pyrimidin-4(3H)-one (1.4t)



¹H-NMR (300 MHz, CDCl₃, 25 °C, TMS): δ (ppm) = 8.01 (d, *J* = 9.0 Hz, 2H), 7.37 (d, *J* = 8.8 Hz, 2H), 7.27 (d, *J* = 7.2 Hz, 3H), 6.98 (m, 7H), 5.29 (s, 2H), 3.88 (s, 6H).

¹³C-NMR (75 MHz, CDCl₃, 25 °C): δ (ppm) = 163.7 (s), 161.8 (s), 161.1 (s), 160.4 (s), 159.6 (s), 136.7 (s), 130.0 (d), 128.9 (d), 128.7 (d), 127.7 (s), 127.5 (s), 126.9 (d), 114.2 (d), 113.9 (d), 106.1 (d), 55.6 (q), 55.5 (q), 49.0 (t).

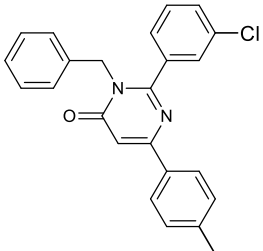
3-Benzyl-2-(4-methoxyphenyl)-6-(*o*-tolyl)pyrimidin-4(3H)-one (1.4u)



¹H-NMR (300 MHz, CDCl₃, 25 °C, TMS): δ (ppm) = 7.51 (dd, *J* = 7.8, 1.8 Hz, 1H), 7.36 – 7.27 (m, 8H), 7.06 (dd, *J* = 7.6, 2.0 Hz, 2H), 6.90 (d, *J* = 8.9 Hz, 2H), 6.64 (s, 1H), 5.31 (s, 2H), 3.85 (s, 3H), 2.51 (s, 3H).

¹³C-NMR (75 MHz, CDCl₃, 25 °C): δ (ppm) = 163.2 (s), 163.1 (s), 161.1 (s), 160.3 (s), 137.6 (s), 136.5 (s), 136.0 (s), 131.0 (d), 129.8 (d), 129.3 (d), 129.2 (d), 128.7 (d), 127.5 (d), 127.3 (s), 126.9 (d), 126.0 (d), 113.9 (d), 112.3 (d), 55.4 (q), 49.1 (t), 20.7 (q).

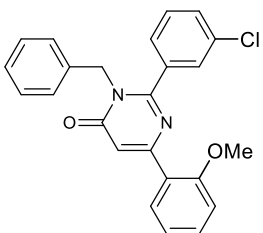
3-Benzyl-2-(3-chlorophenyl)-6-(*p*-tolyl)pyrimidin-4(3H)-one (1.4v)

	<p>Yield = 48%, 74.3 mg (0.2 mmol). Yellow oil.</p> <p>R_f (SiO₂) = 0.5 (Hexane : Ethyl acetate, 8:2).</p> <p>HRMS (ESI): (m/z) calculated for C₂₁H₂₂ClN₂O [M+H]⁺: 386.8872; found: 386.8876.</p>
---	--

¹H-NMR (300 MHz, CDCl₃, 25 °C, TMS): δ (ppm) = 8.28 (d, *J* = 8.1 Hz, 1H), 7.56 (s, 1H), 7.39 (d, *J* = 8.4 Hz, 4H), 7.34 – 7.14 (m, 6H), 7.03 – 6.88 (m, 2H), 5.26 (s, 2H), 2.54 (s, 3H).

¹³C-NMR (75 MHz, CDCl₃, 25 °C): δ (ppm) = 162.4 (s), 155.5 (s), 147.4 (s), 145.9 (d), 136.6 (d), 136.2 (s), 133.9 (s), 129.7 (s), 129.6 (d), 129.1 (d), 128.9 (d), 128.8 (d), 127.7 (d), 127.5 (d), 127.1 (d), 126.9 (s), 126.9 (d), 118.5 (s), 48.8 (t), 22.1 (q).

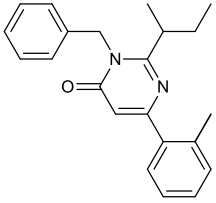
3-Benzyl-2-(3-chlorophenyl)-6-(2-methoxyphenyl)pyrimidin-4(3H)-one (1.4w)

	<p>Yield = 56%, 90.2 mg (0.2 mmol). Yellowish oil.</p> <p>R_f (SiO₂) = 0.1 (Hexane : Ethyl acetate, 8:2).</p> <p>HRMS (ESI): (m/z) calculated for C₂₄H₂₀ClN₂O₂ [M+H]⁺: 403.1208; found: 403.1205.</p>
---	---

¹H-NMR (300 MHz, CDCl₃, 25 °C, TMS): δ (ppm) = 8.06 (dd, *J* = 7.8, 1.8 Hz, 1H), 7.48 – 7.34 (m, 3H), 7.34 – 7.23 (m, 6H), 7.11 – 6.94 (m, 4H), 5.24 (s, 2H), 3.96 (s, 3H).

¹³C-NMR (75 MHz, CDCl₃, 25 °C): 163.4 (s), 158.8 (s), 158.4 (s), 157.3 (s), 136.4 (s), 133.7 (s), 131.6 (d), 131.0 (d), 129.7 (d), 128.8 (d), 127.7 (d), 127.0 (d), 125.1 (s), 120.9 (d), 113.5 (d), 111.5 (d), 55.7 (q), 48.8 (t).

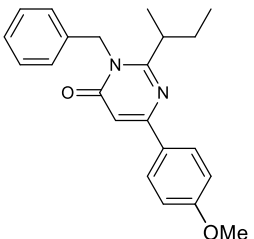
3-Benzyl-2-(*sec*-butyl)-6-(2-methylphenyl)pyrimidin-4(3H)-one (1.4x)

	<p>Yield = 42%, 54.5 mg (0.2 mmol). Yellow oil. R_f (SiO₂) = 0.3 (Hexane : Ethyl acetate, 8:2). HRMS (ESI): (m/z) calculated for C₂₁H₂₂ClN₂O [M+H]⁺: 333.1961; found: 333.1960.</p>
---	---

¹H-NMR (300 MHz, CDCl₃, 25 °C, TMS): δ (ppm) = 7.50 (dd, *J* = 7.8, 1.8 Hz, 1H), 7.41 – 7.29 (m, 6H), 7.25 – 7.20 (m, 2H), 6.57 (s, 1H), 5.55 (d, *J* = 16.0 Hz, 1H), 5.34 (d, *J* = 15.6 Hz, 1H), 2.98 – 2.81 (m, 1H), 2.49 (s, 3H), 1.86 (dt, *J* = 13.5, 7.5 Hz, 1H), 1.60 – 1.45 (m, 1H), 1.18 (d, *J* = 6.7 Hz, 3H), 0.72 (t, *J* = 7.4 Hz, 3H).

¹³C-NMR (75 MHz, CDCl₃, 25 °C): δ (ppm) = 165.8 (s), 163.6 (s), 163.3 (s), 137.8 (s), 136.4 (s), 136.2 (s), 131.1 (d), 130.2 (d), 129.3 (d), 129.2 (d), 128.9 (d), 127.7 (d), 126.5 (d), 125.9 (d), 111.1 (d), 45.8 (t), 39.4 (d), 28.6 (t), 20.8 (t), 19.4 (q), 11.9 (q).

3-Benzyl-2-(*sec*-butyl)-6-(4-methoxyphenyl)pyrimidin-4(3H)-one (1.4y)

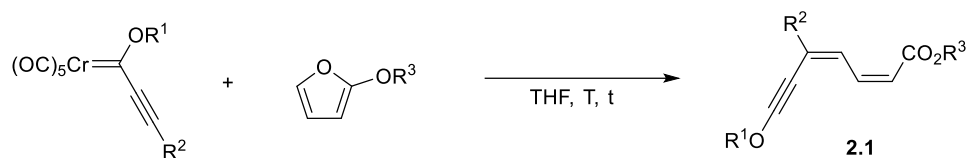
	<p>Yield = 61%, 68.0 mg (0.2 mmol). Yellow solid. mp = 104.0-107.1 °C. R_f (SiO₂) = 0.1 (Hexane : Ethyl acetate, 8:2). HRMS (ESI): (m/z) calculated for C₂₄H₂₀ClN₂O₂ [M+H]⁺: 349.1911; found: 349.1909.</p>
---	--

¹H-NMR (300 MHz, CDCl₃, 25 °C, TMS): δ (ppm) = 8.07 – 7.98 (m, 2H), 7.38 – 7.25 (m, 3H), 7.24 – 7.15 (m, 2H), 7.03 – 6.95 (m, 2H), 6.81 (s, 1H), 5.50 (d, *J* = 15.6 Hz, 1H), 5.34 (d, *J* = 15.8 Hz, 1H), 3.88 (s, 3H), 2.87 (dt, *J* = 7.4, 6.4 Hz, 1H), 1.91 (dt, *J* = 13.5, 7.5 Hz, 1H), 1.63 – 1.49 (m, 1H), 1.21 (d, *J* = 6.6 Hz, 3H), 0.75 (t, *J* = 7.4 Hz, 3H).

¹³C-NMR (75 MHz, CDCl₃, 25 °C): δ (ppm) = 165.8 (s), 163.7 (s), 161.7 (s), 159.3 (s), 136.4 (s), 128.9 (d), 128.9 (d), 128.6 (d), 127.6 (d), 126.4 (d), 114.0 (d), 104.7 (d), 55.4 (q), 45.6 (t), 39.3 (d), 28.8 (t), 19.5 (d), 11.9 (d).

2.2 Experimental procedures described in Chapter II.

2.2.1 Experimental procedure for the synthesis of “push-pull” alkyl 1,3-dien-5-ynecarboxylates **2.1**.⁵



Scheme 3: Synthesis of “push-pull” alkyl 1,3-dien-5-ynecarboxylates **2.1**

2-Methoxyfuran (2 equiv.) was added to a solution of the corresponding chromium carbene complex (1 equiv., 1 mmol) in dry THF (10 mL) at 0 °C. The temperature was raised to rt and the mixture stirred until complete disappearance of the carbene complex was observed by TLC (6-12 h). Solvent was removed under reduced pressure, and the residue purified by flash chromatography (Hexane/EtOAc) to afford the dienynic systems **2.1**.

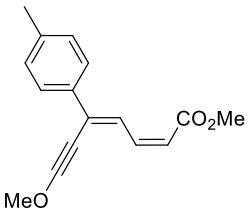
In the case of dienynes **2.1v** and **2.1w**, 2-isopropoxyfuran (2 equiv.) and 2-triisopropylsilyloxyfuran (2 equiv.) were used respectively instead of 2-methoxyfuran to afford the corresponding products, following the same procedure.

“Push-pull” alkyl 1,3-dien-5-ynecarboxylates **2.1a**, **2.1c-d**, **2.n** have been previously prepared according to this procedure and their spectroscopic data are already reported.⁵

“Push-pull” alkyl 1,3-dien-5-ynecarboxylates **2.1o-r** have not been characterised because they did not lead to of alkyl 6-substituted 2-alkoxybenzoate derivatives **2.2**.

⁵ Barluenga, J.; García-García, P.; de Saa, D.; Fernández-Rodríguez, M.A.; Bernardo de la Rúa, R.; Ballesteros, A.; Aguilar, E.; Tomás, M. *Angew. Chem. Int. Ed.* **2007**, *46*, 2610-2612.

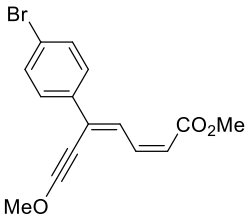
Methyl (2Z,4Z)-7-methoxy-5-(p-tolyl)hepta-2,4-dien-6-ynoate (2.1b)

	<p>Yield = 59%, 151.2 mg (0.6 mmol).</p> <p>Yellow oil.</p> <p>R_f (SiO₂) = 0.5 (Hexane : Ethyl acetate, 8:2).</p> <p>HRMS (ESI): (m/z) calculated for C₁₆H₁₇O₃ [M+H]⁺: 257.1172; found: 257.1177.</p>
---	--

¹H-NMR (300 MHz, CDCl₃, 25 °C, TMS): δ (ppm) = 8.26 (dd, J = 11.7, 1.2 Hz, 1H), 7.80 – 7.59 (m, 2H), 7.35 (t, J = 11.5 Hz, 2H), 7.26 – 7.05 (m, 2H), 5.80 (dd, J = 11.3, 1.1 Hz, 1H), 4.07 (s, 3H), 3.78 (s, 3H), 2.39 (s, 3H).

¹³C-NMR (75 MHz, CDCl₃, 25 °C): δ (ppm) = 167.2 (s), 142.7 (d), 139.1 (s), 135.3 (s), 132.2 (s), 129.1 (d, 2CH), 126.8 (d, 2CH), 126.2 (d), 116.8 (d), 110.6 (s), 66.5 (q), 51.1 (q), 36.6 (s), 21.3 (q).

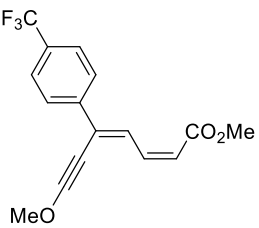
Methyl (2Z,4Z)-5-(4-bromophenyl)-7-methoxyhepta-2,4-dien-6-ynoate (2.1e)

	<p>Yield = 38%, 164.2 mg (0.5 mmol).</p> <p>Yellow oil.</p> <p>R_f (SiO₂) = 0.5 (Hexane : Ethyl acetate, 8:2).</p> <p>HRMS (ESI): (m/z) calculated for C₁₅H₁₄⁷⁹BrO₃ [M+H]⁺: 321.0121; found: 321.0128.</p>
---	---

¹H-NMR (300 MHz, CDCl₃, 25 °C, TMS): δ (ppm) = 8.23 (d, J = 11.6 Hz, 1H), 7.62 (d, J = 8.7 Hz, 2H), 7.46 (d, J = 8.7 Hz, 2H), 7.27 (t, J = 11.5 Hz, 1H), 5.81 (d, J = 11.3 Hz, 1H), 4.05 (s, 3H), 3.74 (s, 3H).

¹³C-NMR (75 MHz, CDCl₃, 25 °C): δ (ppm) = 167.0 (s), 142.3 (d), 137.0 (s), 131.4 (d, 2CH), 130.9 (s), 128.4 (d, 2CH), 127.1 (d), 123.0 (s), 117.8 (d), 110.7 (s), 66.6 (s), 51.3 (s), 36.2 (s).

Methyl (2Z,4Z)-7-methoxy-5-(4-(trifluoromethyl)phenyl)hepta-2,4-dien-6-ynoate (2.1f)

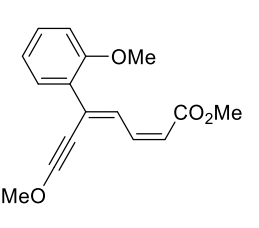
	<p>Yield = 56%, 233.5 mg (0.8 mmol). Yellow oil. R_f (SiO₂) = 0.4 (Hexane : Ethyl acetate, 8:2). HRMS (ESI): (m/z) calculated for C₁₆H₁₄O₃F₃ [M+H]⁺: 311.0890; found: 311.0898.</p>
---	---

¹H-NMR (300 MHz, CDCl₃, 25 °C, TMS): δ (ppm) = 8.29 (d, J = 11.6 Hz, 1H), 7.86 (d, J = 8.0 Hz, 2H), 7.62 (d, J = 8.5 Hz, 2H), 7.31 (t, J = 11.5 Hz, 1H), 5.86 (d, J = 11.3 Hz, 1H), 4.11 (s, 3H), 3.78 (s, 3H).

¹³C-NMR (75 MHz, CDCl₃, 25 °C): δ (ppm) = 167.1 (C), 142.1 (CH), 141.7 (C), 130.8 (q, $^2J_{C-F}$ = 32.6 Hz, C), 130.7 (C), 128.6 (CH), 127.2 (2CH), 125.4 (q, $^3J_{C-F}$ = 4.0 Hz, 2CH), 124.1 (q, $^1J_{C-F}$ = 272.0 Hz, CF₃), 118.8 (CH), 110.9 (C), 66.8 (CH₃), 51.5 (CH₃), 36.3 (C).

¹⁹F-NMR (282 MHz, CDCl₃, 25 °C): δ (ppm) = -62.1.

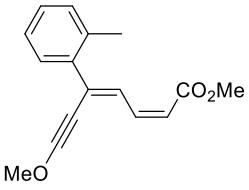
Methyl (2Z,4Z)-7-methoxy-5-(2-methoxyphenyl)hepta-2,4-dien-6-ynoate (2.1g)

	<p>Yield = 49%, 185.7 mg (0.7 mmol). Yellow oil. R_f (SiO₂) = 0.3 (Hexane : Ethyl acetate, 8:2). HRMS (ESI): (m/z) calculated for C₁₆H₁₇O₄ [M+H]⁺: 273.1121; found: 273.1130.</p>
---	--

¹H-NMR (300 MHz, CDCl₃, 25 °C, TMS): δ (ppm) = 8.19 (dd, J = 11.8, 1.2 Hz, 1H), 7.57 (dd, J = 7.7, 1.8 Hz, 1H), 7.45 – 7.24 (m, 2H), 7.05 – 6.87 (m, 2H), 5.78 (dd, J = 11.4, 1.2 Hz, 1H), 4.03 (s, 3H), 3.91 (s, 3H), 3.75 (s, 3H).

¹³C-NMR (75 MHz, CDCl₃, 25 °C): δ (ppm) = 167.1 (s), 157.2 (s), 142.7 (d), 131.5 (d), 130.6 (d), 129.6 (d), 128.3 (s), 120.5 (d), 117.2 (d), 111.4 (d), 109.5 (s), 66.4 (q), 55.7 (q), 51.2 (q), 37.7 (s).

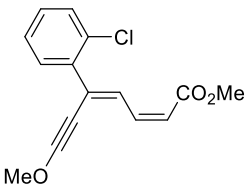
Methyl (2Z,4Z)-7-methoxy-5-(*o*-tolyl)hepta-2,4-dien-6-ynoate (2.1h)

	<p>Yield = 59%, 214.6 mg (0.8 mmol). Yellow oil. R_f (SiO₂) = 0.5 (Hexane : Ethyl acetate, 8:2). HRMS (ESI): (m/z) calculated for C₁₆H₁₇O₃ [M+H]⁺: 257.1172; found: 257.1176.</p>
---	--

¹H-NMR (300 MHz, CDCl₃, 25 °C, TMS): δ (ppm) = 7.70 (dd, *J* = 11.8, 1.2 Hz, 1H), 7.36 – 7.15 (m, 5H), 5.81 (dd, *J* = 11.4, 1.1 Hz, 1H), 4.01 (s, 3H), 3.74 (s, 3H), 2.46 (s, 3H).

¹³C-NMR (75 MHz, CDCl₃, 25 °C): δ (ppm) = 167.1 (s), 141.9 (d), 140.2 (s), 135.7 (s), 133.3 (s), 131.4 (d), 130.6 (d), 128.9 (d), 128.1 (d), 125.9 (d), 117.5 (d), 111.0 (s), 66.5 (q), 51.3 (q), 38.0 (s), 20.6 (q).

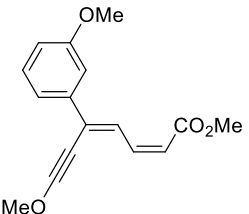
Methyl (2Z,4Z)-5-(2-chlorophenyl)-7-methoxyhepta-2,4-dien-6-ynoate (2.1i)

	<p>Yield = 59%, 224.1 mg (0.8 mmol) Yellow oil. R_f (SiO₂) = 0.4 (Hexane : Ethyl acetate, 8:2). HRMS (ESI): (m/z) calculated for C₁₅H₁₄ClO₃ [M+H]⁺: 277.0626; found: 277.0634.</p>
--	---

¹H-NMR (300 MHz, CDCl₃, 25 °C, TMS): δ (ppm) = 7.81 (dd, *J* = 11.7, 1.2 Hz, 1H), 7.48 – 7.35 (m, 2H), 7.34 – 7.15 (m, 3H), 5.83 (dd, *J* = 11.4, 1.2 Hz, 1H), 4.01 (s, 3H), 3.73 (s, 3H).

¹³C-NMR (75 MHz, CDCl₃, 25 °C): δ (ppm) = 166.9 (s), 141.4 (d), 139.1 (s), 132.35 (s), 132.26 (d), 130.6 (s+d, C + CH), 130.2 (d), 129.2 (d), 126.8 (d), 118.4 (d), 110.8 (s), 66.5 (q), 51.3 (q), 37.4 (s).

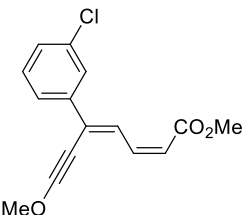
Methyl (2Z,4Z)-7-methoxy-5-(3-methoxyphenyl)hepta-2,4-dien-6-ynoate (2.1j)

	<p>Yield = 39%, 146.6 mg (0.5 mmol). Yellow oil.</p> <p>R_f (SiO₂) = 0.3 (Hexane : Ethyl acetate, 8:2).</p> <p>HRMS (ESI): (m/z) calculated for C₁₆H₁₇O₄ [M+H]⁺: 273.1121; found: 273.1130.</p>
---	--

¹H-NMR (300 MHz, CDCl₃, 25 °C, TMS): δ (ppm) = 8.23 (dd, J = 11.7, 1.1 Hz, 1H), 7.43 – 7.35 (m, 1H), 7.35 – 7.24 (m, 3H), 6.90 (ddd, J = 8.1, 2.5, 1.0 Hz, 1H), 5.80 (dd, J = 11.3, 1.1 Hz, 1H), 4.09 (s, 3H), 3.86 (s, 3H), 3.77 (s, 3H).

¹³C-NMR (75 MHz, CDCl₃, 25 °C): δ (ppm) = 167.2 (s), 159.6 (s), 142.5 (d), 139.8 (s), 132.1 (s), 129.4 (d), 127.3 (d), 119.4 (d), 117.6 (d), 114.4 (d), 112.8 (d), 110.6 (s), 66.7 (q), 55.4 (q), 51.4 (q), 36.7 (s).

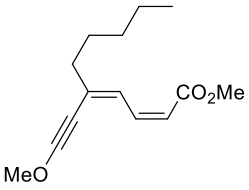
Methyl (2Z,4Z)-5-(3-chlorophenyl)-7-methoxyhepta-2,4-dien-6-ynoate (2.1k)

	<p>Yield = 64%, 246.2 mg (0.9 mmol). Yellow oil.</p> <p>R_f (SiO₂) = 0.4 (Hexane : Ethyl acetate, 8:2).</p> <p>HRMS (ESI): (m/z) calculated for C₁₅H₁₄ClO₃ [M+H]⁺: 277.0626; found: 277.0636.</p>
---	--

¹H-NMR (300 MHz, CDCl₃, 25 °C, TMS): δ (ppm) = 8.22 (dd, J = 11.7, 1.2 Hz, 1H), 7.84 – 7.49 (m, 2H), 7.44 – 7.09 (m, 3H), 5.83 (dd, J = 11.3, 1.2 Hz, 1H), 4.10 (s, 3H), 3.78 (s, 3H).

¹³C-NMR (75 MHz, CDCl₃, 25 °C): δ (ppm) = 167.1 (s), 142.2 (d), 140.1 (s), 134.5 (s), 130.8 (s), 129.6 (d), 128.9 (d), 127.9 (d), 127.1 (d), 125.0 (d), 118.3 (d), 110.8 (s), 66.7 (q), 51.4 (q), 36.3 (s).

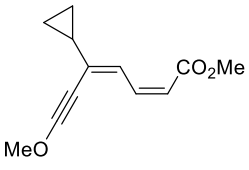
Methyl (2Z,4Z)-5-(methoxyethynyl)deca-2,4-dienoate (2.1l)

	<p>Yield = 64%, 474.0 mg (2.0 mmol). Yellow oil. R_f (SiO₂) = 0.7 (Hexane : Ethyl acetate, 8:2). HRMS (ESI): (m/z) calculated for C₁₄H₂₁O₃ [M+H]⁺: 237.1485; found: 237.1493.</p>
---	--

¹H-NMR (300 MHz, CDCl₃, 25 °C, TMS): δ (ppm) = 7.44 (dd, J = 11.7, 1.2 Hz, 1H), 7.07 (t, J = 11.5 Hz, 1H), 5.60 (dd, J = 11.4, 1.0 Hz, 1H), 3.99 (s, 3H), 3.71 (s, 4H), 2.24 (t, J = 7.6 Hz, 2H), 1.54 (p, J = 7.3 Hz, 2H), 1.34 – 1.23 (m, 4H), 0.88 (t, J = 6.9 Hz, 3H).

¹³C-NMR (75 MHz, CDCl₃, 25 °C): δ (ppm) = 167.3 (s), 142.8 (d), 136.1 (s), 127.8 (d), 115.3 (d), 109.8 (s), 66.5 (q), 51.2 (q), 38.9 (t), 37.8 (s), 31.3 (t), 28.2 (t), 22.6 (t), 14.1 (q).

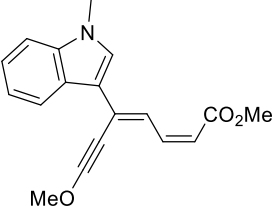
Methyl (2Z,4Z)-5-cyclopropyl-7-methoxyhepta-2,4-dien-6-ynoate (2.1m)

	<p>Yield = 81%, 334.9 mg (1.6 mmol). Yellow oil. R_f (SiO₂) = 0.5 (Hexane : Ethyl acetate, 8:2). HRMS (ESI): (m/z) calculated for C₁₂H₁₅O₃ [M+H]⁺: 207.1016; found: 207.1027.</p>
---	--

¹H-NMR (300 MHz, CDCl₃, 25 °C, TMS): δ (ppm) = 7.63 (dd, J = 11.7, 1.2 Hz, 1H), 7.08 (t, J = 11.6 Hz, 1H), 5.55 (dd, J = 11.4, 1.1 Hz, 1H), 3.98 (s, 3H), 3.72 (s, 3H), 1.71 (tt, J = 7.9, 5.0 Hz, 1H), 0.92 – 0.61 (m, 4H).

¹³C-NMR (75 MHz, CDCl₃, 25 °C): δ (ppm) = 167.4 (s), 142.5 (d), 138.9 (s), 126.7 (d), 114.0 (d), 109.3 (s), 66.6 (q), 51.2 (q), 33.7 (s), 18.3 (d), 7.4 (t, 2CH₂).

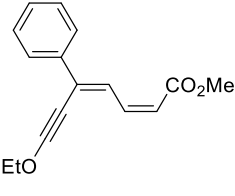
Methyl (2Z,4Z)-7-methoxy-5-(1-methyl-1H-indol-3-yl)hepta-2,4-dien-6-ynoate (2.1s)

	<p>Yield = 47%, 140.0 mg (0.5 mmol). Yellow oil. R_f (SiO₂) = 0.5 (Hexane : Ethyl acetate, 8:2). HRMS (ESI): (m/z) calculated for C₁₈H₁₈NO₃ [M+H]⁺: 296.1281; found: 296.1291.</p>
---	---

¹H-NMR (300 MHz, CDCl₃, 25 °C, TMS): δ (ppm) = 8.39 (dd, *J* = 11.8, 1.1 Hz, 1H), 8.22 (ddd, *J* = 7.0, 3.6, 1.7 Hz, 1H), 7.52 (s, 1H), 7.47 – 7.35 (m, 1H), 7.35 – 7.25 (m, 3H), 5.70 (dd, *J* = 11.2, 1.1 Hz, 1H), 4.11 (s, 3H), 3.81 (s, 3H), 3.81 (s, 3H).

¹³C-NMR (75 MHz, CDCl₃, 25 °C): δ (ppm) = 167.8 (s), 143.5 (d), 138.2 (s), 131.8 (s), 127.3 (s), 125.3 (d), 123.9 (d), 122.6 (d), 121.3 (d), 121.2 (d), 115.8 (d), 113.9 (d), 109.8 (s), 107.7, 66.5 (q), 51.2 (q), 36.8 (s), 33.2 (q).

Methyl (2Z,4Z)-7-ethoxy-5-phenylhepta-2,4-dien-6-ynoate (2.1t)

	<p>Yield = 54%, 140.1 mg (0.5 mmol). Yellow oil. R_f (SiO₂) = 0.5 (Hexane : Ethyl acetate, 8:2). HRMS (ESI): (m/z) calculated for C₁₆H₁₇O₃ [M+H]⁺: 257.1172; found: 257.1174.</p>
---	--

¹H-NMR (300 MHz, CDCl₃, 25 °C, TMS): δ (ppm) = 8.24 (dt, *J* = 11.6, 0.9 Hz, 1H), 7.81 – 7.75 (m, 2H), 7.43 – 7.23 (m, 4H), 5.79 (dt, *J* = 11.4, 0.9 Hz, 1H), 4.30 (q, *J* = 7.1 Hz, 2H), 3.76 (s, 3H), 1.48 (t, *J* = 7.1 Hz, 3H).

¹³C-NMR (75 MHz, CDCl₃, 25 °C): δ (ppm) = 167.2 (s), 142.7 (d), 138.3 (s), 132.6 (s), 128.9 (d), 128.4 (d), 127.0 (d), 126.8 (d), 117.2 (d), 109.5 (s), 75.8 (t), 51.2 (q), 37.9 (s), 14.7 (q).

Methyl (2Z,4Z)-7-isopropoxy-5-phenylhepta-2,4-dien-6-ynoate (2.1u)

	<p>Yield = 59%, 224.1 mg (0.8 mmol). Yellow oil. R_f (SiO₂) = 0.4 (Hexane : Ethyl acetate, 8:2). HRMS (ESI): (m/z) calculated for C₁₇H₁₉O₃ [M+H]⁺: 271.1329; found: 271.1331.</p>
--	--

¹H-NMR (300 MHz, CDCl₃, 25 °C, TMS): δ (ppm) = 8.28 (dd, J = 11.7, 1.2 Hz, 1H), 7.90 – 7.70 (m, 2H), 7.48 – 7.26 (m, 4H), 5.81 (dd, J = 11.4, 1.2 Hz, 1H), 4.53 (hept, J = 6.3 Hz, 1H), 3.77 (d, J = 0.8 Hz, 3H), 1.48 (d, J = 6.3 Hz, 6H).

¹³C-NMR (75 MHz, CDCl₃, 25 °C): δ (ppm) = 167.1 (s), 142.7 (d), 138.4 (s), 132.9 (s), 128.8 (d), 128.3 (d), 126.9 (d), 126.5 (d), 117.0 (d), 108.4 (s), 83.3 (d), 51.1 (q), 39.1 (s), 21.5 (q).

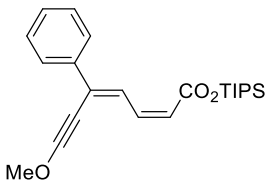
Isopropyl (2Z,4Z)-7-methoxy-5-phenylhepta-2,4-dien-6-ynoate (2.1v)

	<p>Yield = 33%, 303.1 mg (1.1 mmol). Yellow oil. R_f (SiO₂) = 0.5 (Hexane : Ethyl acetate, 8:2). HRMS (ESI): (m/z) calculated for C₁₅H₁₄O₃ [M+H]⁺: 271.1329; found: 271.1330.</p>
--	--

¹H-NMR (300 MHz, CDCl₃, 25 °C, TMS): 8.28 (d, J = 11.8 Hz, 1H), 7.79 (d, J = 8.2 Hz, 2H), 7.49 – 7.18 (m, 4H), 5.77 (d, J = 11.2 Hz, 1H), 5.11 (hept, J = 6.3 Hz, 1H), 4.10 (s, 3H), 1.32 (d, J = 6.3 Hz, 6H).

¹³C-NMR (75 MHz, CDCl₃, 25 °C): δ (ppm) = 166.2 (s), 141.9 (d), 138.1 (s), 131.7 (s), 128.8 (d), 128.3 (d), 127.0 (d), 126.8 (d), 118.4 (d), 110.5 (s), 67.2 (q), 66.4 (d), 36.5 (s), 21.9 (q).

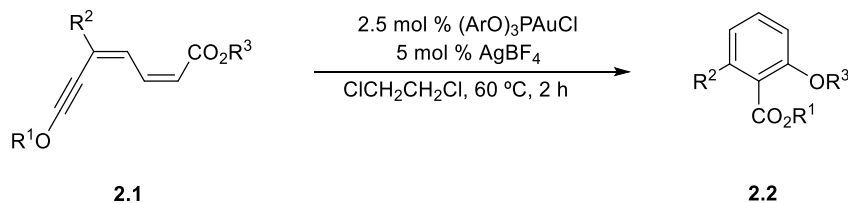
Triisopropylsilyl (2Z,4Z)-7-methoxy-5-phenylhepta-2,4-dien-6-ynoate (2.1w)

	<p>Yield = 15%, 162.9 mg (0.4 mmol). Yellow oil. R_f (SiO₂) = 0.3 (Hexane : Ethyl acetate, 8:2). HRMS (ESI): (m/z) calculated for C₁₅H₁₄O₃ [M+H]⁺: 385.2193; found: 385.2201.</p>
---	--

¹H-NMR (300 MHz, CDCl₃, 25 °C, TMS): δ (ppm) = 8.21 (d, *J* = 11.7 Hz, 1H), 7.79 (dd, *J* = 7.5, 1.9 Hz, 2H), 7.54 – 7.17 (m, 4H), 5.85 (d, *J* = 11.3 Hz, 1H), 4.10 (s, 3H), 1.39 (hept, *J* = 7.4 Hz, 3H), 1.15 (d, *J* = 7.4 Hz, 18H).

¹³C-NMR (75 MHz, CDCl₃, 25 °C): δ (ppm) = 166.5 (s), 142.3 (d), 138.4 (s), 132.0 (s), 128.9 (d), 128.4 (d), 127.4 (d), 127.1 (d), 120.0 (d), 110.7 (s), 66.6 (d), 36.8 (s), 18.0 (q), 12.2 (d).

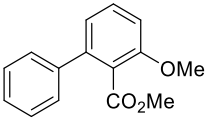
2.2.2 Experimental procedure for the synthesis of alkyl 6-substituted 2-alkoxybenzoate derivatives 2.2.



Scheme 5-4: Gold (I)-catalysed cycloisomerization of “push-pull” alkyl 1,3-dien-5-ynecarboxylates **2.1**.

A solution of AgBF₄ (5 mol%, 0.14 mL, 178.3 mM in dry DCE, 0.025 mmol) was added to (RO)₃PAuCl (2.5 mol%, 11.0 mg, 0.0125 mmol) in a Schlenk flask under argon atmosphere and the reaction mixture was stirred for 30 minutes. The corresponding “push-pull” alkyl 1,3-dien-5-ynecarboxylate **2.1** (0.5 mmol) in dry DCE (3 mL) was subsequently added and the reaction mixture heated at 60 °C for 2 hours. Then, the reaction was allowed to cool down to room temperature, silica gel was added, and solvent was evaporated under reduced pressure. The crude residue was purified by flash column chromatography on silica gel (Hexane/EtOAc: 10/1 to 4/1) to afford alkyl 6-substituted 2-alkoxybenzoate derivatives **2.2**.

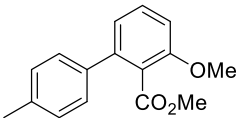
Methyl 3-methoxy-[1,1'-biphenyl]-2-carboxylate (2.2a)

	<p>Yield = 96%, 93.0 mg (0.4 mmol).</p> <p>Yellow oil.</p> <p>R_f (SiO₂) = 0.5 (Hexane : Ethyl acetate, 8:2).</p> <p>HRMS (ESI): (m/z) calculated for C₁₅H₁₅O₃ [M+H]⁺: 243.1016; found: 243.1020.</p>
---	---

¹H-NMR (300 MHz, CDCl₃, 25 °C, TMS): δ (ppm) = 7.47 – 7.36 (m, 6H), 7.02 (dd, *J* = 7.7, 1.0 Hz, 1H), 6.97 (dd, *J* = 8.4, 1.0 Hz, 1H), 3.91 (s, 3H), 3.65 (s, 3H).

¹³C-NMR (75 MHz, CDCl₃, 25 °C): δ (ppm) = 168.6 (s), 156.6 (s), 141.4 (s), 140.2 (s), 130.6 (d), 128.5 (d, 2CH), 128.4 (d, 2CH), 127.7 (d), 123.2 (s), 122.1 (d), 110.0 (d), 56.2 (q), 52.2 (q)

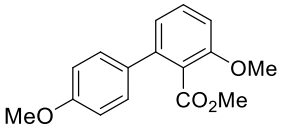
Methyl 3-methoxy-4'-methyl-[1,1'-biphenyl]-2-carboxylate (2.2b)

	<p>Yield = 89%, 70.7 mg (0.3 mmol).</p> <p>Yellowish oil.</p> <p>R_f (SiO₂) = 0.4 (Hexane : Ethyl acetate, 8:2).</p> <p>HRMS (ESI): (m/z) calculated for C₁₆H₁₇O₃ [M+H]⁺: 257.1172; found: 257.1179.</p>
---	--

¹H-NMR (300 MHz, CDCl₃, 25 °C, TMS): δ (ppm) = 7.42 (dd, *J* = 8.4, 7.7 Hz, 1H), 7.34 – 7.28 (m, 2H), 7.25 – 7.18 (m, 2H), 7.00 (dd, *J* = 7.8, 0.9 Hz, 1H), 6.94 (dd, *J* = 8.4, 1.0 Hz, 1H), 3.90 (s, 3H), 3.68 (s, 3H), 2.40 (s, 3H).

¹³C-NMR (75 MHz, CDCl₃, 25 °C): δ (ppm) = 169.1 (s), 156.8 (s), 141.6 (s), 137.8 (s), 137.5 (s), 130.9 (d), 129.5 (d, 2CH), 128.5 (d, 2CH), 123.4 (s), 122.4 (d), 110.0 (d), 56.5 (q), 52.6 (q), 21.6 (q).

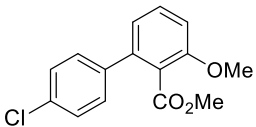
Methyl 3,4'-dimethoxy-[1,1'-biphenyl]-2-carboxylate (2.2c)

	<p>Yield = 98%, 93.4 mg (0.4 mmol). Yellowish oil. R_f (SiO₂) = 0.3 (Hexane : Ethyl acetate, 8:2). HRMS (ESI): (m/z) calculated for C₁₆H₁₇O₄ [M+H]⁺: 273.1121; found: 273.1120.</p>
---	--

¹H-NMR (300 MHz, CDCl₃, 25 °C, TMS): δ (ppm) = 7.48 – 7.25 (m, 3H), 7.03 – 6.87 (m, 4H), 3.89 (s, 3H), 3.85 (s, 3H), 3.68 (s, 3H).

¹³C-NMR (75 MHz, CDCl₃, 25 °C): δ (ppm) = 168.9 (s), 159.3 (s), 156.5 (s), 140.9 (s), 132.6 (s), 130.6 (d), 129.5 (d, 2CH), 123.1 (s), 122.1 (d), 113.9 (d, 2CH), 109.6 (d), 56.2 (q), 55.4 (q), 52.3 (q).

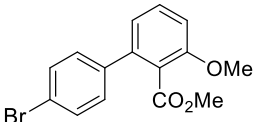
Methyl 3-methoxy-4'-chloro-[1,1'-biphenyl]-2-carboxylate (2.2d)

	<p>Yield = 95%, 94.7 mg (0.4 mmol). Yellowish oil. R_f (SiO₂) = 0.4 (Hexane : Ethyl acetate, 8:2). HRMS (ESI): (m/z) calculated for C₁₅H₁₄ClO₃ [M+H]⁺: 277.0626; found: 277.0626.</p>
---	--

¹H-NMR (300 MHz, CDCl₃, 25 °C, TMS): δ (ppm) = 7.57 – 7.24 (m, 5H), 7.09 – 6.87 (m, 2H), 3.91 (s, 3H), 3.68 (s, 3H).

¹³C-NMR (75 MHz, CDCl₃, 25 °C): δ (ppm) = 168.4 (s), 156.7 (s), 140.1 (s), 138.6 (s), 133.8 (s), 130.7 (d), 129.7 (d, 2CH), 128.7 (d, 2CH), 123.2 (s), 121.9 (d), 110.3 (d), 56.2 (q), 52.4 (q).

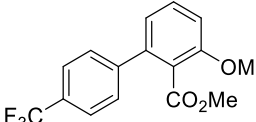
Methyl 3-methoxy-4'-bromo-[1,1'-biphenyl]-2-carboxylate (2.2e)

	<p>Yield = 71%, 82.1 mg (0.3 mmol). Yellowish oil. R_f (SiO₂) = 0.3 (Hexane : Ethyl acetate, 8:2). HRMS (ESI): (m/z) calculated for C₁₅H₁₄⁷⁹BrO₃ [M+H]⁺: 321.0121; found: 321.0119.</p>
---	---

¹H-NMR (300 MHz, CDCl₃, 25 °C, TMS): δ (ppm) = 7.53 (d, *J* = 8.5 Hz, 2H), 7.45 – 7.37 (m, 1H), 7.28 (d, *J* = 8.5 Hz, 2H), 7.01 – 6.93 (m, 2H), 3.90 (s, 3H), 3.68 (s, 3H).

¹³C-NMR (75 MHz, CDCl₃, 25 °C): δ (ppm) = 168.4 (s), 156.7 (s), 140.1 (s), 139.1 (s), 131.6 (d, 2CH), 130.8 (d), 130.0 (d, 2CH), 123.1 (s), 122.1 (s), 121.9 (d), 110.4 (d), 56.2 (q), 52.4 (q).

Methyl 3-methoxy-4'-trifluoromethyl-[1,1'-biphenyl]-2-carboxylate (2.2f)

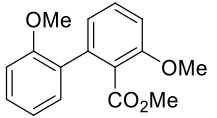
	<p>Yield = 85%, 73.6 mg (0.2 mmol). Yellowish oil. R_f (SiO₂) = 0.4 (Hexane : Ethyl acetate, 8:2). HRMS (ESI): (m/z) calculated for C₁₆H₁₄F₃O₃ [M+H]⁺: 311.0890; found: 311.0888.</p>
---	---

¹H-NMR (300 MHz, CDCl₃, 25 °C, TMS): δ (ppm) = 7.67 (d, *J* = 8.1 Hz, 2H), 7.59 – 7.37 (m, 3H), 7.09 – 6.91 (m, 2H), 3.92 (s, 3H), 3.67 (s, 3H).

¹³C-NMR (75 MHz, CDCl₃, 25 °C): δ (ppm) = 168.2 (C), 156.7 (C), 143.8 (C), 139.9 (C), 130.9 (CH), 129.9 (C, q, ²*J*_{C-F} = 32.8 Hz), 128.8 (2CH), 125.4 (q, ³*J*_{C-F} = 3.8 Hz, 2CH), 124.3 (q, ¹*J*_{C-F} = 272.0 Hz, CF₃), 123.2 (C), 121.9 (CH), 110.8 (CH), 56.2 (CH₃), 52.4 (CH₃).

¹⁹F-NMR (282 MHz, CDCl₃, 25 °C): δ (ppm) = -62.5.

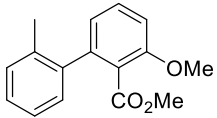
Methyl 2',3-dimethoxy-[1,1'-biphenyl]-2-carboxylate (2.2g)

	<p>Yield = 63%, 58.1 mg (0.2 mmol).</p> <p>Yellowish oil.</p> <p>R_f (SiO₂) = 0.2 (Hexane : Ethyl acetate, 8:2).</p> <p>HRMS (ESI): (m/z) calculated for C₁₆H₁₇O₄ [M+H]⁺: 273.1121; found: 273.1123.</p>
---	---

¹H-NMR (300 MHz, CDCl₃, 25 °C, TMS): δ (ppm) = 7.42 (dd, J = 8.4, 7.7 Hz, 1H), 7.37 – 7.30 (m, 1H), 7.23 (dd, J = 7.5, 1.8 Hz, 1H), 7.05 – 6.91 (m, 4H), 3.90 (s, 3H), 3.77 (s, 3H), 3.59 (s, 3H).

¹³C-NMR (75 MHz, CDCl₃, 25 °C): δ (ppm) = 168.1 (s), 156.6 (s), 156.3 (s), 138.6 (s), 130.6 (d), 130.5 (d), 129.2 (d), 129.1 (s), 123.4 (s), 123.2 (d), 120.5 (d), 110.7 (d), 110.0 (d), 56.1 (q), 55.5 (q), 51.9 (q).

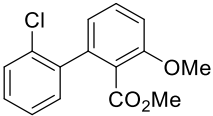
Methyl 3-methoxy-2'-methyl-[1,1'-biphenyl]-2-carboxylate (2.2h)

	<p>Yield = 66%, 54.7 mg (0.3 mmol).</p> <p>Greenish oil.</p> <p>R_f (SiO₂) = 0.3 (Hexane : Ethyl acetate, 8:2).</p> <p>HRMS (ESI): (m/z) calculated for C₁₅H₁₄ClO₃ [M+H]⁺: 257.1172; found: 257.1172.</p>
---	--

¹H-NMR (300 MHz, CDCl₃, 25 °C, TMS): δ (ppm) = 7.41 (dd, J = 8.4, 7.6 Hz, 1H), 7.30 – 7.11 (m, 4H), 6.96 (dd, J = 8.4, 1.0 Hz, 1H), 6.86 (dd, J = 7.6, 0.9 Hz, 1H), 3.91 (s, 3H), 3.52 (s, 3H), 2.18 (s, 3H).

¹³C-NMR (75 MHz, CDCl₃, 25 °C): δ (ppm) = 168.1 (s), 156.3 (s), 141.3 (s), 139.4 (s), 136.1 (s), 130.2 (d), 129.9 (d), 129.2 (d), 127.8 (d), 125.2 (d), 123.8 (s), 122.1 (d), 109.7 (d), 56.0 (q), 52.0 (q), 20.1 (q).

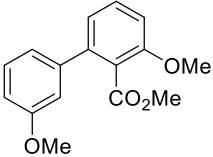
Methyl 2'-chloro-3-methoxy-[1,1'-biphenyl]-2-carboxylate (2.2i)

	<p>Yield = 80%, 79.7 mg (0.3 mmol). Yellowish oil. R_f (SiO₂) = 0.4 (Hexane : Ethyl acetate, 8:2). HRMS (ESI): (m/z) calculated for C₁₅H₁₄ClO₃ [M+H]⁺: 277.0626; found: 277.0627.</p>
---	---

¹H-NMR (300 MHz, CDCl₃, 25 °C, TMS): δ (ppm) = 7.53 – 7.40 (m, 2H), 7.37 – 7.20 (m, 3H), 7.00 (dd, *J* = 8.4, 0.9 Hz, 1H), 6.95 (dd, *J* = 7.7, 0.9 Hz, 1H), 3.92 (s, 3H), 3.56 (s, 3H).

¹³C-NMR (75 MHz, CDCl₃, 25 °C): δ (ppm) = 167.7 (s), 156.7 (s), 139.1 (s), 138.7 (s), 133.2 (s), 130.9 (d), 130.4 (d), 129.6 (d), 129.1 (d), 126.4 (d), 123.6 (s), 122.6 (d), 110.6(s), 56.1 (q), 52.1 (q).

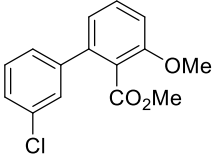
Methyl 3,3'-dimethoxy-[1,1'-biphenyl]-2-carboxylate (2.2j)

	<p>Yield = 80%, 59.0 mg (0.2 mmol). Yellowish oil. R_f (SiO₂) = 0.3 (Hexane : Ethyl acetate, 8:2). HRMS (ESI): (m/z) calculated for C₁₆H₁₇O₄ [M+H]⁺: 273.1121; found: 273.1130.</p>
---	---

¹H-NMR (300 MHz, CDCl₃, 25 °C, TMS): δ (ppm) = 7.43 (t, *J* = 8.1 Hz, 1H), 7.31 (t, *J* = 7.9 Hz, 1H), 7.15 – 6.79 (m, 5H), 3.91 (s, 3H), 3.84 (s, 3H), 3.68 (s, 3H).

¹³C-NMR (75 MHz, CDCl₃, 25 °C): δ (ppm) = 168.6 (s), 159.6 (s), 156.6 (s), 141.6 (s), 141.2 (s), 130.6 (d), 129.5 (d), 123.2 (s), 122.0 (d), 120.8 (d), 113.75 (d), 113.65 (d), 110.1 (d), 56.2 (q), 55.4 (q), 52.3 (q).

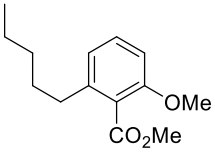
Methyl 3'-chloro-3-methoxy-[1,1'-biphenyl]-2-carboxylate (2.2k)

	<p>Yield = 62%, 76.3 mg (0.3 mmol).</p> <p>Yellowish oil.</p> <p>R_f (SiO₂) = 0.3 (Hexane : Ethyl acetate, 8:2).</p> <p>HRMS (ESI): (m/z) calculated for C₁₅H₁₄ClO₃ [M+H]⁺: 277.0626; found: 277.0636.</p>
---	--

¹H-NMR (300 MHz, CDCl₃, 25 °C, TMS): δ (ppm) = 7.50 – 7.39 (m, 2H), 7.38 – 7.24 (m, 3H), 6.98 (d, *J* = 8.0 Hz, 2H), 3.90 (s, 3H), 3.69 (s, 3H).

¹³C-NMR (75 MHz, CDCl₃, 25 °C): δ (ppm) = 168.3 (s), 156.6 (s), 141.9 (s), 139.8 (s), 134.3 (s), 130.8 (d), 129.7 (d), 128.5 (d), 127.8 (d), 126.5 (d), 123.1 (s), 121.8 (d), 110.5 (d), 56.2 (q), 52.4 (q).

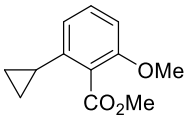
Methyl 2-methoxy-6-pentylbenzoate (2.2l)

	<p>Yield = 73%, 519.8 mg (2.3 mmol).</p> <p>Yellowish oil.</p> <p>R_f (SiO₂) = 0.5 (Hexane : Ethyl acetate, 8:2).</p> <p>HRMS (ESI): (m/z) calculated for C₁₄H₂₁O₃ [M+H]⁺: 237.1485; found: 237.1491.</p>
--	---

¹H-NMR (300 MHz, CDCl₃, 25 °C, TMS): δ (ppm) = 7.28 (t, *J* = 8.0 Hz, 1H), 6.84 (d, *J* = 7.7 Hz, 1H), 6.77 (d, *J* = 8.3 Hz, 1H), 3.92 (s, 3H), 3.82 (s, 3H), 2.56 (t, *J* = 7.9 Hz, 2H), 1.60 (p, *J* = 7.3 Hz, 2H), 1.44 – 1.21 (m, 4H), 0.89 (t, *J* = 6.8 Hz, 3H).

¹³C-NMR (75 MHz, CDCl₃, 25 °C): δ (ppm) = 169.0 (s), 156.3 (s), 141.4 (s), 130.3 (d), 123.6 (s), 121.5 (d), 108.4 (d), 55.9 (q), 52.1 (q), 33.5 (t), 31.7 (t), 30.9 (t), 22.5 (t), 14.0 (q).

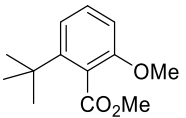
Methyl 2-cyclopropyl-6-methoxybenzoate (2.2m)

	<p>Yield = 84%, 139.8 mg (0.7 mmol).</p> <p>Yellowish oil.</p> <p>R_f (SiO₂) = 0.4 (Hexane : Ethyl acetate, 8:2).</p> <p>HRMS (ESI): (m/z) calculated for C₁₂H₁₅O₃ [M+H]⁺: 207.1016; found: 207.1020.</p>
---	--

¹H-NMR (300 MHz, CDCl₃, 25 °C, TMS): δ (ppm) = 7.25 (t, J = 8.1 Hz, 1H), 6.75 (d, J = 8.3 Hz, 1H), 6.58 (d, J = 7.9 Hz, 1H), 3.95 (s, 3H), 3.83 (s, 3H), 1.89 (tt, J = 8.4, 5.2 Hz, 1H), 1.03 – 0.81 (m, 2H), 0.82 – 0.58 (m, 2H).

¹³C-NMR (75 MHz, CDCl₃, 25 °C): δ (ppm) = 169.1 (s), 156.1 (s), 142.0 (s), 130.5 (d), 124.7 (s), 117.4 (d), 108.5 (d), 56.0 (q), 52.3 (q), 13.2 (d), 8.1 (t, 2CH₂).

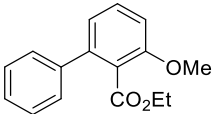
Methyl 2-(tert-butyl)-6-methoxybenzoate (2.2n)

	<p>Yield = 84%, 184.3 mg (0.8 mmol).</p> <p>Yellowish oil.</p> <p>R_f (SiO₂) = 0.5 (Hexane : Ethyl acetate, 8:2).</p> <p>HRMS (ESI): (m/z) calculated for C₁₃H₁₉O₃ [M+H]⁺: 223.1329; found: 223.1336.</p>
---	--

¹H-NMR (300 MHz, CDCl₃, 25 °C, TMS): δ (ppm) = 7.30 (t, J = 8.2 Hz, 1H), 7.09 (d, J = 8.1 Hz, 1H), 6.81 (d, J = 8.2 Hz, 1H), 3.91 (s, 3H), 3.82 (s, 3H), 1.38 (s, 9H).

¹³C-NMR (75 MHz, CDCl₃, 25 °C): δ (ppm) = 170.8 (s), 156.8 (s), 148.3 (s), 129.8 (d), 123.1 (s), 119.3 (d), 108.7 (d), 56.2 (q), 52.2 (q), 36.1 (s), 31.5 (q, 3CH₃).

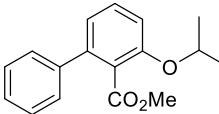
Ethyl 3-methoxy-[1,1'-biphenyl]-2-carboxylate (2.2t)

	<p>Yield = 89%, 78.6 mg (0.3 mmol). Yellowish oil. R_f (SiO₂) = 0.4 (Hexane : Ethyl acetate, 8:2). HRMS (ESI): (m/z) calculated for C₁₆H₁₇O₃ [M+H]⁺: 257.1172; found: 257.1178.</p>
---	--

¹H-NMR (300 MHz, CDCl₃, 25 °C, TMS): δ (ppm) = 7.43 – 7.31 (m, 6H), 6.98 (dd, J = 7.7, 1.0 Hz, 1H), 6.94 (dd, J = 8.4, 0.9 Hz, 1H), 4.10 (q, J = 7.1 Hz, 2H), 3.89 (s, 3H), 0.98 (t, J = 7.2 Hz, 2H).

¹³C-NMR (75 MHz, CDCl₃, 25 °C): δ (ppm) = 168.0 (s), 156.6 (s), 141.5 (s), 140.3 (s), 130.5 (d), 128.5 (d), 128.4 (d), 127.7 (d), 123.5 (s), 122.1 (d), 110.1 (d), 61.2 (t), 56.2 (q), 13.8 (q).

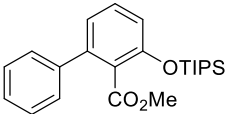
Methyl 3-isopropoxy-[1,1'-biphenyl]-2-carboxylate (2.2v)

	<p>Yield = 96%, 461.0 mg (1.7 mmol). Yellow oil. R_f (SiO₂) = 0.5 (Hexane : Ethyl acetate, 8:2). HRMS (ESI): (m/z) calculated for C₁₆H₁₇O₃ [M+H]⁺: 271.1329; found: 271.1330.</p>
---	--

¹H-NMR (300 MHz, CDCl₃, 25 °C, TMS): δ (ppm) = 7.55 – 7.32 (m, 6H), 7.09 – 6.87 (m, 2H), 4.63 (hept, J = 6.1 Hz, 1H), 3.69 (s, 3H), 1.39 (d, J = 6.0 Hz, 6H).

¹³C-NMR (75 MHz, CDCl₃, 25 °C): δ (ppm) = 168.6 (s), 155.1 (s), 141.2 (s), 140.2 (s), 130.3 (d), 128.4 (d), 128.3 (d), 127.6 (d), 124.8 (s), 121.9 (d), 112.8 (d), 71.6 (d), 52.0 (q), 22.1 (q).

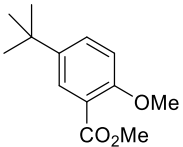
Methyl 3-((triisopropylsilyl)oxy)-[1,1'-biphenyl]-2-carboxylate (2.2w)

	<p>Yield = 61%, 235.4 mg (0.3 mmol). Yellowish oil. R_f (SiO₂) = 0.8 (Hexane : Ethyl acetate, 8:2). HRMS (ESI): (m/z) calculated for C₁₆H₁₇O₃ [M+H]⁺: 385.2193; found: 385.2212.</p>
---	---

¹H-NMR (300 MHz, CDCl₃, 25 °C, TMS): δ (ppm) = 7.47 – 7.32 (m, 4H), 7.29 (t, *J* = 4.0 Hz, 2H), 6.97 (dd, *J* = 7.7, 1.0 Hz, 1H), 6.88 (dd, *J* = 8.2, 1.0 Hz, 1H), 3.64 (s, 3H), 1.43 – 1.22 (m, 3H), 1.14 (d, *J* = 7.2 Hz, 18H).

¹³C-NMR (75 MHz, CDCl₃, 25 °C): δ (ppm) = 168.7 (s), 153.0 (s), 141.4 (s), 140.3 (s), 130.1 (d), 128.4 (d), 128.4 (d), 127.6 (d), 125.8 (s), 122.0 (d), 117.5 (d), 51.9 (q), 18.0 (q), 13.0 (d).

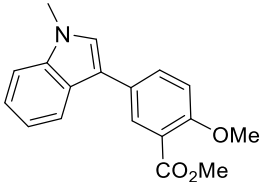
Methyl 5-(*tert*-butyl)-2-methoxybenzoate (2.4n)

	<p>Yield = 16%, 34.2 mg (0.15 mmol). Yellowish oil. R_f (SiO₂) = 0.5 (Hexane : Ethyl acetate, 8:2). HRMS (ESI): (m/z) calculated for C₁₃H₁₉O₃ [M+H]⁺: 223.1329; found: 223.1334.</p>
---	---

¹H-NMR (300 MHz, CDCl₃, 25 °C, TMS): δ (ppm) = 7.77 (d, *J* = 8.1 Hz, 1H), 7.12 – 6.87 (m, 2H), 3.94 (s, 3H), 3.89 (s, 3H), 1.35 (s, 9H).

¹³C-NMR (75 MHz, CDCl₃, 25 °C): δ (ppm) = 166.7 (s), 159.3 (s), 157.9 (s), 131.7 (d), 117.6 (d), 117.2 (s), 109.5 (d), 56.1 (q), 52.0 (q), 35.4 (s), 31.2 (q, 3CH₃).

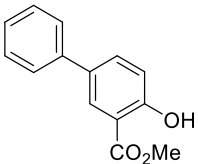
Methyl 2-methoxy-5-(1-methyl-1H-indol-3-yl)benzoate (2.4s)

	<p>Yield = 92%, 120.0 mg (0.40 mmol). Yellowish oil. R_f (SiO₂) = 0.3 (Hexane : Ethyl acetate, 8:2). HRMS (ESI): (m/z) calculated for C₁₄H₂₁O₃ [M+H]⁺: 237.1485; found: 237.1491.</p>
---	--

¹H-NMR (300 MHz, CDCl₃, 25 °C, TMS): δ (ppm) = 8.02 – 7.88 (m, 2H), 7.46 – 7.39 (m, 2H), 7.38 – 7.21 (m, 4H), 4.02 (s, 3H), 3.94 (s, 3H), 3.89 (s, 3H).

¹³C-NMR (75 MHz, CDCl₃, 25 °C): δ (ppm) = 166.7 (s), 160.1 (s), 141.8 (s), 137.8 (s), 132.6 (d), 127.6 (d), 126.1 (s), 122.5 (d), 120.6 (d), 119.9 (d), 119.0 (d), 116.8 (s), 116.0 (s), 110.7 (d), 110.0 (d), 56.3 (q), 52.0 (q), 33.2 (q).

Methyl 4-hydroxy-[1,1'-biphenyl]-3-carboxylate (2.4u)

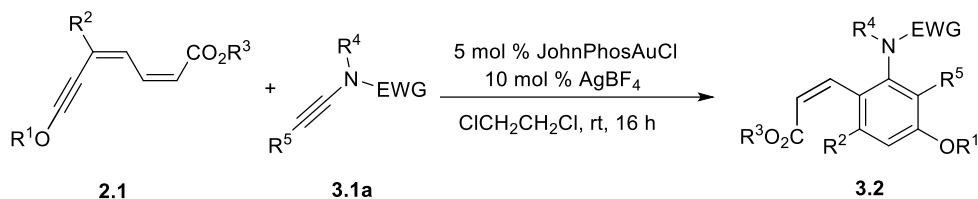
	<p>Yield = 50%, 104.3 mg (0.5 mmol). Yellow oil. R_f (SiO₂) = 0.3 (Hexane : Ethyl acetate, 8:2). HRMS (ESI): (m/z) calculated for C₁₄H₁₃O₃ [M+H]⁺: 229.0859; found: 229.0861.</p>
--	--

¹H-NMR (300 MHz, CDCl₃, 25 °C, TMS): δ (ppm) = 10.92 (s, 1H), 7.90 (d, *J* = 8.3 Hz, 1H), 7.70 – 7.61 (m, 2H), 7.55 – 7.40 (m, 3H), 7.28 (d, *J* = 1.8 Hz, 1H), 7.15 (dd, *J* = 8.3, 1.8 Hz, 1H), 3.97 (s, 3H).

¹³C-NMR (75 MHz, CDCl₃, 25 °C): δ (ppm) = 170.5 (s), 161.8 (s), 148.4 (s), 139.6 (s), 130.3 (d), 128.9 (d), 128.4 (d), 127.2 (d), 118.1 (d), 115.7 (d), 111.2 (s), 52.2 (q).

2.3 Experimental procedures described in Chapter III.

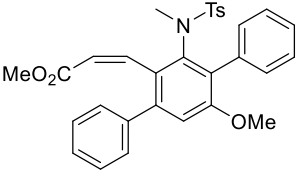
2.3.1 Experimental procedure for the gold (I)-catalysed tetrahydro-Diels-Alder reaction.



Scheme 5. Gold (I)-catalysed tetrahydro-Diels-Alder transformation to obtain tetrasubstituted anilines **3.2**.

A solution of $AgBF_4$ (10 mol%, 0.28 mL, 178.3 mM in dry DCE, 0.05 mmol) was added to JohnPhosAuCl (5 mol%, 13.0 mg, 0.025 mmol) in a Schlenk flask under argon atmosphere and the reaction mixture was stirred for 30 minutes. The mixture was cooled down to 0 °C and the corresponding ynamide **3.1** (2.0 equiv., 1 mmol) and diene carboxylic ester **2.1** (1.0 equiv., 0.5 mmol) in dry DCE (3 mL) were subsequently added. Then, the reaction was allowed to warm to room temperature and the stirring was continued for 16 h. Silica gel was added, and the solvent was evaporated under reduced pressure. The crude residue was purified by flash column chromatography on silica gel (Hexane/EtOAc: 10/1 to 4/1) to afford isolated tetrasubstituted aniline derivatives **3.2**.

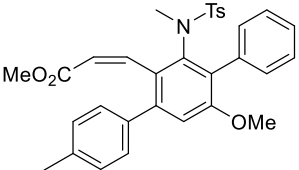
Methyl (Z)-3-(3'-((N,4-dimethylphenyl)sulfonamido)-5'-methoxy-[1,1':4',1''-terphenyl]-2'-yl)acrylate (3.3a)

	<p>Yield = 98%, 124.1 mg (0.2 mmol). Yellow solid. mp = 204.0-210.2 °C. R_f (SiO₂) = 0.2 (Hexane : Ethyl acetate, 8:2). HRMS (ESI): (m/z) calculated for C₃₁H₃₀NO₅S [M+H]⁺: 528.1839; found: 528.1836.</p>
---	--

¹H-NMR (300 MHz, CDCl₃, 25 °C, TMS): δ (ppm) = 7.50 – 7.19 (m, 11H), 7.15 (d, *J* = 8.3 Hz, 2H), 7.07 (d, *J* = 8.2 Hz, 2H), 6.95 (s, 1H), 5.81 (d, *J* = 11.8 Hz, 1H), 3.74 (s, 3H), 3.46 (s, 3H), 2.96 (s, 3H), 2.40 (s, 3H).

¹³C-NMR (75 MHz, CDCl₃, 25 °C): δ (ppm) = 165.8 (s), 157.1 (s), 142.9 (s), 142.4 (s), 141.1 (s), 138.4 (s), 136.9 (s), 135.3 (s), 131.5 (s), 129.9 (d), 129.3 (d), 129.2 (s), 127.9 (d), 127.9 (d), 127.6 (d), 127.3 (d), 127.2 (d), 123.4 (d), 113.0 (d), 56.1 (q), 51.1 (q), 39.0 (q), 21.6 (q).

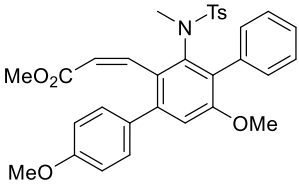
Methyl (Z)-3-(3'-((N,4-dimethylphenyl)sulfonamido)-5'-methoxy-4-methyl-[1,1':4',1''-terphenyl]-2'-yl)acrylate (3.3b)

	<p>Yield = 85%, 138.3 mg (0.3 mmol). White solid. mp = 366.0-374.1 °C. R_f (SiO₂) = 0.2 (Hexane : Ethyl acetate, 8:2). HRMS (ESI): (m/z) calculated for C₃₂H₃₂NO₅S [M+H]⁺: 542.1996; found: 542.2014.</p>
---	---

¹H-NMR (300 MHz, CDCl₃, 25 °C, TMS): δ (ppm) = 7.43 – 7.11 (m, 12H), 7.07 (d, *J* = 8.1 Hz, 2H), 6.93 (s, 1H), 5.81 (d, *J* = 11.7 Hz, 1H), 3.73 (s, 3H), 3.47 (s, 3H), 2.96 (s, 3H), 2.41 (s, 3H), 2.40 (s, 3H).

¹³C-NMR (75 MHz, CDCl₃, 25 °C): δ (ppm) = 165.8 (s), 157.0 (s), 142.9 (s), 143.4 (s), 142.3 (s), 138.3 (s), 138.2 (s), 137.0 (s), 135.3 (s), 131.3 (s), 129.7 (d), 129.3 (d), 129.2 (s), 128.6 (d), 127.9 (d), 127.6 (d), 127.1 (d), 123.3 (d), 113.0 (d), 56.0 (q), 51.1 (q), 39.0 (q), 21.6 (q), 21.3 (q).

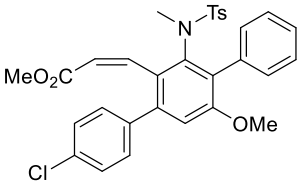
Methyl (Z)-3-(3'-((N,4-dimethylphenyl)sulfonamido)-4,5'-dimethoxy-[1,1':4',1''-terphenyl]-2'-yl)acrylate (3.3c)

	<p>Yield = 59%, 95.5 mg (0.2 mmol). Yellow solid. mp = 275.6-283.1 °C. R_f (SiO₂) = 0.1 (Hexane : Ethyl acetate, 8:2). HRMS (ESI): (m/z) calculated for C₃₂H₃₂NO₆S [M+H]⁺: 558.1945; found: 558.1934.</p>
---	--

¹H-NMR (300 MHz, CDCl₃, 25 °C, TMS): δ (ppm) = 7.37 – 7.19 (m, 8H), 7.12 (d, *J* = 8.4 Hz, 2H), 7.04 (d, *J* = 8.2 Hz, 2H), 6.90 (d, *J* = 2.7 Hz, 2H), 6.87 (s, 1H), 5.79 (d, *J* = 11.7 Hz, 1H), 3.84 (s, 3H), 3.71 (s, 3H), 3.44 (s, 3H), 2.92 (s, 3H), 2.37 (s, 3H).

¹³C-NMR (75 MHz, CDCl₃, 25 °C): δ (ppm) = 165.8 (s), 158.9 (s), 157.1 (s), 144.0 (s), 142.9 (s), 142.1 (s), 138.4 (s), 136.9 (s), 135.4 (s), 133.5 (s), 131.2 (s), 130.9 (d), 129.3 (d), 127.9 (d), 127.6 (d), 127.1 (d), 123.2 (d), 113.3 (d), 113.0 (d), 56.0 (q), 55.4 (q), 51.1 (q), 39.0 (q), 21.6 (q).

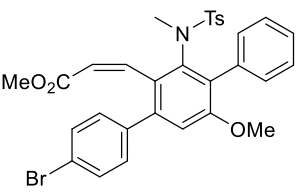
Methyl (Z)-3-(4-chloro-3'-((N,4-dimethylphenyl)sulfonamido)-5'-methoxy-[1,1':4',1''-terphenyl]-2'-yl)acrylate (3.3d)

	<p>Yield = 59%, 139.1 mg (0.3 mmol). Yellowish solid. mp = 254.6-257.8 °C. R_f (SiO₂) = 0.3 (Hexane : Ethyl acetate, 8:2). HRMS (ESI): (m/z) calculated for C₃₁H₂₉ClNO₅S [M+H]⁺: 562.1449; found: 562.1449.</p>
---	--

¹H-NMR (300 MHz, CDCl₃, 25 °C, TMS): δ (ppm) = 7.42 – 7.11 (m, 10H), 7.10 (d, *J* = 8.4 Hz, 2H), 7.04 (d, *J* = 8.2 Hz, 2H), 6.87 (s, 1H), 5.82 (d, *J* = 11.8 Hz, 1H), 3.71 (s, 3H), 3.45 (s, 3H), 2.92 (s, 3H), 2.37 (s, 3H).

¹³C-NMR (75 MHz, CDCl₃, 25 °C): δ (ppm) = 165.7 (s), 157.2 (s), 143.0 (s), 141.2 (s), 139.5 (s), 138.6 (s), 136.8 (s), 135.1 (s), 133.4 (s), 131.9 (s), 131.2 (d), 129.3 (d), 129.1 (s), 128.1 (d), 127.9 (d), 127.6 (d), 127.2 (d), 123.6 (d), 112.8 (d), 56.1 (q), 51.2 (q), 39.0 (q), 21.6 (q).

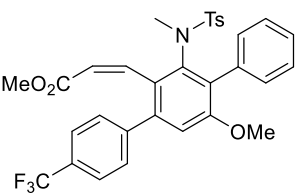
Methyl (Z)-3-(4-bromo-3'-((N,4-dimethylphenyl)sulfonamido)-5'-methoxy-[1,1':4',1''-terphenyl]-2'-yl)acrylate (3.3e)

	<p>Yield = 96%, 174.7 mg (0.3 mmol). Yellow solid. mp = 254.7-260.5 °C. R_f (SiO₂) = 0.3 (Hexane : Ethyl acetate, 8:2). HRMS (ESI): (m/z) calculated for C₃₁H₂₉BrNO₅S [M+H]⁺: 606.0944; found: 606.0944.</p>
---	---

¹H-NMR (300 MHz, CDCl₃, 25 °C, TMS): δ (ppm) = 7.51 (d, *J* = 8.4 Hz, 2H), 7.44 – 7.18 (m, 8H), 7.13 (d, *J* = 8.4 Hz, 2H), 7.07 (d, *J* = 8.4 Hz, 2H), 6.90 (s, 1H), 5.85 (d, *J* = 11.7 Hz, 1H), 3.74 (s, 3H), 3.48 (s, 3H), 2.95 (s, 3H), 2.39 (s, 3H).

¹³C-NMR (75 MHz, CDCl₃, 25 °C): δ (ppm) = 165.7 (s), 157.2 (s), 143.0 (s), 141.1 (s), 140.0 (s), 138.6 (s), 136.7 (s), 135.1 (s), 131.9 (s), 131.5 (d), 131.0 (d), 129.3 (d), 129.0 (s), 127.9 (d), 127.8 (d), 127.5 (d), 127.2 (d), 123.6 (d), 121.5 (d), 112.6 (d), 56.0 (q), 51.2 (q), 39.0 (q), 21.5 (q).

Methyl (Z)-3-(3'-((N,4-dimethylphenyl)sulfonamido)-5'-methoxy-4-(trifluoromethyl)-[1,1':4',1''-terphenyl]-2'-yl)acrylate (3.3f)

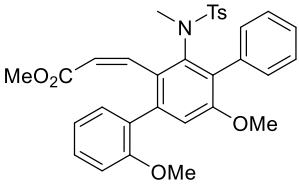
	<p>Yield = 87%, 196.8 mg (0.3 mmol). Yellow solid. mp = 295.2-299.9 °C. R_f (SiO₂) = 0.4 (Hexane : Ethyl acetate, 8:2). HRMS (ESI): (m/z) calculated for C₃₂H₂₉F₃NO₅S [M+H]⁺: 596.1713; found: 596.1716.</p>
---	--

¹H-NMR (300 MHz, CDCl₃, 25 °C, TMS): δ (ppm) = 7.62 (d, *J* = 8.1 Hz, 2H), 7.44 (d, *J* = 8.0 Hz, 2H), 7.41 – 7.15 (m, 6H), 7.11 (d, *J* = 8.4 Hz, 2H), 7.04 (d, *J* = 8.2 Hz, 2H), 6.89 (s, 1H), 5.82 (d, *J* = 11.8 Hz, 1H), 3.72 (s, 3H), 3.43 (s, 3H), 2.93 (s, 3H), 2.37 (s, 3H).

¹³C-NMR (75 MHz, CDCl₃, 25 °C): δ (ppm) = 165.7 (C), 157.3 (C), 144.7 (C), 143.1 (C), 141.0 (C), 138.7 (C), 136.7 (C), 135.0 (C), 132.3 (C), 130.2 (CH), 129.3 (CH), 129.1 (C), 128.0 (CH), 127.9 (q, *J* = 272 Hz, C), 127.6 (CH), 127.3 (CH), 124.8 (q, *J* = 3.8 Hz, CH), 123.9 (CH), 112.7 (CH), 56.1 (CH₃), 51.2 (CH₃), 39.0 (CH₃), 21.6 (CH₃).

¹⁹F-NMR (282 MHz, CDCl₃, 25 °C): δ (ppm) = -62.4.

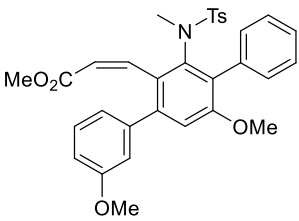
Methyl (Z)-3-(3'-((N,4-dimethylphenyl)sulfonamido)-2,5'-dimethoxy-[1,1':4',1''-terphenyl]-2'-yl)acrylate (3.3g)

	<p>Yield = 56%, 127.9 mg (0.2 mmol). Green oily solid. R_f (SiO₂) = 0.5 (Hexane : Ethyl acetate, 8:2). HRMS (ESI): (m/z) calculated for C₃₂H₃₂NO₆S [M+H]⁺: 558.1945; found: 558.1947.</p>
---	---

¹H-NMR (300 MHz, CDCl₃, 25 °C, TMS): δ (ppm) = 7.42 – 7.10 (m, 10H), 7.05 (d, *J* = 7.8 Hz, 2H), 6.97 (t, *J* = 7.3 Hz, 1H), 6.91 (q, *J* = 4.2 Hz, 2H), 5.64 (d, *J* = 11.7 Hz, 1H), 3.82 (s, 3H), 3.71 (s, 3H), 3.43 (s, 3H), 2.99 (s, 3H), 2.38 (s, 3H).

¹³C-NMR (75 MHz, CDCl₃, 25 °C): δ (ppm) = 166.0 (s), 157.0 (s), 155.8 (s), 143.3 (d), 142.7 (s), 138.5 (s), 137.7 (s), 137.2 (s), 135.4 (s), 131.6 (d), 131.2 (s), 130.6 (s), 129.8 (d), 129.2 (d), 129.2 (d), 127.8 (d), 127.5 (d), 127.0 (d), 121.2 (d), 120.2 (d), 113.2 (d), 110.7 (d), 56.0 (q), 55.4 (q), 51.2 (q), 39.0 (q), 21.6 (q).

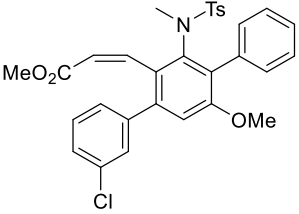
Methyl (Z)-3-(3'-((N,4-dimethylphenyl)sulfonamido)-3,5'-dimethoxy-[1,1':4',1''-terphenyl]-2'-yl)acrylate (3.3h)

	<p>Yield = 62%, 45.8 mg (0.08 mmol). Yellow solid. mp = 299.2-308.1 °C. R_f (SiO₂) = 0.4 (Hexane : Ethyl acetate, 8:2). HRMS (ESI): (m/z) calculated for C₃₂H₃₂NO₆S [M+H]⁺: 558.1945; found: 558.1947.</p>
---	---

¹H-NMR (300 MHz, CDCl₃, 25 °C, TMS): δ (ppm) = 7.44 – 7.17 (m, 7H), 7.11 (d, *J* = 8.1 Hz, 2H), 7.04 (d, *J* = 8.1 Hz, 2H), 6.95 – 6.80 (m, 4H), 5.80 (d, *J* = 11.7 Hz, 1H), 3.82 (s, 3H), 3.71 (s, 3H), 3.46 (s, 3H), 2.93 (s, 3H), 2.37 (s, 3H).

¹³C-NMR (75 MHz, CDCl₃, 25 °C): δ (ppm) = 165.9 (s), 159.2 (s), 157.1 (s), 142.9 (s), 142.5 (s), 142.1 (s), 138.4 (s), 136.9 (s), 135.3 (s), 131.6 (s), 129.3(d), 128.9 (d), 127.9 (d), 127.6 (d), 127.2 (d), 123.4 (d), 122.3 (d), 115.5 (d), 112.9 (d), 56.1 (q), 55.4 (q), 51.2 (q), 39.0 (q), 21.6 (q).

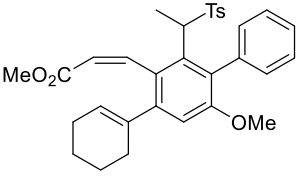
Methyl (Z)-3-(3-chloro-3'-((N,4-dimethylphenyl)sulfonamido)-5'-methoxy-[1,1':4',1''-terphenyl]-2'-yl)acrylate (3.3i)

	<p>Yield = 74%, 182.7 mg (0.3 mmol). Greenish solid. mp = 314.0-317.1 °C. R_f (SiO₂) = 0.4 (Hexane : Ethyl acetate, 200:1). HRMS (ESI): (m/z) calculated for C₃₁H₂₉ClNO₅S [M+H]⁺: 562.1449; found: 562.1450.</p>
---	---

¹H-NMR (300 MHz, CDCl₃, 25 °C, TMS): δ (ppm) = 7.41 – 7.22 (m, 8H), 7.18 (m, 2H), 7.10 (d, *J* = 8.4 Hz, 2H), 7.04 (d, *J* = 8.2 Hz, 2H), 6.87 (s, 1H), 5.82 (d, *J* = 11.8 Hz, 1H), 3.72 (s, 3H), 3.48 (s, 3H), 2.93 (s, 3H), 2.37 (s, 3H).

¹³C-NMR (75 MHz, CDCl₃, 25 °C): δ (ppm) = 165.8 (s), 157.2 (s), 143.0 (s), 142.8 (s), 140.9 (s), 138.6 (s), 136.8 (s), 135.1 (s), 133.7 (s), 132.1 (s), 129.9 (d), 129.3 (d), 129.2 (d), 129.1 (d), 128.5 (d), 128.4 (d), 128.2 (d), 127.9 (d), 127.6 (d), 127.3 (d), 127.2 (d), 123.8 (d), 112.7 (d), 56.1 (q), 51.3 (q), 39.0 (q), 21.6 (q).

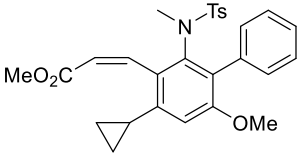
Methyl (Z)-3-(3'-((N,4-dimethylphenyl)sulfonamido)-5'-methoxy-2,3,4,5-tetrahydro-[1,1':4',1''-terphenyl]-2'-yl)acrylate (3.3j)

	<p>Yield = 97%, 299.1 mg (0.6 mmol). White solid. mp = 214.6-217.6 °C. R_f (SiO₂) = 0.6 (Hexane : Ethyl acetate, 8:2). HRMS (ESI): (m/z) calculated for C₃₁H₃₄NO₅S [M+H]⁺: 532.2152; found: 532.2160.</p>
---	--

¹H-NMR (300 MHz, CDCl₃, 25 °C, TMS): δ (ppm) = 7.42 – 7.20 (m, 6H), 7.10 (d, *J* = 8.3 Hz, 2H), 7.04 (d, *J* = 8.1 Hz, 2H), 6.78 (s, 1H), 6.02 (d, *J* = 11.6 Hz, 1H), 5.58 (s, 1H), 3.72 (s, 3H), 3.61 (s, 3H), 2.95 (s, 3H), 2.38 (s, 3H), 2.12 (s, 3H), 1.81 – 1.56 (m, 5H).

¹³C-NMR (75 MHz, CDCl₃, 25 °C): δ (ppm) = 166.5 (s), 157.0 (s), 144.9 (s), 143.5 (d), 142.8 (s), 138.7 (s), 137.9 (s), 137.0 (s), 135.6 (s), 130.7 (s), 129.3 (d), 128.7 (s), 128.1 (d), 127.8 (d), 127.6 (d), 127.0 (d), 122.6 (d), 111.7 (d), 56.0 (q), 51.3 (q), 38.9 (q), 29.7 (t), 25.7 (t), 23.1 (t), 22.1 (t), 21.6 (q).

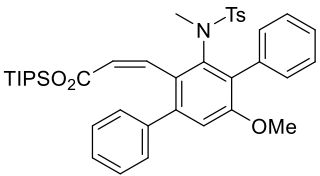
Methyl (Z)-3-(4-cyclopropyl-2-((N,4-dimethylphenyl)sulfonamido)-6-methoxy-[1,1'-biphenyl]-3-yl)acrylate (3.3k)

	<p>Yield = 70%, 278.7 mg (0.6 mmol). White solid. mp = 274.0-276.5 °C. R_f (SiO₂) = 0.5 (Hexane : Ethyl acetate, 8:2). HRMS (ESI): (m/z) calculated for C₂₉H₂₉NO₅S [M+H]⁺: 237.1485; found: 237.1491.</p>
---	--

¹H-NMR (300 MHz, CDCl₃, 25 °C, TMS): δ (ppm) = 7.38 (d, J = 11.8 Hz, 1H), 7.31 – 7.19 (m, 5H), 7.12 (d, J = 8.2 Hz, 2H), 7.05 (d, J = 8.2 Hz, 2H), 6.56 (s, 1H), 6.20 (d, J = 11.8 Hz, 1H), 3.69 (s, 3H), 3.66 (s, 3H), 2.95 (s, 3H), 2.39 (s, 3H), 1.92 (td, J = 8.5, 4.2 Hz, 1H), 1.02 – 0.84 (m, 2H), 0.81 – 0.62 (m, 1H).

¹³C-NMR (75 MHz, CDCl₃, 25 °C): δ (ppm) = 166.2 (s), 157.2 (s), 143.7 (d), 142.8 (s), 141.8 (s), 137.7 (s), 137.0 (s), 135.5 (s), 131.2 (s), 129.9 (s), 129.3 (d), 127.8 (d), 127.5 (d), 127.0 (d), 123.3 (d), 107.8 (d), 55.9 (q), 51.4 (q), 39.0 (q), 21.6 (q), 14.1 (d), 9.2 (t), 8.1 (t).

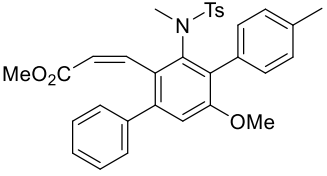
Tert-butyldimethylsilyl (Z)-3-(3'-((N,4-dimethylphenyl)sulfonamido)-5'-methoxy-[1,1':4',1''-terphenyl]-2'-yl)acrylate (3.2o)

	<p>Yield = 98%, 418.3 mg (0.6 mmol). Yellow solid. mp = 304.6-309.1 °C. R_f (SiO₂) = 0.5 (Hexane : Ethyl acetate, 8:2). HRMS (ESI): (m/z) calculated for C₃₉H₄₈NO₅SSi [M+H]⁺: 670.3017; found: 670.3023.</p>
---	---

¹H-NMR (300 MHz, CDCl₃, 25 °C, TMS): δ (ppm) = 7.45 – 7.19 (m, 10H), 7.12 (d, J = 8.1 Hz, 2H), 7.05 (d, J = 8.2 Hz, 2H), 6.95 (s, 1H), 5.88 (d, J = 11.8 Hz, 1H), 3.73 (s, 3H), 2.97 (s, 3H), 2.39 (s, 3H), 1.32 – 1.12 (m, 2H), 1.08 – 0.90 (m, 16H).

¹³C-NMR (75 MHz, CDCl₃, 25 °C): δ (ppm) = 164.4 (s), 156.9 (s), 145.0 (d), 142.9 (s), 142.0 (s), 141.1 (s), 138.0 (s), 136.9 (s), 135.4 (s), 131.3 (s), 129.7 (d), 129.6 (s), 129.3 (d), 127.9 (d), 127.6 (d), 127.2 (d), 127.1 (d), 124.9 (d), 113.0 (d), 56.0 (q), 39.2 (q), 21.6 (q), 17.9 (q), 17.9 (q), 12.0 (d).

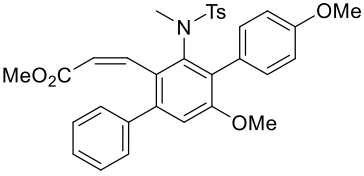
Methyl (Z)-3-(3'-((N,4-dimethylphenyl)sulfonamido)-5'-methoxy-4''-methyl-[1,1':4',1''-terphenyl]-2'-yl)acrylate (3.2p)

	<p>Yield = 92%, 119.7 mg (0.2 mmol). Greenish solid. mp = 344.7-347.1 °C. R_f (SiO₂) = 0.3(Hexane : Ethyl acetate, 8:2). HRMS (ESI): (m/z) calculated for C₃₂H₃₂NO₅S [M+H]⁺: 542.1996; found: 542.2002.</p>
---	--

¹H-NMR (300 MHz, CDCl₃, 25 °C, TMS): δ (ppm) = 7.49 – 7.25 (m, 8H), 7.17 (d, *J* = 8.3 Hz, 2H), 7.06 (d, *J* = 7.7 Hz, 4H), 6.94 (s, 1H), 5.83 (d, *J* = 11.8 Hz, 1H), 3.75 (s, 3H), 3.46 (s, 3H), 3.01 (s, 3H), 2.41 (s, 3H), 2.40 (s, 3H)

¹³C-NMR (75 MHz, CDCl₃, 25 °C): δ (ppm) = 165.8 (s), 157.2 (s), 142.7 (s), 142.2 (s), 141.1 (s), 138.6 (s), 137.2 (s), 136.7 (s), 132.1 (s), 131.4 (s), 129.9 (d), 129.1 (s), 128.6 (d), 127.8 (d), 127.5 (d), 127.2 (d), 123.4 (d), 112.9 (d), 56.0 (q), 51.1 (q), 39.2 (q), 21.6 (q), 21.5 (q).

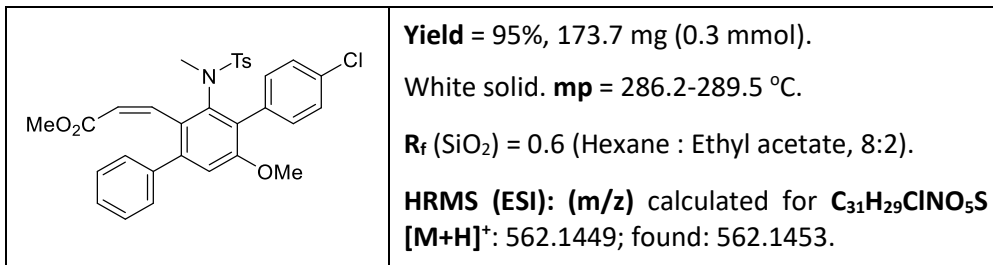
Methyl (Z)-3-(3'-((N,4-dimethylphenyl)sulfonamido)-4''-5'-dimethoxy-[1,1':4',1''-terphenyl]-2'-yl)acrylate (3.2q)

	<p>Yield = 61%, 108.9 mg (0.2 mmol). Yellowish solid. mp = 318.8-320.1 °C. R_f (SiO₂) = 0.1 (Hexane : Ethyl acetate, 8:2). HRMS (ESI): (m/z) calculated for C₃₂H₃₂NO₆S [M+H]⁺: 558.1945; found: 558.1938.</p>
---	--

¹H-NMR (300 MHz, CDCl₃, 25 °C, TMS): δ (ppm) = 7.41 – 7.27 (m, 6H), 7.22 – 6.99 (m, 2H), 7.17 (d, *J* = 8.3 Hz, 2H), 7.06 (d, *J* = 8.1 Hz, 2H), 6.92 (s, 1H), 6.76 (d, *J* = 8.3 Hz, 2H), 5.81 (d, *J* = 11.8 Hz, 1H), 3.82 (s, 3H), 3.73 (s, 3H), 3.43 (s, 3H), 3.00 (s, 3H), 2.38 (s, 3H).

¹³C-NMR (75 MHz, CDCl₃, 25 °C): δ (ppm) = 165.8 (s), 158.8 (s), 157.2 (s), 142.7 (s), 143.7 (s), 142.1 (s), 141.0 (s), 138.8 (s), 137.1 (s), 130.9 (s), 129.8 (d), 129.1 (d), 127.8 (d), 127.4 (d), 127.2 (d), 127.1 (s), 123.3 (d), 113.3 (d), 112.9 (d), 56.0 (q), 55.1 (q), 51.1 (q), 39.1 (q), 21.5 (q).

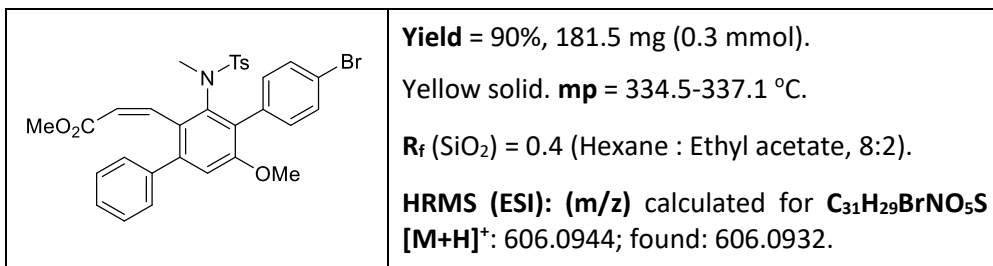
Methyl (Z)-3-(4''-chloro-3'-((N,4-dimethylphenyl)sulfonamido)-5'-methoxy-[1,1':4',1''-terphenyl]-2'-yl)acrylate (3.2r)



¹H-NMR (300 MHz, CDCl₃, 25 °C, TMS): δ (ppm) = 7.57 – 7.02 (m, 14H), 6.94 (d, *J* = 3.6 Hz, 1H), 5.86 (d, *J* = 11.5 Hz, 1H), 3.74 (s, 3H), 3.45 (s, 3H), 3.06 (s, 3H), 2.45 (s, 3H).

¹³C-NMR (75 MHz, CDCl₃, 25 °C): δ (ppm) = 165.8 (s), 165.7 (s), 156.8 (s), 143.1 (s), 142.8 (s), 140.8 (s), 138.6 (s), 137.1 (s), 133.4 (s), 133.4 (s), 129.8 (s), 129.3 (d), 128.0 (d), 127.9 (d), 127.3 (d), 127.0 (d), 123.6 (d), 112.9 (d), 56.0 (q), 51.2 (q), 39.4 (q), 21.6 (q).

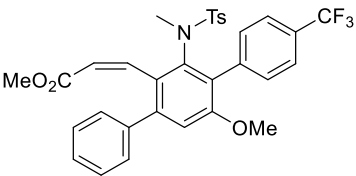
Methyl (Z)-3-(4''-bromo-3'-((N,4-dimethylphenyl)sulfonamido)-5'-methoxy-[1,1':4',1''-terphenyl]-2'-yl)acrylate (3.2s)



¹H-NMR (300 MHz, CDCl₃, 25 °C, TMS): δ (ppm) = 7.32 (m, 10H), 7.14 (t, *J* = 6.5 Hz, 4H), 6.91 (s, 1H), 5.84 (d, *J* = 11.7 Hz, 1H), 3.71 (s, 3H), 3.43 (s, 3H), 3.03 (s, 3H), 2.44 (s, 3H).

¹³C-NMR (75 MHz, CDCl₃, 25 °C): δ (ppm) = 165.8 (s), 156.8 (s), 143.2 (s), 142.9 (s), 140.9 (s), 138.6 (s), 137.1 (s), 134.0 (s), 130.9 (d), 129.9 (s), 129.8 (d), 129.4 (s), 129.4 (d), 127.9 (d), 127.3 (d), 127.0 (d), 123.7 (d), 121.7 (s), 113.0 (s), 56.0 (q), 51.2 (q), 39.4 (q), 21.7 (q).

Methyl (Z)-3-(3'-((N,4-dimethylphenyl)sulfonamido)-5'-methoxy-4''-(trifluoromethyl)-[1,1':4',1''-terphenyl]-2'-yl)acrylate (3.2t)

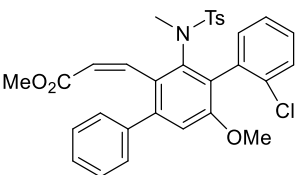
	<p>Yield = 86%, 230.5 mg (0.4 mmol). Greenish solid. mp = 304.5-309.2 °C. R_f (SiO₂) = 0.4 (Hexane : Ethyl acetate, 8:2). HRMS (ESI): (m/z) calculated for C₃₂H₂₉F₃NO₅S [M+H]⁺: 596.1713; found: 596.1716.</p>
---	--

¹H-NMR (300 MHz, CDCl₃, 25 °C, TMS): δ (ppm) = 7.48 – 7.28 (m, 10H), 7.12 (d, *J* = 8.4 Hz, 2H), 7.03 (d, *J* = 8.2 Hz, 2H), 6.94 (s, 1H), 5.86 (d, *J* = 11.7 Hz, 1H), 3.71 (s, 3H), 3.44 (s, 3H), 3.03 (s, 3H), 2.36 (s, 3H).

¹³C-NMR (75 MHz, CDCl₃, 25 °C): δ (ppm) = 165.8 (C), 156.7 (C), 143.3 (C), 143.2 (C), 140.8 (C), 139.1 (q, *J* = Hz, C), 138.5 (C), 136.9 (C), 129.8 (CH), 129.7 (C), 129.5 (C), 129.3 (CH), 128.9 (C), 127.9 (CH), 127.4 (CH), 127.0 (CH), 124.6 (q, *J* = 3.8 Hz, C), 124.4 (q, *J* = 272 Hz, C), 127.7 (CH), 113.0 (CH), 56.0 (CH₃), 51.2 (CH₃), 39.4 (CH₃), 21.4 (CH₃).

¹⁹F-NMR (282 MHz, CDCl₃, 25 °C): δ (ppm) = -62.3.

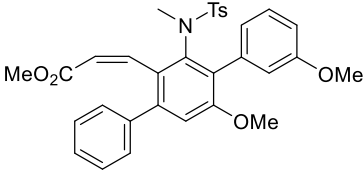
Methyl (Z)-3-(2''-chloro-3'-((N,4-dimethylphenyl)sulfonamido)-5'-methoxy-[1,1':4',1''-terphenyl]-2'-yl)acrylate (3.2u)

	<p>Yield = 68%, 187.1 mg (0.3 mmol). White solid. mp = 294.0-297.1 °C. R_f (SiO₂) = 0.3 (Hexane : Ethyl acetate, 8:2). HRMS (ESI): (m/z) calculated for C₃₁H₂₉ClNO₅S [M+H]⁺: 562.1449; found: 562.1450.</p>
---	--

¹H-NMR (300 MHz, CDCl₃, 25 °C, TMS): δ (ppm) = 7.42 (dd, *J* = 8.0, 1.2 Hz, 1H), 7.39 – 7.27 (m, 9H), 7.19 – 7.12 (m, 4H), 6.93 (s, 1H), 5.63 (d, *J* = 11.8 Hz, 1H), 3.74 (s, 3H), 3.44 (s, 3H), 2.85 (s, 3H), 2.40 (s, 3H).

¹³C-NMR (75 MHz, CDCl₃, 25 °C): δ (ppm) = 165.7 (s), 157.2 (s), 143.3 (s), 141.0 (s), 137.4 (s), 134.3 (s), 134.1 (s), 133.4 (s), 129.8 (d), 129.4 (d), 129.0 (d), 128.9 (d), 128.7 (s), 128.0 (d), 127.6 (d), 127.4 (d), 126.5 (d), 123.6 (s), 112.9 (d), 56.3 (q), 51.2 (q), 37.6 (q), 21.6 (q).

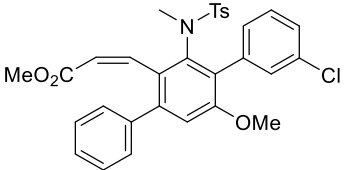
Methyl (Z)-3-(3'-((N,4-dimethylphenyl)sulfonamido)-3'',5'-dimethoxy-[1,1':4',1''-terphenyl]-2'-yl)acrylate (3.2v)

	<p>Yield = 80%, 200.6 mg (0.4 mmol). White solid. mp = 283.5-289.6 °C. R_f (SiO₂) = 0.3 (Hexane : Ethyl acetate, 8:2). HRMS (ESI): (m/z) calculated for C₃₂H₃₂NO₆S [M+H]⁺: 558.1945; found: 558.1938.</p>
---	---

¹H-NMR (300 MHz, CDCl₃, 25 °C, TMS): δ (ppm) = 7.35 (m, 8H), 7.17 (d, *J* = 7.8 Hz, 3H), 7.06 (d, *J* = 8.1 Hz, 2H), 6.92 (s, 1H), 6.83 (dd, *J* = 8.2, 2.5 Hz, 1H), 5.78 (d, *J* = 11.6 Hz, 1H), 3.73 (s, 6H), 3.43 (s, 3H), 2.98 (s, 3H), 2.37 (s, 3H).

¹³C-NMR (75 MHz, CDCl₃, 25 °C): δ (ppm) = 165.8 (s), 159.1 (s), 157.0 (s), 143.2 (d), 142.8 (s), 142.4 (s), 141.0 (s), 138.5 (s), 137.0 (s), 136.4 (s), 131.2 (s), 129.8 (d), 129.2 (d), 128.8 (d), 127.8 (d), 127.4 (d), 127.2 (d), 123.4 (d), 113.0 (d), 56.1 (q), 55.2 (q), 51.1 (q), 39.1 (q), 21.6 (q).

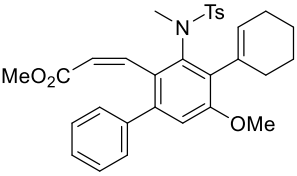
Methyl (Z)-3-(3''-chloro-3'-((N,4-dimethylphenyl)sulfonamido)-5'-methoxy-[1,1':4',1''-terphenyl]-2'-yl)acrylate (3.2w)

	<p>Yield = 98%, 187.1 mg (0.3 mmol). White solid. mp = 304.7-307.8 °C. R_f (SiO₂) = 0.3 (Hexane : Ethyl acetate, 8:2). HRMS (ESI): (m/z) calculated for C₃₁H₂₉ClNO₅S [M+H]⁺: 562.1449; found: 562.1450.</p>
---	---

¹H-NMR (300 MHz, CDCl₃, 25 °C, TMS): δ (ppm) = 7.43 – 7.27 (m, 5H), 7.24 – 7.03 (m, 6H), 6.92 (s, 1H), 5.80 (d, *J* = 11.8 Hz, 1H), 3.72 (s, 3H), 3.44 (s, 3H), 3.02 (s, 3H), 2.39 (s, 3H).

¹³C-NMR (75 MHz, CDCl₃, 25 °C): δ (ppm) = 165.8 (s), 156.9 (s), 143.1 (s), 142.9 (s), 140.9 (s), 138.6 (s), 137.1 (s), 137.0 (s), 133.6 (s), 129.9 (s), 129.8 (d), 129.4 (d), 129.3 (d), 129.0 (d), 127.9 (d), 127.4 (d), 127.3 (d), 127.1 (d), 123.6 (d), 113.0 (d), 56.1 (q), 51.2 (q), 39.4 (q), 21.6 (q).

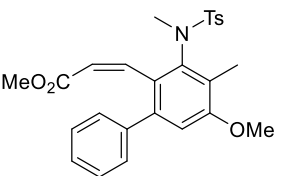
Methyl (Z)-3-(3'-((N,4-dimethylphenyl)sulfonamido)-5'-methoxy-2'',3'',4'',5''-tetrahydro-[1,1':4',1''-terphenyl]-2'-yl)acrylate (3.2x)

	<p>Yield = 63%, 123.5 mg (0.2 mmol)</p> <p>White solid. mp = 264.4-267.1 °C.</p> <p>R_f (SiO₂) = 0.4 (Hexane : Ethyl acetate, 8:2).</p> <p>HRMS (ESI): (m/z) calculated for C₃₁H₃₄NO₅S [M+H]⁺: 532.2152; found: 532.2160.</p>
---	---

¹H-NMR (300 MHz, CDCl₃, 25 °C, TMS): δ (ppm) = 7.78 (d, *J* = 7.9 Hz, 2H), 7.43 – 7.10 (m, 8H), 6.82 (s, 1H), 5.59 (s, 2H), 3.82 (s, 3H), 3.42 (s, 3H), 3.08 (s, 3H), 2.46 (s, 3H), 2.40 – 2.00 (m, 3H), 1.69 (s, 5H).

¹³C-NMR (75 MHz, CDCl₃, 25 °C): δ (ppm) = 165.7 (s), 157.2 (s), 143.1 (s), 141.2 (s), 138.3 (s), 129.8 (d), 129.5 (d), 127.8 (d), 127.5 (d), 127.1 (d), 122.9 (d), 112.6 (d), 56.0 (q), 51.1 (q), 29.8 (t), 29.0 (t), 22.9 (t), 21.9 (t), 21.6 (q).

Methyl (Z)-3-(3'-((N,4-dimethylphenyl)sulfonamido)-5-methoxy-4-methyl-[1,1'-biphenyl]-2-yl)acrylate (3.2y)

	<p>Yield = 66%, 98.5 mg (0.2 mmol).</p> <p>Yellow solid. mp = 227.0-228.5 °C.</p> <p>R_f (SiO₂) = 0.2 (Hexane : Ethyl acetate, 8:2).</p> <p>HRMS (ESI): (m/z) calculated for C₂₆H₂₈NO₅S [M+H]⁺: 466.1683; found: 466.1674.</p>
---	--

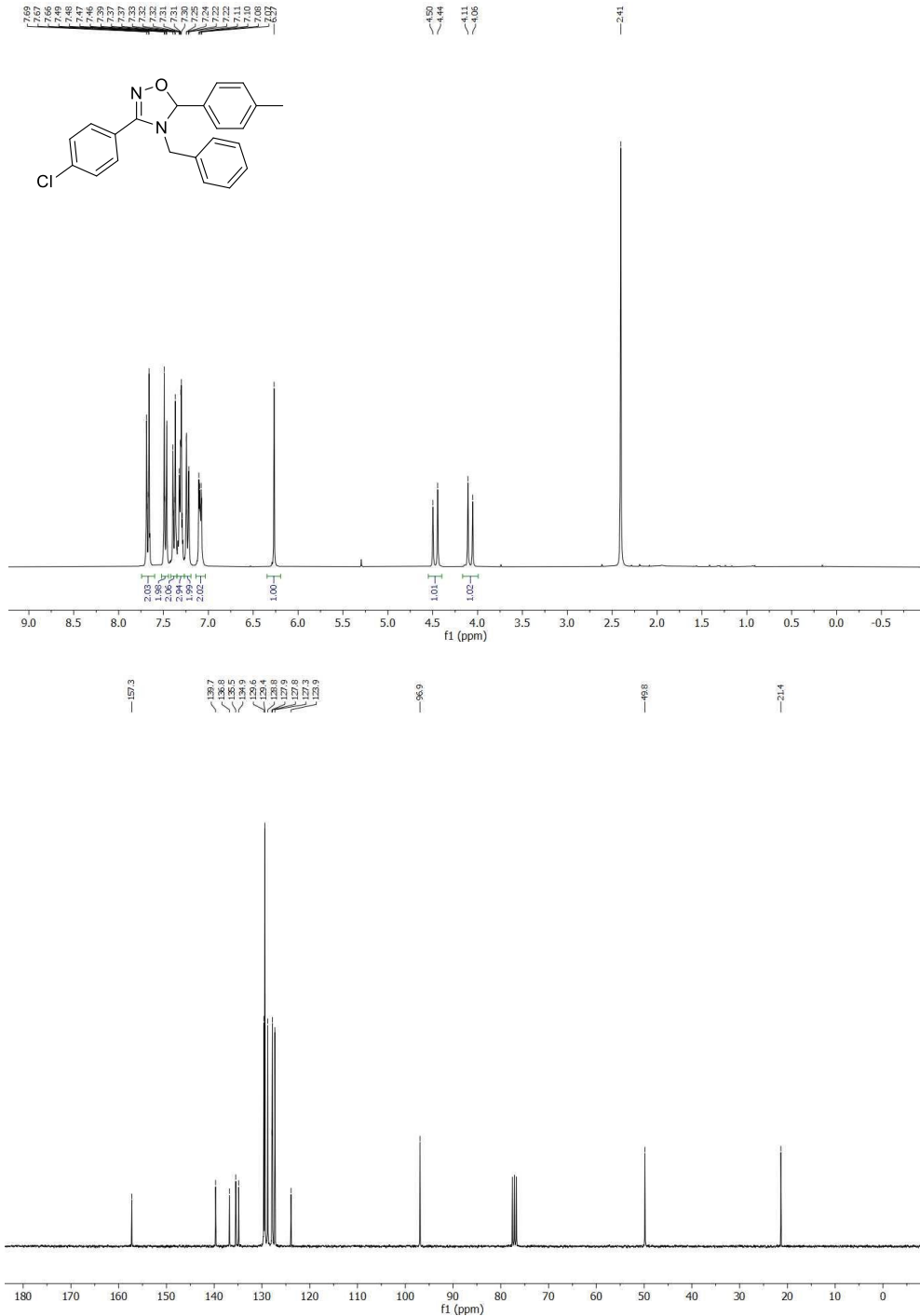
¹H-NMR (300 MHz, CDCl₃, 25 °C, TMS): δ (ppm) = 7.61 – 7.44 (m, 2H), 7.21 – 6.98 (m, 8H), 6.93 (d, *J* = 11.6 Hz, 1H), 6.58 (s, 1H), 5.54 (d, *J* = 11.8 Hz, 1H), 3.63 (s, 3H), 3.22 (s, 3H), 2.91 (s, 3H), 2.26 (s, 3H), 1.56 (s, 3H).

¹³C-NMR (75 MHz, CDCl₃, 25 °C): δ (ppm) = 165.8 (s), 157.8 (s), 143.4 (s), 141.2 (s), 139.9 (s), 138.0 (s), 129.7 (d), 127.8 (d), 127.3 (d), 127.1 (d), 126.0 (s), 122.7 (d), 111.7 (d), 55.6 (q), 51.0 (q), 37.7 (q), 21.7 (q), 11.8 (q).

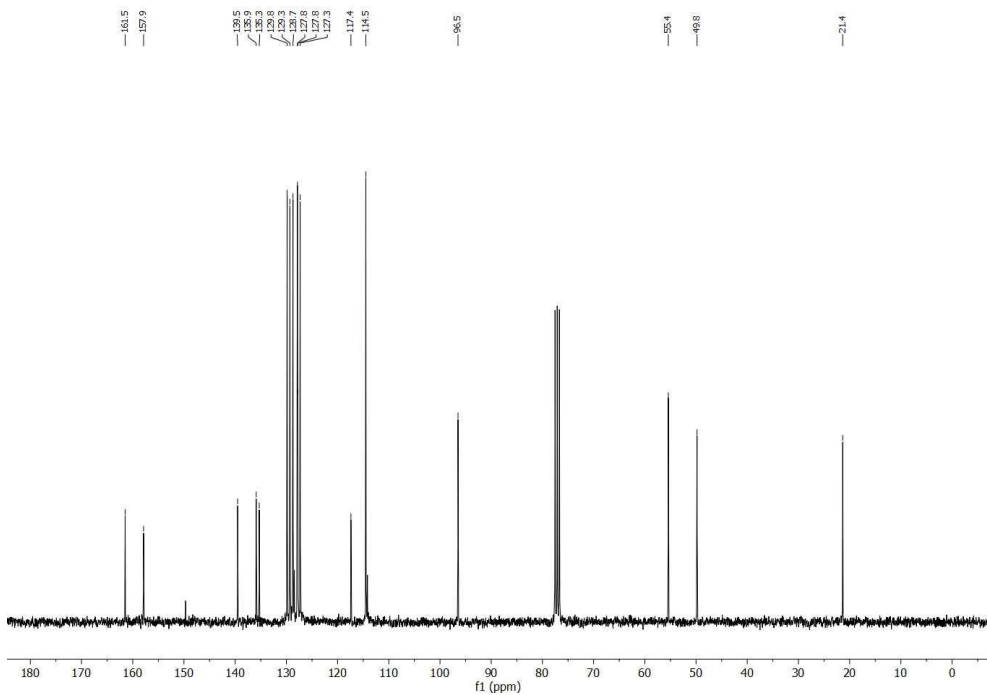
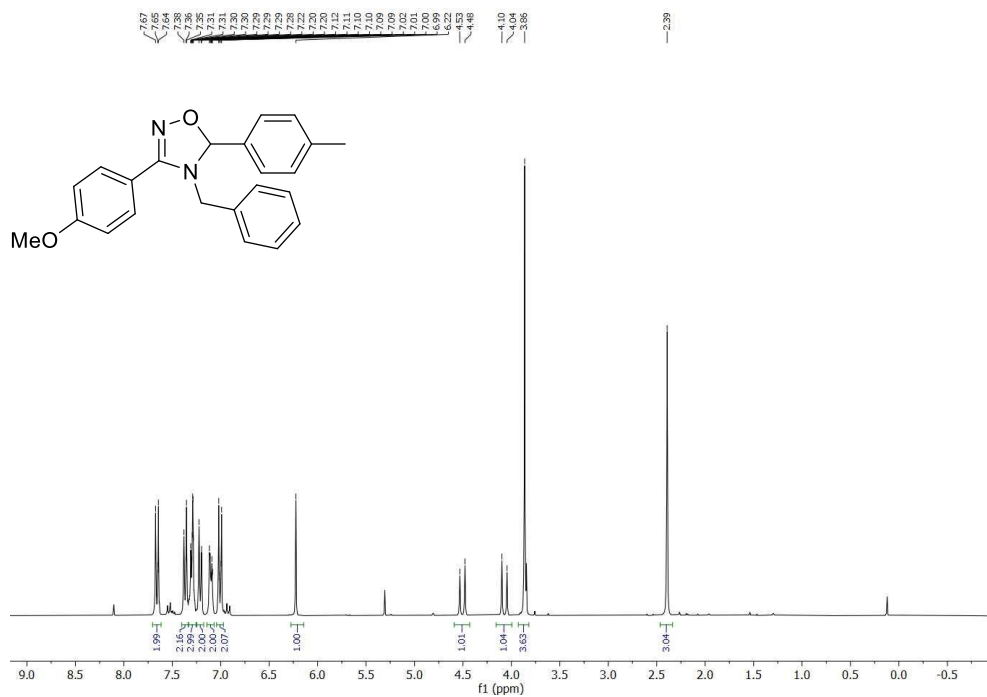
Annex I:
Nuclear Magnetic Resonance (NMR) spectra

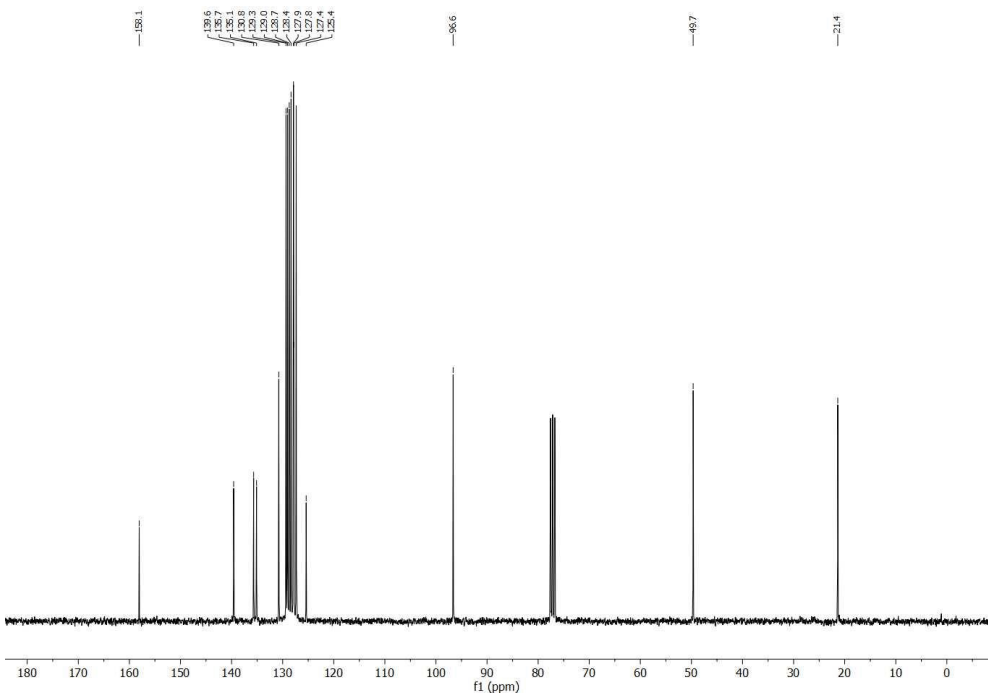
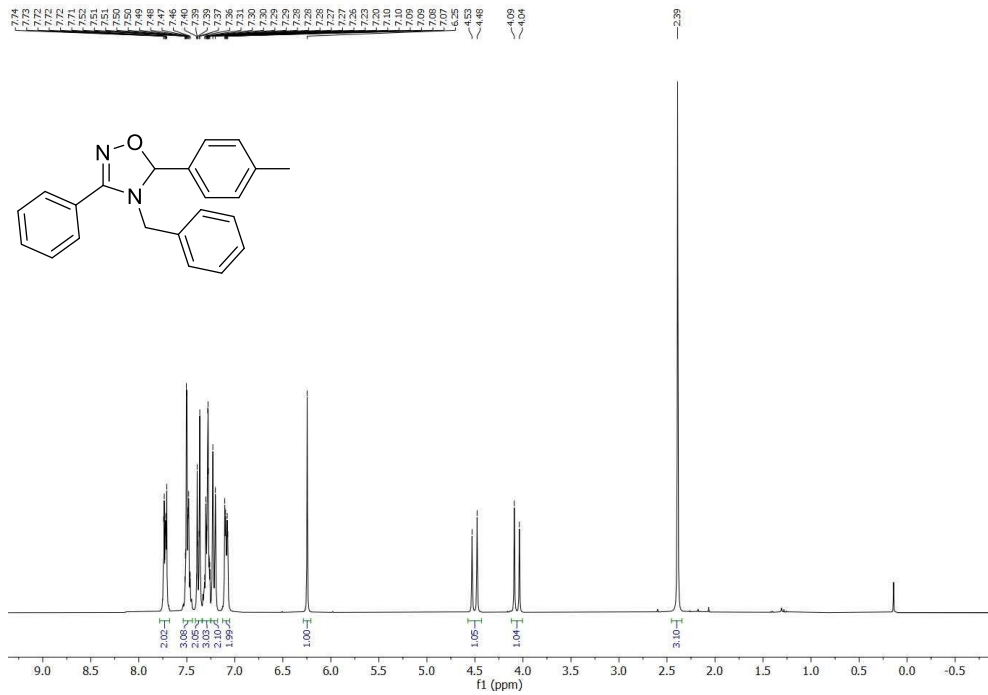
1 Chapter I

4-Benzyl-3-(4-chlorophenyl)-5-(*p*-tolyl)-4,5-dihydro-1,2,4-oxadiazole (1.3a)

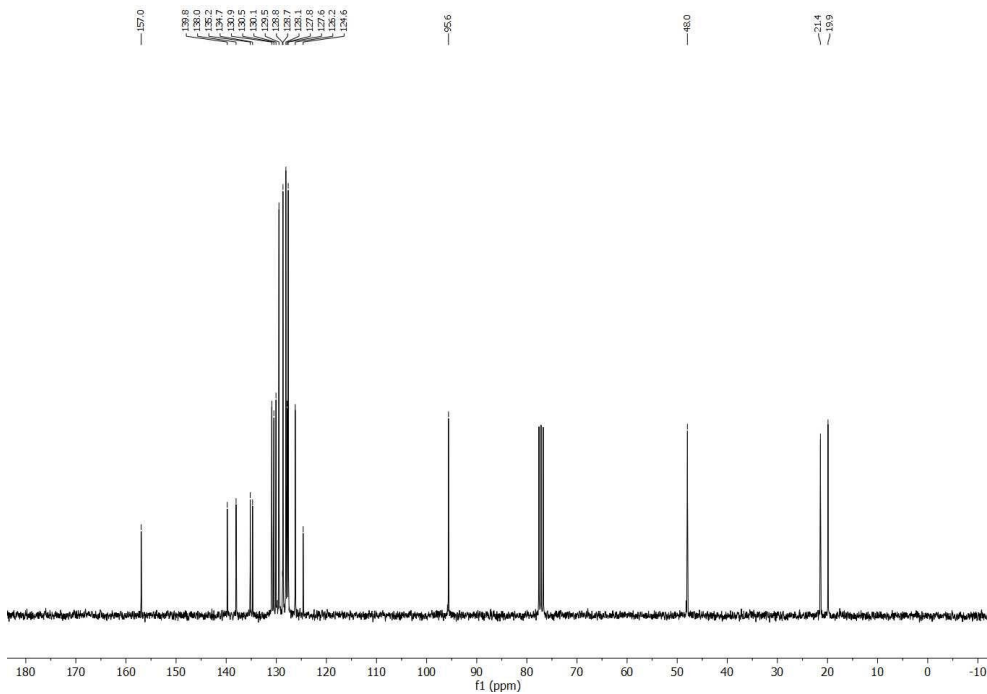
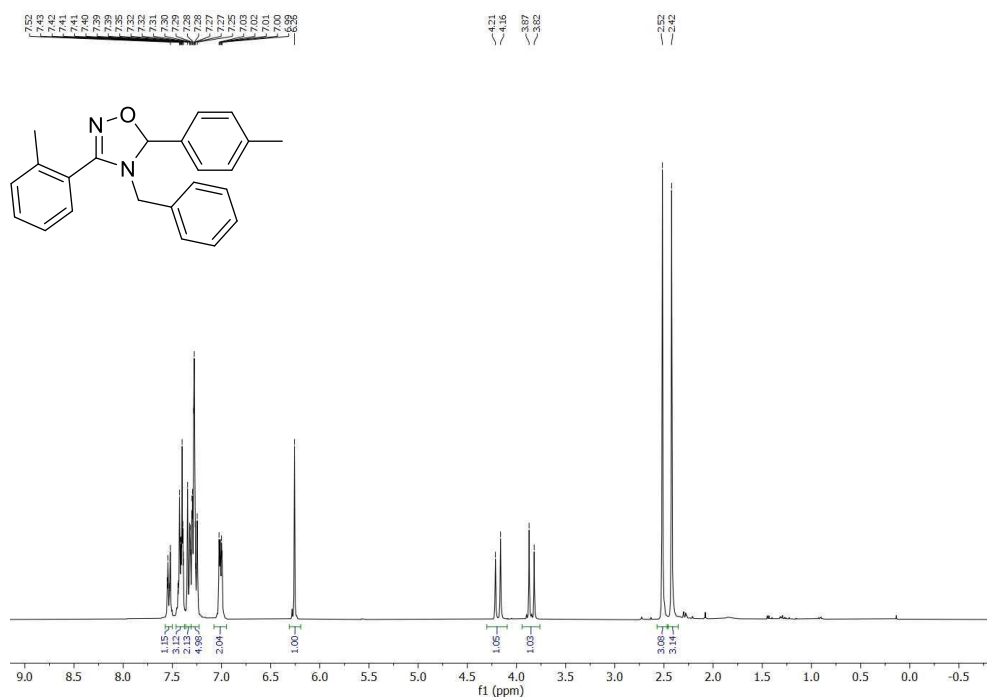


4-Benzyl-3-(4-methoxyphenyl)-5-(*p*-tolyl)-4,5-dihydro-1,2,4-oxadiazole (1.3b)

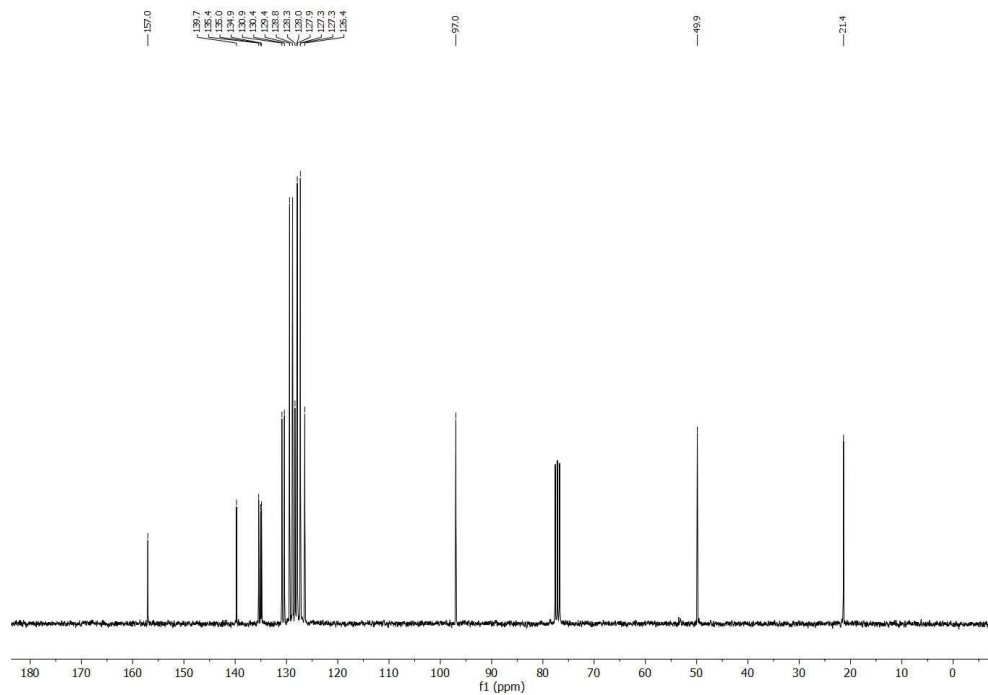
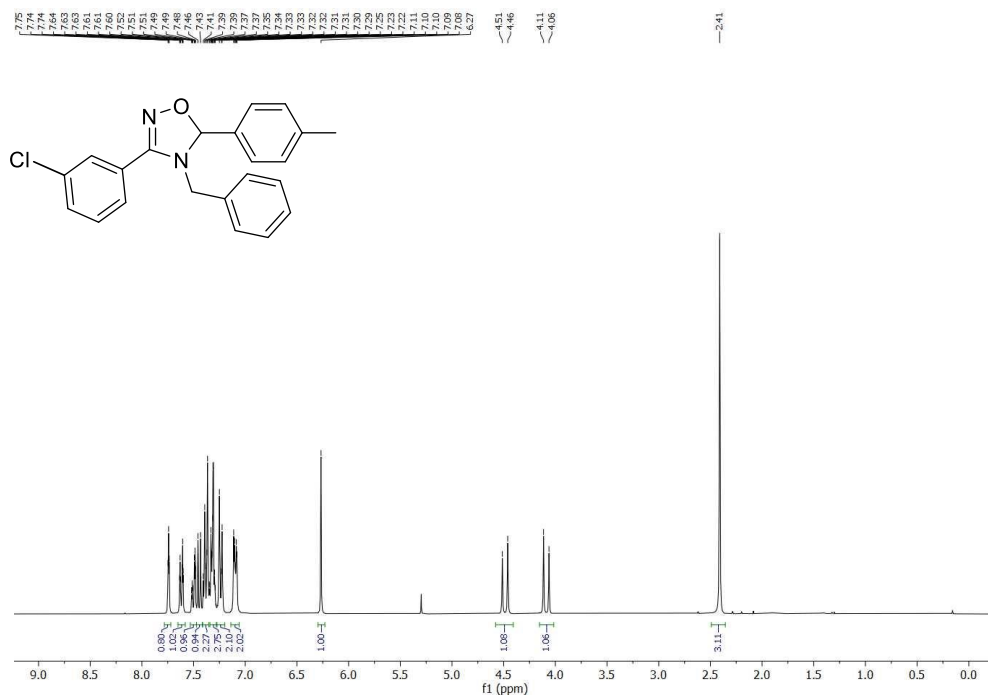


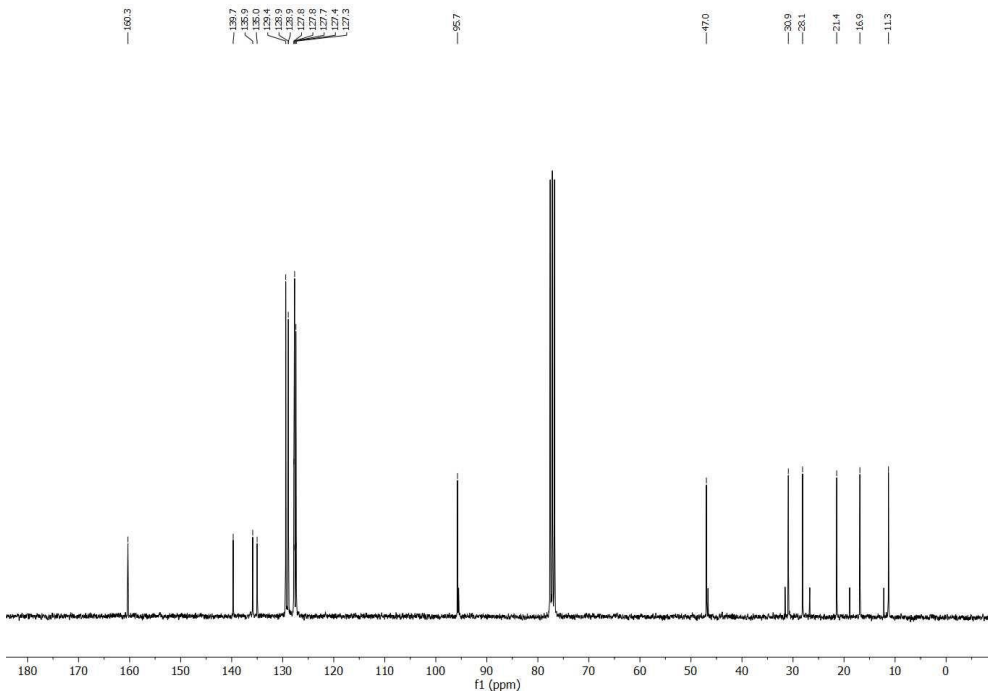
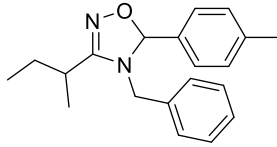
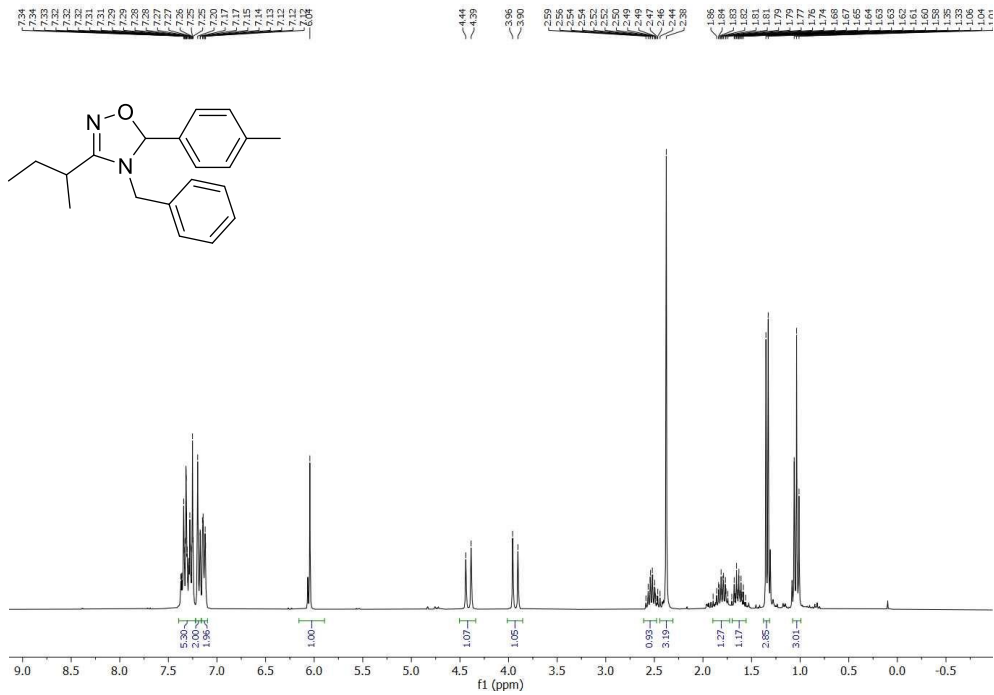
4-Benzyl-3-phenyl-5-(*p*-tolyl)-4,5-dihydro-1,2,4-oxadiazole (1.3c)

4-Benzyl-3-(*o*-tolyl)-5-(*p*-tolyl)-4,5-dihydro-1,2,4-oxadiazole (1.3d)

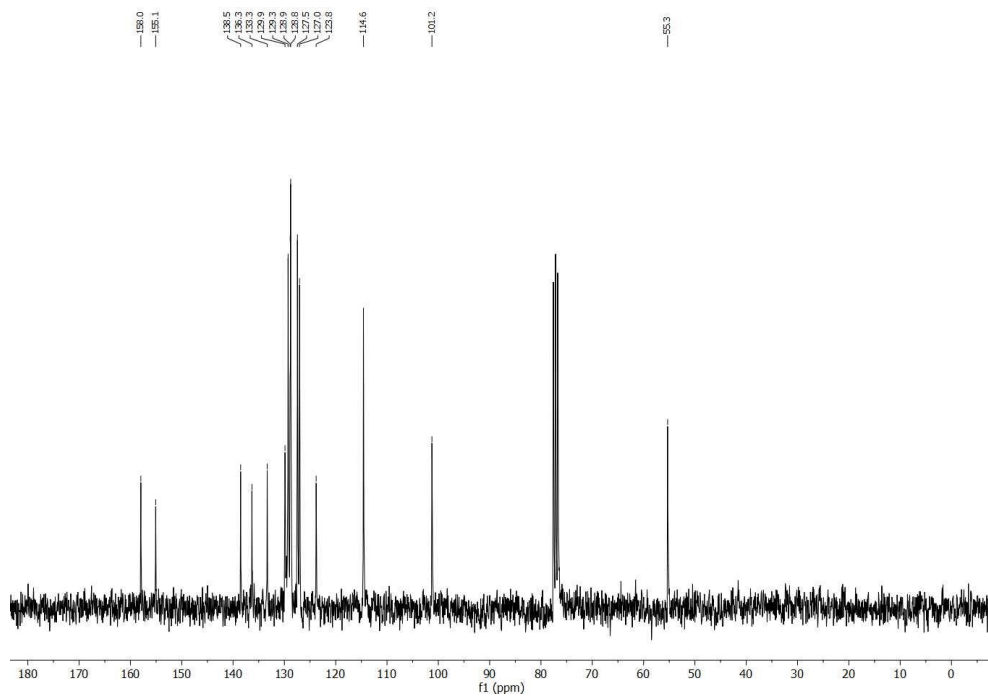
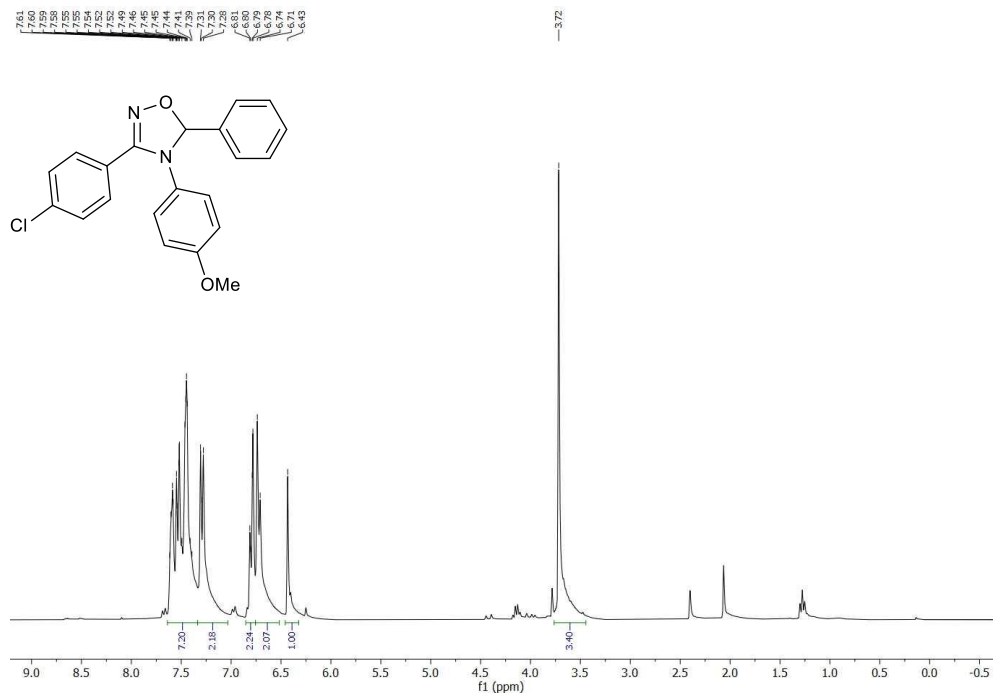


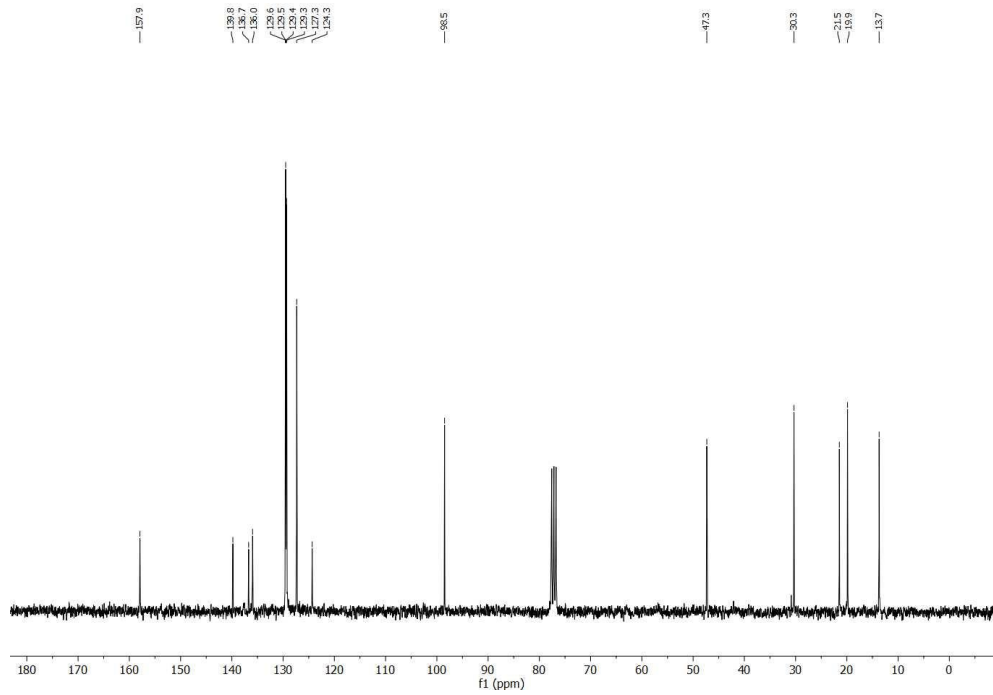
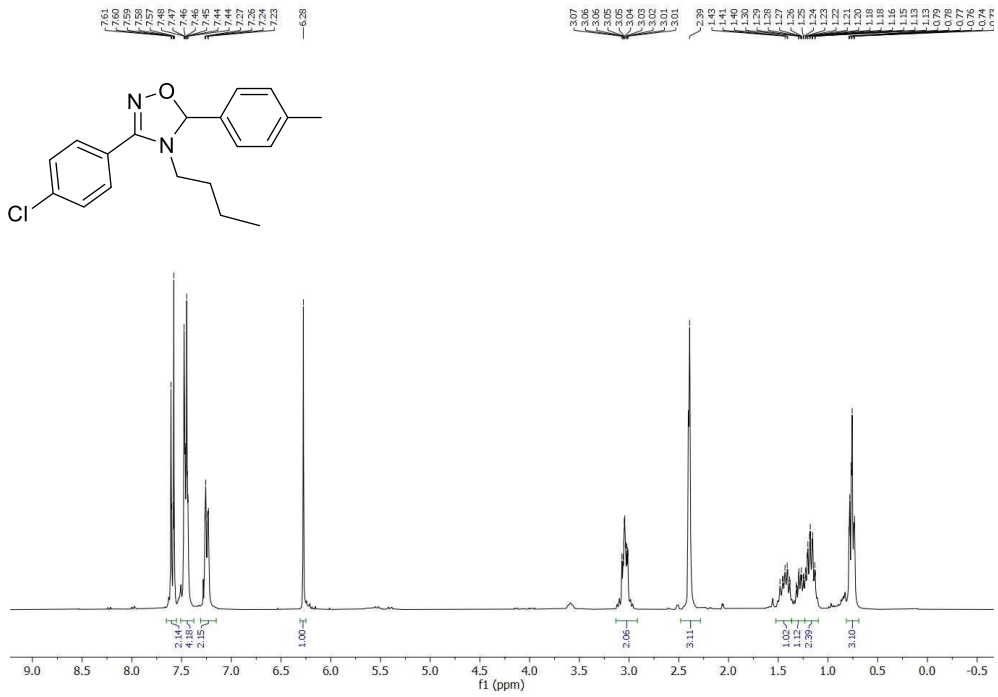
4-Benzyl-3-(3-chlorophenyl)-5-(*p*-tolyl)-4,5-dihydro-1,2,4-oxadiazole (1.3f)



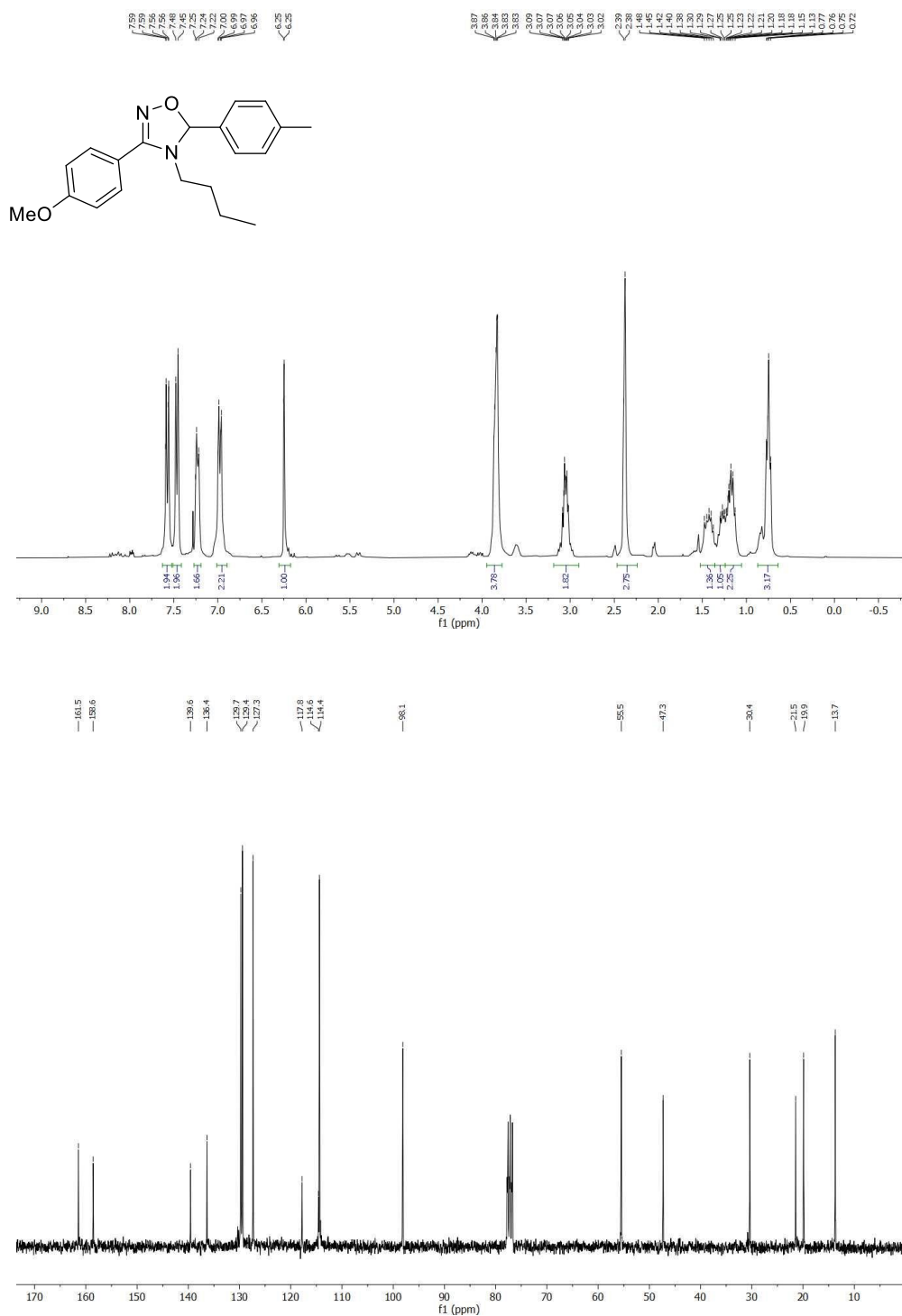
4-Benzyl-3-(*sec*-butyl)-5-(*p*-tolyl)-4,5-dihydro-1,2,4-oxadiazole (1.3g)

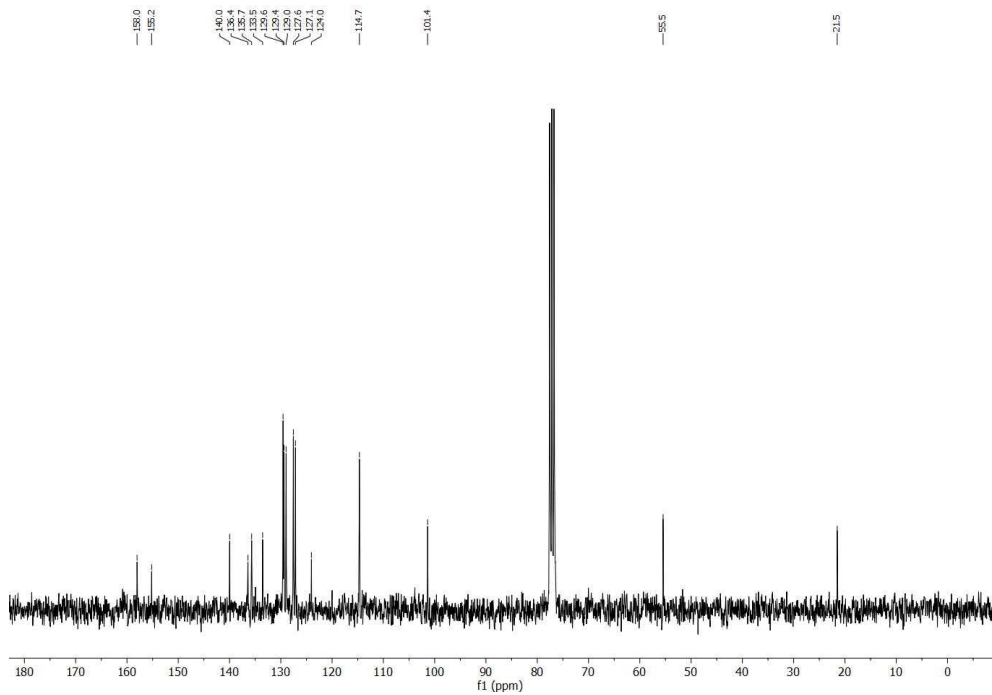
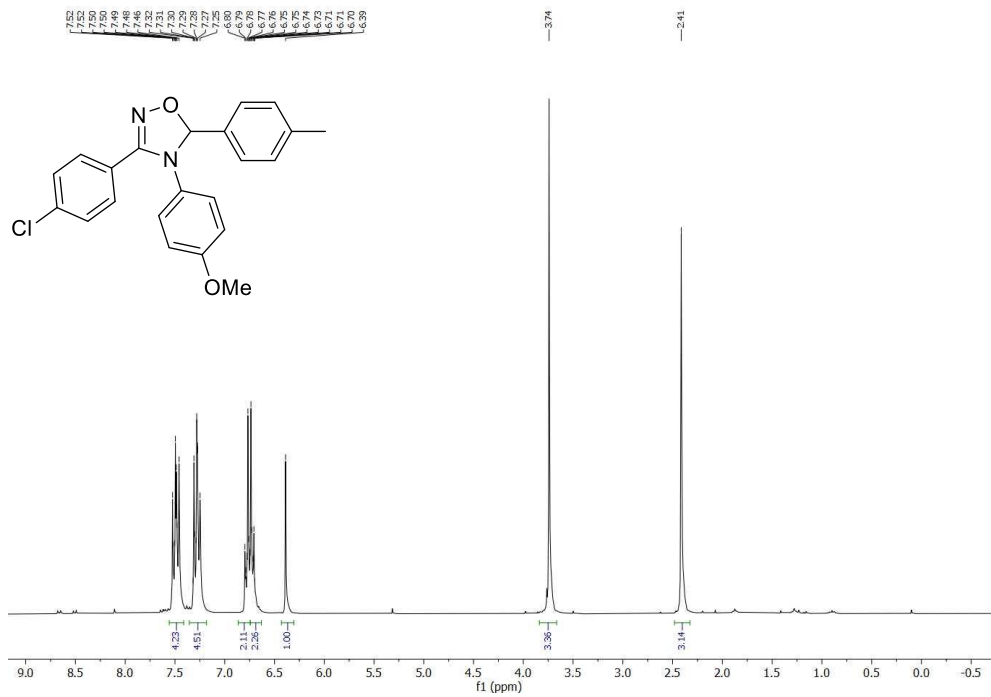
3-(4-Chlorophenyl)-4-(4-methoxyphenyl)-5-(*p*-phenyl)-4,5-dihydro-1,2,4-oxadiazole (1.3h)



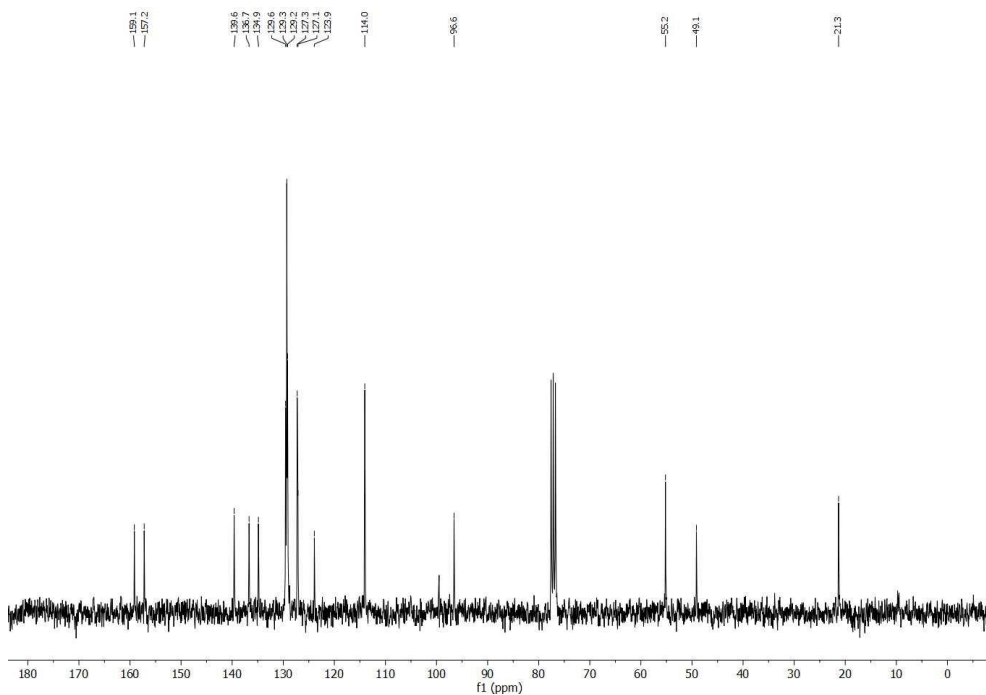
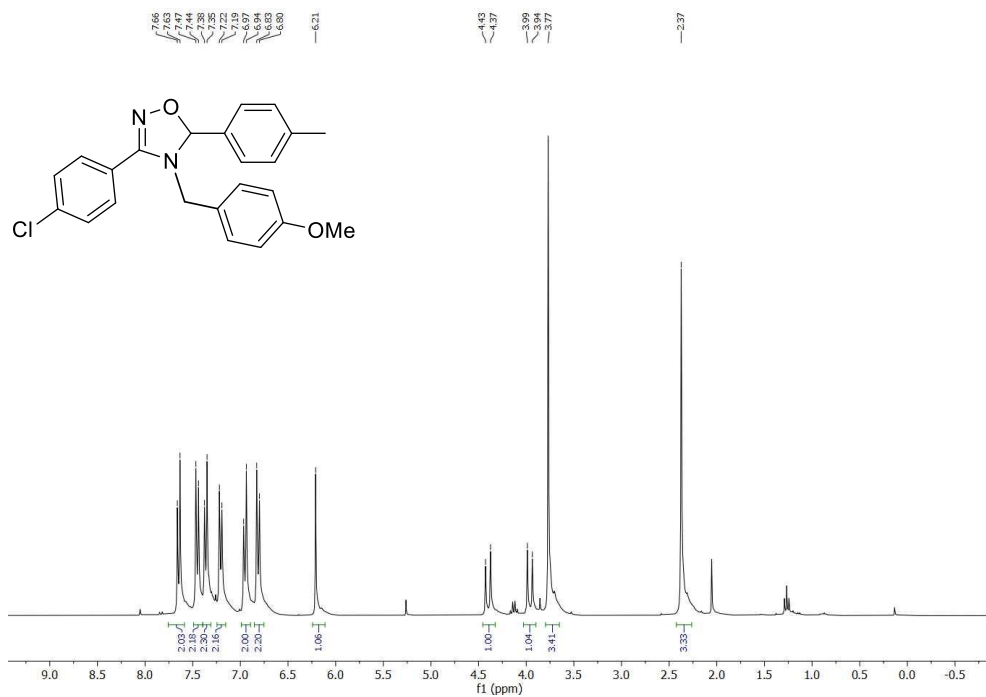
4-Butyl-3-(4-chlorophenyl)-5-(*p*-tolyl)-4,5-dihydro-1,2,4-oxadiazole (1.3j)

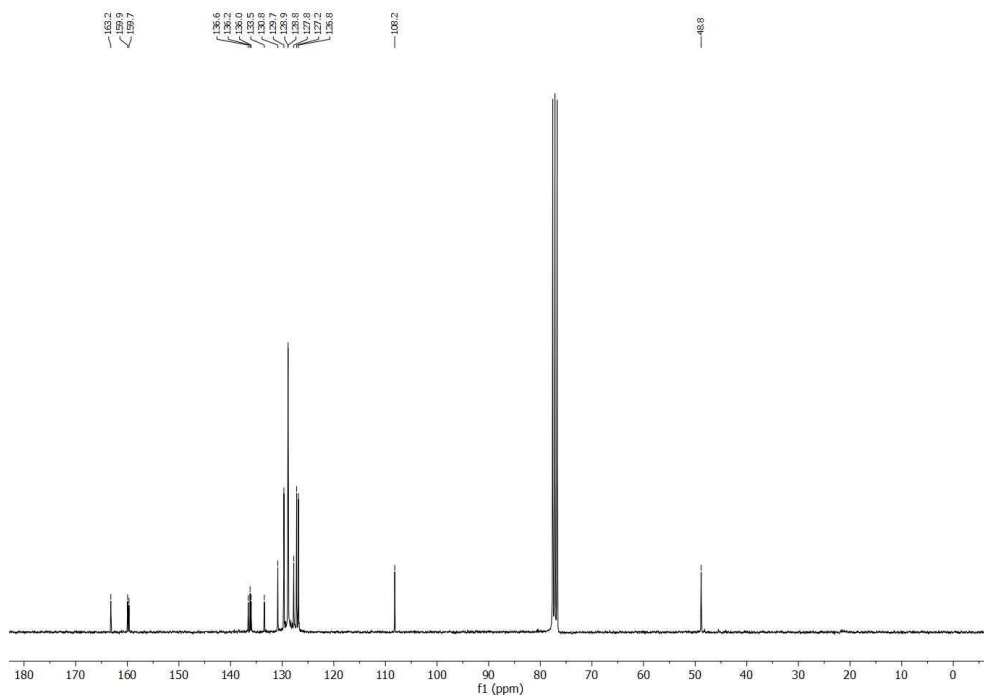
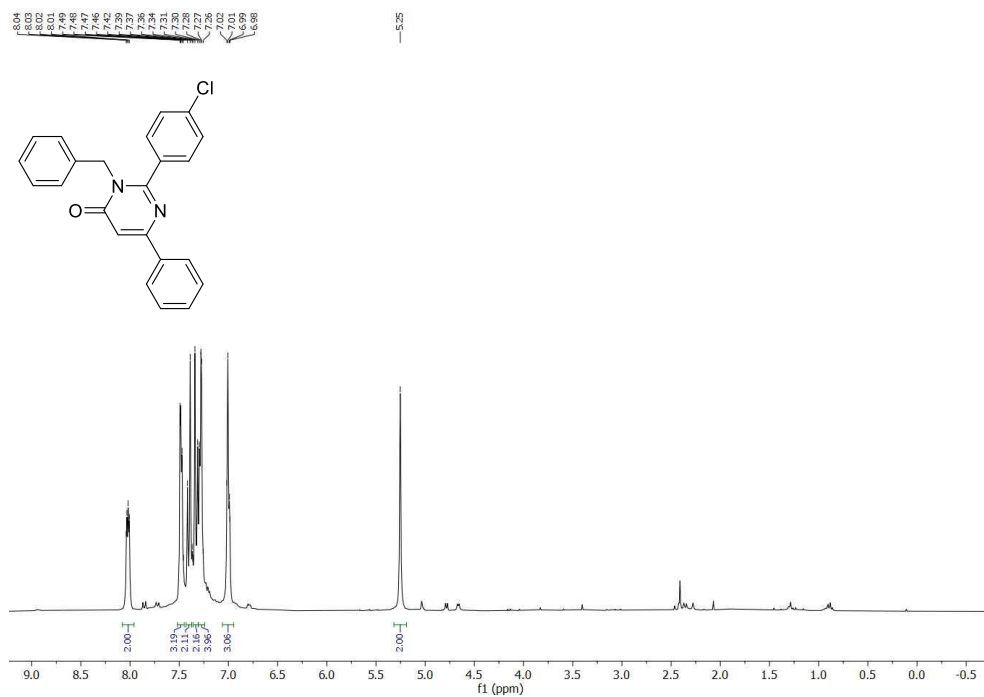
4-Butyl-3-(4-methoxyphenyl)-5-(*p*-tolyl)-4,5-dihydro-1,2,4-oxadiazole (1.3k)



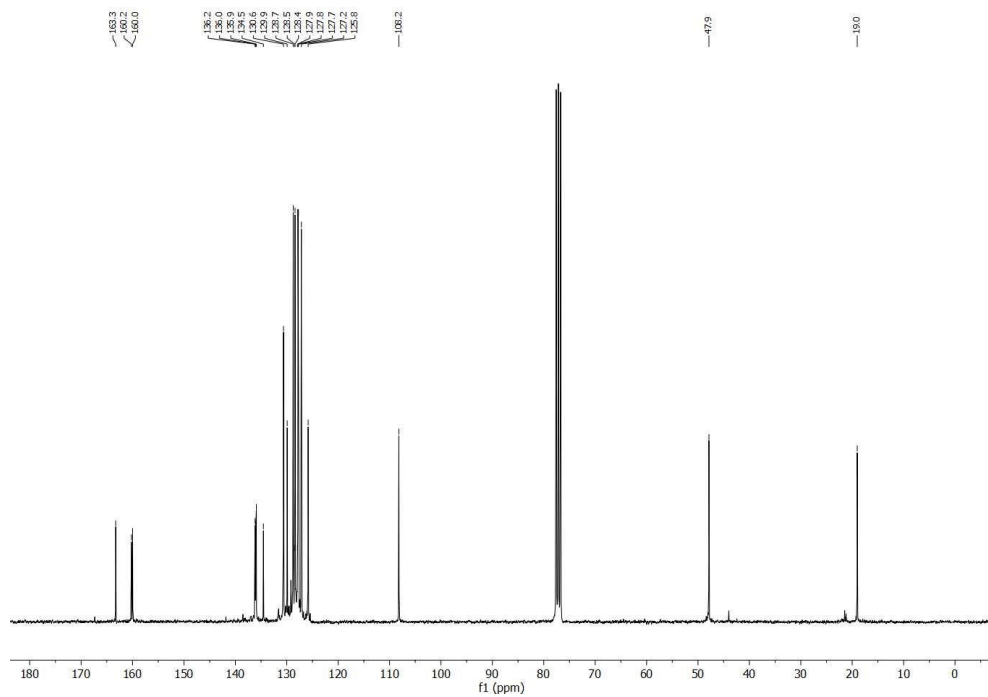
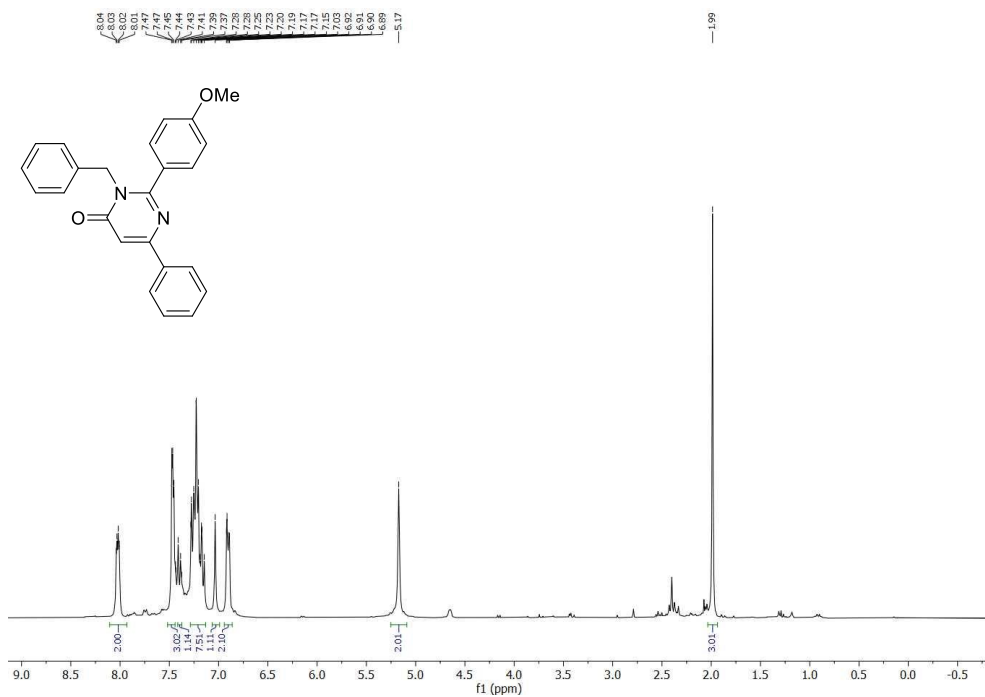
3-(4-Chlorophenyl)-4-(4-methoxyphenyl)-5-(*p*-tolyl)-4,5-dihydro-1,2,4-oxadiazole (1.3I)

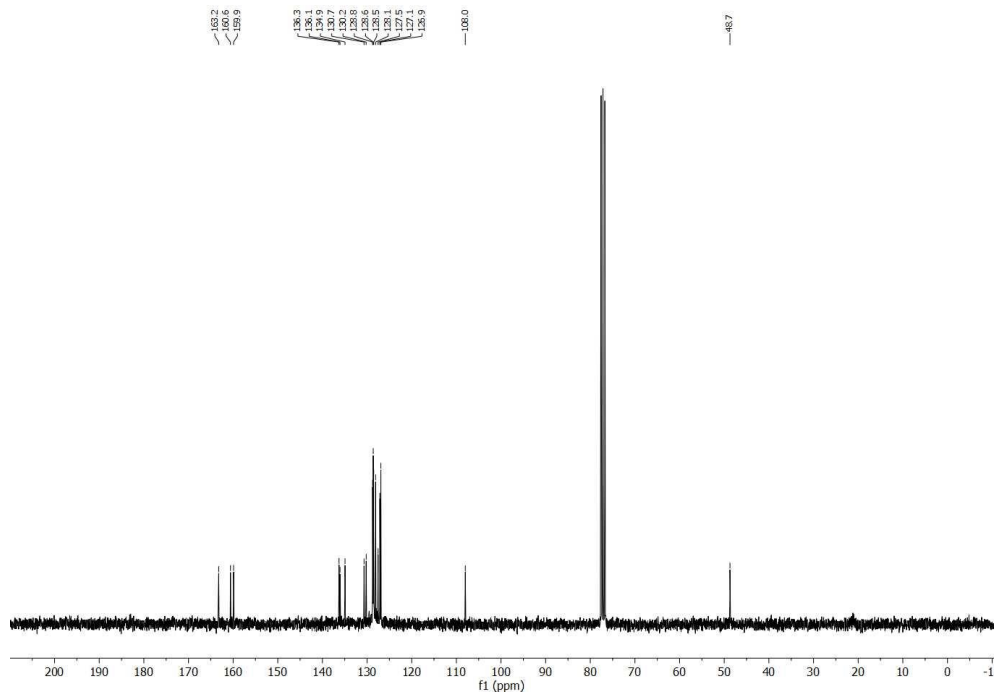
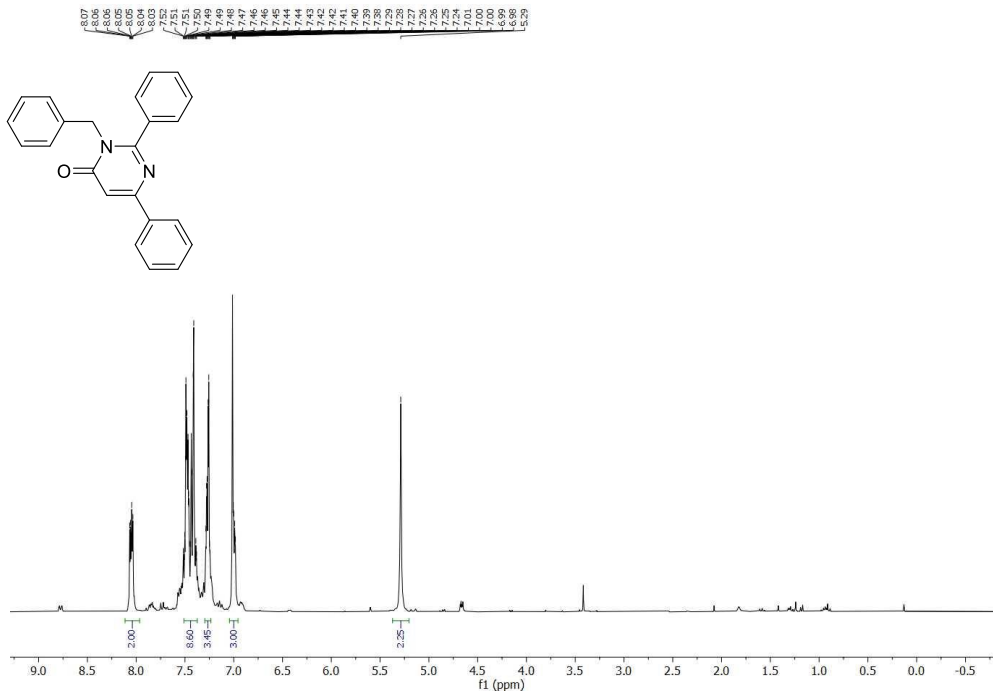
3-(4-chlorophenyl)-4-(4-methoxybenzyl)-5-(p-tolyl)-4,5-dihydro-1,2,4-oxadiazole (1.3m)



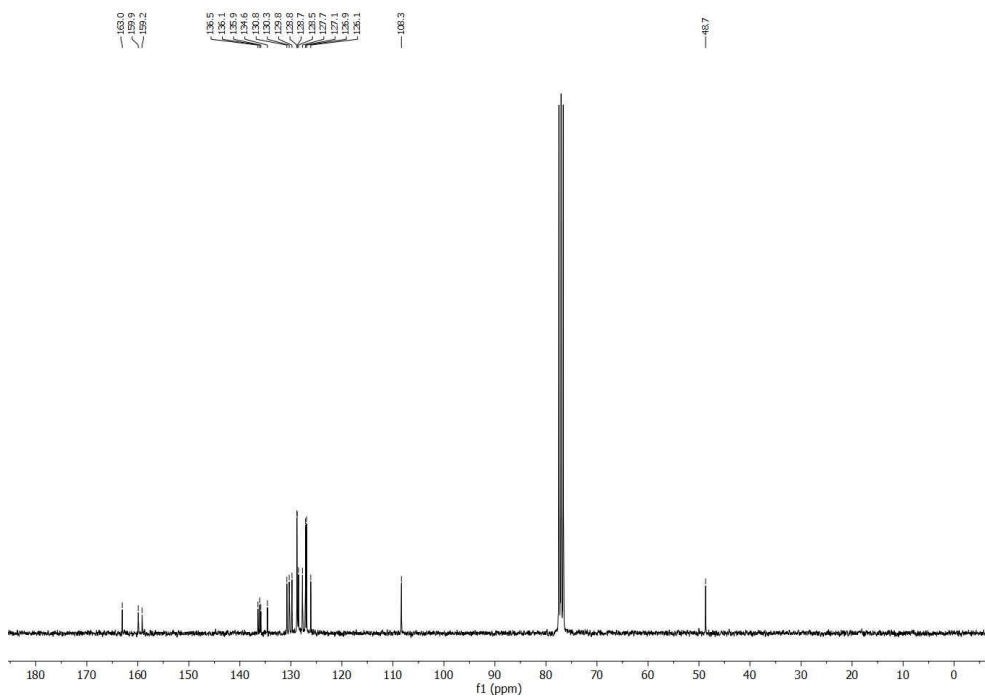
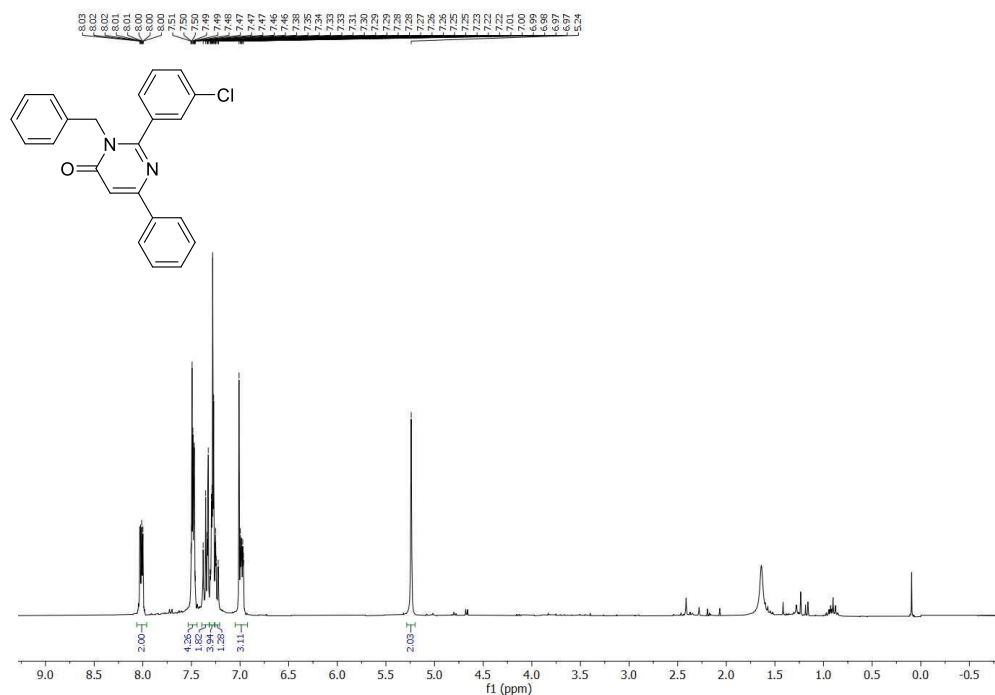
3-Benzyl-2-(4-chlorophenyl)-6-phenylpyrimidin-4(3H)-one (1.4a)

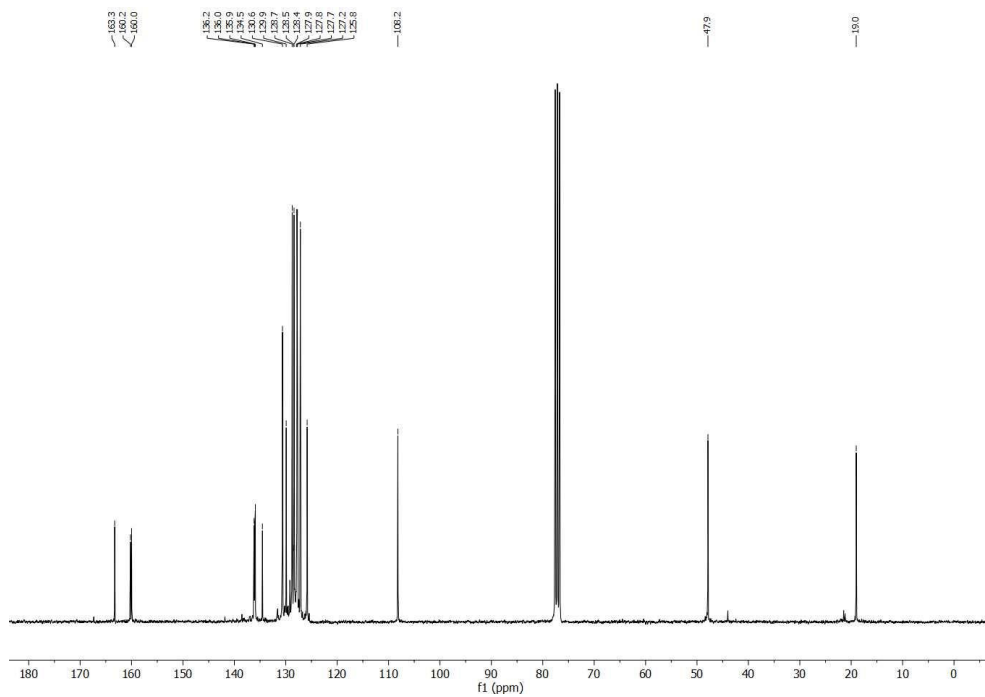
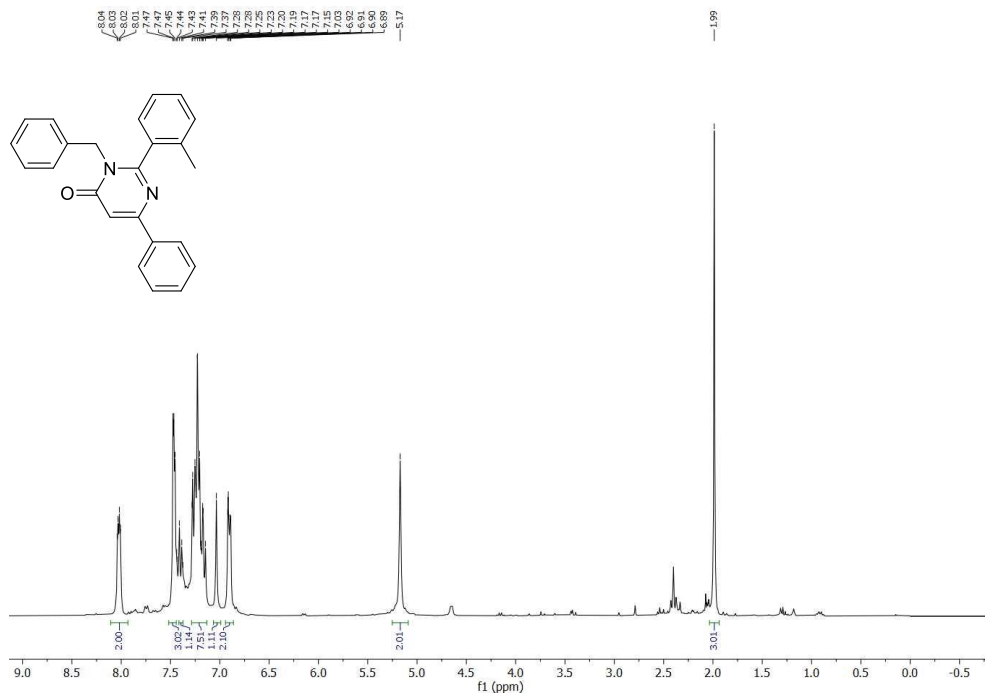
3-Benzyl-2-(4-methoxyphenyl)-6-phenylpyrimidin-4(3H)-one (1.4b)



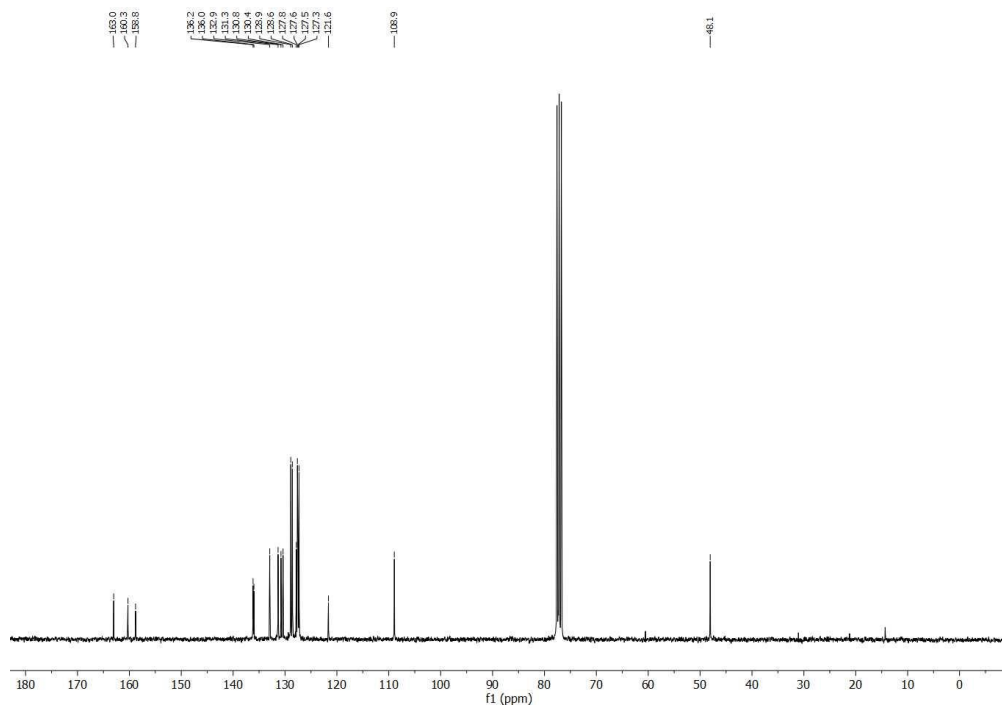
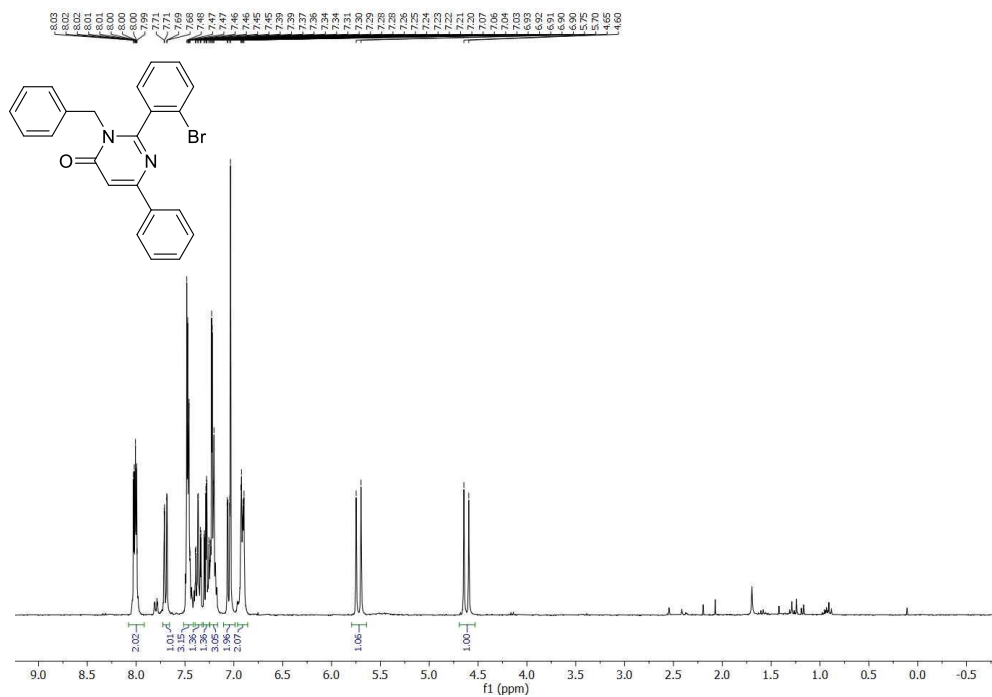
3-Benzyl-2,6-diphenylpyrimidin-4(3H)-one (1.4c)

3-Benzyl-2-(3-chlorophenyl)-6-phenylpyrimidin-4(3H)-one (1.4d)

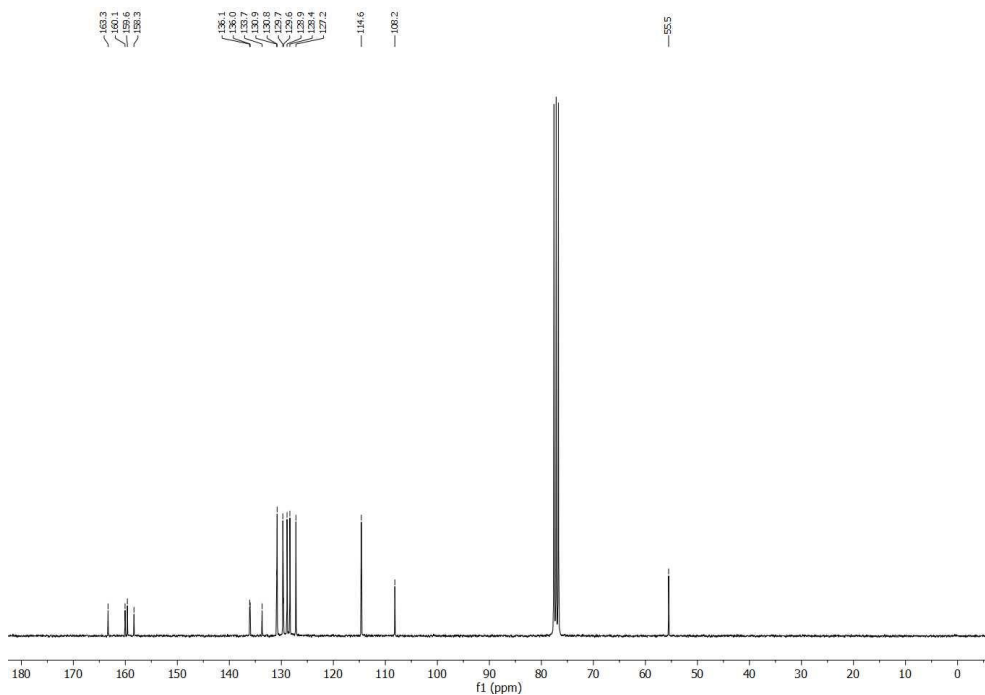
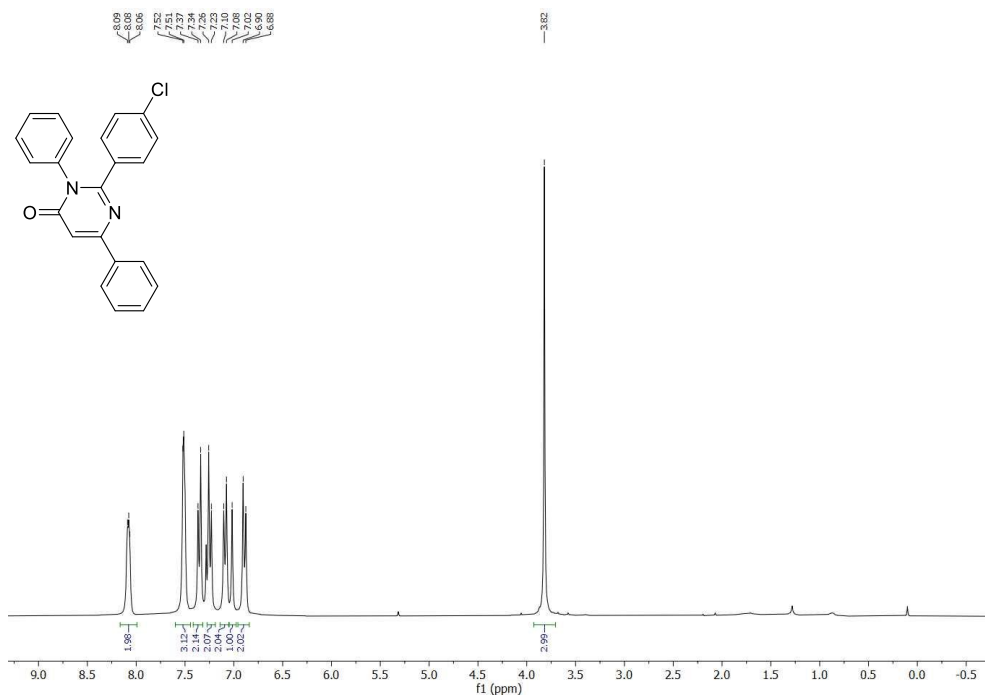


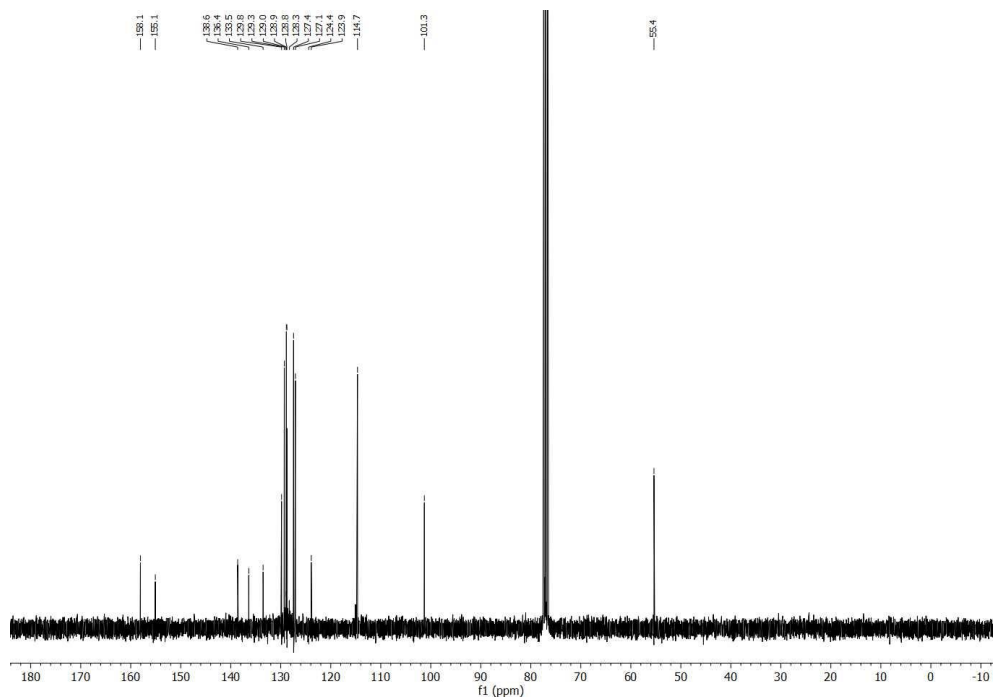
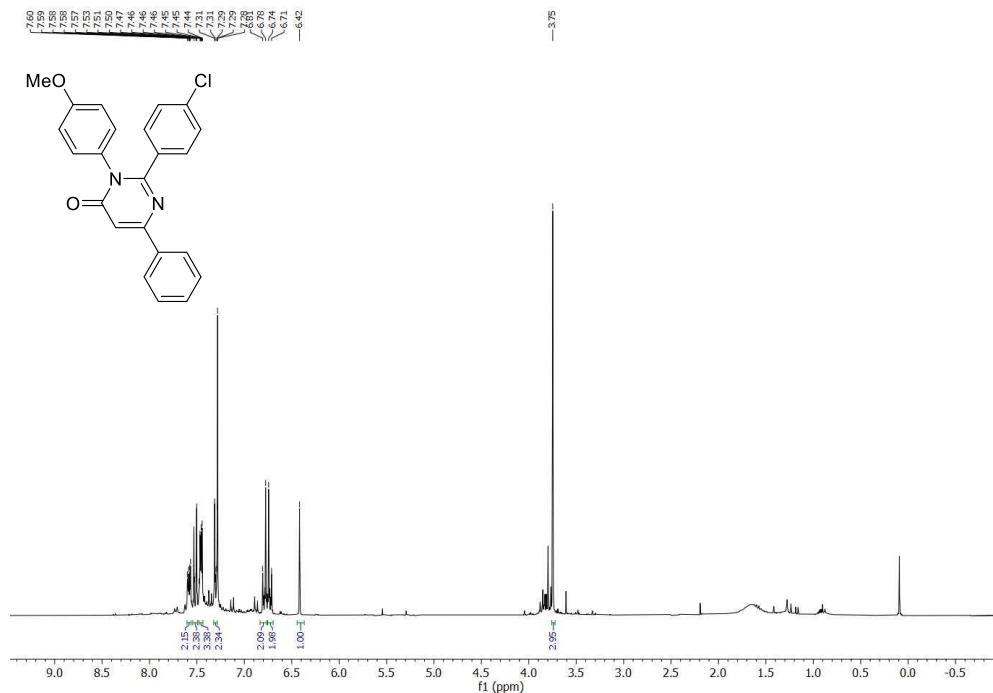
3-Benzyl-6-phenyl-2-(*o*-tolyl)pyrimidin-4(3*H*)-one (1.4e)

3-Benzyl-2-(2-bromophenyl)-6-phenylpyrimidin-4(3H)-one (1.4f)

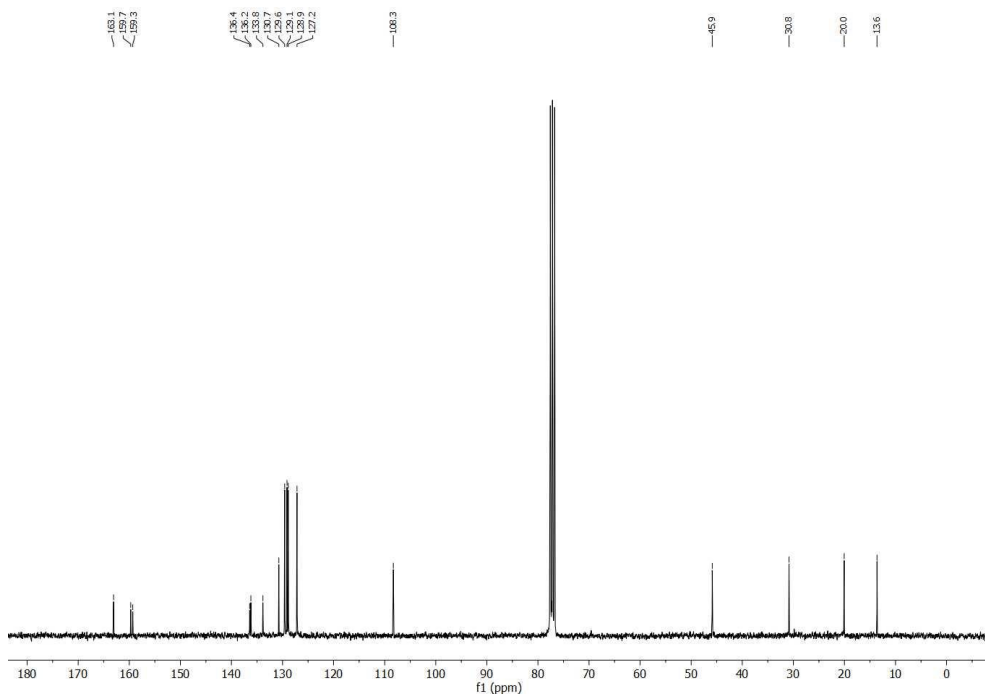
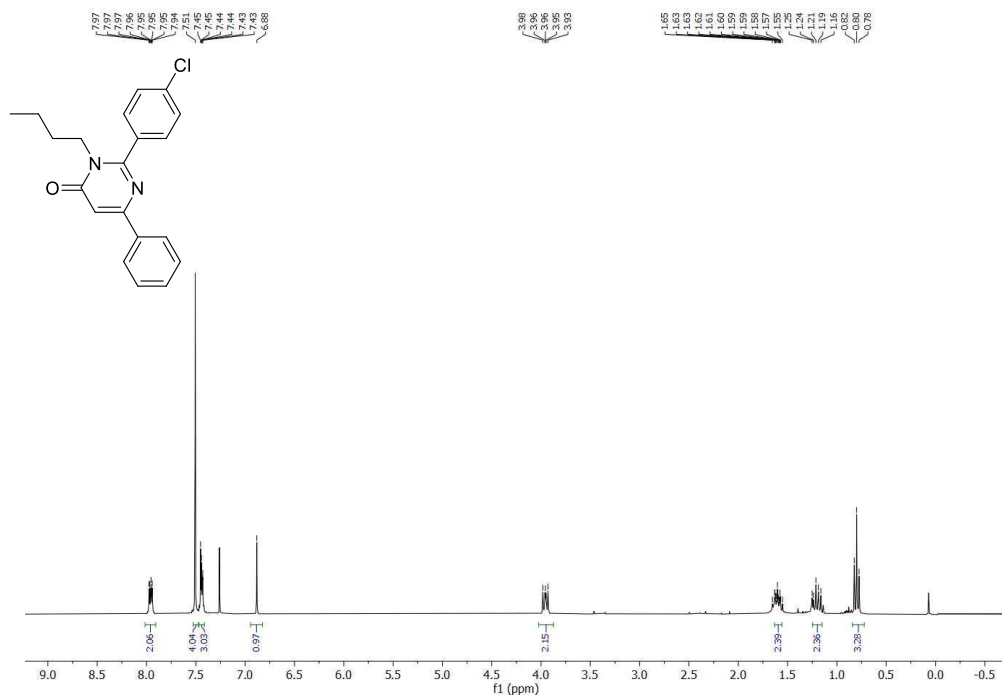


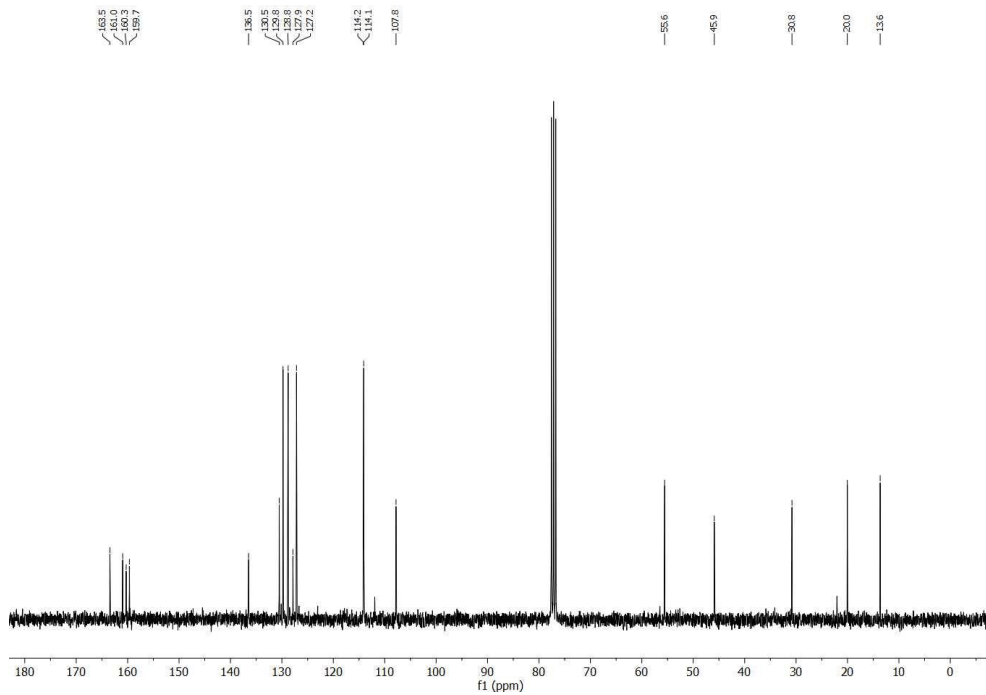
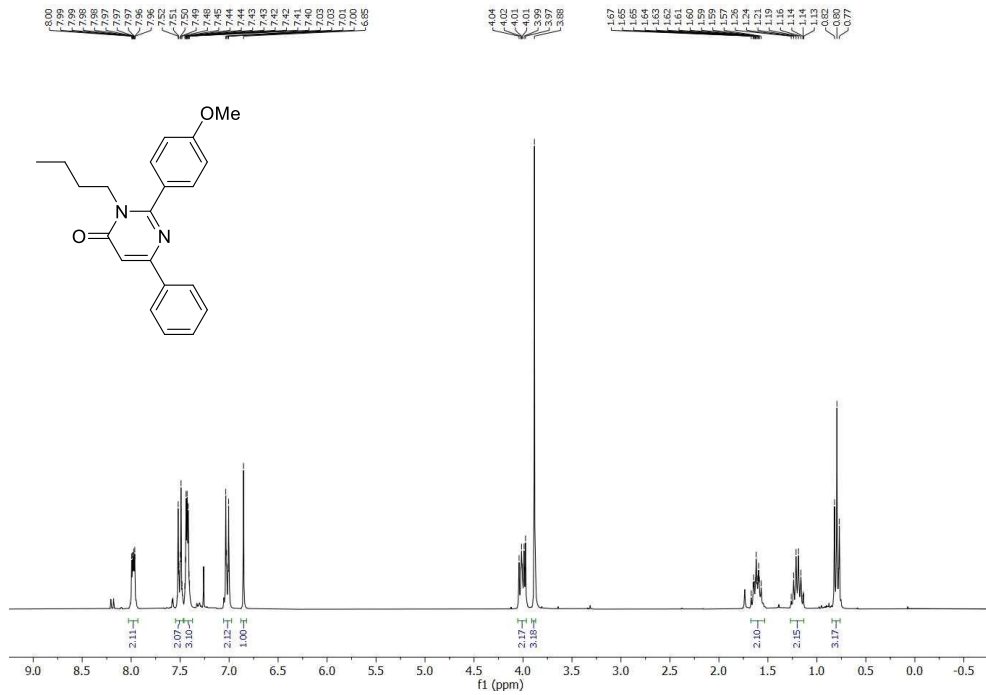
2-(4-Chlorophenyl)-3,6-diphenylpyrimidin-4(3H)-one (1.4h)



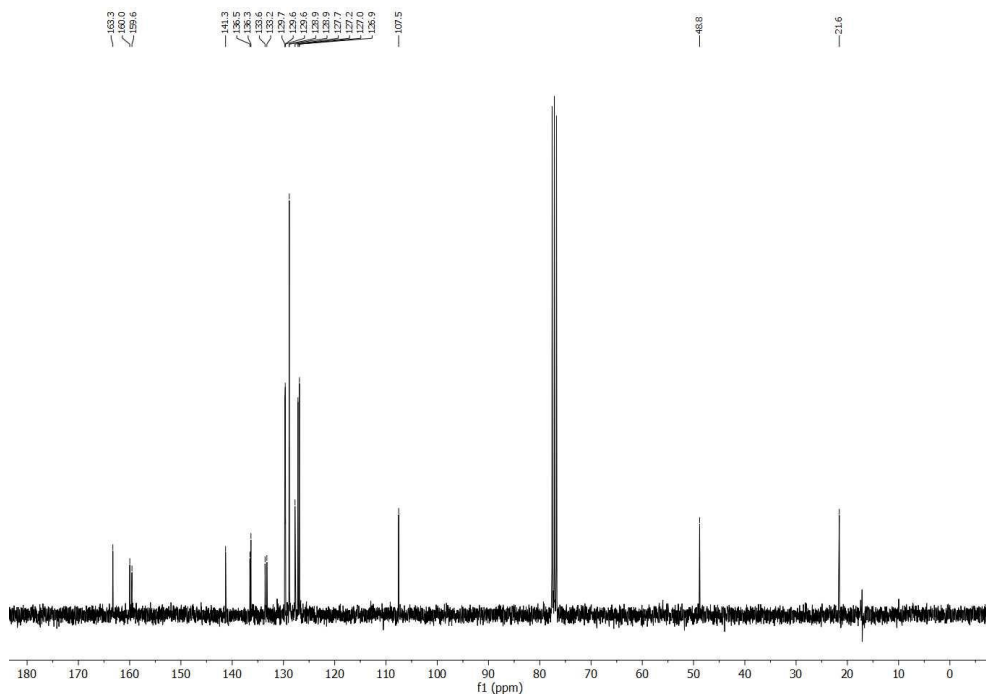
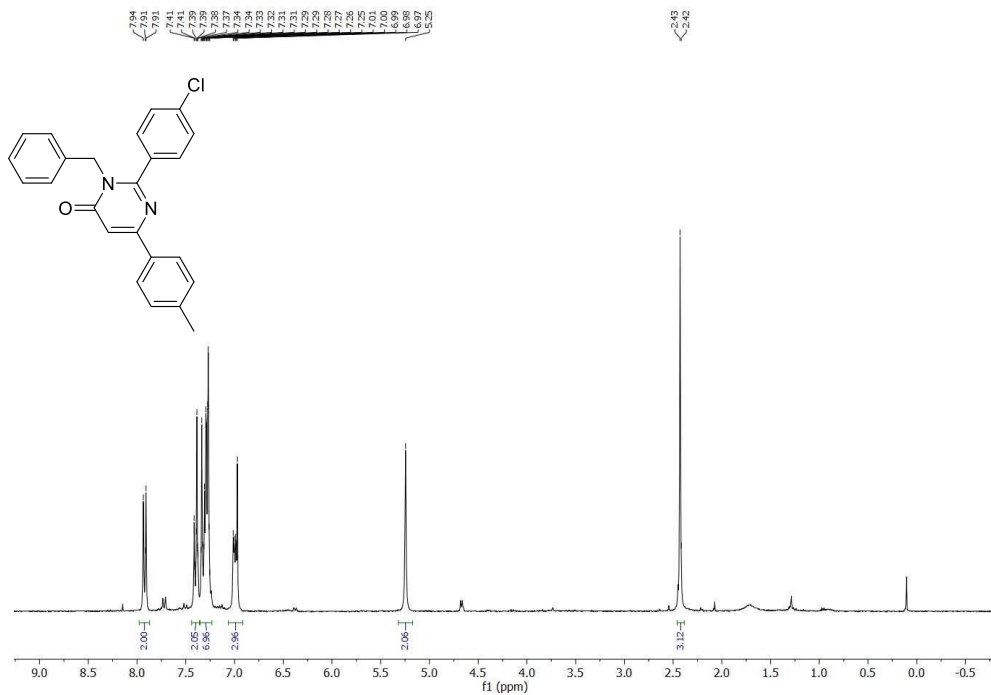
2-(4-Chlorophenyl)-3-(4-methoxyphenyl)-6-phenylpyrimidin-4(3H)-one (1.4i)

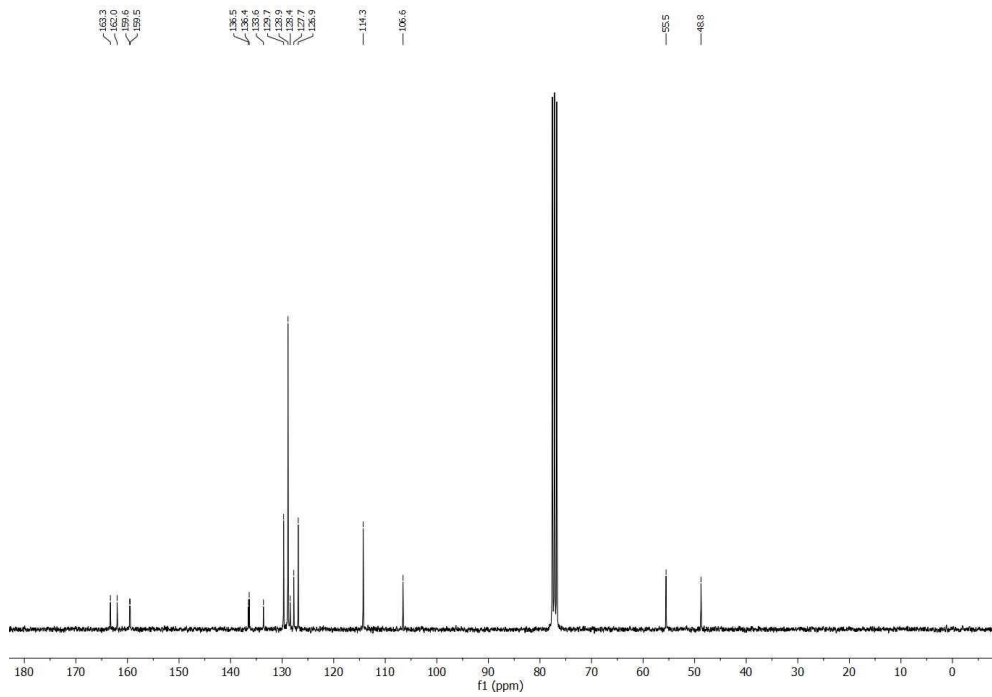
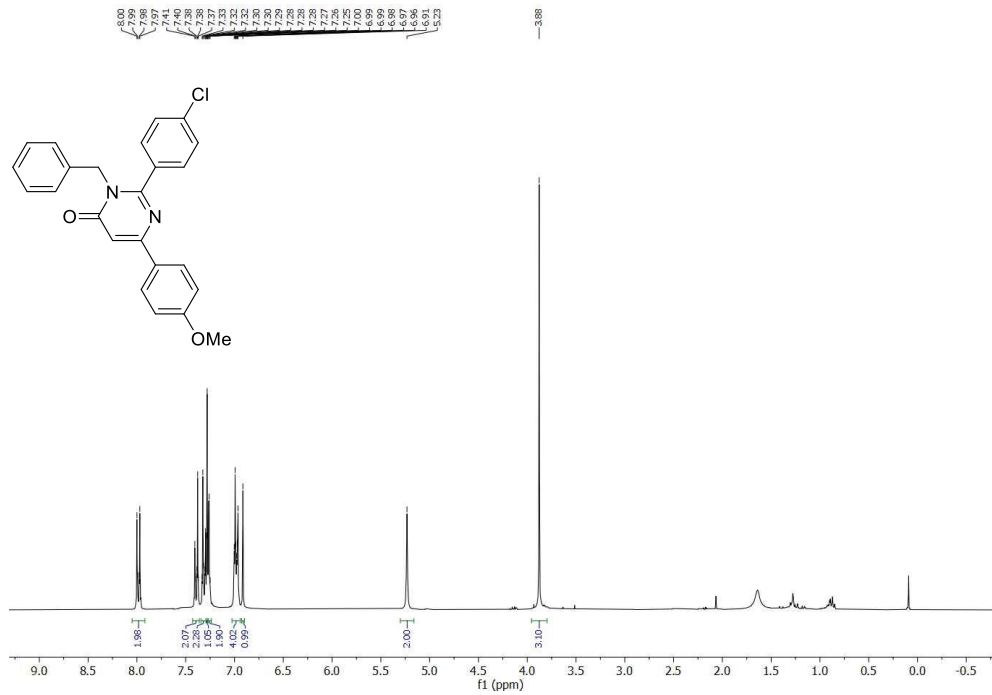
3-Butyl-2-(4-chlorophenyl)-6-phenylpyrimidin-4(3H)-one (1.4j)



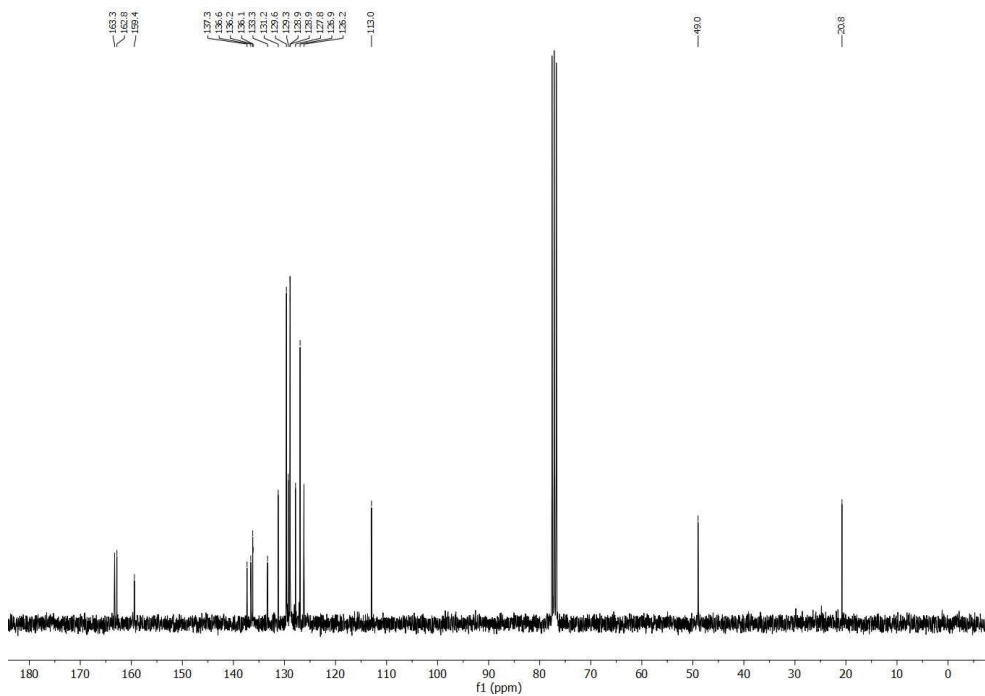
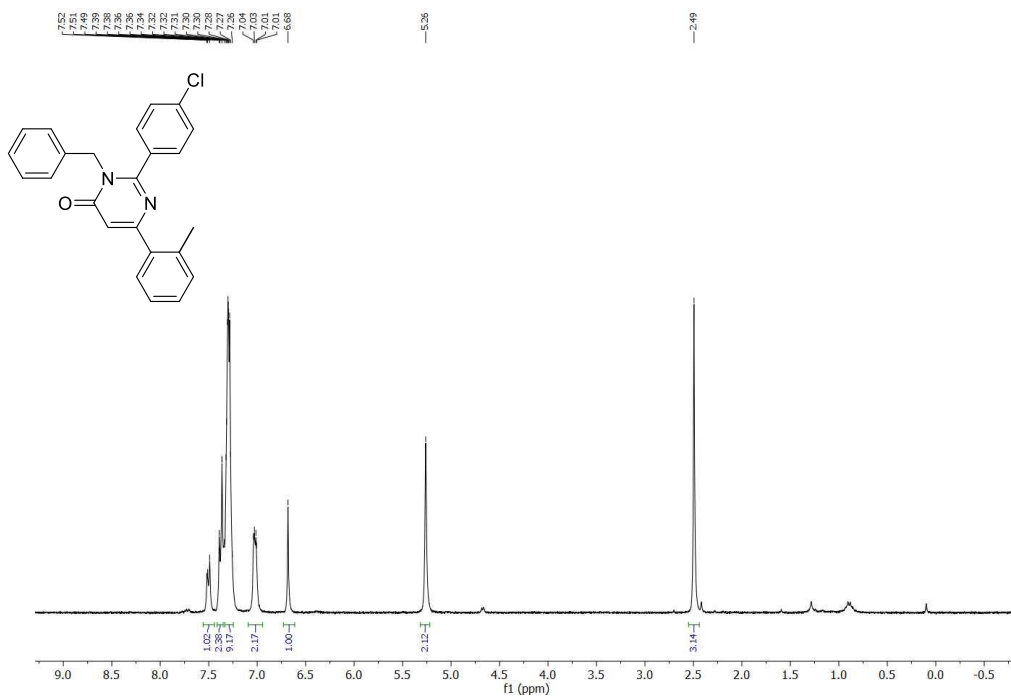
3-Butyl-2-(4-methoxyphenyl)-6-phenylpyrimidin-4(3H)-one (1.4k)

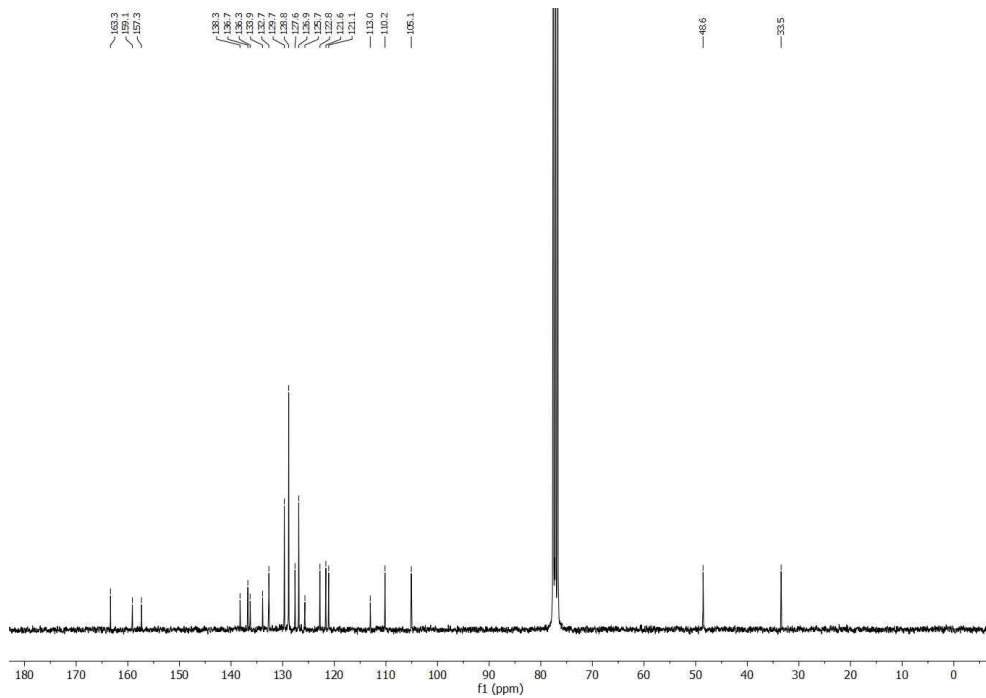
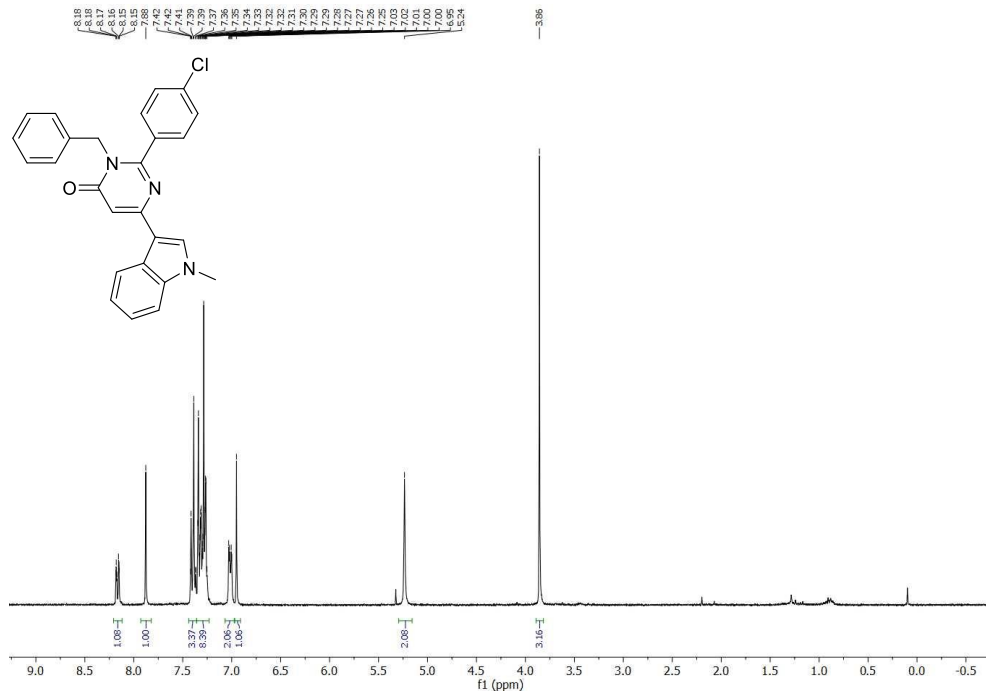
3-Benzyl-2-(4-chlorophenyl)-6-(*p*-tolyl)pyrimidin-4(3*H*)-one (1.4I)



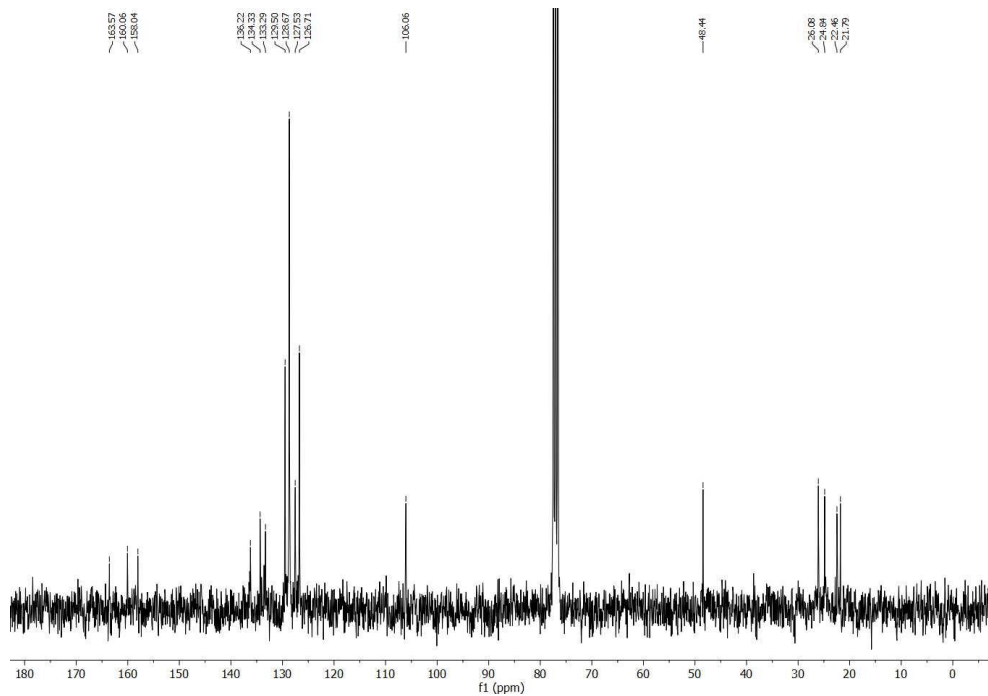
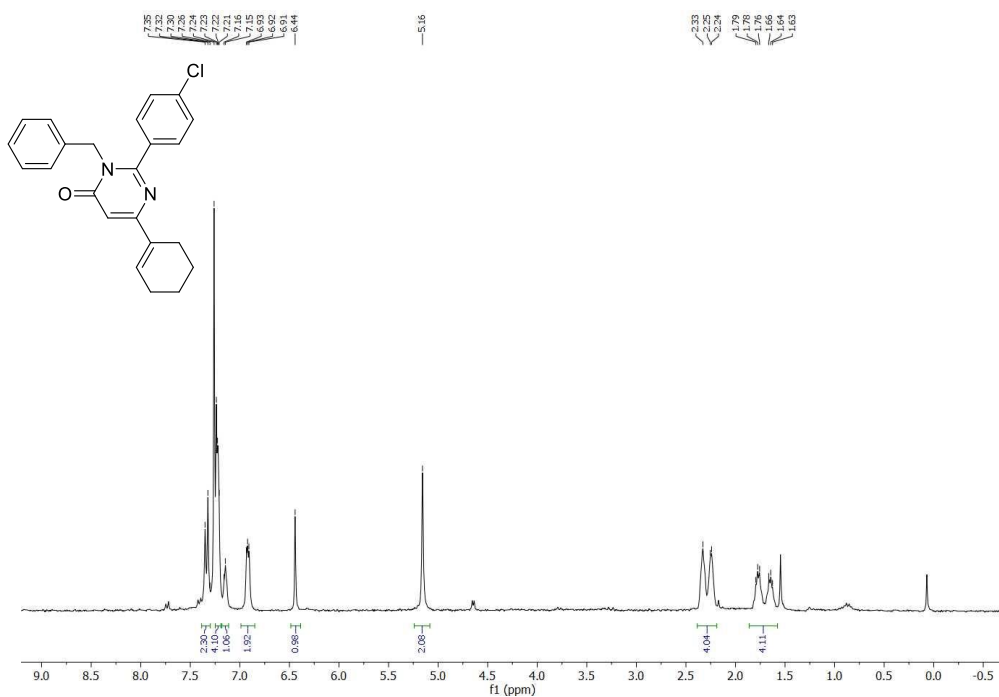
3-Benzyl-2-(4-chlorophenyl)-6-(4-methoxyphenyl)pyrimidin-4(3H)-one (1.4m)

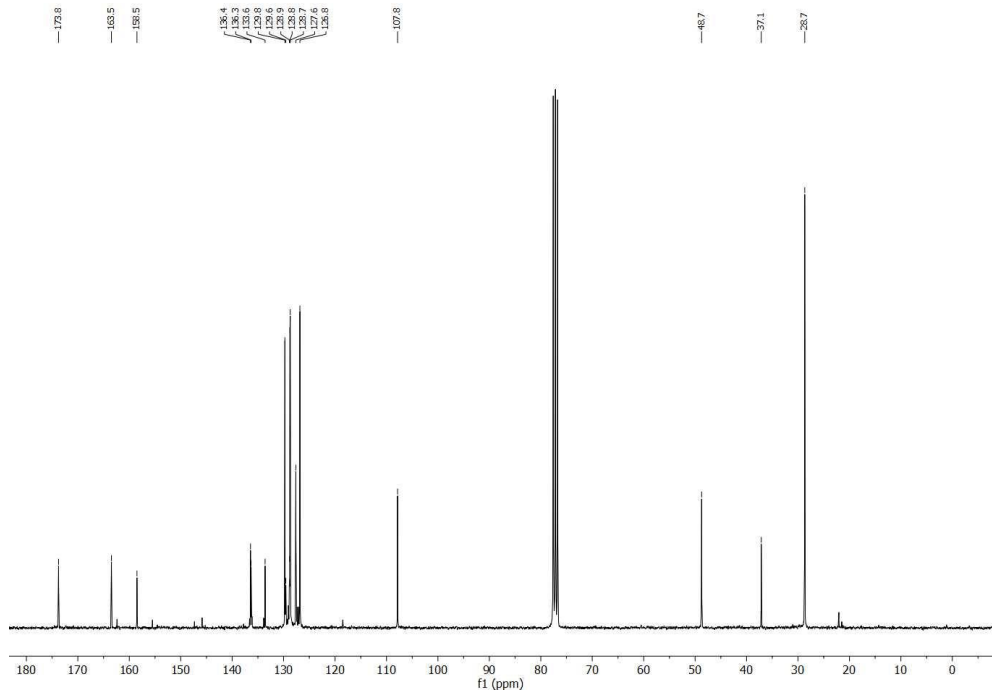
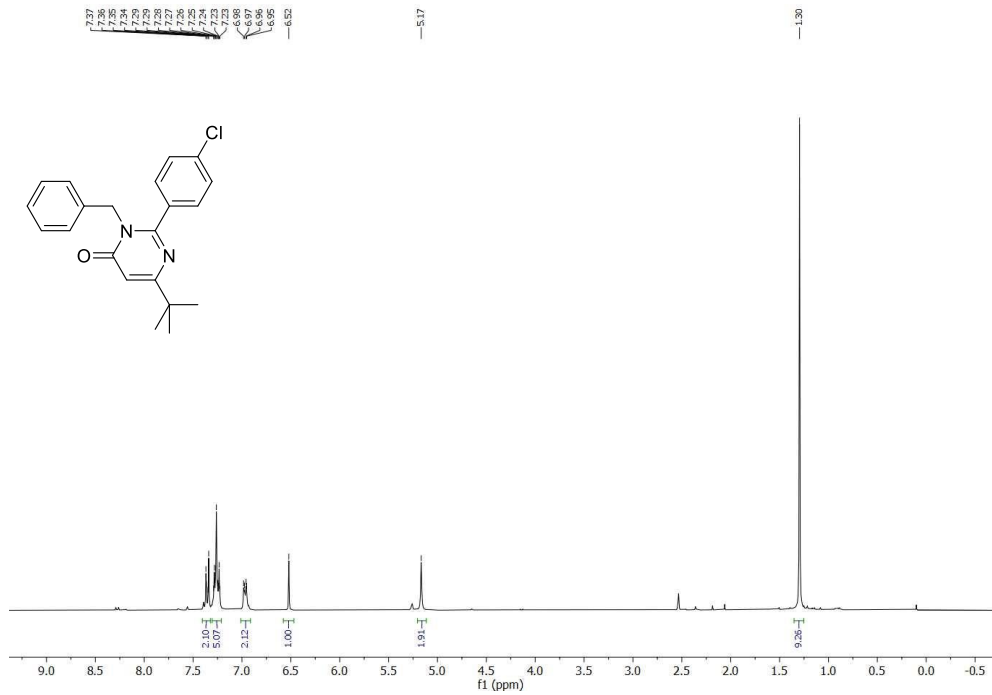
3-Benzyl-2-(4-chlorophenyl)-6-(*o*-tolyl)pyrimidin-4(3*H*)-one (1.4n)



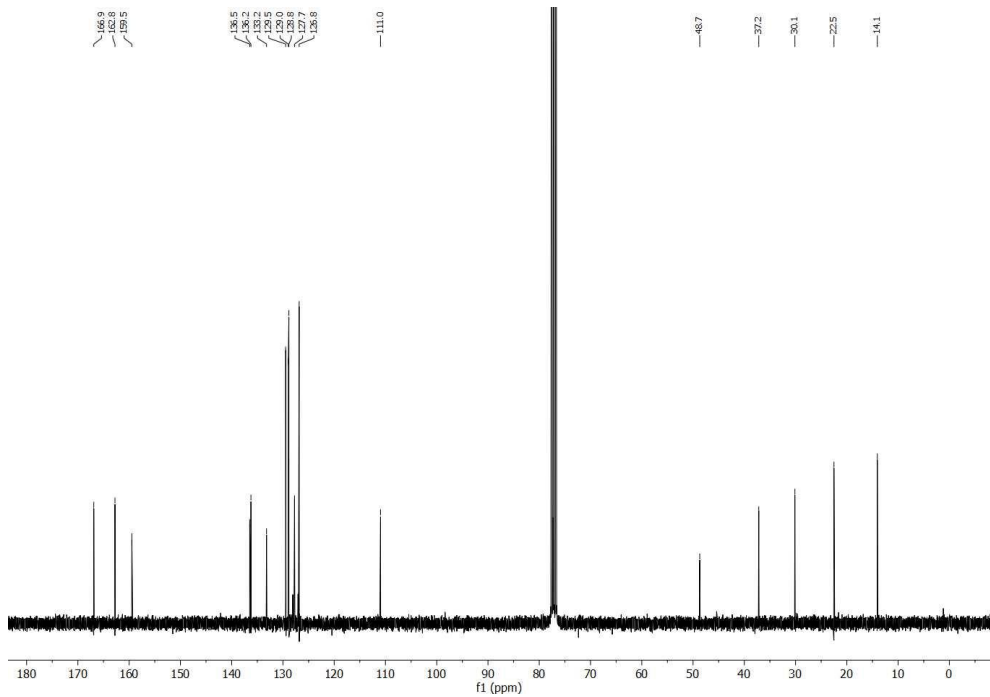
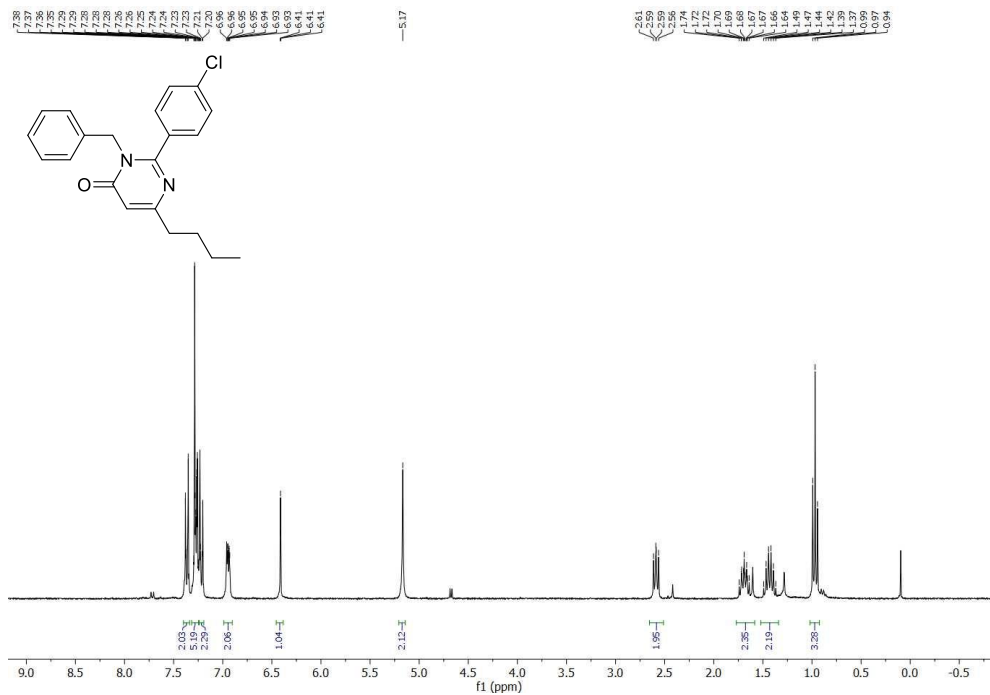
3-Benzyl-2-(4-chlorophenyl)-6-(1-methyl-1H-indol-3-yl)pyrimidin-4(3H)-one (1.4o)

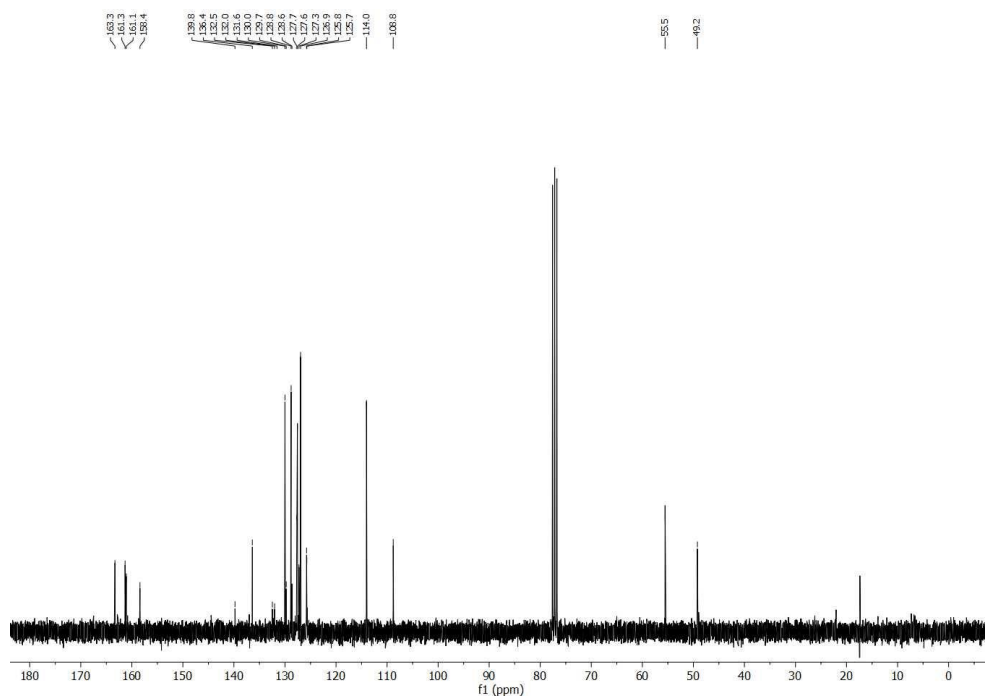
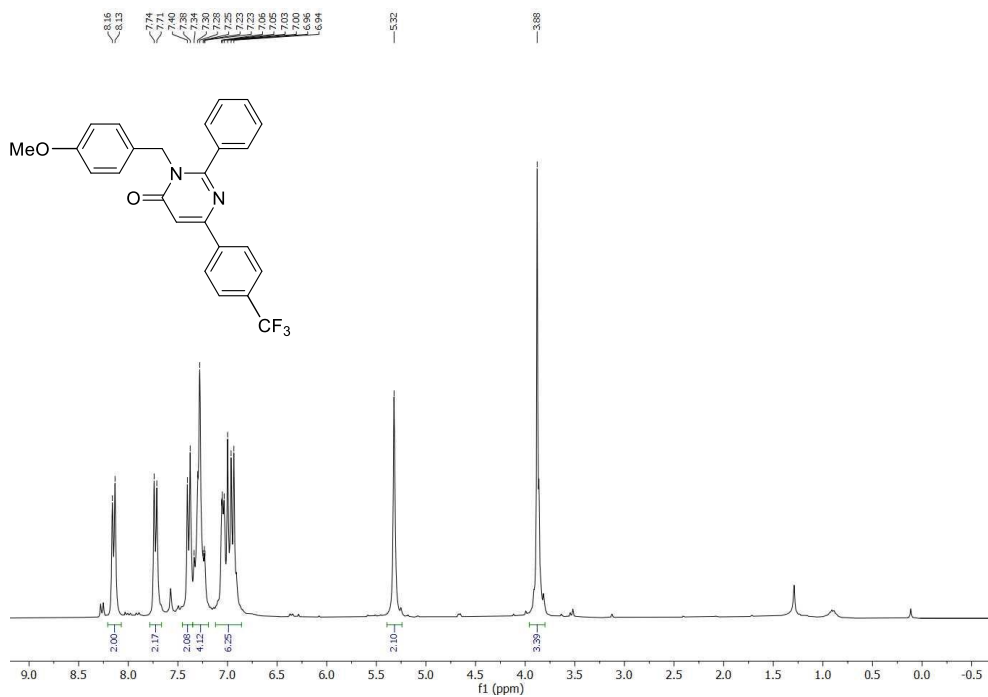
3-Benzyl-2-(4-chlorophenyl)-6-(cyclohex-1-en-1-yl)pyrimidin-4(3H)-one (1.4p)



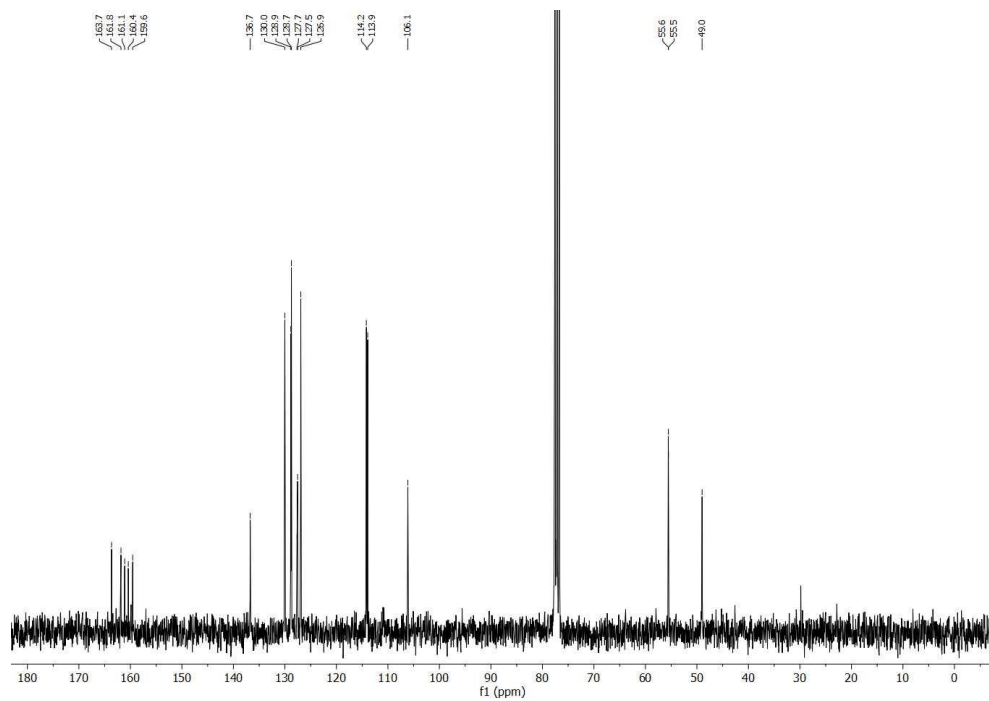
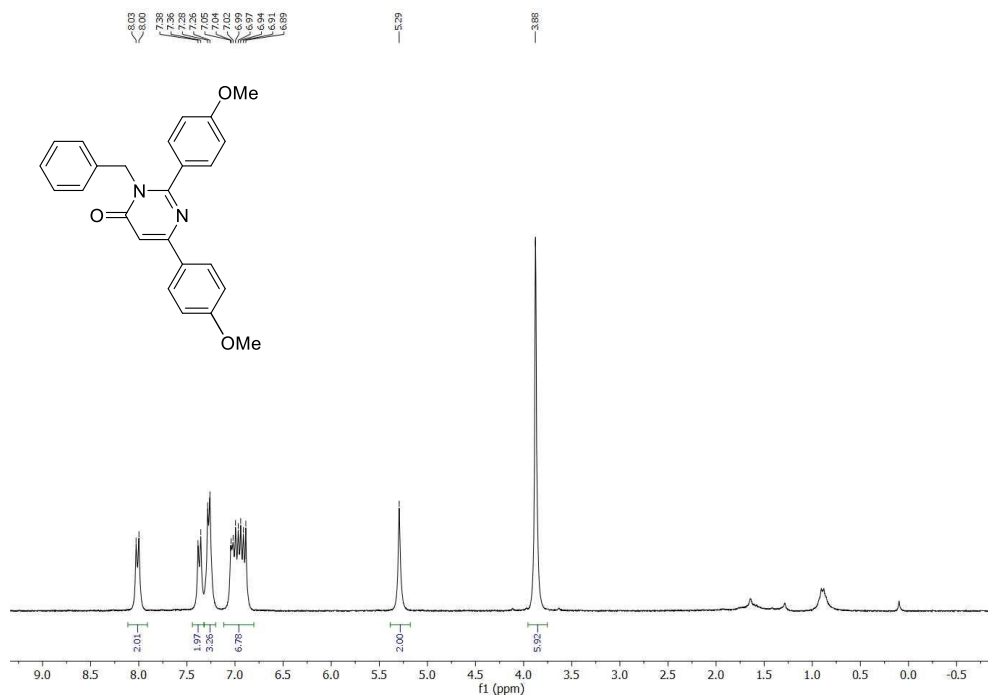
3-Benzyl-6-(*tert*-butyl)-2-(4-chlorophenyl)pyrimidin-4(3H)-one (1.4q)

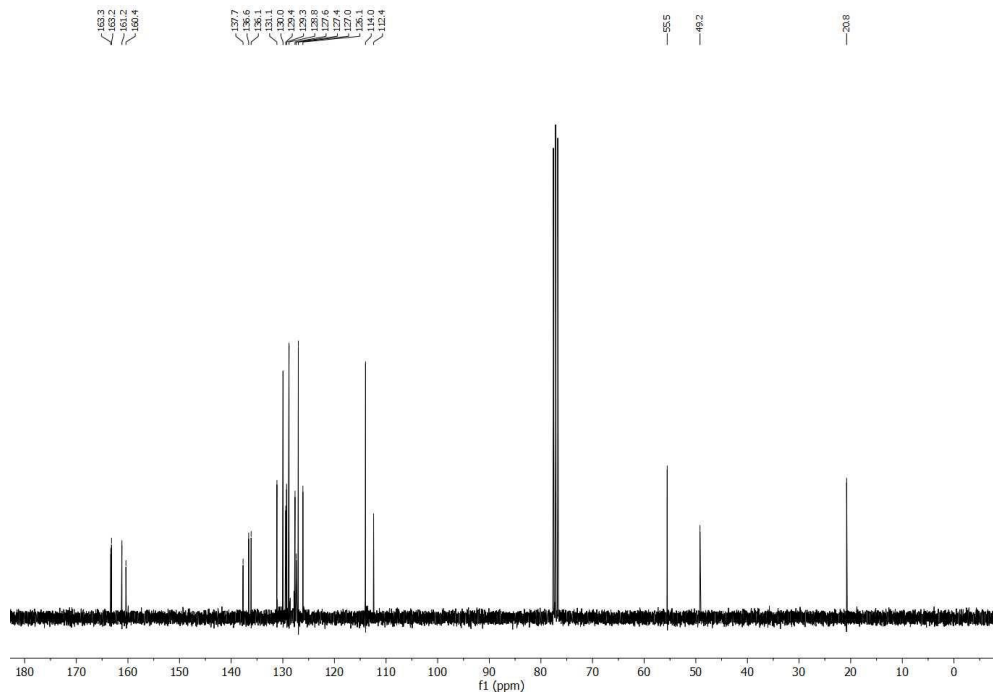
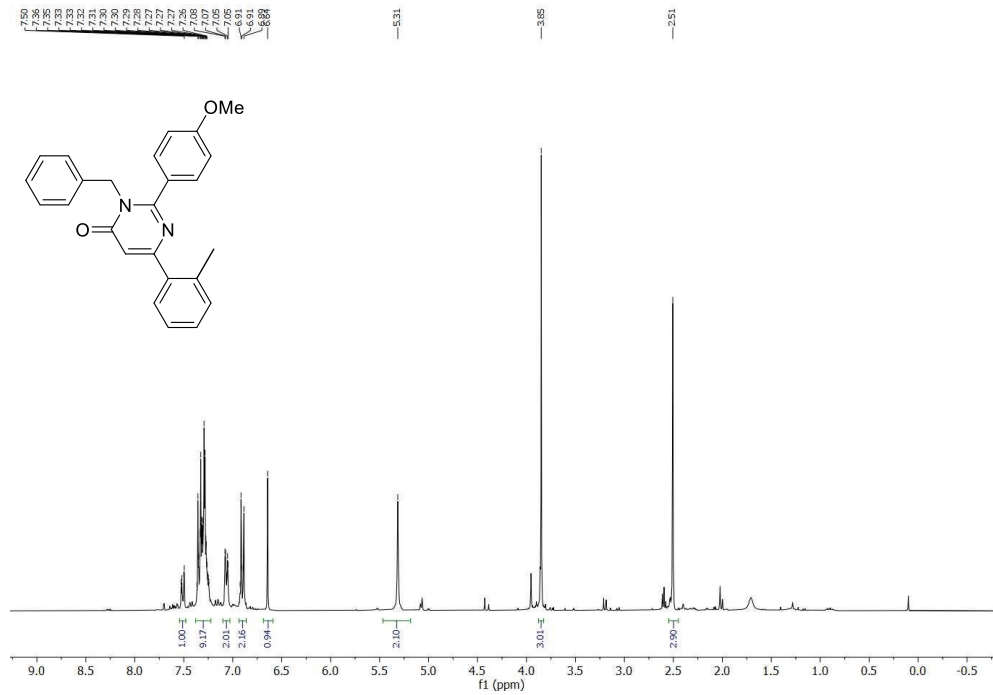
3-Benzyl-6-butyl-2-(4-chlorophenyl)pyrimidin-4(3H)-one (1.4r)



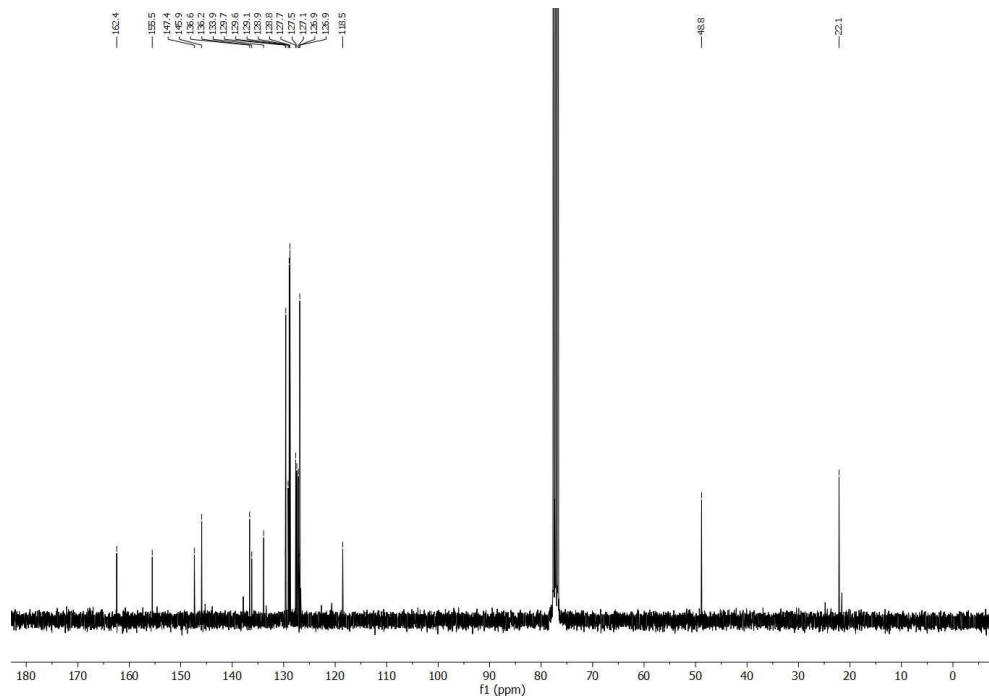
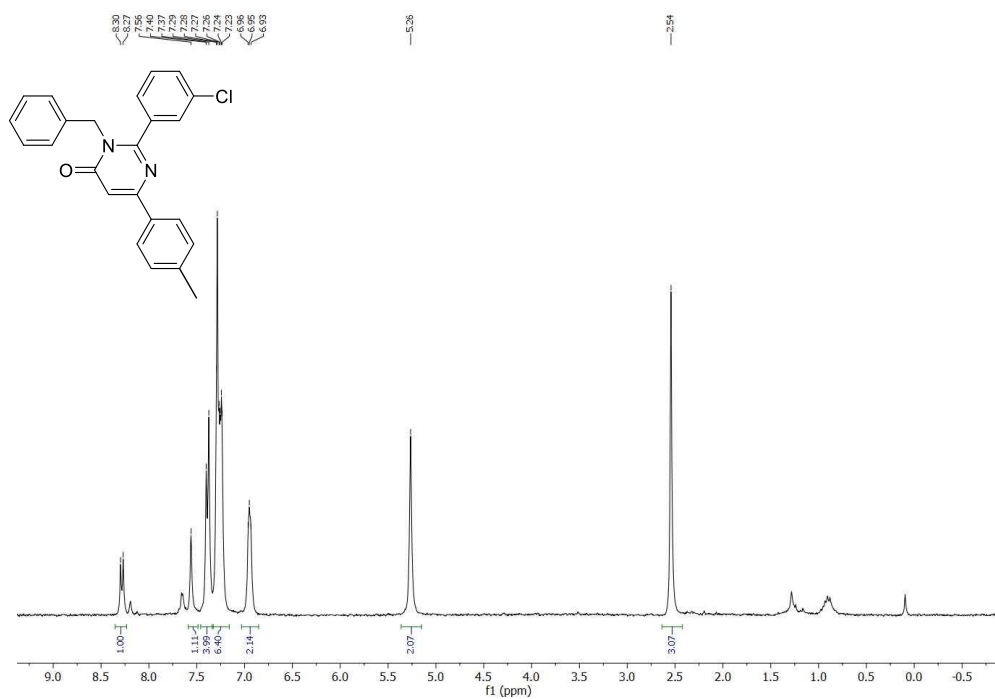
3-(4-Methoxybenzyl)-2-phenyl-6-(4-(trifluoromethyl)phenyl)pyrimidin-4(3H)-one (1.4s)

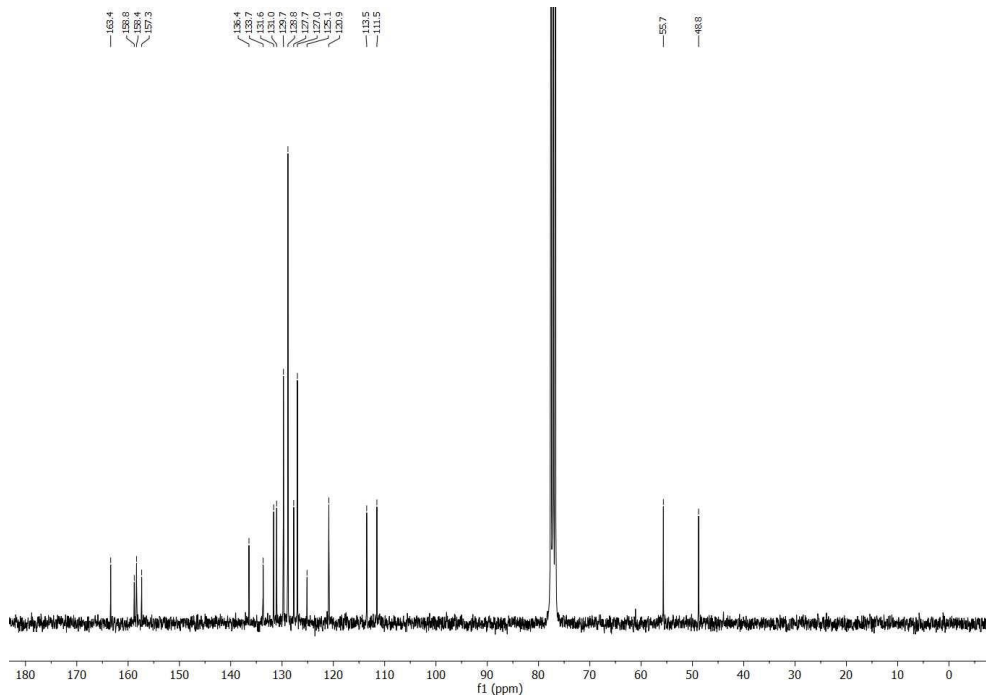
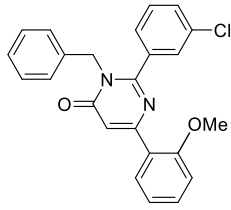
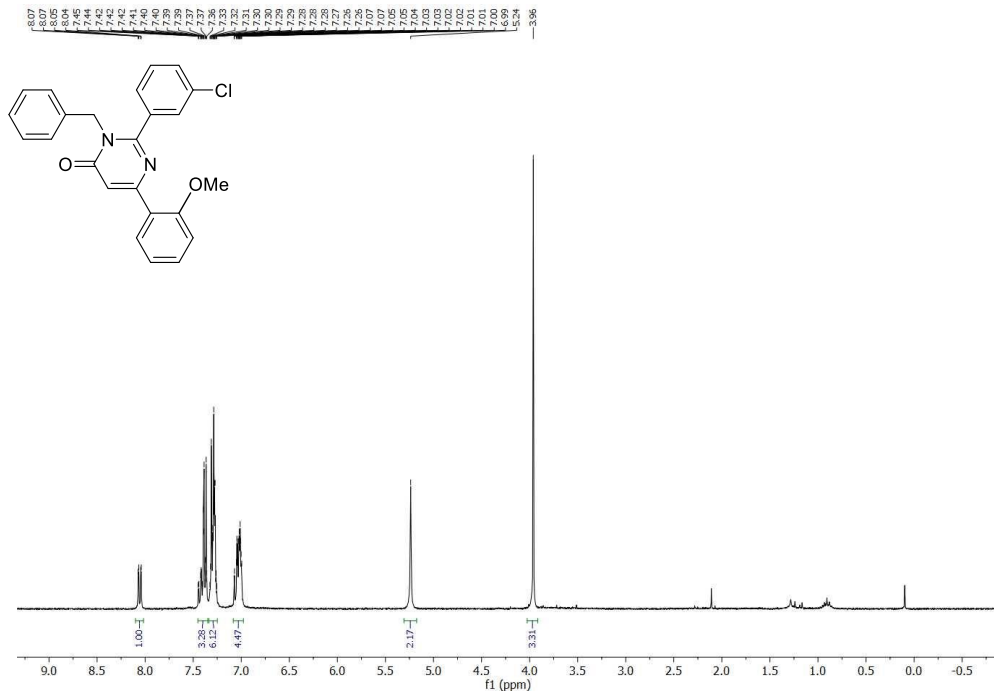
3-Benzyl-2-(4-methoxyphenyl)-6-(4-methoxyphenyl)pyrimidin-4(3H)-one (1.4t)



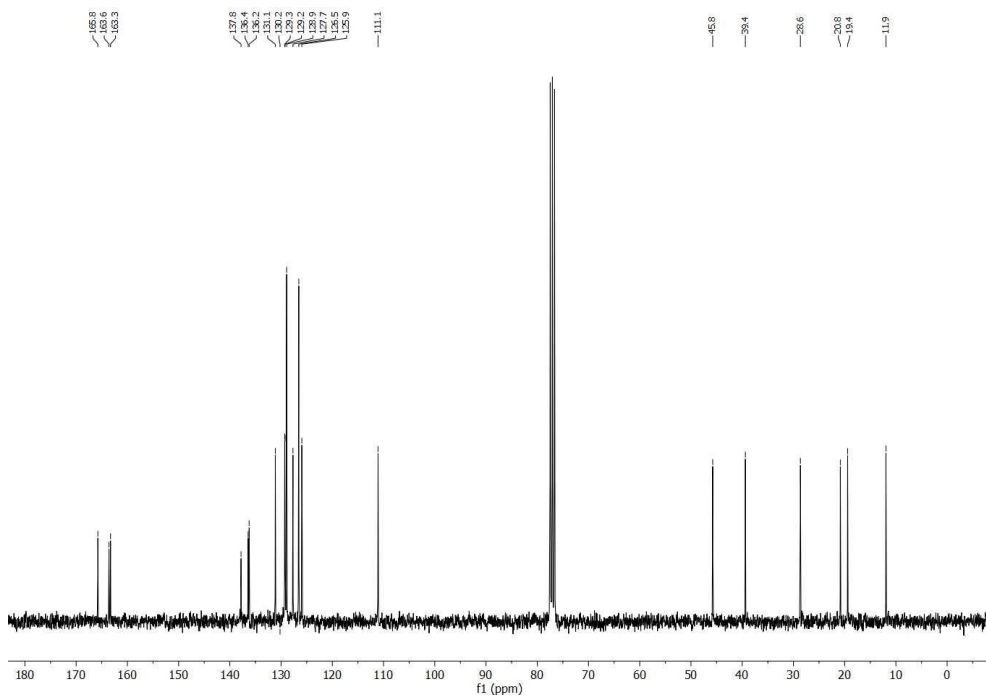
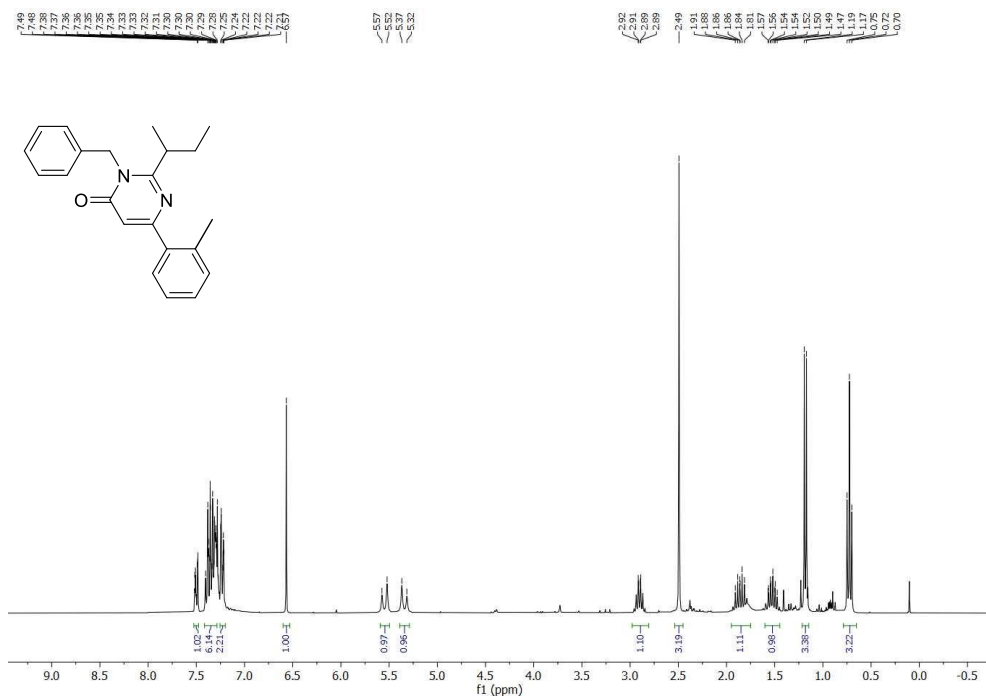
3-Benzyl-2-(4-methoxyphenyl)-6-(*o*-tolyl)pyrimidin-4(3H)-one (1.4u)

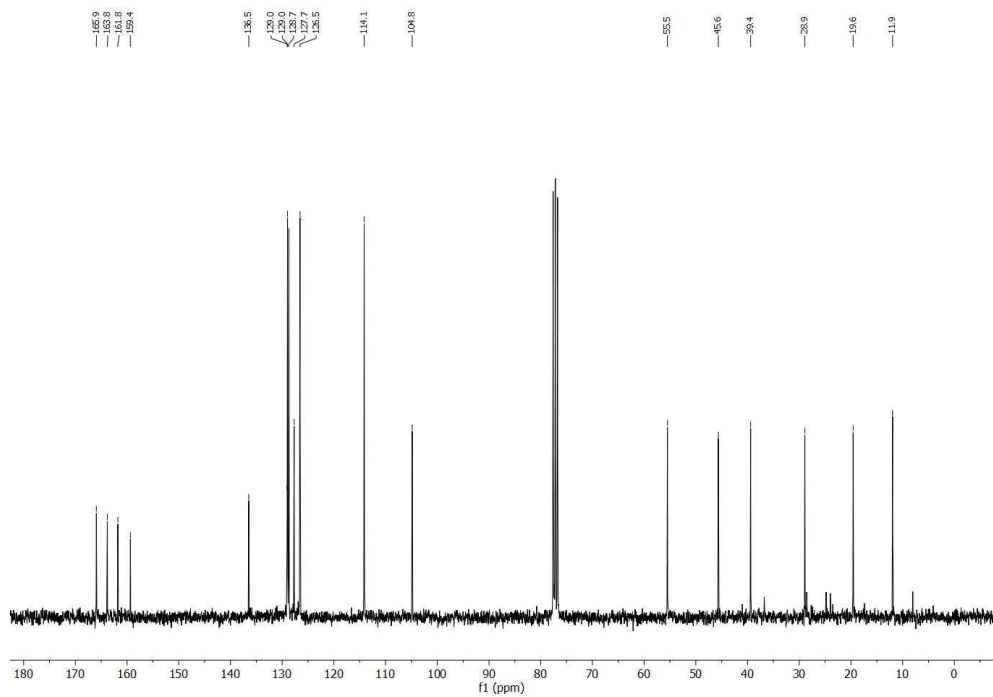
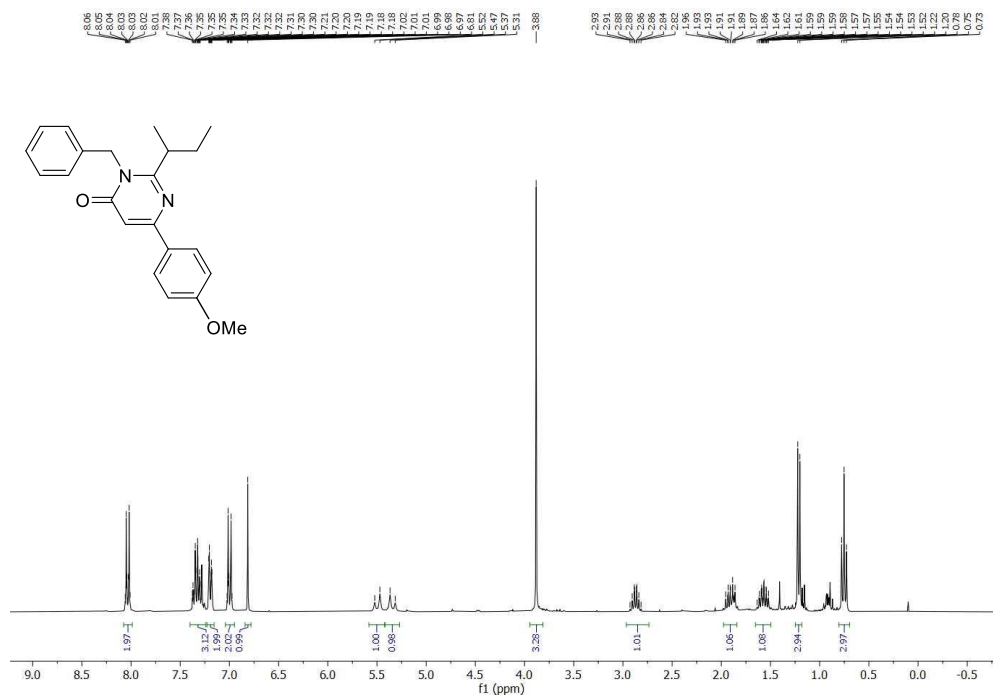
3-Benzyl-2-(3-chlorophenyl)-6-(*p*-tolyl)pyrimidin-4(3*H*)-one (1.4v)



3-Benzyl-2-(3-chlorophenyl)-6-(2-methoxyphenyl)pyrimidin-4(3H)-one (1.4w)

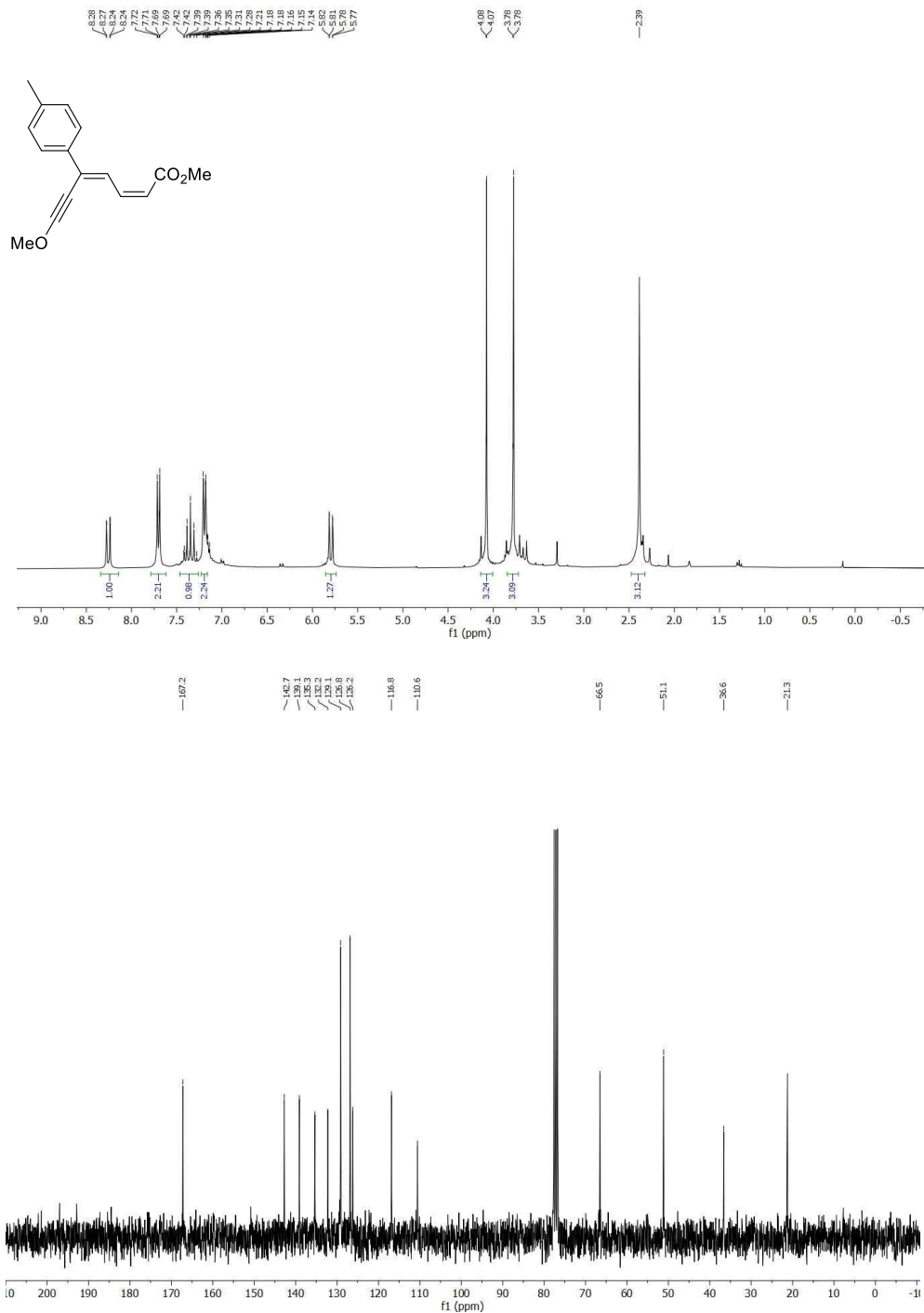
3-Benzyl-2-(*sec*-butyl)-6-(2-methylphenyl)pyrimidin-4(3*H*)-one (1.4x)

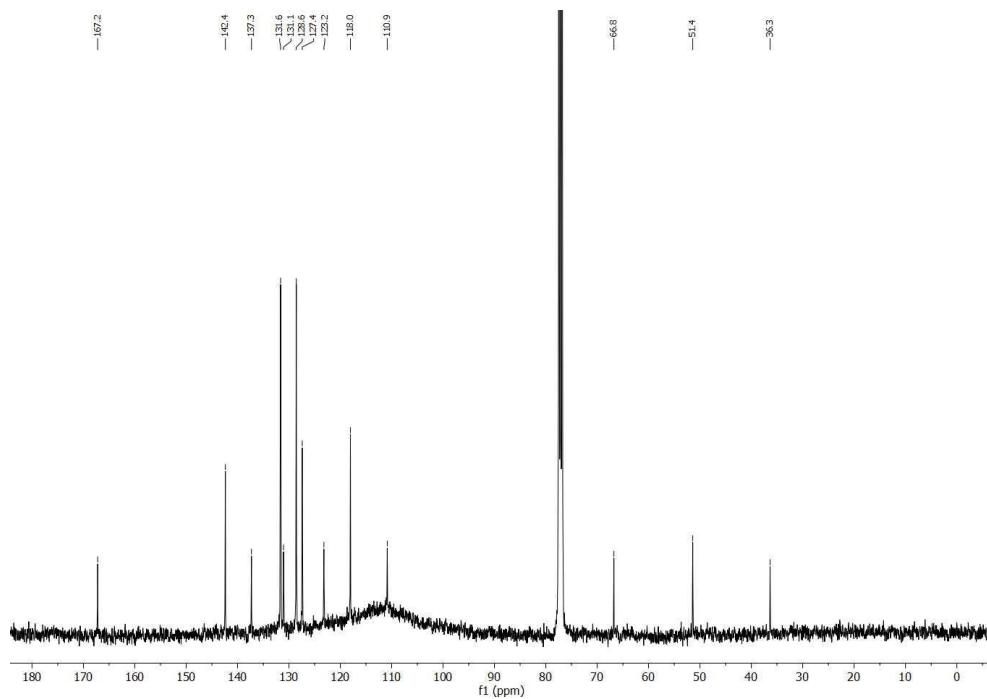
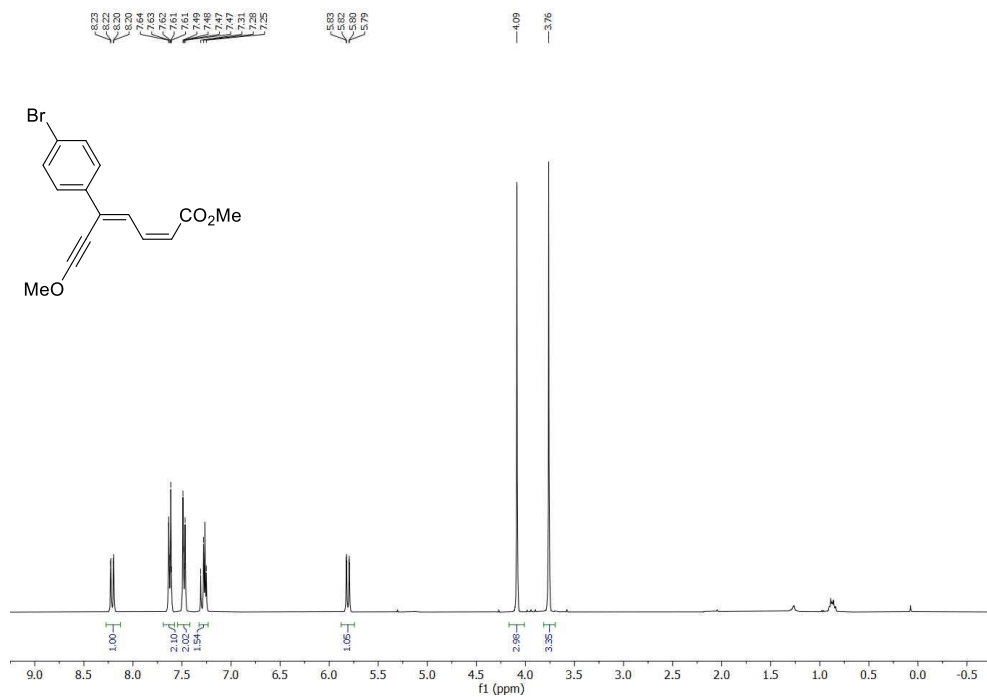


3-Benzyl-2-(*sec*-butyl)-6-(4-methoxyphenyl)pyrimidin-4(3*H*)-one (1.4y)

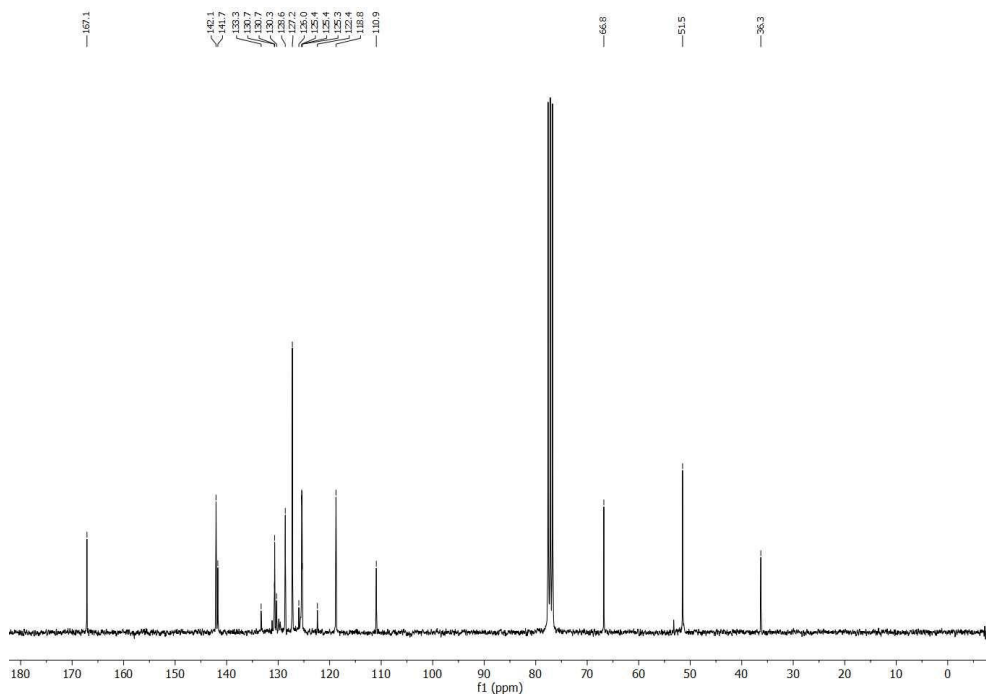
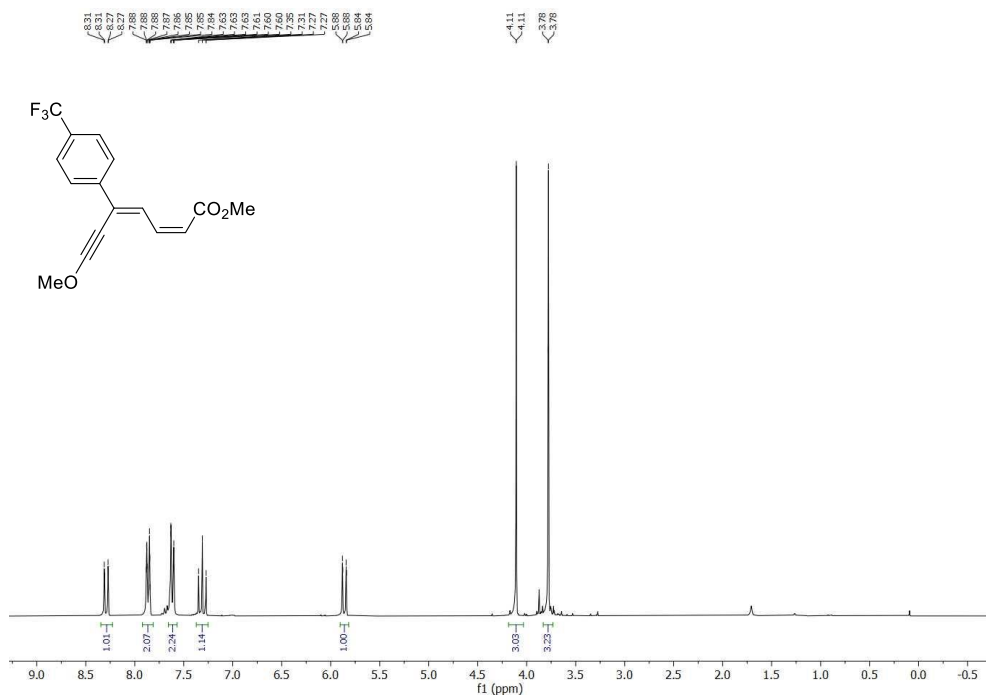
2 Chapter II

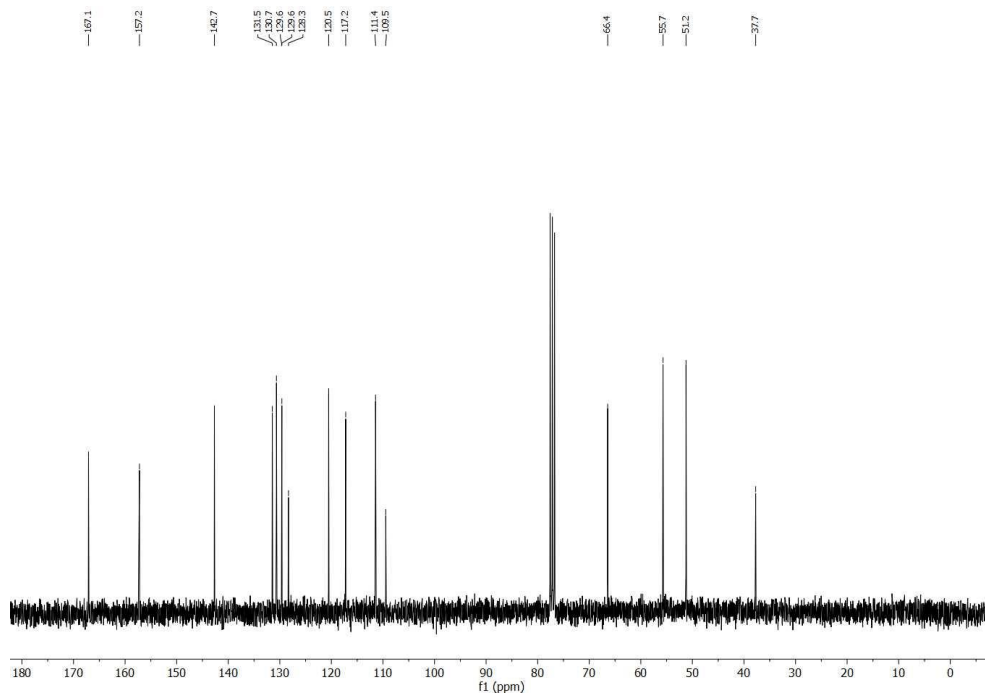
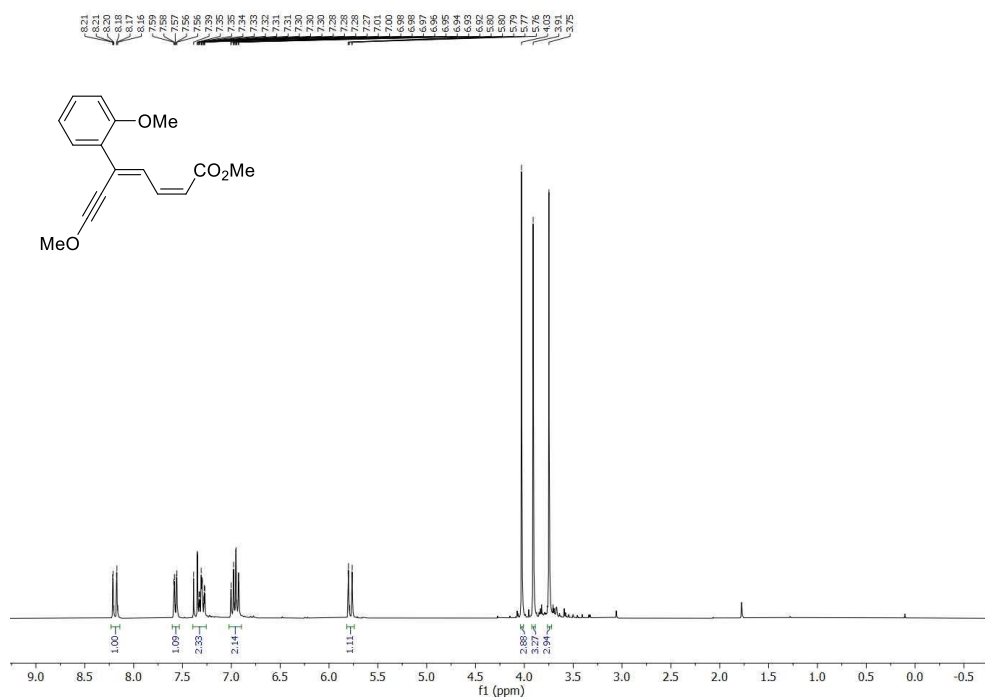
Methyl (2Z,4Z)-7-methoxy-5-(*p*-tolyl)hepta-2,4-dien-6-ynoate (2.1b)



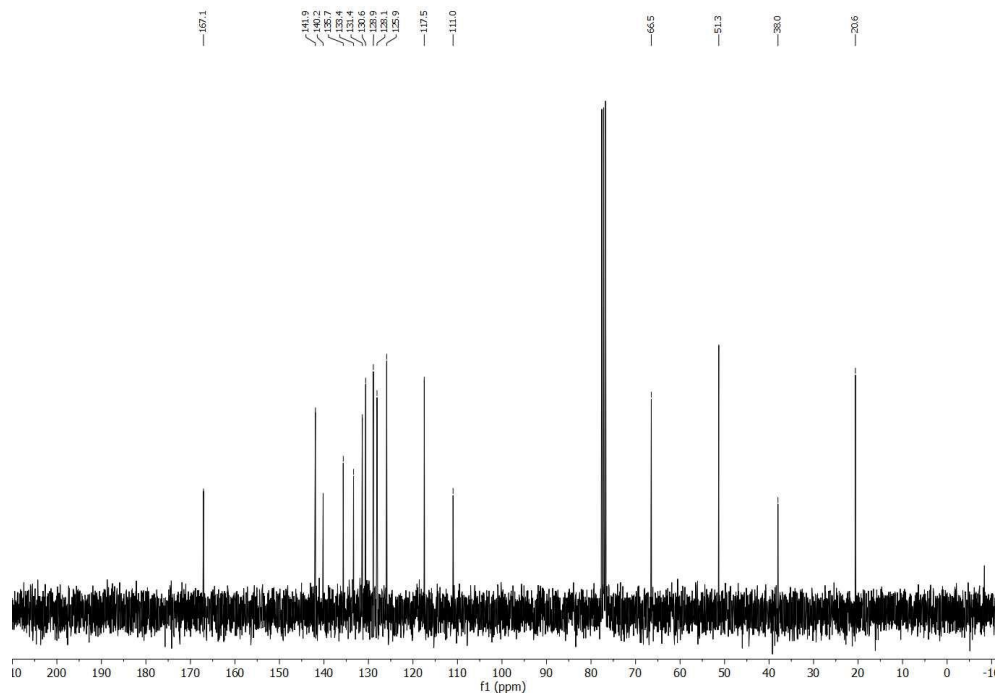
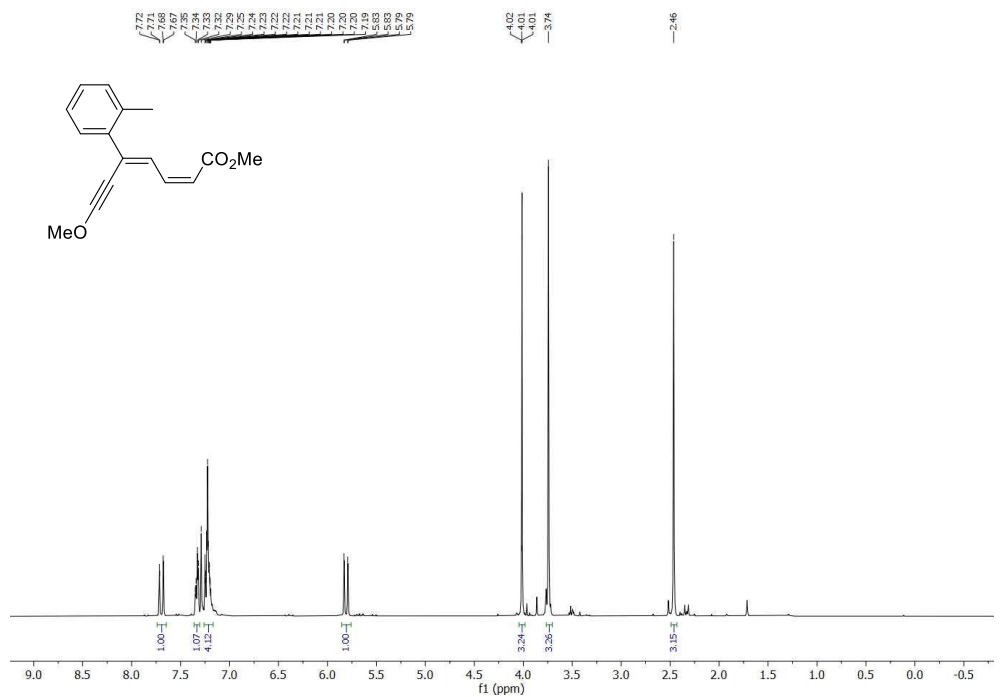
Methyl (2Z,4Z)-5-(4-bromophenyl)-7-methoxyhepta-2,4-dien-6-ynoate (2.1e)

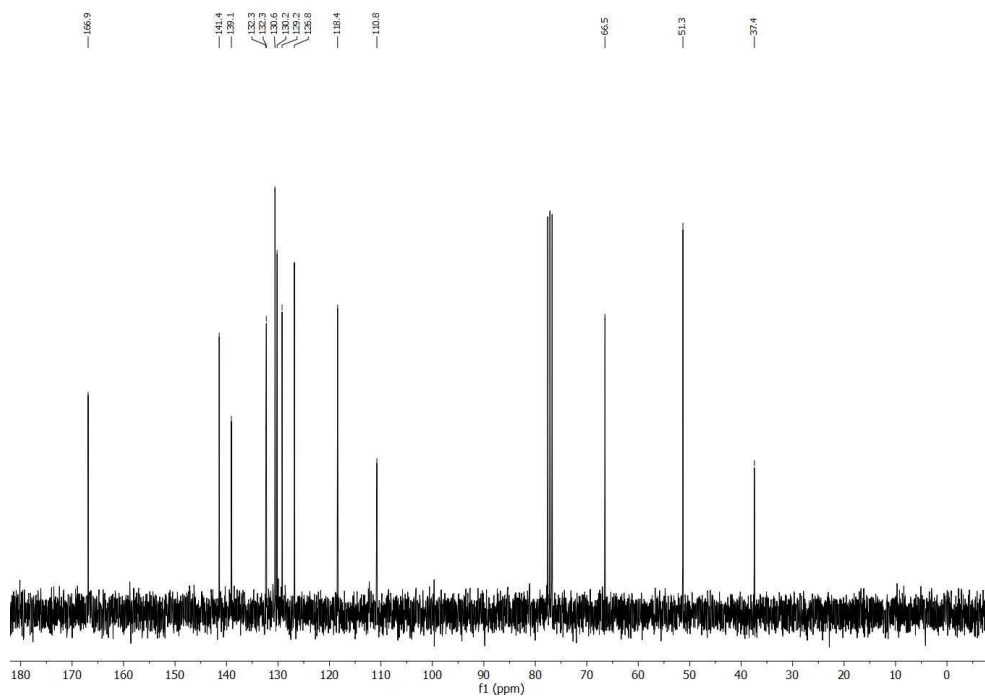
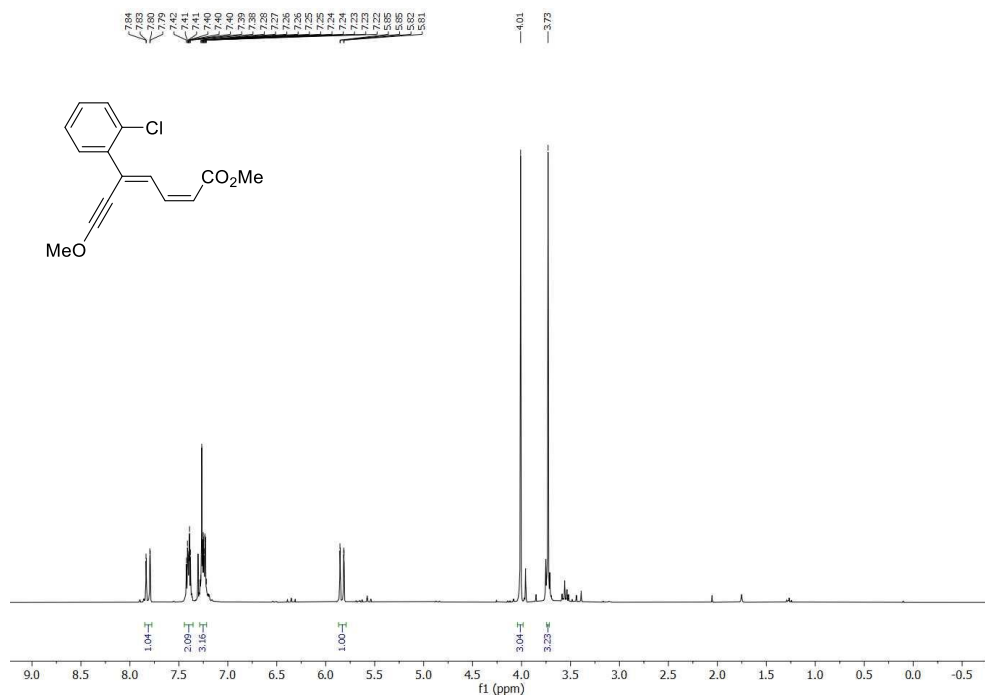
Methyl (2Z,4Z)-7-methoxy-5-(4-(trifluoromethyl)phenyl)hepta-2,4-dien-6-ynoate (2.1f)



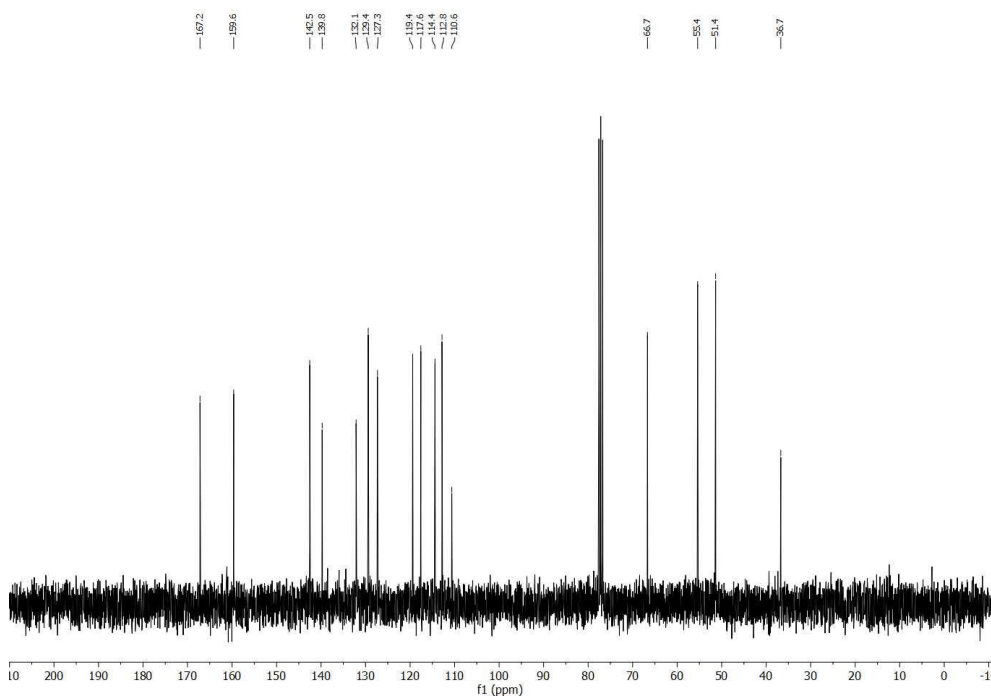
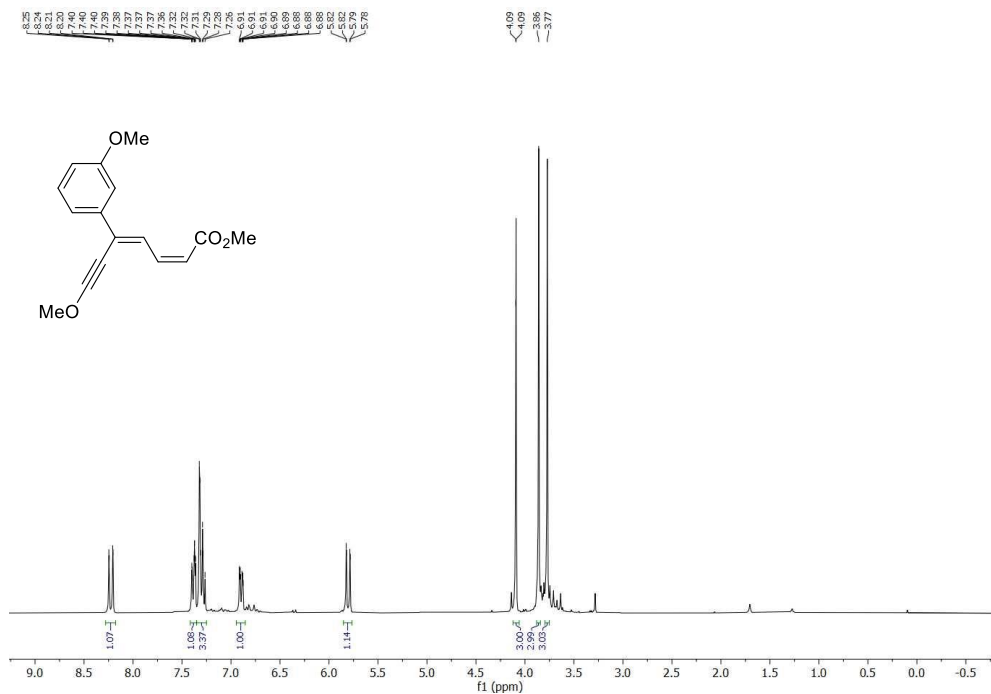
Methyl (2Z,4Z)-7-methoxy-5-(2-methoxyphenyl)hepta-2,4-dien-6-ynoate (2.1g)

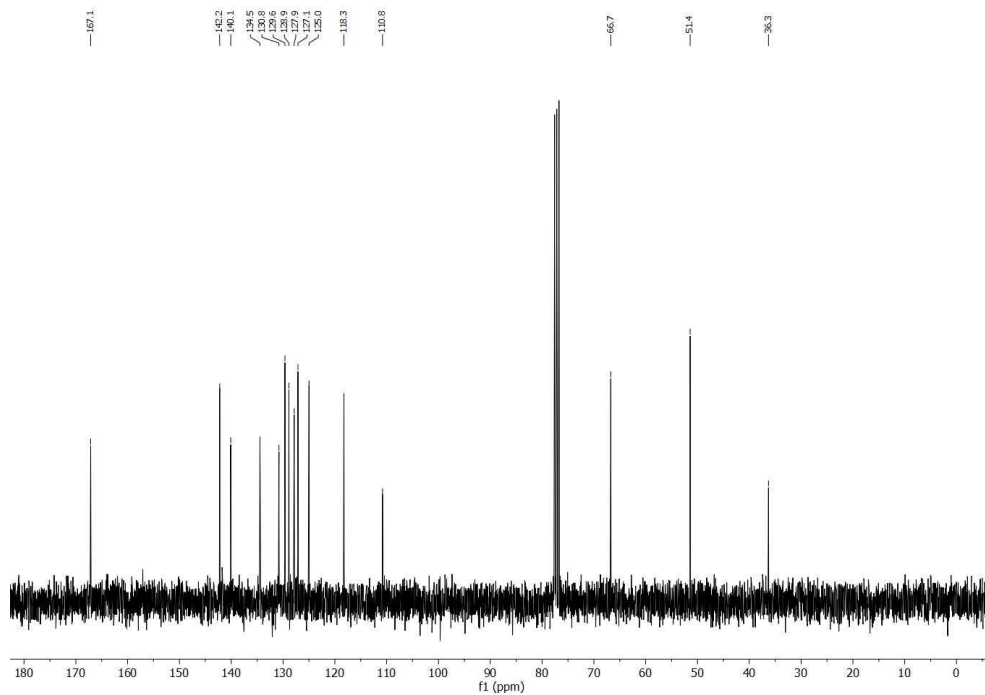
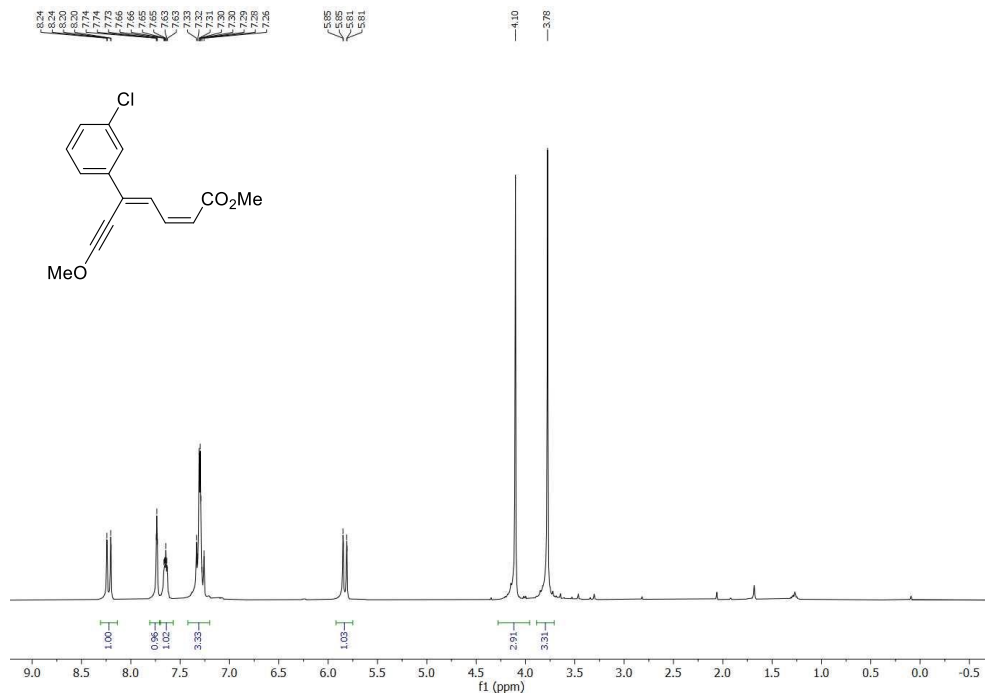
Methyl (2Z,4Z)-7-methoxy-5-(*o*-tolyl)hepta-2,4-dien-6-ynoate (2.1h)



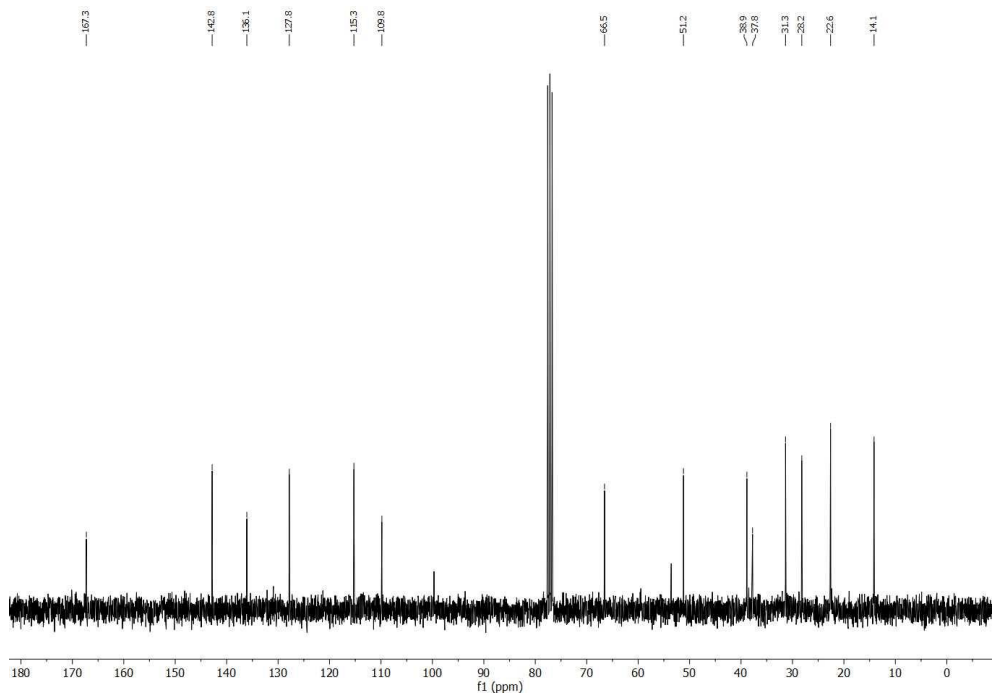
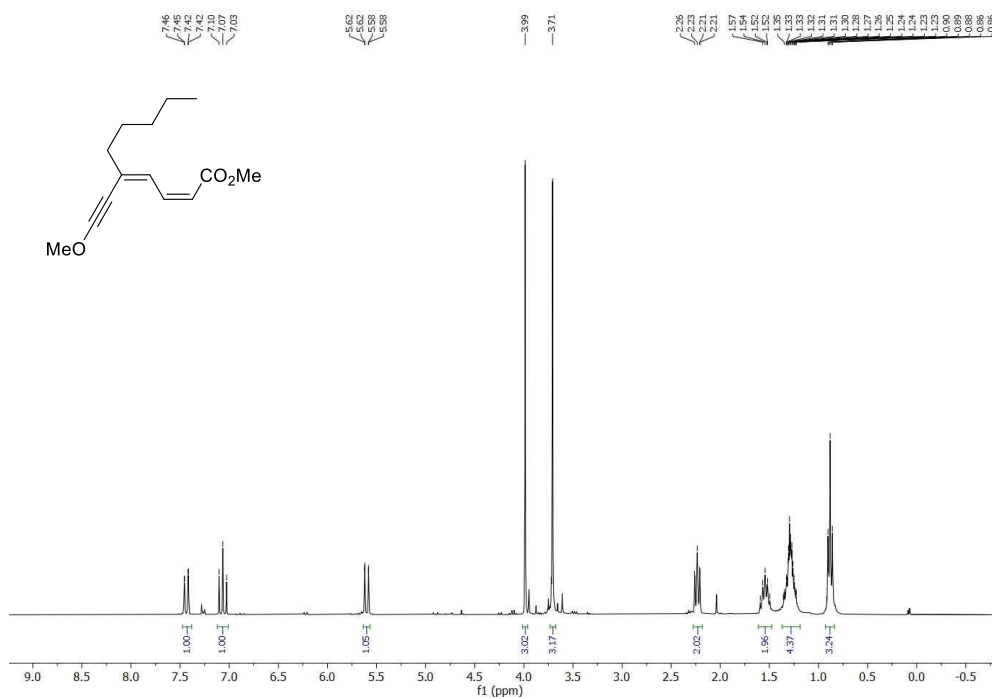
Methyl (2Z,4Z)-5-(2-chlorophenyl)-7-methoxyhepta-2,4-dien-6-ynoate (2.1i)

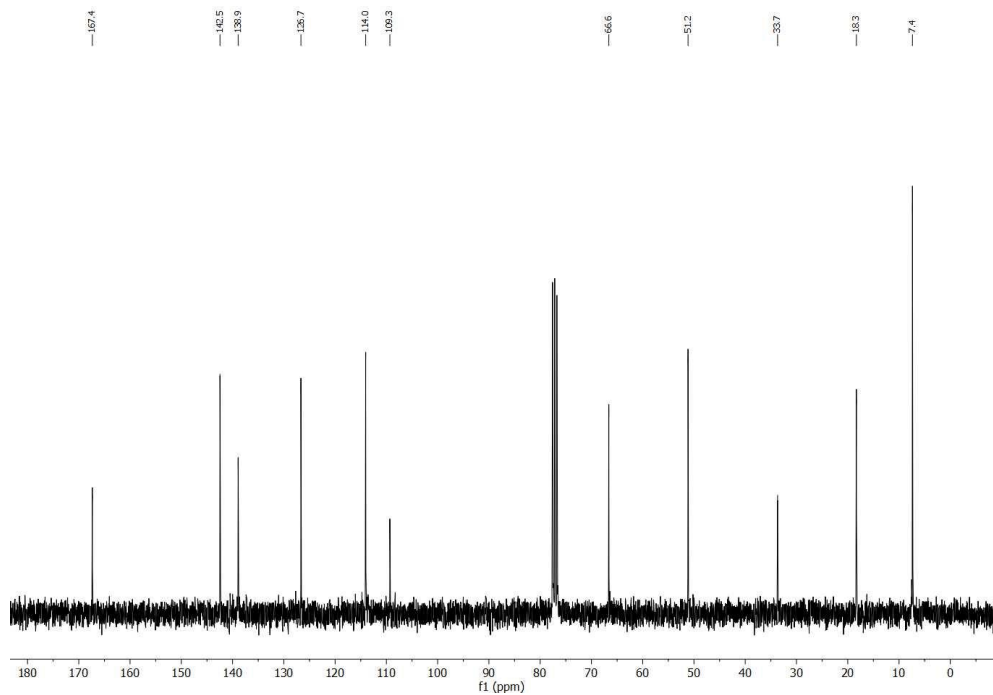
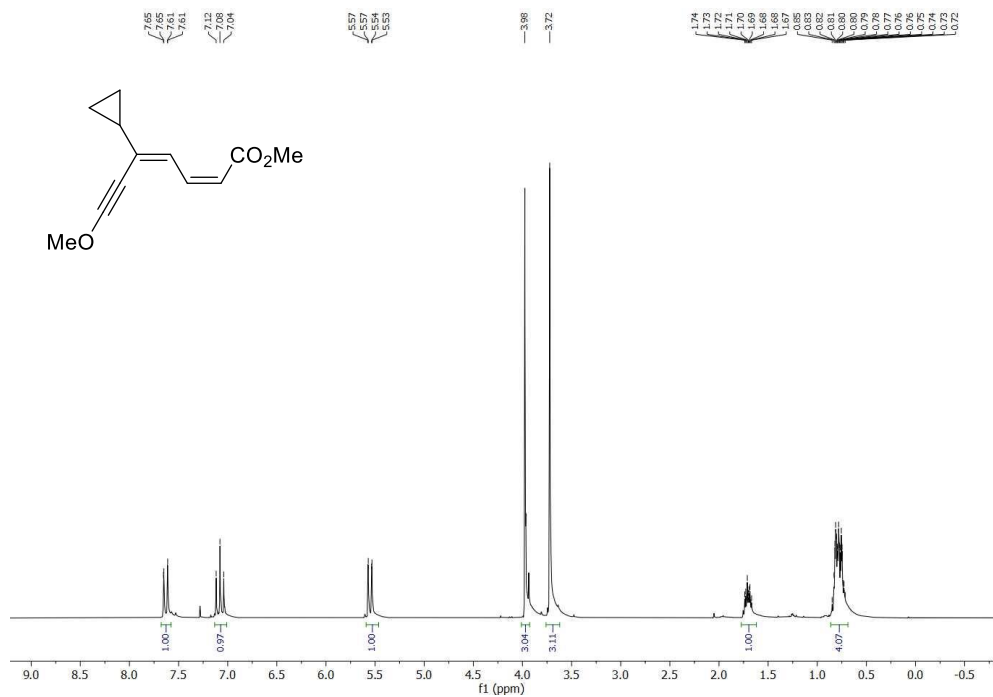
Methyl (2Z,4Z)-7-methoxy-5-(3-methoxyphenyl)hepta-2,4-dien-6-ynoate (2.1j)



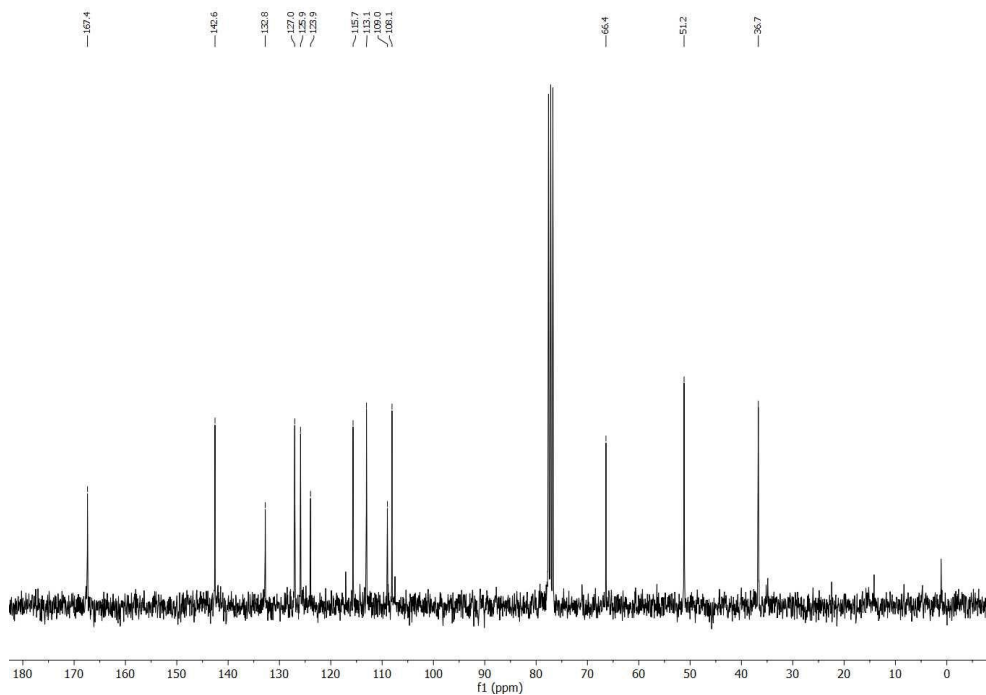
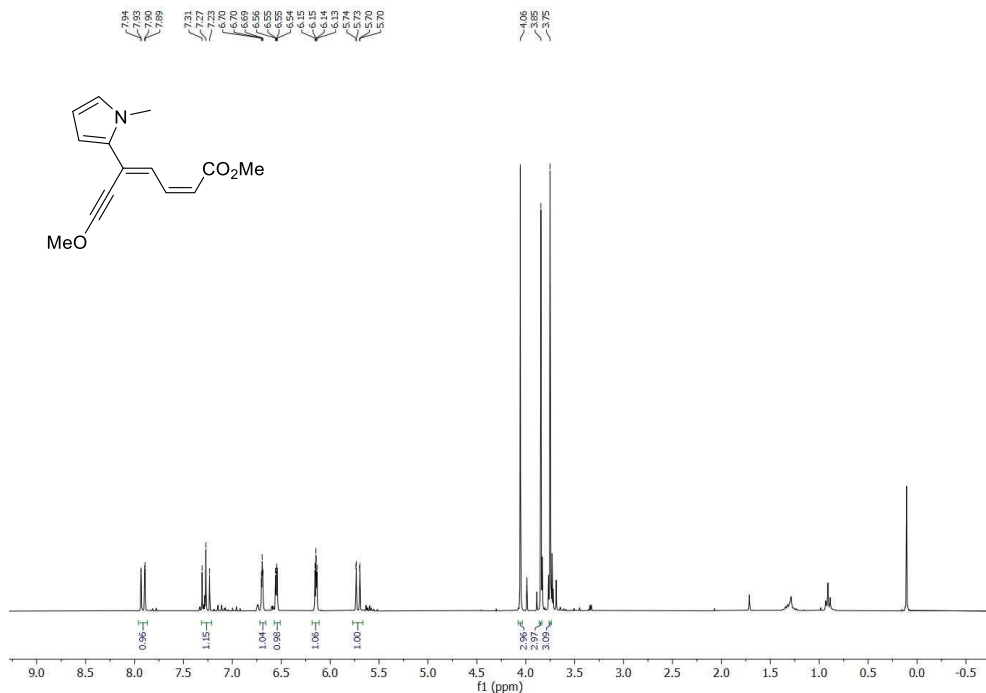
Methyl (2Z,4Z)-5-(3-chlorophenyl)-7-methoxyhepta-2,4-dien-6-ynoate (2.1k)

Methyl (2Z,4Z)-5-(methoxyethynyl)deca-2,4-dienoate (2.1I)

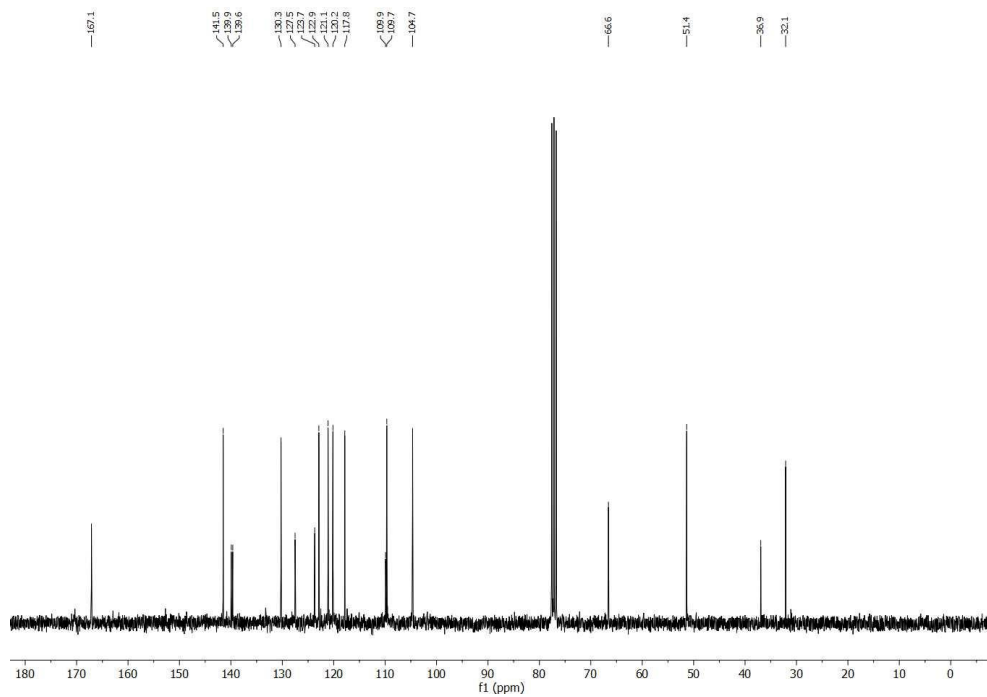
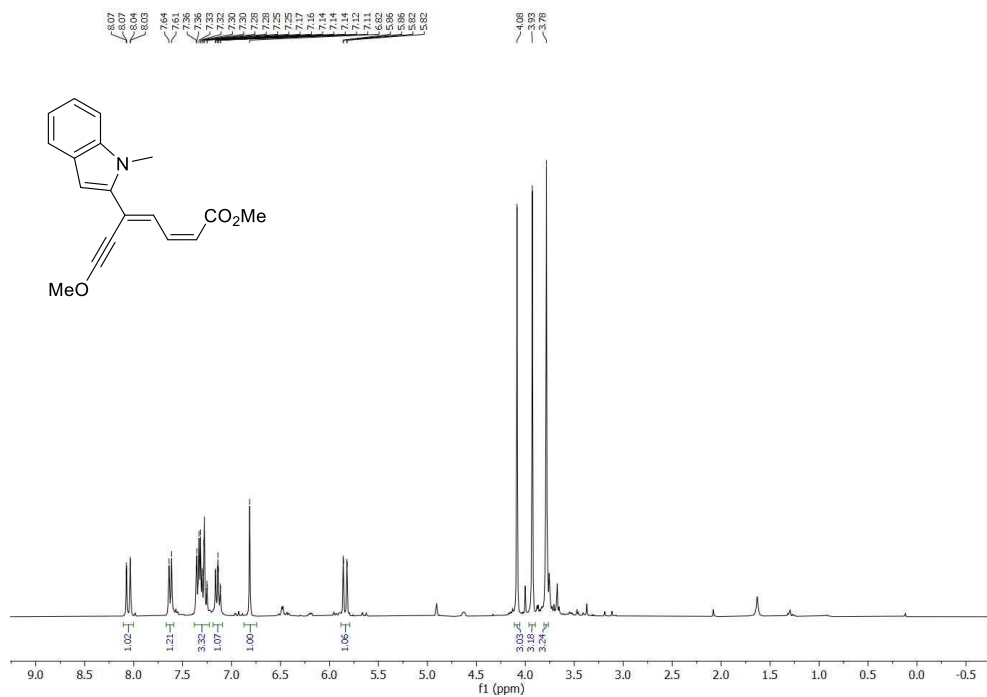


Methyl (2Z,4Z)-5-cyclopropyl-7-methoxyhepta-2,4-dien-6-ynoate (2.1m)

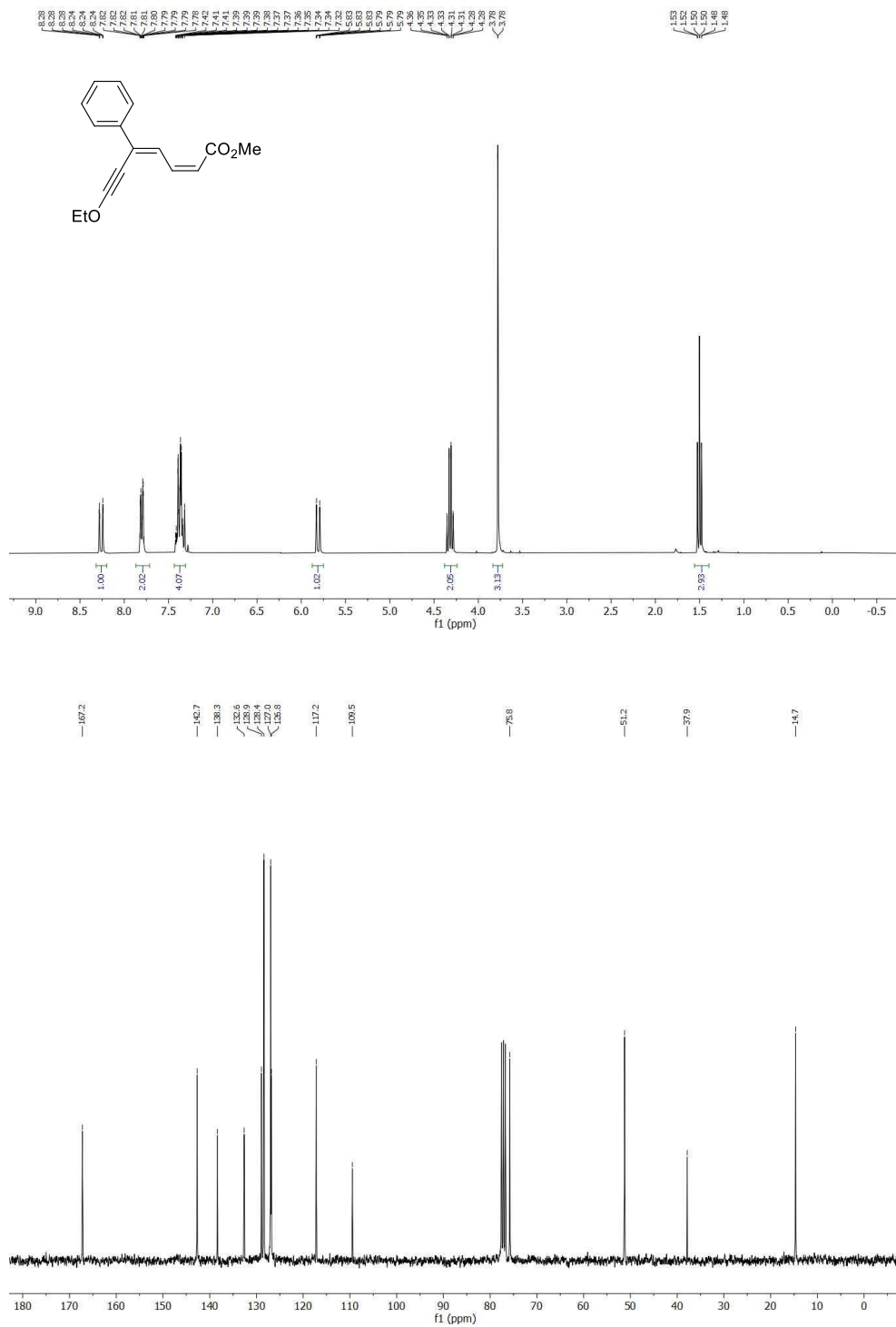
Methyl (2Z,4E)-7-methoxy-5-(1-methyl-1H-pyrrol-2-yl)hepta-2,4-dien-6-ynoate (2.1p)



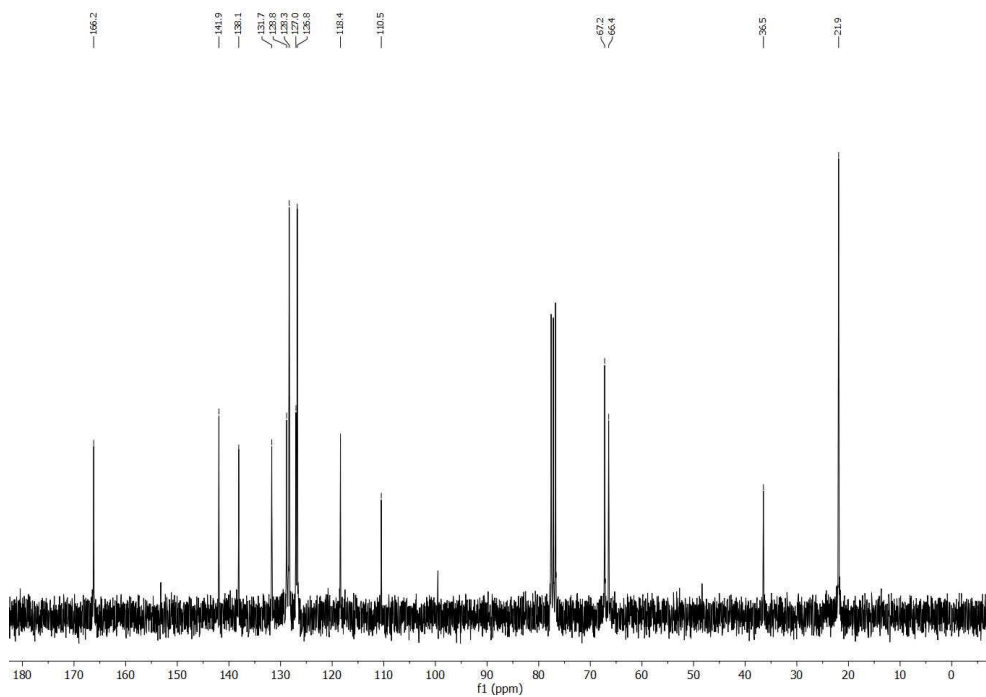
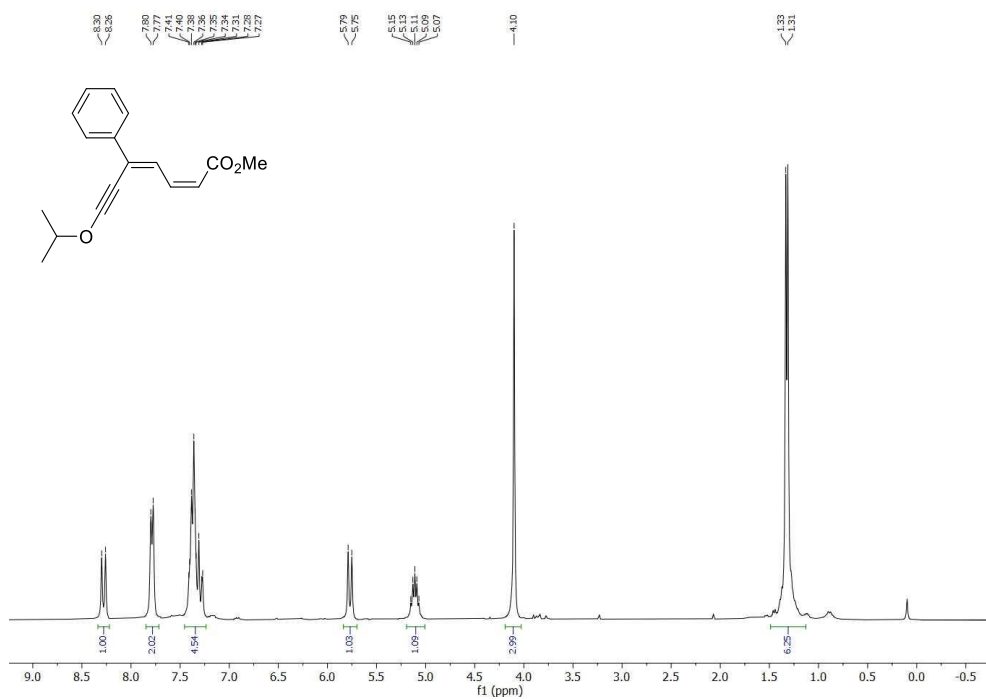
Methyl (2Z,4E)-7-methoxy-5-(1-methyl-1H-indol-2-yl)hepta-2,4-dien-6-ynoate (2.1r)



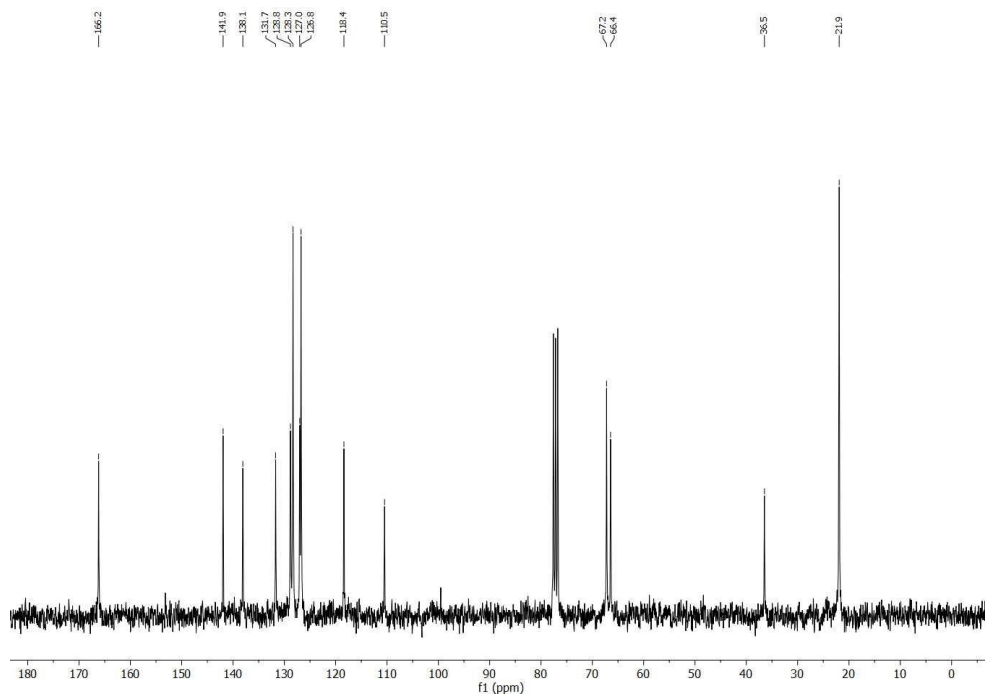
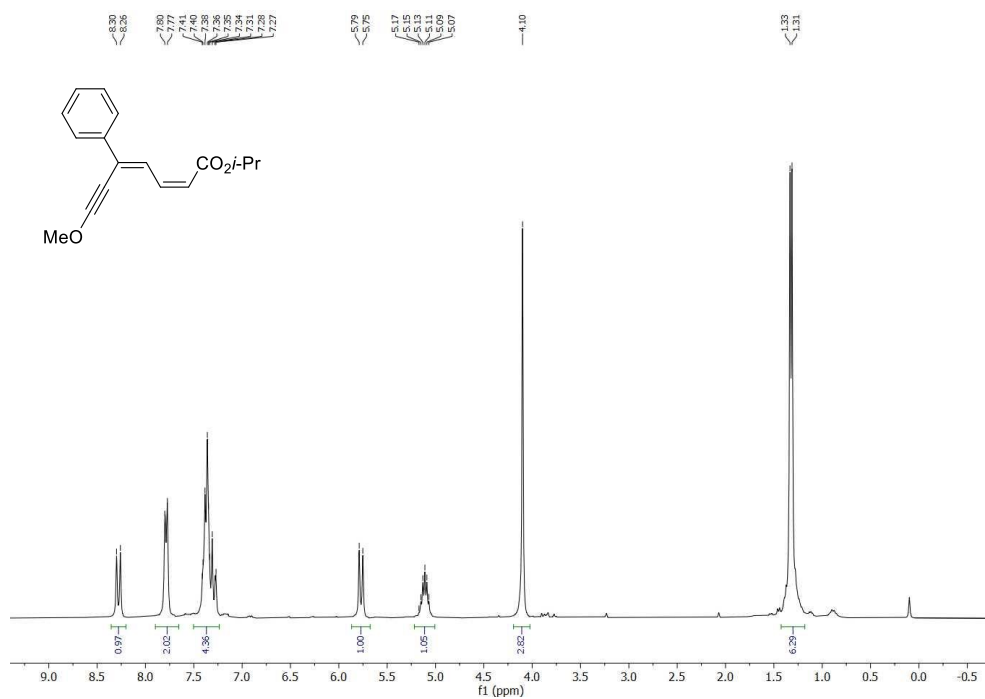
Methyl (2Z,4Z)-7-ethoxy-5-phenylhepta-2,4-dien-6-ynoate (2.1t)



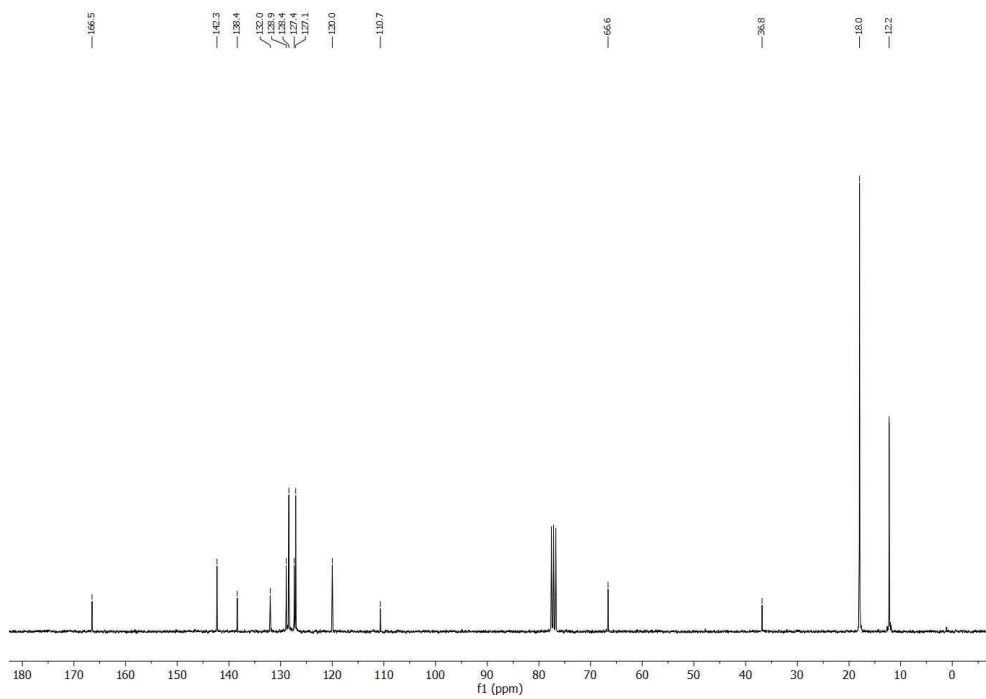
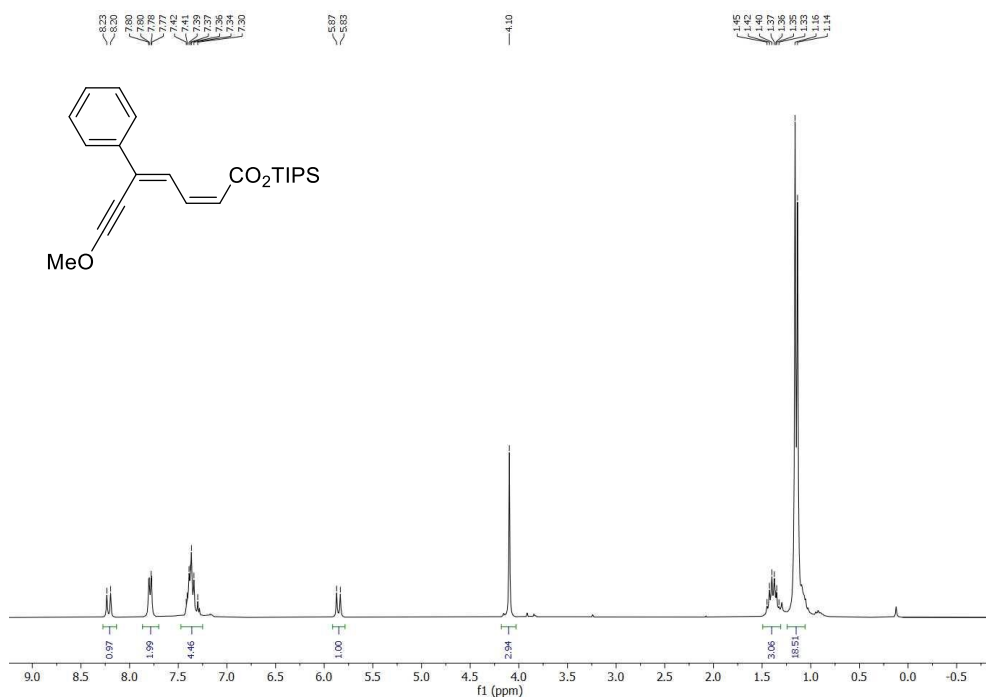
Methyl (2Z,4Z)-7-isopropoxy-5-phenylhepta-2,4-dien-6-ynoate (2.1u)

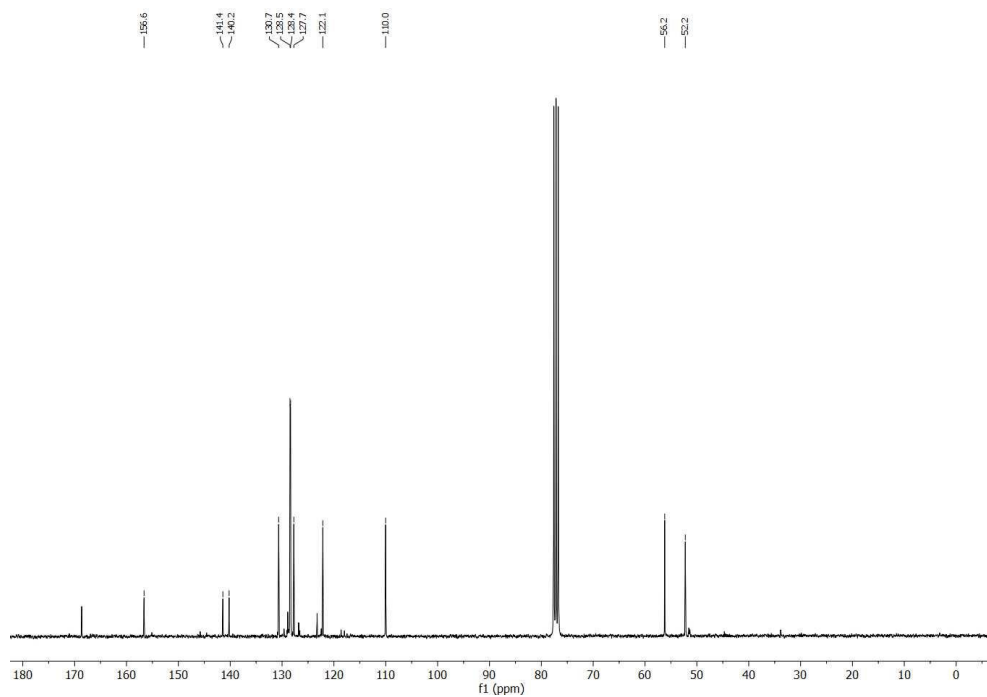
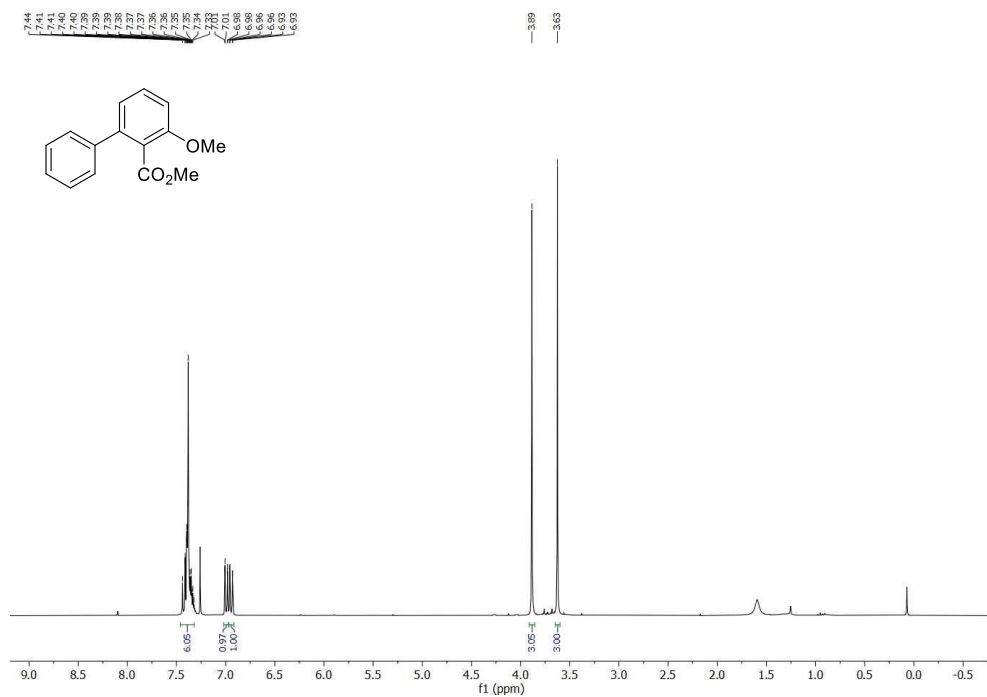


Isopropyl (2Z,4Z)-7-methoxy-5-phenylhepta-2,4-dien-6-ynoate (2.1v)

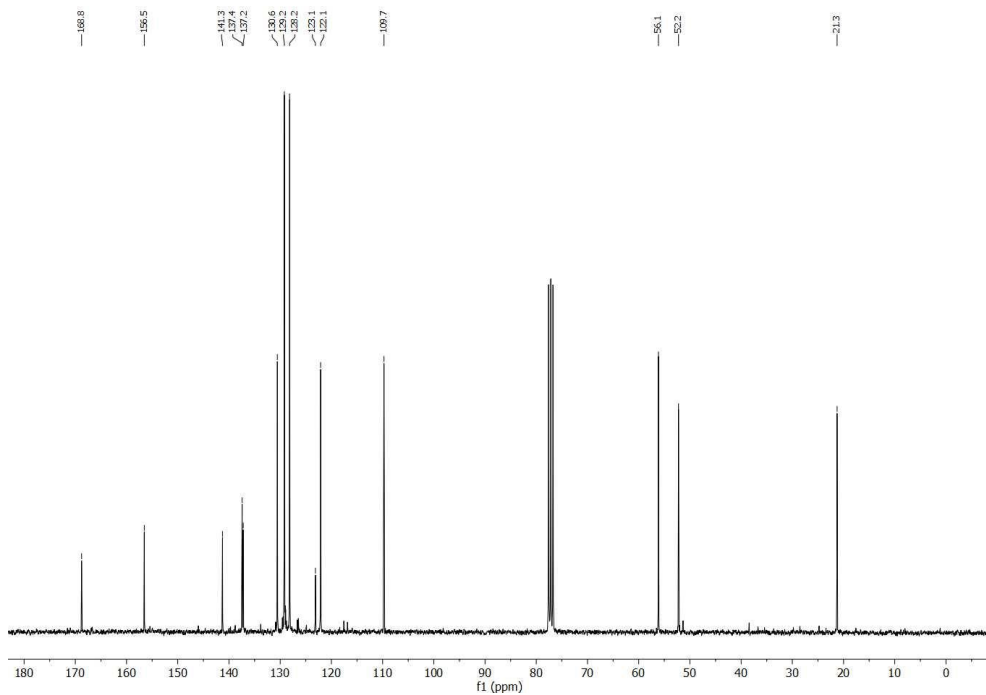
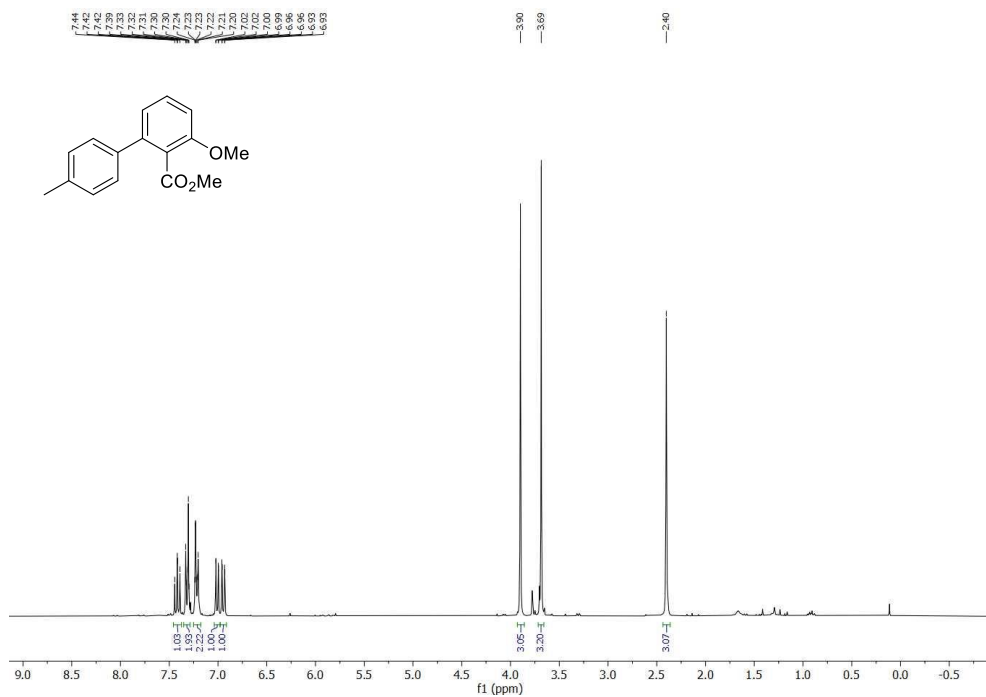


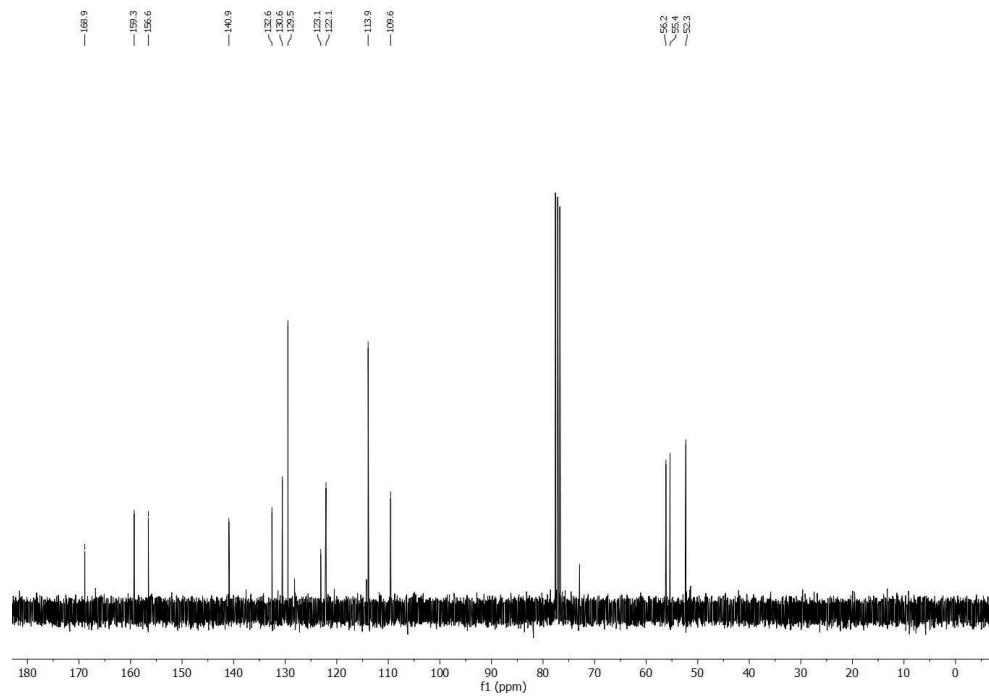
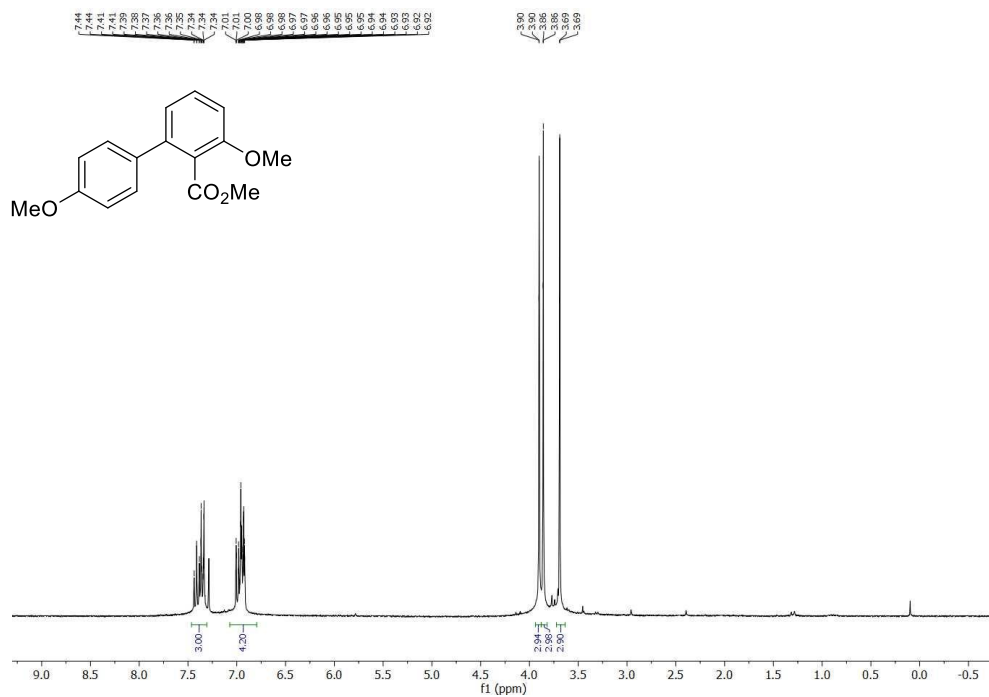
Triisopropylsilyl (2Z,4Z)-7-methoxy-5-phenylhepta-2,4-dien-6-ynoate (2.1w)



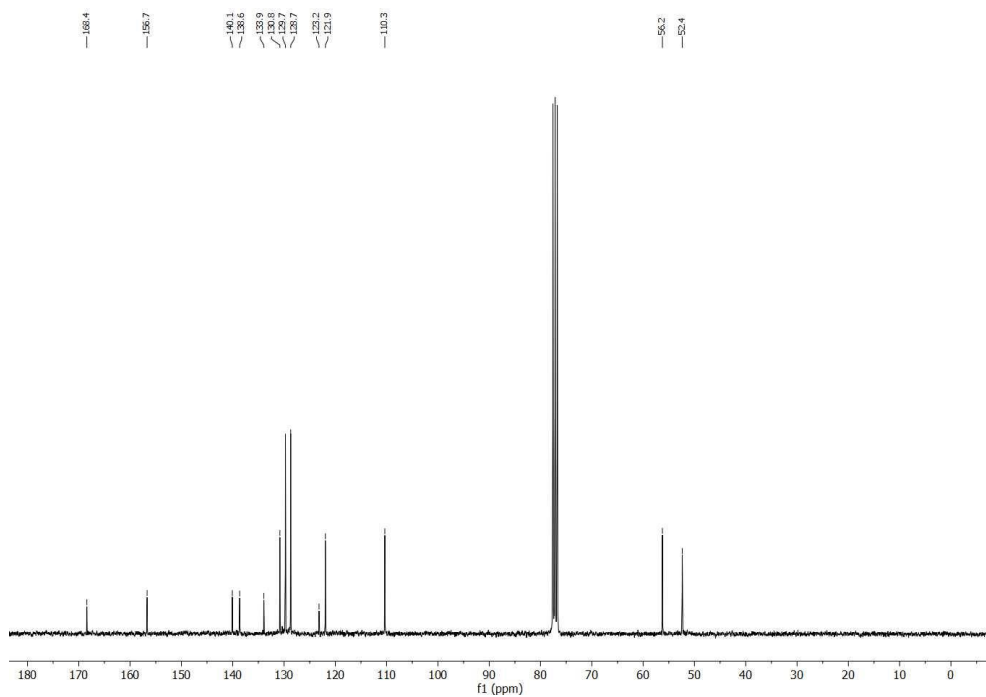
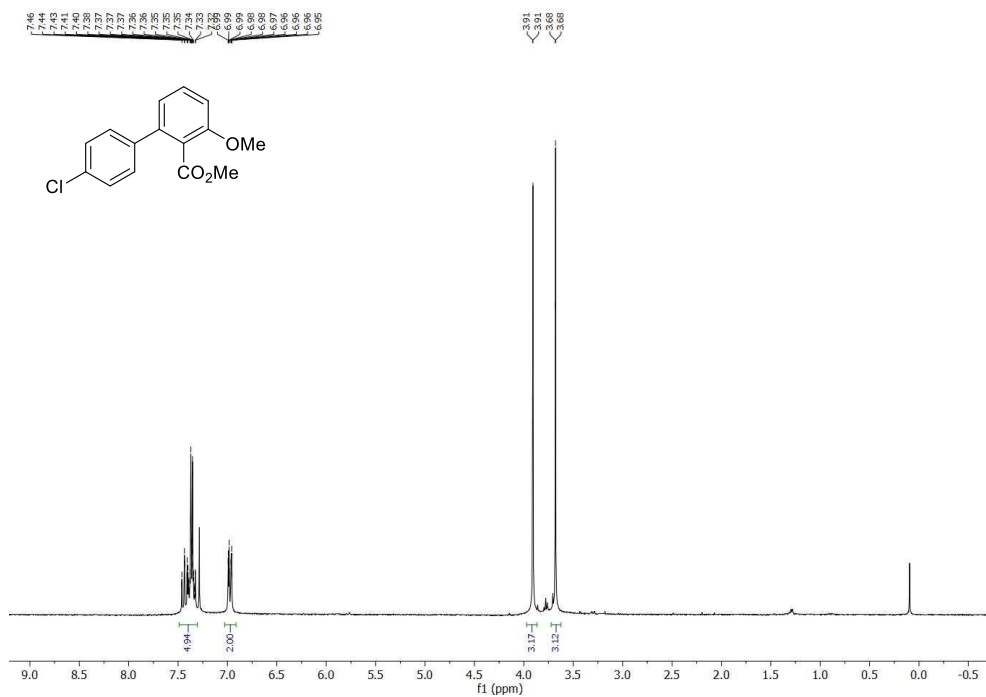
Methyl 3-methoxy-[1,1'-biphenyl]-2-carboxylate (2.2a)

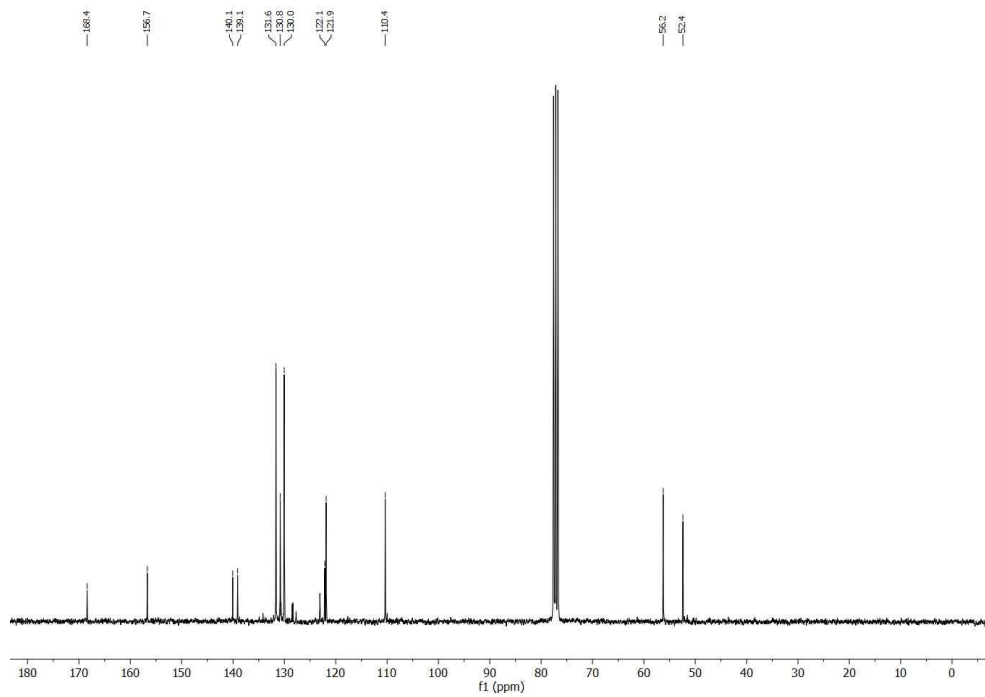
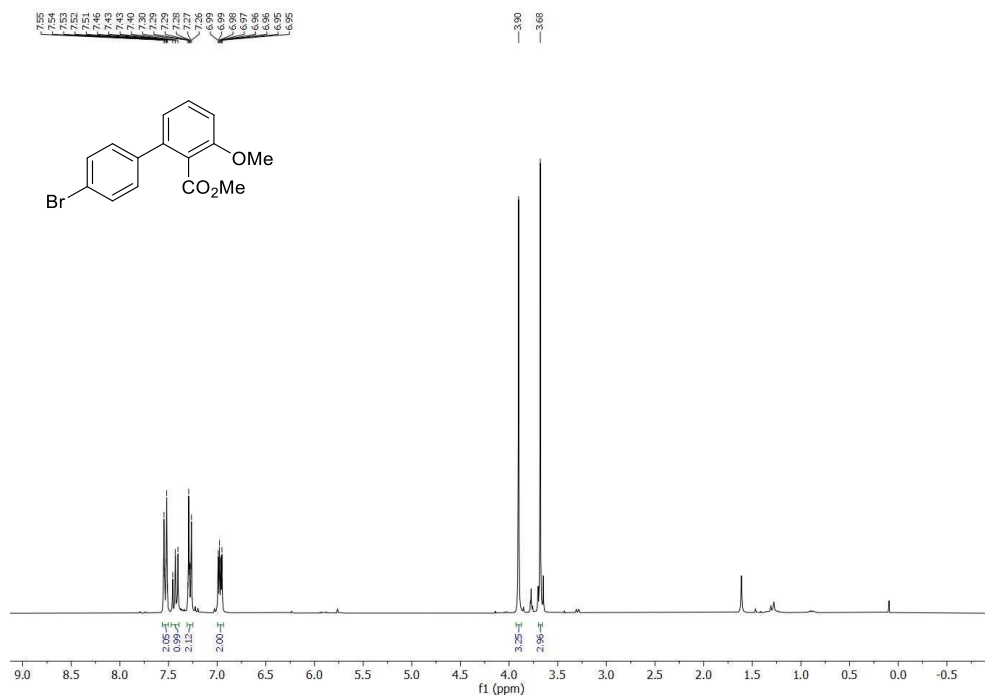
Methyl 3-methoxy-4'-methyl-[1,1'-biphenyl]-2-carboxylate (2.2b)



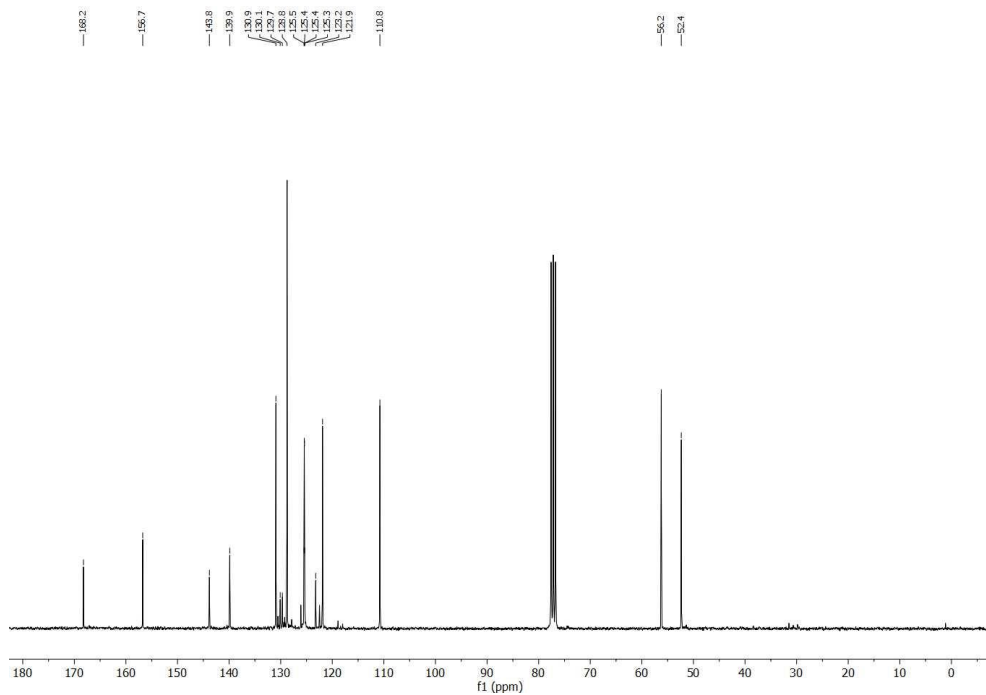
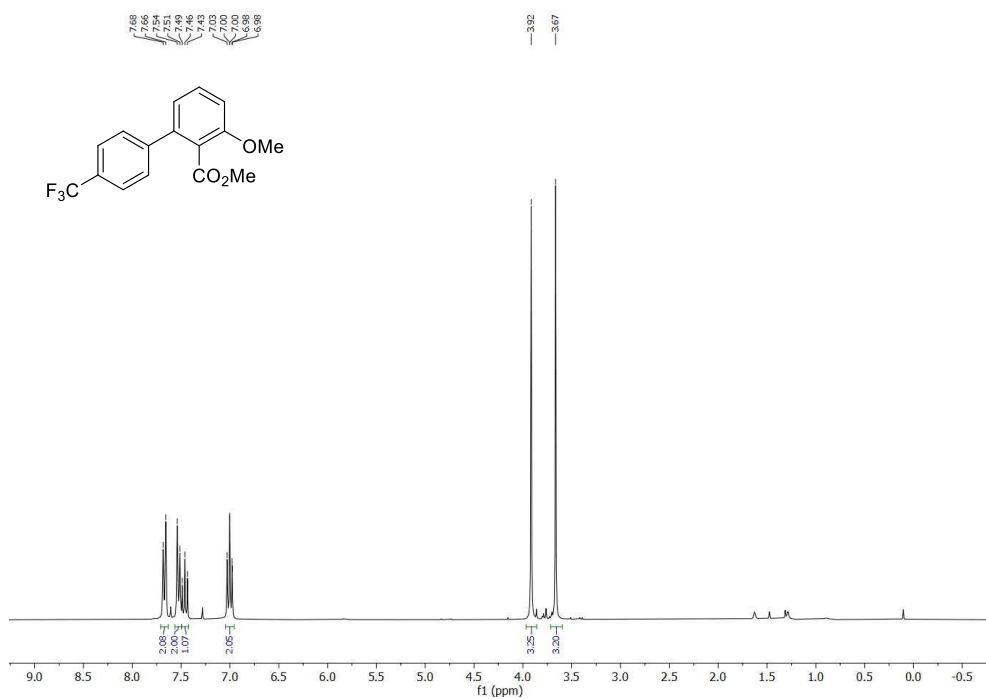
Methyl 3,4'-dimethoxy-[1,1'-biphenyl]-2-carboxylate (2.2c)

Methyl 3-methoxy-4'-chloro-[1,1'-biphenyl]-2-carboxylate (2.2d)

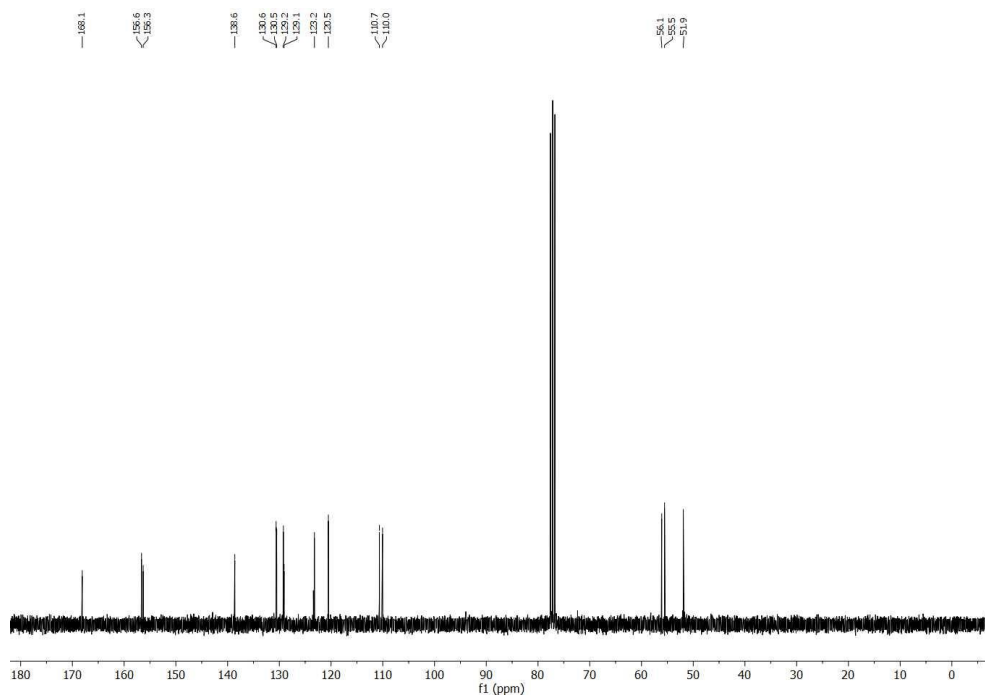
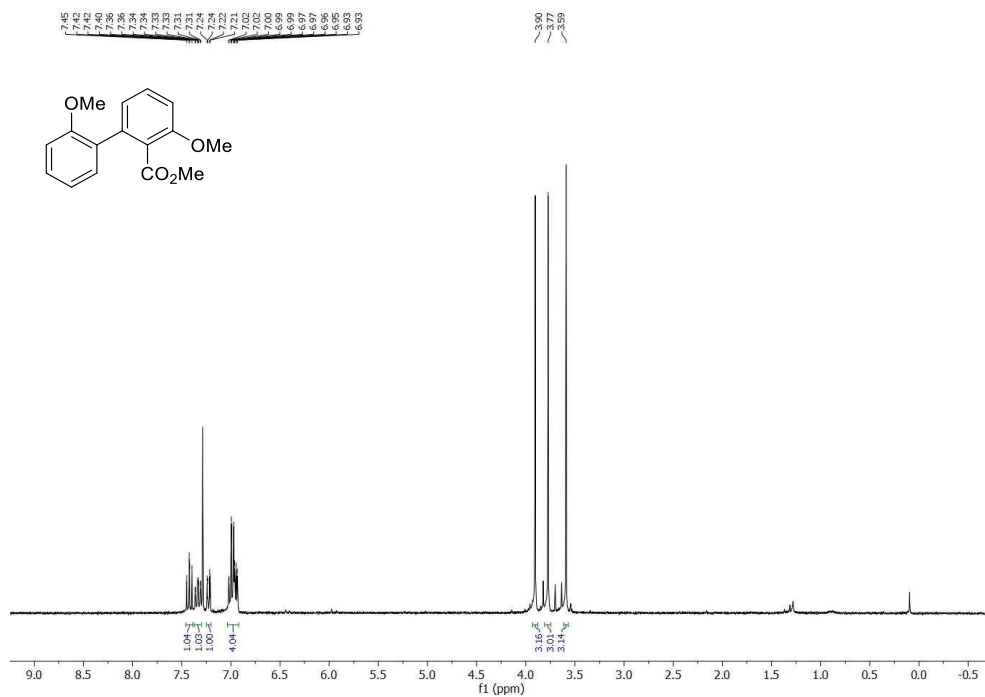


Methyl 3-methoxy-4'-bromo-[1,1'-biphenyl]-2-carboxylate (2.2e)

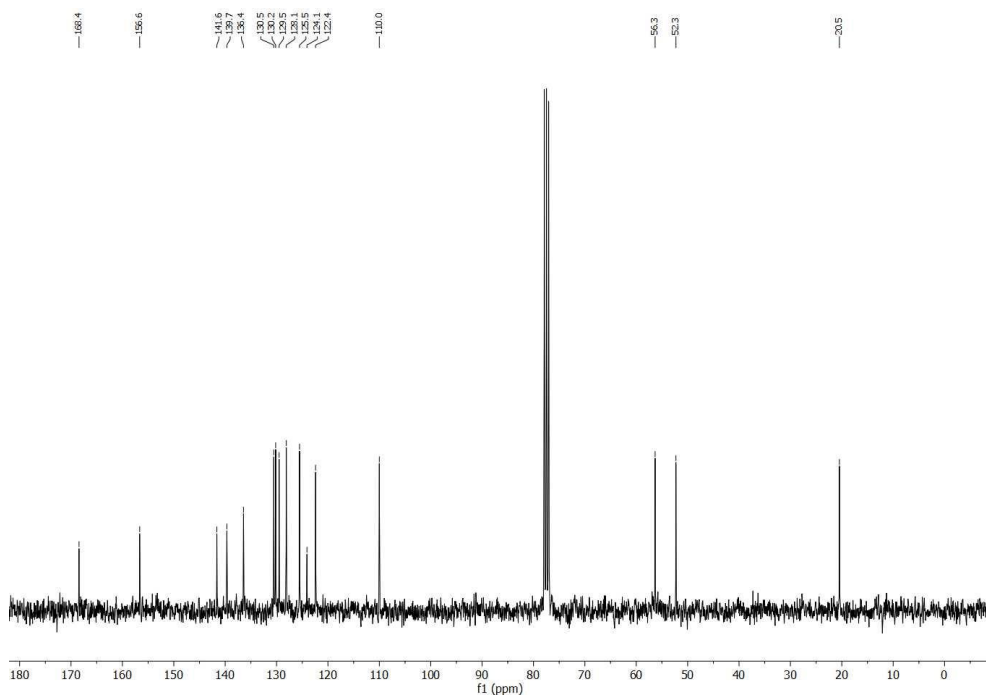
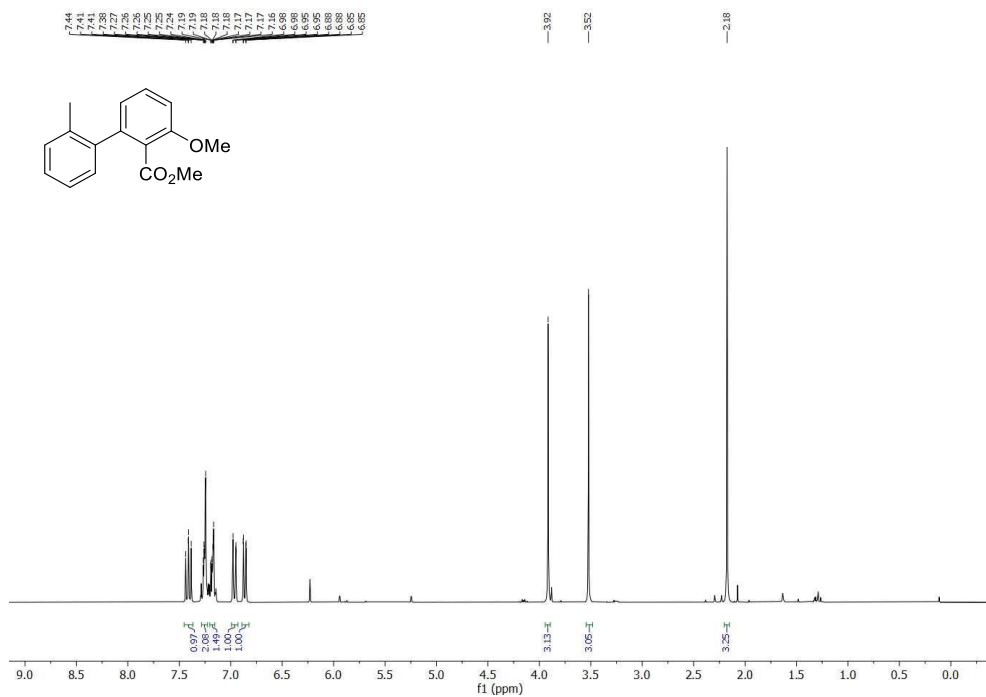
Methyl 3-methoxy-4'-trifluoromethyl-[1,1'-biphenyl]-2-carboxylate (2.2f)

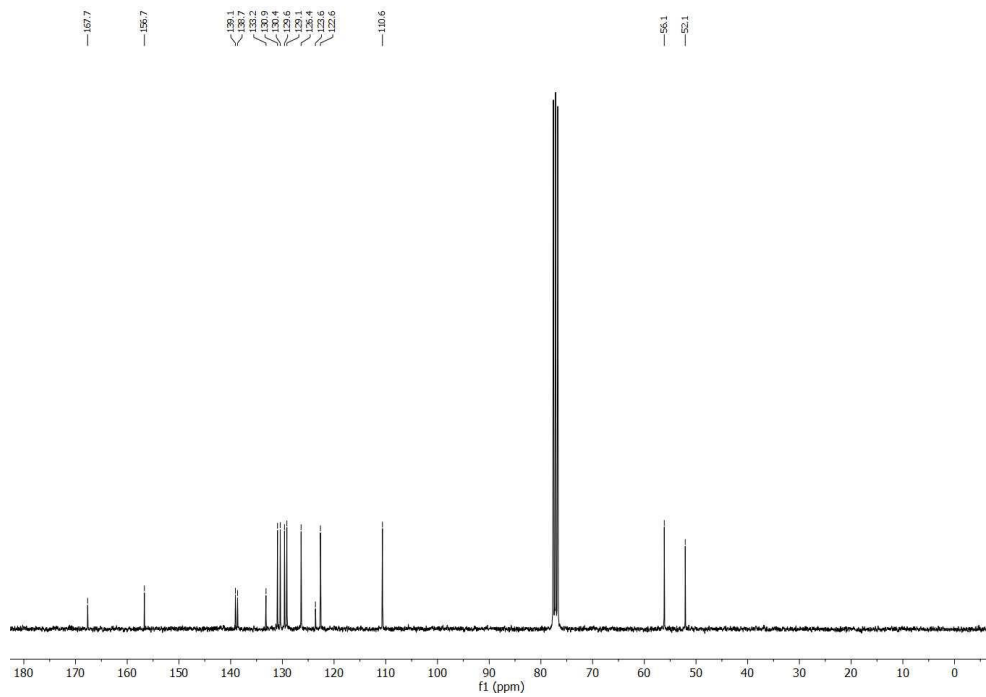
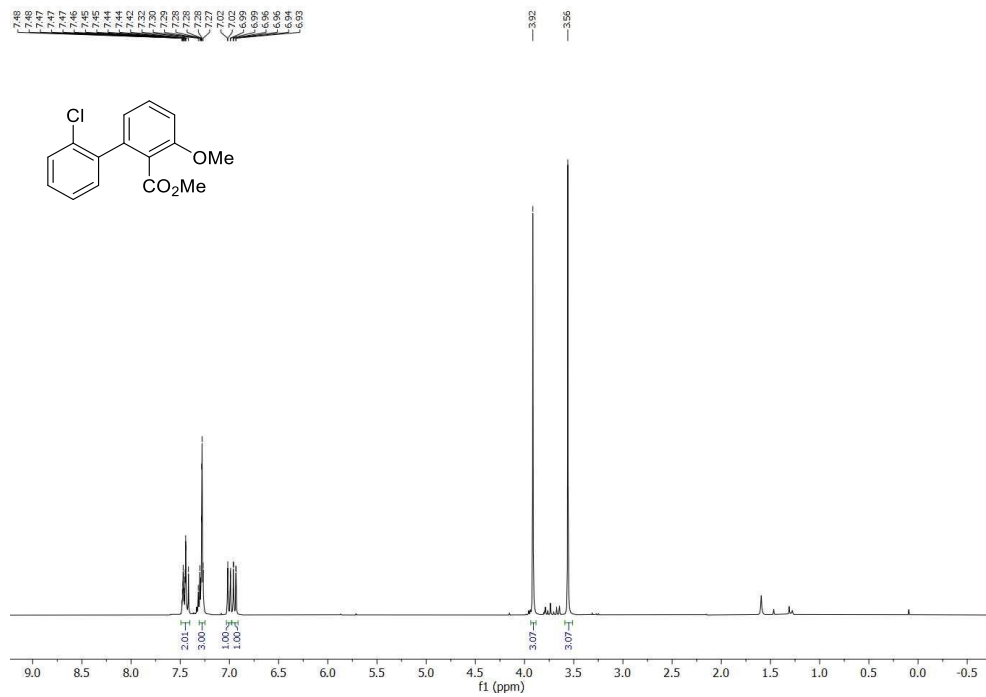


Methyl 2',3-dimethoxy-[1,1'-biphenyl]-2-carboxylate (2.2g)

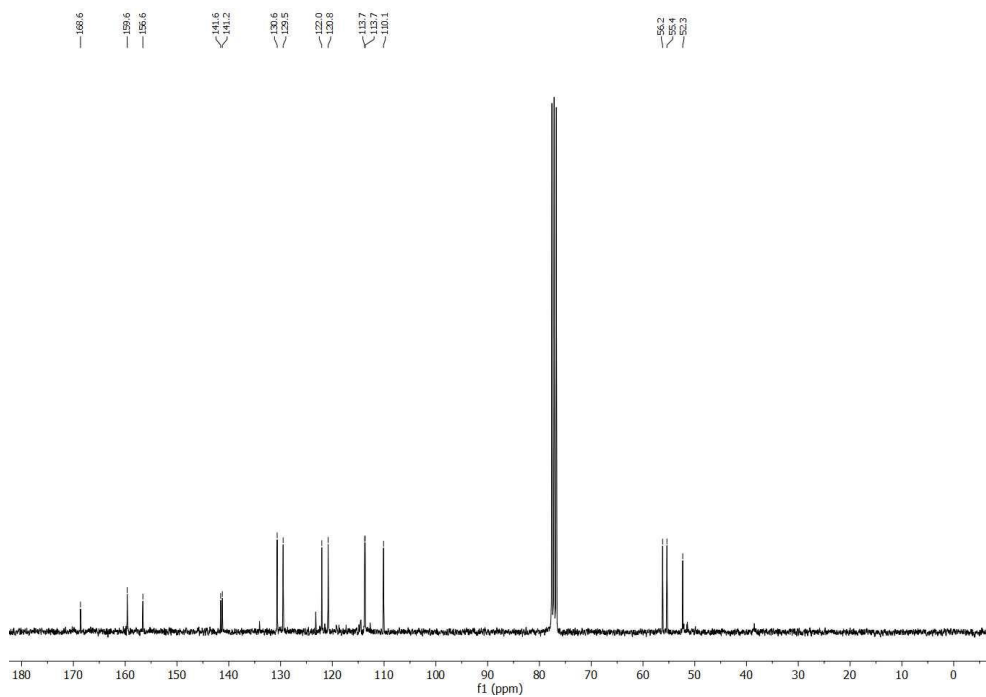
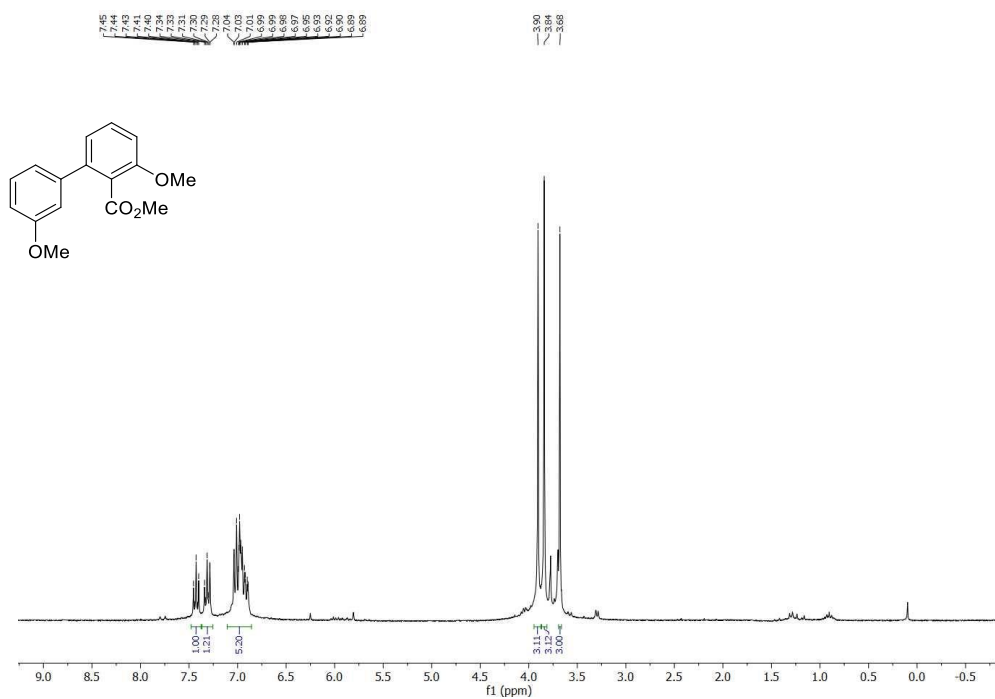


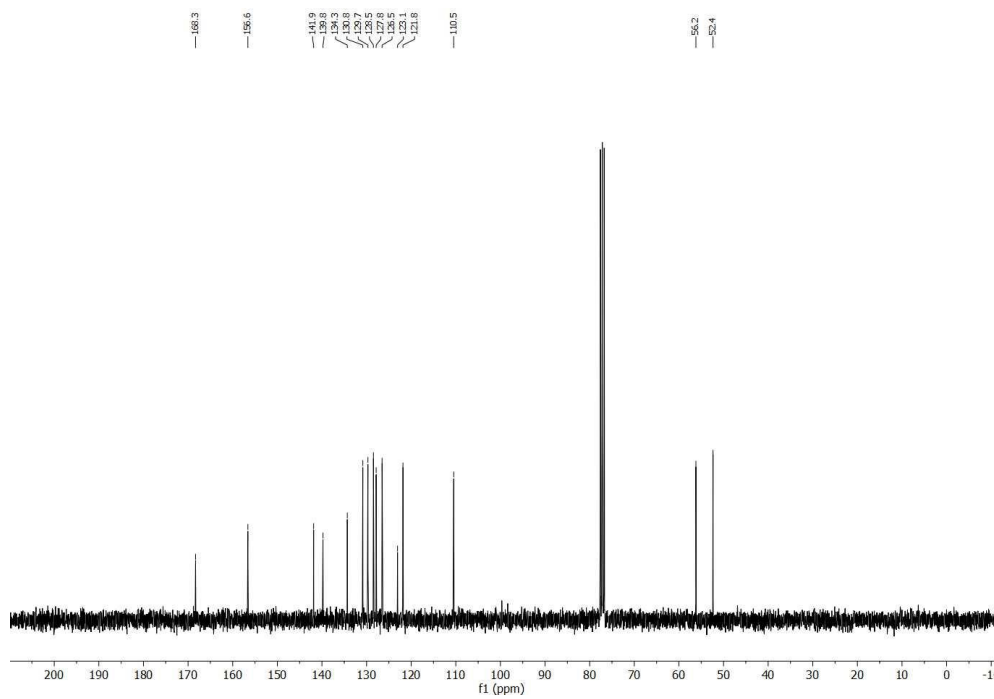
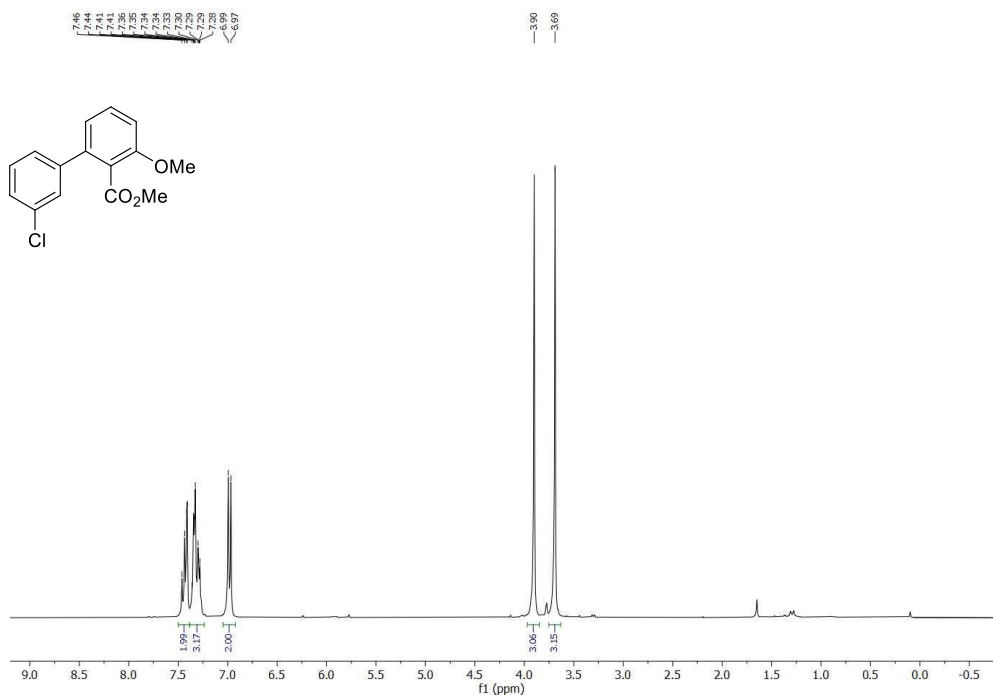
Methyl 3-methoxy-2'-methyl-[1,1'-biphenyl]-2-carboxylate (2.2h)



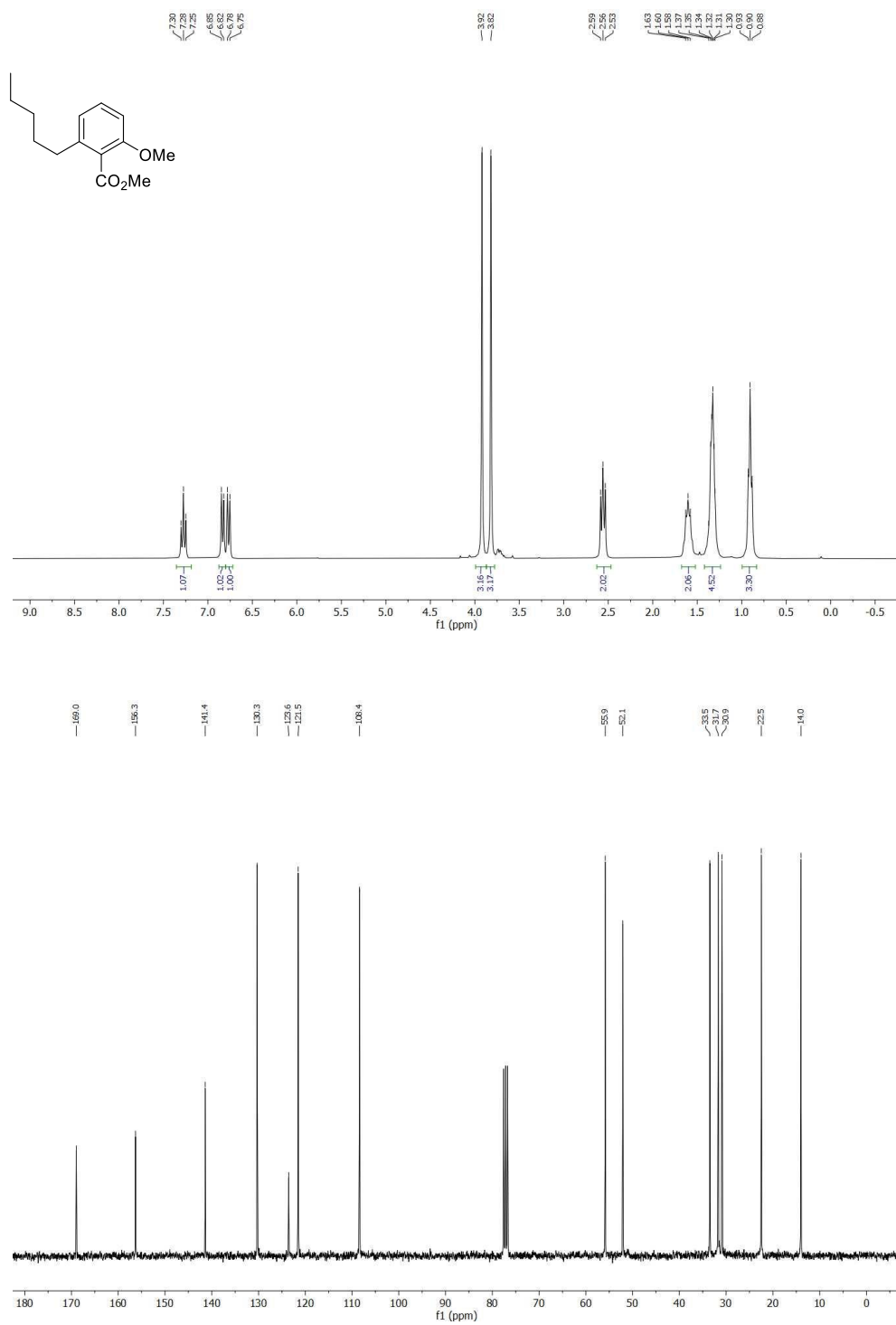
Methyl 2'-chloro-3-methoxy-[1,1'-biphenyl]-2-carboxylate (2.2i)

Methyl 3,3'-dimethoxy-[1,1'-biphenyl]-2-carboxylate (2.2j)

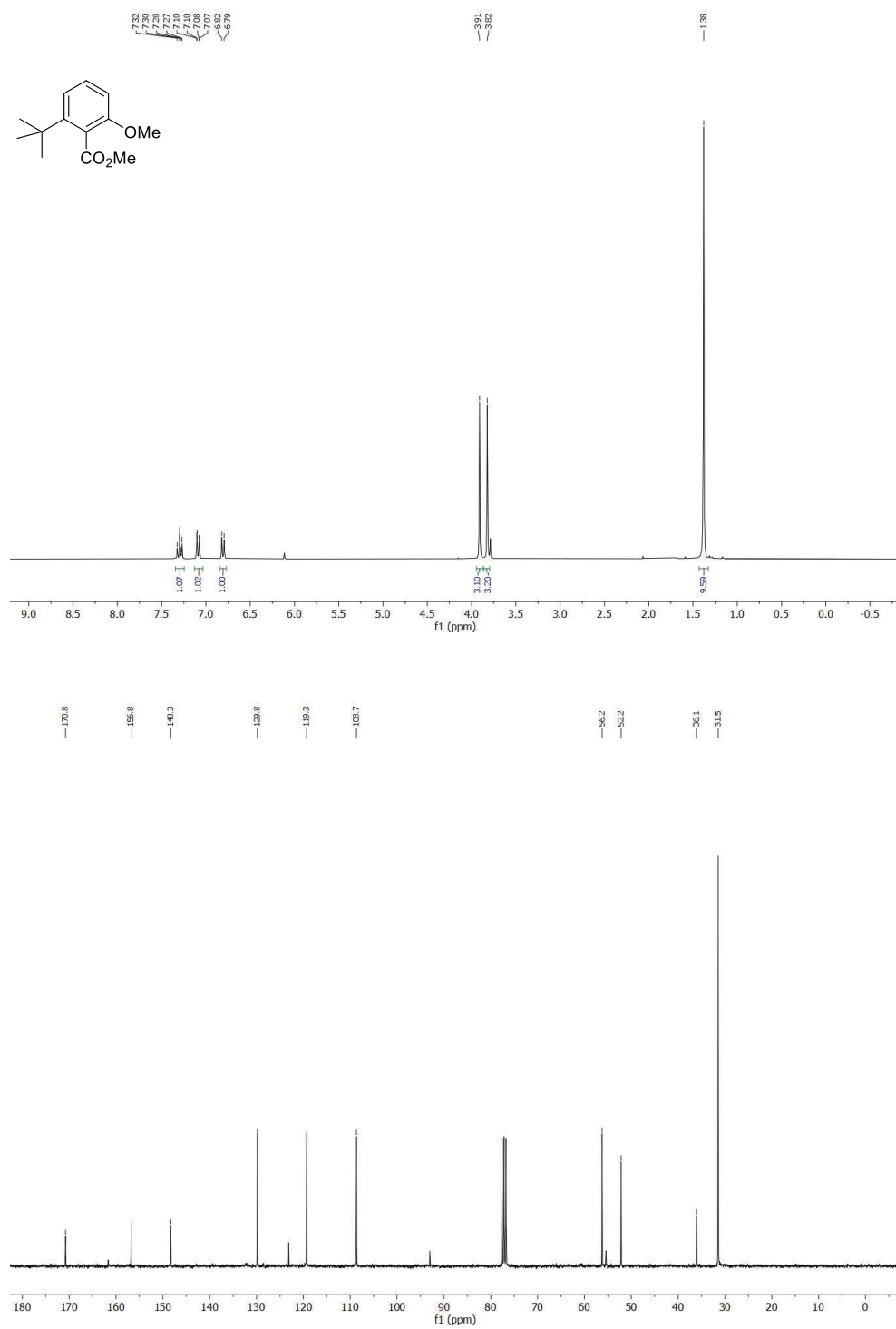


Methyl 3'-chloro-3-methoxy-[1,1'-biphenyl]-2-carboxylate (2.2k)

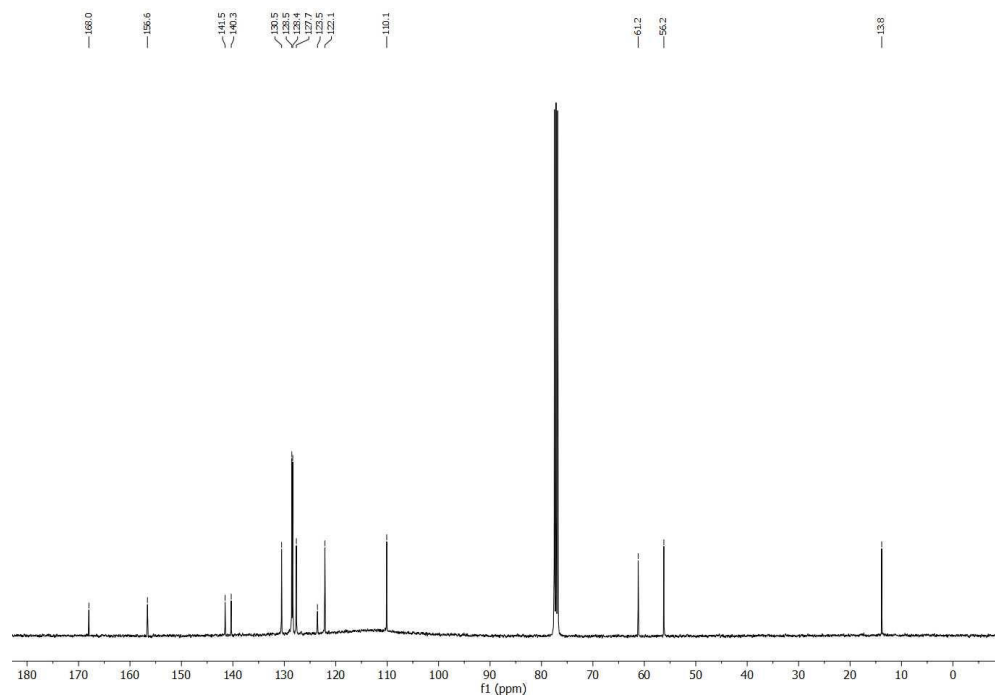
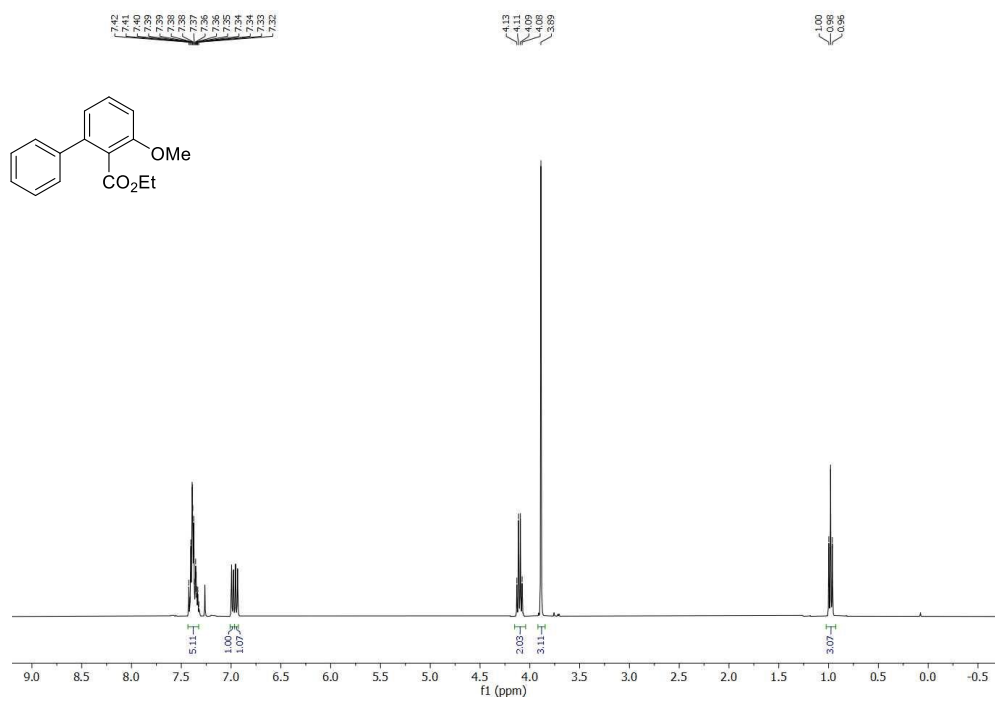
Methyl 2-methoxy-6-pentylbenzoate (2.21)



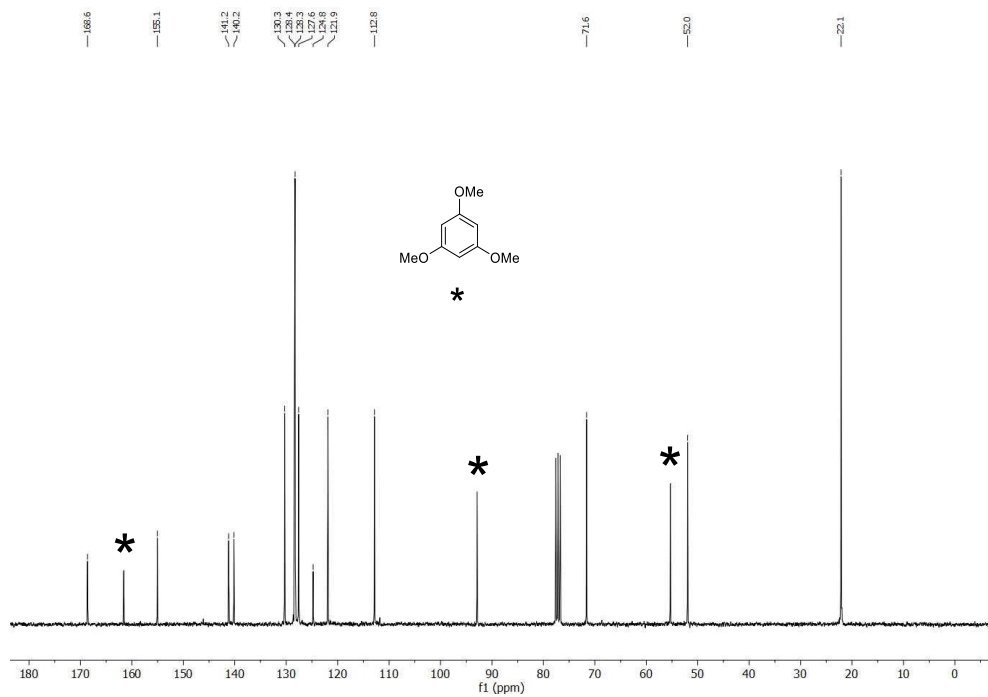
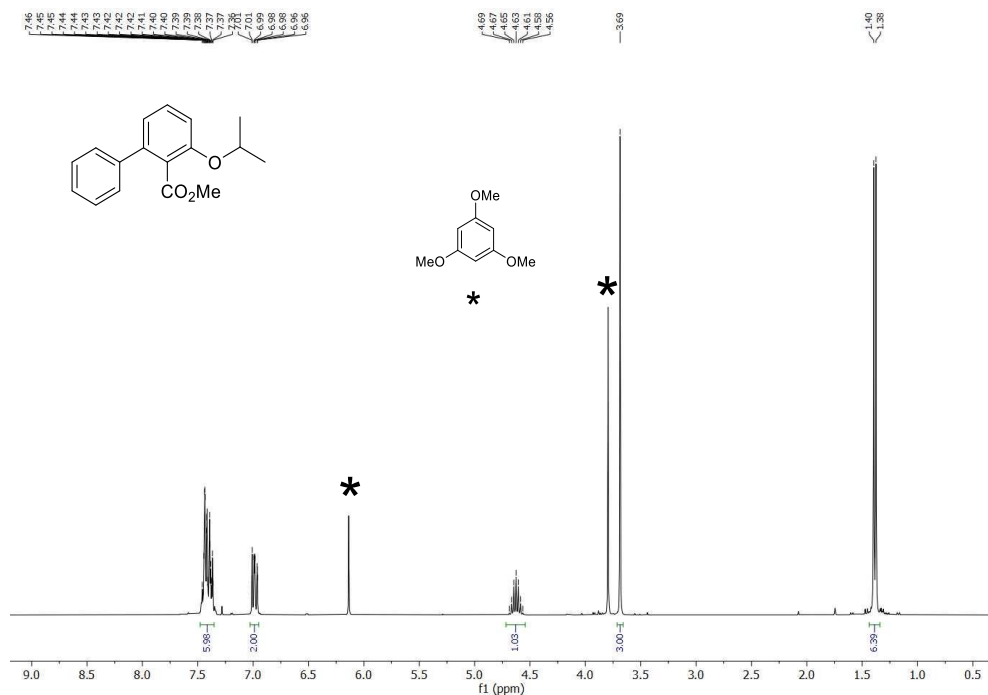
Methyl 2-(*tert*-butyl)-6-methoxybenzoate (2.2n)

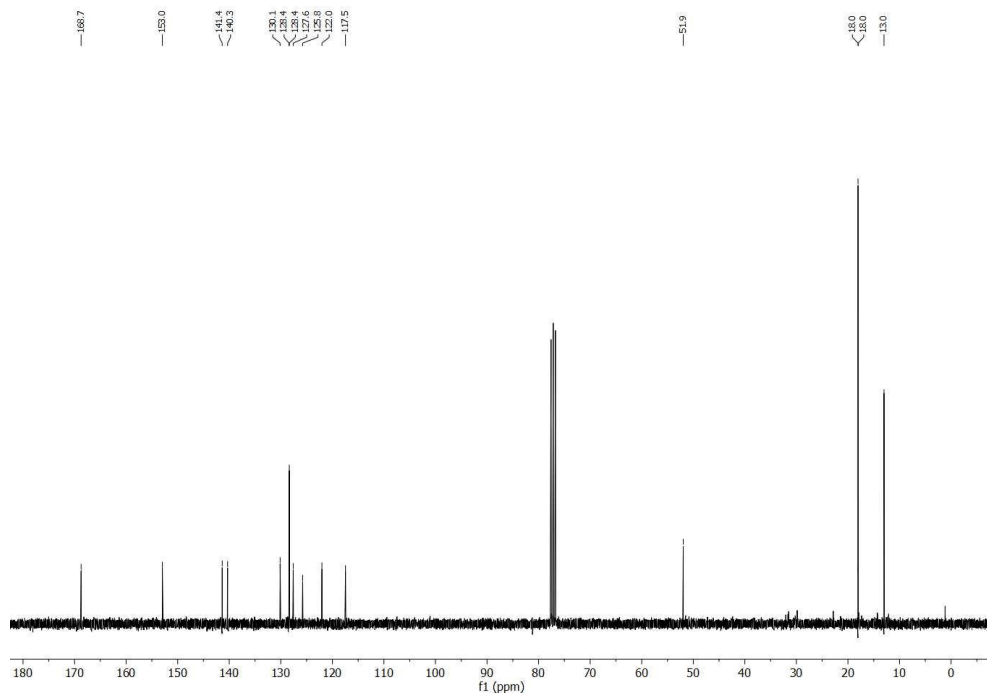
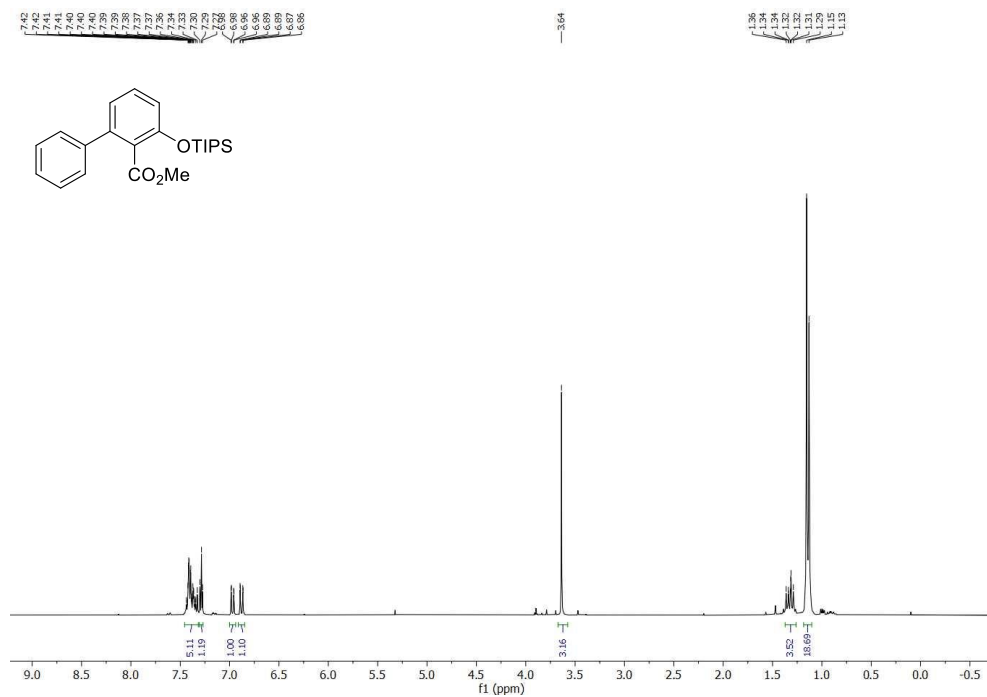


Ethyl 3-methoxy-[1,1'-biphenyl]-2-carboxylate (2.2t)

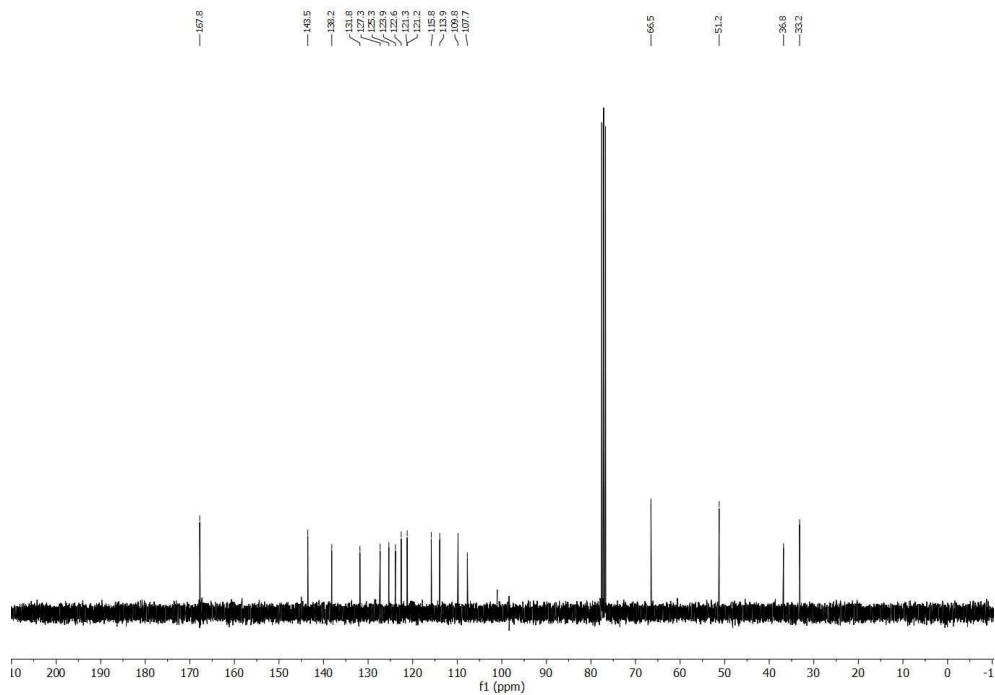
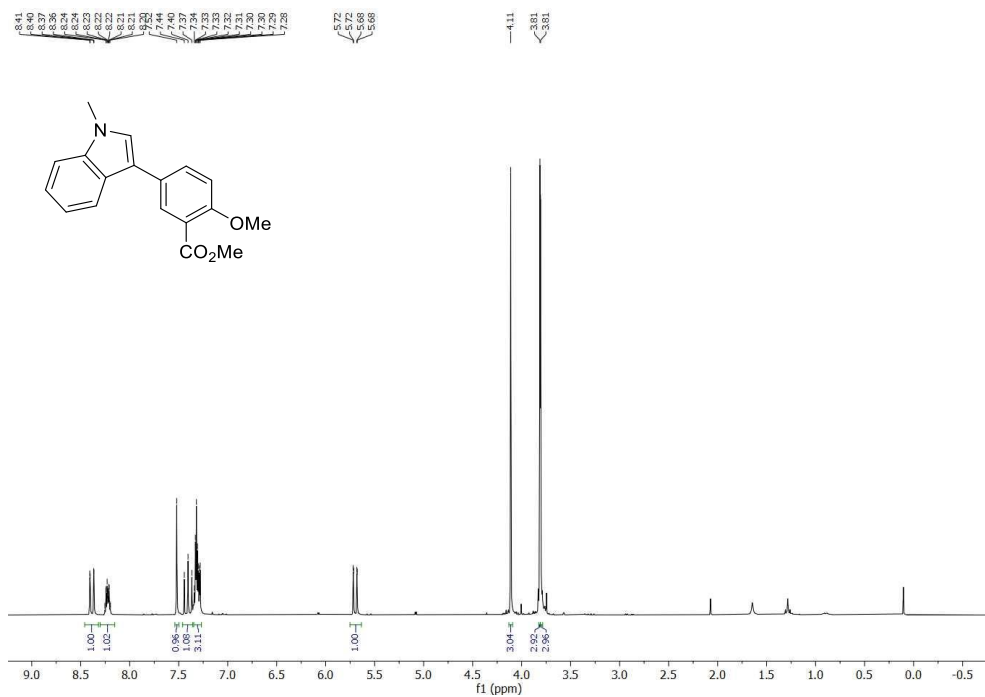


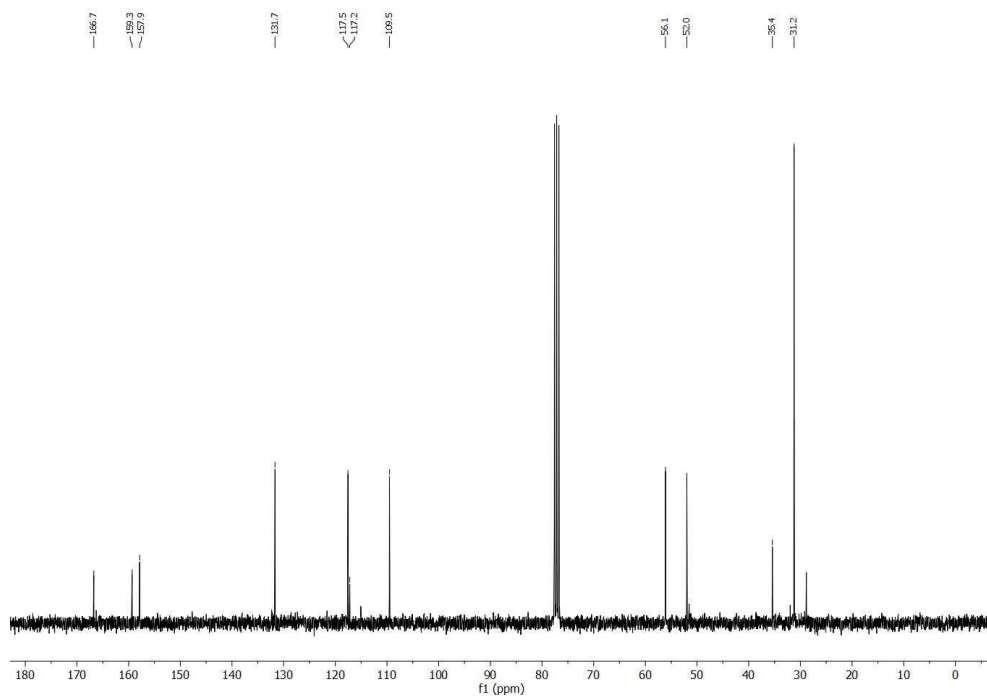
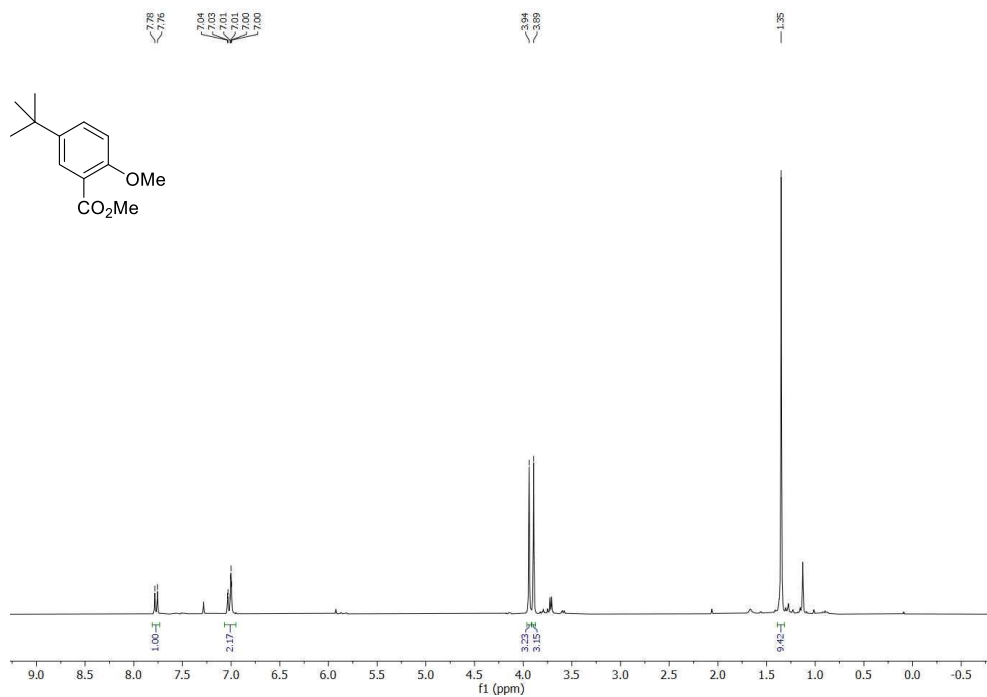
Methyl 3-isopropoxy-[1,1'-biphenyl]-2-carboxylate (2.2v)



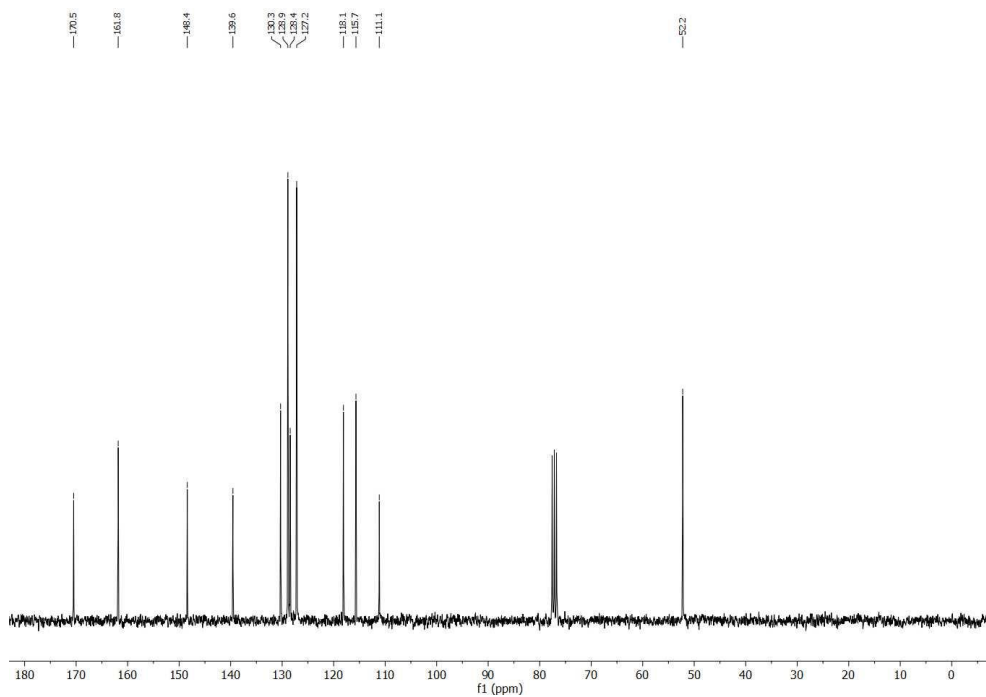
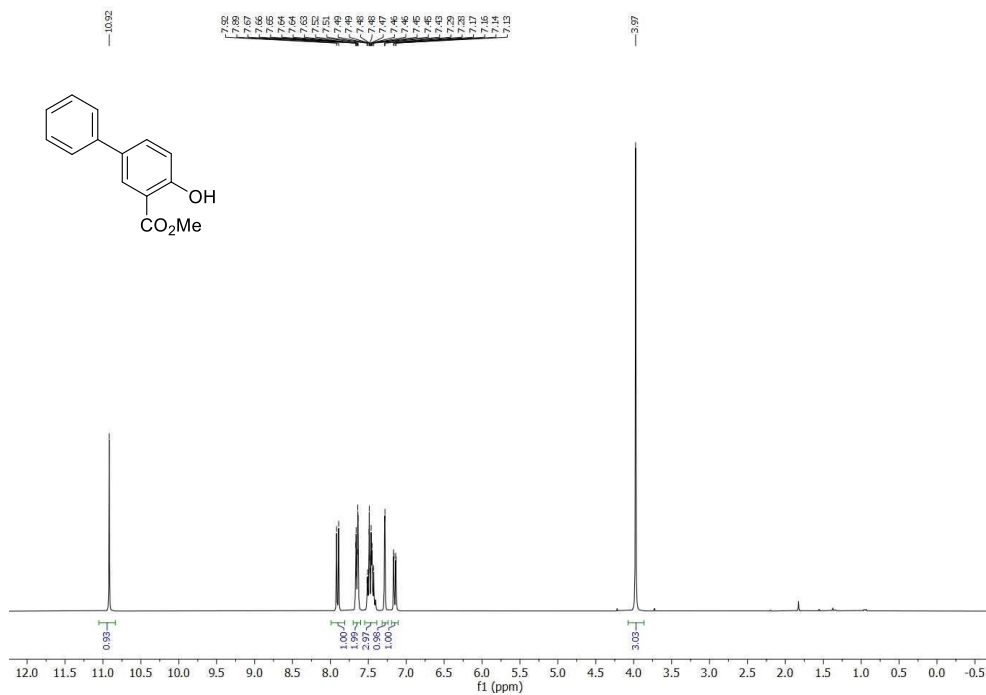
Methyl 3-((triisopropylsilyl)oxy)-[1,1'-biphenyl]-2-carboxylate (2.2w)

Methyl 2-methoxy-6-(1-methyl-1H-indol-3-yl)benzoate (2.4s)



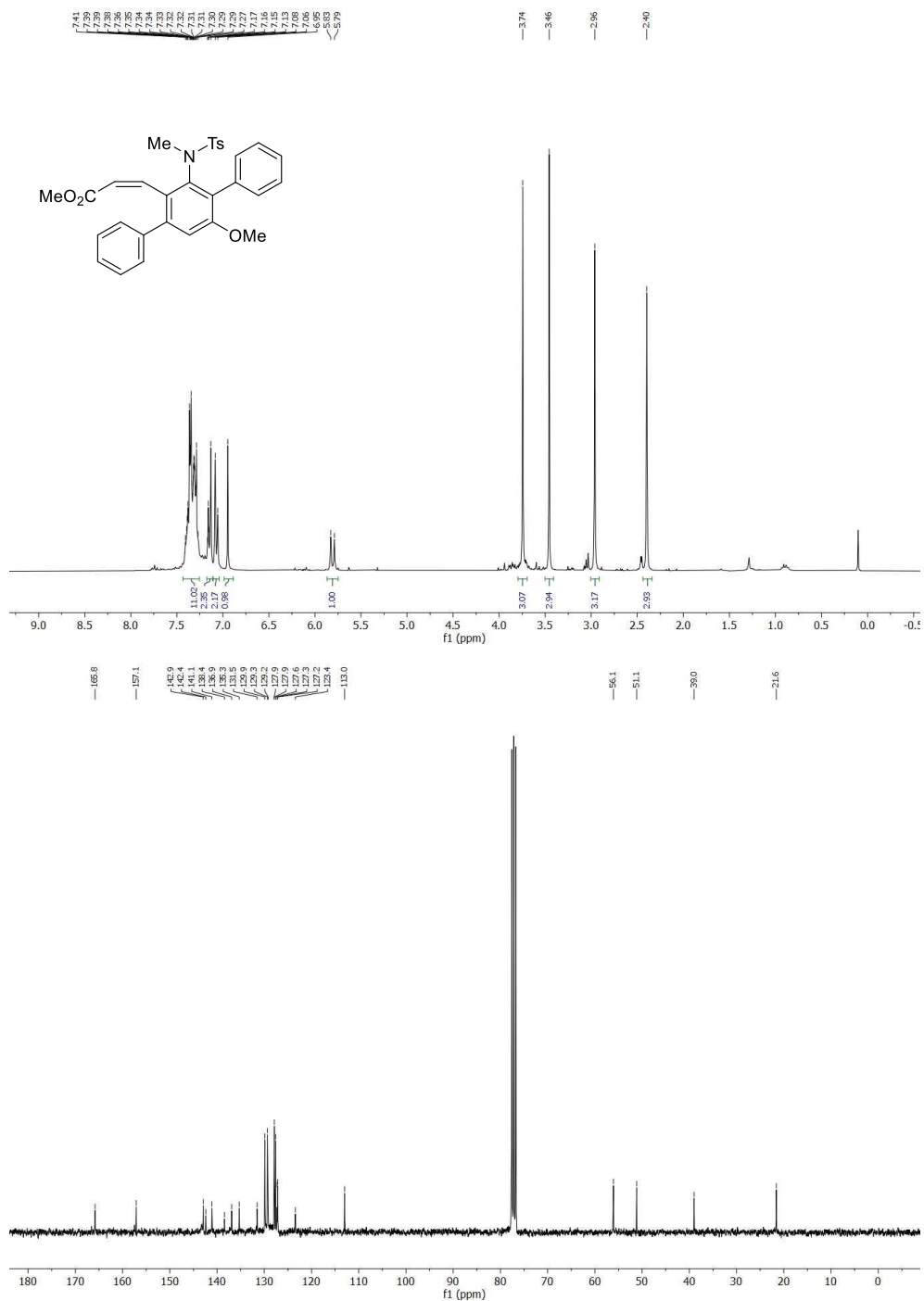
Methyl 5-(*tert*-butyl)-2-methoxybenzoate (2.4n)

Methyl 4-hydroxy-[1,1'-biphenyl]-3-carboxylate (2.4u)

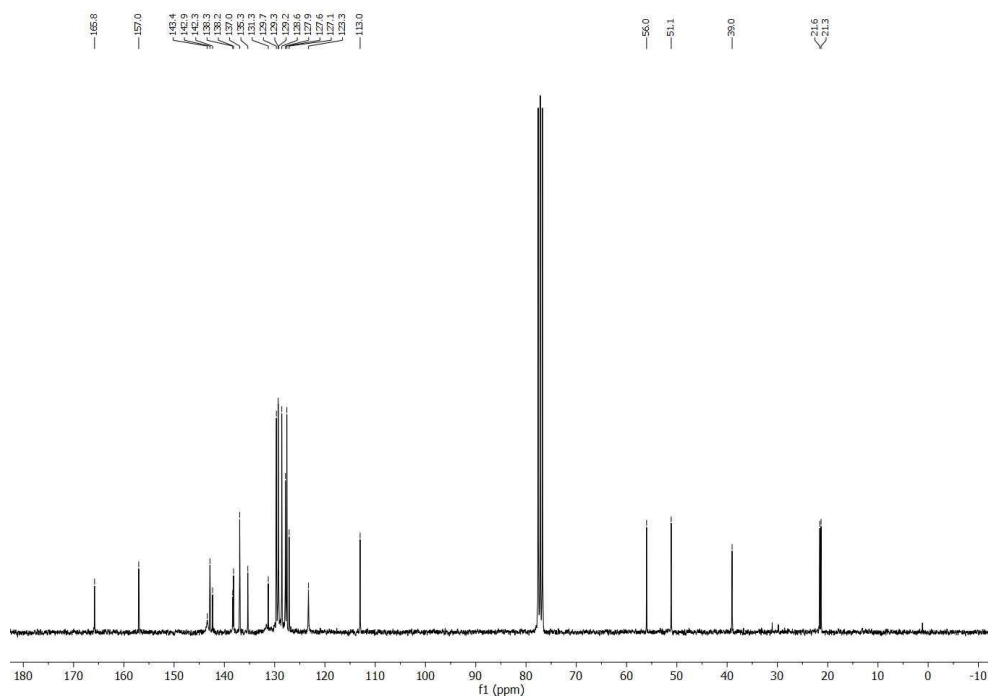
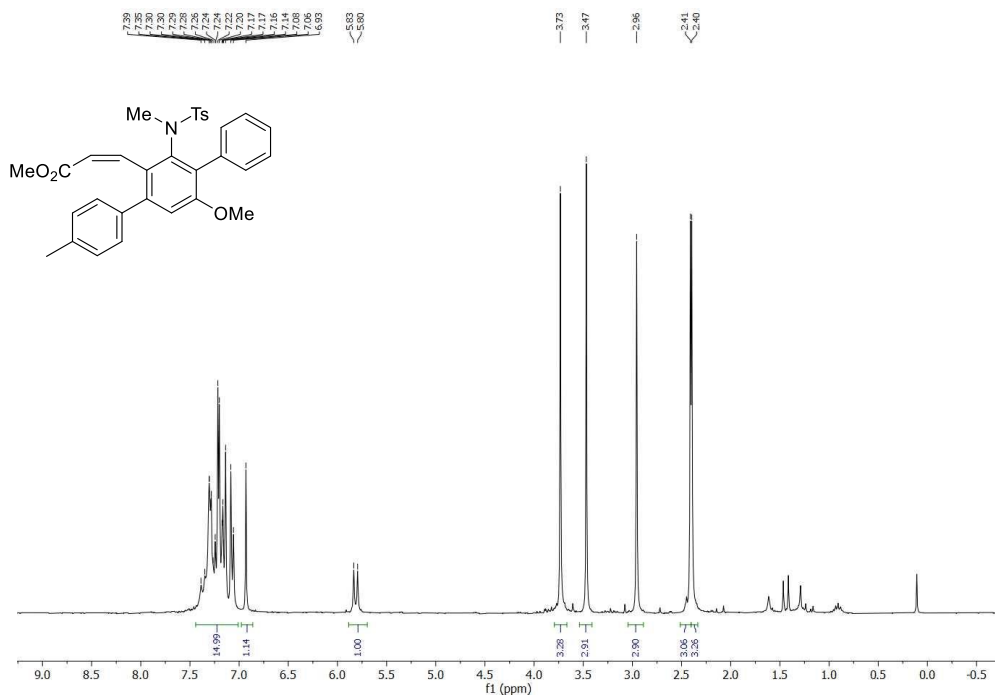


3 Chapter III

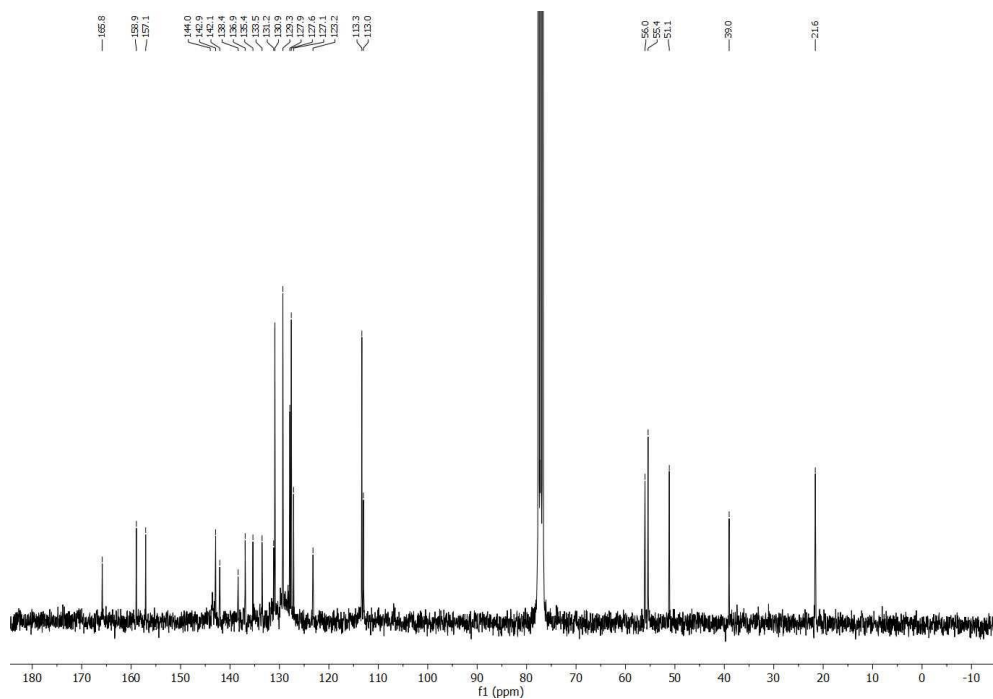
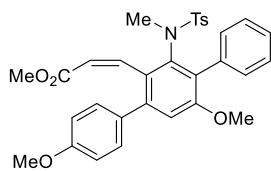
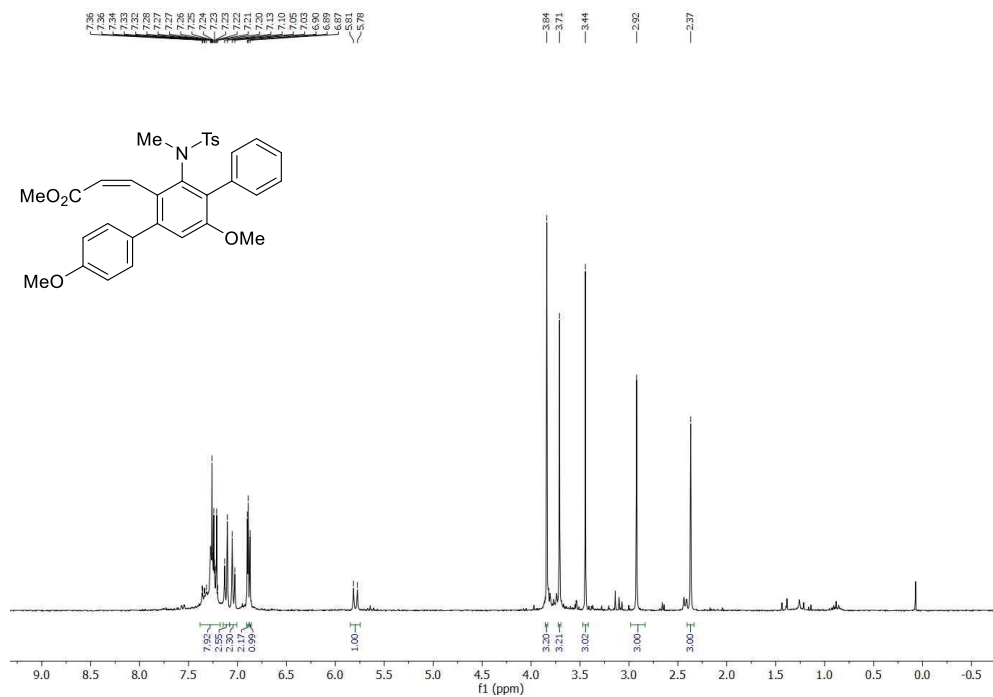
Methyl (Z)-3-(3-((N,4-dimethylphenyl)sulfonamido)-5'-methoxy-[1,1':4',1''-terphenyl]-2'-yl)acrylate (3.2a)



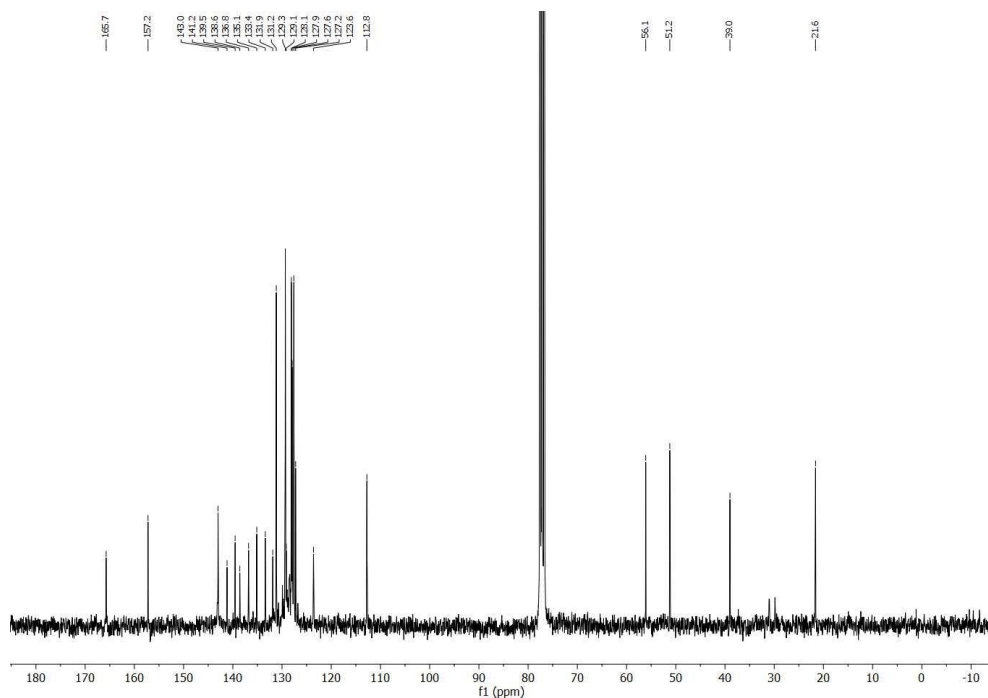
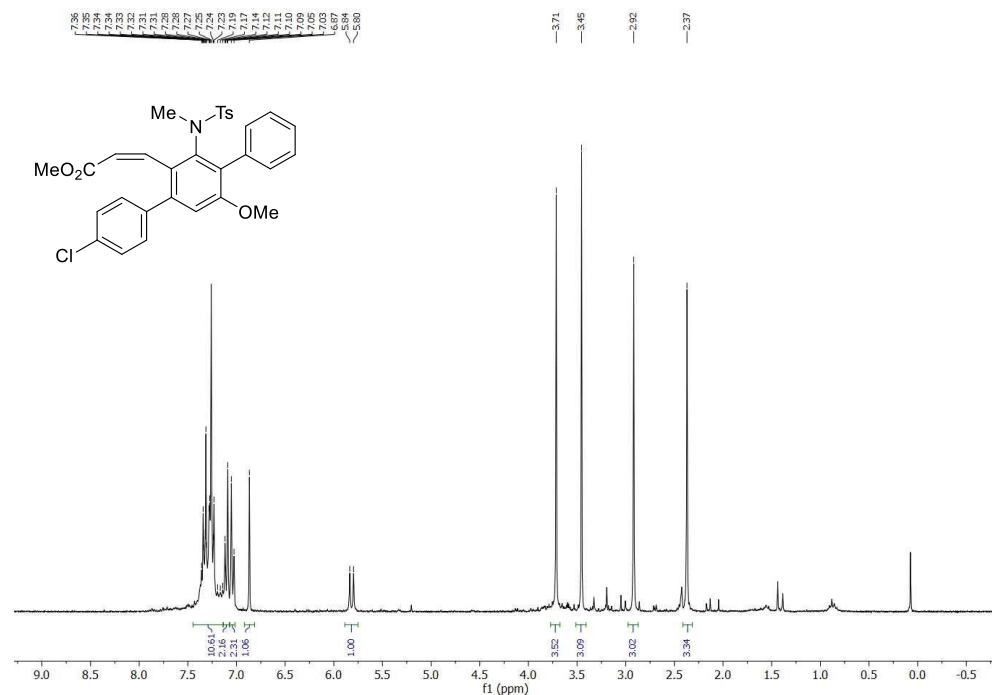
Methyl (Z)-3-(3'-((N,4-dimethylphenyl)sulfonamido)-5'-methoxy-4-methyl-[1,1':4',1''-terphenyl]-2'-yl)acrylate (3.2b)



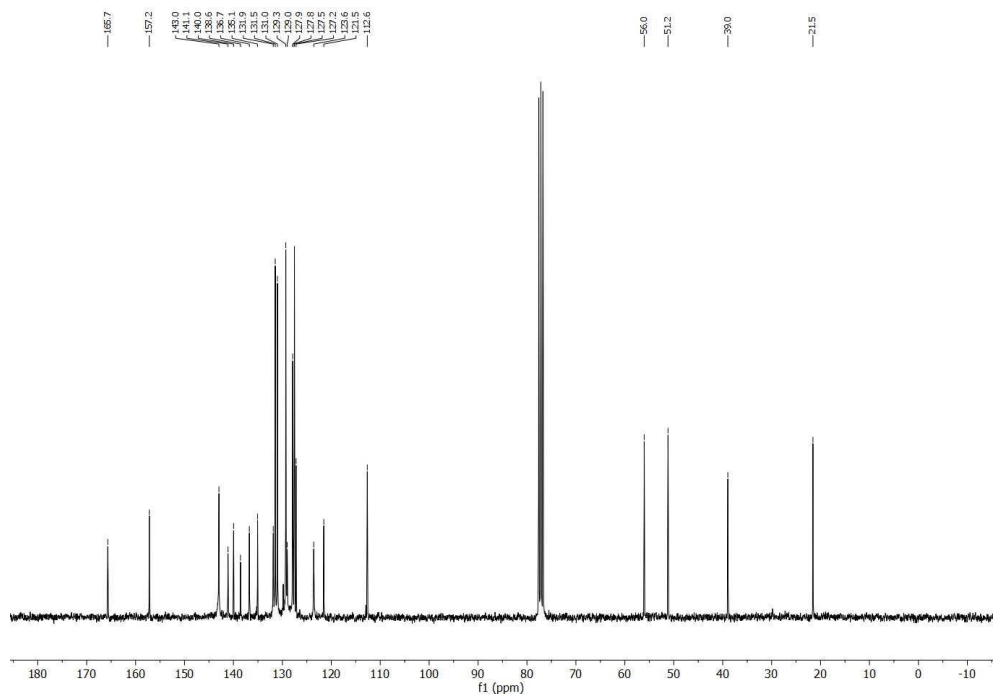
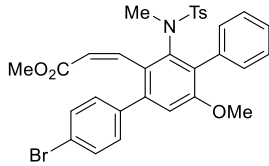
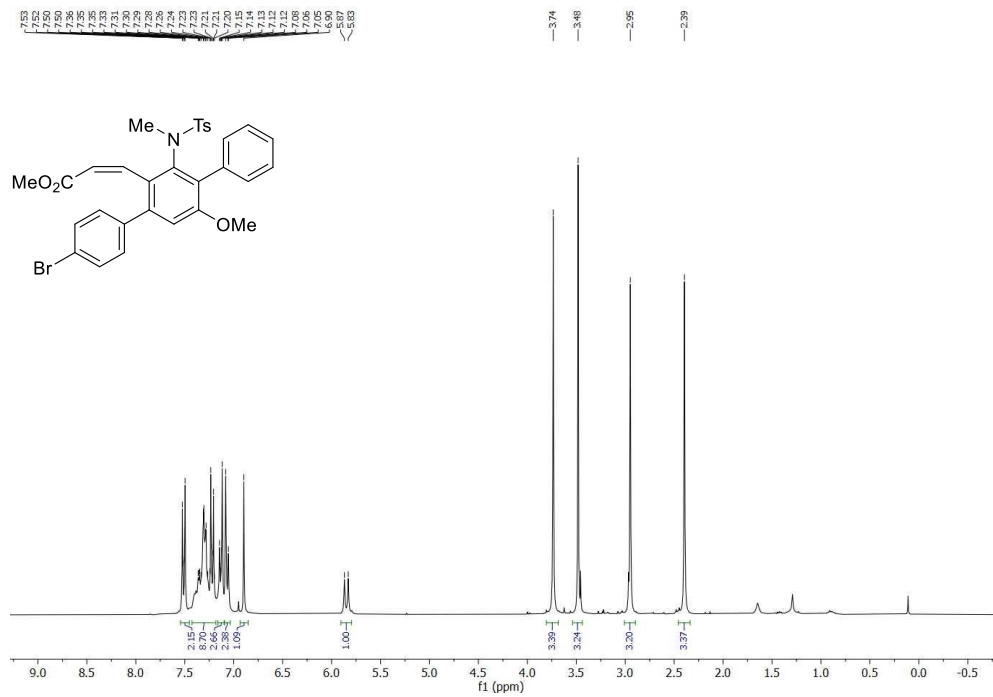
Methyl (Z)-3-(3'-((N,4-dimethylphenyl)sulfonamido)-4,5'-dimethoxy-[1,1':4',1''-terphenyl]-2'-yl)acrylate (3.2c)



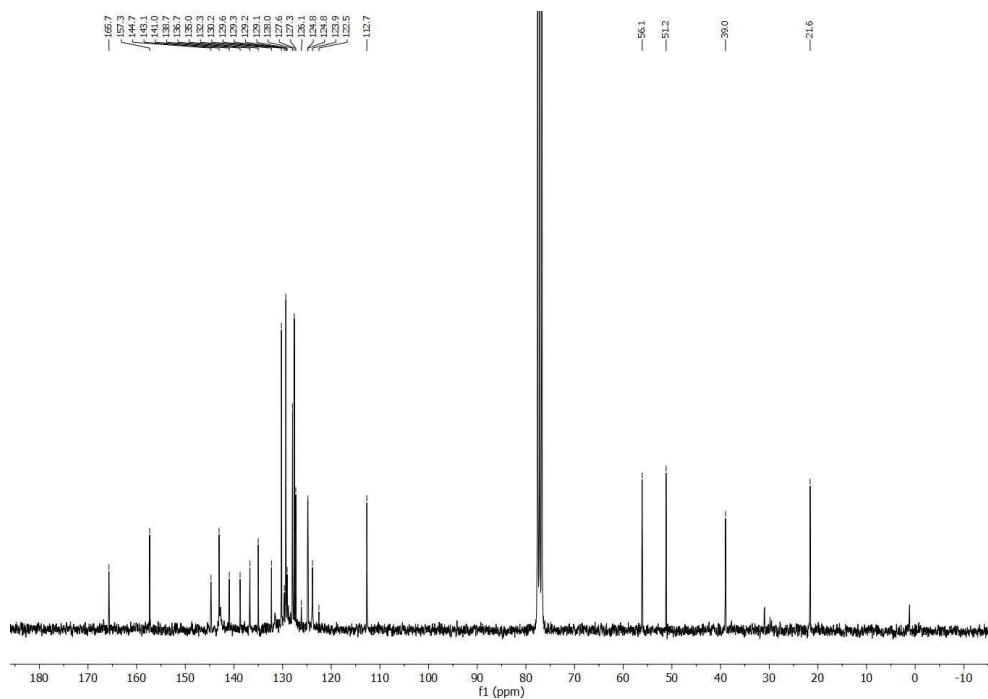
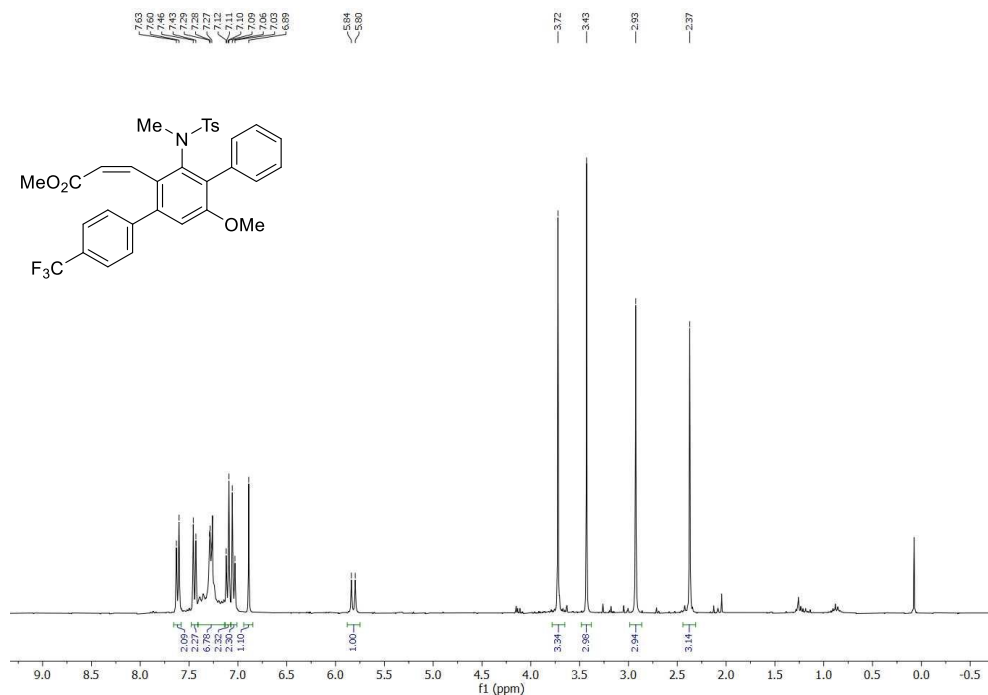
Methyl (Z)-3-(4-chloro-3'-((N,4-dimethylphenyl)sulfonamido)-5'-methoxy-[1,1':4',1''-terphenyl]-2'-yl)acrylate (3.2d)



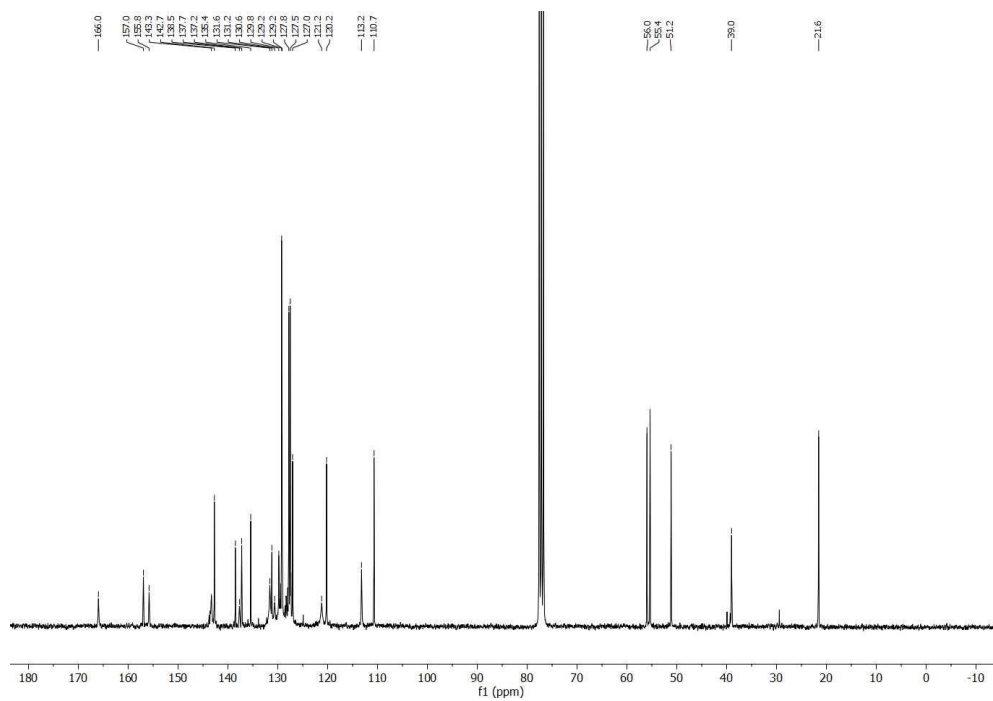
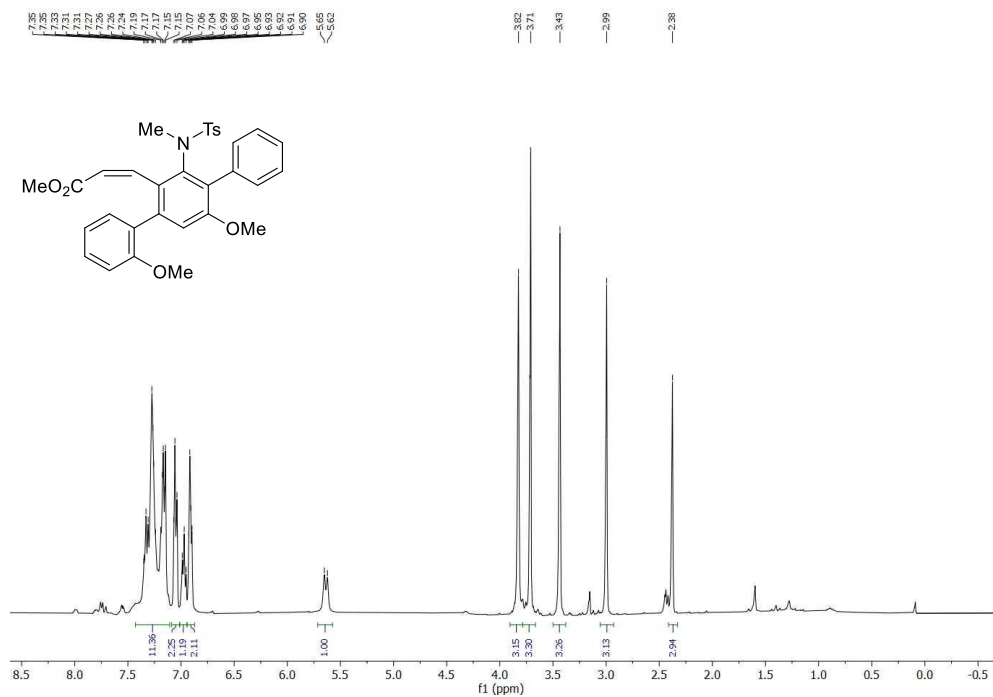
Methyl (Z)-3-(4-bromo-3'-((N,4-dimethylphenyl)sulfonamido)-5'-methoxy-[1,1':4',1''-terphenyl]-2'-yl)acrylate (3.2e)



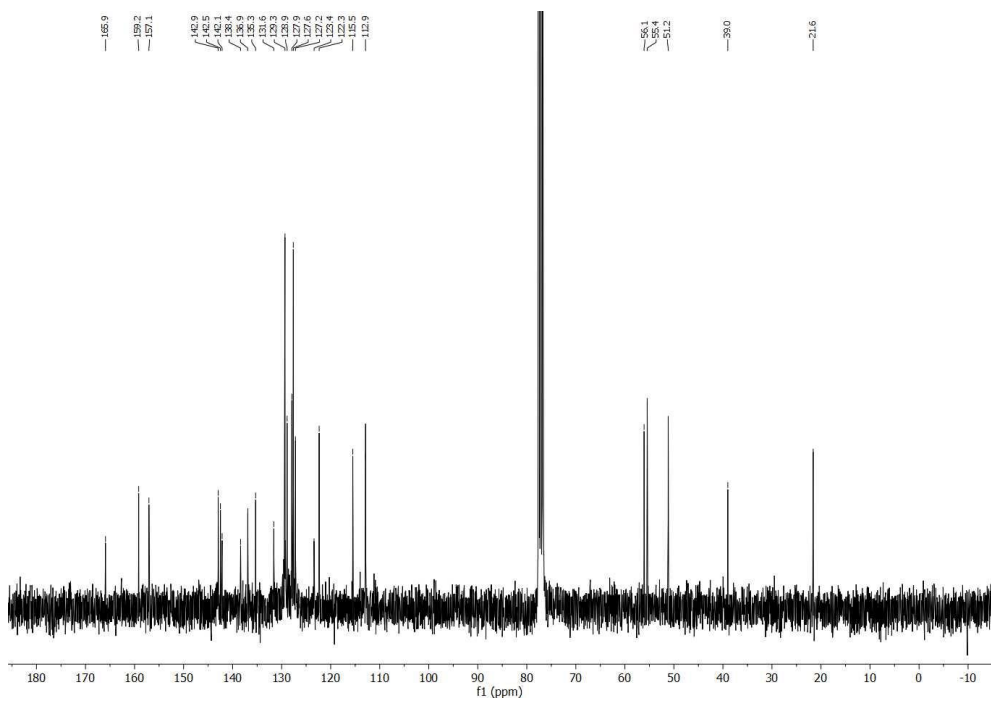
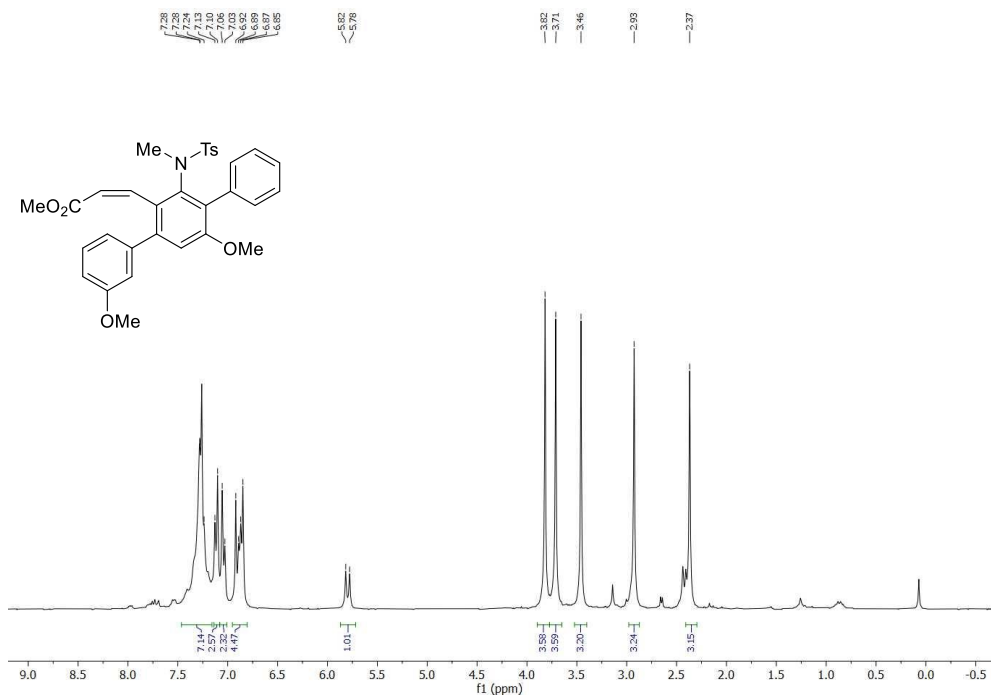
Methyl (Z)-3-(3'-((N,4-dimethylphenyl)sulfonamido)-5'-methoxy-4-(trifluoromethyl)-[1,1':4',1''-terphenyl]-2'-yl)acrylate (3.2f)

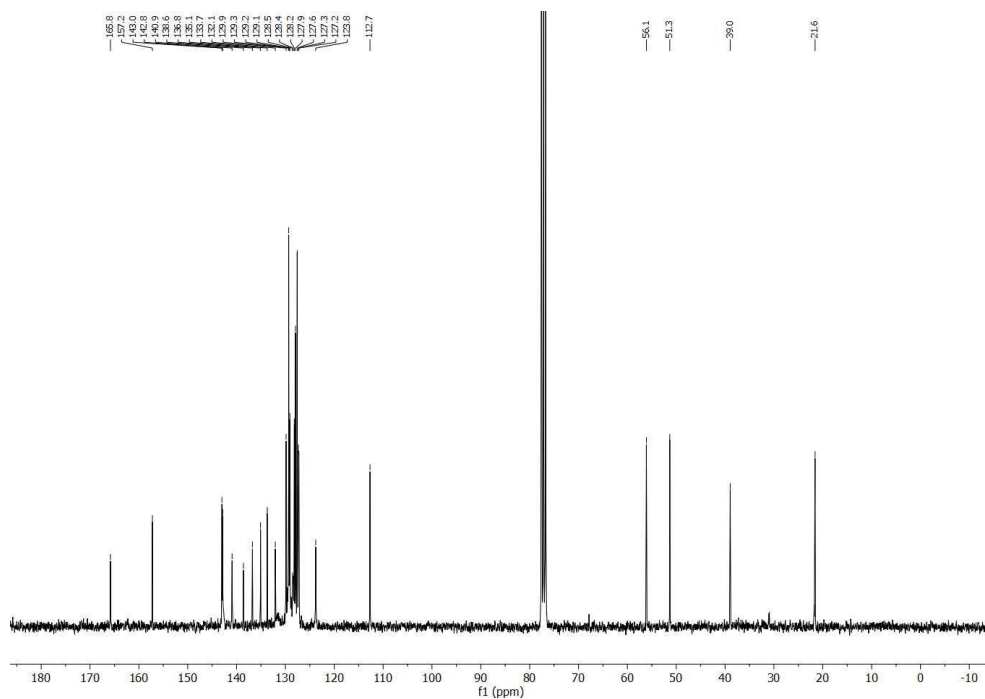
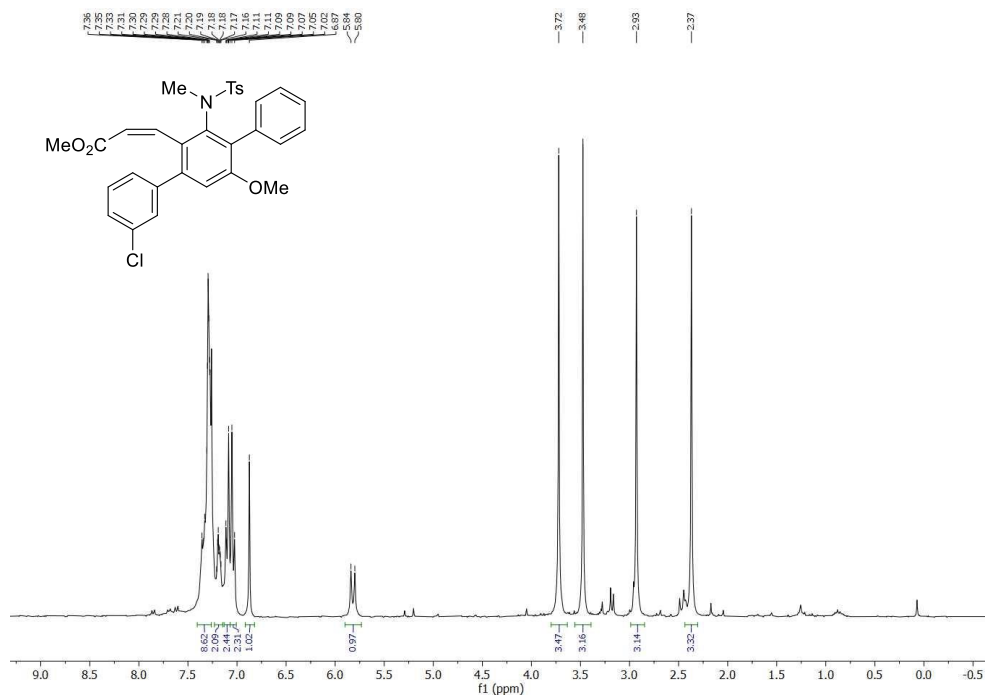


Methyl (Z)-3-(3'-((N,4-dimethylphenyl)sulfonamido)-2,5'-dimethoxy-[1,1':4',1''-terphenyl]-2'-yl)acrylate (3.2g)

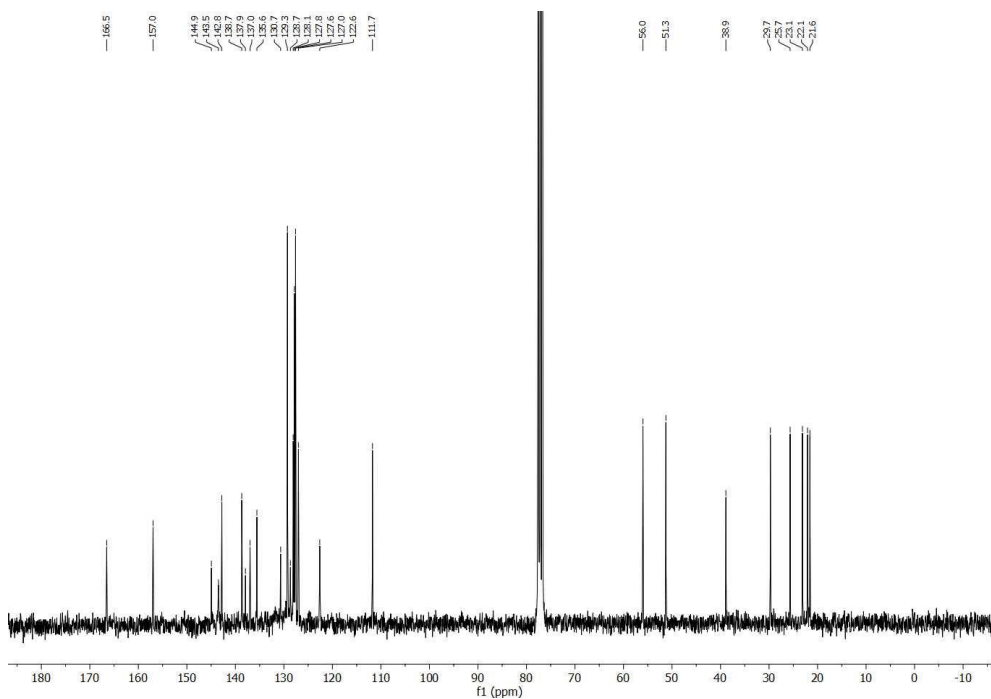
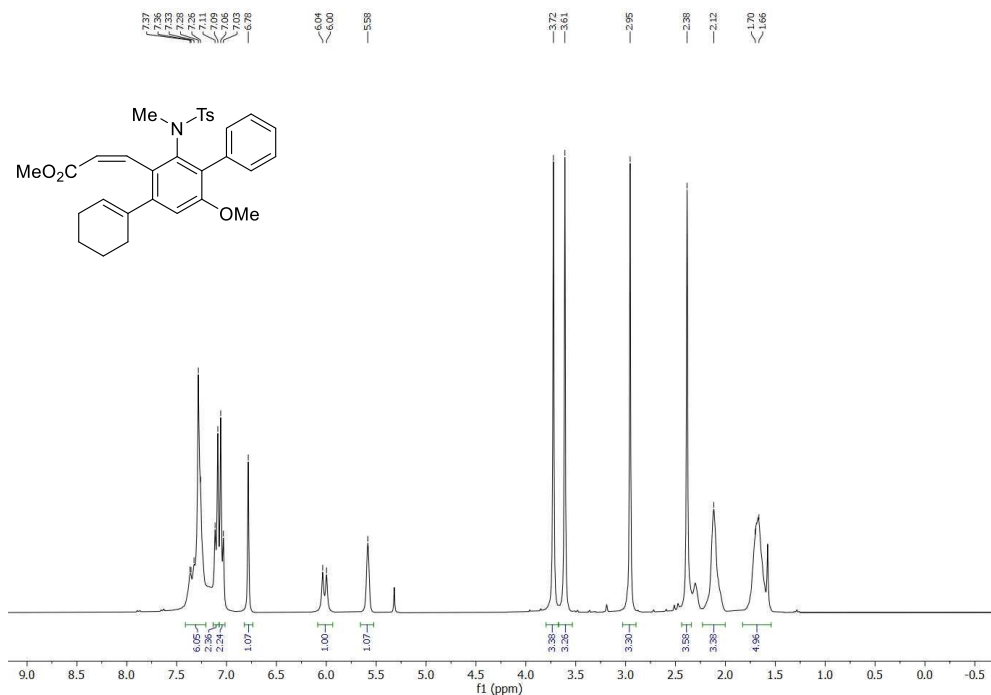


Methyl (Z)-3-(3'-((N,4-dimethylphenyl)sulfonamido)-3,5'-dimethoxy-[1,1':4',1''-terphenyl]-2'-yl)acrylate (3.2h)

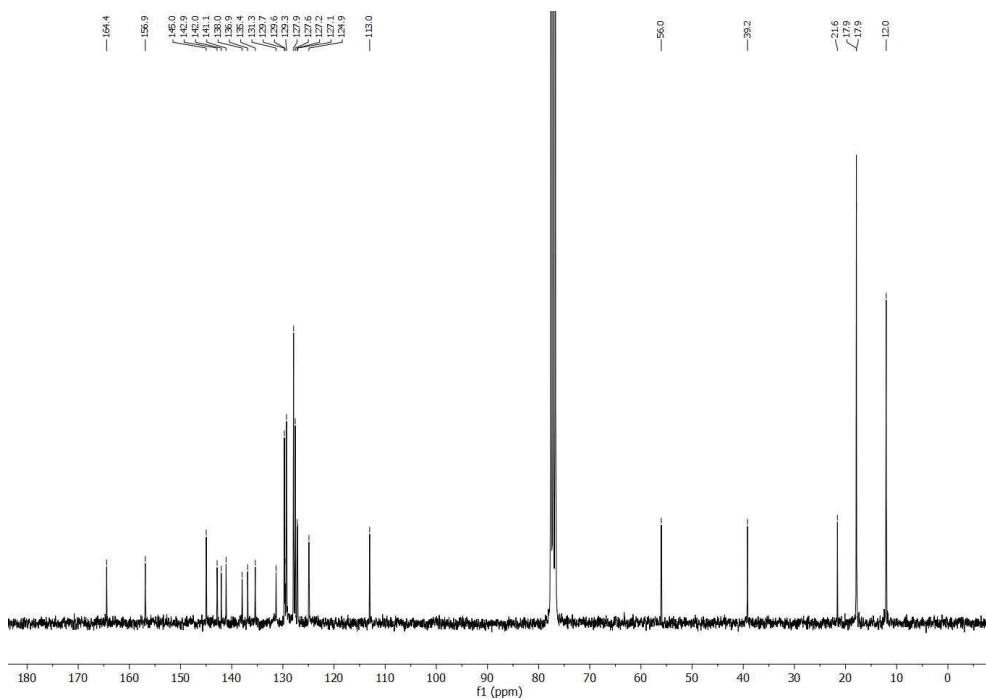
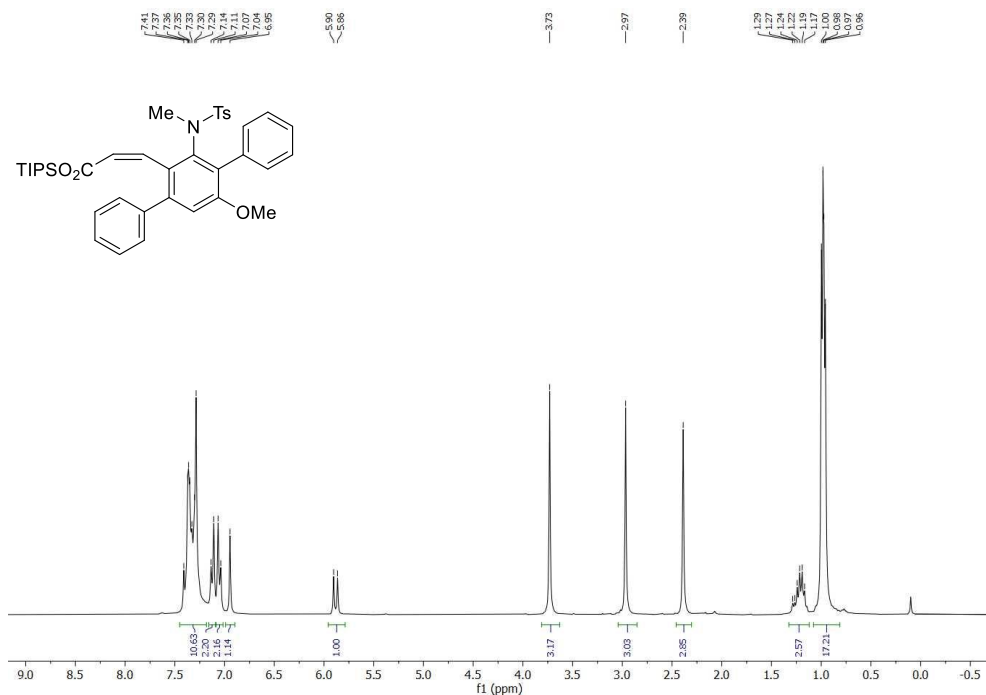


Methyl (Z)-3-(3-chloro-3'-((N,4-dimethylphenyl)sulfonamido)-5'-methoxy-[1,1':4',1''-terphenyl]-2'-yl)acrylate (3.2i)

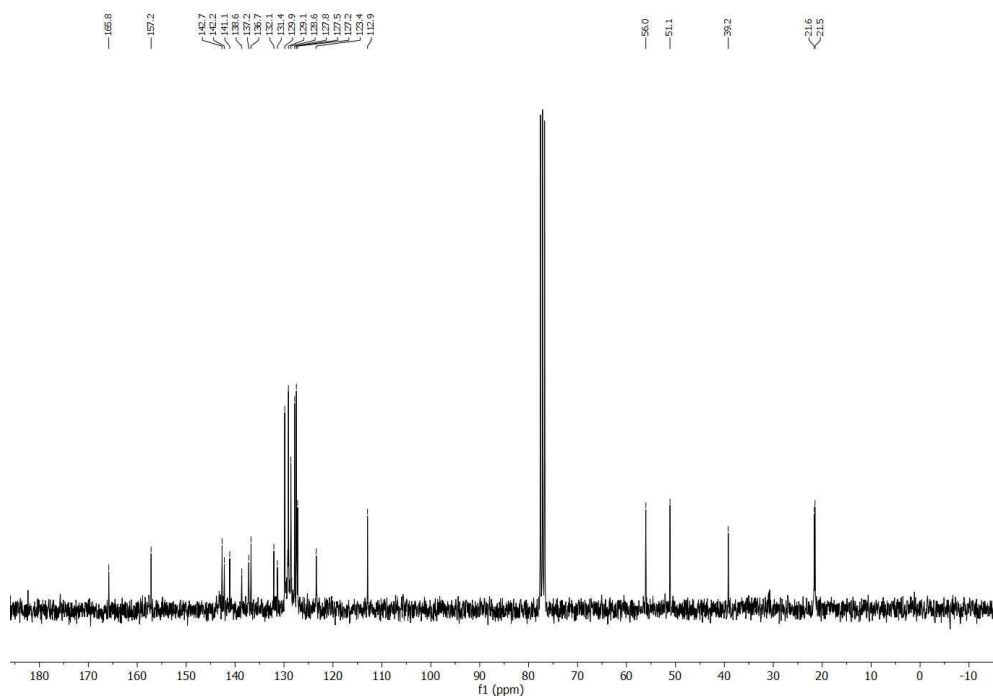
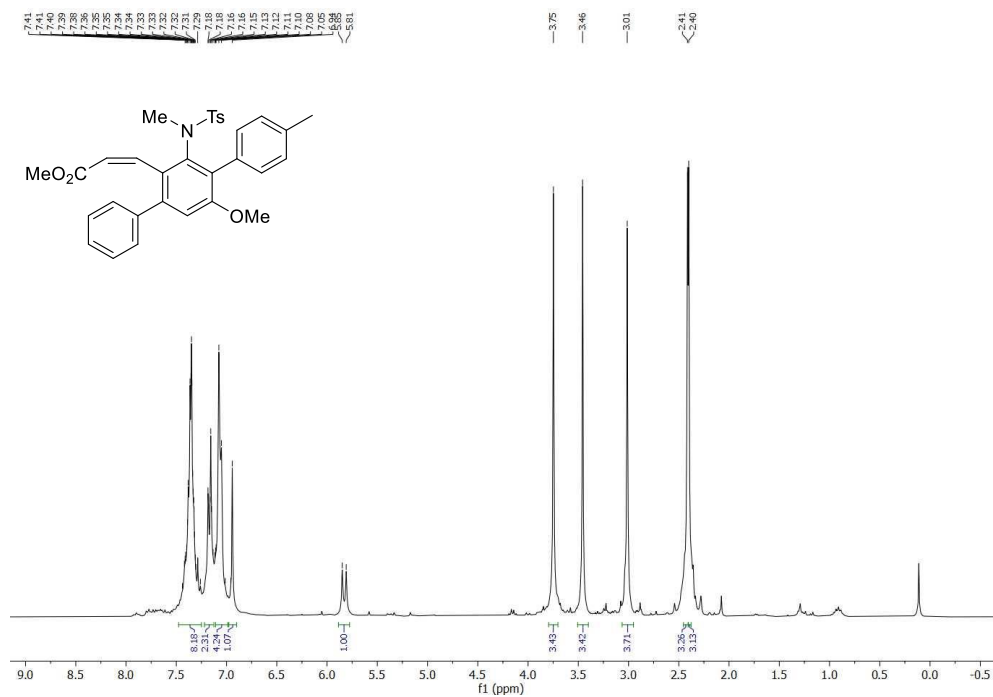
Methyl (Z)-3-(3'-((N,4-dimethylphenyl)sulfonamido)-5'-methoxy-2,3,4,5-tetrahydro-[1,1':4,1''-terphenyl]-2'-yl)acrylate (3.2j)



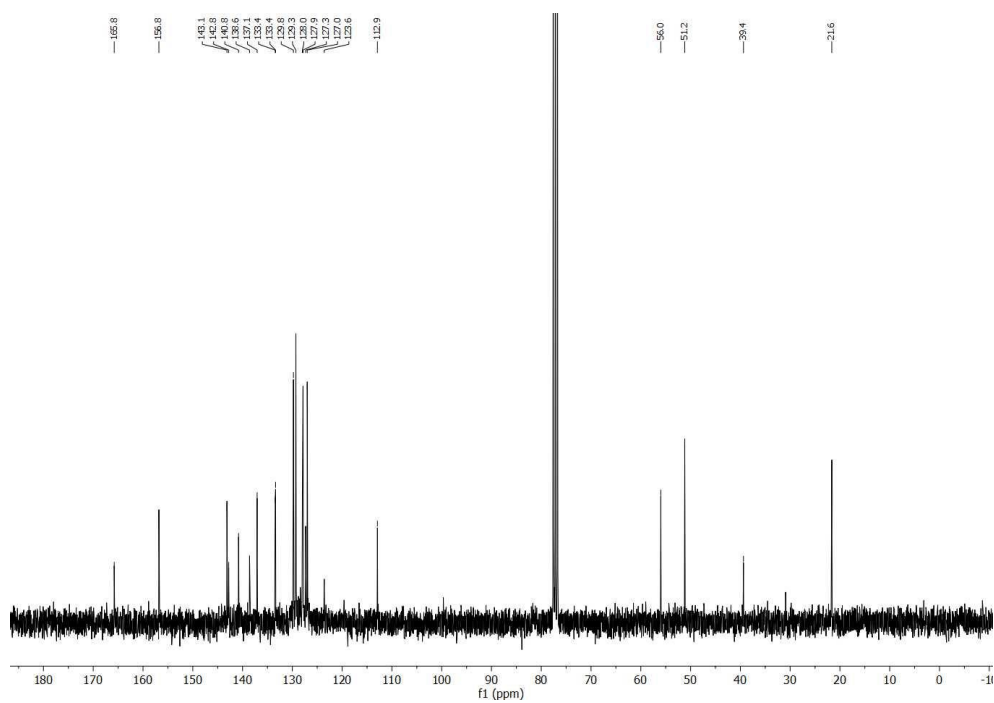
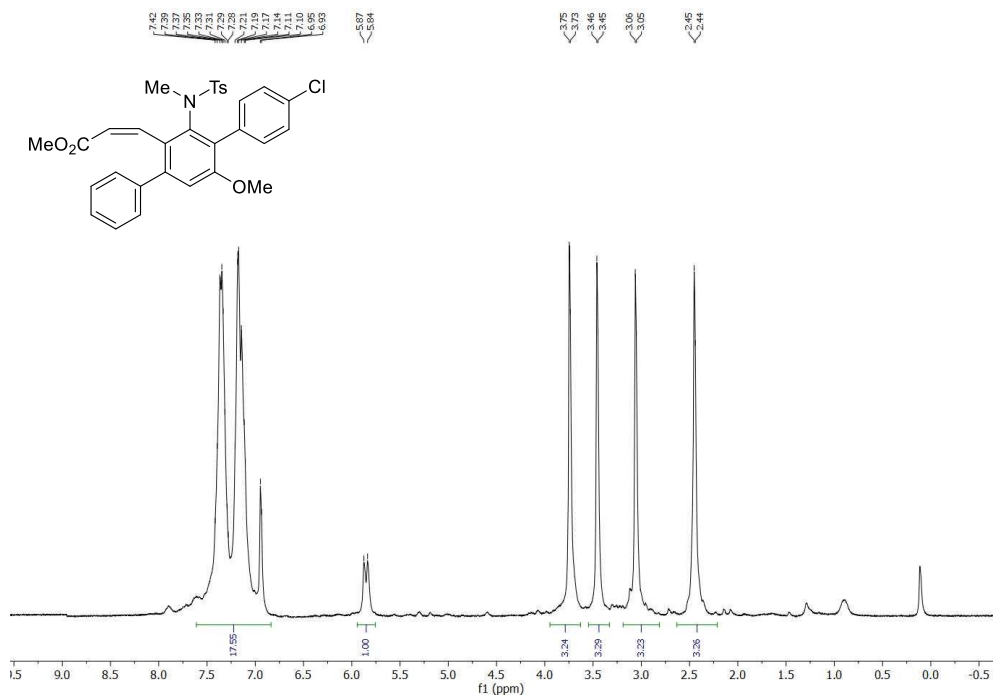
Tert-butyl dimethylsilyl (Z)-3-(3'-((N,4-dimethylphenyl)sulfonamido)-5'-methoxy-[1,1':4',1''-terphenyl]-2'-yl)acrylate (3.20)

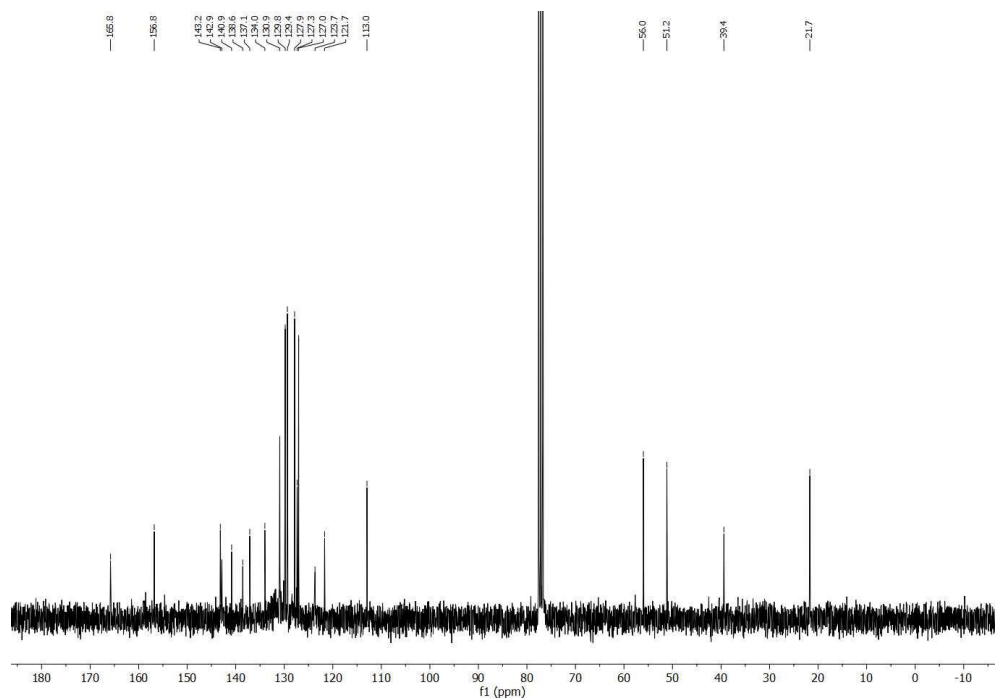
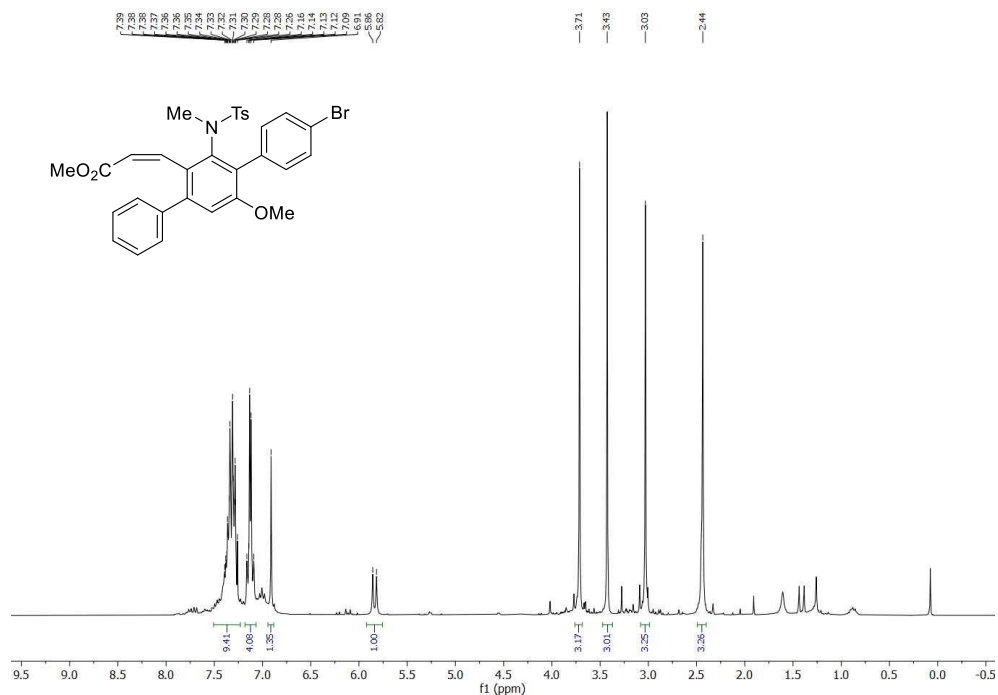


Methyl (Z)-3-(3'-((N,4-dimethylphenyl)sulfonamido)-5'-methoxy-4''-methyl-[1,1':4',1''-terphenyl]-2'-yl)acrylate (3.2p)

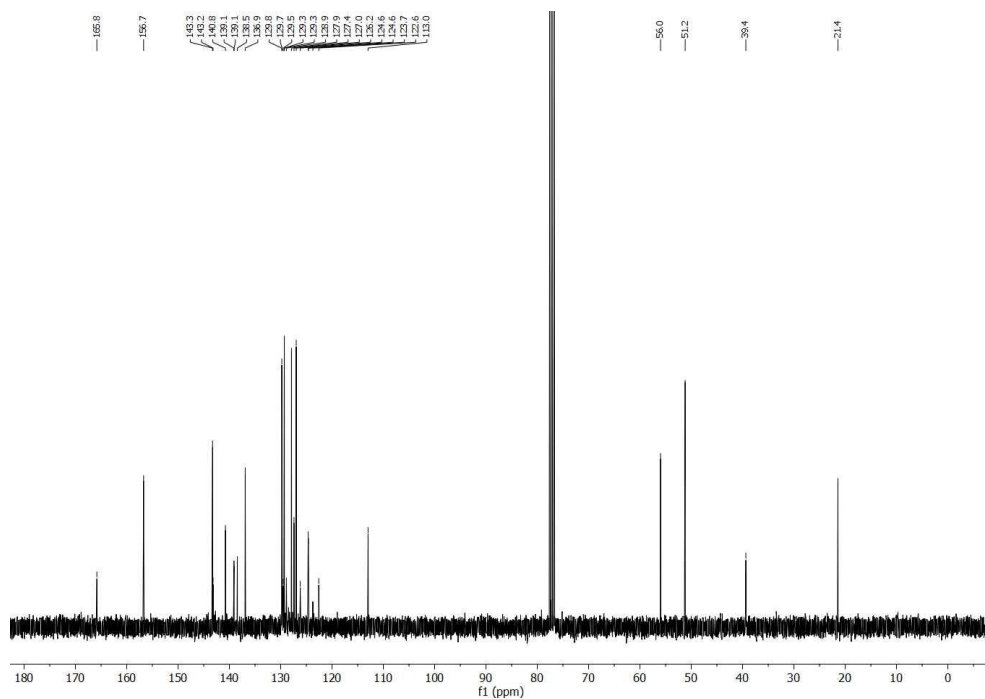
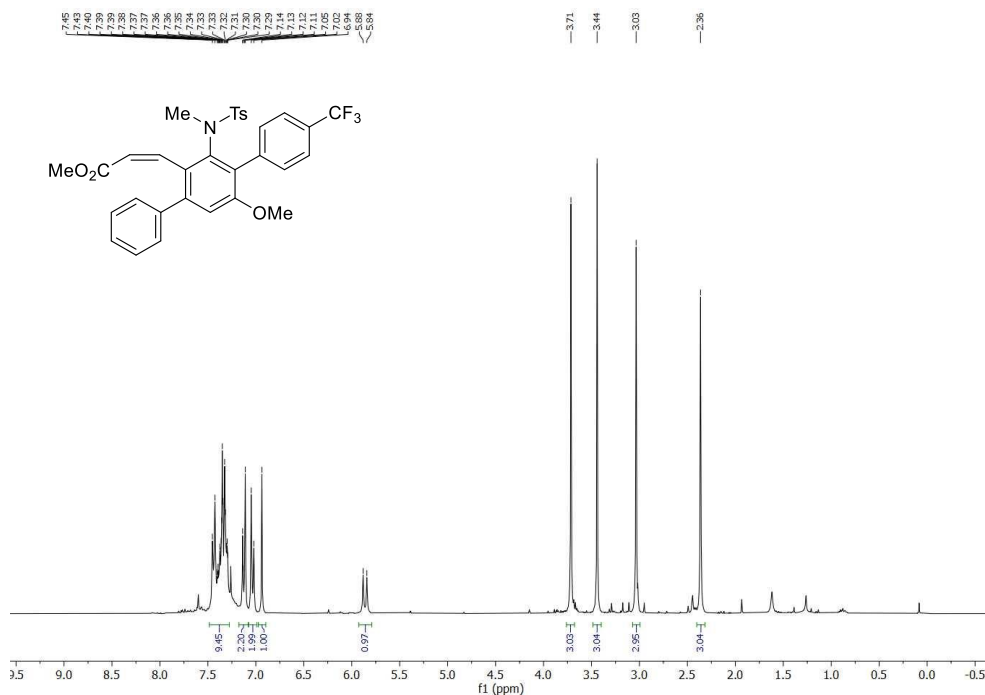


Methyl (Z)-3-(4'-chloro-3'-((N,4-dimethylphenyl)sulfonamido)-5'-methoxy-[1,1':4',1''-terphenyl]-2'-yl)acrylate (3.2r)

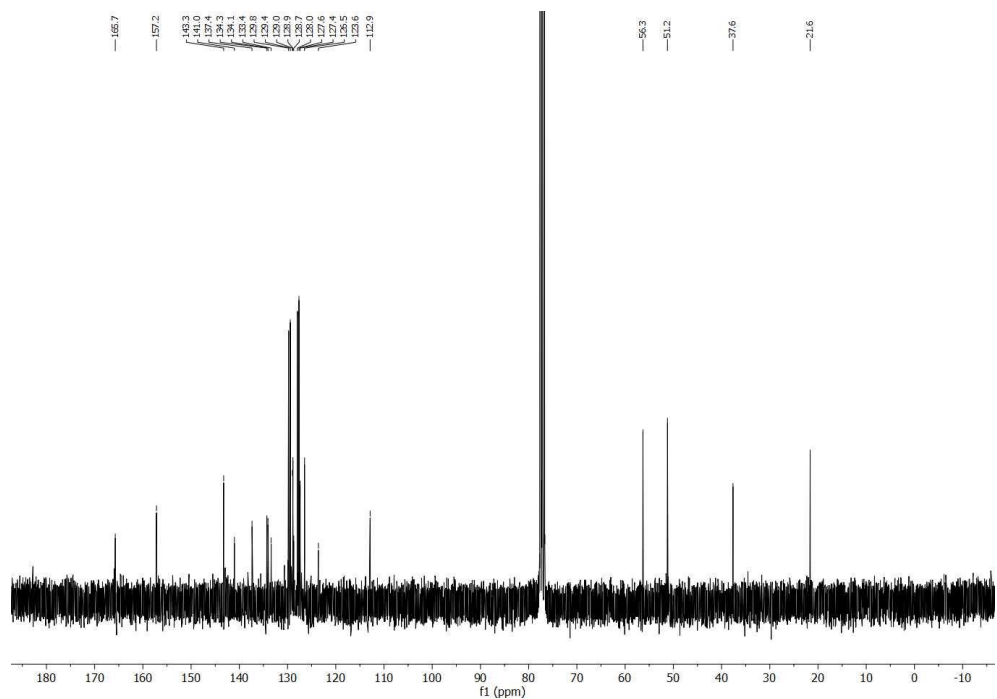
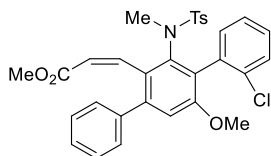
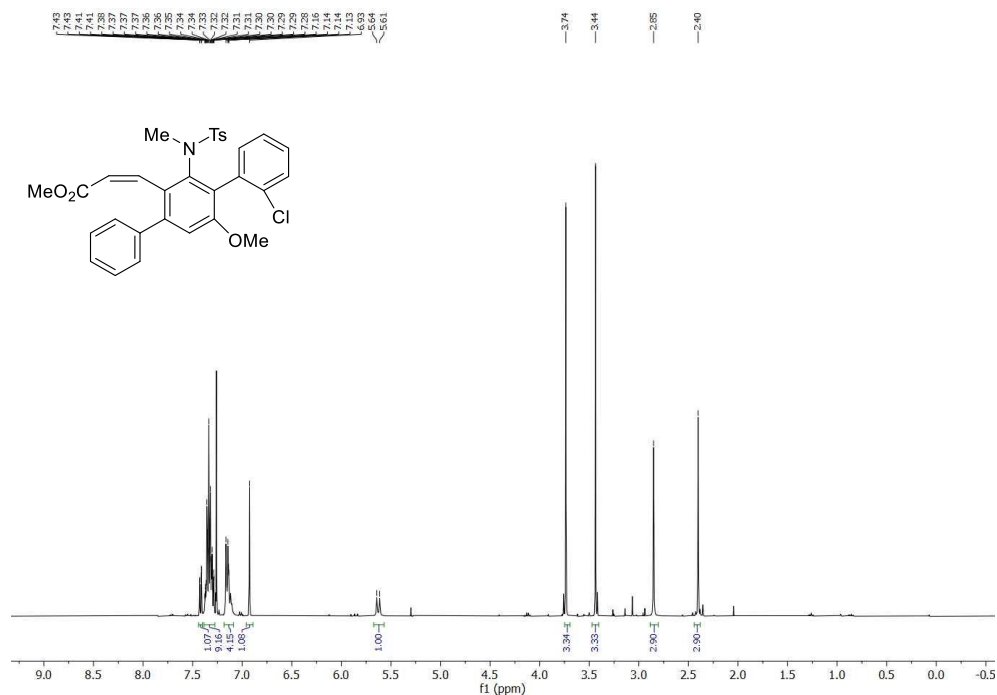


Methyl (Z)-3-(4''-bromo-3'-((N,4-dimethylphenyl)sulfonamido)-5'-methoxy-[1,1':4',1''-terphenyl]-2'-yl)acrylate (3.2s)

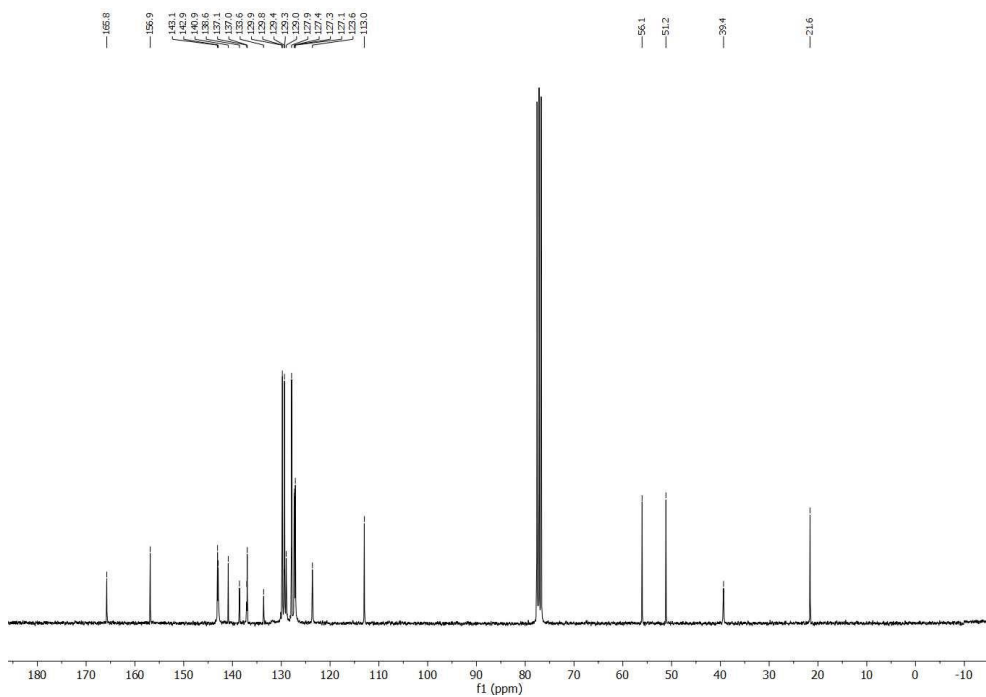
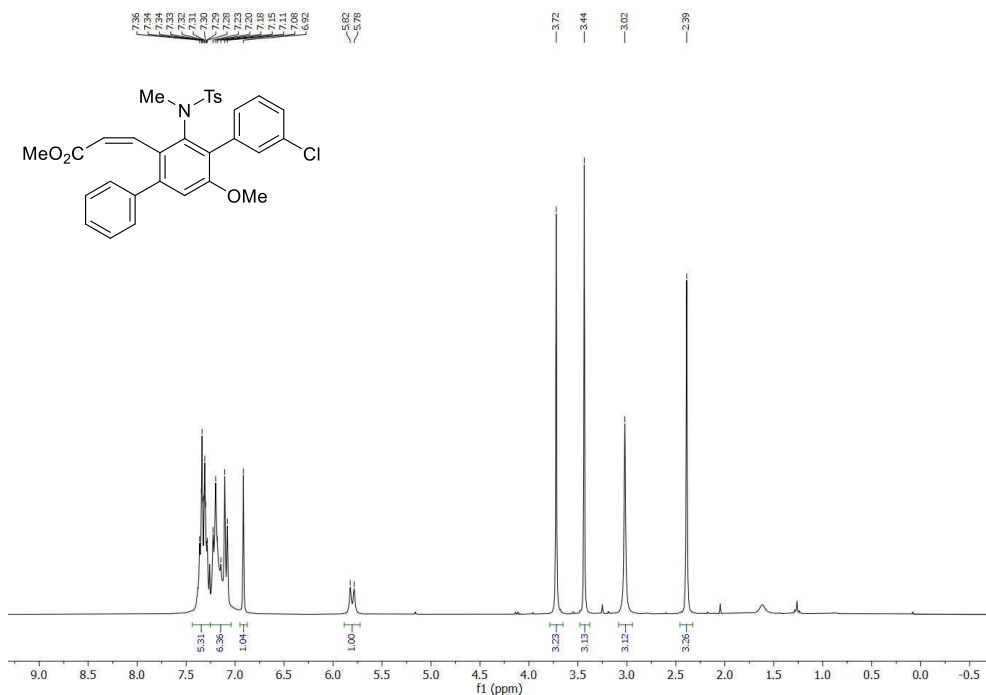
Methyl (Z)-3-(3'-((N,4-dimethylphenyl)sulfonamido)-5'-methoxy-4''-(trifluoromethyl)-[1,1':4',1''-terphenyl]-2'-yl)acrylate (3.2t)

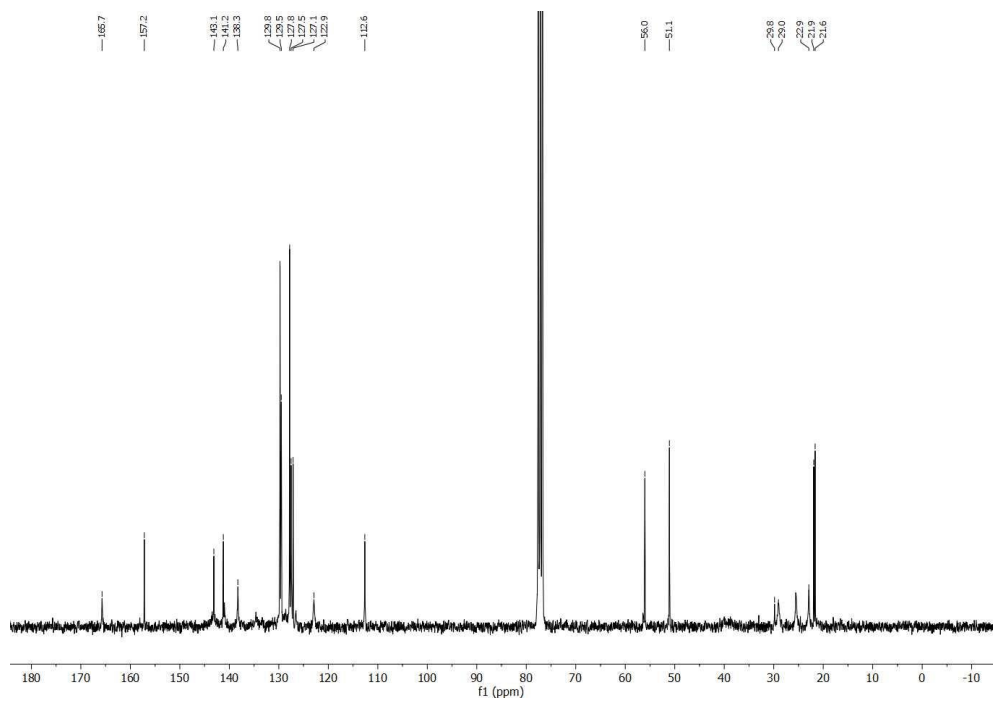
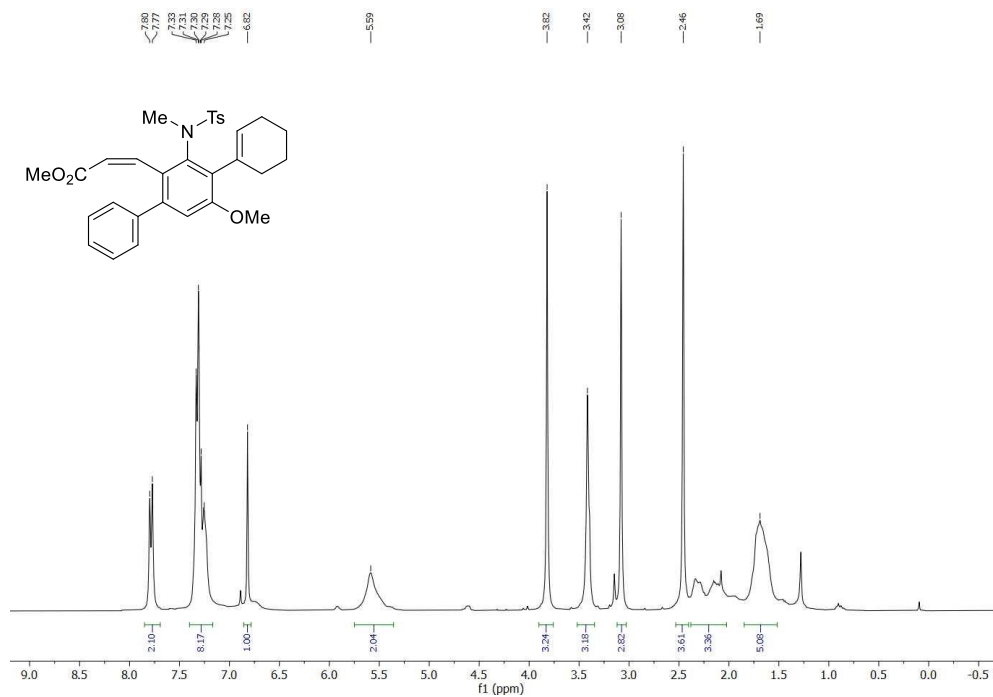


Methyl (Z)-3-(2''-chloro-3'-((N,4-dimethylphenyl)sulfonamido)-5'-methoxy-[1,1':4',1''-terphenyl]-2'-yl)acrylate (3.2u)

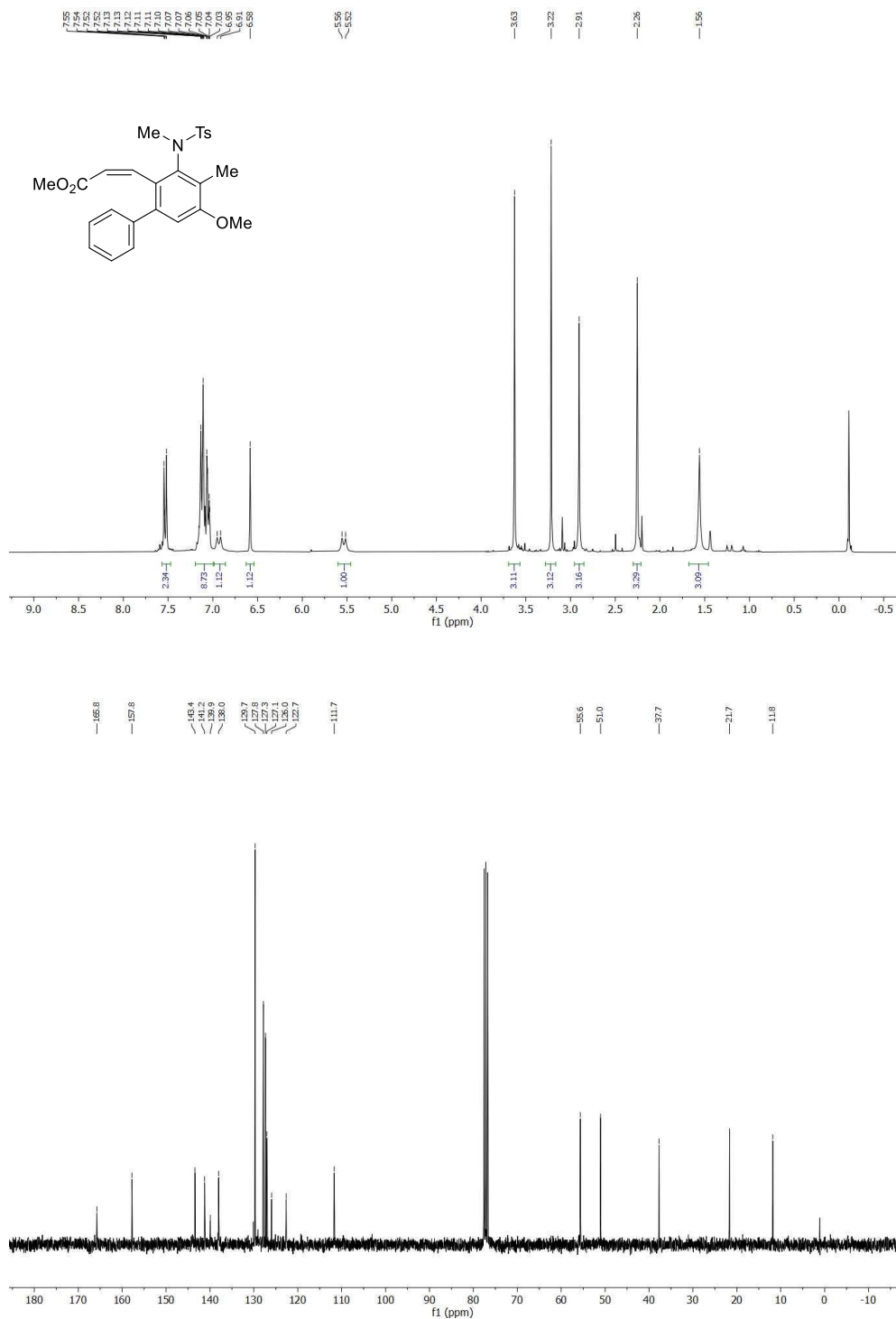


Methyl (Z)-3-(3''-chloro-3'-((N,4-dimethylphenyl)sulfonamido)-5'-methoxy-[1,1':4',1''-terphenyl]-2'-yl)acrylate (3.2w)



Methyl (Z)-3-(3'-((N,4-dimethylphenyl)sulfonamido)-5'-methoxy-2'',3'',4'',5''-tetrahydro-[1,1':4',1''-terphenyl]-2'-yl)acrylate (3.2x)

Methyl (Z)-3-(3-((N,4-dimethylphenyl)sulfonamido)-5-methoxy-4-methyl-[1,1'-biphenyl]-2-yl)acrylate (3.2y)



Annex II:
Complete computational data

General Methods. All the calculations presented here have been performed with the density functional theory, using B3LYP functional,¹ as implemented in the *Gaussian09* suit of programs.² The 6-31G(d) basis set³ was used for all atoms involved but for gold, which has been described with the LANL2DZ pseudopotential.⁴ All stationary points located in the potential energy surface of the reactions studied were fully optimized and characterized to be either minima or transition states (first-order saddle points) by the calculation of the corresponding harmonic vibrational frequencies. Thermal free energy corrections in CH₂Cl₂ solution (G_{therm}) were calculated using the Polarizable Continuum model (PCM)⁵ and the standard procedure starting from the molecular partition functions developed for computing gas-phase thermodynamics properties within the ideal gas, rigid rotor, and harmonic oscillator approximations at a pressure of 1 atm and a temperature of 298.15 K.⁶ Unless stated otherwise, energies discussed in the following sections are Gibbs energies in CH₂Cl₂ solution referred to the corresponding initial activated substrate. Energy values are indicated in Kcal/mol.

¹ a) Becke, A. D. *Phys. Rev. A: At., Mol., Opt. Phys.* **1988**, *38*, 3098-3100; b) Lee, C.; W. Yang, W.; Parr, R. G. *Phys. Rev. B: Condens. Matter Mater. Phys.* **1988**, *37*, 785-789; c) Becke, A. D. *J. Chem. Phys.* **1993**, *98*, 5648-5652.

² Frisch, M. J.; Trucks, G. W.; Schlegel, H. B.; Scuseria, G. E.; Robb, M. A.; Cheeseman, J. R.; Scalmani, G.; Barone, V.; Mennucci, B.; Petersson, G. A.; Nakatsuji, H.; Caricato, M.; Li, X.; Hratchian, H. P.; Izmaylov, A. F.; Bloino, J.; Zheng, G.; Sonnenberg, J. L.; Hada, M.; Ehara, M.; Toyota, K.; Fukuda, R.; Hasegawa, J.; Ishida, M.; Nakajima, T.; Honda, Y.; Kitao, O.; Nakai, H.; Vreven, T.; Montgomery Jr., J. A.; Peralta, J. E.; Ogliaro, F.; Bearpark, M.; Heyd, J. J.; Brothers, E.; Kudin, K. N.; Staroverov, V. N.; Kobayashi, R.; Normand, J.; Raghavachari, K.; Rendell, A.; Burant, J. C.; Iyengar, S. S.; Tomasi, J.; Cossi, M.; Rega, N.; Millam, J. M.; Klene, M.; Knox, J. E.; Cross, J. B.; Bakken, V.; Adamo, C.; Jaramillo, J.; Gomperts, R.; Stratmann, R. E.; Yazyev, O.; Austin, A. J.; Cammi, R.; Pomelli, C.; Ochterski, J. W.; Martin, R. L.; Morokuma, K.; Zakrzewski, V. G.; Voth, G. A.; Salvador, P.; Dannenberg, J. J.; Dapprich, S.; Daniels, A. D.; Farkas, O.; Foresman, J. B.; Ortiz, J. V.; Cioslowski, J.; Fox, D. J. *Gaussian 09, Revision A.1*, Gaussian, Inc., Wallingford CT, **2009**.

³ Hehre, W. J.; Radom, L.; Pople, J. A.; Schleyer, P. V. R. *Ab Initio Molecular Orbital Theory*; Wiley: New York, **1986**.

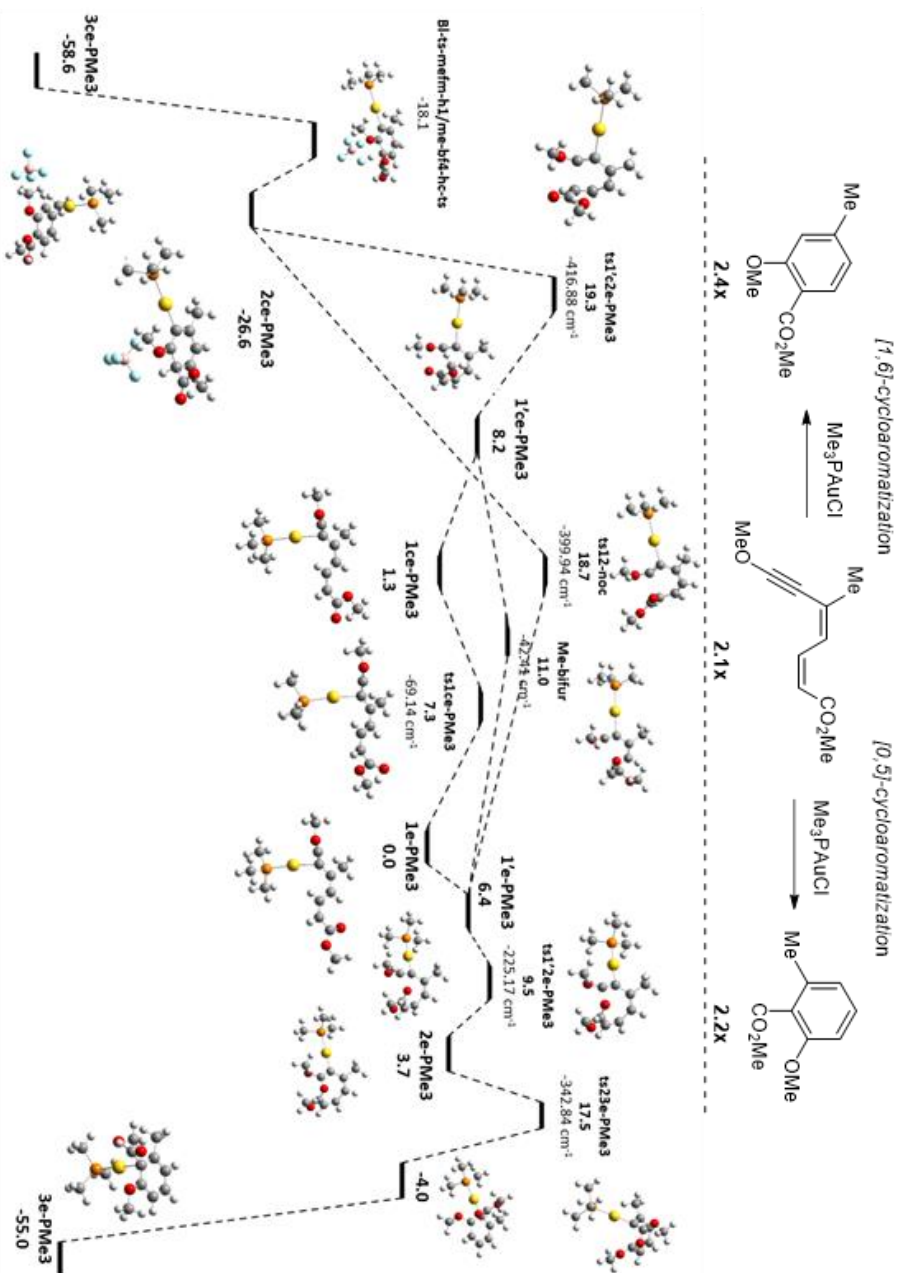
⁴ Hay, P. J.; Wadt, W. R. *J. Chem. Phys.* **1985**, *82*, 270-283.

⁵ a) Mennucci, B.; Tomasi, J. *J. Chem. Phys.* **1997**, *106*, 5151-5158; b) Barone, V.; Cossi, M.; Tomasi, J. *J. Chem. Phys.* **1997**, *107*, 3210-3221; c) Cancès, M. T.; Mennucci, B.; Tomasi, J. *J. Chem. Phys.* **1997**, *107*, 3032-3041; d) Barone, V.; Cossi, M.; Tomasi, J. *J. Comput. Chem.* **1998**, *19*, 404-417; e) Tomasi, J.; Mennucci, B.; Cancès, M. T. *J. Mol. Struct.: THEOCHEM* **1999**, *464*, 211-226; f) Scalmani, G.; Frisch, M. J. *J. Chem. Phys.* **2010**, *132*, 114110.

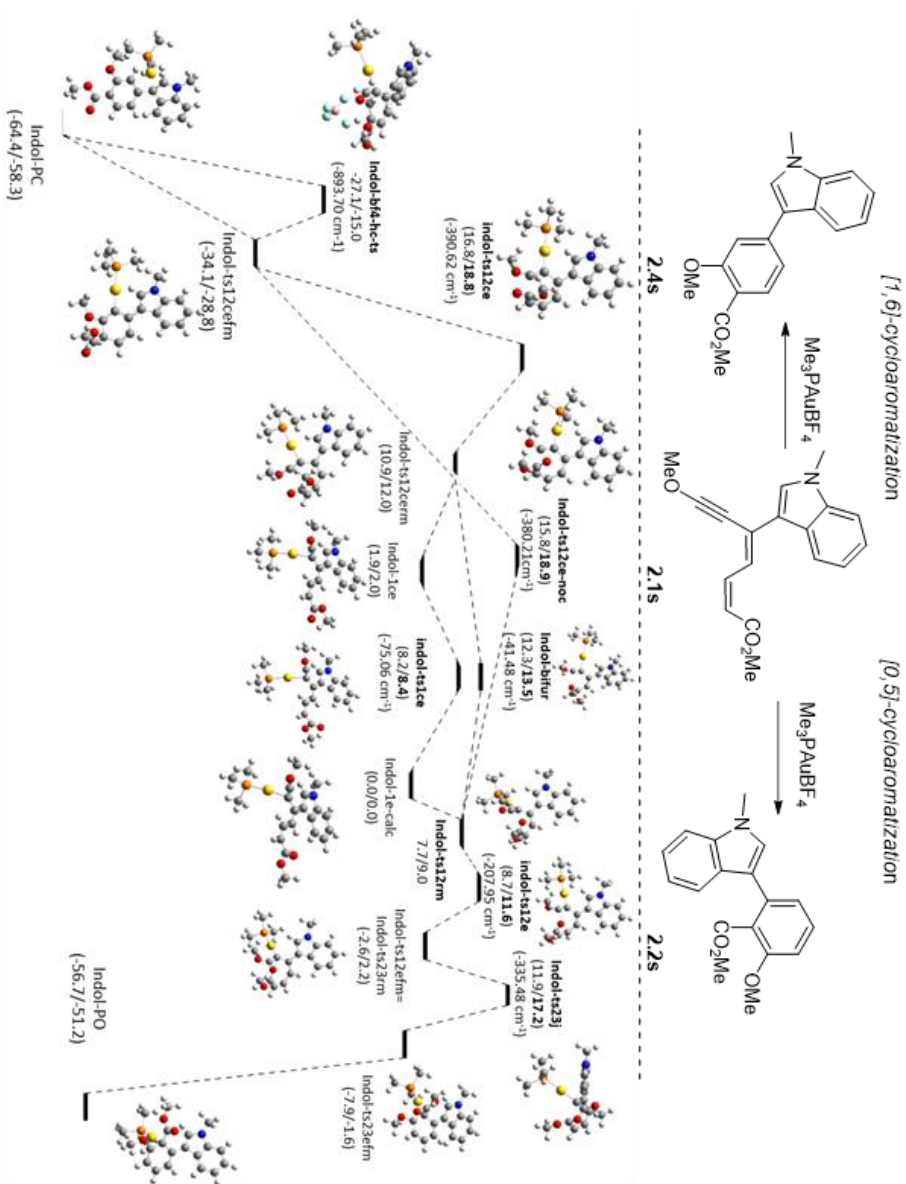
⁶ a) McQuarrie, D. A. *Statistical Mechanics, Harper and Row: New York*, **1976**; b) Ribeiro, R. F.; Marenich, A. V.; Cramer, C. J.; Truhlar, D. G. *J. Phys. Chem. B* **2011**, *115*, 14556-14562.

1 Chapter II.

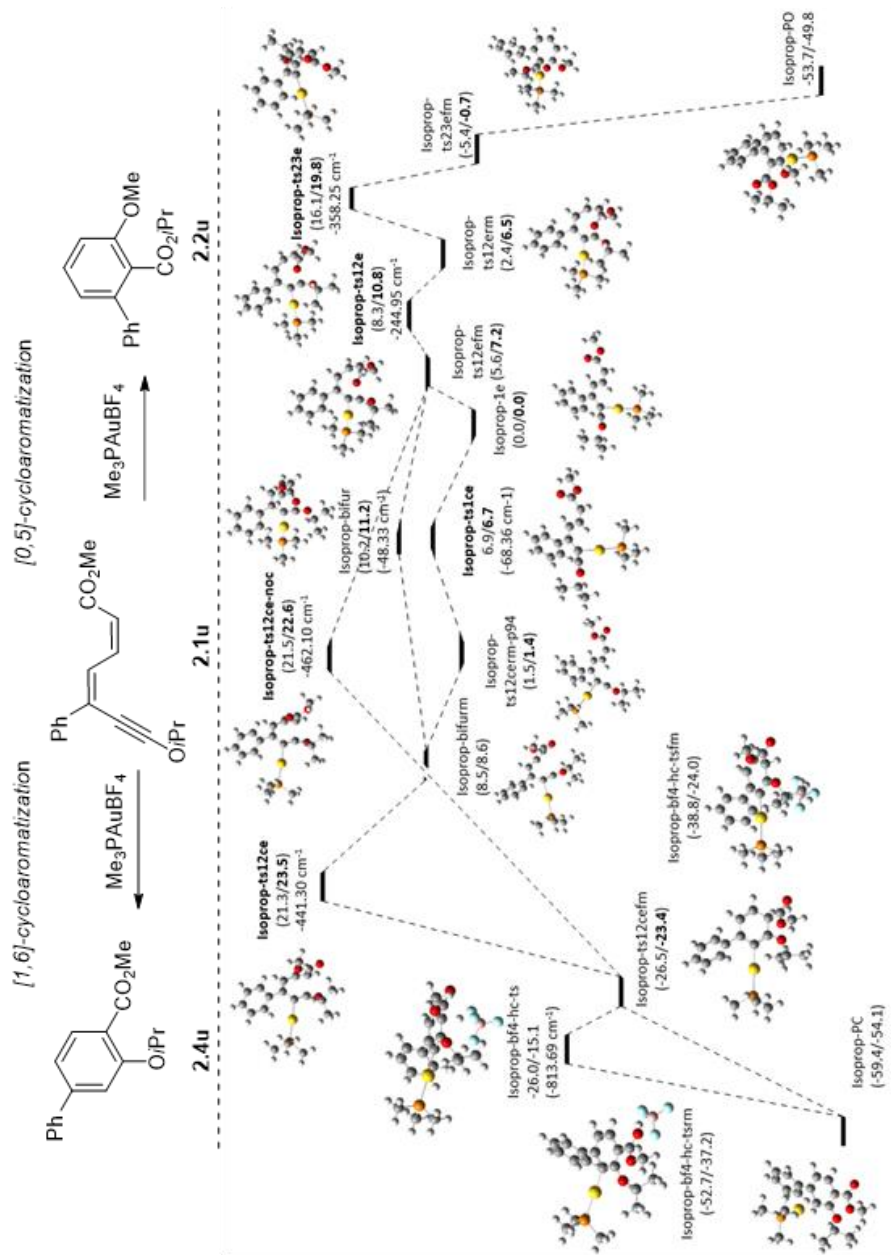
“Push-pull” 2,4-dien-6-ynecarboxylic acid **2.3x** and *“push-pull”* 2,4-dien-6-ynecarboxylic esters **2.1n, s, u, and x** were selected as reaction models for the calculations, with AlCl_3 and PMe_3AuCl as catalyst (see Schemes S1-4 for the reaction profiles for the cyclizations with both ball-and-stick, for clarity).



Scheme 1: Intermediates and transition states for the two cycloisomerisation pathways of "push-pull" 2,4-dien-6-ynecarboxylic ester 2.1x ($\text{R}^2 = \text{Me}$), catalysed by Me_3PAuCl , obtained using B3LYP/6-31(G) (LANL2DZ for gold).

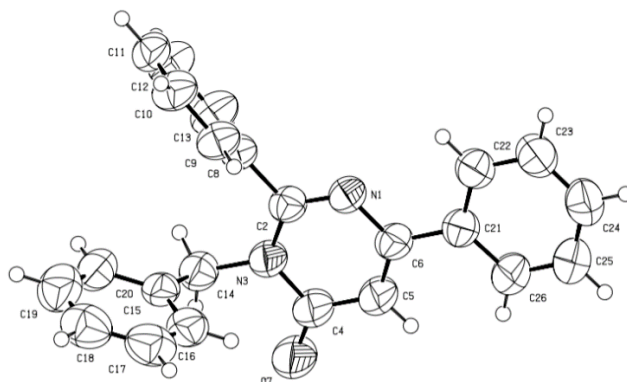


Scheme 3: Intermediates and transition states for the two cycloisomerisation pathways of "push-pull" 2,4-dien-6-ynecarboxylic ester 2.1s ($\text{R}^2 = \text{N-methylindol-3-yl}$), catalysed by $\text{Me}_3\text{PAuBF}_4$, obtained using B3LYP/6-31(G) (LANL2DZ for gold).



Scheme 4: Intermediates and transition states for the two coisomerisation pathways of "push-pull" 2,4-dien-6-ynecarboxylic ester 2.1u ($R^1 = iPr$), catalysed by Me_3PAuBF_4 , obtained using B3LYP/6-31(G) (LANL2DZ for gold).

Annex III:
Crystallographic data

3-Benzyl-2,6-diphenylpyrimidin-4(3H)-one (1.4c)

Empirical formula: C ₂₃ H ₁₈ N ₂ O	Formula weight: 338.14
Temperature: 297.0 K	Wavelength: 1.54184 Å
Crystal system, space group:	Monoclinic, P2(1)/c
Unit cell dimensions:	a = 12.2026 (3) Å α = 90.0 deg.
	b = 5.6291(2) Å β = 92.225(2) deg.
	c = 25.8032(7) Å γ = 90.0 deg.
Volume: 1771.08(9) Å ³	Z, Calculated density: 2, 1.087 Mg/m ³
F(000): 476	Absorption coefficient: 1.299 mm ⁻¹
Crystal size:	0.05x0.1x0.28 mm
Theta range for data collection:	-43.0 to 94.50 deg.
Limiting indices:	-14<=h<=14, -6<=k<=6, -26<=l<=26
Reflections collected / unique:	11255 / 4953 [R(int) = 0.0247]
Completeness to theta = 97.27	99.4 %
Absorption correction:	Semi-empirical from equivalents
Max. and min. Transmission:	1.00000 and 0.6974
Refinement method:	Full-matrix least-squares on F ²
Data / restraints / parameters:	3154 / 0 / 235
Goodness-of-fit on F²:	1.039
Final R indices [I>4σ(I)]:	R ₁ = 0.0460, wR ₂ = 0.1444
R indices (all data):	R ₁ = 0.0570, wR ₂ = 0.1444
Largest diff. peak and hole:	0.147 and -0.149 e.Å ⁻³

